2003

Piles embedded in soft clay located below the water table subjected to lateral cyclic loadings: Sensitivity analysis.

Deni Gunawan. Priyanto Putro
University of Windsor

PILES EMBEDED IN SOFT CLAY LOCATED BELOW THE WATER TABLE SUBJECTED TO LATERAL CYCLIC LOADINGS – SENSITIVITY ANALYSIS

by

Deni G. Priyanto P.

A Thesis
Submitted to Faculty of Graduate Studies and Research through the
Department of Civil and Environmental Engineering
in Partial Fulfillment of the
Requirements for the Degree of
Masters of Applied Science
at the
University of Windsor

Windsor, Ontario, Canada

2002

ABSTRACT

This study presents the theoretical formulation and numerical investigations of sensitivity analysis of laterally loaded piles embedded in soft clay located below the water table. Single piles with various lengths and boundaries subjected to cyclic lateral forces and bending moments are analyzed. The groups of 3×3 piles with various spacing (2D, 3D, 4D, and 5D) are also analyzed in this study. For single piles, the pile structure is considered as one-dimensional beam and the supporting soft clay is defined by means of p-y model. For groups of piles, the pile members are considered as one-dimensional beams and the pile cap is considered as plate finite elements. The behaviour of a pile-soil-pile system in the pile group is simulated by means of p-y relationship modified by the f_m factor that is dependent on the spacing of the groups of piles and the location of the pile member in a group of piles. The pile stiffness and characteristics of soil p-y relationship are taken as the design variables. They are considered as distributed parameters of continuous type. The pile-soil model subjected to lateral loading is analyzed in the framework of sensitivity theory by means of adjoint method for nonlinear system. The first variation of functional of maximum deformations due to the changes of the design variables is formulated based on virtual work theorem with aid of variational calculus. The unknown variations of generalized deformations imposed on the pile-soil system are determined by reference to constitutive relationships that are extended in the framework of sensitivity theory on the dependence on the design variables. The sensitivities of maximum generalized lateral deflections are determined in terms of sensitivity integrands ated with suitable variations of the design variables. The sensitivity integrands and

the numerical assessments of the integrations of the sensitivity integrands and the relative sensitivity factors are determined and discussed. Some comparatives analyses for single piles and groups of piles with various conditions are developed.

Dedicated to

The Almighty GOD

ACKNOWLEDGEMENTS

I would like to express my sincere thanks and appreciation to my supervisor **Dr. B.B. Budkowska** for her persistent support and guidance throughout the progress of this thesis, and also for her contribution on the derivation of formulas of the sensitivity analysis in **Chapter 4** and **Appendix A**. I would also like to express my profound gratitude towards my committee members **Dr. M. K. Madugula** and **Dr. N. G. Zamani** for their constructive suggestions and encouragements.

Thanks to the **librarians in the Leddy Library of the University of Windsor** who helped me finding the resources for my thesis.

My special thanks are due to my best friend **Amina Radyastuti**, my Canadian parents **Pastor & Mrs. McCready**, my brothers and sisters **Imelda, Octa, Ester, Hengki**, and **Yongki**, and **my grandmother** for their advice, encouragement, and prayer. My very special thanks are due to **my parents in Indonesia** for their financial support, advice, encouragement, and prayers. Finally, I would like to give thanks to my **God.**

TABLE OF CONTENTS

LIST OF TABLES

LIST OF FIGURES

LIST OF SYMBOLS

$(A_b)_i$	The quantitative assessments of sensitivity of b for each soil stage *i*.
$(A_c)_i$	The quantitative assessments of sensitivity of c for each soil stage *i*.
$(A_{EI})_i$	The quantitative assessments of sensitivity of EI for each soil stage *i*.
$(A_{tot})_i$	The total quantitative assessments of sensitivities of EI, c, γ', ε_{50} and b for each soil stage *i*.
A_y	Deflection coefficient for lateral force loading.
$(A_{\varepsilon_{50}})_i$	The quantitative assessments of sensitivity of ε_{50} for each soil stage *i*.
$(A_{\gamma'})_i$	The quantitative assessments of sensitivity of γ' for each soil stage *i*.
b	The width of the pile.
B_y	Deflection coefficient for bending moment loading.
c	The undrained cohesion of soil at the depth x.
c_u	The undrained cohesion of the soil.
C_b	The sensitivity operators/ integrands of the pile member due to the changes of the width of the pile b.
C_c	The sensitivity operators/ integrands of the pile member due to the changes of cohesion of soil c.
C_{EI}	The sensitivity operators/ integrands of the pile member due to the changes of stiffness of the pile EI.
C_m	Moment amplification factor (dimensionless).

C_y Deflection amplification factor (dimensionless).

$C_{\varepsilon_{50}}$ The sensitivity operators/ integrands of the pile member due to the changes of ε_{50}.

$C_{\gamma'}$ The sensitivity operators/ integrands of the pile member due to the changes of submerged unit weight of the soil γ'.

D The vector of maximum deformation of the pile soil system.

E Denotes the modulus of elasticity of the pile material.

EI Stiffness of the pile.

f_m p-multiplier.

f_{mi} p-multiplier for row i.

f_r The percentage of forces carried by the top of pile member.

$(F_b)_u$ The relative sensitivity factor of b connected with each stage i.

$(F_c)_u$ The relative sensitivity factor of c connected with each stage i.

$(F_{EI})_u$ The relative sensitivity factor of EI connected with each stage i.

F_y The yield strength of steel.

$(F_{\varepsilon_{50}})_u$ The relative sensitivity factor of ε_{50} connected with each stage i.

$(F_{\gamma'})_u$ The relative sensitivity factor of γ' connected with each stage i.

G_e Pile group efficiency.

H_c The characteristic shear load.

H_t	Lateral force load applied at the top of the pile.
i	The soil stages (nonlinear elastic stage, linear softening stage, and plastic flow stage).
I_{xx}	The moment of inertia in the x-direction.
J	Model constant that has recommended value is equal 0.5.
k	The modulus of the subgrade reaction of the soil.
l_i	The range where the specific soil's phase can develop.
m	Exponent.
M	The bending moment.
M_c	The characteristic moment load.
M_g	Maximum moment in a pile in the group (F.L).
M_s	Maximum moment in a single pile under the same load (F.L).
M_t	Bending moment load applied at the top of the pile.
M_y	The moment capacity of the pile.
$\tilde{M}$	Internal bending moment of the adjoint system generated by application of $\bar{1}$.
n	Exponent.
n_c	Number of column.
n_h	Constant of modulus of horizontal subgrade reaction.
N_r	The number of rows.

p	Soil reaction.
p_{gp}	The lateral load resistance of a pile in a group.
p_{sp}	The lateral load resistance of a single pile.
p_{top}	The soil resistance at the top of correlated pile member due to the lateral force Pg_i.
p_u	The ultimate soil resistance.
$\tilde{p}$	Internal soil resistance of the adjoint system generated by application of $\bar{1}$.
Pg_i	Lateral forces applied at the pile cap of the group of piles.
Pg_l	Lateral forces applied at the pile cap that result in the reaction on such a pile member is equal to unity.
P_i	Lateral forces applied at the single pile.
q_u	The unconfined compressive strength of the soft clay.
Q	The performace functional/ the potential functional, which is defined as a potential energy maximum deformation.
$(Q_u)_g$	Ultimate lateral load capacity of the group.
$(Q_u)_s$	Ultimate lateral load capacity of a single pile.
s_u	The shear strength of the soil.
$\mathbf{t}$	The design variables vector.
T	The relative stiffness factor.

R_I	Moment of inertia ratio.
V_{top}	The shear force at the top of the correlated pile member due to the lateral force Pg_i.
x	Depth from ground surface to p-y curve.
x_r	The depth where the transitition occurs in the distribution of the ultimate soil resistance for softclay.
y	Lateral displacement.
y_g	Group deflection (L).
y_s	Single pile deflection under the same load (L).
y_{50}	The deflection at one-half the ultimate soil resistance.
δb_n	The normalized value of the design component b with respect to initial value.
δc_n	The normalized value of the design component c with respect to initial value.
$\delta(EI)_n$	The normalized value of the design component EI with respect to initial value.
δt	The changes of the design variables.
δy	Variations of deformations imposed on the primary system.
$\delta y''$	Variations of the second derivative of deformations imposed on the primary system.

R_I	Moment of inertia ratio.
V_{top}	The shear force at the top of the correlated pile member due to the lateral force Pg_i.
x	Depth from ground surface to p-y curve.
x_r	The depth where the transitition occurs in the distribution of the ultimate soil resistance for softclay.
y	Lateral displacement.
y_g	Group deflection (L).
y_s	Single pile deflection under the same load (L).
y_T	Lateral deflection at the top of the pile.
y_{50}	The deflection at one-half the ultimate soil resistance.
δb_n	The normalized value of the design component b with respect to initial value.
δc_n	The normalized value of the design component c with respect to initial value.
$\delta(EI)_n$	The normalized value of the design component EI with respect to initial value.
$\delta \mathbf{t}$	The changes of the design variables.
δy	Variations of deformations imposed on the primary system.

$\delta y''$	Variations of the second derivative of deformations imposed on the primary system.
δy_T	The first variations (changes) of top lateral displacement.
$\delta\varepsilon_{50n}$	The normalized value of the design component ε_{50} with respect to initial value.
$\delta\gamma'_n$	The normalized value of the design component γ' with respect to initial value.
$\delta\varphi_T$	The first variations (changes) of top angle of rotation.
ε_{50}	The strain corresponding to 50% of maximum deviator in triaxial test.
γ'	The submerged unit weight of soft clay.
γ_s	The saturated unit weight.
γ_w	The unit weight of water.
λ	A constant that describes type of p-y curve.
λ_c	A scalar and the characteristic length.
λ_s	The characteristic length.
φ_T	Angle of rotation at the top of the pile.
σ_p	Representative passive pressure of soil.
$\bar{1}$	The generalized unit load that corresponds to the type of deformation component.

δy_T	The first variations (changes) of top lateral displacement.
$\delta \varphi_T$	The first variations (changes) of top angle of rotation.
$\delta \gamma'_n$	The normalized value of the design component γ' with respect to initial value.
$\delta \varepsilon_{50n}$	The normalized value of the design component ε_{50} with respect to initial value.
ε_{50}	The strain corresponding to 50% of maximum deviator in triaxial test.
γ'	The submerged unit weight of soft clay.
γ_s	The saturated unit weight.
γ_w	The unit weight of water.
λ	A constant that describes type of p-y curve.
λ_c	A scalar and the characteristic length.
λ_s	The characteristic length.
σ_p	Representative passive pressure of soil.
$\bar{1}$	The generalized unit load that corresponds to the type of deformation component.

CHAPTER 1
INTRODUCTION

1.1. PROBLEM STATEMENT

Although vertical piles are usually designed to support axial loads, in some cases, they have to support lateral loads or bending moments. Unlike the analysis of axially loaded piles that can be adequately designed by simple static methods, the analysis of laterally loaded piles is more complex. The solution must ensure that equilibrium and soil-structure interaction compatibility are satisfied and nonlinear soil response makes the analysis more complicated.

Many researches have been done to understand the response of pile to lateral load. There are two categories of serviceability design methods, the first is continuum method (Paulos 1971, Randolph 1981) and the second one is the subgrade reaction or p-y method. Both of those methods measure the structural responses, which are:

- The displacement
- The stress
- The internal forces (i.e. bending moments, shear forces, and soil reactions of the piles).
- The natural frequencies

The lateral loading that is exerted on the piles can result from the followings:

- Wind forces on buildings, bridges, or large signs,
- Centripetal force from vehicular traffic on curved highway bridges,
- Lateral seismic forces from earthquakes,
- Backfill loads behind walls, and
- Force of ocean waves, water currents and various forces subject on the substructure of bridges.

As a part of infrastructure that supports the upper structure, laterally loaded piles have to be properly designed. Designers should consider the maintenance services, future rehabilitations, renovations, and replacement activities in overall planning and costing. The structure will have a good performance when the quality of the structure is same as or better than the quality of the structure when it was designed and it also give an acceptable level of serviceability along its designed lifetime. Traditionally, the design of infrastructure have only considered initial condition, load, and material properties as the primary input variables for structural design without taking into account the effect of environmental and material degradation after time. Such an approach does not adequately assess the actual service life of the structure.

The performance of the design of the structure is affected by the performance of models. The development of a good performance model depends on the condition and assessment methods, loads, material predictions, and climatic and environmental conditions. The deterioration of the structure during in-service can be revealed by excessive deformations or various distresses of strength type. The key factors that caused deterioration of the structure are load, material degradation, environment, construction

quality and other mechanism. The primary factors in most deteriorations of deformation type are load and material aging. It is therefore essential to develop a method that provides a theoretical basis for assessment of maximum deformations expressed in terms of possible changes of material properties. It is particularly useful to refer such analysis to the structural model that is employed in the design process, which defines an initial condition. The discussed criteria can be suitable introduced to the distributed parameter sensitivity theory.

1.2 BACKGROUND

The application of sensitivity theory to laterally loaded piles is useful because of the following reasons:

- It is developed in the vicinity of the initial solution that is considered during design of the structure,
- The material characteristics are considered as a spatial functions,
- It is able to indicate the locations of the changes of material properties of the system that are critical for increase of maximum deformations,
- The performance functional of maximum deformation that is formulated in the scope of variational calculus makes the analysis transparent with respect to spatial variables,
- It is possible quantitatively assess the impact each of the change of the material property has on the change of maximum deformations.

1.3 OBJECTIVES

The objectives of this study are the followings:

- To perform the sensitivity analysis of lateral displacements and angles of rotation at the top of the piles embedded in the soft clay located below the water table subjected to laterally cyclic loading.
- To understand the behaviour of the laterally loaded piles based on the results of the sensitivity analysis.
- To determined the soil phases of the pile along the depth due to such loads.
- To demonstrate the distributions of the sensitivity operators along the depth of the piles in order to give information for engineers in design/ redesign/ rehabilitation of the pile structure (sensitivity of EI) and the information on the most effective and rational improvement of the soil (sensitivity due to c, γ', ε_{50}, and b).
- To assess the effect of the changes of the sensitivity operators on the lateral deformation at the top of the pile.
- Based on the results of the sensitivity analysis, perform the comparative analysis of the laterally loaded piles for the followings conditions:
  - The piles with various lengths (short piles and long piles).
  - The piles with various boundary conditions at the top of the piles (free head and fixed head).
  - To understand the behaviour of the laterally loaded pile with different type of loadings (bending moment M or lateral forces P).
  - The sensitivity analysis of the top lateral displacement δy_t and the top angle of rotation $\delta\varphi_t$ of laterally loaded piles due to the changes of the design variables.
  - Single piles and the groups of piles.
  - Between the pile members in a group.

- Pile members of groups with various spacings.

- To give possible application of the results of the sensitivity analysis and recommendations for laterally loaded piles design.

1.4 SCOPE

1. Piles used in this study are H-Piles, which are made of carbon steel A514, and soil type is soft clay below the water table. The properties of piles and soil parameters are presented in Chapter 5.
2. The design parameters that are used in the sensitivity analysis are the following:
   - The stiffness of piles, EI
   - The diameter of piles, b
   - The cohesion of soil, c
   - The strain corresponding to one-half the maximum principles stress difference, ε_{50}
   - The effective unit weight of the soil, γ'

1.5 REPORT ORGANIZATION

The organization of this report is the following:

Chapter 1 presents the Introduction. Chapter 2 contains the literature review on the laterally loaded pile. The literature review on sensitivity analysis of the pile and raft foundations is presented in Chapter 3. Chapter 4 discusses theoretical formulation of sensitivity analysis of laterally loaded pile embedded in soft clay below the water table subjected to cyclic loading. Numerical investigation on the sensitivity analysis is presented in Chapter 5. The results of numerical investigation on single pile are presented

in Chapter 6, while those on groups of piles are presented in Chapter 7. Chapter 8 discusses the result of both Chapters 6 and 7, and the conclusions of this research are presented in Chapter 9.

CHAPTER 2
LITERATURE REVIEW ON THE METHODS OF ANALYSIS OF LATERALLY LOADED PILES

2.1 CURRENT ANALYSIS OF LATERALLY LOADED SINGLE PILE

Determination of the models used in analysis of laterally loaded piles is significant in the accuracy of the results of the analysis. There are some models for use in analysis of laterally loaded single piles defined by Reese and Van Impe (2001). They are the following: (1) Elastic pile and elastic soil, (2) Elastic pile and finite elements for soil, (3) Rigid pile and plastic soil, (4) Characteristic load method, and (5) Nonlinear pile and p-y model for soil. The following section will review each of the models.

2.1.1 Elastic pile and elastic soil

In this model, pile is embedded in an elastic soil as show in Fig. 2.1a. Terzaghi (1955) proposed the values of subgrade modulus that can be used to solve deflection and bending moment, however these cannot be used for loads that are larger than the ones that produce one-half of bearing capacity of the soil. The standard beam equation, such as the one suggested by Hetenyi (1946) can be applied in this model. Although, this model has been widely used, but there is neither recommendation for the computation of

the bearing capacity under lateral load nor the comparison between the results of this method and experiments.

The computations using the elastic model and several variations of this model for various cases of loading of single pile and for the interaction of piles with close spacing have been developed by Paulos and his colleagues (Paulos and Davis 1980, Paulos and Hull 1989). Even though the solutions have got considerable attention, but they cannot directly be used for the computation of larger deformation and collapse of nonlinear soil (Reese and Van Impe 2001).

2.1.2 Elastic pile and finite elements for soil

This case is similar to the first model, but the soil is modelled by the finite elements. As shown in Fig. 2.1b, it seems that this model is ideal to analyze laterally loaded pile, because we can used various kinds of elements, whether three dimensional and nonlinear for all elements, or even nonlinear geometry can be used.

However, there are some problems in using this model (Reese and Van Impe 2001): (1) The selection of the basic nonlinear element of soil, (2) Coding to disregarding tensile stresses, (3) Modeling layered soils, (4) Accounting the separation of soil and pile when repeated loading applied, and (5) Accounting for the changes of soil characteristics due to various types of loadings. All the problems mentioned have not been solved satisfactory.

Some researchers have performed some analysis using this model. Brown, Shie, and Kumar (1989), Kooijman (1989) developed p-y curves using 3D finite elements models. The research in using 3D and nonlinear finite elements is still continuing,

however, there is no proposal being made for practical application (Reese and Van Impe 2001).

To apply this model in application, there should be some recommendations in appropriate size of the map, boundary constraints, special interface elements, most favourable shape and size of elements, or other details (Reese and Van Impe, 2001).

2.1.3 Rigid pile and plastic soil

Broms (1964a,b, 1965) used the model at Fig. 2.1c to predict the loading that produces ultimate bending moment. The pile is assumed to be rigid. The solution is solved by means of the equation of static for the distribution of the ultimate resistance of the soil that sets the pile in equilibrium. After ultimate loading is found for particular dimension of pile, the deflection in working load may be computed by using the first model. This method can be applied for either cohesive or cohesionless soils and for either long or short piles.

Even though, there are several simplified assumptions in this method, but it is very useful for preliminary design of laterally loaded pile. Another benefits of this method are: the mechanics of the problem of lateral loading can be seen clearly and this method can be used as a check of the result of p-y analysis method (Van Impe and Reese 2001).

2.1.4 Characteristic load method

The characteristic load method (CLM) was developed by Duncan and his colleagues in 1994, after the previous work of Evan and Duncan (1982). Using p-y

curves, they analyzed the laterally loaded piles for various kinds of soil and pile-head conditions. Then, the series of this solution was analyzed in order to find some simple equations that could be used in determination of response of pile under lateral loading easily for preliminary design. Dimensionless variables were used in the prediction equations. This method can be used to find the lateral deflections of the ground line of single piles with free-head, fixed-head, and 'flag-pole' (i.e. partially embedded) conditions due to lateral load, the values and the locations of the maximum moments for those three conditions, and the ground line lateral deflection when the pile subjected bending moment at the ground line. The determination of the length of the piles used as the samples in this study is based on this method, so that the more detail explanation of this method is presented in Chapter 4.

2.1.5 Nonlinear pile and p-y model for soil

In the model shown in the Fig. 2.2, loading on the pile commonly refers to the 2D case, no torsion or out-of-plane bending is assumed. The section of the piles is homogeneous, but made up of different cross section, as shown by the horizontal line across the pile. In the actual case the changes of cross section can be applied by using different wall thickness along the length of steel pipe. Hetenyi (1946) presented the solution for beams on foundation with linear response to solve this analysis.

The p-y method that was proposed by McClelland and Focht (1958) and Reese and Matlock (1956) is very useful and gives a practical method for design. In p-y curve, p represents soil reaction and y stands for lateral displacement at an arbitrary depth.

During the 1950's, the development of the digital computer to solve non-linear problem and the remote-reading strain gauge to develop soil-response (p-y) curves from the field experiment made the application of this method possible. This method has been used in the design of pile-supported platforms that subjected large lateral load from waves and wind by petroleum industry. Recommendations and rules in application of this method were presented by American Petroleum Institute (1987) and Det Norske Veritas (1977). The application of this method is extended for onshore foundation, such as in the publication of the Federal Highway Administration (USA) (Reese 1984).

2.2 CURRENT ANALYSIS OF LATERALLY LOADED GROUP OF PILES

O'Neill (1983) classified pile group into two types: (1) Groups of widely spaced piles, where the deflection of one pile in the group does not affect the other piles, because there is enough space between the pile members, so that piles interact only through the pile cap; (2) Group of closely spaced piles, where the response of one pile affect the nearby piles, because there is pile-soil-pile interaction.

There are several methods of analyses of pile-soil-pile interaction in the behaviour of pile groups (Dunnavant and O'Neill 1986, Davisson 1970): (1) continuum methods; (2) the Winkler interaction model; (3) the modified unit load transfer method; (4) the empirical stiffness distribution model; (5) the group reduction factor method; (6) the hybrid model; (7) the group amplification procedure; (8) p-multiplier concept. Each of the method will be discussed in the following section.

2.2.1 Continuum methods

One of the continuum methods is presented by Poulos (1971). The methods were developed to predict the pile-head response at the surface support. The variations of deflection and bending moment along the length of the piles are not taking into account. This method uses Mindlin's three-dimensional elasticity equations to calculate the stresses and displacements due to horizontal point loads applied in an elastic half space. Soil is assumed being elastic and the effect of the pile to other pile is taken into account by using linear elastic theory. The methods only can be used if the piles have constant cross sections, the pile head restraints have to be either fully-fixed (no rotation) or fully free (no bending moment). The other difficulty of this approach is the determination of the soil modulus between two piles.

Other kinds of continuum methods are the boundary element method (Banerjee and Davies, 1988) and the finite element method. Shibata et al. (1988) did 3-D finite element analysis for analysis of pile groups. This method can incorporate nonlinear soil behaviour and account the stiffness of the soil and piles separately and precisely. The complexity of is the disadvantage of this method.

2.2.2 Winkler interaction model

Nogami and Paulson (1985) and Hariharan and Kumarasamy (1982) presented a network of springs to represent the pile-soil-pile reaction. This method only considers the pile-soil-pile interaction in horizontal direction.

2.2.3 Modified unit load transfer method

The modified unit transfer load method (Bogard and Matlock 1983) developed p-y curves for a group of piles from a single pile. The modified single pile has diameter that same as the width of the pile group. The width is equal the width of the piles and the soils in between the piles. This procedure is used for circular pile embedded in soft clay, with the assumption that the distribution of the lateral resistance is equal among the piles.

2.2.4 Empirical stiffness model

The method, which developed by Dunnavant and O'Neill (1986), considers the effect of "shadowing" that is the effect that piles in the leading row are more heavily loaded than trailing row. This method depends on the proper selection of the soil elastic modulus. This method is the most reliable method to determine the load distribution among the piles in the group (Ooi and Duncan, 1994).

2.2.5 Group reduction factor method

In this method, the lateral load behaviour of the pile group is determined by a single pile analysis with the reduced modulus. Based on the model tests of pile groups in sands by Prakash (1962), Davisson (1970) concluded that there was no pile-soil-pile interaction when the space is more than eight diameters of the piles. Davisson (1970) proposed that for groups of piles with the spacing are equal tree diameters, the subgrade reactions were equal 75% of those of single pile. While, from spacing is equal to 3 to 8 diameters, the reduction factor can be linearly interpolated.

2.2.6 Hybrid model

The procedure is based on the concept that the deflection of a group of piles consists of the results of two mechanisms: (1) a mechanism due to nonlinear soil behaviour occurring close to the individual piles; (2) a mechanism due to pile-soil-pile interaction through the less highly stressed soil further from the piles. Focht and Koch (1973) proposed hybrid model that combined Poulos (1971) elastic continuum model and nonlinear p-y analysis. The estimation of deflections and bending moments in pile groups can be obtained with this method.

2.2.7 Group amplification procedure (GAP)

Group Amplification Procedure (GAP) (Ooi and Duncan 1994) is based on the original Focht and Koch (1973) procedure. The deflections and bending moments of pile groups will be greater than those of single piles, so that this procedure tried to determine amplification factor for deflection C_y and amplification factor for moments C_m, that formulated as:

$$y_g = C_y y_s \tag{2.1}$$

$$M_g = C_m M_s \tag{2.2}$$

where C_y = deflection amplification factor (dimensionless);

C_m = moment amplification factor (dimensionless);

y_g = group deflection (L);

y_s = single pile deflection under the same load (L);

M_g = maximum moment in a pile in the group (F.L);

M_s = maximum moment in a single pile under the same load (F.L);

The value of C_y and C_m is greater than or equal to 1.0. The values of C_y and C_m depend on the soil type (sand or clay), diameter of single pile, spacing of piles, passive earth pressure coefficient, angle of internal friction for sand and undrained shear strength for clay.

This procedure has the following limitations: (1) it can be used for rectangular (but not circular) group with uniform or non-uniform spacing, if the average pile or drilled shaft spacing is used in the calculation; (2) it can be applied only for vertical pile, not the batter ones; (3) it can be applied for free-head or fixed-head pile; (4) it cannot determine the distribution of load; (5) the arrangement of piles in a group is not taken into account, but the difference is not significant; (6) it is applied for long pile and embedded in a uniform soil. It has been found that there is a good agreement between the result of this method and in field load test (Ooi and Duncan 1994).

2.2.8 Pile group analysis using p-multipliers

The most commonly used method of the laterally loaded pile analysis is the application of finite difference or finite element method to solve the beam equation and the soil is modelled as nonlinear soil-response (p-y) curves.

The deflections of pile in a group are greater that those of single isolated pile, if they are subjected the same load. The loss of efficiency of the piles in the group was related principally to "shadowing"(i.e., the loss of soil resistance of piles in the trailing

rows) (Brown et al., 1988). This fact indicates that the p-y curves of the soil should be modified when it is used for the analysis of the piles in a group.

Brown et al. (1988) proposed the p-y multiplier concept. This concept, as shown in Fig.2.3, introduced the using of p-multiplier (f_m) to indicate the loss of soil resistance. This value modifies the single-pile p-y curve to obtain a group-pile p-y curve. In this approach, the p-y curve is stretched in the direction of deflection, so that the deflection of pile group will be bigger than that of single pile due to similar loading.

The values of p-multiplier proposed by Brown et al. (1988) are the result of a large-scale test for pile-group and isolated pile embedded in dense sand subjected to cyclic loading. Brown and Shie (1991) also performed the p-multiplier from the result of 3-D finite element analysis. They also performed the values of y-multiplier. While p-multiplier is less than or equal to 1.0, y-multiplier is greater than or equal to 1.0.

Mokwa and Duncan (2001) proposed *p*-multiplier design curves (Fig. 2.4) that make this concept can be applied for various kind of soil. They collected and reviewed over 350 journal articles and other publications pertaining to lateral resistance, testing and analysis of pile caps, piles, and pile groups. They also did full-scale field lateral load tests, 1g model laboratory tests, and geotechnical centrifuge test. The description of pile group arrangements for this approach is shown in Fig. 2.5.

Mokwa and Duncan (2001) formulated *p*-multiplier in Eq. (2.3). They also proposed the relationship between *p*-multiplier (f_m) and the pile group efficiency (G_e) as shown in Eqs. (2.4)~(2.5).

$$p_{gp} = f_m p_{sp} \tag{2.3}$$

$$G_e = \frac{(Q_u)_g}{n(Q_u)_s} \tag{2.4}$$

$$G_e = \frac{\sum_{i=1}^{N_r} f_{mi}}{N_r} \tag{2.5}$$

where p_{gp} = the lateral load resistance of a pile in a group

p_{sp} = the lateral load resistance of a single pile;

f_m = p-multiplier;

G_e = pile group efficiency;

$(Q_u)_g$ = ultimate lateral load capacity of the group;

$(Q_u)_s$ = ultimate lateral load capacity of a single pile;

n = the number of piles in the group;

N_r = the number of rows;

f_{mi} = the p-multiplier for row i.

The value of the pile group efficiency G_e obtained by using Eq. (2.4) can be different from using Eq. (2.5). However, from both method of the calculation of G_e result in the same trends that can be considered as a same value for practical purpose.

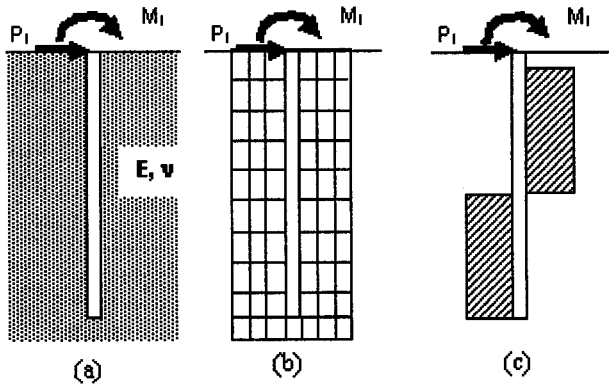

Figure 2.1 Models for a pile under lateral loading (Reese and Van Impe 2001).

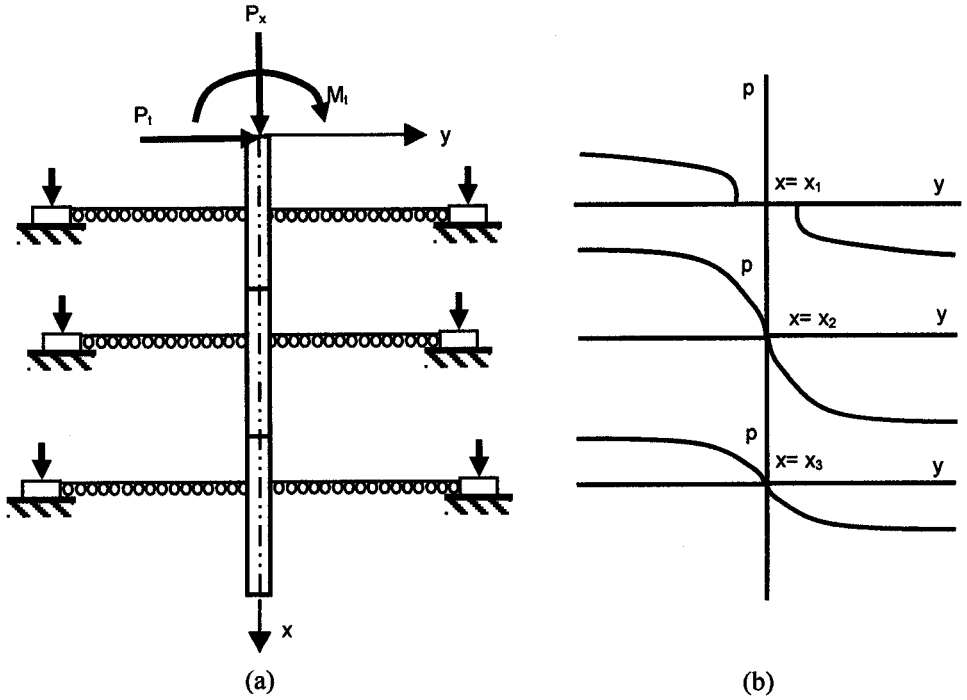

Figure 2.2 Model for a pile under lateral loading with p-y curves (Reese and Van Impe 2001)

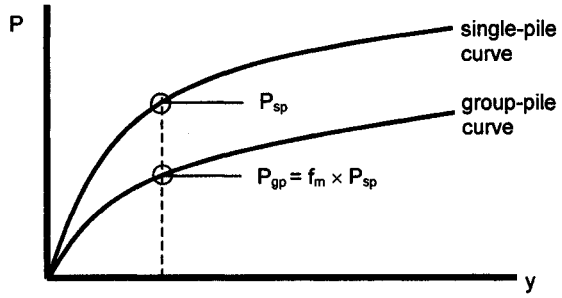

Figure 2.3 p-multiplier (f_m) concept (Brown et al. 1988)

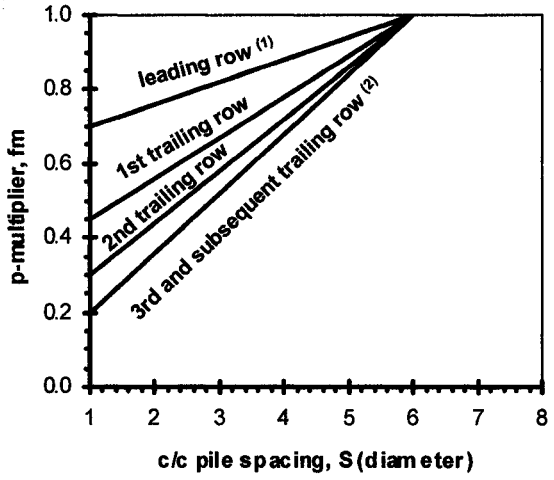

Notes:

(1) The term row used in this chart refers to piles aligned perpendicular to the direction of applied load (see Fig. 2.5).

(2) Use the f_m values recommended for the 3rd trailing row for all rows beyond the third trailing row.

(3) Bending moments and shear forces computed for the leading row corner piles should be adjusted as follows:

Side by spacing	Corner pile factor
3D	1.0
2D	1.2
1D	1.6

Figure 2.4 Proposed p-multiplier design curves (Mokwa and Duncan 2001)

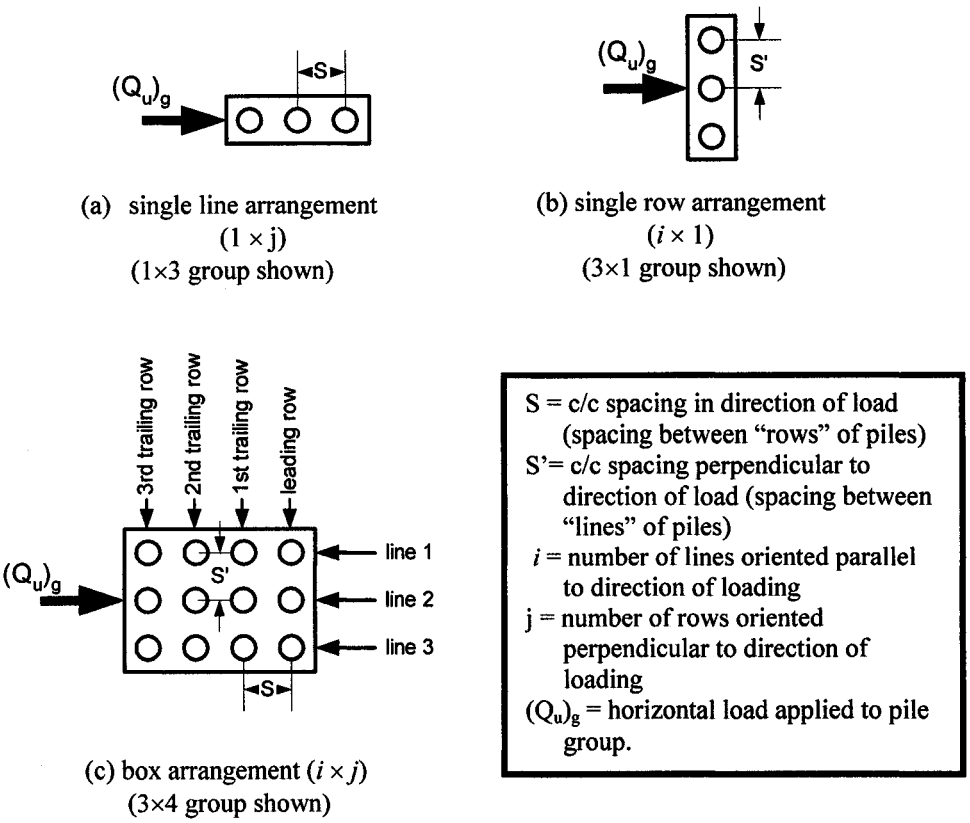

(a) single line arrangement ($1 \times j$) (1×3 group shown)

(b) single row arrangement ($i \times 1$) (3×1 group shown)

(c) box arrangement ($i \times j$) (3×4 group shown)

Figure 2.5 Description of term used to describe pile group arrangement (Mokwa and Duncan 2001)

CHAPTER 3
LITERATURE REVIEW ON THE SENSITIVITY ANALYSIS OF PILE FOUNDATION

3.1 GENERAL

The loose definition of the sensitivity analysis is the study of the relationships between information flowing in and out of the models (Saltelli et al. 2000). The models can be developed as physical experimentations or mathematical models. In some cases, the physical experimentations are not effective and even impossible to be done because the process is too complex. In such these cases, the investigators can employ the mathematical or computational models. A mathematical model is defined by a series of equations, input factors, parameters, and variables aimed to characterize the investigated processes.

Kleiber et al. (1997) state that there are two major reasons of doing sensitivity analysis: (1) The overall computational cost required by such algorithms depends strongly on the efficiency of gradient evaluation, because the gradients of functions describing system behaviour with respect to parameters are essential for system optimization and reliability assessment. (2) It is now broadly accepted that any realistic large-scale engineering simulation has to be completed by an extensive study on response

sensitivity to system parameters just to broaden our understanding of the system behaviour.

Sensitivity analysis means very different things to different people (after Saltelli et al. 2000). In civil engineering, the sensitivity analysis is used in terms of the structural optimization. The optimal design is the best feasible design according to a preselected quantitative measure of effectiveness. The minimum cost may be the primary consideration in doing structural optimization in civil engineering (Haftka et al. 1990).

Although this study does not take cost as the primary consideration, by characterization of the effect of the changes of the soil and pile parameters, we can define the most effective way to improve the strength of the laterally loaded piles, and then the cost considerations become the responsibility of the designers.

3.2 DESIGN VARIABLES, PERFORMANCE FUNCTIONAL, AND CONSTRAINTS

Design variables are defined as a group of parameters that have potential for change in a permissible range in order to improve or optimize a structure (Haftka et al. 1990). Design variables are available to the engineer at the onset of the investigation process. The examples of the design variables can be physical parameters of the structure (stiffness), strength parameters of the soil model, or geometric parameters (cross-section dimensions, length). The design variables employed in this study are the followings:

- The pile stiffness EI
- The cohesion c
- The submerged unit weight γ'

- The ε_{50}
- The width of the pile b.

The notion of optimization also implies that there are some merit functions or functions that can be improved. The common terminology for such functions is objective functions or performance functions (Haftka et al. 1990). The sensitivity analysis is concerned with the variation of a performance function with respect to changes (variations) of the design variables. The examples of the performance function can be deformation function, internal forces function, etc.

Determination of constraint approximations, such as displacement and stresses is the next important stages in structural optimization after performing the sensitivity analyses. The sensitivity analyses are performed to determine the derivatives of the physical responses of a structure regarding the design variables when the value of one or more design of the design variables is disturbed. The constraint approximations are used to predict the physical responses of the structure in terms of their design variables and the derivatives of the responses of the structure.

3.3 CLASSIFICATION OF SENSITIVITY METHODS

There are two methods of sensitivity analyses commonly identified in the literature. They are discrete methods and variational methods. The discrete methods, adopted for finite element analysis, can be classified into three groups, i.e. finite difference, semi-analytical and analytical methods. In the finite difference method, after analysis using the original design variables and their perturbed values has been performed, the derivatives

of the physical responses with respect to the design variables are computed. In semi-analytical method, the derivatives of the physical responses are obtained directly from the modification of the finite element formulations in which the finite difference equation is applied to calculate the derivatives of the stiffness matrix. The analytical method is identical to the semi-analytical method except that the first derivative of the stiffness matrix regarding to the design variables is calculated analytically. In the variational methods, the gradients of objective and constraint functions regarding to the design variables are expressed analytically, and the governing equations of the structure are differentiated to carry out the design sensitivity analysis. (Haftka et al. 1990, Choi and Chang 1992, Mota Soares and Leal 1992).

The discrete methods are only applicable to non-structural sensitivity analysis involving systems of linear equations, eigen value problems, etc (Haftka et al. 1990). For structural applications, they have two disadvantages, which are: (1) Not all structural analysis solutions methods lead to the type of discretized equation; (2) Operating on the discretized equations often required access to the source code of the structural analysis that are usually not provided in most structural analysis programs (Haftka et al. 1990).

Variational methods differentiate the equations governing the structure before they are discretized, so that the source code of the structural analysis program is not required. The variational methods can be defined into two groups, i.e. the direct differentiation method and the adjoint method. The direct differentiation method differentiates the system equations with respect to the design variables to obtain the first-order equations for displacement sensitivities. In the adjoint method, a system subjected to initial action, i.g. deformation, and the evaluated the sensitivity response of the system.

The Lagrange multipliers allow the evaluation the sensitivity response without explicit calculation of the displacement sensitivity.

3.4 PREVIOUS WORKS

The applications of the sensitivity analysis can be used in many different areas. In civil engineering, some researchers have employed the sensitivity analyses in the pile and raft foundations with a various conditions of loadings and design parameters.

3.4.1 Raft foundation

Valliappan et al. (1997, 1999) have done the sensitivity analyses of the raft foundations. Valliappan et al. (1997) proposed an algorithm for the semi-analytical sensitivity method applied to non-linear analysis and a modification of the two-point constraint approximation, named bi-point constraint approximation. A raft foundation on a soil medium has been analyzed and the results have been compared to validate the proposed method.

Valliappan et al. (1999) applied a structural optimization combined with the finite element method for the optimal design of a raft-pile foundation system. For the optimization process, the sensitivity analysis is carried out using the approximate semi-analytical method while the constraint approximation is obtained from the combination of extended Bi-point and Lagrangian polynomial approximation methods. The objective function of the problem is the cost of the foundation. The design variables are the raft thickness, cross-section, length and number of piles. The maximum displacement and

differential displacement are selected as constraints. The proposed method is shown to achieve an optimum design of raft-pile foundation efficient and accurately.

3.4.2 Pile foundations

3.4.2.1 Introduction

The sensitivity analyses of the piles foundations that have been done can be classified by the types of loading, i.e. piles under axial loading, piles undergoing torsion, piles under bending load condition, piles partially embedded in soil, and piles under lateral loading. The following section presents the previous works in sensitivity analyses in each of them.

3.4.2.2 Piles under axial loading

Budkowska and Szymczak (1993a, 1994b) derived first variations of a vertical displacement and axial force of axially loaded piles due to changes of the design variables. The design parameters in this sensitivity analysis are the pile material and the soil behaviour. A simple one-dimensional idealization of the pile in conjunction with the soil model consisting of a continuously distributed system of springs and a spring located on the pile toe or Winkler-type model of the soil behaviour is assumed. The considerations based on the virtual work theorems are valid for both linear and nonlinear in the pile material and the soil behaviour. The first variations of the displacements and the internal forces enables us to assess the quantities under consideration due to the design variables increment without carrying out full reanalysis of the pile. The numerical

examples presented in this researches show the good performance of the accuracy of the approximation of the change of the design variables.

Budkowska and Szymczak (1995b) employed the same models of the pile and soil, but different design variables, i.e. the location of end-points of the piles. The numerical examples presented in this study show that the accuracy of the approximation of the changes is also good, even for 30% changes of the pile length.

3.4.2.3 Piles undergoing torsion

Budkowska and Szymczak (1993b) derived first order variations of an angle of the pile twist and a torque at a specified cross-section of the pile due to design variable variations. The cross-section dimensions and the parameters determining both the pile material and the soil behaviour are assumed to be the design variables. The considerations based on some variational theorems of mechanics are restricted to the linear range of the structure behaviour.

Budkowska and Szymczak (1994b) also presented the sensitivity analysis for piles undergoing torsion, but different design variables are employed, i.e. an increment of the pile length. A pile of circular cross-section, made of a linear elastic material subjected to torsional loadings is considered. The considerations are based on calculus of variations with moving boundaries. The sensitivity analysis enables the calculation of changes in the quantities under consideration due to the pile end shifts without a full re-analysis of the pile. A detailed discussion of a pile embedded in multilayered soil is also presented. The accuracy of the approximation of the change of the angle of the pile top twist due to the pile length variation is investigated and shows a good accuracy.

3.4.2.4 Piles under bending load condition

Budkowska (1998a) presented the sensitivity analysis of piles subject to bending due to variable length. The pile structure is modeled as a beam element and the soil is simulated by the elastic foundation of Winkler type. The functionals of bending and shear energy are defined in the scope of variational calculus based on the principle of virtual energy. They employ the concept of the adjoint structure subject to unit dummy load. The first variations of deformation and static field components are formulated with moving ends. The evaluation of changes of kinematic and static fields utilizes Taylor's mean value theorem, as well as approximate values of variations of deformation field component not defined within the intervals of shift of soil of support conditions. The final forms of sensitivity equations are accompanied with set of equations defining the behaviour of natural boundary conditions for primary and adjoint structure. They form the basis of the numerical investigations of the piles penetrating homogeneous and nonhomogeneous soil as well. The obtained sensitivity results are compared with exact solutions and accuracy of the results is examined from the error analysis standpoint.

Employed the same methods but different design variables, Budkowska (1998b) performed the sensitivity analysis of the long piles embedded in homogeneous elastic soils under bending moments. The derived sensitivity equations are valid for arbitrary distribution of the design variable vector. The obtained sensitivity equations resulted in formulation of the underintegral sensitivity operators associated with each of the design variables. The determined underintegral sensitivity operators enable one to localize the most effective domains where the variations of the design variables affect mostly the changes of the quantity under consideration.

3.4.2.5 Buckling of piles partially embedded in soil

Budkowska and Szymczak (1996, 1997) presented the first variation of the critical buckling load of a pile partially embedded in a soil. Pile is idealized as one-dimensional column and the soil represented by Winkler-type elastic foundation. The effect of negative skin friction is neglected. The design variables are the pile material and the soil properties, and also the pile ends locations. The accuracy of the approximation of the change of the critical buckling load due to some design variable variations is also investigated and shown that the first-order sensitivity analysis leads to a good approximation of the change of the critical load, due to the design variable variations within broad limits of its changes.

3.4.2.6 Piles under lateral loading

Budkowska and Szymczak (1992a, 1992b; 1995) proposed an approximate procedure for calculation of changes of maximum values of an arbitrary displacement and an internal force of laterally loaded piles due to some increments of the pile cross-section dimensions, the pile material constants and the soil parameters is proposed. The pile is simulated as one dimesional beam element, and the response of soil is modeled as the Winkler type foundation. The method presented can be applied to both linear and nonlinear behaviour of the pile material and the soil. The first order variation of the maximum value of quantity under consideration is evaluated with the aid of the adjoint structure concept. The accuracy of the calculation of the changes of the maximum value of the flexural moment of the pile by means of its first variation is discussed. Using the same models of piles and soils. The results of the numerical examples given dealing with

the linear structures allow the conclusion to be drawn that the approximation of the exact results by means of the first variations are reasonable good (Budkowska and Szymczak, 1992a)

Budkowska and Cean (1996) presented the theoretical formulation of the sensitivity analysis of laterally loaded long piles embedded in a homogeneous sandy soil employed the same models and methods. The design variables are taken as the stiffness of the pile EI and the modulus of the subgrade reaction of the soil k. They did the comparative analysis of the pile loaded by the horizontal force and the bending moment. The effects of changes of the design variables on the components of kinematic field for pile due to both types of loadings have quantitatively the same value. They also performed the distribution of the sensitivity operators that can be used for engineering practice in design/ redesign/ rehabilitation of the shape of the pile structure (sensitivity due to EI) and the information on the most effective and rational improvement of the soil (sensitivity due to k).

Using the same models of piles and soil, and also the similar methods, the theoretical formulation of sensitivity analysis of laterally loaded piles due to variable location of a soil layer are presented (Budkowska 1999, Budkowska, Sekulovic, and Saha 1999a). The result of the sensitivity analysis enables one to analyze the effect of the changes of the internal forces and generalized displacements of laterally loaded piles for various scenarios of changes of boundaries of the arbitrary soil layer resulting in expansion/ shrinkage, as well as translation upwards/ downwards. The numerical investigations (Budkowska, Sekulovic, and Saha 1999b) were compared with the exact solutions obtained by means of reanalysis of the problem. The accuracy of the sensitivity

outcomes has been examined in the framework of the error analysis. It enables one to determine the acceptable range of variability of the depth of soil layers assuring acceptable error of approximation.

Budkowska (1997a) presented the general formulation of the sensitivity analysis of laterally loaded pile embedded in a homogeneous soil medium. This approached is also based on the principles of variational calculus. The central point of analysis is connected with the concept of functional with constraints, which is then transformed into augmented functional without constraints, however dependent on the Lagrange multipliers vector. The other part of this paper (Budkowska 1997b) investigated the short steel piles subjected to a bending type of load. The pile structures are embedded in homogeneous sand and clayey soil modeled as a one-dimensional structural element supported by Winkler type foundation. The modulus of subgrade reaction for clayey is constant, while that for sandy soil varies linearly. The design variables are taken as the bending stiffness of the pile structure and modulus of subgrade reaction. Based on the distributions of underintegral sensitivity operators for short piles embedded in clayey and sandy soils, some conclusions of considerable importance for engineering practice are presented.

Budkowska and Suwarno (2002a) presented a sensitivity analysis of lateral displacements of long single pile subjected to static horizontal forces applied at the soil surface. Soil is stiff clay below the water table that modeled by means of a p-y model. The material characteristics of the pile-soil system are taken as the design variables. The sensitivity functional of a nonlinear pile-soil system is formed with the aid of the adjoint system that demonstrates the nonlinear features. The determination of the first variation

of lateral displacement functional due to the changes of the design variables resulted in formulation of the sensitivity integrands associated with each design variables.

Budkowska and Suwarno (2002b) performed a sensitivity analysis of pile group subjected to horizontal loading embedded in stiff clay located below the water table. They use the same methods for single piles and take into account the group effect by introducing suitable f_m factor. The quantitative assessment of the locations of the soil phases, integrations of the sensitivity operators, and the relative sensitivity factors are also presented and come to the conclusions of the comparisons of the design variables' importance for each soil phase.

Budkowska and Priyanto (2002a) compared the sensitivity integrands for short piles and long piles embedded in soft clay located below the water table. The type of load is cyclic loading that applied at the soil surface. The p-y model is employed to simulate the soil effect on the behaviour of the pile-soil system. The design variables chosen for investigation are those connected with pile-soil strength parameters. The pile-soil system is a five parametric sensitivity system. It is analyzed based on the adjoint pile method that has nonlinear features. The equation of first variation of deformation determined depend on the sensitivity operators connected to each of the design variables. The sensitivity operators presented are strongly dependent on the magnitude of the applied load.

Budkowska and Priyanto (2002b) presented the behaviour of a pile-soil system in the pile group embedded in the soft clay below the water table under cyclic lateral loading. The soil is simulated by means of a p-y relationship modified by the f_m factor that is dependent on spacing and location. The design variables are taken as the bending stiffness of the pile and soil strength parameters that appear in the p-y constitutive

relationship. The adjoint structure method is adopted for sensitivity investigations. Special approaches are developed for the purpose of sensitivity analysis to assure that the pile investigated is the nonlinear member of pile group. It assures that the kinematic and static fields produced by unit-generalized load depend on the magnitude of the load applied to the primary pile group system. The first variation of kinematic functional due to variations of the design variables vector is formed with the aid of variational calculus. It leads to the determination of nonlinear sensitivity integrands that are strongly dependent on the magnitude of the applied load. The last two papers mentioned are parts of this research.

Barakat et al. (1999) presented a general approach to the reliability-based analyses and the optimum designs of laterally loaded piles. All behaviour and side constraints specified by standard specifications for piles are taken into account by this approach. The casual effect of corrosion of piles with time is considered in formulation with limiting state functions. The solution to reliability-based problems is obtained by a computer program (RELLOP). A general reliability based methodology is developed and implemented in the developed computer program (RELLOP) for both element and system limit states. Numerical examples demonstrating the feasibility of considering multiple limit states and system reliability requirements in the design of laterally loaded piles are presented. Effects on the reliability-based design solution of allowable reliability levels, and time of exposure to corrosion are also illustrated.

3.5 SENSITIVITY ANALYSIS METHODS EMPLOYED IN THIS STUDY

In this study, the theoretical approach of sensitivity analysis is formulated in the framework of variational calculus that allows for appropriate involvement of sensitivity parameters of a continuous type. The behaviour of the loading-deformation of the laterally loaded pile, although highly nonlinear, is path independent. For such a condition, the adjoint system method is the most effective methods (Kleiber et al. 1997). Because of that, the first variation of functional of the top lateral deflection and the angle of rotation is formed based on the adjoint structure method (Budkowska 1997a). It incorporates the virtual work theorem. It is assumed that in the scope of sensitivity theory, the constitutive relationships of the pile-soil interaction system depend on the state and design variables. The formulation employs the fact that the variations of δy and $\delta\varphi$ are imposed on the primary pile structure that is subjected to a constant load. This approach enables one to determine the first variations of functional of generalized deformations by means of sensitivity operators of the design variables. The adjoint structure has to satisfy the same constitutive relationship that the original primary structure does (Dems and Mroz 1983), so that it is very important to determined the models and loading of the adjoint structure that appropriate in this definition. The models and loadings of the adjoint structures are discussed in Chapter 6 and 7.

CHAPTER 4
THEORETICAL FORMULATION

4.1 INTRODUCTION

This chapter is divided into two parts. The first part presents the constitutive behaviour of soft clay located below the water table after Matlock (1970), and the second part is the derivation of equations for sensitivity analysis of the first part.

4.2 P-Y CURVE OF SOFT CLAY LOCATED BELOW THE WATER TABLE SUBJECTED TO LATERAL CYCLIC LOADING

The determination of p-y curve is very important in modelling the soil resistance. Matlock (1970) provided p-y curve for analysis of pile embedded in soft clay below the water table subjected to lateral cyclic loading. He performed lateral load tests employing a steel pipe pile that was 12.75 inches in diameter and 42 ft long. It was driven into clays near Lake Austin that had shear strength of about 800 lb/ft^2. The pile was recovered, taken to Sabine Pass, Texas, and driven into clay with a shear strength that averaged about 300 lb/ft^2 in the significant upper zone. Based on this research, the characteristic

shapes of the p-y curves for soft clay below the water table subjected cyclic loading is shown in Fig. 4.2.

The soil strength parameters are not explicitly presented in the constitutive model but are presented by means of the ultimate soil resistance p_u. The values of p_u varies in linear fashion along the depth of pile as shown in Fig. 4.2, they are formulated in Eqs. (4.1)-(4.2).

For $x < x_r$:

$$p_u = \left(3 + \frac{\gamma'}{c}x + \frac{J}{b}x\right)cb \tag{4.1}$$

For $x \geq x_r$:

$$p_u = 9cb \tag{4.2}$$

where γ' is the submerged unit weight of soft clay, c is undrained cohesion of soil, b is the width of the pile, and J is model constant that has recommended value is equal 0.5.

Based on the continuity of p_u, x_r is formulated in Eq. (4.3) from the comparison of Eqs. (4.1) and (4.2). The variability of p_u is shown in Fig. 4.1.

$$x_r = \frac{6cb}{(\gamma' b + Jc)} \tag{4.3}$$

The horizontal displacement of the soil y is defined in term of y/y_{50}, the value of y_{50} for soft clay is formulated in Eq. (4.4).

$$y_{50} = 2.5\ \varepsilon_{50} \cdot b \tag{4.4}$$

where ε_{50} is the strain corresponding to 50% of maximum deviator in triaxial test, Wang and Reese (1993) recommended the value of ε_{50} for soft clay located below the water table is equal 0.02.

For $x \leq x_r$ the soil model is able to simulate the nonlinear elastic p-y relationship that is followed by linear softening which is then transformed into plastic flow. The soil response can be localized in any of these stages depending on the lateral deflection y of the pile produced by the applied load. The constitutive behaviour of soft clay for $x \leq x_r$ is defined by set of the following relationships that require the fulfillment constraints imposed on the lateral displacement y.

Thus for $0 < y < 3y_{50}$:

$$p = 0.5\ p_u \left(\frac{y}{y_{50}}\right)^{1/3} \tag{4.5}$$

and for $3\ y/y_{50} \leq y \leq 15y/y_{50}$

$$p = p_u \left[\left(0.9 - 0.18\frac{x}{x_r}\right) - 0.06\left(\frac{y}{y_{50}}\right)\left(1 - \frac{x}{x_r}\right)\right] \tag{4.6}$$

whereas for $y > 15y_{50}$

$$p/p_u = 0.72\, x/x_r \tag{4.7}$$

Eq. (4.5) with the same lateral constrains describes the soil behaviour also for $x \geq x_r$. However, when lateral displacement y reaches value $3y_{50}$, Eq. (4.6) ceases to be valid for $x \geq x_r$ and Eq. (4.6) becomes:

$$p = 0.72\, p_u \tag{4.8}$$

The graphical representation of the soil model for soft clay located below the water table subjected to cyclic loading is presented in Fig. 4.2.

Reviewing the diagrams presented in Fig. 4.2 shows, for $x < x_r$ that the soil has three stages which are nonlinear elastic stage, linear softening stage, and plastic flow, while for $x \geq x_r$ that the nonlinear soil behaviour is transformed into plastic flow at $y = 3y_{50}$ passing by the softening stage along the depth, so that there is no softening stage. The important features of each soil stage are:

1. In nonlinear elastic stage, there exists the unique relationship p-y such that the increase of p implies the increase of y,
2. In linear softening stage, the relationship p-y that is also unique means that the increase of y implies the decrease of p,
3. In plastic stage, there is no unique p-y relationship which denotes that single value of p is related to infinite numbers of y,

4. The intensity (rate of softening) depends on the ratio (x/x_r). It has highest value for $x = 0$ and disappears for $x = x_r$.

The examination of constitutive Eqs. (4.5)~(4.8) together with Eqs. (4.1), (4.2), and (4.4) shows that the parameters that contribute to p-y relationship are: cohesion c, submerged unit weight γ', width of the pile b and ε_{50}. The increase of first three parameters in nonlinear elastic stage results in increase of the soil reaction p. However, the increase of ε_{50} is associated with decrease of soil reaction. The ε_{50} can be called weakness parameter or deformability parameter. Its small value defines strong cohesive soil like stiff clay that has brittle behaviour, while large value of ε_{50} indicates the weak cohesive soil such as soft clay that has ability to deform.

4.3 THEORETICAL FORMULATION OF SENSITIVITY ANALYSIS OF LATERALLY LOADED PILES SUPPORTED BY SOFT CLAY LOCATED BELOW THE WATER TABLE

The behaviour of laterally loaded pile embedded in a soil is considered as a soil-structure interaction system. The pile is modeled as one dimensional beam element. The surrounding soil is simulated by means of nonlinear p-y springs distributed in continuous fashion along the pile length. The suitable differential equation of the pile-soil system shown in Fig. 4.3A is the following:

$$EI\,y^{IV} - p = 0 \tag{4.9}$$

where EI is the bending stiffness of the pile, p stands for soil reaction and y is the lateral deflection.

The constitutive equation for the pile material subjected to bending moment is given as:

$$EI\,y'' = -M \tag{4.10}$$

where M is the bending moment.

The soil response for soft clay located below the water table is described by Eqs. (4.5)~(4.8) completed by Eqs. (4.1)~(4.4). The parameters of constitutive relations of pile-soil system are taken as the design variables that are arranged in the design variables vector **t** defined as follows:

$$\mathbf{t} = [\, EI,\ c,\ \gamma',\ \varepsilon_{50},\ b \,] \tag{4.11}$$

The performance functional Q is defined as a potential energy of maximum deformation. It depends on the state variables (y, y'') and the design variables (**t**). This dependence is extended also to the constitutive relationships of the system analyzed. The performance functional can change due to the changes of states variables or the design variables. The former scenario covers the case when the load changes whereas the design variables are maintained constant, while latter case occurs when the load is constant however the design variables change. The change of the performance functional

associated with second case is defined as a sensitivity of the performance functional due to the changes of the design variables. The vector of maximum deformation **D** of the pile-soil system is linked to the top pile point. It consists of two components, i.e. the top lateral displacement y_T and angle of rotation φ_T. Thus:

$$\mathbf{D} = [\, y_T, \varphi_T \,]^T \tag{4.12}$$

Based on the virtual work theorem (Washizu, 1976), the potential functional Q is defined as:

$$Q = \bar{1} \cdot \mathbf{D} \tag{4.13}$$

where as its first variation δQ is given as:

$$\delta Q = \bar{1} \cdot \delta \mathbf{D} \tag{4.14}$$

The first variation of deformation vector $\delta \mathbf{D}$ is designated as:

$$\delta \mathbf{D} = [\, \delta y_T, \delta \varphi_T]^{-1} \tag{4.15}$$

where δy_T and $\delta \varphi_T$ stand for first variations (changes) of top lateral displacement and angle of rotation respectively.

The pile-soil system subjected to external load P (or M) of constant value (called the primary pile-system shown in Fig. 4.3A) is in a state of deformation. Some variations of deformation δy_T, $\delta \varphi_T$ are imposed on the primary structure. They are associated with the changes of the design variables $\delta \mathbf{t}$. The variation of $\delta \mathbf{D}$ can be determined based on the virtual work theorem (Washizu, 1976) when the generalized unit load is applied to the adjoint pile-soil system being in the same state of deformation as the primary structure (shown in Fig. 4.3B).

For linear elastic systems the state of deformation and internal forces generated in adjoint system by application of generalized unit load is constant (Budkowska, 1997). However, for nonlinear elastic systems this rule does not apply. This means that deformations and internal forces the unit generalized load produces in the adjoint system are strongly dependent on the state of deformation of primary system. This is translated to the dependence on the magnitude of the applied load to the primary structure.

The following relationship is employed for determination of the components of $\delta \mathbf{D}$.

$$\bar{1}\,\delta \mathbf{D} = -\int_0^l \tilde{M}\,\delta y''\,dx + \int_0^l \tilde{p}\,\delta y\,dx \tag{4.16}$$

where $\bar{1}$ is the generalized unit load that corresponds to the type of deformation component; $\tilde{M}$, $\tilde{p}$ stand for internal forces of the adjoint system generated by application of $\bar{1}$; δy, $\delta y''$ denote variations of deformations imposed on the primary system.

The variations δy and δy″ can be determined from constitutive relationship of the pile structure and the supporting soil extended to the dependence on the design variables.

The constitutive equations written in incremental (variational) form are the following:

$$\delta M = \frac{\partial M}{\partial y''}\delta y'' + \frac{\partial M}{\partial t}\delta t \tag{4.17}$$

$$\delta p = \frac{\partial p}{\partial y}\delta y + \frac{\partial p}{\partial t}\delta t \tag{4.18}$$

The variations δy and δy″ are imposed on the primary structure in the presence of constant load; therefore the increments of internal forces are equal to zero. This means that:

$$\delta M = 0 \tag{4.19}$$

$$\delta p = 0 \tag{4.20}$$

Equations (4.19) and (4.20) allow for determination δy″ and δy. Thus:

$$\delta y'' = -\frac{\partial y''}{\partial M}\left(\frac{\partial M}{\partial t}\right)\delta t \tag{4.21}$$

$$\delta y = -\frac{\partial y}{\partial p}\left(\frac{\partial p}{\partial t}\right)\delta t \tag{4.22}$$

Substituting Eqs. (4.21) and (4.22) into Eq. (4.16) results in:

$$\bar{1}\,\delta\mathbf{D} = \int_0^l \tilde{M}\frac{\partial M}{\partial(EI)}\left(\frac{\partial y''}{\partial M}\right)\delta\mathbf{t}\,dx - \int_0^l \tilde{p}\frac{\partial y}{\partial p}\left(\frac{\partial p}{\partial \mathbf{t}}\right)\delta\mathbf{t}\,dx \tag{4.23}$$

The partial derivatives with respect to state variables such as $(\partial M/\partial y'')^{-1}$ and $(\partial p/\partial y)^{-1}$ that are under integrals of Eq. (4.23) are determined for constant values of the design variables. This means that they are obtained based on Eqs. (4.5)~(4.8) and (4.10) with suitable inclusion of Eqs. (4.1)~(4.4). Eq. (4.23) indicates that $\delta\mathbf{t}$ under first integral implies application of $\delta(EI)$ while $\delta\mathbf{t}$ under second integral requires introducing the remaining components of the changes of the design variables vector $\delta\mathbf{t}$, i.e. δc, $\delta\gamma'$, $\delta\varepsilon_{50}$ and δb. Consequently, the second integral of Eq. (4.23) is represented by four integrals that contain various variations of the design variables vector. Eq. (4.23) is now reshaped in a new form that contains explicitly shown all variations of the design variables vector. Thus:

$$\begin{aligned}\bar{1}\,\delta\mathbf{D} = &-\int_0^l \tilde{M}y''(EI)\delta EI\,dx - \int_0^l \tilde{p}\left(\frac{\partial y}{\partial p}\right)\left(\frac{\partial p}{\partial c}\right)\delta c\,dx - \int_0^l \tilde{p}\left(\frac{\partial y}{\partial p}\right)\left(\frac{\partial p}{\partial \gamma'}\right)\delta\gamma'\,dx \\ &- \int_0^l \tilde{p}\left(\frac{\partial y}{\partial p}\right)\left(\frac{\partial p}{\partial \varepsilon_{50}}\right)\delta\varepsilon_{50}\,dx - \int_0^l \tilde{p}\left(\frac{\partial y}{\partial p}\right)\left(\frac{\partial p}{\partial b}\right)\delta b\,dx\end{aligned} \tag{4.24}$$

The products of functions appearing under each integrand associated with suitable variation of the design variable are defined as follows:

$$C_{EI} = \tilde{M}\, y''(1/EI) \tag{4.25}$$

$$C_c = \tilde{p}\,(\partial y/\partial p)(\partial p/\partial c) \tag{4.26}$$

$$C_{\gamma'} = \tilde{p}\,(\partial y/\partial p)(\partial p/\partial \gamma') \tag{4.27}$$

$$C_b = \tilde{p}\,(\partial y/\partial p)(\partial p/\partial b) \tag{4.28}$$

$$C_{\varepsilon_{50}} = \tilde{p}\,(\partial y/\partial p)(\partial p/\partial c) \tag{4.29}$$

Substituting the relationships (4.25)~(4.29) into Eq. (4.24) we arrived at the following equation:

$$\bar{1}\,\delta\mathbf{D} = -\int_0^l C_{EI}\delta(EI)_n\,dx - \int_0^l C_c\delta c_n\,dx - \int_0^l C_{\gamma'}\delta\gamma'_n\,dx - \int_0^l C_{\varepsilon_{50}}\delta\varepsilon_{50n}\,dx - \int_0^l C_b\delta b_n\,dx \tag{4.30a}$$

$$\delta(EI)_n = \frac{\delta EI}{EI} \tag{4.30b}$$

$$\delta c_n = \frac{\delta c}{c} \tag{4.30c}$$

$$\delta\gamma'_n = \frac{\delta\gamma'}{\gamma'} \tag{4.30d}$$

$$\delta\varepsilon_{50n} = \frac{\delta\varepsilon_{50}}{\varepsilon_{50}} \tag{4.30e}$$

$$\delta b_n = \frac{\delta b}{b} \tag{4.30f}$$

where

C_{EI}, C_c, $C_{\gamma'}$, $C_{\varepsilon_{50}}$, and C_b are the sensitivity operators of the pile member due to the changes of EI, c, γ', ε_{50}, and b respectively.

$\delta(EI)_n$, δc_n, $\delta\gamma'_n$, $\delta(\varepsilon_{50})_n$, and δb_n denote the normalized vavariations of the design component specified with respect to their initial values. These values are formulated in Eqs. (4.30b)-(4.30f)

The normalized variations of the design variables are scalars and can be expressed in fractions or percents. In this way all sensitivity operators/ integrands that are specified in Eq. (4.30) carry unit of a force.

The equations of C_{EI}, C_c, $C_{\gamma'}$, $C_{\varepsilon_{50}}$, and C_b are presented in the Eqs. (4.31)~(4.42) and the applications of those equations are summarized in the Table 4.1. The detail derivation of Eqs.(4.31)~(4.42) are shown in Appendix A.

$$C_{EI} = \left(-y_a'' y''\right) EI \tag{4.31}$$

$$C_{c1} = \left(-1.5\left(\frac{y_a}{y_{50}}\right)^{\frac{1}{3}} y(3b + Jx)\right) c \tag{4.32}$$

$$C_{c2} = \left(-13.5\left(\frac{y_a}{y_{50}}\right)^{\frac{1}{3}} yb\right) c \tag{4.33}$$

$$C_{c3} = \left(\left(3y_{50}\frac{5x_r - x}{x_r - x} - y_a\right)(3b + Jx)\left\{\left(0.9 - 0.18\frac{x}{x_r}\right) - 0.06\left(\frac{y}{y_{50}}\right)\left(1 - \frac{x}{x_r}\right)\right\}\right) c \tag{4.34}$$

$$C_{\gamma'1} = \left(-1.5\left(\frac{y_a}{y_{50}}\right)^{\frac{1}{3}} y(bx)\right)\gamma' \tag{4.35}$$

$$C_{\gamma'2} = \left(-\left(3y_{50}\frac{5x_r - x}{x_r - x} - y_a\right)(bx)\left\{\left(0.9 - 0.18\frac{x}{x_r}\right) - 0.06\left(\frac{y}{y_{50}}\right)\left(1 - \frac{x}{x_r}\right)\right\}\right)\gamma' \tag{4.36}$$

$$C_{\varepsilon_{50}1} = \left(0.5\left(\frac{y_a}{y_{50}}\right)^{\frac{1}{3}} y\left[(3b + Jx)c + \gamma' bx\right]\left(\frac{1}{\varepsilon_{50}}\right)\right)\varepsilon_{50} \tag{4.37}$$

$$C_{\varepsilon_{50}2} = \left(4.5\left(\frac{y_a}{y_{50}}\right) ycb\left(\frac{1}{\varepsilon_{50}}\right)\right)\varepsilon_{50} \tag{4.38}$$

$$C_{\varepsilon_{50}3} = \left(-\left(3y_{50}\frac{5x_r - x}{x_r - x} - y_a\right)\frac{1}{\varepsilon_{50}}\left(1 - \frac{x}{x_r}\right)\left(\frac{y}{y_{50}}\right)\cdot 0.06\left[3cb + \gamma' bx + Jcx\right]\right)\varepsilon_{50} \tag{4.39}$$

$$C_{b1} = \left(3\left(\frac{y_a}{y_{50}}\right)^{\frac{1}{3}} y\left(c + \tfrac{1}{3}\gamma' x - \frac{Jxc}{6}\right)\right)b \tag{4.40}$$

$$C_{b2} = \left(9\left(\frac{y_a}{y_{50}}\right)^{\frac{1}{3}} yc\right)b \tag{4.41}$$

$$C_{b3} = \left(\left(3y_{50}\frac{5x_r - x}{x_r - x} - y_a\right)\left\{\begin{array}{l}\left[3c + \gamma' x\right]\left[\left(0.9 - 0.18\frac{x}{x_r}\right) - 0.06\left(\frac{y}{y_{50}}\right)\left(1 - \frac{x}{x_r}\right)\right] \\ + 0.06\left[3c + \gamma' x + \frac{Jxc}{b}\right]\left(\frac{y}{y_{50}}\right)\left(1 - \frac{x}{x_r}\right)\end{array}\right\}\right)b \tag{4.42}$$

The graphical representation of the sensitivity operators defined in Eqs. (4.31)-(4.42) is essential in whole analysis because of the following reasons:

- The distributions of sensitivity operators directly give insight in the spatial localization of the changes of the design variables,

- They form the basis for quantitative appraisal of the effect each of the design variables has on the change of the deformation,
- They allow the identification of various soil's state (starting from linear elastic and end up at plastic flow),
- They enable one to assess the size of each soil's state along the pile axis.

The graphical representations for single pile are presented in Chapter 6 and for groups of pile are presented in Chapter 7.

It is worth nothing that Eqs. (4.26)~(4.30) are written in symbolic fashion. Each of the last four integrals of Eq. (4.30a) is combined with a suitable number of Eqs. (4.26)~(4.29) that are connected with variable soil phases which can develop along the pile axis depending on the value of the loading applied to the pile-soil system. Equation (4.30) is used for determination of δy_T and $\delta \varphi_T$ when the pile-soil system is subjected either to horizontal force P or bending moment M.

These combinations are taken into account by introducing suitable superscripts (P_y, P_φ, M_y, M_φ) to the integrands of Eq. (4.30a). The analysis of sensitivity integrands/ sensitivity operators defined by formulas (4.25)~(4.29) is considered as important part of sensitivity investigations. The graphical representation of sensitivity integrands enables one to assess effectively, the changes of the specific design variables have on the changes of deformations of the pile-soil system. The visual inspection of the sensitivity integrands allows for immediate detection of areas of critical importance the changes of the design variables have on the changes of deformations. Moreover they are able to indicate the location and size where soil is in nonelastic, softening or plastic stage. The examinations of sensitivity integrands allows Eq. (4.30a) be applied with respect to various soil phases

that can develop as a result of application of an increasing load. Therefore it is possible to evaluate quantitatively the contributions of the design variables changes of each soil phase on the changes of top deflections. The quantitative assessment of $\delta\mathbf{D}$ associated with each soil phase can be obtained as (with the assumption that all variations of the design variables are constant):

$$(A_{EI})_i = \int_{li} C_{EI}\,dx \tag{4.43}$$

$$(A_c)_i = \int_{li} C_c\,dx \tag{4.44}$$

$$(A_{\gamma'})_i = \int_{li} C_{\gamma'}\,dx \tag{4.45}$$

$$(A_{\varepsilon_{50}})_i = \int_{li} C_{\varepsilon_{50}}\,dx \tag{4.46}$$

$$(A_b)_i = \int_{li} C_b\,dx \tag{4.47}$$

where l_i means range where the specific soil's phase can develop.

In doing the numerical investigation, the integration in Eqs. (4.43)-(4.47) are solved by Simpson's method. The idea behind Simpson's method is to evaluate the function at three points within each little interval, and then to calculate the area underneath a parabola fitted to those three points. An English mathematician Thomas Simpson (1710-1761) introduced this method.

This method can be explained by Fig 4.4 (Purcell and Varberg 1987) that shows the graph of y = f(*x*) on [*a, b*]. The interval [*a, b*] is divided into n subintervals, so that the length of each interval *h* is:

$$h = (b - a)/n \tag{4.48a}$$

where n is an even number.

Then, this method can be formulated as:

$$\int_a^b f(x)dx \approx \frac{h}{3}\left[f(x_0) + 4f(x_1) + 2f(x_2) + \cdots + 4f(x_{n-1}) + f(x_n)\right] \tag{4.48b}$$

Equation (4.30a) can be written for each soil stage and suitably integrated. Assuming constant values of normalized variations of the design variables, Eq. (4.30) for each stage i can be expressed as:

$$\left(\bar{1}\,\delta\mathbf{D}_T\right)_i = \left(A_{EI}\,\delta(EI)_n + A_c\delta c_n + A_{\gamma'}\delta\gamma'_n + A_{\varepsilon_{50}}\delta(\varepsilon_{50})_n + A_b\delta b_n\right)_i \tag{4.49}$$

where $A_{EI}, A_c, A_{\gamma'}, A_{\varepsilon_{50}}$ and A_b are the quantitative assessments of sensitivities of EI, c, γ′, ε_{50} and b respectively.

The next modification of Eq. (4.49) is obtained by introducing the following relationship for each stage i:

$$\left(A_{tot}\right)_i = \left(A_{EI} + A_c + A_{\gamma'} + A_{\varepsilon_{50}} + A_b\right)_i \tag{4.50}$$

Then, Eq. (4.49) can be written as:

$$\bar{1}\delta\mathbf{D}_T = \sum_i \left(A_{tot}\right)_i \left(\frac{A_{EI}}{A_{tot}} \delta\left(EI\right)_n + \frac{A_c}{A_{tot}} \delta c_n + \frac{A_{\gamma'}}{A_{tot}} \delta\gamma'_n + \frac{A_{\varepsilon_{50}}}{A_{tot}} \delta\left(\varepsilon_{50}\right)_n + \frac{A_b}{A_{tot}} \delta b_n \right)_i \tag{4.51a}$$

$$= \sum_i \left(A_{tot}\right)_i \left(\left(F_{EI}\right)_u \delta\left(EI\right)_n + \left(F_c\right)_u \delta c_n + \left(F_{\gamma'}\right)_u \delta\gamma'_n + \left(F_{\varepsilon_{50}}\right)_u \delta\left(\varepsilon_{50}\right)_n + \left(F_b\right)_u \delta b_n \right)_i \tag{4.51b}$$

where $\left(F_{EI}\right)_u$, $\left(F_c\right)_u$, $\left(F_{\gamma'}\right)_u$, $\left(F_{\varepsilon_{50}}\right)_u$ and $\left(F_b\right)_u$ are relative sensitivity factors connected with each stage i. They show in percent the contribution of the specified design variable in total change of the deformation investigated. The graphical representations of those values for single pile are presented in Chapter 6 and for groups of pile are presented in Chapter 7.

Table 4.1. The application Eqs. (4.31)~(4.42) to calculate the value of C_i

		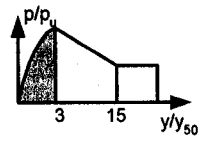 Nonlinear elastic	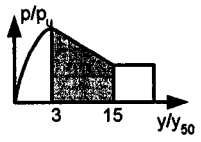 Softening	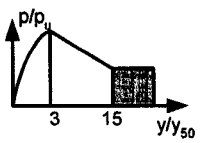 Plastic flow
$x < x_r$		**$0 < y/y_{50} < 3$**	**$3 < y/y_{50} < 15$**	**$y/y_{50} > 15$**
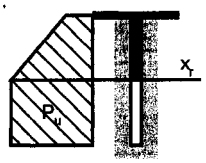	**EI**	EI (Eq. 4.31)	EI (Eq. 4.31)	EI (Eq. 4.31)
	c	c_1 (Eq. 4.32)	c_3 (Eq. 4.34)	0
	γ'	γ'_1 (Eq. 4.35)	γ'_2 (Eq. 4.36)	0
	ε_{50}	$\varepsilon_{50\text{-}1}$(Eq. 4.37)	$\varepsilon_{50\text{-}3}$(Eq. 4.39)	0
	b	b_1 (Eq. 4.40)	b_3 (Eq. 4.42)	0
		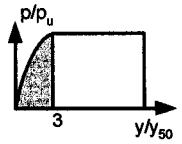 Nonlinear elastic	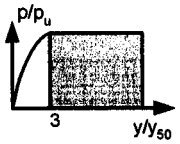 Plastic flow	
$x > x_r$		**$0 < y/y_{50} < 3$**	**$y/y_{50} > 3$**	
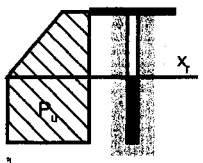	**EI**	EI (Eq. 4.31)	EI (Eq. 4.31)	
	c	c_2 (Eq. 4.33)	0	
	γ'	0	0	
	ε_{50}	$\varepsilon_{50\text{-}2}$(Eq. 4.38)	0	
	b	b_2 (Eq. 4.41)	0	

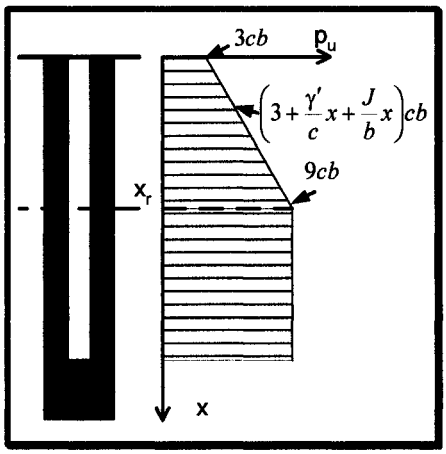

Figure 4.1 Variability of ultimate soil resistance along the pile axis

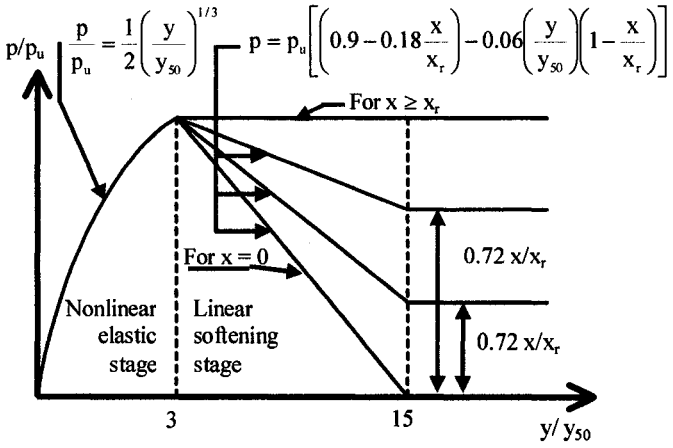

Figure 4.2 Constitutive p-y model of soft clay located below the water table subjected to lateral cyclic loadings (after Matlock, 1970)

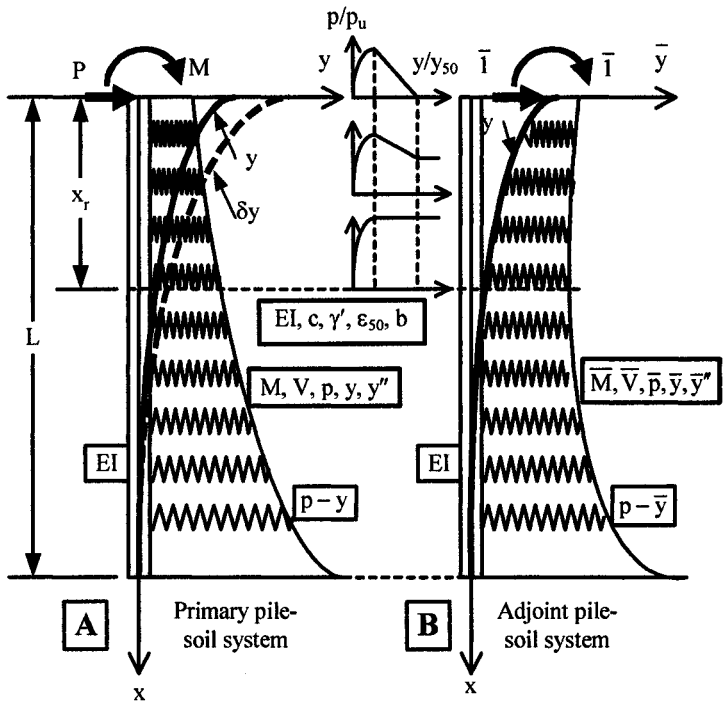

Figure 4.3 The concept of the primary and adjoint nonlinear pile-soil system.

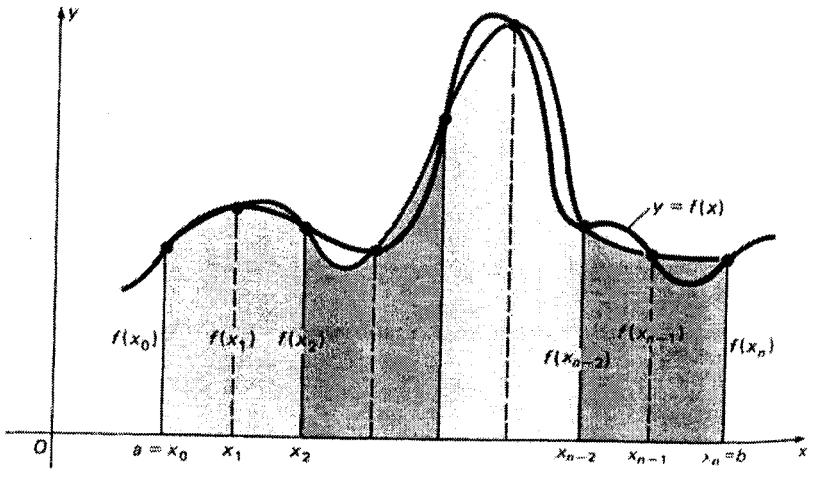

Figure 4.4 Numerical integration using Simpson's rule (Purcell and Varberg, 1987)

CHAPTER 5
NUMERICAL INVESTIGATION

5.1 INTRODUCTION

The process in doing the numerical investigation of the sensitivity analysis of laterally loaded piles embedded in the soft clay below the water table is presented in Fig. 5.1 as a flow chart. Some of the steps are discussed in the following sections, and the others are presented in Chapter 6 and 7.

5.2 DETERMINATION OF SOIL PROPERTIES, PILE PROPERTIES, CONSTRAINT TYPE AND LOAD TYPES.

5.2.1 Soil properties

The soil that used in this study is defined as a homogenous soil, which is soft clay or soft glacial soil below the water table. Based on Terzaghi (1967), the typical properties of soft glacial soil are the followings: porosity n is 55 %, void ratio e is 1.2, water content w is 45 %, and saturated unit weight γ_s is 17.7 kN/m^3. Because the soil is located below the water table, so that the effective unit weight γ' of the soil can be determined from the

value of the saturated unit weight γ_s and unit weight of water γ_w is equal to 9.81 kN/m^3 as:

$$\gamma' = \gamma_s - \gamma_w$$

$$= 17.7 - 9.81 = 7.89 \text{ kN/m}^2. \quad (5.1)$$

Das (1995) defined the unconfined compressive strength of the soft clay q_u in the range of 24 – 48 kPa, so that in this case it is assumed as 36 kPa. The undrained cohesion c_u or shear strength s_u of the soil is defined as:

$$c_u = s_u = q_u / 2 = 36 / 2 = 18 \text{ kPa} \quad (5.2)$$

The other properties that needed to be determined is ε_{50} which is the strain corresponding to one-half of the maximum principal stress difference. Wang and Reese (1993) recommended that if there is no stress-strain curve available, the typical value of ε_{50} is 0.02.

5.2.2 Pile properties

The determination of the pile properties used in this analysis is based on the previous numerical analyses of laterally loaded piles done by COM624P version 2.0 programs presented in the manual of the programs (Wang and Reese 1993). The pile properties used in this study are determined as steel H-pile 14HP89 or HP 360 × 1.295, which is described in Table. 5.1. The moment of inertia in the x-direction is equal to 374×10^{-6} m^4, and the modulus of elasticity is equal to 2×10^5 MPa (AISC, 1999). This

pile is made of carbon steel A514 that has the yield strength is equal to 480×10^3 kPa, so that the moment capacity M_y of this pile is defined as:

$$M_y = F_y I_{xx} / y$$
$$= 480 .10^3 \times 374.10^{-6} / (0.373 / 2)$$
$$= 962.6 \text{ kNm.} \quad (5.3)$$

The pile properties and soil properties used in this study are summarized in Table 5.1.

5.2.3 Constraint type and load type

The types of constraints and loads, which are investigated in this sensitivity analysis, are the followings:

1. Sensitivity analyses of lateral displacement and angle of rotation at the top of the piles for free head single isolated piles subjected to lateral forces and bending moments at the top of the piles.
2. Sensitivity analyses of lateral displacement at the top of the piles for fixed head single isolated piles subjected to of lateral forces.
3. Sensitivity analyses of lateral displacement at the top of the piles for groups of 9 piles subjected to lateral forces.

5.3 DETERMINATION OF LENGTH OF THE PILES

The behaviour of laterally loaded piles depends on their length. The classification of piles into long and short piles implies their different applications. The determination of

length of the laterally loaded pile-soil interaction system of linear elastic type is readily obtainable from the linear theory of subgrade reaction. In this theory, the soil response is modelled by means of Winkler type foundation that involves the coefficient of subgrade reaction k. For strong cohesive soils coefficient of subgrade reaction k has constant value (Terzaghi, 1956). Then the length of the laterally loaded pile can be determined as a product of a scalar and the characteristic length λ_c that is given (Davisson and Gill, 1963, Das, 1999) as:

$$\lambda_c = \sqrt[4]{\frac{EI}{kb}} \tag{5.4}$$

where EI is the bending stiffness of the pile, b stands for the width of the pile.

There is a common agreement that for cohesionless soils (Matlock and Reese, 1960) the coefficient of subgrade reaction k varies in linear fashion with depth of the pile according to following rule:

$$k = n_h \cdot x \tag{5.5}$$

where n_h is called constant of modulus of horizontal subgrade reaction (Das, 1999).

Then the characteristic length λ_s is given (Das, 1999) as:

$$\lambda_s = \sqrt[5]{\frac{EI}{n_h}} \tag{5.6}$$

The laterally loaded pile-soil interaction system in which the soil reaction is characterized either by k (Matlock and Reese, 1960) or n_h (Davisson and Gill, 1963) has closed form solution. However, when the pile is embedded in soft clay located below the water table that is described by the p-y relationship, the closed form solution does not exist.

The evaluation of a length of laterally loaded pile embedded in a soil described by p-y curve can be done by means of the relative stiffness factor T proposed by Matlock and Reese (1960). It depends on the type of loading (lateral force H_t or the bending moment M_t, type of pile constraints (free pile's head or fixed pile's head), bending stiffness of the pile EI and the top horizontal displacement y_t. The relative stiffness factor T is equivalent to the characteristic length of a pile λ_c and λ_s when analyzed in the scope of linear elastic theory.

The lateral loading (H_t and M_t) that is associated with the top lateral displacement y_t can be determined by means of the characteristic load method proposed by Evans and Duncan (1982). When the pile embedded in p-y soil is subjected to horizontal force H_t that is applied to free or fixed head, then

$$T = \sqrt[3]{\frac{y_t EI}{A_y H_t}} \tag{5.7}$$

where $A_y = 2.43$ for a free head pile, and

$A_y = 0.93$ for a fixed head pile.

Application of bending moment M_t to the pile's top implies that the relative stiffness factor T is defined as:

$$T = \sqrt[2]{\frac{y_t EI}{B_y M_t}} \tag{5.8}$$

where $B_y = 1.62$

When the embedded length of the pile is larger than 5T, the pile is considered as a long pile. If the length of a pile is smaller than 4, the pile is regarded as short one. Long piles subjected to lateral loadings behave as fixed at the bottom. For relatively flexible piles such as timber piles, this corresponds to a length of at least twenty diameters, whereas for relatively stiff piles such as those made of steel or concrete, the length should be at least thirty-five diameters. The characteristic load and moment method of Evans and Duncan (1982) enables one to determine H_t and M_t required by Formula (5.7) and (5.8) for any value y_t needed.

The characteristic shear load H_c and characteristic moment M_c are defined as follows:

$$H_c = \lambda B^2 E R_I \left(\frac{\sigma_p}{E R_I}\right)^m (\varepsilon_{50})^n \tag{5.9}$$

and

$$M_c = \lambda B^3 E R_I \left(\frac{\sigma_p}{E R_I}\right)^m (\varepsilon_{50})^n \tag{5.10}$$

where I is the moment of inertia of a pile,

B is the width of a pile,

λ is a constant that describes type of p-y curve,

R_I stands for moment of inertia ratio,

σ_p means representative passive pressure of soil,

E denotes the modulus of elasticity of the pile material,

ε_{50} defines a strain at which 50% of soil strength is mobilized.

The exponent m and n depends on the type of characteristic load (H_c or M_c) and the type of soil (cohesive or frictional). The moment of inertia ratio R_I is defined as:

$$R_I = \frac{I}{\pi B^4/64} \tag{5.11}$$

For plastic clay and sand λ=1.0 whereas for brittle clay $\lambda = (0.14)^n$. The mean representative passive pressure for cohesive soils is given as:

$$\sigma_p = 4.2\, c_u \tag{5.12}$$

where c_u is the undrained cohesion. The exponent m, n associated with Formula (5.9) and (5.10) are specified in Table 5.2.

By assuming that y_t / B is equal to 0.05 the value of T for the soil properties and pile properties defined in Section 5.2 for various types of the constraints of the pile and the different types of loads are shown in Table 5.3. The length of the piles used in the

sensitivity analysis is also presented in Table 5.3. The detail calculation of the length of the pile using the CLM methods is presented in Appendix B.

5.4 ANALYSIS OF LATERALLY LOADED PILE USED IN THIS STUDY

The distributions of deflection and bending moment along the length of the pile are needed as input of sensitivity analysis. Computer programs employed in analyses of laterally loaded pile are COM624P version 2.0 (Wang and Reese, 1993) for single pile analysis and FB-Pier program (2001) for groups of piles analysis. The overview of the program will be discussed in the following section. Both of these computer programs use the p-y curve from Matlock (1970) defined in section 4.2 in the analysis of laterally loaded piles embedded in the soft clay below the water table subjected to cyclic loadings.

5.4.1 COM624p version 2.0

Wang and Reese (1993), sponsored by the Federal Highway Administration developed COM624p version 2.0 at The University of Texas at Austin. In this program, the p-y curve method is employed to analyze the pile subjected lateral load. The beam-column equation is solved by finite difference method. This program can determine the pile deflection, rotation, bending moment, shearing forces, and soil reactions using an iterative process that considers the nonlinear response of the soil surrounding the pile. This program can be used not only to analyze laterally loaded single pile with various types of pile head condition and various types of loadings, but also groups of piles by applying the p-multiplier to the pile. Although this program can be used to analyze

groups of piles but the effect pile arrangement is just shown by different value of p-multiplier.

5.4.2 FB-Pier Program

The University of Florida, Bridge Software Institute (BSI), with the support of the Florida Department of Transportation and the Federal Highway Administration, developed FB-Pier program (2001). The program also employs p-y method, but it uses non-linear finite element analysis. The program is a complete substructure design program that includes both geotechnical and structural aspects of foundation and pier design. Program design and analysis features include single pile/shaft, pile/shaft groups, pile bents, sound walls, retaining walls, signs, and high mast lighting structures. Analysis capabilities include combined axial, lateral, and rotation resistance of the piles/shafts, pile cap, and pier components. The structural model includes both linear and non-linear (concrete cracking, steel yielding) capabilities, as well as biaxial interaction diagrams for all sections. The latter models (linear or non-linear) are available for prestressed piles, composite piles, drilled shafts, composite shafts, H-piles, pipe piles, and various concrete sections, reinforced and/or prestressed generally used for bridge piers. Although there is a difference of pile head connection behaviour of FB-Pier and COM624P, but the study in comparison of the results of both of the programs does not have unacceptable difference.

Table 5.1 Soil properties and pile properties

SOIL PROPERTIES

Soil type : Soft clay below the water table

- Effective unit weight γ' 7.86 kN/m^3
- Undrained cohesion c_u 18 kPa
- ε_{50} 0.02

PILE PROPERTIES

Pile type: Steel H-Pile 14HP89 / HP 360×1.295

- weight : 1.295 kN/m
- d_1 : 351 mm
- d_2 : 373 mm
- w : 15.62 mm
- I_{xx} : 374×10^{-6} m^4
- I_{yy} : 109×10^{-6} m^4
- Modulus of elasticity E: 2 × 10^8 kPa
- Stiffness EI : 74,800 kNm^2
- Area A : 16.8 × 10-3 m^2
- Diameter b : 373 mm

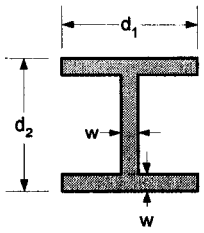

Table 5.2. Values of exponents m and n

Soil Type	For H_c		For M_c	
	m	N	m	n
Cohesive	0.683	-0.22	0.46	-0.15
Frictional	0.57	-0.22	0.40	-0.15

Table 5.3 The lengths of piles used in the sensitivity analysis

	Constraint	Free head		Fixed head
	Load type	P	M	P
	T	2.3 m	2.135 m	2.49 m
	Pile length (m)			
short pile	2T	4.60	4.27	4.98
	3T	6.90	6.41	7.47
	4T	9.20	8.54	9.96
	4.5T	10.35	9.61	11.21
long pile	5T	11.50	10.68	12.45
	6T	13.80	12.81	14.94
	7T	16.10	14.95	17.43
	8T	18.40	17.08	19.92
	9T	20.70	19.22	22.41
	10T	23.00	21.35	24.90

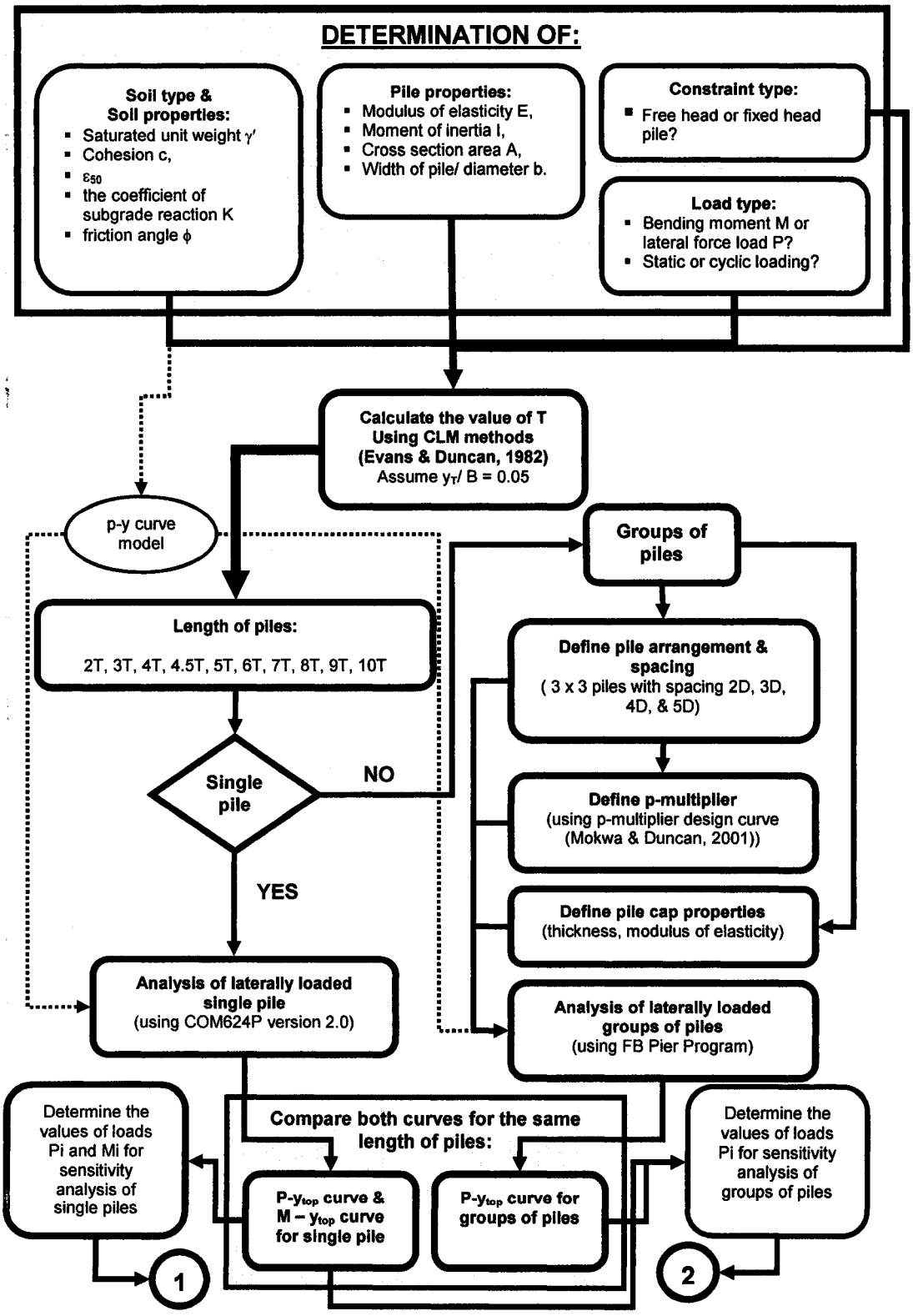

Figure 5.1a. Numerical investigation process of the sensitivity analysis of laterally loaded single piles and groups of piles (continued).

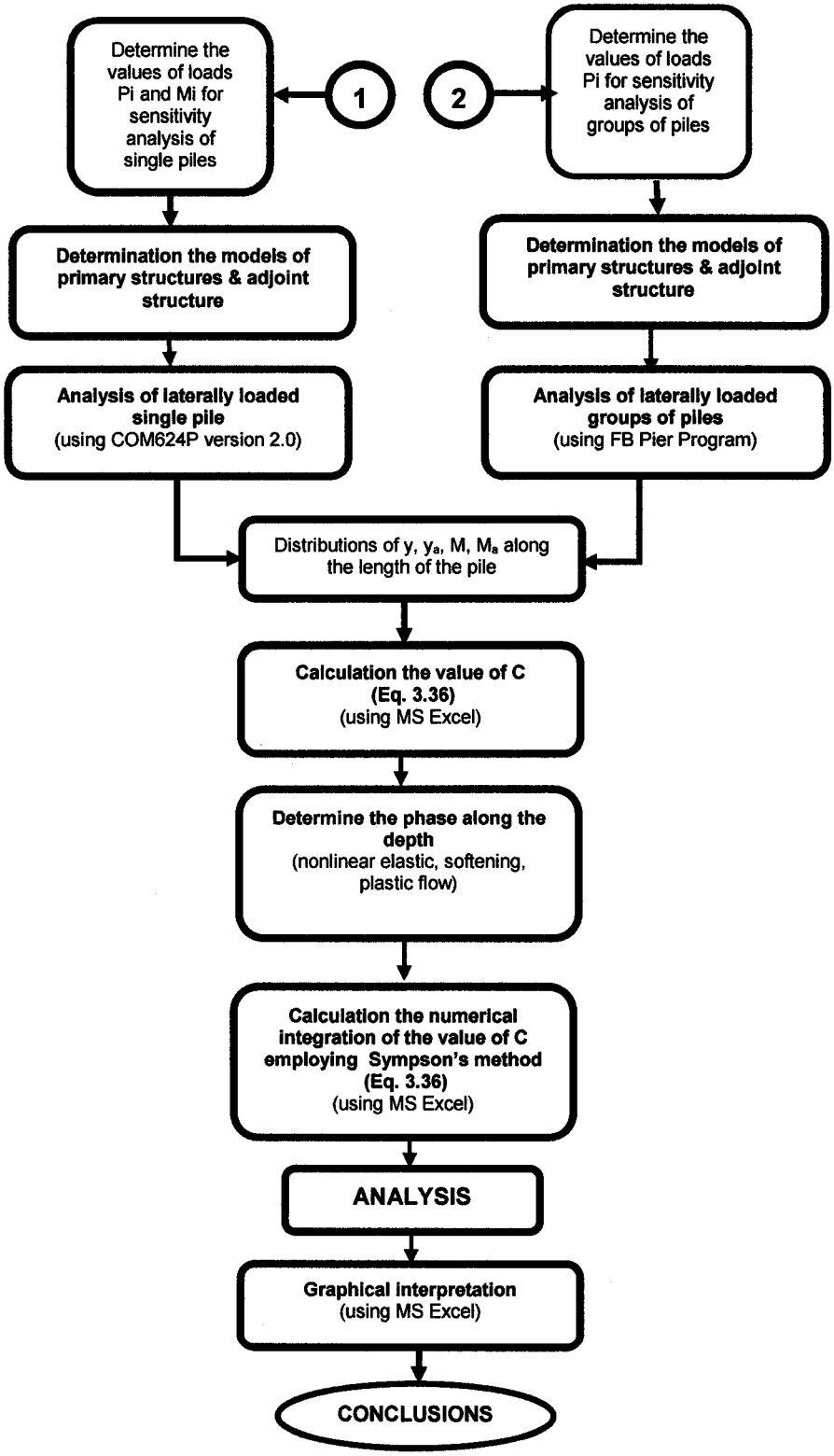

Figure 5.1b. Numerical investigation process of the sensitivity analysis of laterally loaded single piles and groups of piles (continue).

CHAPTER 6
SENSITIVITY ANALYSIS OF SINGLE PILE

6.1 SCOPE

The sensitivity analyses of single pile which are done in this study are the followings:

1. Sensitivity analysis of top lateral deflection δy_t for free head piles subjected to lateral forces P_i at the top of the pile.
2. Sensitivity analysis of top angle of rotation $\delta\varphi_t$ for free head piles subjected to lateral forces P_i at the top of the pile.
3. Sensitivity analysis of top lateral deflection δy_t for free head piles subjected to bending moments M_i at the top of the pile.
4. Sensitivity analysis of top angle of rotation $\delta\varphi_t$ for free head piles subjected to bending moments M_i at the top of the pile.
5. Sensitivity analysis of top lateral deflection δy_t for fixed head piles subjected to lateral forces P_i at the top of the pile.

The length of 2T, 3T, 4T, 4.5T, 5T, 6T, 7T, 8T, 9T, and 10T are employed in this analysis. The lengths of 3T and 10T are presented in this report. The length of 3T

represents a short pile, while 10T is considered as a long pile. The choice of short and long piles for sensitivity analysis is dictated by the different types of behaviour developed when used in any applications of practical importance.

The lateral forces and bending moments applied at the top of the piles are cyclic loading with 1000 cycles. However the number of cycles is not important for the soft clays below the water table. The loss of resistance in comparison to that from static loading is more important than the effect of cyclic loading (Reese, L.C. and Van Impe, W.F., 2001).

6.2 DETERMINATION OF P_i AND M_i

The preliminary study is made to determine the values of load series P_i and M_i. The curves of top lateral displacement vs. the series of forces or bending moments applied to the top of the piles are used to determine the values of load series P_i and M_i. In doing this analyses, COM624P version 2.0 (Wang and Reese, 1993) are employed. The models employed in this analysis are shown in Fig. 6.1, and the input data for the analysis are presented in Appendix C. The result of this analysis for free head pile subjected to P_i is shown in Fig. 6.2, for free head pile subjected to M_i is shown in Fig. 6.3, and for fixed head pile subjected to P_i is presented in Fig. 6.4.

6.3 MODEL OF PRIMARY STRUCTURE AND ADJOINT STRUCTURE

The model of primary structure is same as the models used in determination of P_i and M_i. The primary and adjoint structures models are shown in Fig. 6.5. The nination of deformations and internal forces of the adjoint system associated with

any state of deformation of the primary structure is obtained as the result of validity of superposition principle in the vicinity of any loading applied to the primary structure. This concept for various kinds of loading and the objects of sensitivity analysis is presented in Fig. 6.6. Models determined are analyzed using COM624P version 2.0 Program (Wang and Reese, 1993).

6.4 SENSITIVITY ANALYSES AND NUMERICAL ASSESSMENTS

The graphical presentations of the sensitivity analyses and the numerical assessments for single piles for each cases defined in section 6.1 are presented in Appendix D – Appendix M. The summary of the numerical assessments of A and F of the free head single pile with various lengths is presented in Appendix R.The discussions of the result of this chapter are presented in Chapter 8.

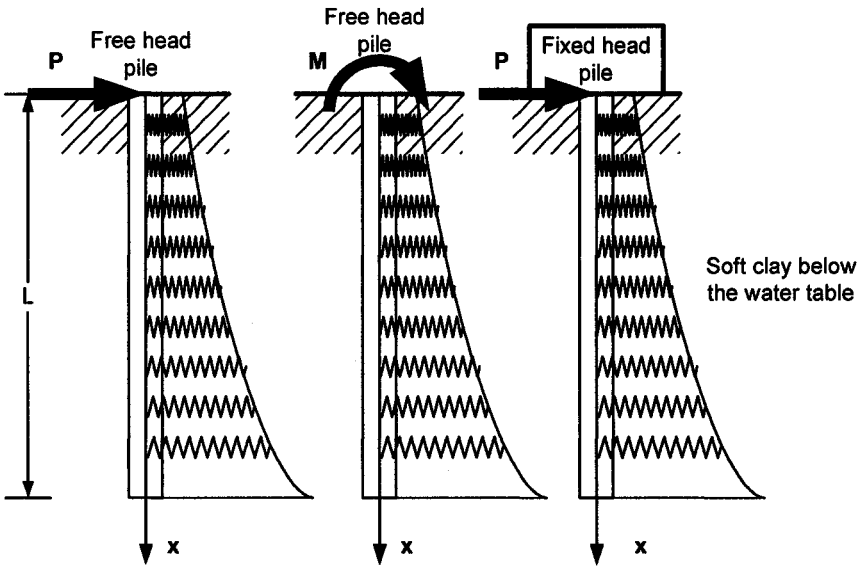

Figure 6.1. Single piles models employed to determined P_i and M_i

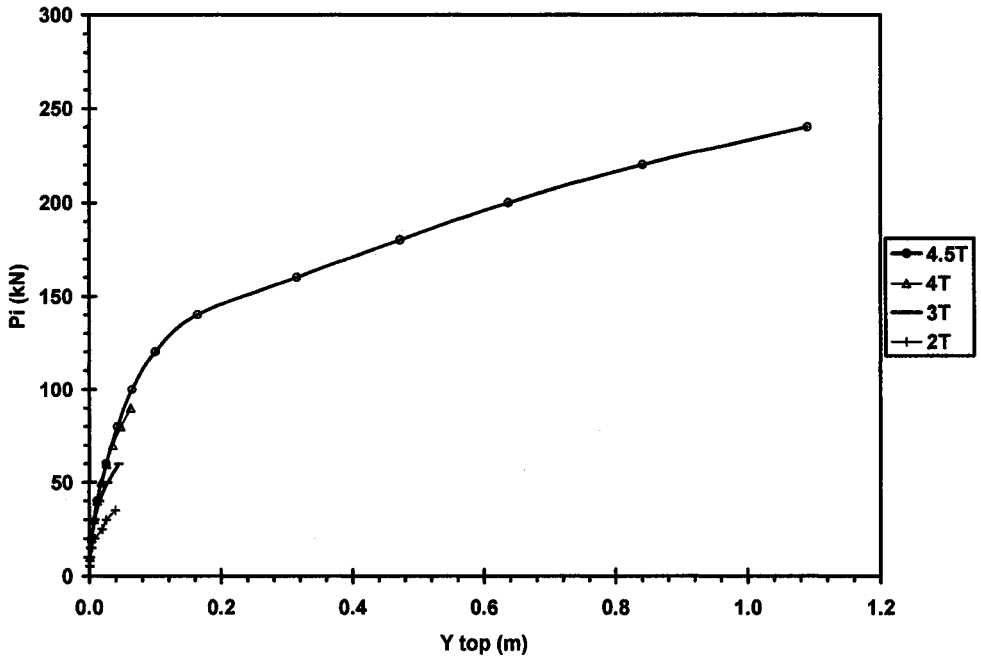

(a) Short piles

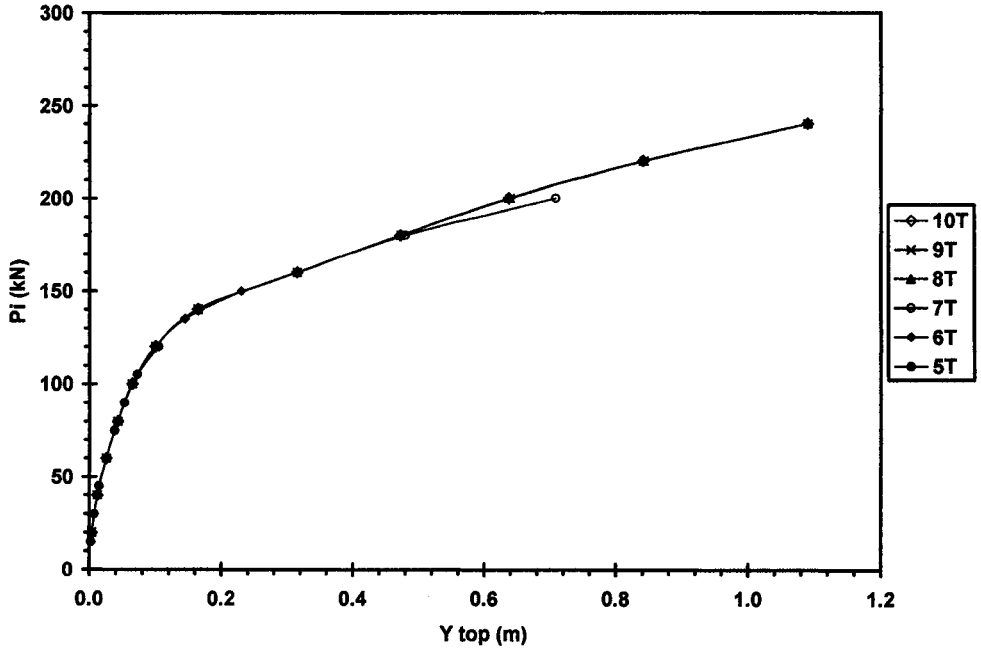

(b) Long piles

Figure 6.2 Discrete forces P_i vs. lateral displacement of the top of the pile y_{top} for free head pile subjected to lateral forces P_i (continued)

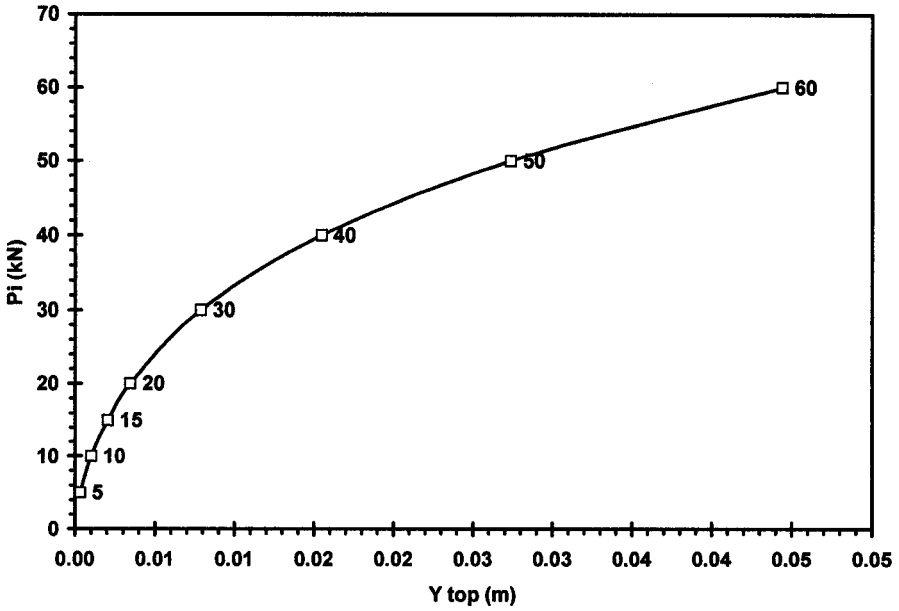

(c) L = 3T

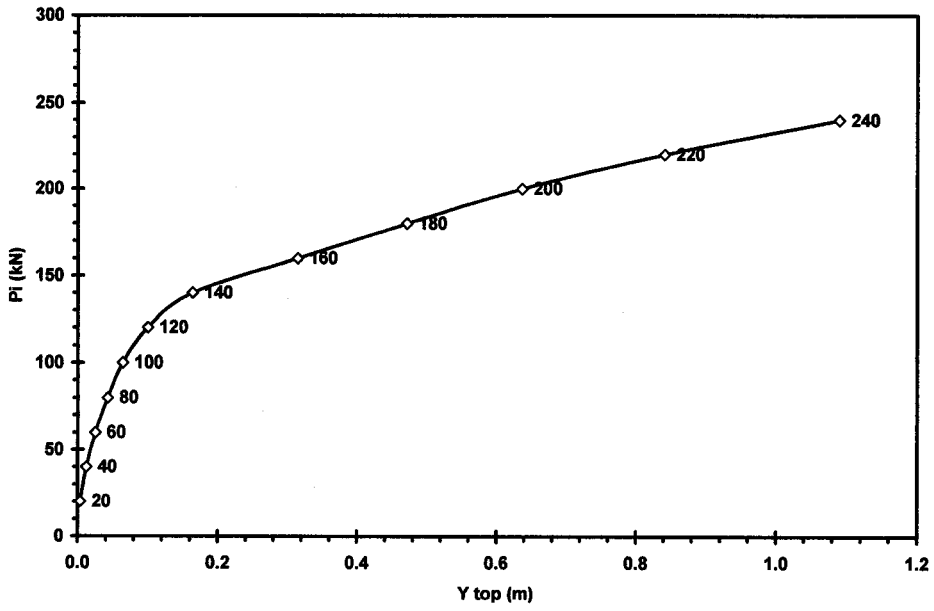

(d) L = 10T

Figure 6.2 Discrete forces P_i vs. lateral displacement of the top of the pile y_{top} for free head pile subjected to lateral forces P_i

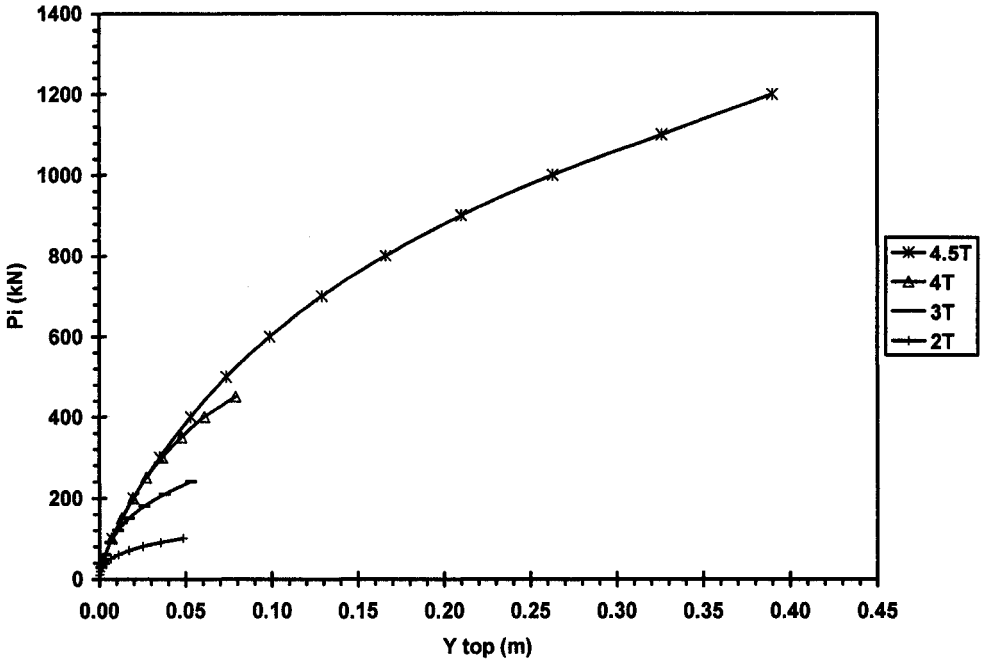

(a) Short piles

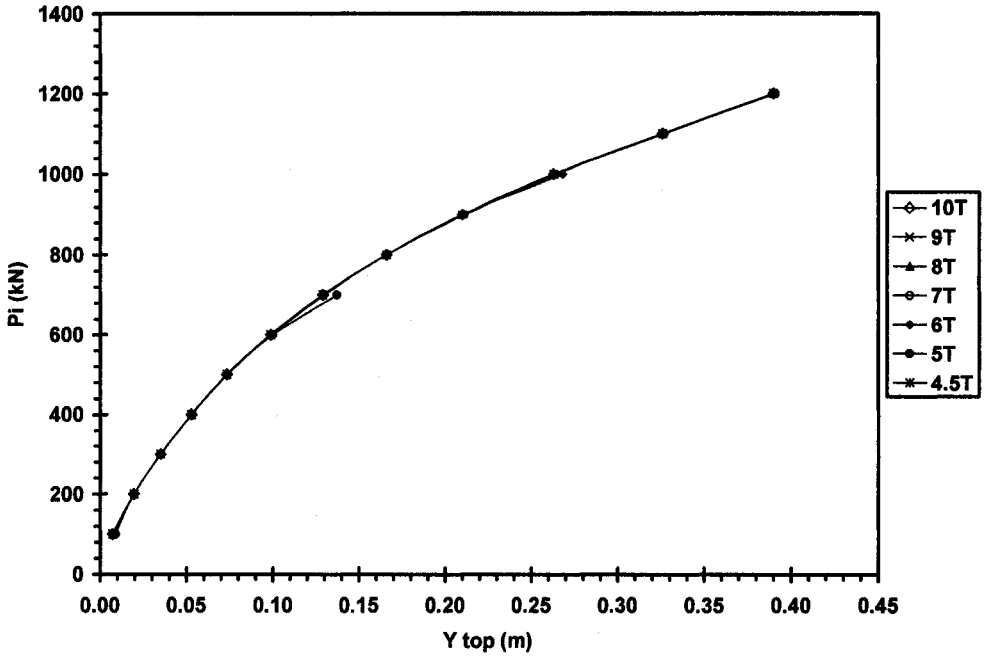

(b) Long piles

Figure 6.3 Discrete forces P_i vs. lateral displacement of the top of the pile y_{top} for free head pile subjected to bending moment M_i (continued)

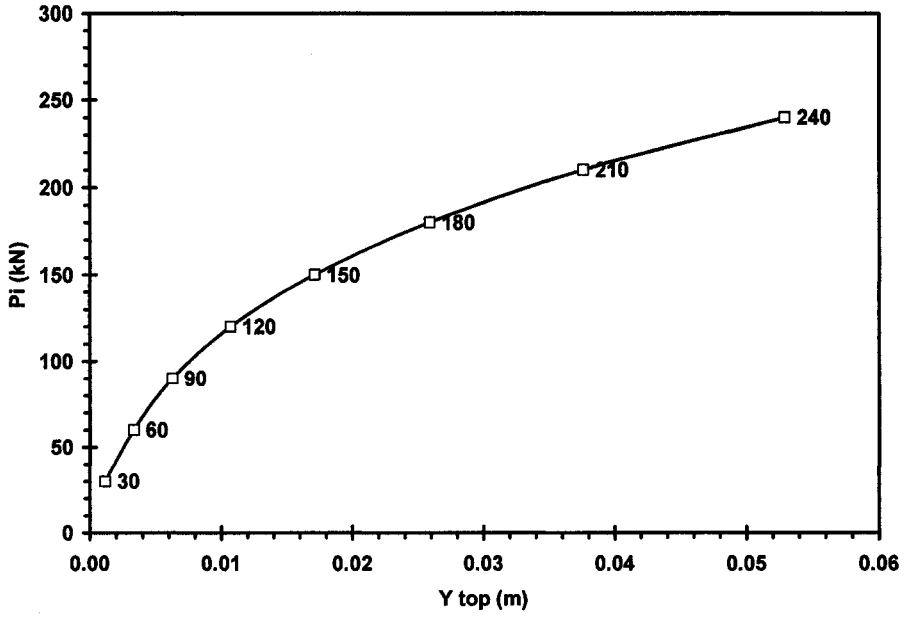

(c) L = 3T

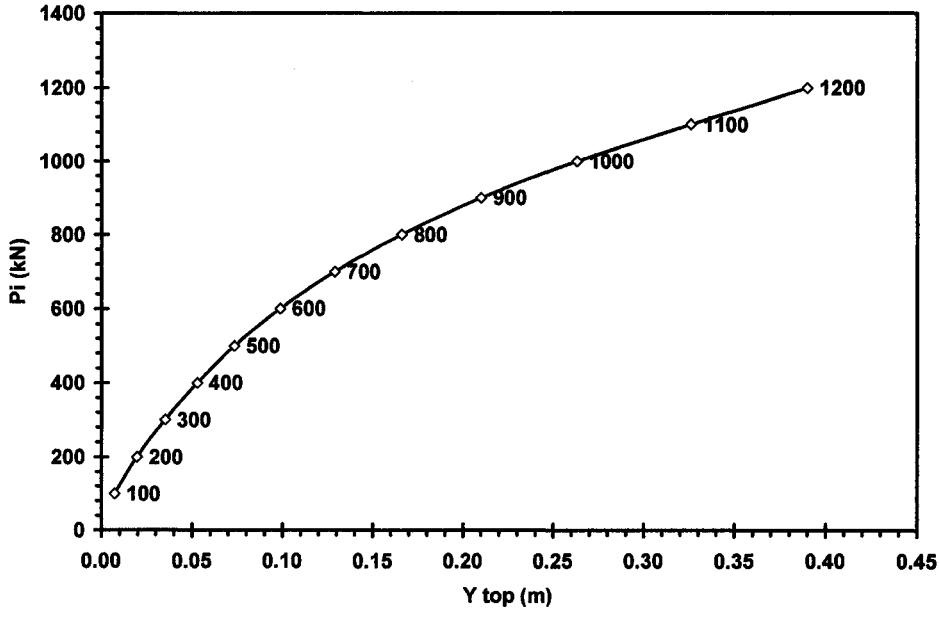

(d) L = 10T

Figure 6.3 Discrete forces P_i vs. lateral displacement of the top of the pile y_{top} for fixed head pile subjected to lateral forces P_i

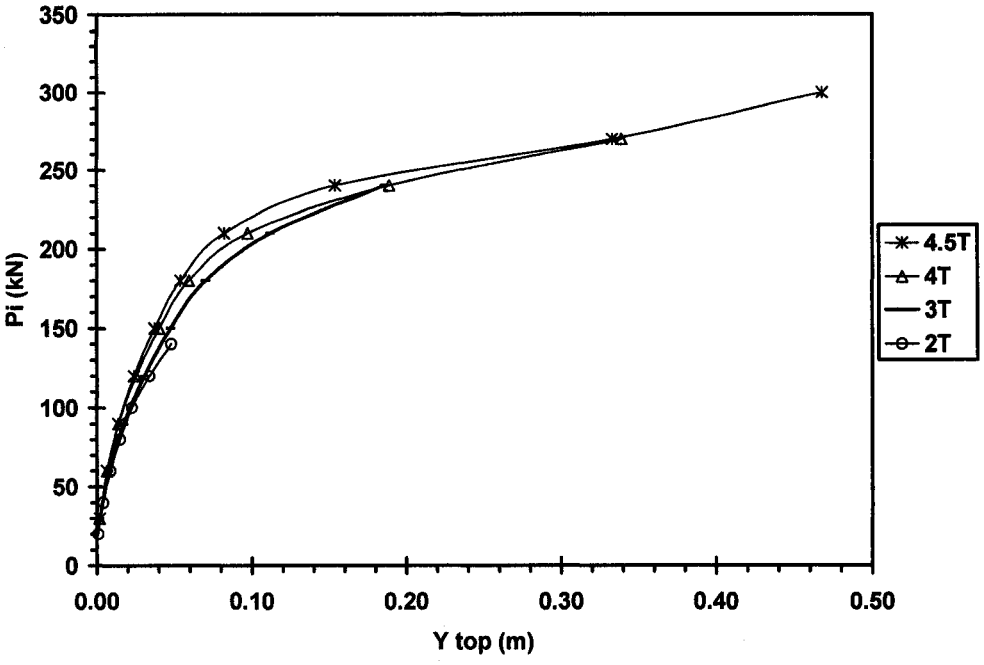

(a) Short piles

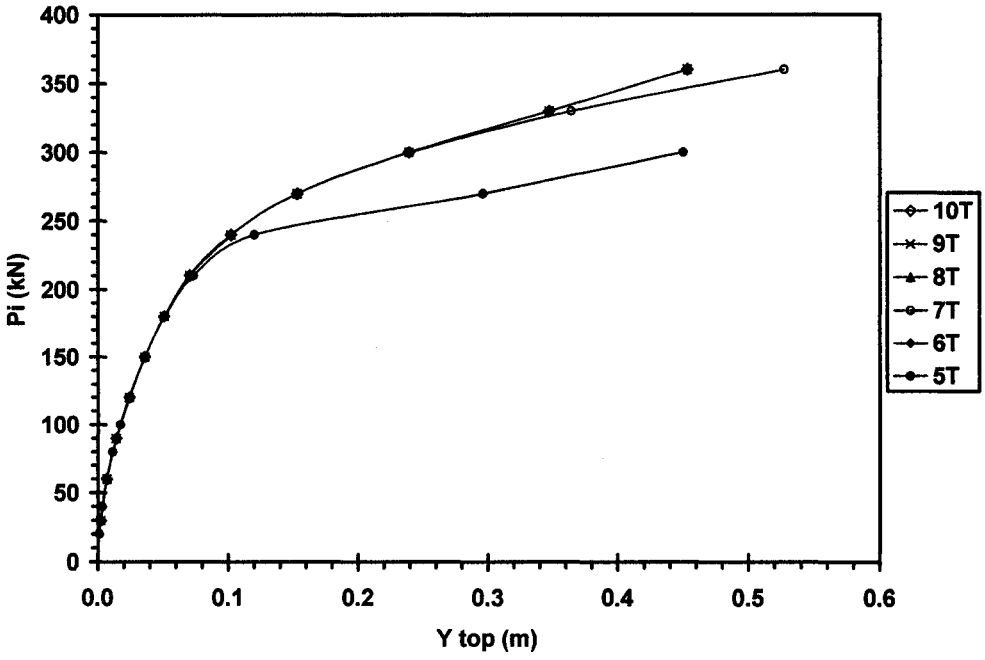

(b) Long piles

Figure 6.4 Discrete forces P_i vs. lateral displacement of the top of the pile y_{top} for fixed head pile subjected to lateral forces P_i (continued)

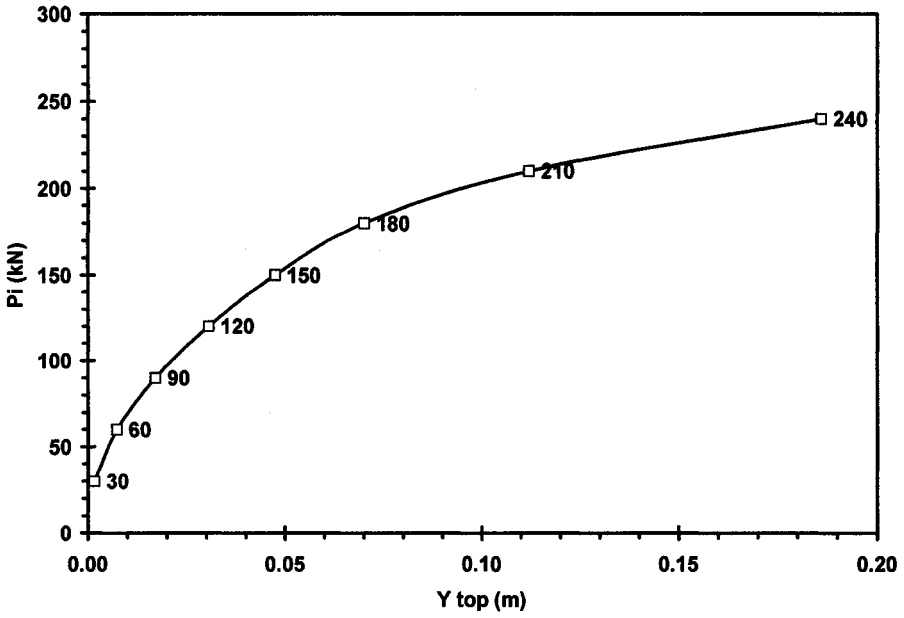

(c) L = 3T

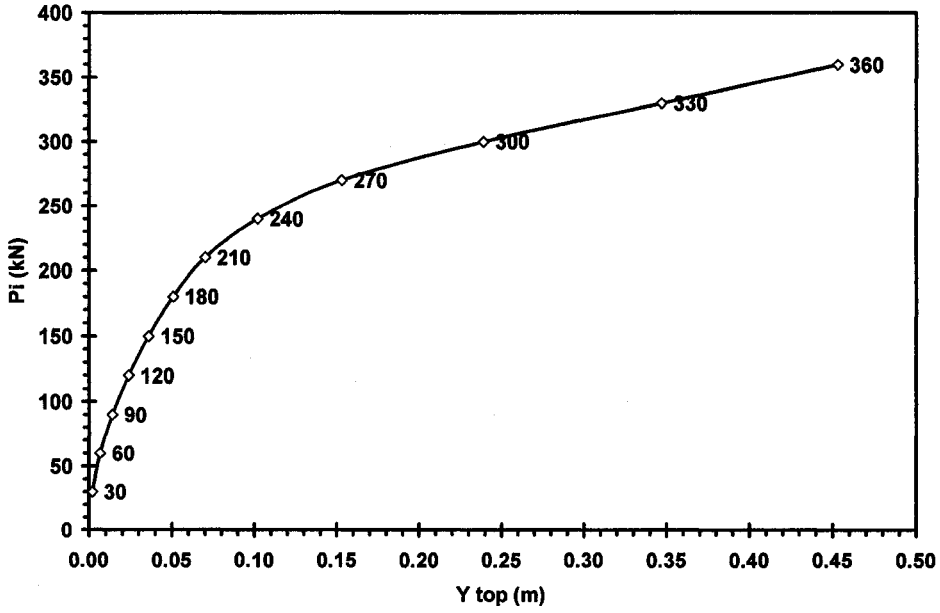

(d) L = 10T

Figure 6.4 Discrete forces P_i vs. lateral displacement of the top of the pile y_{top} for fixed head pile subjected to lateral forces P_i

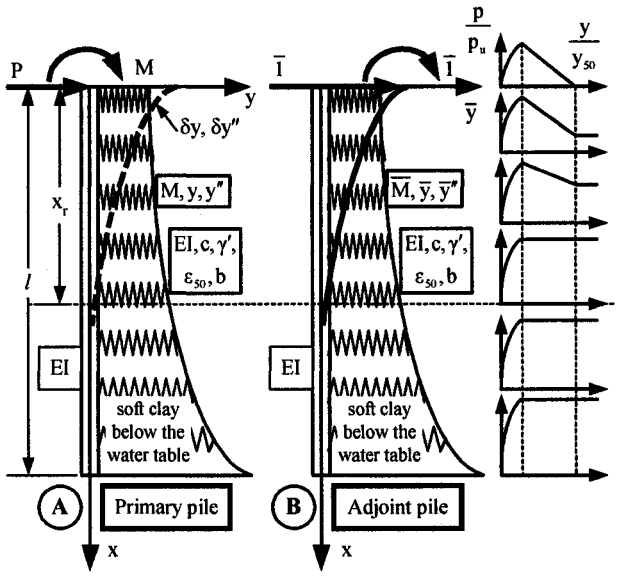

Figure 6.5 Primary and adjoint pile structures used in sensitivity analysis of single isolated pile. The p-y curves for discrete depth locations are also shown.

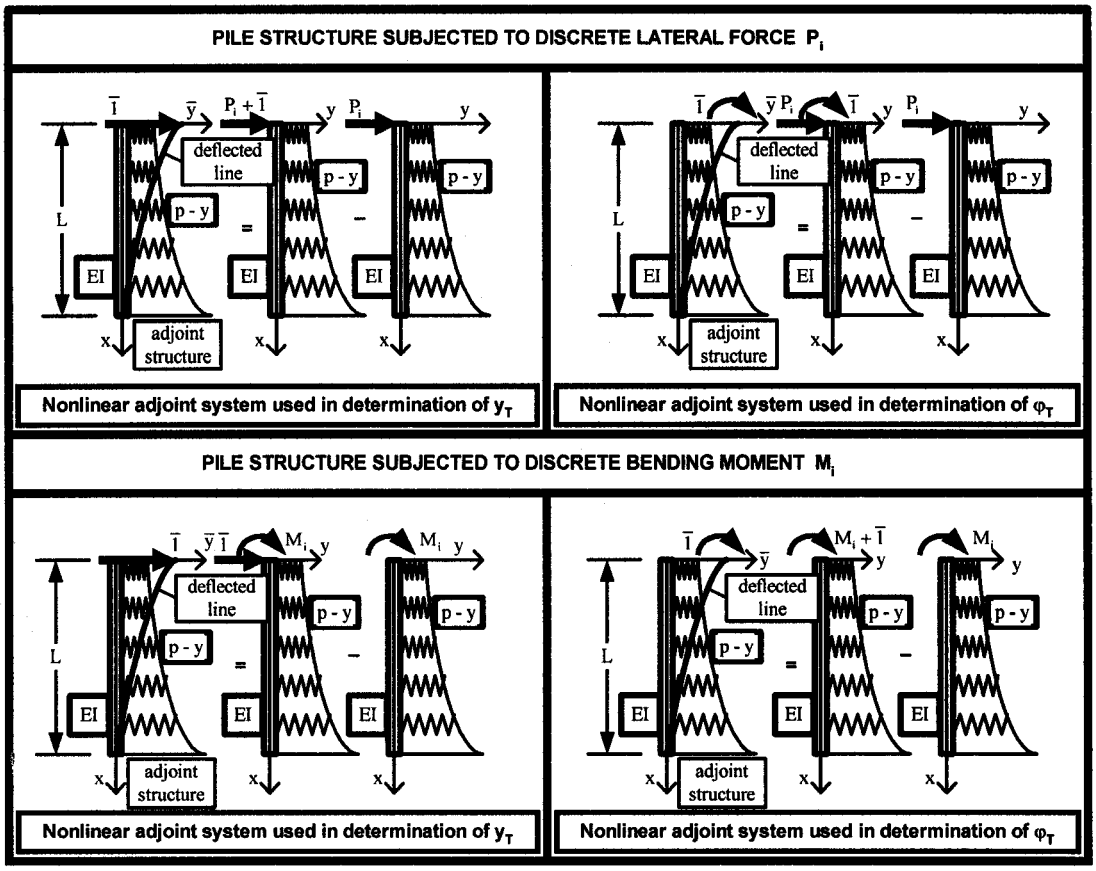

Figure 6.6 Four cases of application of the generalized unit load employed in sensitivity analysis of nonlinear adjoint pile structure being in the state of deformation corresponding to primary structure.

CHAPTER 7

SENSITIVITY ANALYSIS OF GROUPS OF PILES

7.1 SCOPE

The groups of piles employed in this study are shown in Fig. 7.1.a. The piles are arranged as 3×3 groups of piles with various spacing s, which are equal to 2D, 3D, 4D, and 5D. The length of the pile is equal to 10T, which is 23 m. The pile cap is reinforced concrete with modulus of elasticity E is equal 3×10^7 kPa and Poisson's ratio μ is equal to 0.2. Thickness t of the pile cap is equal 2 m. Lateral forces Pg_i applied at the cap of the groups of piles are cyclic loading with 1000 cycles. Each pile members has the same section properties as the single pile defined in Chapter 5, and the soil surrounded the pile is soft clay below the water table that also defined in Chapter 5. Sensitivity analyses of lateral deflection δy_t at the top of the following pile members are employed in this study: A (2^{nd} trailing row-middle), B (1^{st} trailing row - middle), C (leading row-middle), and D (leading row-corner). The locations of each pile members are described in Fig. 7.1.a.

7.2 DETERMINATION OF Pg_i

In order to compare the results of single pile analyses and those of groups of piles analyses, the lateral forces Pg_i that applied to the pile group should produce the same displacement as the results of the lateral forces P_i that applied to the single pile. Comparison of the curves of top lateral displacement y_t vs. the series of lateral forces for single pile P_i and groups of piles Pg_i are done in order to find the values of lateral forces Pg_i. Laterally loaded piles analyses are needed in order to obtain these curves. For single piles, they are specified in Chapter 6. The model for the analyses of laterally loaded piles for the groups of piles in this study is shown in Fig. 7.1.b. The pile members are modeled as 50 elements and analyzed by means of FEM using the FB-Pier Program (2001). The input data for these analyses are presented in Appendix C.2. The connections between pile members and pile cap are assumed as pinned joint in order to compare the results of sensitivity analyses with those of the free head single piles. The p-multiplier f_m and the corner pile factor f are applied for the pile group using the curves in Fig. 2.4 from Mokwa and Duncan (2001), for this study the values of f_m and f are presented in Table 7.1. The curves of top lateral displacement y_t vs. the series of lateral forces for single pile P_i and groups of piles Pg_i as the results of this analysis are presented in Fig. 7.2 and the values of lateral forces applied at the top of the pile groups are presented in Table 7.2.

7.3 MODEL OF PRIMARY AND ADJOINT STRUCTURE

There are two different possibilities in analysis of laterally loaded groups of piles. The first (Fig. 7.3a), each of pile members are modeled as a single isolated pile and apply the p-multiplier on the p-y curve of the soils and then apply the distributed lateral forces.

The distributions of lateral forces Pg_i applied in the pile cap in each pile members are based on the values of the p-multiplier. This method is used in analysis of pile group by mean of COM624P version 2.0 programs. The second as shown in Fig 7.3b, the group of piles are analyzed concurrently and the p-multipliers f_m are applied for each row. This method is used in analysis of pile group by means of FB-Pier Programs. The results of both methods are almost similar. This study uses the second method in analysis of laterally loaded pile group for either primary or adjoint structure.

Using the first method, the analyses of primary and adjoint structure for the groups of piles are relatively same as those of the single piles; the different is only the application of p-multiplier f_m. For primary structure, the forces to each pile are needed to be determined, but we can just apply the unit force in the adjoint structure. By means of the second method, the analysis of primary structure is easier, because we do not need to determine the distributed force for each pile member. However, in analysis of adjoint structure we need to determine the values of lateral forces Pg_1 applied at the pile cap that result in the reaction on such a pile member is equal to unity. The determinations of the lateral forces Pg_1 that applied to the adjoint structures are needed. The values of Pg_1 vary with the rows of pile member as result of the fact that that each pile member resists different amount of forces because of the different values of f_m. The unit lateral forces applied in the adjoint structures Pg_1 for such a pile member are the forces applied to the pile cap that result in the reaction of the top of the same pile member is equal to 1 unit force. This concept can be explained in Fig. 7.4. The value of unit force Pg_1 can be formulated as:

$$Pg_1 = \frac{n_c}{f_r} \tag{7.1}$$

and

$$f_r = \frac{p_{top} + V_{top}}{Pg_i} \tag{7.2}$$

where:

n_c is number of column,

f_r is the percentage of forces carried by the top of pile member,

p_{top} is the soil resistance at the top of correlated pile member due to the lateral force Pg_i,

V_{top} is the shear force at the top of the correlated pile member due to the lateral force Pg_i,

Pg_i is the lateral forces applied at the pile cap.

The results of the calculation of unit force Pg_1 for each case are presented in the graphical form in Appendix N.

7.4 SENSITIVITY ANALYSES AND NUMERICAL ASSESSMENTS

The results of the sensitivity analyses of top lateral displacement δy_t for pile member A (2nd trailing row) of group 3×3 piles with length L = 10T and spacing 2D when subjected to lateral forces Pg_i and their numerical assessment are presented in Appendix O. The comparison of the sensitivity analysis of each pile members A, B, C, and D of the same groups is presented in Appendix P. Appendix Q presents the

comparison of sensitivity analysis of pile member A in various spacing, and Appendix R. The summary of the numerical assessments of A and F of the pile groups with various spacing is presented in Appendix S. The discussion of this result is presented in Chapter 8.

Table 7.1 The values of f_m and f for various spacing s

Spacing s	The corner pile factor F	p- multiplier f_m		
		Pile member A (2^{nd} trailing row)	Pile member B (1^{st} trailing row)	Pile member C (leading row)
2D	1.2	0.44	0.56	0.76
3D	1.0	0.58	0.67	0.82
4D	1.0	0.72	0.78	0.88
5D	1.0	0.86	0.89	0.94

Table 7.2 The values of lateral forces applied at the top of single pile P_i and pile group Pg_i employed in sensitivity analysis

Y top	Pi	Pgi			
	single pile	group pile (s=2D)	group pile (s=3D)	group pile (s=4D)	group pile (s=5D)
m	kN	kN	kN	kN	kN
0.0000	0	0	0	0	0
0.0034	20	115	126	145	157
0.0120	40	270	290	315	342
0.0251	60	387	447	479	523
0.0426	80	515	577	637	692
0.0646	100	644	723	796	866
0.0998	120	795	895	980	1070
0.1640	140	948	1065	1171	1275
0.3150	160	1107	1240	1365	1483
0.4720	180	1204	1345	1479	1605
0.6370	200	1328	1485	1630	1768

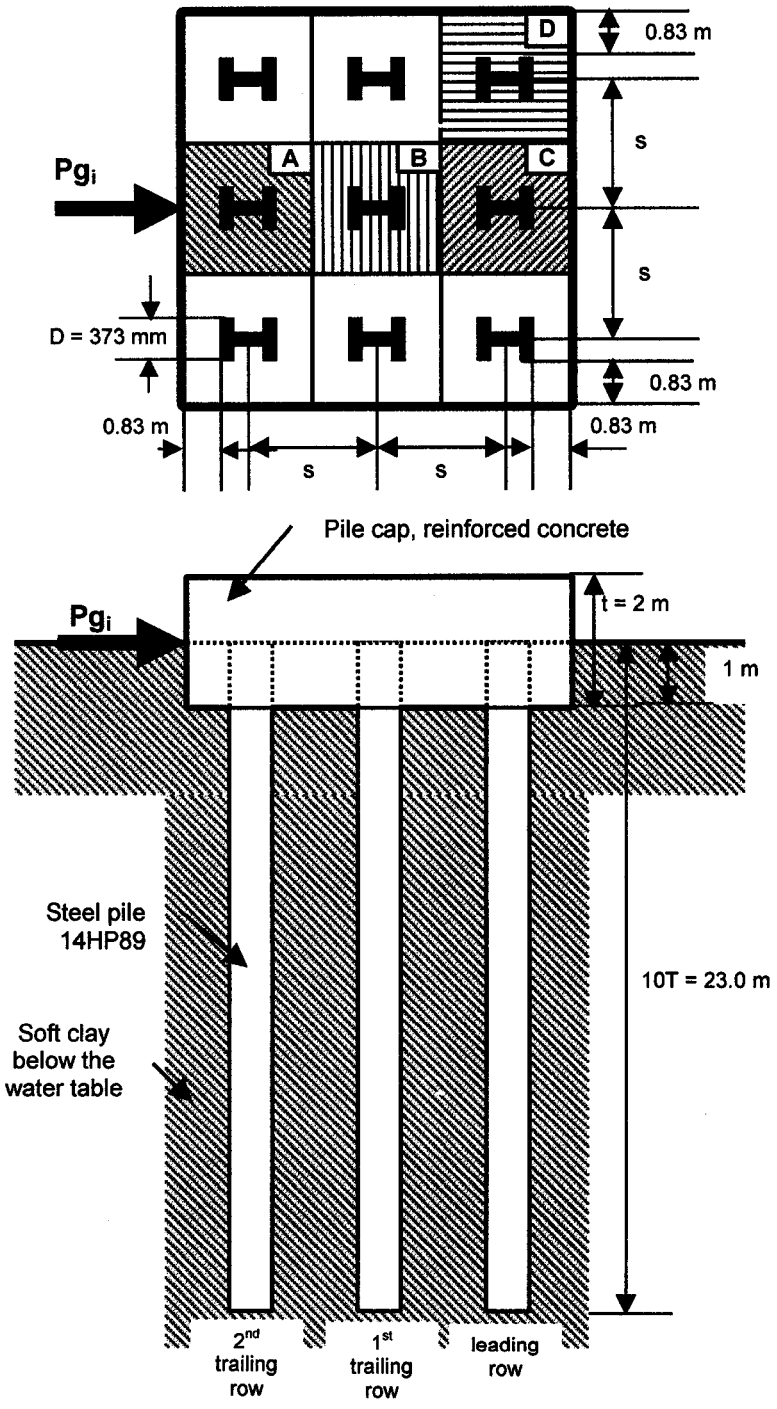

Figure 7.1a Pile group properties employed in the sensitivity analysis

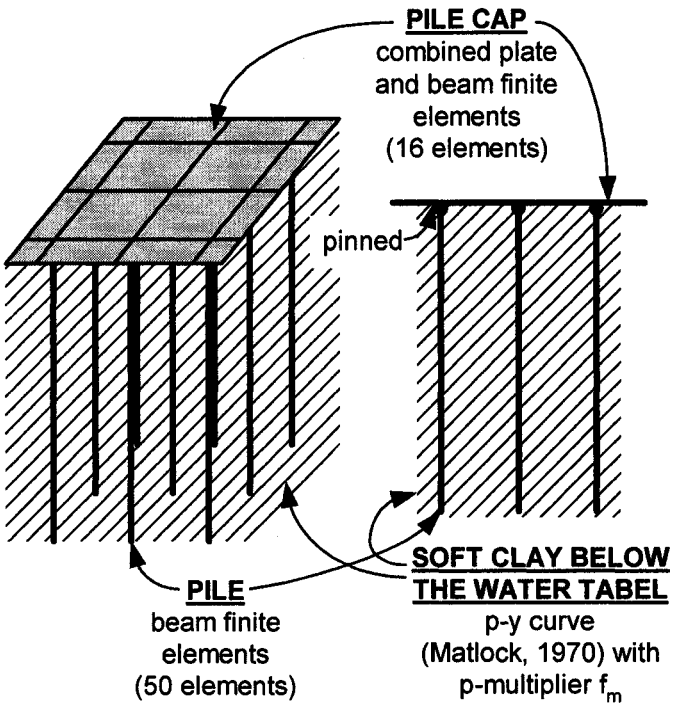

Figure 7.1b Pile group model employed in the laterally loaded pile analysis using FB-Pier Program (FDT and FHA, 2001) employed in sensitivity analysis

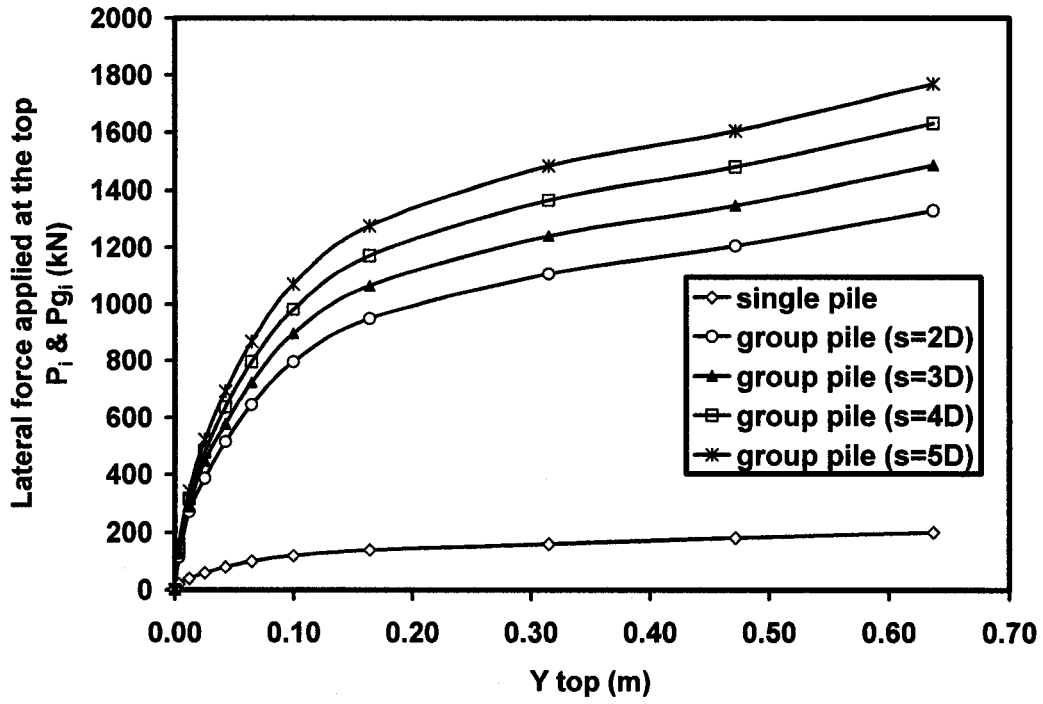

Figure 7.2. Discrete forces P_i and Pg_i vs. the lateral displacement at the top of the pile y_{top} for single pile and groups of piles subjected to lateral forces.

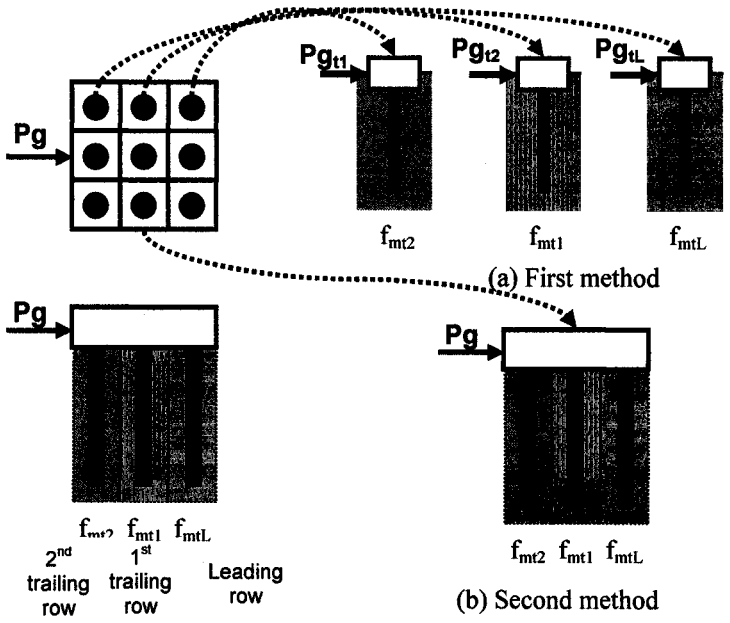

Figure 7.3. Two different methods in analysis of laterally loaded group of piles

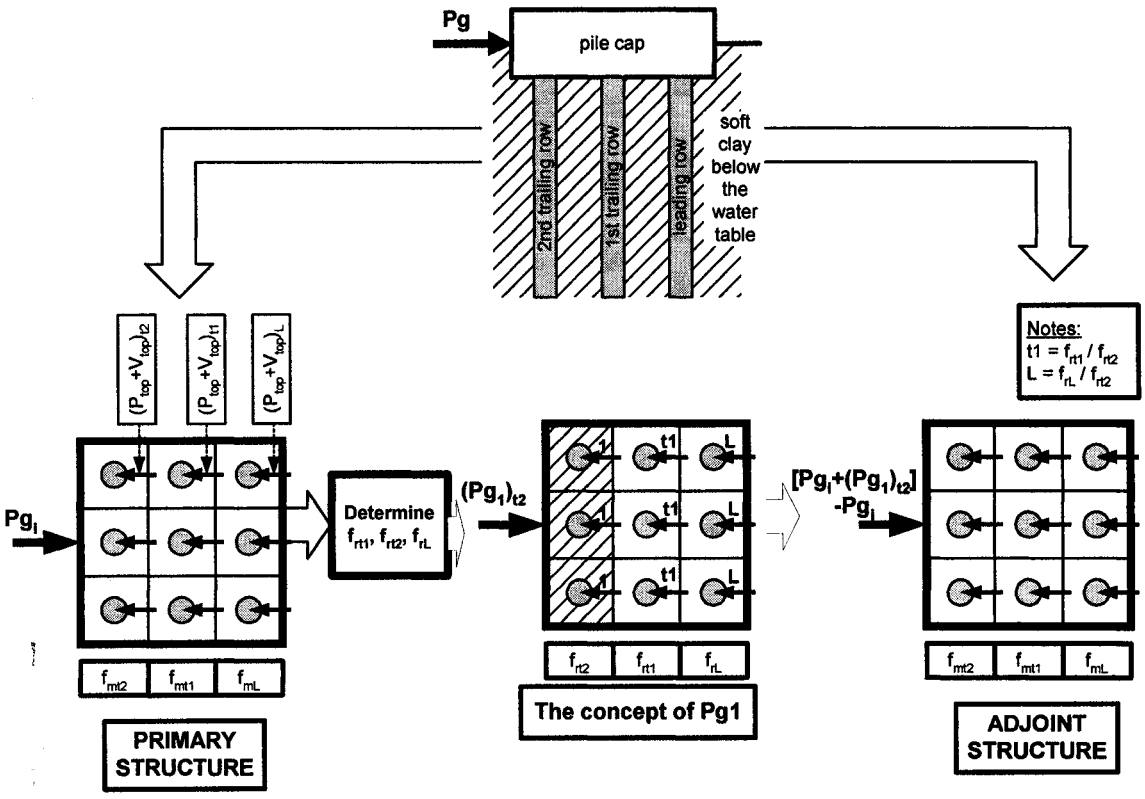

Figure 7.4 The approach of analysis of the pile member based on the distribution of lateral load Pg and Pg_I applied to the pile cap and transferred to the pile members.

CHAPTER 8
DISCUSSION

8.1 VERIFICATION OF THE RESULT OF SENSITIVITY ANALYSIS

The numerical investigation in this study requires so many analyses of laterally loaded piles due to a series of load that are highly possible to be miscalculated. The verification of the result of the sensitivity analysis is quite necessary to avoid this error. The result of the sensitivity analysis can be verified by the followings: (1) the verification of the loads applied at the primary structures, (2) the verification of the displacements at the primary and the adjoint structures, and (3) the evaluations of the distribution of the soil stages along the depth of the piles due to such a loading.

For single piles, the quantities of the lateral forces applied at the primary structures are equal to the shear forces at the top of the piles. Those values can be observed by means of the distributions of the shear force along the depth (Figs. D.12, E.12, F.12, G.12, H.12, I.12, J.12, K.12, L.12). For free head single piles, the quantities of the bending moments applied at the primary structure are equal to the bending moments at the top of the piles and those values can be observed by means the distributions of the bending moments at the primary structures (Figs. D.2, E.2, F.2, G.2,

H.2, I.2, J.2, K.2, L.2). For groups of piles, the loads applied are equal to the summation of the soil reactions and the shear forces at the top of the pile members, so that the distributions of the soil reactions and shear forces for each pile members are required for this verification.

The displacement at the top of the primary structure can be verified by means of the Figs. 6.2 and 7.2 that show the curves of lateral load applied at the ground line vs. the lateral deflection at the top of the pile.

The distributions of the lateral displacements along the depth of the adjoint pile structures are not explicitly verified. However, they can be verified by evaluation of Figs. 6.2 and 7.2. These figures show that the lateral displacements of the piles do not increase linearly due to the series of loads. The quantities of lateral displacement at the adjoint structures for such a loading depend on the quantities of the change of the top lateral displacement due to the change of the quantities of loads. This can be explained as the following. For the sensitivity analysis of the top lateral displacement of free head pile subjected lateral forces P_i with length L = 10T, it shown in Fig. 6.2b that the increments of top lateral displacement y_{top} due to lateral forces P_i which are less than 140 kN are relatively small if they are compared with those due to the lateral forces P_i which are greater than 140 kN. Based on that fact, the values of the distributions of lateral displacements (Fig. E.5) are also varied in the same way as Fig. 6.2b.

As defined in Chapter 4, the constitutive behaviour of the soil in this study has three different loading stages when the depth x is above x_r and two stages when the depth x is below x_r. Using the conditions defined in Table 4.1 and the distribution of the lateral displacement at the primary structure, the soil stages along the depth of the piles due to

such a loadings can be determined by evaluations of the distributions of the lateral displacements. In some case, in such a depth of the pile the displacement of the pile is relatively small that can be consider as undeformed structure. The assessment of the locations and the size of the soil stages for the sensitivity analyses of δy_t for free head pile with length L = 10T is presented in the graphical forms in Fig. E.13. This figure gives a significant instrument to examine the verification of the sensitivity analysis results, because it shows the depth where the distributions of the sensitivity integrands change the stage.

8.2 GENERAL DISCUSSION ON THE RESULT OF SENSIVITY ANALYSIS

8.2.1 Introduction

This discussion is focussed on the case of the sensitivity analysis of lateral deflection at the top of the pile with the length L = 10T subjected to lateral forces P_i, while other cases will be discussed in the next section. This section discusses each of the sensitivity operators and the physical interpretations of them are also described.

8.2.2 Discussion on the sensitivity operators C

The examination of the distribution of the bending moments at the adjoint structure (as shown in Fig. E.4) provides the valuable information on the effect of the magnitude of lateral load on the deformation of the systems. Three families of curves that are identified are connected with three ranges of loads that can be distinguished. For this the first family is connected with loading less than 80 kN. The second family of

loadings is localized in the interval 100-160 kN, and the third family is associated with the remaining highest values of loads, which are greater than 180 kN. For the same case, these loads when located on the p-y curve associated with x = 0 are shown in Figure E.1. This figure also shown that when load is less than 80 kN the ground line is in the nonlinear elastic stage, for loads (100-160) kN the ground line is in the linear softening stage, and for loads (> 180 kN) it is in the plastic flow stage.

The sensitivity operators C show the effects of the change of the design parameters on the displacement at the top of the piles and they carry units of loads correlated to the unit of loads (forces (kN) or moments (kN.m)) applied at the top of the pile. Design parameters EI represents the strength of the pile and design parameters c, γ', and b represent the strength of the soil. The increase of those four parameters can reduce the displacement due to the same loading. The other parameter ε_{50} denotes the weakness of the soil. From those facts, it shows that in the distributions of the sensitivity operators C_{EI}, C_c, $C_{\gamma'}$, and C_b have negative sign which means that the increase of these design parameters under constant load result in the decrease of δy_t or $\delta\varphi_t$. The positive sign in the sensitivity operator $C_{\varepsilon 50}$ at the nonlinear elastic stage means that the increase of $\delta\varepsilon_{50}$ will increase the δy_t or $\delta\varphi_t$. The changes of the sign positive to negative in the distribution of sensitivity operator $C_{\varepsilon 50}$ occurs as the result of the change from the stage of nonlinear elastic to linear softening or nonlinear elastic to plastic flow. In the stages of linear softening and plastic flow this change does not mean that the increase of $\delta\varepsilon_{50}$ will decrease of δy_t or $\delta\varphi_t$, but it denotes the dissipation of energy. It shows that design parameter ε_{50} has a unique characteristic. In the elastic stage, it denotes the weakness of

the soil, but in the linear softening and the plastic flow stages the changes of ε_{50} only affect slightly to the top lateral displacement due to such a lateral force.

The development of softening and plastic flow process starts from the top surface and propagates in depth when the applied load increases. This situation reflects on the distributions and magnitudes of the sensitivity integrands. Thus through properly performed integration process of the sensitivity integrands it is possible to identify and assess the changes of the maximum deformation caused by the changes of the design variables when some of the soil surrounding the piles is in nonlinear elastic, softening or plastic flow stage.

The evaluation of the distributions of C_{EI} (Fig. E.6) shows that its distribution is predictable because it follows the distribution of the bending moments at the primary and adjoint structure. The distribution of C_{EI} is not really affected by the soil stage.

From Fig. (E.7a), the distributions of C_c shows that in the interval of load (20-80) kN the soil surrounding the pile is in the elastic stage. An increase in load produces an increase in the dependence of δc on δy_t. In the interval of loads (100 – 120) kN (Fig. E.7b), the soil at the top part is in the linear softening stage. As the result of it, the distribution of C_c increases dramatically that means the change of δc can effect spectacularly on the δy_t. Below this linear softening part, the soil is in the elastic stage that the value of C_c will decrease dramatically.

Due to load 140 kN (Fig. E.7c) the distribution of C_c consists of three soil stages which are the followings: for the depth above x_r it is in the elastic softening stage, for the

depth x_r –3.45 m (x_r) it is in the plastic flow stage, and for the depth below 3.45 m it is in the nonlinear elastic stage.

Due to the loadings (160-180) kN (Fig. E.7c), the distributions of C_c consist of four soil stages, which are 1st plastic flow stage, linear softening stage, 2nd plastic flow stage, and nonlinear elastic stage from the top to the bottom. The linear softening stage and the 2nd plastic flow stage are separated by the depth x_r.

For only both stages are separated by x_r, the plastic flow stage can be located below the linear softening stage. It happens because of the change of conditions, in the depth upper the depth x_r soil has three stages, where at the displacement $y > 3y_{50}$ and $y < 15y_{50}$, the soil is in the linear softening stage, while in the depth below x_r the same condition is in the plastic flow stage.

The distribution of C_c due to loading (140-180) kN is presented in Fig. E. 7c. It is shown that in the plastic flow stage C_c is equal to zero, which means that δc is independent of δy_t.

Due to the loading of (200-240) kN, the distribution of C_c as shown in Fig. E.7d consists only the two soil stages, which are the plastic flow and the nonlinear elastic stages. It is shown that in these cases of loading that the effect of δc on δy_t decreases dramatically.

The plastic flow stage can also be indicated by means of the distribution of soil resistance p at the primary structure (Fig. E.11). From the evaluation of the distributions of C_c, the effect of δc on δy from the largest to the smallest can be ordered as follows: the linear softening stage, the nonlinear elastic stage, and the plastic flow stage, which is

equal zero. The quantitative assessment of the location and the size of the soil stages due to the series of loading are described in Fig. E. 13. This figure is developed from the evaluations of the displacements of the primary structure.

The examination of distributions of C_b (Figs. E.10a-E.10c) results in the same stages determinations. The major differences between the distributions of C_b and C_c are the magnitude and the shape of the figure. Based on the loading of (80, 120 and 180) kN, the magnitude of C_b is about 65-80 % of the magnitude of C_c. The other difference is that the value of C_b in the nonlinear elastic stage increases severely (more that 200%) near the depth below x_r. This fact shows that the effect of δb on δy_t in the nonlinear elastic stage is much greater when the depth is below x_r. In the plastic flow stage, the value of C_b is also equal zero. However, the highest increase of the value of C_b occurs when the soil in the linear softening stage as it is shown in Figs. E.10b-E.10c.

The distributions of $C_{\gamma'}$ (Figs. E.8a-E.8c) only exist for the depth above x_r. For the depth below x_r the sensitivity operator $C_{\gamma'}$ is equal to zero. This fact indicates that δy_t only depends on $\delta\gamma'$ for the depth above x_r and is independent of $\delta\gamma'$ for the depth below x_r. The evaluation the distribution of $C_{\gamma'}$ also indicates that the maximum effect of $\delta\gamma'$ on δy_t occurs in the linear softening stage, and it is equal to zero in the plastic softening stage.

Unlike the distributions of C_b in the nonlinear elastic stage that increase severely near the depth below x_r, the distributions of $C_{\varepsilon 50}$ in the nonlinear elastic stage (Fig. E.9a) have a perfect continuity at the depth x_r. It indicates that the effect of $\delta\varepsilon_{50}$ on δy_t is not really affected by the depth x_r. In the linear softening stage (Figs. E.9b-E.9c), the values

of $C_{\varepsilon 50}$ change their signs from positive to negative and their magnitude increase dramatically as it occurs to the other sensitivity operators. The $C_{\varepsilon 50}$ is also equal to zero when the soil is in the plastic flow stage.

In conclusion, the distributions of C_{EI} follow the distributions of bending moments at the primary and the adjoint structures. Unlike the distributions of C for the others parameters (c, γ', ε_{50}, and b) which are really affected by the soil stage, they are not affected by the soil stages. The distributions of C for other parameters (c, γ', ε_{50}, and b) increase dramatically in the linear softening stage and are equal to zero in the plastic flow stage. The zero value demonstrates that a plastic flow of soil does not affect the lateral deformations, which can be interpreted that the soil's plastic flow is uncontrollable. The depth x_r also has significant effect on their distributions. The linear softening of soft clay can develop only for $x \leq x_r$. The distribution of $C_{\gamma'}$ is equal to zero below the depth x_r. In the nonlinear elastic stage, the sensitivity operators C_c and C_b increase dramatically below the depth x_r, but the sensitivity operator $C_{\varepsilon 50}$ in this soil stage is not affected by x_r.

8.2.3 Discussion on the quantitative assessment of the sensitivity A due to the changes of the design variables

The value of the sensitivities A is the result of the numerical integration of the value of sensitivity operator C.

As shown in Fig. E.14a, the quantitative assessment of A_{EI} in the nonlinear elastic stage increases gradually until the load is equal to 160 kN, and then tend to be constant

when the load increases. The peak value of this stage occurs when the load is equal to 160 kN and A_{EI} is equal to 0.241 kN.m.

In the linear softening stage, A_{EI} starts existing in the load 100 kN and the value A_{EI} increases until the load 160 kN, then decreases and vanishes when the loads is greater than 200 kN. Due to the increase of loadings, the soil changes its stages from linear softening stage to the plastic flow stage. The peak value of A_{EI} in this stage is equal to 0.0288 kN.m at the load is equal to 160 kN. The value of A_{EI} in the plastic flow stage starts in the load 160 kN and increases when the load increases and A_{EI} for the plastic flow stage is equal to 0.689 kN.m for the load 240 kN.

The quantitative assessment of A_c in the nonlinear elastic stage (Fig. E.14b) increases regularly until the load equal to 140 kN when it has the value equal to 3.48 kN.m, and then decrease when the load increase, because some of the elastic part has changed to the linear softening and plastic flow stage due to the increase of displacements. The linear softening stage starts existing when the load is equal to 100 kN and the value of A_c in this stage increases until the peak value 70.3 kN.m when the loads is equal to 140 kN and then start decrease when the load is greater than 140 kN because some of the softening part change to the plastic flow. In the plastic flow stage, the value of A_c is equal to zero.

The values of $A_{\gamma'}$, $A_{\varepsilon 50}$, and A_b (as shown in Figs. E.14c-E.14e) have the same trend as the value of A_c but they have different peak value and magnitude. In the nonlinear elastic stage, $A_{\gamma'}$ has the peak value 0.265 kN.m at the load is equal to 100 kN, $A_{\varepsilon 50}$ has the peak value 1.16 kN.m at the load is equal to 140 kN, and A_b has the peak value 2.32 kN.m at the load is equal to 140 kN. In the linear softening stage, $A_{\gamma'}$ has the peak value

11.9 kN.m at the load is equal to 140 kN, $A_{\varepsilon 50}$ has the peak value 17.2 kN.m at the load is equal to 160 kN, and A_b has the peak value 56.5 kN.m at the load is equal to 140 kN. The values of $A_{\gamma'}$, $A_{\varepsilon 50}$, and A_b are equal to zero at the plastic flow stage.

In conclusion, the values of A increase with the increase of the load when whole soil is in the nonlinear elastic stage. When the load increase and the soil consist of the various soil stages, variation of the value of A is not regular with the increase of the load and it is hard to be predicted.

In the nonlinear elastic stage and the linear softening stage (as shown in Figs. E.14f-E.14g), the value of A_c most dominates between the five design parameters that indicate the most effective way to decrease the top lateral displacement is to improve the soil cohesion c. Fig. E.14a shown that in the plastic flow stage only A_{EI} exists. This fact explains that when the soil has already failed (in the plastic flow stage), only pile strength resists the external forces. As shown in Fig. E.14i, without considering the stages of the soils, the value of A_c is the most dominant in each loading.

The summation of the sensitivities $(A_{tot})_i$ due to the changes of five design parameters (EI, c, γ', ε_{50}, and b) for each soil stages as it is formulated in Eq. (4.50) is compared in Fig E.14j. From this figure, the value of A_{tot} in the linear softening stage gives the greatest value followed by A_{tot} in the elastic stage and A_{tot} in the plastic flow. It means that the change of the design variables has the highest effect on δy_t in the linear softening stage followed by the nonlinear elastic stage and the plastic flow stage. The sensitivity value A_i in the linear softening stage is equal to zero, except for A_{EI}. It makes sense, because when the soil is in the plastic flow stage, only the pile's strength that the load.

8.2.4 Discussion in the relative sensitivity factor F

Equation 4.51b defines the relative sensitivity factor $(F_i)_u$ of such a design variable for a specified soil phase. $(F_i)_u$ is the ratio of the quantitative assessment of A of such a design variable for a specified soil stage with the total of the quantitative assessment of A for the same soil stage, so that F describes the level of importance of a specified design variable to the others design variables.

The relative sensitivity factor F_{EI} (as shown in Fig. E.15a) has a very small value (less than 3 %) when the load is less than 180 kN, while when the loads increase F_{EI} increases dramatically up to 21% for the load 240 kN. The spectacular increase of F_{EI} occurs due to the change of the soil stage from the linear softening stage to the plastic flow stage. Unlike the sensitivity operators C_i of other design variables, which are related to the soil strength that vanish in the plastic flow stage, C_{EI} still exists in this stage because EI is independent to the soil strength. This fact shows when the soil is failled, the strength of the pile EI becomes more dominant.

Due to the load less than 80 kN where the whole part of the pile is in the nonlinear elastic stage (as shown in Fig. E.15b), the relative sensitivity factor F_c has a relatively constant value which is 52%. Due to loads (100-180) kN the soil consists of two different soil stages, which are the nonlinear elastic stage and the linear softening stage. If we compare with the previous condition, F_c decreases its value and is not constant anymore. When the load is greater than 180 kN, the soil consists of two stages, which are the linear softening stage and the plastic flow stage. As it is defined previously that the value of A_c in the plastic flow stage is equal to zero, so that only the elastic stage under that stage which still contribute in the values of A_c. As a result, F_c for the load greater

than 180 kN decreases when the load increases, because the soil in the nonlinear elastic stage portion change to the plastic flow stage due to the increase of load.

The relative sensitivity factor $F_{\varepsilon 50}$ (shown in Fig. E.15d) has the same characteristic as F_c, the different is only its magnitude. Its value in the elastic stage is about 19%.

The relative sensitivity factor $F_{\gamma'}$ (shown in Fig. E.15c) also has the relatively constant value in the elastic stage that is about 5%. For the load is equal to 80 kN the linear softening stage starts existing. $F_{\gamma'}$ decreases and then it tends to increase until the linear softening stage changes to the plastic softening stage. In this stage as shown in the loads (200 – 240 kN), unlike the other parameters which C still exists in the depth below x_r when the soil is in the nonlinear elastic stage, the value of $C_{\gamma'}$ vanishes in this stage below x_r, so that the value of $F_{\gamma'}$ is equal to zero.

As it is shown in Fig. E.15e, the value of F_b has the same trend as F_c, except when the linear softening stage exists it tends to increase. The value of F_b in the elastic stage is about 22%.

From Fig E.15f that show the relative sensitivity factor in the nonlinear elastic portion F_e for the load in the range of (20-160 kN), the design variables from the most dominant to the less dominant can be ordered as follows: cohesion c, diameter b, ε_{50}, saturated unit weight γ', and stiffness of the pile EI. The relative sensitivity factor in the linear softening portion F_s (Fig. E15g) have similar order of the design variables as that in the nonlinear elastic portion, except for the load is equal to 180 kN where the sensitivity parameter γ' overcomes ε_{50}. When the load increase, the linear softening stage

changes to the plastic flow stage, so that F_s is vanished for the loads is greater than 180 kN.

The relative sensitivity factor in the plastic flows stage F_f starts existing for load is equal 160 kN. As shown in Fig. E.15h, F_f is not significant, because only C_{EI}, which still exists in this stage. In the range of loads (160-180) kN, the value of F_f is very small, because only small part of the soil is in plastic flow stage. When the load increases, the plastic flow portion will increase, so that the quantity of F_f increases. However, this increase is not significant because only C_{EI} exists in this stage and EI has small portion compared with other parameters.

If we combine the relative sensitivity factor F from all the soil stages, as shown in Fig. E.15i, when the load is less than 120 kN, the order of the design variables from the most significant to the least significant is c, b, ε_{50}, γ', and EI. For the load in the range (80-180) kN, F is irregular due to the various stage of soil exist along the pile. However it is still in the same order until the load is equal to 160 kN. For the load is equal to 180 kN, $F_{\gamma'}$ overlaps $F_{\varepsilon 50}$. In the load (200-240) kN, soil is in the plastic flow and elastic stage. The value of F_{EI} increases, $F_{\gamma'}$ vanishes, and the others decrease with the similar portions, except for F_{EI} that will become more dominant.

From the same figure, it is shown that when whole part of the soil is in the elastic stage (represent the load 20-80) the value of F for each parameter has the relatively constant values, but when the load increases and the soil consists of various soil stages, F varies arbitrarily with the increase of the load. These values are important because most of the pile design is in the elastic stage. The values of the relative sensitivity factor for

tion $y < 3\ y_{50}$ are the followings:

F_{EI} : 1 – 2 %

F_c : 52 %

$F_{\gamma'}$: 5 %

$F_{\varepsilon 50}$: 20 %

F_b : 22 – 23 %

8.3 COMPARATIVE ANALYSIS

8.3.1 Introduction

By means of the results of the sensitivity analyses, the discussion of this section will be focused the comparative analysis on the followings:

1. For single piles, the comparative analysis are on the followings:
   - The various lengths of the piles (short and long piles),
   - The various boundary conditions of the piles (free head and fixed head piles),
   - The different types of loads applied at the top of the piles.
   - The comparison of the sensitivity analysis of top lateral displacement δy_t and top angle of rotation $\delta \varphi_t$.
2. For groups of piles, the comparative analysis are on the followings:
   - The single isolated piles and pile group's member,
   - The effect of location of the piles in a group,

     The various spacing s of the pile groups.

8.3.2 Single isolated piles

8.3.2.1 Comparison of the short pile and the long pile

In doing this comparative analysis, the pile with length L=3T and length L=10T is employed to represent the short pile and long piles.

The difference between the short pile and long pile is the distribution of the lateral displacement at of the pile both in the adjoint or primary structures. As shown in Figs. D.3; D.5; E.3; and E.5, for the short piles the tips of the piles are deformed, while for the long piles they are not deformed. The distributions of the moments at the primary and adjoint structure (as shown in Figs. D.2; D.4; E.2; E.4) also have the same pattern for short or long pile the different is only the magnitude. The distributions of the bending moment at the adjoint structure for the short pile have only in one family curve, because whole of the pile is in the elastic stage for all loading, while for the long pile, they are in the three families of curves. The family curves are described in Section 8.2.2.

The comparative analysis based on the distribution of the sensitivity integrands of the long pile and short pile has been done by Budkowska and Priyanto (2001), as part of the results of this study. The evaluations of the distributions of sensitivity operators C presented in Figs. (D.5-D.10; E.5-E.10; H.5-H.10; H.5-H.10) leads to the following conclusions:

- For short piles the changes of the design variables affecting the top deformations are distributed along the entire length of the pile (except of γ'). The changes of c, ε_{50}, and b at the point of rotation of a short pile do not affect the changes of top deflection.

- For long piles, the distributions of sensitivity integrands are localized in the upper 50% of the length of long piles.
- The increase of magnitude of load acting on the long pile results in the development of elastic stage that moves deeper and deeper along the pile axis.
- The numerical values of sensitivity integrands are larger for long piles than for short piles.
- Based on the examination of $C_{(...)}^{P}$ and $C_{(...)}^{M}$ for short and long piles, the effect of changes of the design variables on the top lateral displacement of piles can be arranged in the following descending order of importance: cohesion c, ε_{50}, γ' and EI.

As shown in Figs. D.14-15 and Figs. E.14-15, the values of A and F for both short and long pile vary in the same pattern as discussed in the previous section, except the short pile is only in the nonlinear elastic stage.

The comparison of the quantitative assessment of the sensitivities A_i and the relative sensitivity factor F_i for the various length (2T, 3T, 4T, 4.5T, 5T, 6T, 7T, 8T, 9T, and 10T) for free head pile subjected to lateral forces, and it is shown in Appendix R. The value of A_i for various lengths varies slightly due to the change of length as it is shown in Figs. R.1a-R.1e. Figures R.1b-R.1e show that the values of A for the lengths L = 7T and 10T are less than those for length L = 8T and 9T and they show inaccuracy. However, these results can be explained as the followings. In the numerical integration, constant numbers of elements (100 elements) are used in the analysis of laterally loaded piles using COM624P, which means the use of different size of the elements. In doing

numerical integration, we only calculate the sensitivity integrands at the end of each element, so that the use of the different sizes of element causes the depth x_r is not always at the similar depth. It does not affect significantly in the nonlinear elastic stage and plastic flow, because the sensitivity operators C in these stages only varies slightly. However, in the linear softening stage it can affect the value of A and F considerably, because at the depth close above to x_r the value of C_c, $C_{\gamma'}$, $C_{\varepsilon 50}$, and C_b can increase drastically. Increasing the numbers of elements or using the same size of elements for the analysis of each pile length can reduce this inaccuracy. However, this result is still reasonable.

The relative sensitivity factor F for various lengths of piles in each stage has the same characteristic, as it is shown in Figs. R.2a-R.4a. It indicates that the relative sensitivity factors F is affected slightly by the length of the pile.

If we determined that the maximum displacement of the top of the pile is equal to 5 cm, which means that whole of the pile is in the nonlinear elastic stage, we can generate Figs. R.5a-R.5e. From these figures, we can conclude the followings:

- The values of Fe_{EI} and $Fe_{\gamma'}$ increase with the increase of the length of the pile for short piles ($L < 5T$), while for long pile ($L > 5T$) it remains constant.
- The values of Fe_b decreases with the increase of the length of the pile for short piles ($L < 5T$), while for long pile ($L > 5T$) it remains constant.
- The values of Fe_c and $Fe_{\varepsilon 50}$ are independent of the lengths of the piles.

This fact indicates that it is possible to develop the design chart to simplify the sensitivity analysis.

8.3.2.2 Comparison of the free head piles and fixed head piles

The major difference due to the boundary conditions at the top of the pile is the distributions of the bending moments along the depth of the primary and adjoint pile structures. For fixed head pile the maximum value of bending moment is at the top of the pile (Figs. F.2 and G.2), while for free head pile the maximum bending moment occurs at the middle part of the pile (Fig. D.2 and E.2). The values of bending moment at the primary and adjoint structures affect directly on the distributions of C_{EI}. As it is shown in Figs. F.5 and G.5, the distributions of C_{EI} for fixed head piles have maximum values at the top of the pile, which means that the highest effect of δEI on δy is in the top part of the pile, while for free head piles C_{EI} is equal to zero at the top of the piles. Even though this fact consequently affects the values of A_i and F_i, it does not affect the order of significance of the sensitivity operators.

The distributions of lateral displacements at the primary and adjoint structures of the fixed head piles have the same trend as the free head piles. This fact results in the similar shape of the others sensitivity operators C_c, $C_{\gamma'}$, $C_{\varepsilon 50}$, and C_b (as shown in Figs. F.6-F.10 and Figs.G.6-G.10) for free head and fixed head piles. The differences are only in the magnitude of them and the lateral forces applied. Fixed head piles required greater loads to produce the same displacement. It is shown in Fig. 6.4.

In conclusion, the major difference of the free head pile and fixed head pile is on the distributions of C_{EI}. For fixed head pile C_{EI} maximum at the top of the pile, while for free head pile C_{EI} is equal to zero at the top of the pile. The sensitivity operators C of other design variables have the same characteristics for both free head piles and fixed piles.

8.3.2.3 Comparison of the different loads

The types of loads compared in this study are lateral forces and bending moment loads applied at the top of the free head single piles. The major difference in the results of laterally loaded pile analysis for both cases is in the distributions of the bending moments at the primary structure. For the piles subjected to bending moments the maximum value of the bending moment is at the top of the pile, while for pile subjected to lateral forces it is at the middle part of the pile. This is shown when we compare Figs. (D.2 and H.2; E.2 and I.2). Consequently this affects the distributions of C_{EI} (as shown in Figs. H.5 and I.5).

For long piles the trends of deformation at the primary structure due to bending moments are different from those due to lateral forces, this is shown in Figs. E.3 and I.3, while the distributions of bending moment and displacement at the adjoint structures are similar to the piles subjected lateral load (Fig. I.4-I.5). The main difference of those two cases is in the distribution of the lateral displacement. For long piles, free head pile subjected bending moments deflects in two directions and only the upper part that piles deflects (Fig. I.4), while the similar piles subjected lateral forces deflects only in one direction and the deeper part of the pile deflects (Fig. E.4). Consequently, this affects the distribution of C_c, $C_{\gamma'}$, $C_{\varepsilon 50}$, and C_b (as it is shown in Figs. I.6 – I.10). For short piles, the difference in the characteristic of the displacement at the primary structure is unnoticeable (Figs. D.3 and H.3), so that their distributions of C_c, $C_{\gamma'}$, $C_{\varepsilon 50}$, and C_b for both cases have the same trends.

In conclusion, the major differences in the sensitivity analyses of δy_t for laterally loaded free head long piles due to different types of loadings are in the followings: (1) istributions of the bending moments at the primary structure, where the maximum

value of the bending moment is at the top of the pile for the piles subjected to bending moments, while it is at the middle part of the pile for pile subjected to lateral forces. Consequently, this affects the distribution of the sensitivity operators. (2) The distribution of the sensitivity integrands of the free head pile subjected to bending moments are localized in the upper part than the free head pile subjected to lateral forces.

8.3.2.4 Comparison of the sensitivity analysis of δy_t and $\delta\varphi_t$

The major difference in doing sensitivity analysis of δy_t and $\delta\varphi_t$ is the loading applied at the adjoint structures. For sensitivity analysis of δy_t, the adjoint structure is subjected to the lateral forces, while it is subjected to bending moments for sensitivity analysis of $\delta\varphi_t$. As the result of it, the distributions of bending moments at the adjoint structures have maximum value at the top (as shown in Fig. J.4; K.4; L.4; M.4). When the piles are subjected to lateral forces, the difference is only in the magnitude of the distributions of C_{EI} (as shown in Figs. J.5; K.5), C_{EI} for the sensitivity analysis of δy_t is larger than those of the sensitivity analysis of $\delta\varphi_t$. For the piles subjected to bending moments as shown in Figs. L.5 and M.5, the difference is also in the characteristics of the distributions of C_{EI}, it has the maximum value at the top of the piles.

The distributions of the lateral displacement at the adjoint structure for the sensitivity analysis of $\delta\varphi_t$ have the same trend as those for the sensitivity analysis of δy_t. Therefore, the distributions of C_c, $C_{\gamma'}$, $C_{\varepsilon 50}$, and C_b for both have similar characteristic, as they are shown in Figs. J.6-J.10; K.6-K.10; L.6-L.10; M.6-M.10.

When whole part of the soil is in the nonlinear elastic stage, the magnitude of C of the sensitivity of δy_t is relatively greater than the sensitivity of $\delta\varphi_t$ (Figs. J.6-J.10; K.6a, 7a, 8a, 9a, 10a; L.6-L.10, M.6a, 7a, 8a, 9a, 10a) while when some part of them is in the linear softening or plastic flow, they have relatively similar magnitude (Figs. K.6b-6d, 7b-7d, 8b-8c, 9b-9c, 10b-10c and Figs. K.6b-6c, 7b-7c, 8b-8c, 9b-9c, 10b-10c).

In conclusion, the differences of the sensitivity analysis of δy_t and $\delta\varphi_t$ are the followings: (1) For the sensitivity analysis of $\delta\varphi_t$ for free head pile subjected moment load, the sensitivity operator C_{EI} has the maximum value at the top of the pile, while it has maximum value in the middle part of the pile for the followings: sensitivity analysis of $\delta\varphi_t$ for free head piles subjected to lateral forces, sensitivity analysis of δy_t for free head piles subjected to bending moments or lateral forces separately. (2) The value of sensitivity operators C for the other design variables (c, γ', ε_{50}, and b) of δy_t and $\delta\varphi_t$ only vary in magnitude but have similar characteristics. When the whole soil is in the elastic stage, the magnitude of sensitivity operators $C_{c,\ \gamma',\ \varepsilon 50,\ b}$ of the sensitivity of δy_t are relatively greater than the sensitivity of $\delta\varphi_t$, but when the load increases and the soil consists of various stages they are relatively similar.

8.3.3 Groups of piles

8.3.3.1 Comparison of the single isolated pile and pile group's member

The characteristics of the distributions of bending moment and displacements at either the primary and adjoint structures are similar for groups of pile and single pile. The main difference is only the magnitude of them. Therefore the distributions of the

sensitivity operators C for pile groups also have the same pattern as those of single pile, but they have different magnitude. These values for pile member A of the group of 3×3 piles with spacing s = 2D are shown in Figs. O.1-O.13.

The values of sensitivities A and relative sensitivity factors F of groups of pile for arbitrary loads have the same characteristics as those of the single pile, as it has been discussed in the previous section, but they have different magnitude. These values for pile member A of the group of 3×3 piles with spacing s = 2D are shown in Figs. O.14a-O.15i.

In conclusion, the distributions of the sensitivity operators C, sensitivity A, and relative sensitivity factors F for pile groups have the same characteristics as those of single pile, but they have different magnitudes.

8.3.3.2 Comparative analysis of the effect of location of the piles in a group of piles

The comparative analysis of the effect of location of the piles in a group of piles is done by the comparison of the behaviour of pile member A (i.e. middle pile located at the 2nd trailing row), B (i.e. middle pile located at the 1st trailing row), C (middle pile located at the leading row), and D (corner pile located at the leading row).

The comparison of the pile members A, B, C, and D in a group of 3×3 piles with spacing s = 2D is shown in Appendix P. The pile cap is subjected to three different values of forces that produce y_t as shown in Fig. P.1. It is shown that pile C and D, which are in the leading row have the greatest value of f_m, that indicate the strongest soil strength if it is compared to piles A and B.

The distributions of the bending moments M and the shear forces V at the primary structure (as show in Fig. P.2 and P.12) demonstrate that for spacing s = 2D, pile D has the largest bending moment followed by pile C, B, and A. The distribution of the bending moment M of pile D is larger than that of pile C because of the corner pile factor indicate in Fig. 2.4. For others spacing s > 3D, the distributions of the bending moments M and the shear forces V for the pile C will be similar to those of pile D, because the corner pile factor is equal to unity. Unlike the bending moment at the primary structure M, pile A has the largest bending moments at the adjoint structure M_a followed by pile B and C, as it is shown in Fig. P.4.

The distribution of the displacement at the adjoint and primary structure (as shown in Figs. P.3 and P.5) can be ordered from the largest to the smallest as follows: pile A, B, C and D. Pile C and D have the same value, because the corner pile factor only affects on M and V. Because of the constraints imposed on the pile cap, the displacement at the top of all the pile is similar for the primary pile groups. Although the constraint is also imposed at the adjoint structures, but the quantity of loads that applied at the adjoint structures are different for different rows.

The value of C_{EI} (as shown in Fig. P.6) can be ordered from the largest to smallest as follows: pile D, C, B, and A. For the loads P1 and P2, the difference in the value C_{EI} is very small, they almost coincide each other. As the result of it the value of A_{EI} (as shown in Fig. P.14a) does not have the same order as the value of sensitivity operators C. The value of sensitivity A_{EI} due to P3 can be ordered from the largest to the smallest as: pile D, A, C, and B.

The value of sensitivity operators C for others design variables c, γ', ε_{50}, and b (as shown in Figs.P.7-P.10) for pile C is same as those for pile D. Consequently, the value of sensitivities A for both piles C and D are also similar. The sensitivity operator C of these parameters are ordered from the largest to the smallest: pile A, B, and C. When the loads increase to P3, the difference of the values C vanishes except for the sensitivity operator $C_{\varepsilon 50}$. Due to loads P1 and P2, the values of sensitivities $A_{c,\ \gamma',\ \varepsilon 50,\ b}$ (as shown in Fig. P.14b-P.14e) can be ordered from the largest to the smallest as: pile A, B, C and D. When the load increases to P3, the difference in the values of sensitivities $A_{c,\ \gamma',\ \varepsilon 50,\ b}$ is diminished. Even though each pile member has different values of sensitivities $A_{c,\ \gamma',\ \varepsilon 50,\ b}$, but the quantitative assessment of relative sensitivity factors $F_{c,\ \gamma',\ \varepsilon 50,\ b}$ is similar for each pile as shown in Figs. P.15a-P.15i.

The comparative analysis of the effect of the location of the piles in a group results in the following conclusions:

- The corner pile factor applied to the corner pile in the leading row caused the pile in the corner-leading row has larger value of bending moments and shear forces that the middle-leading row, however it does not affect the displacement of it.
- The piles located in the leading row have the largest bending moment at the primary structure followed by the piles in the 1st trailing row and 2nd trailing row constitutively. However the bending moments at the adjoint structure are ordered oppositely from the largest to smallest as: the piles in the 2nd trailing row, the 1st trailing row, and the leading row.

- The lateral displacement at the top of the piles at the primary structure is similar for each row due to the constraint imposed on the pile cap, but the distributions of the lateral displacements vary for each row. The piles located in the 2nd trailing row have the largest distribution of lateral displacements at the primary and adjoint structures followed by the piles in the 1st trailing row and in the leading row constitutively.
- The value of the sensitivity operator C_{EI} and the quantitative assessment of the sensitivity A_{EI} of each row due to load P1 and P2 (i.e. loads that cause the top surface of the soil being in the elastic and linear softening stages) are relatively similar, but due to the loads increase to P3 (i.e. load that cause the top surface of the soil being in the plastic flow stage) these values at leading row, 1st trailing row, and 2nd trailing row vary from the largest to the smallest.
- The value of $C_{(c,\ \gamma',\ \varepsilon 50,\ b)}$ and $A_{(c,\ \gamma',\ \varepsilon 50,\ b)}$ for each row due to load P3 (i.e. load that cause the top surface of the soil being in the plastic flow stage) are relatively similar, but due to the smaller loads P1 and P2 (i.e. loads that cause the top surface of the soil being in the elastic and linear softening stages) these values at leading row, 1st trailing row, and 2nd trailing row vary from the largest to the smallest.
- The relative sensitivity factors F are independent to the locations of the piles in a group.

8.3.3.3 Comparison of the various spacing s of the pile groups

Due to the effect of shadowing in the pile group p-multiplier f_m is applied to the pile members in the analysis of laterally loaded pile. The value of f_m varies for different

spacing s and the location of the piles in the pile groups. The value f_m for leading row is larger than that for trailing row. The larger is the spacing s, the larger is the value of f_m and f_m is equal to one for spacing s is greater than 6D, which means that each pile member behaves as a single isolated pile (as shown in Table 7.1). As a result, the greater the spacing s, the greater the load required to produce the same displacement so that it is required smaller loads to produce the same displacement for group of piles than single isolated piles, as it is shown in Fig. N.3a-N.3d.

Based on Figs. N.3a-N.3d, we can determine the efficiency of the pile group G_e. The value of G_e for different spacing s is presented in Fig. N.1a. This figure shows that the greater the spacing s, the greater is the efficiency of the pile groups. The values of efficiency of the pile G_e calculated using Eq. (2.4) and Eq. (2.5) are compared in Fig. N.2b. Using Eq. (2.4) the efficiency of pile groups G_e depends on the quantity of load applied, while using Eq. (2.5) this value is constant for different loads. The efficiency of the pile groups G_e from Eq. (2.4) is greater than that from Eq. (2.5). The value of G_e from Eq. (2.4) is quite bigger than that from Eq. (2.5) as stated by Mokwa and Duncan (2001).

The shear forces at the top of each pile members V_t for various spacing s are compared in Figs. N.2a-N.2d. These figures indicate that the greater the spacing s, the smaller is the difference of the shear forces at the top of each pile members V_t. These figures also compare V from pile groups' members with V from single pile that they also indicate that the greater is the spacing of the pile groups, the greater is G_e.

The summation of the shear forces at the top of the pile V_t and the soil resistance at the top of the pile p_t determine the percentage of the load carried by each pile members. Figures N.4a-N.4b demonstrate that the greater spacing results in the load

distributed equally to each pile members. The pile member C, which is in the leading row supports the largest amount of load. The percentage of loads carried by each pile member in the pile groups with different spacing is quite constant for arbitrary loadings. Consequently, the unit force of the pile groups due to such a loading Pg_1 for different load quantity calculated by Eq. (7.1) has relatively constant value for different loading. When the spacing s increases, the difference between the unit force of the pile group Pg_1 for different pile members decreases. This fact is shown in Figs. N.5a-N.5d.

To compare the effect of different spacing, the pile member A of the groups of 3×3 piles with various spacing (s = 2D, 3D, 4D, and 5D) are subjected to lateral forces on the pile cap P1, P2, and P3. Lateral forces P1, P2, and P3 are forces that generate top lateral displacement y_t equal to 0.0426 m, 0.0998 m, and 0.315 m respectively, as it is shown in Fig. Q.1. It is also shown in this figure that the greater the spacing s, the greater is the value f_m.

Refer to Figs. Q.2a-Q.2c and Figs. Q.4a-Q.4c, the bending moment at the primary structure increases when the spacing increases, but at the adjoint structure it decreases when the spacing increases. It is also shown that the bending moment at the primary structure for group of piles relatively smaller than that of the single pile, but at the adjoint structure it is relatively greater than that of the single pile. At both primary and adjoint structures, the displacement of the single pile is also relatively smaller than that of the single pile at both primary or adjoint structures and the greater the spacing the smaller the lateral displacement is (as shown in Figs. Q.3a-Q.3c and Figs. Q.5a-Q.5c). The difference in the displacement at the primary and adjoint structures is that there is constraint imposed on the pile cap at the primary structure that the displacement at the top of the

piles is constant, while for the adjoint structure although the constraint is still imposed on the pile cap but the different quantity of loads are applied at the pile cap, so that the top lateral displacement varies with the spacing.

As shown in Fig. Q.6a-Q.6c, the magnitudes of the sensitivity operator C_{EI} for three cases of loading increase with the increase of spacing; consequently C_{EI} for single pile is greater than that for pile groups. As shown in Figs. Q.7a, Q.8a, Q.9a and Q.10a, due to the load P1, the sensitivity operators C_c, $C_{\gamma'}$, $C_{\varepsilon 50}$, and C_b decrease when the spacing of the pile groups increases, that also means that those values of single pile is smaller than those of groups of piles. Refer to Figs. Q.7b-c, Q.8b-c, Q.9b-c, and Q.10b-c, when the loads increase to P2 and P3 their differences tend to vanish due to the decrease of the difference in displacement of the adjoint and primary structures. The exception for load P2, there is a big increment of those values at the depth 2.3 m. This big difference is caused by the different soil stage in that point, because the displacement at that depth for pile group with spacing s = 2D is greater than the others spacing, so that the pile group with spacing s = 2D is in the linear softening stage and the other piles are in the nonlinear elastic space. The discrete element used in program FB-Pier cannot recognize the exact depth when the soil is in the different stage. This error can be avoided if we can use more dense elements in the analysis of laterally loaded pile.

As shown in Figs. Q.13a-c, the undeformed pile structure starts from the lower depth if the spacing decreases. It due to the effect of shadowing that lowers the strength of the soil by decreasing f_m so that the greater deflection is generated by the same quantity of loads.

As show in Fig. Q.14a, in the nonlinear elastic stage and in the linear softening, the quantitative assessment of sensitivity A_{EI} due to loads P1 and P2 of the groups of piles differ slightly with different spacing and that value for groups of piles is greater than that of single pile. When the load increase to P3, A_{EI} for the elastic portions of the pile groups still greater than that of single pile, but these values of the plastic flow and the nonlinear softening portions of the single pile are greater that those of the groups of piles.

As shown in Figs. Q.14b-e, due to loads P1 and P2, the quantitative assessments of sensitivities A_c, $A_{\gamma'}$, $A_{\varepsilon 50}$, and A_b in the elastic portions and softening portions decrease with the increase of the spacing and those values of pile groups are greater than those of single pile. When the load increases to P3, the quantitative assessments of sensitivities A_c, $A_{\gamma'}$, and A_b vary slightly, but the quantitative assessment of sensitivity $A_{\varepsilon 50}$ decrease with the increase of the spacing and these values for single pile are greater than those of groups of piles, because the single pile has smaller displacement than the groups of piles so where the soil in a particular depth of the groups of piles is in the plastic flow stage, this of the single pile is still in the softening stage.

As shown in Fig. Q.14f, the portions of the quantitative assessments of sensitivities Ae_i (which is A in the elastic portion) due to three quantity of loadings decreases with the increases of spacing and have the portions from the largest to the smallest as follows: Ae_c, Ae_b, $Ae_{\varepsilon 50}$, $Ae_{\gamma'}$ and Ae_{EI}, except $Ae_{\gamma'}$ vanishes for load P3.

As shown in Fig. Q.14g, due to load P1 there is no quantitative assessments of sensitivities in the linear softening portion *As*, because no depth of the pile is in the linear softening portion. Due to load P2, *As* decreases with the increase of spacing so that *As* for

pile group is greater than that for single pile. Due to load P3, *As* is relatively constant with the spacing and *As* for single pile is greater than that of pile group.

As shown in Fig. Q.14h, Af only exists for design variable EI varying arbitrary fashion with respect to the spacing, because it is connected with the portion of the plastic stage and the magnitude of sensitivity operator C_{EI}. Although the magnitude of sensitivity operator C_{EI} for spacing s = 2D is smaller than that for s = 3D, but the plastic flow portion is longer and located in the deeper part where the magnitude of the C_{EI} is located. Without considering the soil stages, the spacing does not effect the quantitative assessments of sensitivities A of each parameter, as shown in Fig. Q.14i.

As shown Figs. Q.15a-I, the relative sensitivity factors F of all parameters except of parameter EI are only slightly vary with the spacing or even they can be considered constant. The relative sensitivity factor F due to three loadings (P1, P2, and P3) for parameter EI increases with the increase of the spacing. Their orders from the largest to the smallest are constant with respect to the various spacing, which are the followings: F_c, F_b, $F_{\varepsilon 50}$, $F_{\gamma'}$ and F_{EI}.

8.4 APPLICATIONS OF THE RESULT OF THIS STUDY

The results of this study can be applied in the followings:

1. Determination of the most effective parameter to reduce the top lateral displacement.

The results of this study show that the changes on the design variables that result in the reduction of the lateral displacement at the top of the piles from the largest to

minimum are the followings: c, ε_{50}, b, γ', and EI. Based on this fact, the increase of the soil strength is more effective to reduce the top lateral displacement than to improve the strength of the piles.

2. **Determination of the effective depth of the soil strength and the pile strength improvement.**

This study show that the changes of the design parameters to reduce the top lateral displacements are not effective from the top to the bottom, but they are only effective up to a particular depth that can be determine through the sensitivity analysis done by this study.

CHAPTER 9
CONCLUSION AND FUTURE RESEARCH

9.1 CONCLUSION

1. The verification of the results of the sensitivity analysis depends on the verification of the inputs on the sensitivity analysis (i.e. distributions of the moment and lateral displacements at the primary and adjoints structures: M, M_a, y, y_a). This can be observed by evaluation of the correlation of the figures produced in this study.
2. The evaluation of the distributions of bending moment at the adjoint structure M_a for free head single pile with L=10T subjected to lateral forces at the top shows that there are three ranges of loads distinguished (i.e. 1st family of loads (<80 kN), 2nd family of loads (100-160)kN, and 3rd family of loads (>180 kN)). These families are connected with the development of various stages of lateral displacements in the soil that are produced by these loads (i.e. 1st range is in the nonlinear elastic stage, 2nd range is in the linear softening stage, and 3rd range is in the plastic flow stage).
3. The design variable EI represents the strength of the pile and design variables c, γ', and b represent the strength of the soil. The other parameter ε_{50} have a specific aracteristic. In the nonlinear elastic stage, it denotes the weakness of the soil, but in

the linear softening and the plastic flow stages the changes of ε_{50} only affect slightly to the top lateral displacement due to such a lateral force.

4. The development of softening and plastic flow process starts from the top surface and propagates in depth when the applied load increases.
5. The evaluation of the sensitivity operators C result in the following conclusions:
   - The distributions of sensitivity operator C_{EI} follow the distributions of bending moments at the primary and the adjoint structures. Unlike the distributions of the sensitivity operators C for the others parameters (c, γ', ε_{50}, and b), which are really affected by the soil stage, the distributions of sensitivity operator C_{EI} are not affected by the soil stages.
   - The distributions of sensitivity operators C for other parameters (c, γ', ε_{50}, and b) increase dramatically in the linear softening stage and are equal to zero in the plastic flow stage. The zero value demonstrates that a plastic flow of soil does not affect the lateral deformations, which can be interpreted that the soil's plastic flow is uncontrollable.
   - The depth x_r also has significant effect on their distributions. The linear softening of soft clay can develop only for $x \leq x_r$. The distribution of $C_{\gamma'}$ is equal to zero below the depth x_r. In the nonlinear elastic stage, the sensitivity operators C_c and C_b increase dramatically below the depth x_r, but the sensitivity operator $C_{\varepsilon 50}$ in this soil stage is not affected by x_r.
6. The evaluation of the quantitative assessment of sensitivities A result in the following conclusions:

- The quantitative assessments of the sensitivities A increase with the increase of the load when whole soil is in the nonlinear elastic stage. When the load increases and the soil consist of the various soil stages, the variation of the quantitative assessment of the sensitivities A is irregular with the increase of the load and it is hard to be predicted. At the plastic flow stage, only the value of A_{EI} exists.
- In the nonlinear elastic stage and the linear softening stage the value of A_c most dominates between the five design parameters, but in the plastic flow stage only A_{EI} exists.
- By comparison of the total of the sensitivities $(A_{tot})_i$ due to the changes of five design parameters (EI, c, γ', ε_{50}, and b) for each soil stages, the value of A_{tot} in the linear softening stage gives the greatest value followed by A_{tot} in the elastic stage and A_{tot} in the plastic flow. It means that the change of the design variables has the highest effect on top lateral displacements δy_t in the linear softening stage followed by the nonlinear elastic stage and the plastic flow stage.

7. When whole part of the soil is in the elastic stage (represent the load 20-80) the value of relative sensitivity factors F for each parameter has the relatively constant values, but when the load increase and the soil consist of various soil stages, the relative sensitivity factors F varies irregularly with the increase of the load. These values for free head piles with the length L = 10T in the nonlinear elastic stage subjected to loads less than 80 kN are important because most of the pile are designed only in the elastic stage. These values can be summarized as follows:

F_{EI} : 1 – 2 %

F_c : 52 %

$F_{\gamma'}$: 5 %

$F_{\varepsilon 50}$: 20 %

F_b : 22 – 23 %

8. From the comparison of the short pile and long pile come the following conclusions:
   - For short piles the changes of the design variables affecting the top deformations are distributed along the entire length of the pile (except of γ'). The changes of c, ε_{50}, and b at the point of rotation of a short pile do not affect the changes of top deflection.
   - For long piles, the distributions of sensitivity integrands are localized in the upper 50% of the length of long piles.
   - The increase of magnitude of load acting on the long pile results in the development of elastic phase that moves deeper and deeper along the pile axis.
   - The numerical values of sensitivity integrands are larger for long piles than for short piles.
   - Based on the examination of $C_{(...)}^{P}$ and $C_{(...)}^{M}$ for short and long piles, the effect of changes of the design variables on the top lateral displacement of piles can be arranged in the following descending order of importance: cohesion c, ε_{50}, γ' and EI.
   - The quantitative assessment of the sensitivities A_i and the relative sensitivity factors F_i for various lengths varies slightly with the different length.

- For the maximum displacement of the top of the pile equal to 5 cm, which means that whole of the pile is in the nonlinear elastic stage;
  - The relative sensitivity factors in the nonlinear elastic stage Fe_{EI} and $Fe_{\gamma'}$ increase with the increase of the length of the pile for short piles ($L < 5T$), while for long pile ($L > 5T$) they remain constant.
  - The relative sensitivity factor in the nonlinear elastic stage Fe_b decreases with the increase of the length of the pile for short piles ($L < 5T$), while for long pile ($L > 5T$) it remains constant.
  - The relative sensitivity factors in the nonlinear elastic stage Fe_c and $Fe_{\varepsilon 50}$ are independent of the lengths of the piles.

9. The major difference of the free head pile and fixed head pile is on the distributions of the sensitivity operator C_{EI}. For fixed head pile C_{EI} maximum at the top of the pile, while for free head pile C_{EI} is equal to zero at the top of the pile. The sensitivity operators of other design variables C_c, $C_{\gamma'}$, $C_{\varepsilon 50}$, and C_b have the same characteristics for both free head piles and fixed head piles.

10. The major differences in the sensitivity analyses of δy_t for laterally loaded free head long piles due to different types of loadings are in the followings:
    - The distributions of the bending moments at the primary structure, where the maximum value of the bending moment is at the top of the pile for the piles subjected to bending moments, while it is at the middle part of the pile for pile subjected to lateral forces. Consequently, this affects the distribution of the sensitivity operators.

- The distribution of the sensitivity integrands of the free head pile subjected to bending moments are localized in the upper part than the free head pile subjected to lateral forces.

11. The differences of the sensitivity analysis of δy_t and $\delta \varphi_t$ are the followings:

    - For the sensitivity analysis of $\delta \varphi_t$ for free head pile subjected moment load, the sensitivity operator C_{EI} has the maximum value at the top of the pile, while it has maximum value in the middle part of the pile for the followings: sensitivity analysis of $\delta \varphi_t$ for free head piles subjected to lateral forces, sensitivity analysis of δy_t for free head piles subjected to bending moments or lateral forces separately.

    - The value of sensitivity operators C for the other design variables (c, γ', ε_{50}, and b) of δy_t and $\delta \varphi_t$ only vary in magnitude but have similar characteristics. When the whole soil is in the elastic stage, the magnitude of sensitivity operators $C_{c, \gamma', \varepsilon 50, b}$ of the sensitivity of δy_t are relatively greater than the sensitivity of $\delta \varphi_t$, but when the load increases and the soil consists of various stages they are relatively similar.

12. The distributions of sensitivity operators C, the quantitative assessment of the sensitivities A, and the relative sensitivity factors F for pile groups have the same characteristics as those of single pile, but they have different magnitude.

13. The comparative analysis of the effect of the location of the piles in a group results in the following conclusions:

- The corner pile factor applied to the corner pile in the leading row caused the pile in the corner-leading row has larger value of bending moments and shear forces that the middle-leading row, however it does not affect the displacement of it.
- The piles located in the leading row have the largest bending moment at the primary structure followed by the piles in the 1st trailing row and 2nd trailing row constitutively. However the bending moments at the adjoint structure are ordered oppositely from the largest to smallest as: the piles in the 2nd trailing row, the 1st trailing row, and the leading row.
- The lateral displacement at the top of the piles at the primary structure is similar for each row due to the constraint imposed on the pile cap, but the distributions of the lateral displacements vary for each row. The piles located in the 2nd trailing row have the largest distribution of lateral displacements at the primary and adjoint structures followed by the piles in the 1st trailing row and in the leading row constitutively.
- The value of the sensitivity operator C_{EI} and the quantitative assessment of the sensitivity A_{EI} of each row due to load P1 and P2 (i.e. loads that cause the top surface of the soil being in the elastic and linear softening stages) are relatively similar, but due to the loads increase to P3 (i.e. load that cause the top surface of the soil being in the plastic flow stage) these values at leading row, 1st trailing row, and 2nd trailing row vary from the largest to the smallest.
- The value of $C_{(c,\ \gamma',\ \varepsilon 50,\ b)}$ and $A_{(c,\ \gamma',\ \varepsilon 50,\ b)}$ for each row due to load P3 (i.e. load that cause the top surface of the soil being in the plastic flow stage) are relatively similar, but due to the smaller loads P1 and P2 (i.e. loads that cause the top

surface of the soil being in the elastic and linear softening stages) these values at leading row, 1st trailing row, and 2nd trailing row vary from the largest to the smallest.

- The relative sensitivity factors F are independent to the locations of the piles in a group.

14. From the comparative analysis of the various spacing s of the pile groups, we can conclude the followings:

- The value of f_m for leading row is greater than that for trailing row, and f_m increases with the increase of spacing s.
- The larger the spacing s of the groups of piles, the larger the load required producing the same displacement.
- The greater the spacing s, the greater is the efficiency of the pile groups G_e.
- The efficiency of pile groups G_e from Eq. (2.4) depends on the quantity of load applied, while this value from Eq. (2.5) is constant for different loads. The efficiency of the pile groups G_e from Eq. (2.4) is greater than that from Eq. (2.5).
- The greater the spacing s, the smaller the difference between the shear forces at the top of each pile members V_t located in different rows.
- The unit force of the pile groups due to such a loading Pg_1 for different load quantity calculated by Eq. (7.1) has relatively constant value for different quantity of loadings. When the spacing s increases, the difference between the unit force of the pile group Pg_1 for different pile members decreases.

- The bending moment at the primary structure increases when the spacing increases, but at the adjoint structure it decreases when the spacing increases. It is also shown that the bending moment at the primary structure for group of piles is relatively smaller than that of the single pile, but at adjoint structure it is relatively greater than that of the single pile.

- At both primary and adjoint structure, the displacement due to such a load of the single isolated pile is relatively smaller than that of the groups of piles, and the greater the spacing the smaller is the lateral displacement.

- The difference in the displacement at the primary and the adjoint structures of the groups of piles because of the followings: there is constraint imposed on in the primary structure that the displacement at the top of each pile members is the same, although the constraint is also imposed on the adjoint structures, but the quantities of loads applied at the adjoint structures depend on the locations of the pile members in a group of piles and the spacing s of the groups of piles.

- For pile is subjected to three quantity of loads P1, P2, and P3, where P1 is the loads that cause the top surface of the soil being in the nonlinear elastic stage, P2 is the loads that cause the top surface of the soil being in the linear softening stage,P3 is the loads that cause the top surface of the soil being in the plastic flow stage:

  - The magnitude of sensitivity operators C_{EI} for three cases of loading increases with the increase of spacing and C_{EI} for single pile is greater than that for pile groups.

- Due to the load P1, the sensitivity operators C_c, $C_{\gamma'}$, $C_{\varepsilon 50}$, and C_b decrease when the spacing of the pile groups increases, that also means that those values for a single pile are smaller than those of groups of piles, while when the loads increase to P2 and P3 their differences tend to vanish.

- The undeformed pile portion starts from the lower depth when the spacing decreases.

- In the elastic stage and in the linear softening, the quantitative assessments of the sensitivity A_{EI} due to loads P1 and P2 of the groups of piles differ slightly with different spacing and that value of A_{EI} for groups of piles is larger than that of single pile. When the load increases to P3, A_{EI} of the pile groups in the nonlinear elastic stage is still larger than that of single pile, but those values of A_{EI} in the plastic flow and the nonlinear softening stages of the single pile are larger than those of the groups of piles.

- Due to P1 and P2, the quantitative assessments of sensitivities A_c, $A_{\gamma'}$, $A_{\varepsilon 50}$, and A_b in the nonlinear elastic stage and linear softening stage decrease with the increase of the spacing and those values of pile groups are larger than those of single pile. When the load increases to P3, the quantitative assessments of sensitivities A_c, $A_{\gamma'}$, and A_b vary slightly, but the quantitative assessment of sensitivity $A_{\varepsilon 50}$ decrease with the increase of the spacing. The values of A_c, $A_{\gamma'}$, $A_{\varepsilon 50}$, and A_b for single pile are greater than those for groups of piles.

- The quantitative assessment of sensitivities in the nonlinear elastic stage Ae_i due to three quantity of loadings decreases with the increases of spacing and Due to loads P1 and P2, they can be ordered from the largest to the smallest as the followings: Ae_c, Ae_b, $Ae_{\varepsilon 50}$, $Ae_{\gamma'}$ and Ae_{EI}. Due to load P3, $Ae_{\gamma'}$ vanishes, but this order remains the same.

- Due to P1 there is no quantitative assessment of sensitivities in the linear softening stage As, because no soil is in the linear softening stage. Due to P2, As decreases with the increases of spacing so that As for the pile group is greater than that for single pile. Due to load P3, As relatively constant with the spacing and As for single pile is greater than that of pile group.

- The relative sensitivity factors F_c, F_b, $F_{\varepsilon 50}$, $F_{\gamma'}$ are only varied slightly with respect to the spacing or even they can be considered constant. The relative sensitivity factor F_{EI} due to three loadings (P1, P2, and P3) increases with the increase of the spacing. The order of the relative sensitivity factors F from the largest to the smallest is not depend on the spacing, they can be ordered as: F_c, F_b, $F_{\varepsilon 50}$, $F_{\gamma'}$ and F_{EI}.

15. The results of this study can be applied in the followings: (1) Determination of the most effective parameter to reduce the top lateral displacement, (2) Determination of the effective depth of the soil strength and the pile strength improvement.

9.2 RECOMMENDATION FOR FUTURE RESEARCH

In order to extend the applicability of this research in the design of the laterally loaded pile design, the following research is suggested:

1. The sensitivity analyses for various types of homogeneous soil, layered soil, and the length of the piles in order to construct a design code that is user friendly.
2. To develop the program on sensitivity analysis of the laterally loaded piles for various types soils, types of loadings, and soil layers that is user friendly.
3. The results of this study show that the soil improvement is very important to decrease the lateral displacements, so that it is really useful to determine and construct a soil improvement technique that is effective and applicable for laterally loaded pile structures.

REFERENCES

American Petroleum Institute (API) (1987). "Recommended practice for planning, designing and constructing fixed offshore platforms." API Recommended Practice2A (RP-2A), 17th edn.

Banerjee, K., and Davies, T. G. (1980). "Analysis of some reported case histories of laterally loaded pile groups." *Proc., Conf. on Numer. Meth. in Offshore Piling*, Inst. of Civil Engineers, London, England, 101-108.

Barakat, S.A., Malkawi, A. I. H., and Tahat, R.H. (1999). "Reliability-based optimization of laterally loaded piles." *Structural Safety* Vol. 21, 45-64.

Bogard, D., and Matlock, H. (1983). "Procedures for analysis of laterally loaded pile group in soft clay." *Proc., Conf. on Geotech. Practice in Offshore Engrg.*, ASCE, New York, N.Y., 499-535.

Broms, B.B. (1964a). "Lateral resistance of piles in cohesive soils." *Journal of the Soil Mechanics and Foundations Division*, ASCE 90 (SM2): 27-63.

Broms, B.B. (1964b). "Lateral resistance of piles in cohesionless soils." *Journal of the Soil Mechanics and Foundations Division*, ASCE 90 (SM3): 123-156.

Broms, B.B. (1965). "Design of laterally loaded piles." *Journal of the Soil Mechanics and Foundations Division*, ASCE 91 (SM3):77-99.

Brown, D.A. and Shie, C.F. (1991). "Modification of p-y curves to account for group effects of laterally loaded piles." *Proceedings of Geotechnical Engineering Congress 1991*,ASCE 1 (Geotechnical Special Publication 27): 479-490.

Brown, D.A., Morrison, C., and Reese, L.C. (1988). "Lateral load behavior of pile group in sand." *J. Geotech. Engrg.*, 114(11), 1261-1276.

Brown, D.A., Shie, C.F.and Kumar, M. (1989). "p-y curves for laterally loaded piles derived from three dimensional finite element model." *Proceedings of the III International Symposium, Numerical Models in Geomechanics (NUMOG III)*, Niagara Falls, Canada. New York: Elsevier Applied Sciences: 683-690.

Budkowska, B.B. (1997a). "Sensitivity analysis of short piles embedded in homogeneous soil. Part I (Theoretical formulation)." *Computers and Geotechnics*, 21(2), 87-101.

Budkowska, B.B. (1997b). "Sensitivity analysis of short piles embedded in homogeneous soil. Part II (numerical investigations)." *Computers and Geotechnics*, 21(2), 103-119.

Budkowska, B.B. (1998a). "Investigation of the effect of variable length of piles during bending – sensitivity analysis." *Archives of Civil Engineering*, 44(3), 315-337.

Budkowska, B.B. (1998b). "Application of sensitivity theory to analysis of piles subject to bending and penetrating a homogeneous soil." *Archives of Civil Engineering*, 44(3), 299-314.

Budkowska, B.B. (1999). "Effect of variable location of soil layers on the behaviour of laterally loaded piles - sensitivity analysis." *Computers and Geotechnics,*. Vol. 25, 25-43.

Budkowska, B.B. and Cean, E. (1996). "Comparative sensitivity analysis of laterally loaded piles." *Proceedings of the Sixth – International Offshore and Polar Engineering Conference*, Los Angeles, USA, May 26-31, 1996, Vol.1, pp. 499-505.

Budkowska, B.B. and Priyanto, D.G. (2002a). "Comparative analysis of lateral deformations of short and long piles embedded in nonlinear soft clay – sensitivity analysis." *International Symposium on Lowland Technology, 2002 (ISLT)*, Saga, Japan.

Budkowska, B.B and Priyanto, D.G. (2002b). "Investigation of pile group in soft clay subjected to horizontal loading – sensitivity analysis." *Proceedings of Eighth International Symposium on Numerical Models in Geomechanics – NUMOG VII*, Rome, Italy, 10-12 April 2002, p. 481-486.

Budkowska, B.B., Sekulovic, D., and Saha, C.R. (1999a). "Sensitivity of piles due to variable thickness and location of the soil layer. Part I. Theoretical Formulation." *Archives of Civil Engineering*, 45(3), 427-441.

Budkowska, B.B., Sekulovic, D., and Saha, C.R. (1999b). "Sensitivity of piles due to variable thickness and location of the soil layer. Part II. Numerical Investigations." *Archives of Civil Engineering*, 45(3), 553-570.

Budkowska, B.B. and Suwarno, D. (2002a). "Assessment of horizontal loading of pile group penetrating stiff clay below the water table – sensitivity analysis." *International Symposium on Lowland Technology, 2002 (ISLT)*, Saga, Japan.

Budkowska, B.B. and Suwarno, D. (2002b). "Sensitivity analysis of nonlinear behaviour of laterally loaded piles." *Proceedings of Eighth International Symposium on Numerical Models in Geomechanics – NUMOG VII*, Rome, Italy, 10-12 April 2002, pp. 475-480.

Budkowska, B.B. and Szymczak, C. (1992a). "Application of reanalysis method of laterally loaded piles." *Numerical Models in Geomechanics*, Balkema Rotterdam, pp. 817-825.

Budkowska, B.B. and Szymczak, C. (1992b). "Sensitivity analysis of laterally loaded piles by means of adjoint method." *Computers and Geotechnics*, Vol. 13, 37-49.

Budkowska, B.B. and Szymczak, C. (1993a). "Sensitivity analysis of axially loaded piles." *Arch. Civ. Engng.* XXXIX (1), 93-105.

Budkowska, B.B. and Szymczak, C. (1993b). "Sensitivity analysis of piles undergoing torsion." *Computers and Structures*, 48(5), 827-834.

Budkowska, B.B. and Szymczak, C. (1994a). "Effect of varying length of pile undergoing torsion." *Computers and Structures*, 52(5), 931-938.

Budkowska, B.B. and Szymczak, C. (1994b). "Some problems of sensitivity analysis of axially loaded piles." *Proceedings of the 4th International Offshore and Polar Engineering Conference. Part 1, Apr 10-15, 1994*, p. 554-558.

Budkowska, B.B. and Szymczak, C. (1995a). "On the first variation of extremum values of displacements and internal forces of laterally loaded piles." *Computers and Structures*, 57(2), 303-307.

Budkowska, B.B. and Szymczak, C. (1995b). "The analysis of an axially loaded pile with account for its varying length." *Computers and Structures* 54(6), 1149-1154.

Budkowska, B.B. and Szymczak, C. (1996). "Partially embedded piles subjected to critical buckling load - sensitivity analysis." *Computers and Structures*. 61(1), 193-196.

Budkowska, B.B. and Szymczak, C. (1997). "Initial post-buckling behaviour of piles partially embedded in soil." *Computers and Structures* 62(5), 831-835.

Choi, K. K., and Chang, K. H. (1992). "Shape design sensitivity analysis and optimization of elastic solids", in M.P. Kamat, Ed., *Structural Optimization: Status and Promise, Progress in Astronautics and Aeronautics,* Vol. 150, The American Institute of Aeronautics and Astronautics, Inc., Washington, pp. 569-609.

Das, B.M. (1997). *Principles of geotechnical engineering, 4th edn.* PWS Publishing Company.

Davisson, M.T. (1970). "Lateral load capacity of piles," *Hwy. Res. Rec. No. 333.* Transportation Research Board, National Research Council, Washington, D.C., 104-112.

Davisson, M. T., and Gill, H. L. (1963). "Laterally loaded piles in a layered soil system." *Journal of the Soil Mechanics and Foundation Division,* ASCE, Vol. 89, No.SM3, pp. 63-94.

Dems, K. and Mroz, Z. (1983). "Variational approach by means of adjoint system to structural optimization and sensitivity analysis." *Intern. J. Solid and Structures* 19: 677-692.

Det Norske Veritas. (1977). "Rules for design, construction and inspections of offshore structures." *Veritsveien* 1, 1322 Hovek, Norway.

Duncan, J.M., Evans L.T., Jr. and P.S.K Ooi. (1994). "Laterally load analysis of single piles and drilled shafts." *Journal of the Geotechnical Division*, ASCE 120(5): 1018-1033

Dunnavant, T. W., and O'Neill, M. W. (1986). "Evaluation of design-oriented methods for analysis of vertical pile groups subjected to lateral loads." *Proc., 3rd Int. Conf. on. Numer. Meth. in Offshore Pilling*, Nantes, France, Editions Technip., Paris, France, 303-316.

Evans, L.T. Jr. and J.M. Duncan. (1982). "Simplified analysis of laterally loaded piles." *UCB/GT/82-04*, University of California, Berkeley.

FB-Pier, User Guide and Manual, 2001. Gainesville: FDT and FHA, USA.

Focht, J. A., and Koch, K. J. (1973). " Rational analysis of the lateral performance of offshore pile groups. "*Proc., 5th Offshore Tech. Conf., 2,* Offshore Technology Conference, Dallas, Tex., 701-708.

Haftka, R.T., Gurdal, Z., and Kamat, M. P (1990). *Elements of structural optimization, 2nd Edn.*, Kluwer Academic Publishers, Dordrecht.

Hariharan, M., and Kumarasamy, K. (1982). "Analysis of pile groups subjected to lateral loads. "*Proc. 3rd Int. Conf. on Behavior of Offshore Struct.,* 2, Hemisphere Publishing Corp., Washington, D.C., 383-390.

Haugh, E.J., Choi, K.K., and Komkov, V. (1986). *Design sensitivity analysis of structural systems*. Orlando Academic Press., Inc.

Hetenyi, M. (1946). *Beams on elastic foundation.* Ann Arbor: The University of Michigan Press.

Kleiber, M., Antunez., H., Hien, T. D and Kowalczyk, P. (1997). *Parameter sensitivity in nonlinear mechanics, theory and finite element computations*, John Wiley and Sons.

Kooijman, A.P. (1989). "Comparison of an elastoplastic quasi three-dimensional model for laterally loaded piles with fields tests." *Proceedings of the III International Symposium, Numerical Models in Geomechanics (NUMOG III)*, Niagara Falls, Canada, Elsevier Applied Science: New York: 675-682.

Matlock, H. (1970). "Correlations for design of laterally loaded piles in soft clay." *Offshore Technology Conference,* Paper No. OTC 1204, Houston.

Matlock, H. and Reese L.C. (1960). "Generalizedsolutions for laterally loaded piles." *Journal of the Soil Mechanics and Foundations Division,* ASCE, SM5.

McClelland, B. and Focht, J.A. Jr. (1958). "Soil modulus for laterally loaded piles." *Transactions*, ASCE 123: 1049-1086.

Mokwa, R.L and Duncan, J.M. (2001). "Laterally Loaded Pile Group Effect and P-Y Multipliers." *Foundations and Ground Improvement (Proceedings of specialty conference: June 9-13, 2001)*, Blacksburg, Virginia: 728-742.

Mota Soares, C. A., and Leal, R. P. (1992). "Mixed elements in shape sensitivity analysis of structures based on local criteria." in M.P. Kamat, Ed., *Structural Optimization: Status and Promise, Progress in Astronautics and Aeronautics,* Vol. 150, The American Institute of Aeronautics and Astronautics, Inc., Washington, pp. 549-567.

Nogami, T., and Paulson, S.K. (1985). "Transfer matrix approach for nonlinear pile group response analysis." *Int. J. Numer. and Analytical Methods in Geomechanics*, (9), 289-316.

Ooi, P. S. K., and Duncan, J. M. (1994). "Lateral load analysis of groups of piles and drilled shafts." *Journal of Geotechnical Engineering,* Vol. 120, No. 6: 1034-1050.

Paulos, H.G. (1971). "Behaviour of laterally loaded piles: I-single piles, and II-pile groups." *J.SMFD. ASCE97.* SM5 711-731. 733-751.

Paulos, H.G. and Davis, E.H. (1980). *Pile foundation analysis and design.* John Wiley and Sons, New York.

Paulos, H.G. and Hull, T.S. (1989). "The role of analytical mechanics in foundation engineering." *Foundation Engineering, Current Principals and Practices*, ASCE2: 1578-1606.

Prakash, S. (1962). "Behaviour of pile groups subjected to lateral loads," PhD thesis, University of Illinois, Urbana, III.

Purcell, E.D. and Varberg, D. (1987). *Calculus and analytic geometry, fifth edition.* Prentice-Hall, New Jersey.

Randolph, M.F. (1981). "The response of flexible piles to lateral loads." *Geotechnique* 31(2): 247-259.

Reèse, L.C. and Matlock, H. (1956). "Nondimesional solutions for laterally loaded piles with soil modulus assumed proportional to depth." *Proceedings of the VIII Texas Conference on Soil Mechanics and Foundation Engineering*, University of Texas, Austin.

Reese, L.C. and Van Impe, W.F. (2001). *Single Pile and Pile Groups Under Lateral Loading.* A.A. Balkema, Rotterdam, Brookfield.

Reese, L.C. (1984). *Handbook on design of piles and drilled shafts under lateral load.* FHWA-IP-84-11, 360 pp. US Department of Transportation, Federal Highway Administration.

Saltelli, A., Chan, K., Scott, E. M. (2000). *Sensitivity analysis.* John Wiley and Sons, Ltd.

Shibata, T., Yashima, A., Kimura, M., and Fukada,H. (1988). "Analysis of laterally loaded piles by quasy-three dimensional finite element method." *Proc., 6th Int. Conf. on Numer. Meth. in Geomech.*, A. A. Balkema, Rotterdam, The Netherlands, 2, 1051-1058.

Terzaghi, K. (1955). "Evaluation of coefficient subgrade modulus." *Geotechnique*, V: 297-326.

Valliappan, S., Tandjiria, V., and Khalili, N. (1997). "Design sensitivity and constraint approximation methods for optimization in non-linear analysis." *Communications in numerical methods in Engineering.* Vol. 13, 999-1008.

Valliappan, S., Tandjiria, V., and Khalili, N. (1999). "Design of raft-pile foundation using combined optimization and finite element approach." *Int. J. Numer. Anal. Meth. Geomech*, Vol. 23, 1043-1065.

Wang, S.T and Reese, L.C.(1993). *COM624P - Laterally loaded pile analysis program for the microcomputer, version 2.0.* U.S Department of Transportation, Federal Highway Administration Report No.FHWA-SA-91-048.

Washizu, K. (1976). *Variational methods in elasticity and plasticity.* Oxford: Pergamon Press.

APPENDIX A:

Derivation of formulas of sensitivity analysis of laterally pile embedded in soft clay located below the water table subjected to cyclic loading

APPENDIX A:

Derivation of formulas of sensitivity analysis of laterally pile embedded in soft clay located below the water table subjected to cyclic loading

The characteristic shapes of the p-y curves for soft clay below the water table subjected cyclic loading is shown in Fig. (A.1) (Matlock, 1970).

1. Distribution of p_u along the depth.

The soil strength parameters are not explicitly present in the constitutive model but are present by means of the ultimate soil resistance p_u. The p_u varies in linear fashion along the depth of pile. The distribution of p_u is shown in Fig. A.1b.

For $x < x_r$

$$p_u = \left(3 + \frac{\gamma'}{c}x + \frac{J}{b}x\right)cb \qquad \text{(A.1)}$$

The second term of Eq. (A.1) is linearly increasing due to only the effect of gravity or the weight of the soil, and the next term due to the effect of cohesion of soil.

For $x \geq x_r$

$$p_u = 9cb \qquad \text{(A.2)}$$

2. Discussion on p-y curve

For x = 0;

$$p_u = 3cb \tag{A.3}$$

and

$$p = p_u \cdot \tfrac{1}{2}\left(\frac{y}{y_{50}}\right)^{\frac{1}{3}} \tag{A.4}$$

Thus, for x = 0 p is soil reaction which is the weakest for the same deformations and the value of p_u is the smallest along the depth. Since y_{50} is a constant, $(y/y_{50})^{1/3}$ has the same value.

Then, we observe increase in the p_u with depth. It is associated with two factors:

- The first is connected with the effective unit weight ($\gamma' b \cdot x$);
- The second is attributed to linear increase in cohesion according to $Jcx \equiv 0.5cx$

For the values of A and B are represented by Eqs. (A.5a & A.5b).

$$A = (\gamma' b) \tag{A.5a}$$

$$B = 0.5c, \tag{A.5b}$$

The comparison of A and B reveals that B is independent of width and depends only in cohesion. A shows that, it depends on b (width). Thus, for large value of b, the effect of $\gamma' \cdot b$ can be larger than c.

Based on the continuity of p_u, x_r is given as:

$$x_r = \frac{6cb}{(\gamma' b + Jc)} \tag{A.6}$$

The p_u increases from $3cb$ at x=0 to the value of $9cb$ at $x = x_r$. However, this increase is due to the contribution of $\gamma' b$ and $0.5c$. From $x \geq x_r$ to reach $p_u = 9cb$ caused by the term Jcx alone, therefore, the term $\gamma' bx$ is added. The analysis of p_u shows, that with depth, for the same value (y/y_{50}), p increases as x increases.

3. The behaviour of p/p_u as a function of (y/y_{50})

Based on the Fig. (A.2), we can determine the behaviour of p/p_u as a function of y/y_{50}.

3.1 For $3<(y/y_{50})< 15$; and arbitrary $x \leq x_r$

From the similarity of the triangles CAB and EDB (Fig. A.2),

$$\frac{\left(\frac{\tilde{p}}{p_u}\right)}{15-\left(\frac{y}{y_{50}}\right)} = \frac{0.72-0.72\frac{x}{x_r}}{(15-3)} \tag{A.7}$$

$$\left(\frac{\tilde{p}}{p_u}\right) = \frac{1}{12}\cdot 0.72\left(1-\frac{x}{x_r}\right)\left(15-\left(\frac{\tilde{y}}{y_{50}}\right)\right)$$

$$= 0.06\left(1-\frac{x}{x_r}\right)\left(15-\left(\frac{\tilde{y}}{y_{50}}\right)\right) \tag{A.8}$$

$$\left(\frac{\tilde{p}}{p_u}\right)_{tot} = \left(\frac{\tilde{p}}{p_u}\right) + 0.72\left(\frac{x}{x_r}\right) \tag{A.9}$$

$$\left(\frac{p}{p_u}\right)_{tot} = 0.06\left(1-\frac{x}{x_r}\right)\left(15-\left(\frac{\tilde{y}}{y_{50}}\right)\right)+0.72\frac{x}{x_r}$$
$$=\left(0.9-0.18\frac{x}{x_r}\right)-0.06\left(\frac{\tilde{y}}{y_{50}}\right)\left(1-\frac{x}{x_r}\right) \quad \text{(A.10)}$$

The bending moment of the pile represents in term of the deformation of the pile,

$$M = -EIy'' \quad \text{(A.11)}$$

the first variation of Eq. (A.11) is given as:

$$\delta M = -EI\delta y'' \quad \text{(A.12)}$$

3.2 Soil reaction for $x \leq x_r$ and $y \leq 3y_{50}$

$$y_{50} = 2.5\ \varepsilon_{50}\ b \quad \text{(A.13)}$$

$$p_u = \left(3+\frac{\gamma'}{c}x+\frac{J}{b}x\right)cb \quad \text{(A.14)}$$

$$\frac{p}{p_u} = 0.5\left(\frac{y}{y_{50}}\right)^{1/3} \quad \text{(A.15)}$$

$$p = 0.5p_u\left(\frac{y}{y_{50}}\right)^{1/3} \quad \text{(A.16)}$$

For $p = p(y/y_{50})$, first variation of p is given as:

$$\delta p = 0.5p_u \cdot \frac{1}{3}\left(\frac{y}{y_{50}}\right)^{-2/3} \cdot \frac{1}{y_{50}}\delta y$$
$$= \frac{1}{6}p_u \cdot \left(y^2 y_{50}\right)^{-1/3}\delta y \quad \text{(A.17)}$$

3.3 Soil reaction for $x \le x_r$; $3 < \left(\frac{\tilde{y}}{y_{50}}\right) < 15$

$$\left(\frac{p}{p_u}\right)_{tot} = \left(0.9 - 0.18\frac{x}{x_r}\right) - 0.06\left(\frac{\tilde{y}}{y_{50}}\right)\left(1 - \frac{x}{x_r}\right) \tag{A.18}$$

$$p_u = \left(3 + \frac{\gamma'}{c}x + \frac{J}{b}x\right)cb \tag{A.19}$$

$$p = \left(3 + \frac{\gamma'}{c}x + \frac{J}{b}x\right)cb\left\{\left(0.9 - 0.18\frac{x}{x_r}\right) - 0.06\left(\frac{\tilde{y}}{y_{50}}\right)\left(1 - \frac{x}{x_r}\right)\right\} \tag{A.20}$$

For $p = p(\tilde{y})$, first variation of p is given as:

$$\begin{aligned}\delta p &= \left(3 + \frac{\gamma'}{c}x + \frac{J}{b}x\right)cb(-0.06)\frac{1}{y_{50}}\left(1 - \frac{x}{x_r}\right)\delta y \\ &= \frac{-0.06}{y_{50}}(3cb + \gamma' bx + Jcx)\left(1 - \frac{x}{x_r}\right)\delta y\end{aligned} \tag{A.21}$$

3.4 Soil reaction for $x \ge x_r$; $y/y_{50} \le 3$

$$p_u = 9cb \tag{A.22}$$

$$\frac{p}{p_u} = 0.5\left(\frac{y}{y_{50}}\right)^{\frac{1}{3}} \tag{A.23}$$

$$p = 4.5cb\left(\frac{y}{y_{50}}\right)^{\frac{1}{3}} \tag{A.24}$$

For $p = p(y)$, first variation of p is given as:

$$\delta p = 4.5 \cdot \tfrac{1}{3} \cdot cb \left(\frac{y}{y_{50}}\right)^{-\frac{2}{3}} \cdot \frac{1}{y_{50}} \delta y$$

$$= 1.5 cb \frac{1}{\left(\frac{y}{y_{50}}\right)^{\frac{2}{3}}} \cdot \frac{1}{y_{50}} \delta y$$

$$= 1.5 cb \frac{1}{\sqrt[3]{\left(\frac{y}{y_{50}}\right)^{2} \cdot y_{50}^{3}}} \delta y$$

$$= 1.5 cb \frac{1}{\sqrt[3]{y^2 y_{50}}} \delta y$$

$$= 1.5 cb \left(y^2 y_{50}\right)^{-\frac{1}{3}} \delta y \qquad \text{(A.25)}$$

3.5 Soil reaction for $x \geq x_r$ and $y/y_{50} > 3$

$$p_u = 9cb \qquad \text{(A.26)}$$

$$\frac{p}{p_u} = 0.72 \qquad \text{(A.27)}$$

$$p = 0.72 \cdot 9cb$$
$$= 6.48cb \qquad \text{(A.28)}$$

p is independent of y, thus $\delta p = 0$, therefore the case for $x \geq x_r$ and $\left(\frac{y}{y_{50}}\right)$>3 is not analyzed.

4. Sensitivity analysis of the top lateral displacement of laterally loaded piles embedded in nonlinear medium

The models of adjoint and primary structures are shown in Fig. A.3. Using adjoint structure method, the δy_{Top}^{force} can be determined using the following relationship.

$$\overline{1}\delta y_{Top}^{force} = -\int_0^l M_a \delta y'' dx + \int_0^{x_r} p_a \delta y dx + \int_{x_r}^l p_a \delta y dx \tag{A.29}$$

where

M and p are dependent on the state variables vector and the design variables vector $\bar{s}$.

$\bar{s} = (s_1, s_2, s_3, s_4, \ldots)$

M_a= distribution of bending moment in adjoint structure subjected to unit load,

p_a = distribution of soil reactions in the adjoint structure subject to unit force.

$$\bar{s} = EI, c, \gamma', \varepsilon_{50}, b \tag{A.30}$$

$$\begin{aligned}\delta M &= M_{,y'} \delta y'' + M_{,\bar{s}} \delta \bar{s} \\ &= -EI\delta y'' + M_{,\bar{s}} \delta \bar{s}\end{aligned} \tag{A.31}$$

$$\begin{aligned}\delta p &= p_{,y} \delta y + p_{,\bar{s}} \delta \bar{s} \\ &= p_u \cdot \tfrac{1}{6}\left(y^2 y_{50}\right)^{-\frac{1}{3}} \delta y + p_{,\bar{s}} \delta \bar{s}\end{aligned} \tag{A.32}$$

The statically admissible variations of the displacement field $\delta y''$ and δy are imposed on the primary structure. The generated variations of the internal forces (given by Eqs. (34, 35)) i.e. δM and δp are equal to zero, since the primary structure is subjected to constant load, thus:

$$\delta M = 0 \tag{A.33}$$

and

$$\delta p = 0 \tag{A.34}$$

The variations $\delta y''$ and δy required by Eq. (A.29) can be determined from Eqs. (A.31) and (A.32) employing the constraints (A.33) and (A.34), thus:

$$\delta y'' = \frac{1}{EI} M_{,\bar{s}}\, \delta\bar{s} \tag{A.35}$$

$$p_u \cdot \tfrac{1}{6}\left(y^2 y_{50}\right)^{-1/3} \delta y = -p_{,\bar{s}}\, \delta\bar{s} \tag{A.36}$$

$$\delta y = -\frac{6\left(y^2 y_{50}\right)^{1/3}}{p_u} p_{,\bar{s}}\, \delta\bar{s} \tag{A.37}$$

Eq. (A.37) is valid for $y \leq 3y_{50}$ in the range $x \leq x_r$. Substitution of Eqs.(A.35) and (A.37) into Eq. (A.29) gives:

$$\bar{1}\delta y_{top}^{force} = -\underbrace{\int_0^l M_a \frac{1}{EI} M_{,\bar{s}}\,\delta\bar{s}\,dx}_{\text{I}} - \underbrace{\int_0^{x_r} p_a \frac{6\left(y^2 y_{50}\right)^{1/3}}{p_u} p_{,\bar{s}}\,\delta\bar{s}\,dx}_{\text{II}} - \underbrace{\int_{x_r}^l p_a \frac{6\left(y^2 y_{50}\right)^{1/3}}{p_u} p_{,\bar{s}}\,\delta\bar{s}\,dx}_{\text{III}} \tag{A.38}$$

In Eqs. (A.35)~(A.38), M and p are connected with the primary structure. For $3y_{50} < y < 15y_{50}$ in the range of $x < x_r$ (note: for $x=x_r$ produces ∞), from Eq. (A.21) combined with Eqs. (A.32) and (A.34), we have:

$$-0.06\frac{1}{y_{50}} p_u \left(1-\frac{x}{x_r}\right)\delta y = -p_{,\bar{s}}\,\delta\bar{s} \tag{A.39}$$

$$\delta y = \frac{y_{50}}{0.06 p_u \left(1-\frac{x}{x_r}\right)} p_{,\bar{s}}\,\delta\bar{s} \tag{A.40}$$

where

$$p_u = \left[3+\frac{\gamma'}{c}x+\frac{J}{b}x\right]cb \tag{A.41}$$

At the same time if $y > 3y_{50}$ for $x \geq x_r$ the soil already flows and automatically the third integral in Eq. (A.38) does not exist. But, if for $x < x_r$; $3y_{50} < y < 15y_{50}$ the third integral exists, it does not mean that below x_r it exists, i.e. for $x > x_r$, $y \geq 3y_{50}$, it is very probable that at the same time $3y_{50} < y < 15y_{50}$ for $x \geq x_r$, that means the prevention of the third integral in Eq. (A.38).

Thus for $3y_{50} < y < 15y_{50}$ in $x \le x_r$ and for $y < 3y_{50}$ in the range of $x \ge x_r$, Eq. (A.38) is modified as follows:

$$\bar{1}\delta y_{top}^{force} = -\int_0^l M_a \frac{1}{EI} M_{,\bar{s}}\, \delta\bar{s}\, dx + \int_0^{x_r} p_a \frac{y_{50}}{0.06 p_u \left(1 - \frac{x}{x_r}\right)} p_{,\bar{s}}\, \delta\bar{s}\, dx - \int_{x_r}^l p_a \frac{6\left(y^2 y_{50}\right)^{1/3}}{p_u} p_{,\bar{s}}\, \delta\bar{s}\, dx \tag{A.42}$$

The value of p_u in second integral of Eq. (A.42) is given as:

$$p_u = \left[3 + \frac{\gamma'}{c}x + \frac{J}{b}x\right]cb \tag{A.43}$$

while in the third integral, p_u is given as :

$$p_u = 9cb \tag{A.44}$$

4.1 First integral of Eq. (42)

From following values:

$$\bar{s} = \left(EI, c, \gamma', \varepsilon_{50}, b\right) \tag{A.45}$$

$$M = -EIy'' \tag{A.46}$$

$$\delta EI \tag{A.47}$$

$$M_{,\bar{s}} = -y'' \tag{A.48}$$

$$M_{,\bar{s}}\,\delta\bar{s} = -y''\delta EI \tag{A.49}$$

$$\frac{M_a}{EI} = -y_a'' \tag{A.50}$$

So that the first integral of Eq. (A.42) is given as:

$$-\int_0^l M_a \frac{1}{EI} M_{,\bar{s}}\,\delta\bar{s}\,dx = -\int_0^l y_a'' y''\delta EI\,dx \tag{A.51}$$

4.2 Second integral in Eq. (42)

4.2.1 For $x \le x_r$ *and* $y \le 3y_{50}$

$$p_a = p_u \tfrac{1}{2}\left(\frac{y_a}{y_{50}}\right)^{1/3} \tag{A.52}$$

$$p_a \frac{6\left(y^2 y_{50}\right)^{1/3}}{p_u} = 3\left(y_a y^2\right)^{1/3} \tag{A.53}$$

$$\begin{aligned} p &= p_u \tfrac{1}{2}\left(\frac{y}{y_{50}}\right)^{1/3} \\ &= 0.5\left[3 + \frac{\gamma'}{c}x + \frac{J}{b}x\right]cb\left(\frac{y}{y_{50}}\right)^{1/3} \\ &= \left[(3b + Jx)c + \gamma' bx\right]\tfrac{1}{2}\left(\frac{y}{y_{50}}\right)^{1/3} \end{aligned} \tag{A.54}$$

$$p_{,\bar{s}}\,\delta\bar{s} = p_{,c}\,\delta c + p_{,\gamma'}\delta\gamma' + p_{,\varepsilon_{50}}\,\delta\varepsilon_{50} + p_{,b}\,\delta b$$

$$= \tfrac{1}{2}(3b + Jx)\left(\frac{y}{y_{50}}\right)^{1/3}\delta c + \tfrac{1}{2}(bx)\left(\frac{y}{y_{50}}\right)^{1/3}\delta\gamma'$$

$$-\tfrac{1}{6}\left[(3b + Jx)c + \gamma' bx\right]\left(\frac{y}{y_{50}}\right)^{1/3} * \left(\frac{1}{\varepsilon_{50}}\right)\delta\varepsilon_{50}$$

$$+\left(c + \tfrac{1}{3}\gamma' x - \frac{Jxc}{6b}\right)\left(\frac{y}{y_{50}}\right)^{1/3}\delta b \qquad \text{(A.55)}$$

Thus:

$$\int_0^{x_r} p_a \frac{6\left(y^2 y_{50}\right)^{1/3}}{p_u} p_{,\bar{s}}\,\delta\bar{s}\,dx$$

$$= \int_0^{x_r} 3\left(y_a y^2\right)^{1/3} \cdot \tfrac{1}{2}(3b + Jx)\left(\frac{y}{y_{50}}\right)^{1/3}\delta c\,dx \qquad \text{(A.56a)}$$

$$+ \int_0^{x_r} 3\left(y_a y^2\right)^{1/3} \cdot \tfrac{1}{2}(bx)\left(\frac{y}{y_{50}}\right)^{1/3}\delta\gamma'\,dx \qquad \text{(A.56b)}$$

$$- \int_0^{x_r} 3\left(y_a y^2\right)^{1/3} \cdot \tfrac{1}{6}\left[(3b + Jx)c + \gamma' bx\right]\left(\frac{y}{y_{50}}\right)^{1/3}\left(\frac{1}{\varepsilon_{50}}\right)\delta\varepsilon_{50}\,dx \qquad \text{(A.56c)}$$

$$+ \int_0^{x_r} 3\left(y_a y^2\right)^{1/3}\left(c + \tfrac{1}{3}\gamma' x - \frac{Jxc}{6b}\right)\left(\frac{y}{y_{50}}\right)^{\frac{1}{3}}\delta b\,dx \qquad \text{(A.56d)}$$

4.2.2 For $x < x_r$ and $3y_{50} \le y \le 15y_{50}$

$$p_a = p_u\left[\left(0.9 - 0.18\frac{x}{x_r}\right) - 0.06\left(\frac{y_a}{y_{50}}\right)\left(1 - \frac{x}{x_r}\right)\right] \qquad \text{(A.57)}$$

From Eq. (A.41)

$$\delta y = \frac{y_{50}}{0.06 p_u \left(1 - \frac{x}{x_r}\right)} p_{,\bar{s}}\, \delta \bar{s} \tag{A.58}$$

$$\begin{aligned} p_a \delta y &= p_u \frac{\left[\left(0.9 - 0.18\frac{x}{x_r}\right) - 0.06\left(\frac{y_a}{y_{50}}\right)\left(1 - \frac{x}{x_r}\right)\right] y_{50}}{0.06 p_u \left(1 - \frac{x}{x_r}\right)} p_{,\bar{s}}\, \delta \bar{s} \\ &= y_{50}\left[\frac{0.18}{0.06} \cdot \frac{\left(5 - \frac{x}{x_r}\right)}{\left(1 - \frac{x}{x_r}\right)} - \frac{y_a}{y_{50}}\right] p_{,\bar{s}}\, \delta \bar{s} \\ &= \left[3 y_{50} \frac{5x_r - x}{x_r - x} - y_a\right] p_{,\bar{s}}\, \delta \bar{s} \end{aligned} \tag{A.59}$$

$$\begin{aligned} p &= \left[3 + \frac{\gamma'}{c} x - \frac{J}{b} x\right] cb \left[\left(0.9 - 0.18\frac{x}{x_r}\right) - 0.06\left(\frac{y}{y_{50}}\right)\left(1 - \frac{x}{x_r}\right)\right] \\ &= \left[3cb + \gamma' bx + Jcx\right]\left\{\left(0.9 - 0.18\frac{x}{x_r}\right) - 0.06\left(\frac{y}{y_{50}}\right)\left(1 - \frac{x}{x_r}\right)\right\} \end{aligned} \tag{A.60}$$

$$p_{,c} = (3b + Jx)\left\{\left(0.9 - 0.18\frac{x}{x_r}\right) - 0.06\left(\frac{y}{y_{50}}\right)\left(1 - \frac{x}{x_r}\right)\right\} \tag{A.61}$$

$$p_{,\gamma'} = (bx)\left\{\left(0.9 - 0.18\frac{x}{x_r}\right) - 0.06\left(\frac{y}{y_{50}}\right)\left(1 - \frac{x}{x_r}\right)\right\} \tag{A.62}$$

$$y_{50} = 2.5\varepsilon_{50} b \tag{A.63}$$

$$p_{,\varepsilon_{50}} = [3cb + \gamma' bx + Jcx]\left\{\left(-0.06\left(\frac{y}{2.5b}\right)(-1)(\varepsilon_{50})^{-2}\right)\cdot\left(1-\frac{x}{x_r}\right)\right\}$$
$$= [3cb + \gamma' bx + Jcx]\cdot 0.06\left(\frac{y}{y_{50}}\right)\cdot\frac{1}{\varepsilon_{50}}\left(1-\frac{x}{x_r}\right) \quad \text{(A.64)}$$

$$p_{,b}\,\delta b = \left\{\begin{array}{l}[3c+\gamma' x]\left[\left(0.9-0.18\frac{x}{x_r}\right)-0.06\left(\frac{y}{y_{50}}\right)\cdot\left(1-\frac{x}{x_r}\right)\right] \\ +0.06\left[3c+\gamma' x+\frac{Jxc}{b}\right]\left(\frac{y}{y_{50}}\right)\left(1-\frac{x}{x_r}\right)\end{array}\right\}\delta b \quad \text{(A.65)}$$

$$\int_0^{x_r} p_a\,\delta y\,p_{,\bar{s}}\,\delta s\,dx =$$

$$= \int_0^{x_r}\left(3y_{50}\frac{5x_r-x}{x_r-x}-y_a\right)(3b+Jx)\left\{\left(0.9-0.18\frac{x}{x_r}\right)-0.06\left(\frac{y}{y_{50}}\right)\left(1-\frac{x}{x_r}\right)\right\}\delta c\,dx \quad \text{(A.66a)}$$

$$+\int_0^{x_r}\left(3y_{50}\frac{5x_r-x}{x_r-x}-y_a\right)(bx)\left\{\left(0.9-0.18\frac{x}{x_r}\right)-0.06\left(\frac{y}{y_{50}}\right)\left(1-\frac{x}{x_r}\right)\right\}\delta\gamma' dx \quad \text{(A.66b)}$$

$$+\int_0^{x_r}\left(3y_{50}\frac{5x_r-x}{x_r-x}-y_a\right)\left(\frac{1}{\varepsilon_{50}}\right)\left(1-\frac{x}{x_r}\right)\left(\frac{y}{y_{50}}\right)\cdot 0.06[3cb+\gamma' bx+Jcx]\delta\varepsilon_{50}\,dx \quad \text{(A.66c)}$$

$$+\int_0^{x_r}\left(3y_{50}\frac{5x_r-x}{x_r-x}-y_a\right)\left\{\begin{array}{l}[3c+\gamma' x]\left[\left(0.9-0.18\frac{x}{x_r}\right)-0.06\left(\frac{y}{y_{50}}\right)\left(1-\frac{x}{x_r}\right)\right] \\ +0.06\left[3c+\gamma' x+\frac{Jxc}{b}\right]\left(\frac{y}{y_{50}}\right)\left(1-\frac{x}{x_r}\right)\end{array}\right\}\delta b\,dx \quad \text{(A.66d)}$$

4.3 Third integral in Eq. (42)

$$\int_{x_r}^{l} p_a\frac{6\left(y^2 y_{50}\right)^{\frac{1}{\beta}}}{p_u}p_{,\bar{s}}\,\delta\bar{s}\,dx \quad \text{(A.67)}$$

Term (A.67) is derived for $x > x_r$ and $y < 3y_{50}$, then:

$$p_u = 9cb \tag{A.68}$$

$$\frac{p_a}{p_u} = \frac{1}{2}\left(\frac{y_a}{y_{50}}\right)^{\frac{1}{3}} \tag{A.69}$$

$$p_a = \frac{p_u}{2}\left(\frac{y_a}{y_{50}}\right)^{\frac{1}{3}} \tag{A.70}$$

$$p_a \cdot \frac{6\left(y^2 y_{50}\right)^{\frac{1}{3}}}{p_u} = \frac{p_u}{2}\left(\frac{y_a}{y_{50}}\right)^{\frac{1}{3}} \cdot \frac{6\left(y^2 y_{50}\right)^{\frac{1}{3}}}{p_u} = 3\left(y_a y^2\right)^{\frac{1}{3}} \tag{A.71}$$

$$\{\bar{s}\}^T = \{c, \varepsilon_{50}, b\} \tag{A.72}$$

$$p_{,\bar{s}}\, \delta\bar{s} = p_{,c}\, \delta c + p_{,\varepsilon_{50}}\, \delta\varepsilon_{50} \tag{A.73}$$

$$\frac{p}{p_u} = \frac{1}{2}\left(\frac{y}{y_{50}}\right)^{\frac{1}{3}} \tag{A.74}$$

$$p = 9cb \cdot \frac{1}{2}\left(\frac{y}{y_{50}}\right)^{\frac{1}{3}} = 4.5cb\left(\frac{y}{y_{50}}\right)^{\frac{1}{3}} \tag{A.75}$$

p is independent of γ', so that:

$$p_{,\gamma'}\, \delta\gamma' = 0 \tag{A.77}$$

$$p_{,c}\, \delta c = 4.5b\left(\frac{y}{y_{50}}\right)^{\frac{1}{3}} \delta c \tag{A.78}$$

$$y_{50} = 2.5\varepsilon_{50} b \tag{A.79}$$

$$p = 4.5cb\left(\frac{y}{2.5\varepsilon_{50} b}\right)^{\frac{1}{3}} \tag{A.80}$$

$$\begin{aligned} p_{,\varepsilon_{50}}\,\delta\varepsilon_{50} &= 4.5cb\cdot\tfrac{1}{3}\left(\frac{y}{2.5\varepsilon_{50} b}\right)^{-\frac{2}{3}}(-1)\frac{y}{2.5b}\varepsilon_{50}{}^{-2}\delta\varepsilon_{50} \\ &= -1.5cb\left(\frac{y}{y_{50}}\right)^{\frac{1}{3}}\frac{1}{\varepsilon_{50}}\delta\varepsilon_{50} \end{aligned} \tag{A.81}$$

$$p_{,b}\,\delta b = 3c\left(\frac{y}{y_{50}}\right)^{\frac{1}{3}}\delta b \tag{A.82}$$

Combining Eq.(A.67) with Eqs. (A.71), (A.77), (A.78), (A.81), and (A.82), we arrive at:

$$\begin{aligned} &\int_{x_r}^{l} p_a \frac{6\left(y^2 y_{50}\right)^{\frac{1}{3}}}{p_u} p_{,\bar{s}}\,\delta\bar{s}\,dx \\ &= \int_{x_r}^{l} 13.5\left(\frac{y_a}{y_{50}}\right)^{\frac{1}{3}} yb\,\delta c\,dx \\ &- \int_{x_r}^{l} 4.5\left(\frac{y_a}{y_{50}}\right) ycb\left(\frac{1}{\varepsilon_{50}}\right)\delta\varepsilon_{50}\,dx \\ &+ \int_{x_r}^{l} 9\left(\frac{y_a}{y_{50}}\right)^{\frac{1}{3}} yc\delta b\,dx \end{aligned} \tag{A.83}$$

Finally Eq.(A.38) can be written as:

For $y < 3y_{50}$ *and* $0 \le x \le l$

$$1\delta y_{top}^{force} = -\int_0^l y_a'' \, y'' \delta EI \, dx \tag{A.84a}$$

$$-\int_0^{x_r} 1.5\left(\frac{y_a}{y_{50}}\right)^{\frac{1}{3}} y(3b + Jx)\delta c \, dx \tag{A.84b}$$

$$-\int_{x_r}^{l} 13.5\left(\frac{y_a}{y_{50}}\right)^{\frac{1}{3}} yb \, \delta c dx \tag{A.84c}$$

$$-\int_0^{x_r} 1.5\left(\frac{y_a}{y_{50}}\right)^{\frac{1}{3}} y(bx)\delta\gamma' dx \tag{A.84d}$$

$$+\int_0^{x_r} 0.5\left(\frac{y_a}{y_{50}}\right)^{\frac{1}{3}} y\left[(3b + Jx)c + \gamma' bx\right]\cdot\left(\frac{1}{\varepsilon_{50}}\right)\delta\varepsilon_{50} \, dx \tag{A.84e}$$

$$+\int_{x_r}^{l} 4.5\left(\frac{y_a}{y_{50}}\right) ycb\left(\frac{1}{\varepsilon_{50}}\right)\delta\varepsilon_{50} \, dx \tag{A.84f}$$

$$+\int_0^{x_r} 3\left(\frac{y_a}{y_{50}}\right)^{\frac{1}{3}} y\left(c + \tfrac{1}{3}\gamma' x - \frac{Jxc}{6}\right)\delta b dx \tag{A.84g}$$

$$+\int_0^{x_r} 9\left(\frac{y_a}{y_{50}}\right)^{\frac{1}{3}} yc\delta b dx \tag{A.84h}$$

For $3y_{50} \le y \le 15y_{50}$ in the range of $0 \le x \le l$, Eq. (A.38) has the following form:

$$1\delta y_{top}^{force} = -\int_0^l y_a'' \, y'' \delta EI \, dx$$

$$-\int_0^{x_r}\left(3y_{50}\frac{5x_r - x}{x_r - x} - y_a\right)(3b + Jx)\left\{\left(0.9 - 0.18\frac{x}{x_r}\right) - 0.06\left(\frac{y}{y_{50}}\right)\left(1 - \frac{x}{x_r}\right)\right\}\delta c dx \tag{A.85a}$$

$$-\int_{x_r}^{l} 13.5\left(\frac{y_a}{y_{50}}\right)^{\frac{1}{3}} yb\,\delta c\,dx \tag{A.85b}$$

$$-\int_{0}^{x_r}\left(3y_{50}\frac{5x_r-x}{x_r-x}-y_a\right)(bx)\left\{\left(0.9-0.18\frac{x}{x_r}\right)-0.06\left(\frac{y}{y_{50}}\right)\left(1-\frac{x}{x_r}\right)\right\}\delta\gamma'\,dx \tag{A.85c}$$

$$-\int_{0}^{x_r}\left(3y_{50}\frac{5x_r-x}{x_r-x}-y_a\right)\frac{1}{\varepsilon_{50}}\left(1-\frac{x}{x_r}\right)\left(\frac{y}{y_{50}}\right)\cdot 0.06\left[3cb+\gamma' bx+Jcx\right]\delta\varepsilon_{50}\,dx \tag{A.85d}$$

$$+\int_{x_r}^{l} 4.5\left(\frac{y_a}{y_{50}}\right)^{\frac{1}{3}} ycb\frac{1}{\varepsilon_{50}}\delta\varepsilon_{50}\,dx \tag{A.85e}$$

$$-\int_{0}^{x_r}\left(3y_{50}\frac{5x_r-x}{x_r-x}-y_a\right)\left\{\begin{array}{l}\left[3c+\gamma' x\right]\left[\left(0.9-0.18\frac{x}{x_r}\right)-0.06\left(\frac{y}{y_{50}}\right)\left(1-\frac{x}{x_r}\right)\right]\\ +0.06\left[3c+\gamma' x+\frac{Jxc}{b}\right]\left(\frac{y}{y_{50}}\right)\left(1-\frac{x}{x_r}\right)\end{array}\right\}\delta b\,dx \tag{A.85f}$$

$$-\int_{x_r}^{l} 9\left(\frac{y_a}{y_{50}}\right)^{\frac{1}{3}} yc\,\delta b\,dx \tag{A.85g}$$

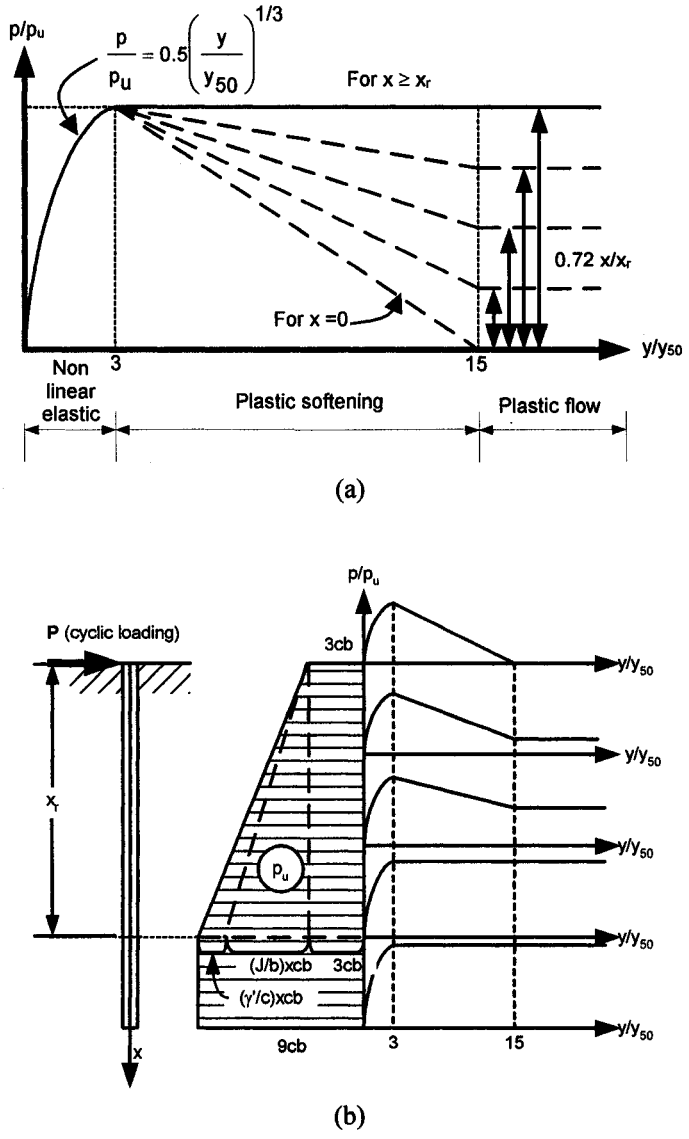

Figure A.1 Characteristic shape of the p-y curves for soft clay below the water table under cyclic loading (after Matlock 1970)

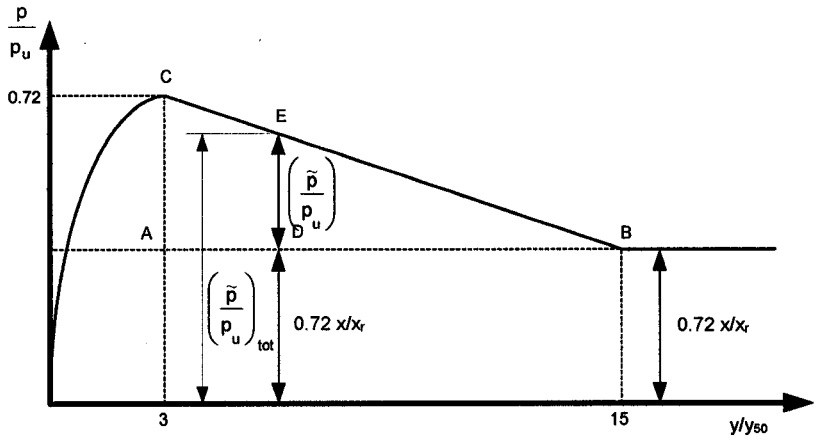

Figure A.2 The p-y curve for soft clay below the water table under cyclic loading shown in terms of p/p_u vs. y/y_{50}

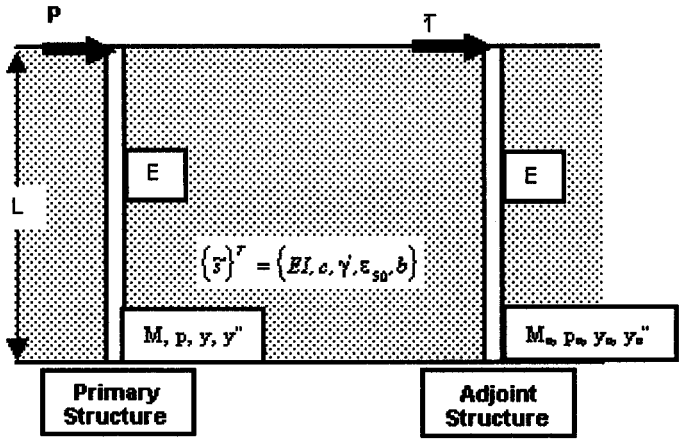

Figure A.3 The models of primary structure and adjoint structure

APPENDIX B:

Determination of the lengths of the piles used in the sensitivity analysis using CLM method

APPENDIX B:

Determination of the lengths of the piles used in the sensitivity analysis using CLM method

1. Calculation of H_c & M_c

The determination of the length of the piles used in this study is determined by CLM methods (Evans & Duncan, 1982). For the pile properties and soil properties presented in Chapter 5, the following values can be determined:

$I = 374 \times 10^{-6}\ m^4$ (B.1)

$B = 0.373\ m$ (B.2)

$$R_I = \frac{I}{\pi B^4/64}$$

$$= \frac{374 \times 10^{-6}}{\pi \times 0.373^4/64} = 0.394 \quad \text{(B.3)}$$

$\sigma_p = 4.2\ c_u = 4.2 \times 18 = 75.06\ kPa$ (B.4)

$E = 2 \times 10^8\ kPa$ (B.5)

$\varepsilon_{50} = 0.02$ (B.6)

m & n from table 5.2

for plastic clay

$\lambda = 1.0$ (B.7)

for brittle clay

- to determine H_c :

$$m = 0.683 \quad \text{and} \quad n = -0.22$$

$$\lambda = (0.14)^n = (0.14)^{-0.22} = 1.541 \tag{B.8}$$

- to determine M_c

$$m = 0.46 \quad \text{and} \quad n = -0.15$$

$$\lambda = (0.14)^n = (0.14)^{-0.15} = 1.343 \tag{B.9}$$

The characteristic shear load H_c and characteristic moment M_c are determined as:

For brittle behaviour:

$$H_c = \lambda B^2 ER_I \left(\frac{\sigma_p}{ER_I}\right)^m (\varepsilon_{50})^n$$

$$= 1.541 \times 0.373^2 \times 2 \cdot 10^8 \times 0.394 \times \left(\frac{75.06}{2 \cdot 10^8 \times 0.394}\right)^{0.683} (0.22)^{-0.22}$$

$$= 3081.87 \text{ kN} \tag{B.10}$$

and

$$M_c = \lambda B^3 ER_I \left(\frac{\sigma_p}{ER_I}\right)^m (\varepsilon_{50})^n$$

$$= 1.343 \times 0.373^3 \times 2 \cdot 10^8 \times 0.394 \times \left(\frac{75.06}{2 \cdot 10^8 \times 0.394}\right)^{0.46} (0.22)^{-0.15}$$

$$= 16{,}745.14 \text{ kNm} \tag{B.11}$$

For plastic behaviour:

$$H_c = \lambda B^2 ER_I \left(\frac{\sigma_p}{ER_I}\right)^m (\varepsilon_{50})^n$$

$$= 1.00 \times 0.373^2 \times 2 \cdot 10^8 \times 0.394 \times \left(\frac{75.06}{2 \cdot 10^8 \times 0.394} \right)^{0.683} (0.22)^{-0.22}$$

$$= 2{,}001.22 \text{ kN} \quad \text{(B.12)}$$

and

$$M_c = \lambda B^3 E R_I \left(\frac{\sigma_p}{E R_I} \right)^m (\varepsilon_{50})^n$$

$$= 1.00 \times 0.373^3 \times 2 \cdot 10^8 \times 0.394 \times \left(\frac{75.06}{2 \cdot 10^8 \times 0.394} \right)^{0.46} (0.22)^{-0.15}$$

$$= 12{,}496.37 \text{ kNm} \quad \text{(B.13)}$$

2. Calculation of H_t, M_{max}, and T

For the all condition, it assumed that

$y_t/B = 0.05$ (B.14)

so:

$y_t = 0.05 \times 373 = 18.65$ mm (B.15)

2.1 Free head pile subjected to lateral force at the top of the piles

2.1.1 Brittle behaviour

$\varepsilon_{50} = 0.02$,

From Fig. B.1:

$H_t/H_c = 0.016$ (B.16)

$H_t = 0.016 \times 3081.87 = 49.31$ kN (B.17)

From Fig. B.4:

$M_t/M_c = 0.006$ (B.18)

$M_{max} = 0.006 \times 16{,}745 = 100.47$ kNm (B.19)

For free head pile $A_y = 2.43$

$$T = \sqrt[3]{\frac{y_t EI}{A_y H_t}}$$

$$= \sqrt[3]{\frac{(18.65 \cdot 10^{-3})(2 \cdot 10^{8})(374 \cdot 10^{-6})}{2.43 \times 49.31}}$$

$= 2.266$ m (B.20)

2.1.2 Plastic behaviour

$\varepsilon_{50} = 0.02$,

From Fig. B.1:

$H_t/H_c = 0.022$ (B.21)

$H_t = 0.0227 \times 2{,}001.22 = 45.43$ kN (B.22)

From Fig. B.4:

$M_{max}/M_c = 0.0068$ (B.23)

$M_{max} = 0.0068 \times 12{,}496.37 = 89.98$ kNm (B.24)

For free head pile $A_y = 2.43$

$$T = \sqrt[3]{\frac{y_t EI}{A_y H_t}}$$

$$= \sqrt[3]{\frac{(18.65 \cdot 10^{-3})(2 \cdot 10^{8})(374 \cdot 10^{-6})}{2.43 \times 45.43}}$$

$= 2.329$ m (B.25)

2.2 Free head pile subjected to bending moment at the top of the piles

2.2.1 Brittle behaviour

$\varepsilon_{50} = 0.02$,

From Fig. B.3:

$M_{max}/M_c = 0.0125$ (B.26)

$H_t = 0.0125 \times 16{,}745.14 = 209.31$ kN (B.27)

For $B_y = 1.62$

$$T = \sqrt[2]{\frac{y_t EI}{B_y M_t}}$$

$$= \sqrt[2]{\frac{(18.65 \cdot 10^{-3})(2 \cdot 10^{8})(374 \cdot 10^{-6})}{1.62 \times 209.31}}$$

$= 2.028$ m (B.28)

2.22 Plastic behaviour

$\varepsilon_{50} = 0.02$

From Fig. B.3

$M_{max}/M_c = 0.01375$ (B.29)

$M_{max} = 0.01375 \times 12{,}496.37 = 171.83$ kNm (B.30)

For $B_y = 1.62$

$$T = \sqrt[2]{\frac{y_t EI}{B_y M_t}}$$

$$= \sqrt[2]{\frac{(18.65 \cdot 10^{-3})(2 \cdot 10^{8})(374 \cdot 10^{-6})}{1.62 \times 171.83}}$$

$= 2.24$ m (B.31)

2.1 Fixed head pile subjected to lateral force at the top of the piles

2.11 Brittle behaviour

$\varepsilon_{50} = 0.02$,

From Fig. B.2:

$H_t/H_c = 0.0325$ (B.32)

$H_t = 0.0325 \times 3081.87 = 100.16$ kN (B.33)

From Fig. B.5:

$M_{max}/M_c = 0.018$ (B.34)

$M_{max} = 0.018 \times 16{,}745 = 301.41$ kNm (B.35)

For fixed head pile $A_y = 0.93$

$$T = \sqrt[3]{\frac{y_t EI}{A_y H_t}}$$

$$= \sqrt[3]{\frac{(18.65 \cdot 10^{-3})(2 \cdot 10^{8})(374 \cdot 10^{-6})}{0.93 \times 49.31}}$$

$= 2.46$ m (B.36)

2.1.2 Plastic behaviour

$\varepsilon_{50} = 0.02$

From Fig. B.1:

$H_t/H_c = 0.047$ (B.37)

$H_t = 0.047 \times 2{,}001.22 = 94.06$ kN (B.38)

From Fig. B.4:

$M_{max}/M_c = 0.018$ (B.39)

$M_{max} = 0.018 \times 12{,}496.37 = 224.93$ kNm (B.40)

For free head pile $A_y = 0.93$

$$T = \sqrt[3]{\frac{y_t EI}{A_y H_t}}$$

$$= \sqrt[3]{\frac{(18.65 \cdot 10^{-3})(2 \cdot 10^{8})(374 \cdot 10^{-6})}{0.93 \times 45.43}}$$

$$= 2.52 \text{ m} \qquad \text{(B.41)}$$

For the piles behave between brittle and plastic behaviour, the values of T are taken as the average of T from brittle and plastic behaviour and formulated as:

$$T = \frac{T_{brittle} + T_{plastic}}{2} \qquad \text{(B.42)}$$

The results of this calculation are summarized in Table B.1.

Table B.1 The values of Ht, M_{max}, and T for various types of loads and constraint using CLM methods (Evans & Duncan, 1981)

Constraint	Load	Behaviour	H_t (kN)	M_{max} (kNm)	T_b & T_p (m)	T (m)
Free head	P	brittle	49.31	100.47	2.27	2.3
		plastic	45.43	84.98	2.33	
	M	brittle	-	209.31	2.03	2.135
		plastic	-	171.83	2.24	
Fixed head	P	brittle	100.16	301.41	2.46	2.49
		plastic	94.06	224.93	2.52	

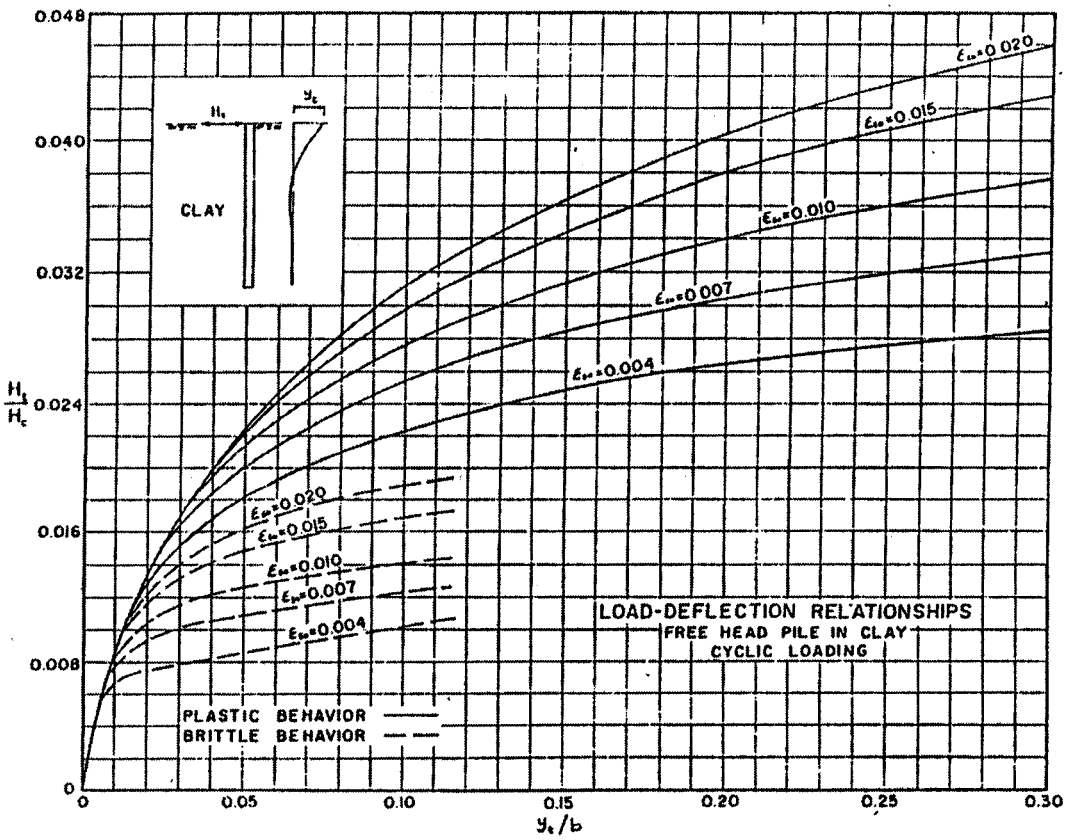

Figure B.1 Load-deformation curves for free head pile in clay-cyclic (Evans & Duncan 1982)

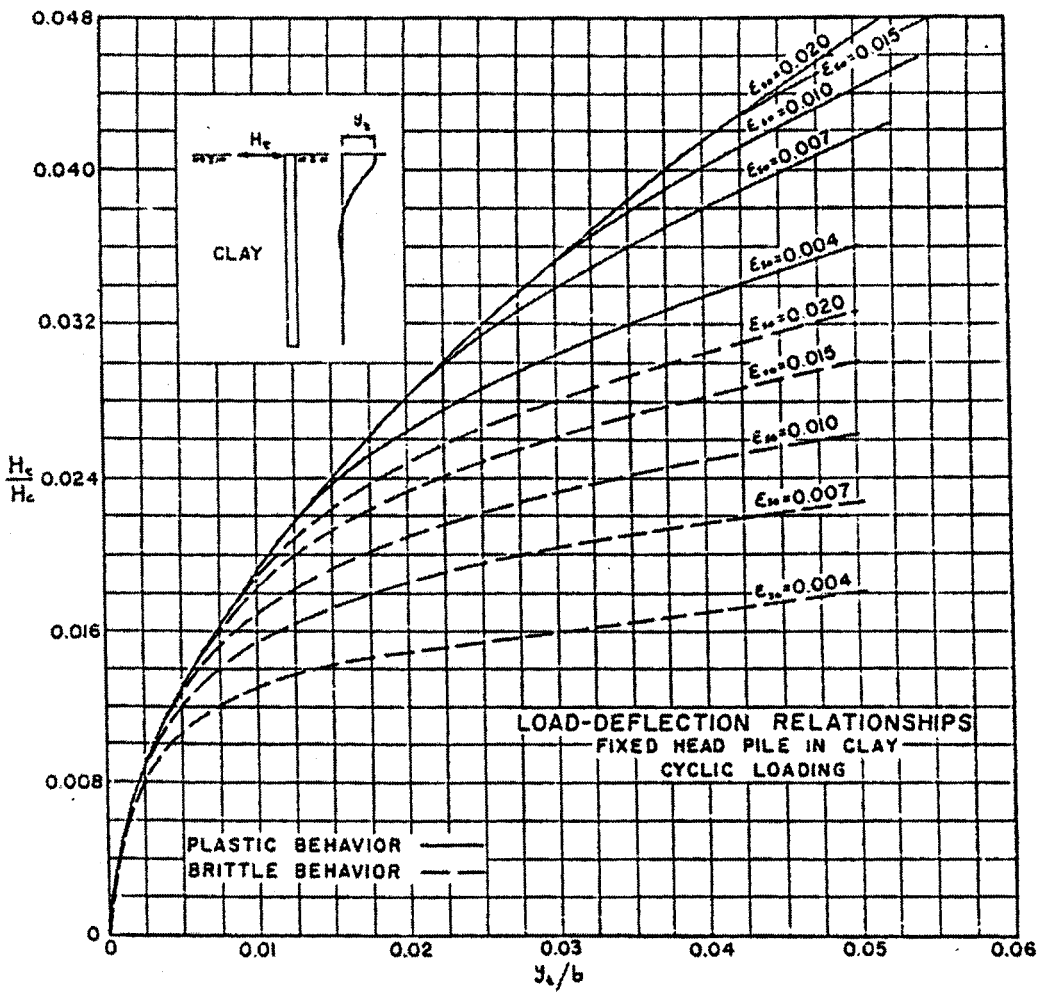

Figure B.2 Load-deformation curves for fixed head pile in clay-cyclic (Evans & Duncan 1982)

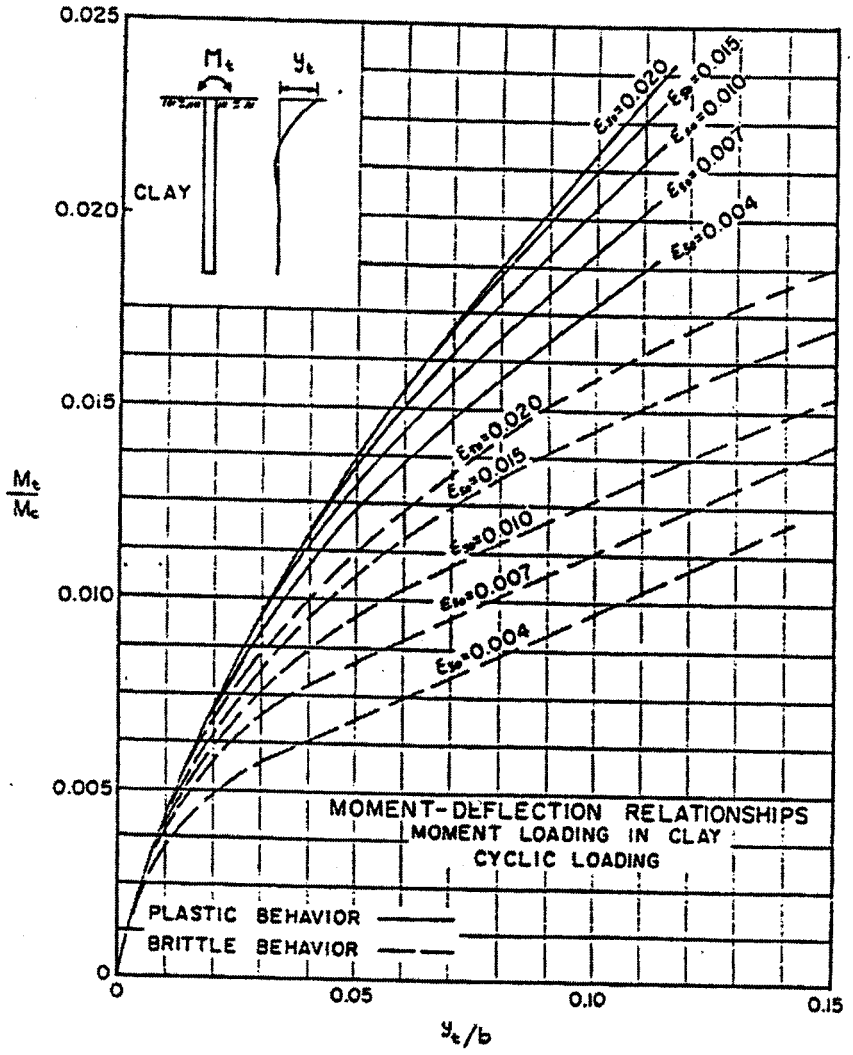

Figure B.3 Moment-deformation curves for moment loading in clay-cyclic (Evans & Duncan 1982)

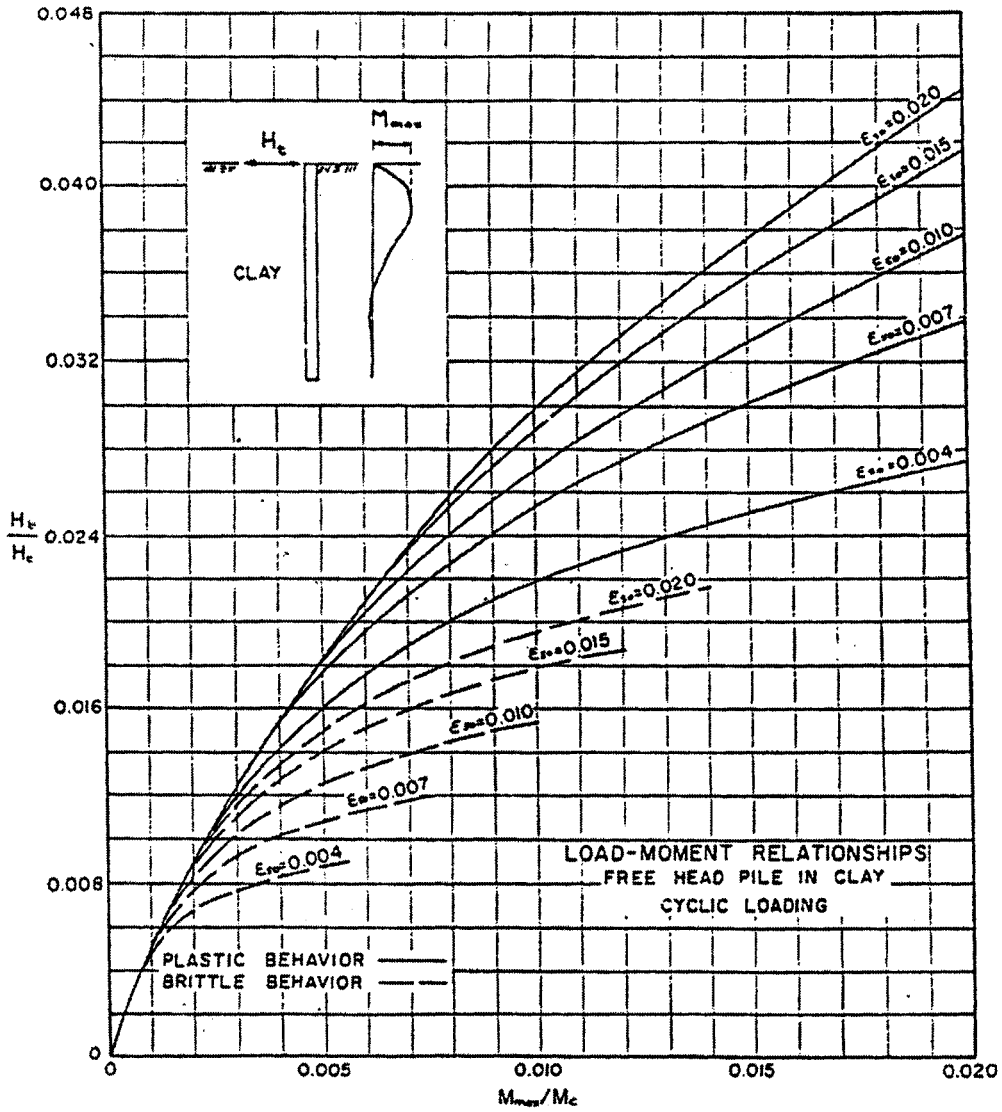

Figure B.4 Load-moment curves for free head pile in clay-cyclic (Evans & Duncan 1982)

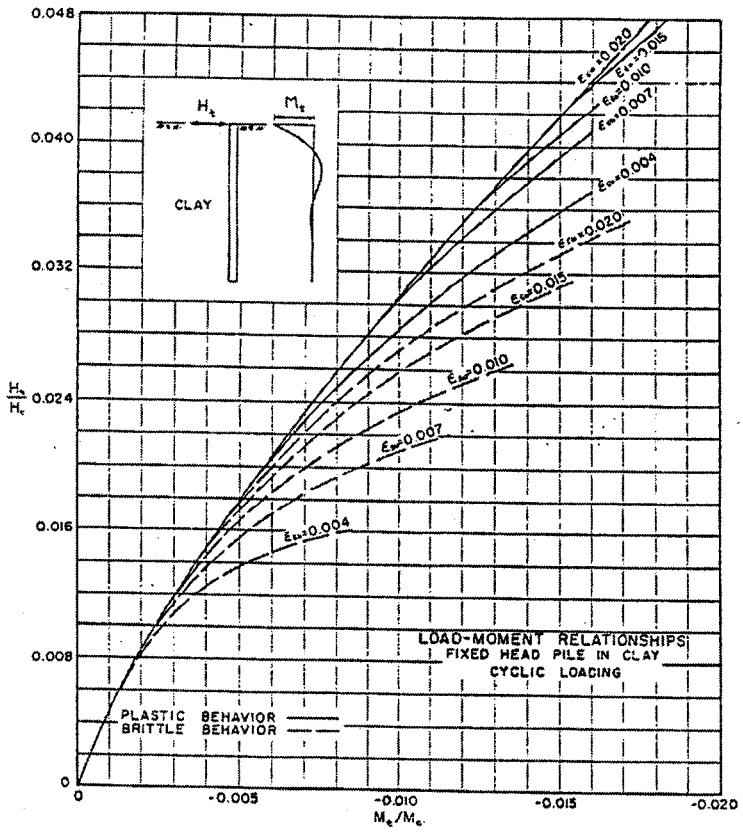

Figure B.5 Load-moment curves for fixed head pile in clay-cyclic (Evans & Duncan 1982)

APPENDIX C:

Input data for laterally loaded piles analyses

APPENDIX C:

Input data for laterally loaded piles analyses

C.1. ANALYSIS OF LATERALLY LOADED SINGLE PILE USING COM624P VERSION 2.0

1. Case

Fixed head pile

Length L = 10T = 24.9 m,

Section properties defined in Chapter 5.

Soil properties is also defined in Chapter 5.

Load : lateral force P_i = 100 kN

Cycle : 10,000

2. Input file

```
FIXED HEAD PILE SUBJECTED LATERAL FORCE P=100kN, L=10T
    2     1     0
  100      1      1      0
    2      2      0
    24.900  200000000      0.000       0.000
    1      1
    2      1      0            10000
  100       0.00010000     100.00000000
    0.0000      0.3730      0.0004      0.0168
    1      1      0.0000     25.0000 100000.0000
    0.0000     7.89000
    5.0000     7.89000
```

```
 0.0000     18.0000      0.0000     0.02000
25.0000     18.0000      0.0000     0.02000
 0
 1
 1    100.0000      0.0000      0.0000
```

C.2. ANALYSIS OF GROUPS OF PILES USING FB-PIER PROGRAM

1. Group of 3x3 piles with spacing is equal 2D and length L=10T=23 m subjected to lateral force P_g = 500 kN

```
Laterally loaded pile-sensitivity analysis

08/05/02
Deni Priyanto

:
PRINT
L=1 M=1 D=1 O=1 S=1 P=1 T=1 F=1 C=1 B=1 I=1 R=0 N=0
:
CONTROL
1 U= 1 D= 0 S= 0 R= 0 N= 51 Z= 0 V=1.0  : NUMLC
S= 0 T= 0 0 P= 2 F= 0
I= 60 T= 1
:
PILE
NSET= 1 S= 0 M= 0 NSEG= 1
C Custom
C T=0 D=2 U=1 : H-Pile - nonlinear
K= 3 L= 23 M= 1 C= 41370 , 3.04414e+007 \
S= 0,0,480000,0,0,0,2e+008,0
OR= 2
D= 0.351 TW= 0.01562 B= 0.373 TF= 0.01562 S= 0
E= 0 H= 0 A= 1 S= 5 G= 0 C= 0
5 5 : NPX, NPY
0.81 0.746 0.746 0.81
0.81 0.91 0.91 0.81
0.44 0.56 0.76
1 1 1
:
MISSING
16 : number of missing piles
1 1
2 1
3 1
4 1
```

```
5 1
1 2
5 2
1 3
5 3
1 4
5 4
1 5
2 5
3 5
4 5
5 5
:
SOIL
L= 1 C= 1000 W= 0 O= 0 S= 0 : Nlayers,kcyc
32 16286 17.7 18 0.02 0 24132 0.3 34.5 25 \
4 1 1 1 0 0 0 0 0 \
E=0,-25 B=0 S=1
32 16286 17.7 18 0.02 0 24132 0.3 34.5
24132 0.35 2846.7 1 : soil tip stiffness info
:
CAP
E= 3e+007 U= 0.2 T= 2 S= 0
:
LOAD
17 L= 1 F= 500 0 0 0 0 0
:
SWFACT
1 F= 0 0
:
```

---

2. Group of 3x3 piles with spacing is equal 3D and length L=10T=23 m subjected to lateral force P_g = 500 kN

```
Laterally loaded pile-sensitivity analysis

08/05/02
Deni Priyanto

:
PRINT
L=1 M=1 D=1 O=1 S=1 P=1 T=1 F=1 C=1 B=1 I=1 R=0 N=0
:
CONTROL
1 U= 1 D= 0 S= 0 R= 0 N= 51 Z= 0 V=1.0  : NUMLC
S= 0 T= 0 0 P= 2 F= 0
I= 60 T= 1
:
PILE
```

```
NSET= 1 S= 0 M= 0 NSEG= 1
C Custom
C T=0 D=2 U=1 : H-Pile - nonlinear
K= 3 L= 23 M= 1 C= 41370 , 3.04414e+007 \
S= 0,0,480000,0,0,0,2e+008,0
OR= 2
D= 0.351 TW= 0.01562 B= 0.373 TF= 0.01562 S= 0
E= 0 H= 0 A= 1 S= 5 G= 0 C= 0
5 5 : NPX, NPY
0.81 1.119 1.119 0.81
0.81 1.119 1.119 0.81
0.58 0.67 0.82
1 1 1
:
MISSING
16 : number of missing piles
1 1
2 1
3 1
4 1
5 1
1 2
5 2
1 3
5 3
1 4
5 4
1 5
2 5
3 5
4 5
5 5
:
SOIL
L= 1 C= 1000 W= 0 O= 0 S= 0 : Nlayers,kcyc
32 16286 17.7 18 0.02 0 24132 0.3 34.5 25 \
4 1 1 1 0 0 0 0 0 \
E=0,-25 B=0 S=1
32 16286 17.7 18 0.02 0 24132 0.3 34.5
24132 0.35 2846.7 1 : soil tip stiffness info
:
CAP
E= 3e+007 U= 0.2 T= 2 S= 0
:
LOAD
17 L= 1 F= 500 0 0 0 0 0
:
SWFACT
1 F= 0 0
:
```

3. Group of 3x3 piles with spacing is equal 4D and length L=10T=23 m subjected to lateral force P_g = 500 kN

```
Laterally loaded pile-sensitivity analysis

08/05/02
Deni Priyanto

:
PRINT
L=1 M=1 D=1 O=1 S=1 P=1 T=1 F=1 C=1 B=1 I=1 R=0 N=0
:
CONTROL
1 U= 1 D= 0 S= 0 R= 0 N= 51 Z= 0 V=1.0  : NUMLC
S= 0 T= 0 0 P= 2 F= 0
I= 60 T= 1
:
PILE
NSET= 1 S= 0 M= 0 NSEG= 1
C Custom
C T=0 D=2 U=1 : H-Pile - nonlinear
K= 3 L= 23 M= 1 C= 41370 , 3.04414e+007 \
S= 0,0,480000,0,0,0,2e+008,0
OR= 2
D= 0.351 TW= 0.01562 B= 0.373 TF= 0.01562 S= 0
E= 0 H= 0 A= 1 S= 5 G= 0 C= 0
5 5 : NPX, NPY
0.81 1.492 1.492 0.81
0.81 1.492 1.492 0.81
0.72 0.78 0.88
1 1 1
:
MISSING
16 : number of missing piles
1 1
2 1
3 1
4 1
5 1
1 2
5 2
1 3
5 3
1 4
5 4
1 5
2 5
3 5
4 5
5 5
:
SOIL
L= 1 C= 1000 W= 0 O= 0 S= 0 : Nlayers,kcyc
22 16286 17.7 18 0.02 0 24132 0.3 34.5 25 \
```

```
4 1 1 1 0 0 0 0 0 \
E=0,-25 B=0 S=1
32 16286 17.7 18 0.02 0 24132 0.3 34.5
24132 0.35 2846.7 1 : soil tip stiffness info
:
CAP
E= 3e+007 U= 0.2 T= 2 S= 0
:
LOAD
17 L= 1 F= 500 0 0 0 0 0
:
SWFACT
1 F= 0 0
:
```

---

4. Group of 3x3 piles with spacing is equal 5D and length L=10T=23 m subjected to lateral force P_g = 500 kN

```
Laterally loaded pile-sensitivity analysis

08/05/02
Deni Priyanto

:
PRINT
L=1 M=1 D=1 O=1 S=1 P=1 T=1 F=1 C=1 B=1 I=1 R=0 N=0
:
CONTROL
1 U= 1 D= 0 S= 0 R= 0 N= 51 Z= 0 V=1.0  : NUMLC
S= 0 T= 0 0 P= 2 F= 0
I= 60 T= 1
:
PILE
NSET= 1 S= 0 M= 0 NSEG= 1
C Custom
C T=0 D=2 U=1 : H-Pile - nonlinear
K= 3 L= 23 M= 1 C= 41370 , 3.04414e+007 \
S= 0,0,480000,0,0,0,2e+008,0
OR= 2
D= 0.351 TW= 0.01562 B= 0.373 TF= 0.01562 S= 0
E= 0 H= 0 A= 1 S= 5 G= 0 C= 0
5 5 : NPX, NPY
0.81 1.865 1.865 0.81
0.81 1.865 1.865 0.81
0.86 0.89 0.94
1 1 1
:
MISSING
16 : number of missing piles
1 1
2 1
3 1
```

```
4 1
5 1
1 2
5 2
1 3
5 3
1 4
5 4
1 5
2 5
3 5
4 5
5 5
:
SOIL
L= 1 C= 1000 W= 0 O= 0 S= 0 : Nlayers,kcyc
32 16286 17.7 18 0.02 0 24132 0.3 34.5 24 \
4 1 1 1 0 0 0 0 0 \
E=0,-25 B=0 S=1
32 16286 17.7 18 0.02 0 24132 0.3 34.5
24132 0.35 2846.7 1 : soil tip stiffness info
:
CAP
E= 3e+007 U= 0.2 T= 2 S= 0
:
LOAD
17 L= 1 F= 500 0 0 0 0 0
:
SWFACT
1 F= 0 0
:
```

APPENDIX D:

Sensitivity analysis of top lateral displacement δy_t for single free head pile with length L = 3T subjected to lateral forces Pi

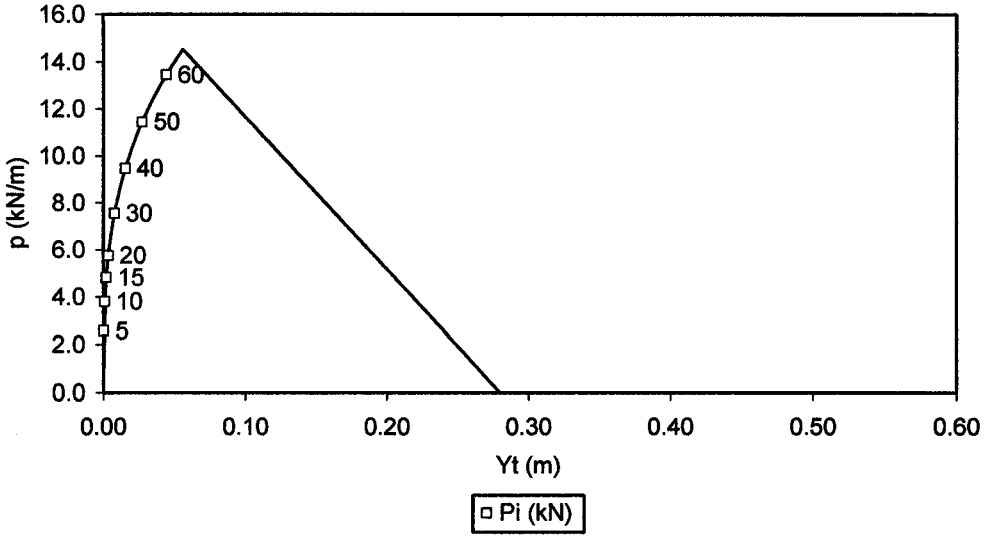

Fig. D.1 Soil reaction p at the top surface (expressed in terms of lateral loading) vs. lateral displacement generated by lateral loading applied to the pile for sensitivity analysis of top lateral displacement δy_t for free head single pile with length L = 3T subjected to lateral forces P_i (kN)

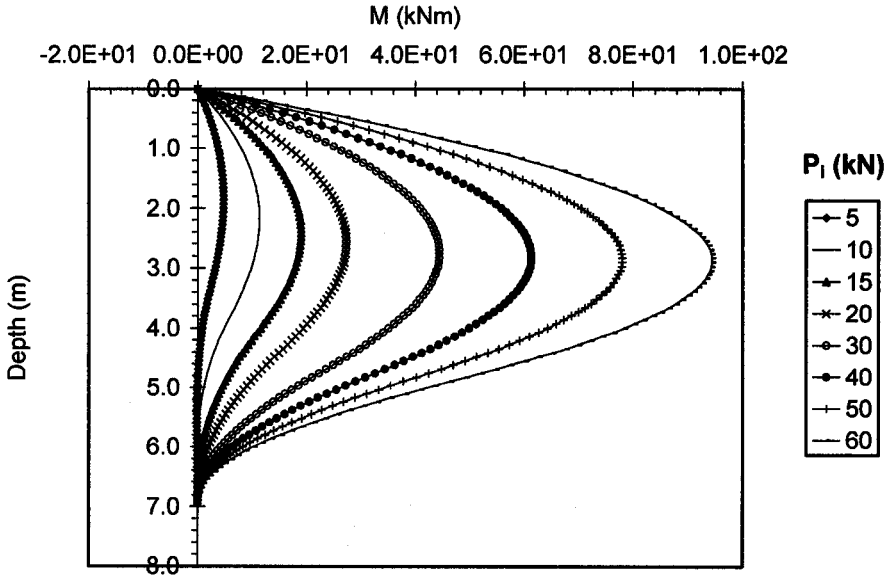

Fig. D.2 Distributions of bending moments at the primary structure M along the depth of the pile for sensitivity analysis of top lateral displacement δy_t for free head single pile with length L = 3T subjected to lateral forces P_i (kN)

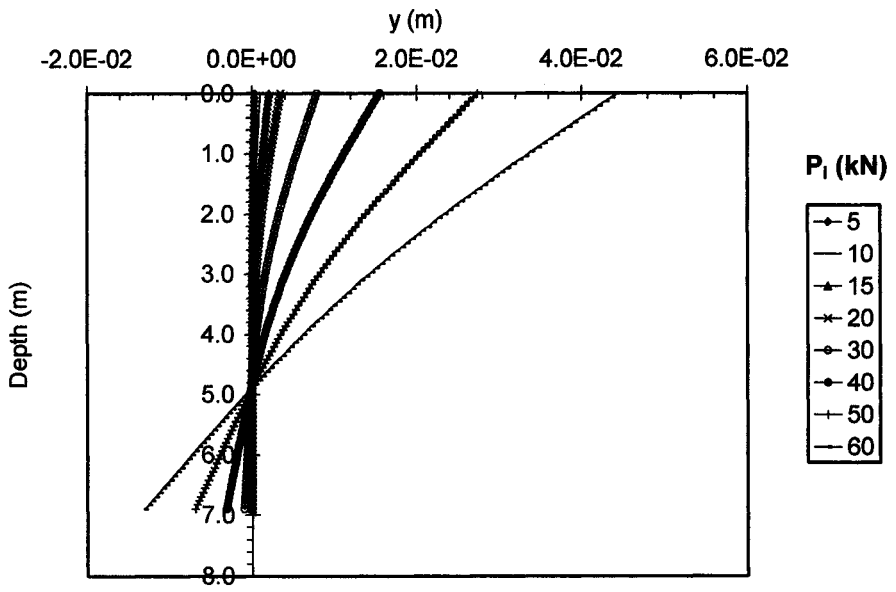

Fig. D.3 Distributions of lateral deflections at the primary structure y along the depth of the pile for sensitivity analysis of top lateral displacement δy_t for free head single pile with length L = 3T subjected to lateral forces P_i (kN)

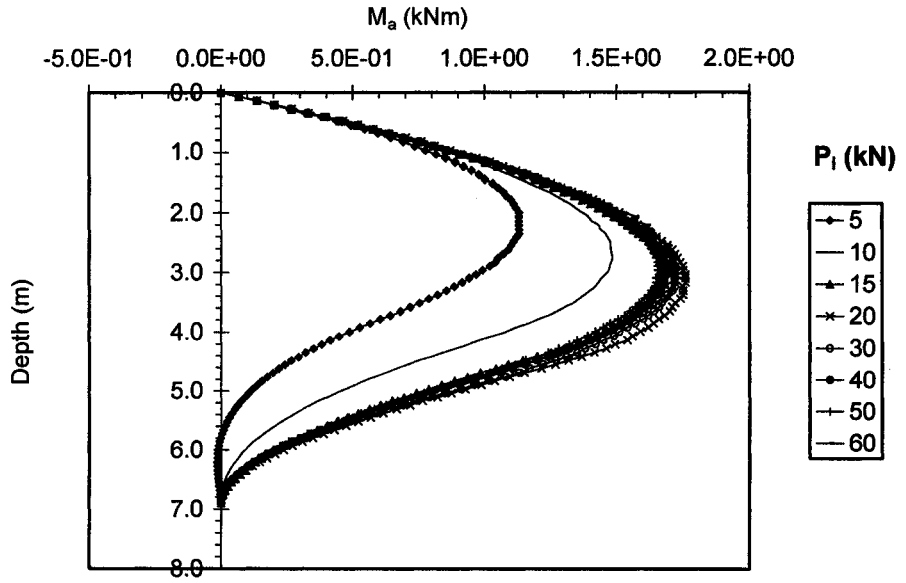

Fig. D.4 Distributions of bending moments M_a along the depth of the pile at the adjoint structure for sensitivity analysis of top lateral displacement δy_t for free head single pile with length L = 3T subjected to lateral forces P_i (kN)

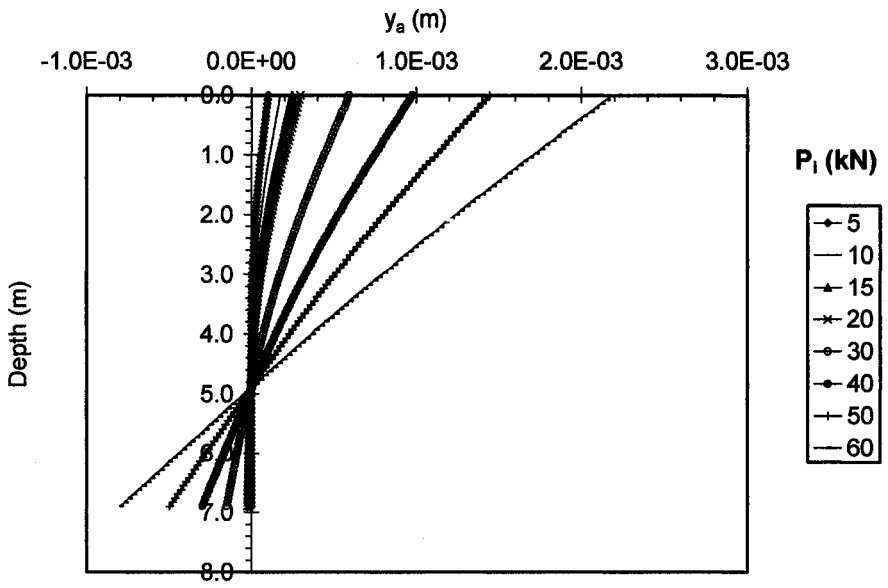

Fig. D.5 Distributions of lateral deflections at the adjoint structure y_a along the depth of the pile for sensitivity analysis of top lateral displacement δy_t for free head single pile with length L = 3T subjected to lateral forces P_i (kN)

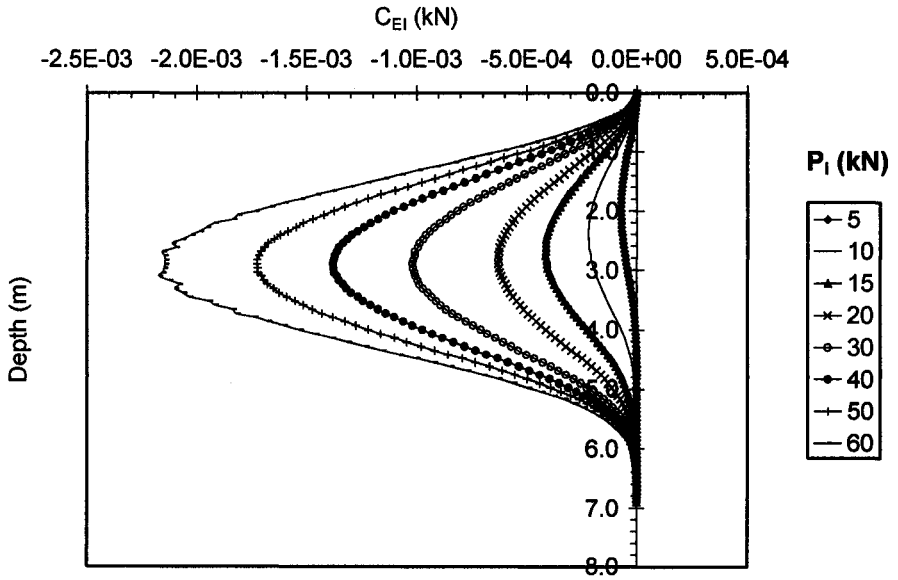

Fig. D.6 Distributions of sensitivity operators C_{EI} affecting the changes of δy_t due to the variations of the design variable δEI for free head single pile with length L = 3T subjected to lateral forces P_i (kN)

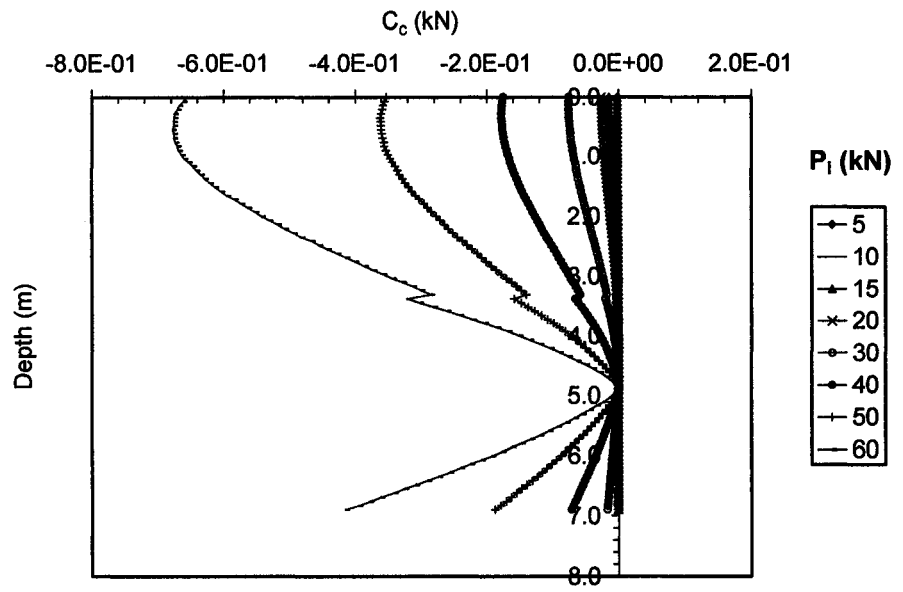

Fig. D.7 Distributions of sensitivity operators C_c affecting the changes of δy_t due to the variations of the design variable δc for free head single pile with length L = 3T subjected to lateral forces P_i (kN)

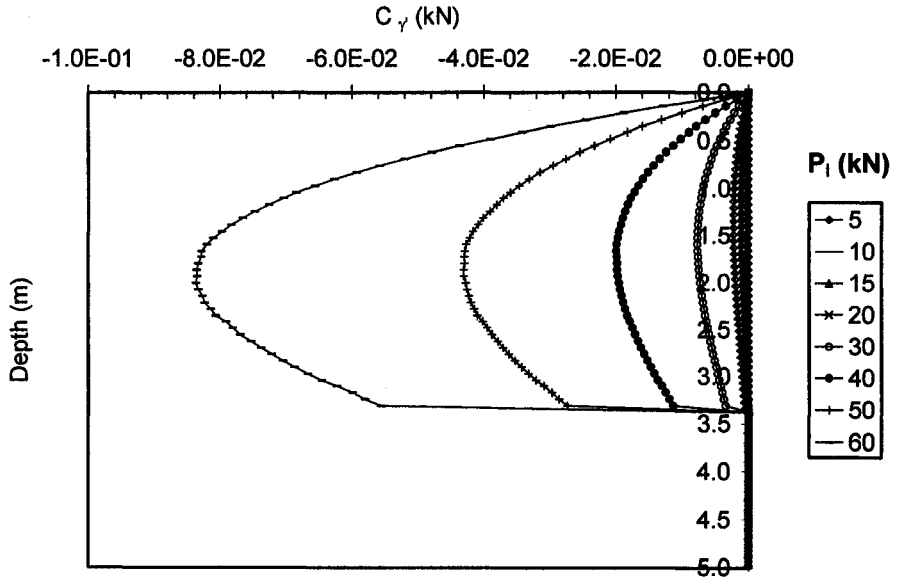

Fig. D.8 Distributions of sensitivity operators $C_{\gamma'}$ affecting the changes of δy_t due to the variations of the design variable $\delta\gamma'$ for free head single pile with length L = 3T subjected to lateral forces P_i (kN)

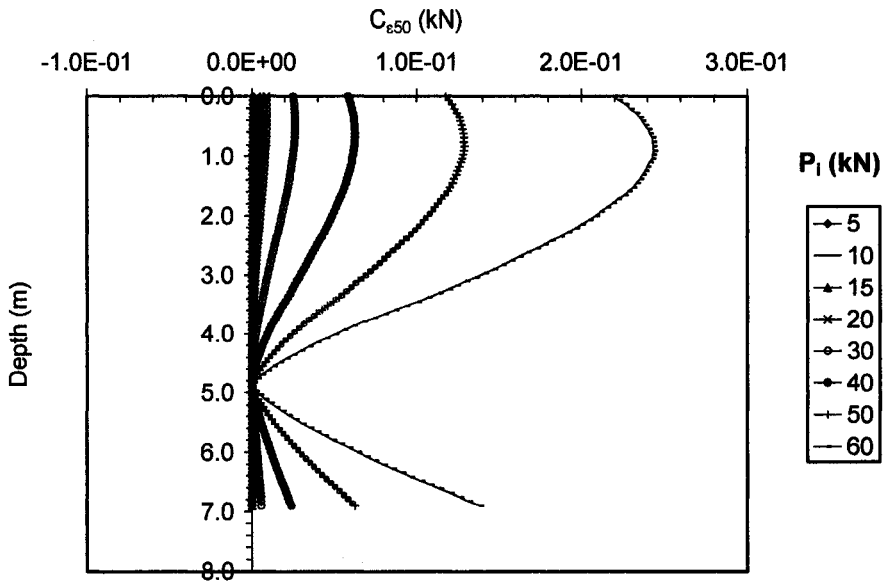

Fig. D.9 Distributions of sensitivity operators $C_{\varepsilon 50}$ affecting the changes of δy_t due to the variations of the design variable $\delta\varepsilon_{50}$ for free head single pile with length L = 3T subjected to lateral forces P_i (kN)

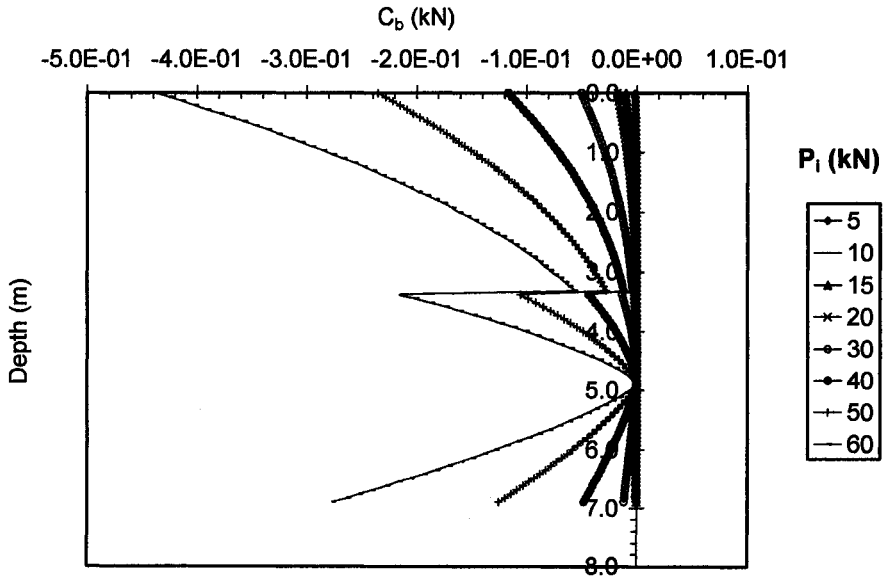

Fig. D.10 Distributions of sensitivity operators C_b affecting the changes of δy_t due to the variations of the design variable δb for free head single pile with length L = 3T subjected to lateral forces P_i (kN)

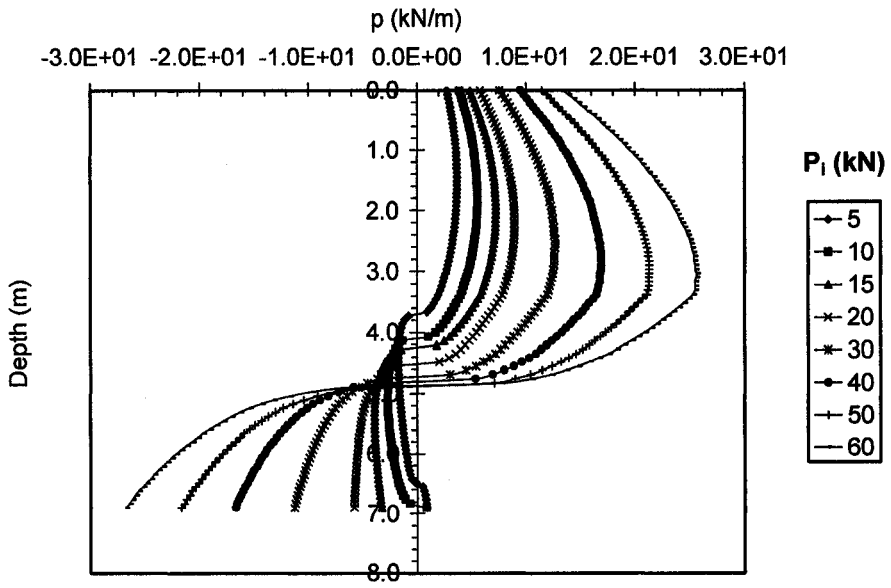

Fig. D.11 Distributions of soil reaction p at the primary structure along the depth of the pile for sensitivity analysis of top lateral displacement δy_t for free head single pile with length L = 3T subjected to lateral forces P_i (kN)

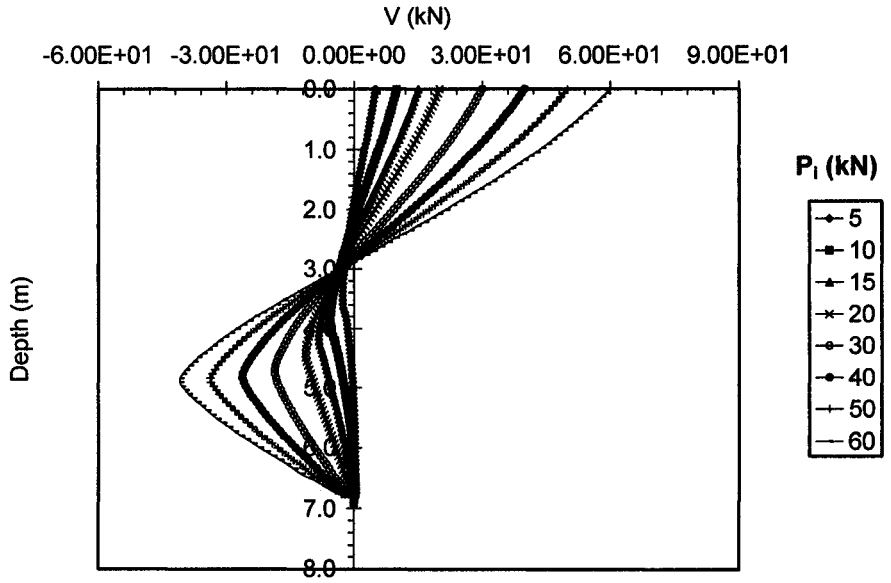

Fig. D.12 Distributions of shear forces V at the primary structure along the depth of the pile for sensitivity analysis of top lateral displacement δy_t for free head single pile with length L = 3T subjected to lateral forces P_i (kN)

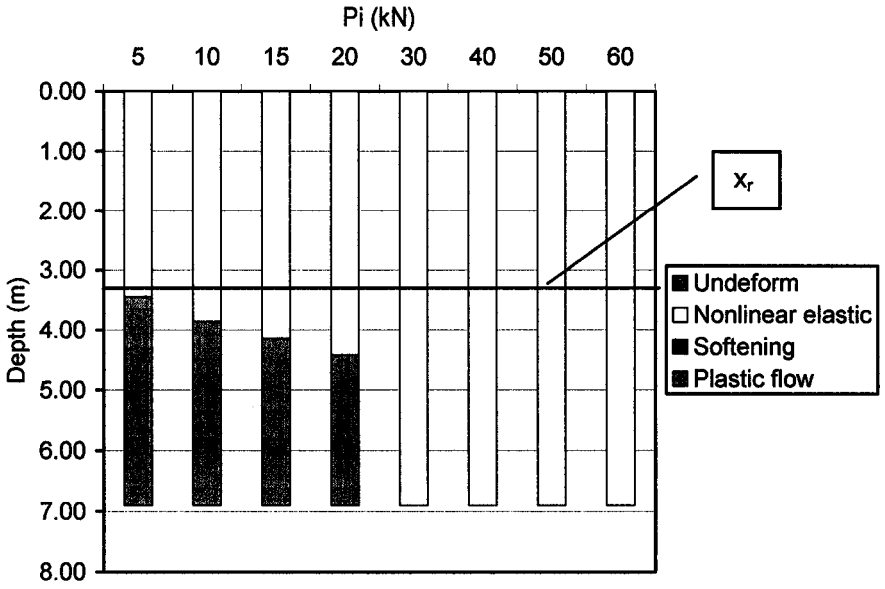

Fig. D.13 Quantitative assessment of the location and the size of soil phases developed with depth determined based on the distributions of sensitivity operators affecting δy_t for free head single pile with length L = 3T subjected to lateral forces P_i (kN)

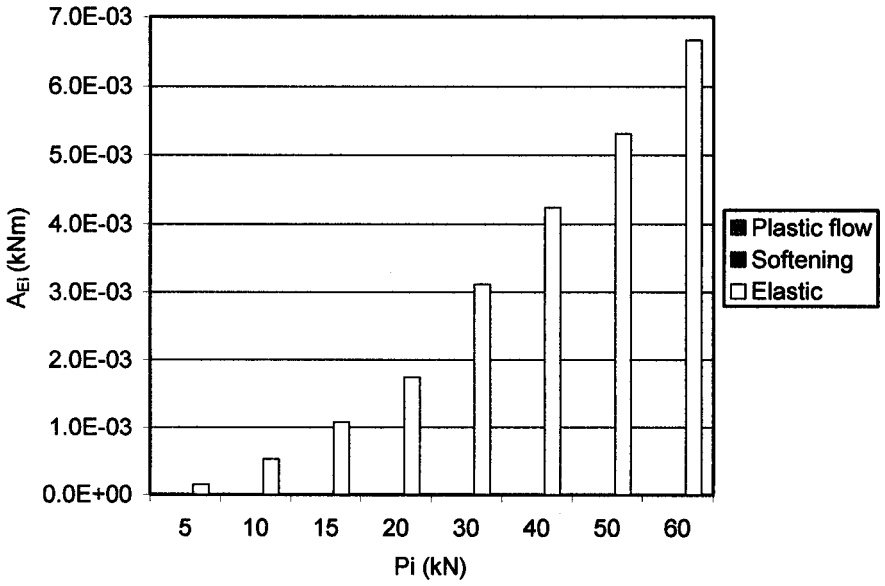

Fig. D.14a Quantitative assessment of sensitivity A_{EI} associated with development of nonlinear elastic, linear softening, and plastic flow stages in the soil along the pile axis that affect δy_t for free head single pile with length L = 3T subjected to lateral forces P_i (kN)

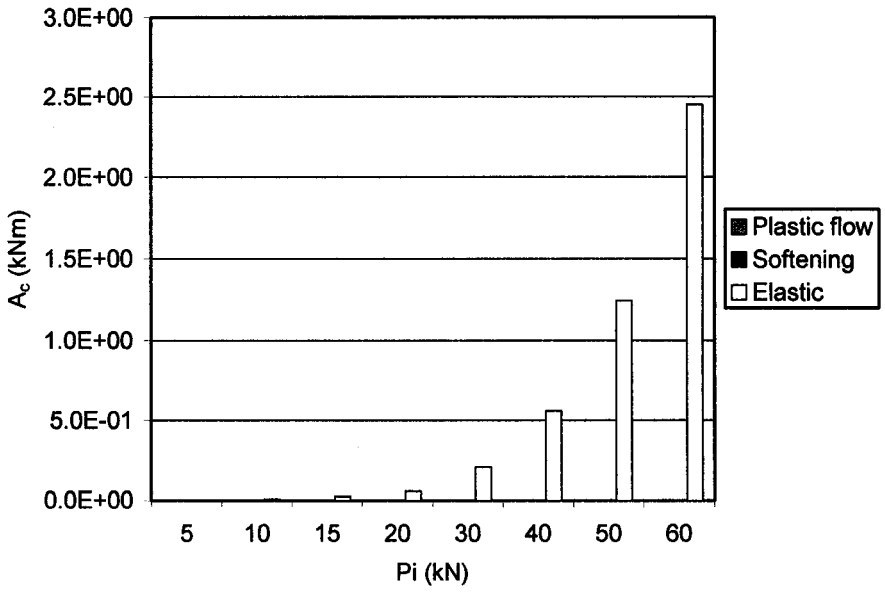

Fig. D.14b Quantitative assessment of sensitivity A_c associated with development of nonlinear elastic, linear softening, and plastic flow stages in the soil along the pile axis that affect δy_t for free head single pile with length L = 3T subjected to lateral forces P_i (kN)

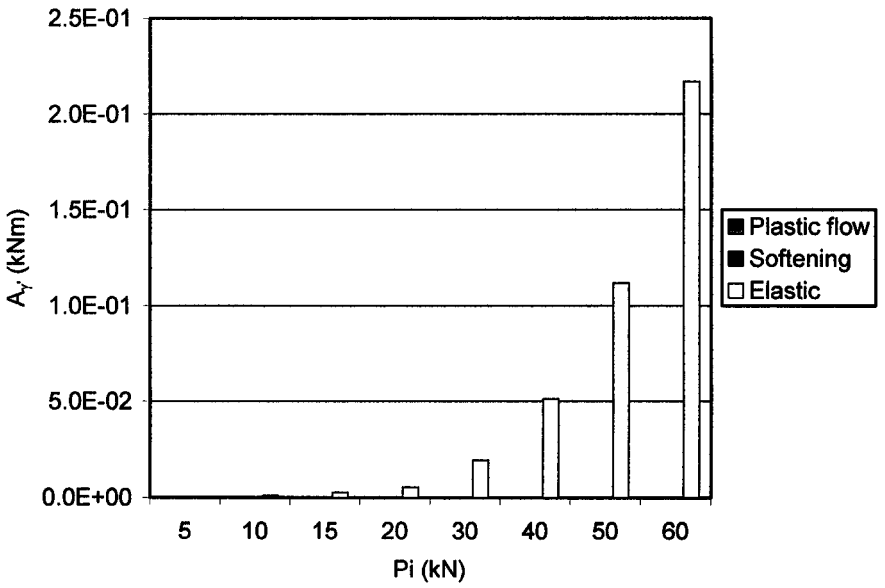

Fig. D.14c Quantitative assessment of sensitivity $A_{\gamma'}$ associated with development of nonlinear elastic, linear softening, and plastic flow stages in the soil along the pile axis that affect δy_t for free head single pile with length L = 3T subjected to lateral forces P_i (kN)

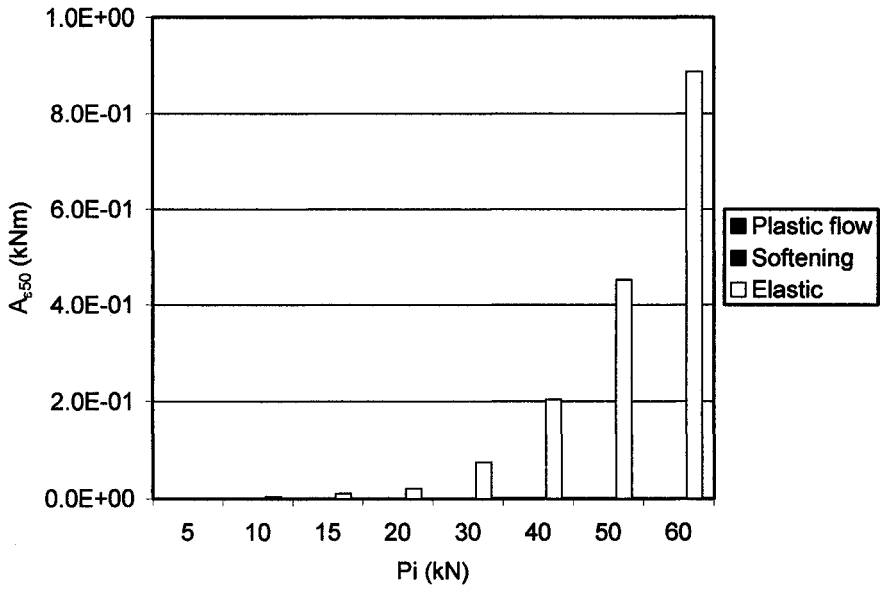

Fig. D.14d Quantitative assessment of sensitivity $A_{\varepsilon 50}$ associated with development of nonlinear elastic, linear softening, and plastic flow stages in the soil along the pile axis that affect δy_t for free head single pile with length L = 3T subjected to lateral forces P_i (kN)

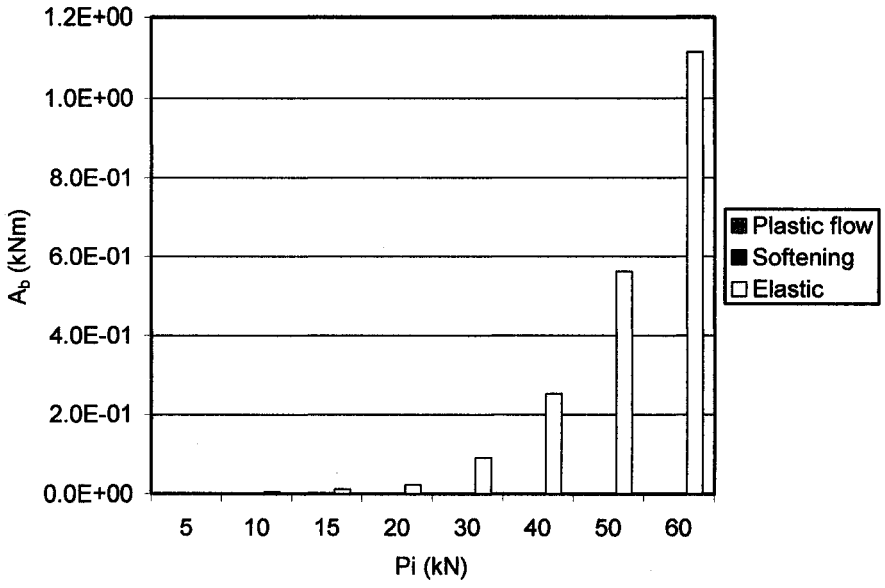

Fig. D.14e Quantitative assessment of sensitivity A_b associated with development of nonlinear elastic, linear softening, and plastic flow stages in the soil along the pile axis that affect δy_t for free head single pile with length L = 3T subjected to lateral forces P_i (kN)

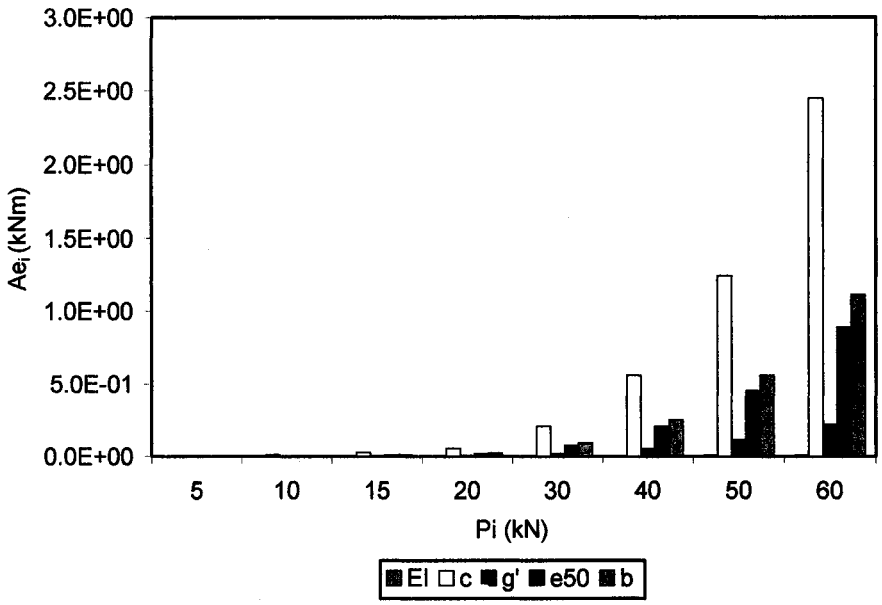

Fig. D.14f Quantitative assessment of sensitivities Ae_i that contains Ae_{EI}, Ae_c, $Ae_{\gamma'}$, $Ae_{\varepsilon 50}$, and Ae_b associated with the development of the nonlinear elastic stage in the soil along the pile axis that affect δy_t for free head single pile with length L = 3T subjected to lateral forces P_i (kN)

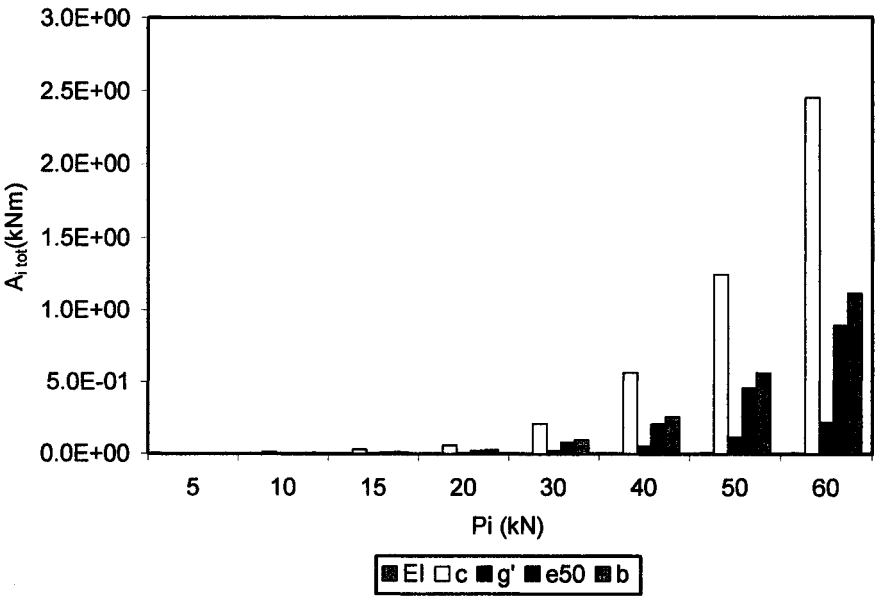

Fig. D.14g Quantitative assessment of sensitivities $A_{i\ tot}$ that contains $(A_{EI}, A_c, A_{\gamma'}, A_{\varepsilon 50}$, and $A_b)_{tot}$ associated with the development of three stages in the soil along the pile axis that affect δy_t for free head single pile with length L = 3T subjected to lateral forces P_i (kN)

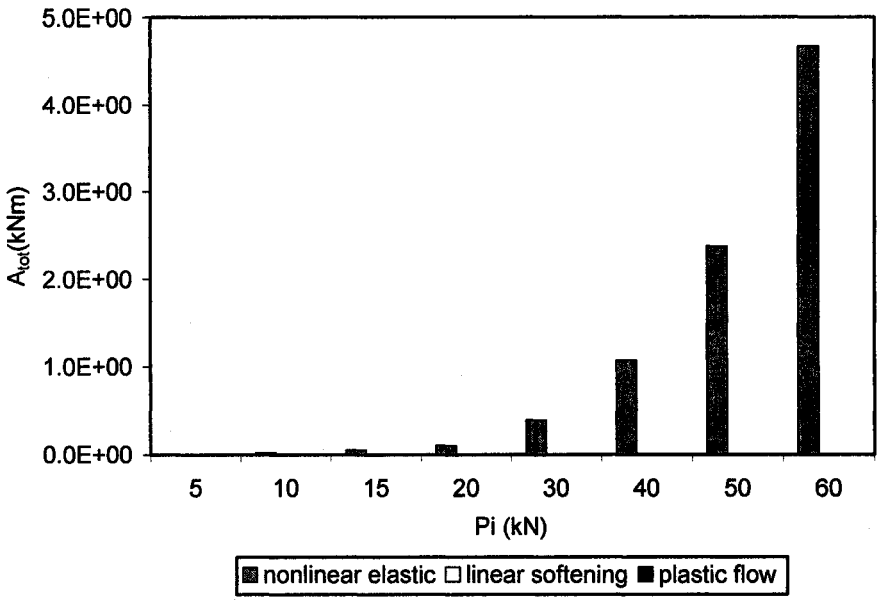

Fig. D.14h Quantitative assessment of sensitivities A_{tot} that is summation of (A_{EI}, A_c, $A_{\gamma'}$, $A_{\varepsilon 50}$, and A_b)$_i$ of each soil stage that affect δy_t for free head single pile with length L = 3T subjected to lateral forces P_i (kN)

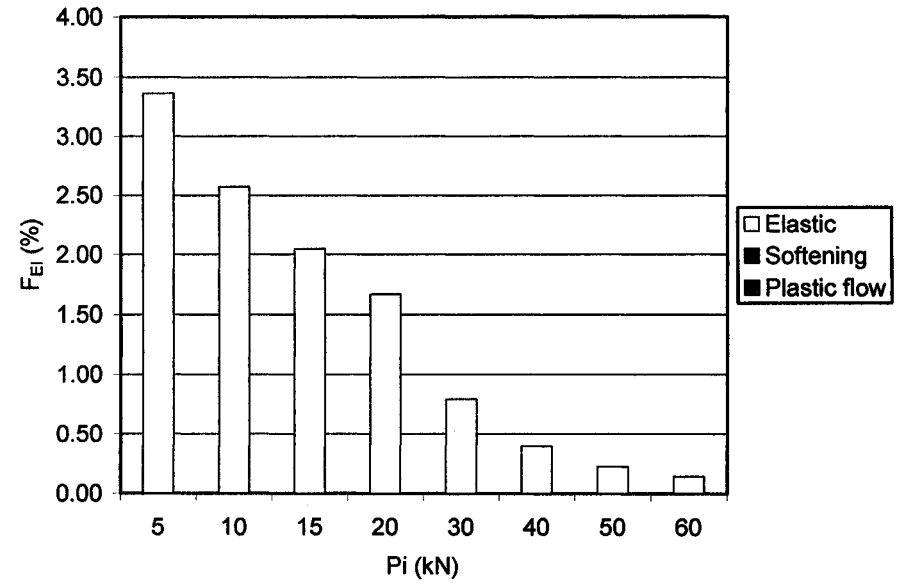

Fig. D.15a Quantitative assessment (in %) of relative sensitivity factors F_{EI} that affect δy_t for free head single pile with length L = 3T subjected to lateral forces P_i (kN)

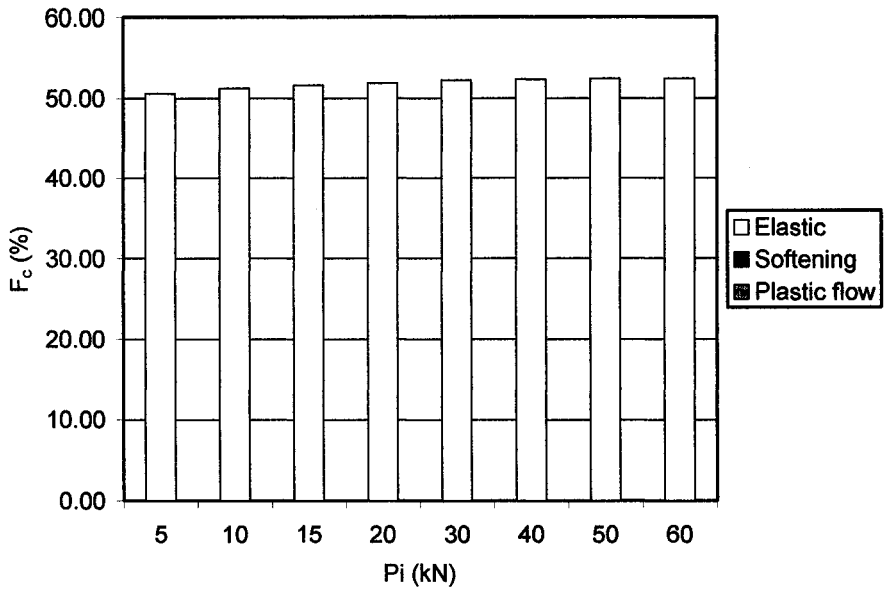

Fig. D.15b Quantitative assessment (in %) of relative sensitivity factors F_c that affect δy_t for free head single pile with length L = 3T subjected to lateral forces P_i (kN)

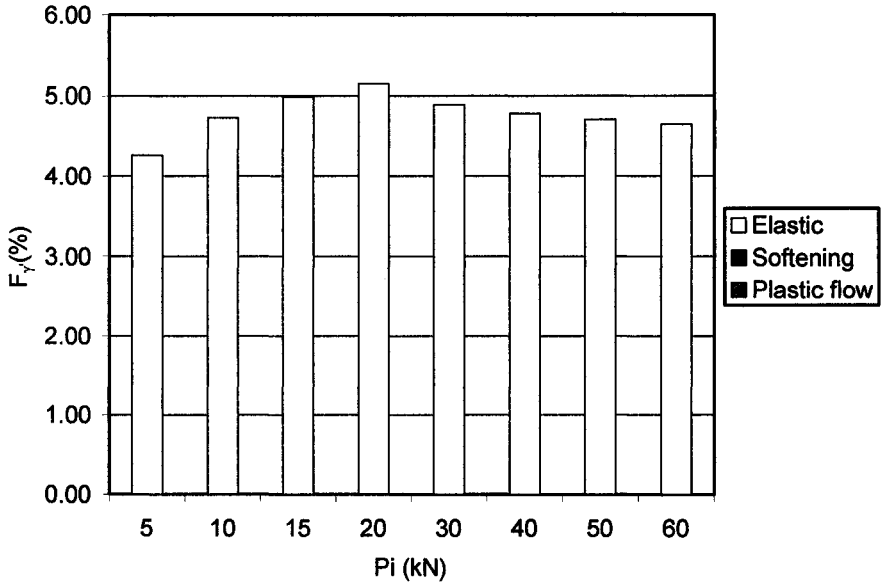

Fig. D.15c Quantitative assessment (in %) of relative sensitivity factors $F_{\gamma'}$ that affect of δy_t for free head single pile with length L = 3T subjected to lateral forces P_i (kN)

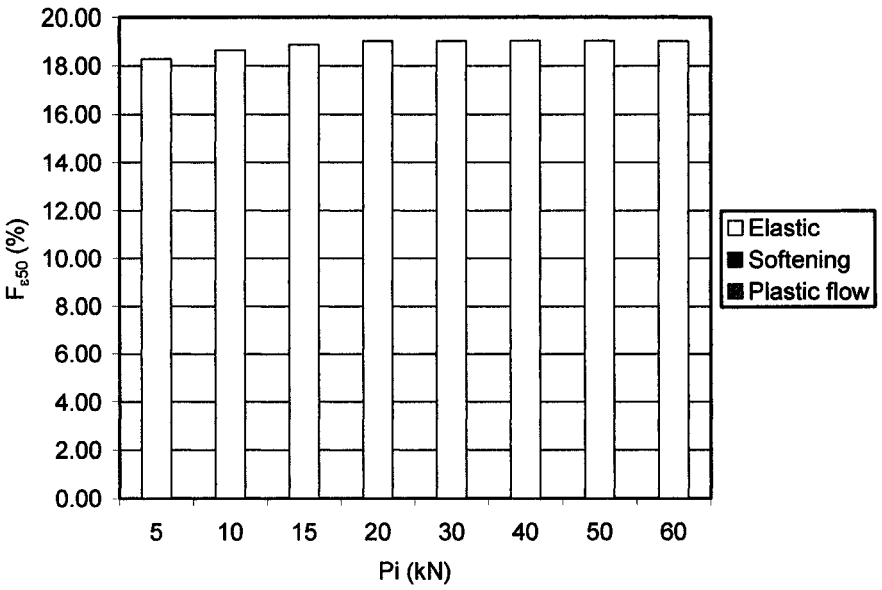

Fig. D.15d Quantitative assessment (in %) of relative sensitivity factors $F_{\varepsilon 50}$ that affect δy_t for free head single pile with length L = 3T subjected to lateral forces P_i (kN)

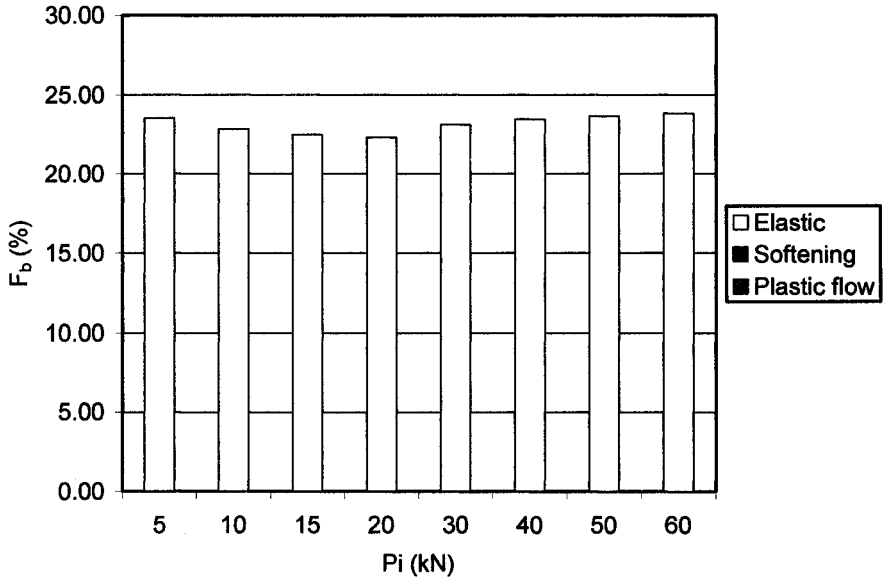

Fig. D.15e Quantitative assessment (in %) of relative sensitivity factors F_b that affect δy_t for free head single pile with length L = 3T subjected to lateral forces P_i (kN)

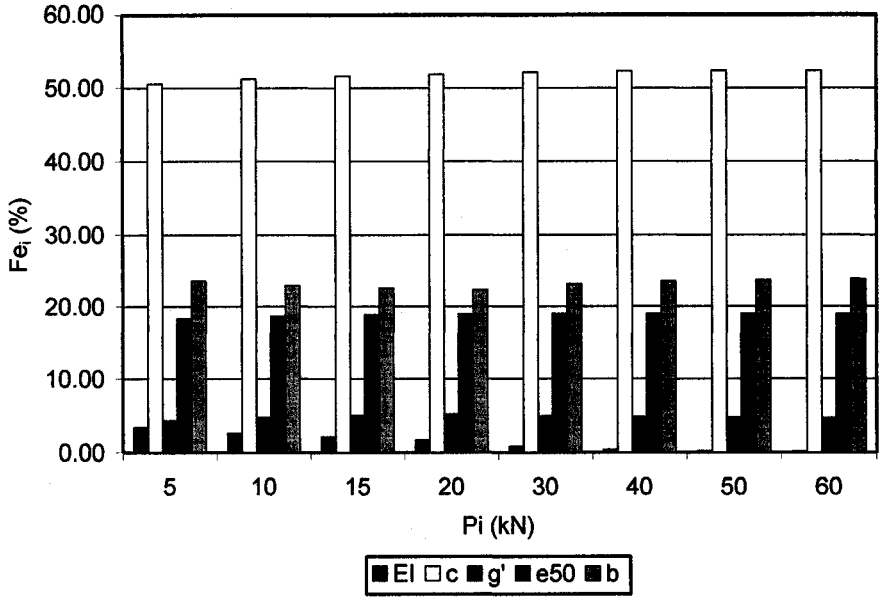

Fig. D.15f Quantitative assessment (in %) of relative sensitivity factors Fe_i that contains Fe_{EI}, Fe_c, $Fe_{\gamma'}$, $Fe_{\varepsilon 50}$, and Fe_b associated with the nonlinear elastic soil stage developed along the pile axis that affect δy_t for free head single pile with length L = 3T subjected to lateral forces P_i (kN)

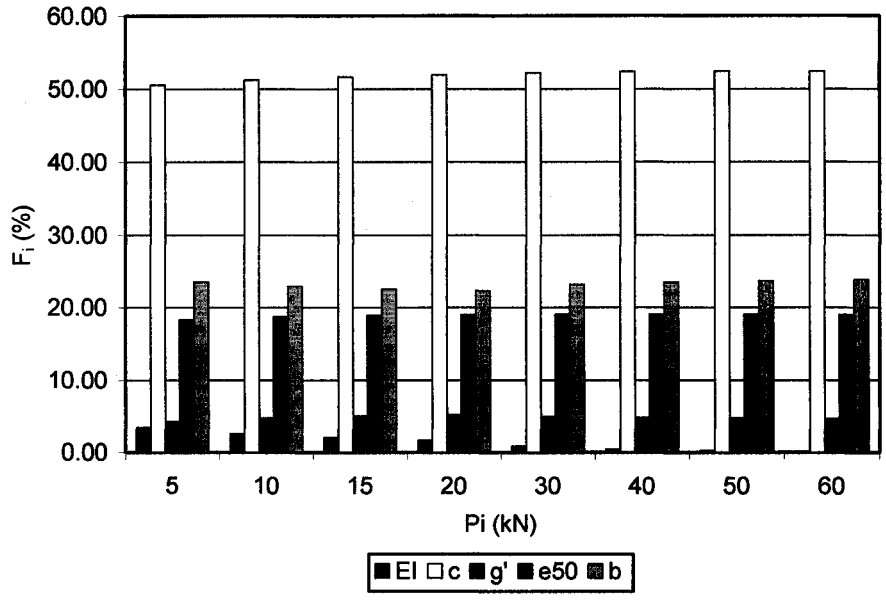

Fig. D.15g Quantitative assessment (in %) of relative sensitivity factors F_i that contains F_{EI}, F_c, $F_{\gamma'}$, $F_{\varepsilon 50}$, and F_b associated with all soil stages developed along the pile axis that affect δy_t for free head single pile with length L = 3T subjected to lateral forces P_i (kN)

APPENDIX E:

Sensitivity analysis of top lateral displacement δy_t for single free head pile with length L = 10T subjected to lateral forces Pi

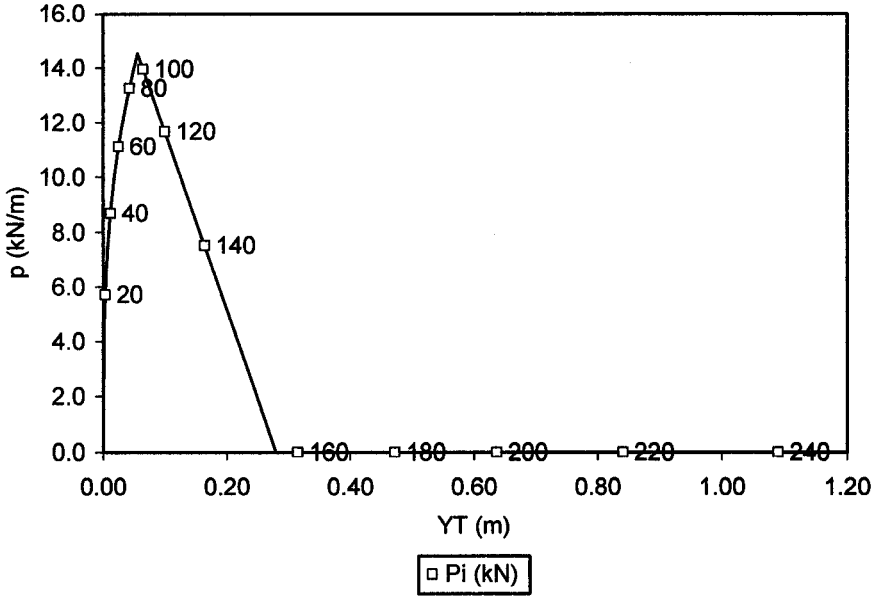

Fig. E.1 Soil reaction p at the top surface (expressed in terms of lateral loading) vs. lateral displacement generated by lateral loading applied to the pile for sensitivity analysis of top lateral displacement δy_t for free head single pile with length L = 10T subjected to lateral forces P_i (kN)

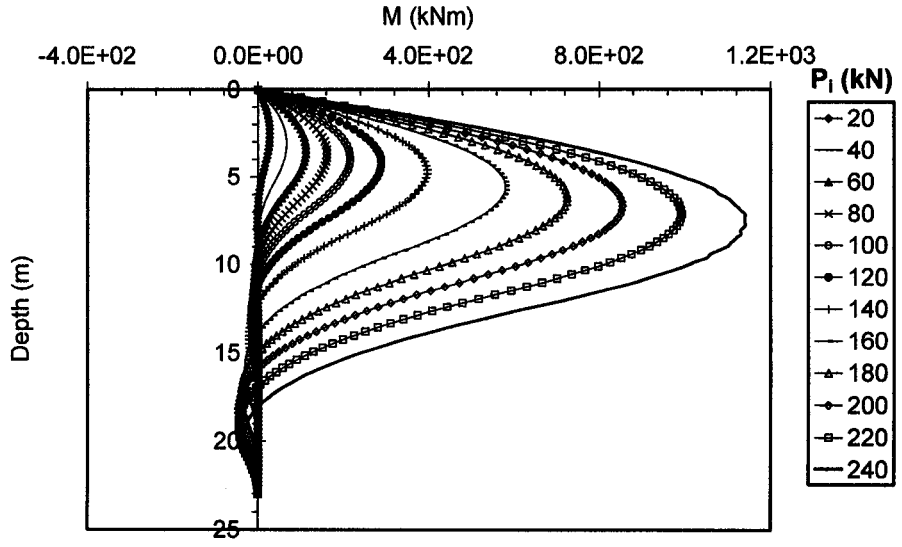

Fig. E.2 Distributions of bending moments at the primary structure M along the depth of the pile for sensitivity analysis of top lateral displacement δy_t for free head single pile with length L = 10T subjected to lateral forces P_i (kN)

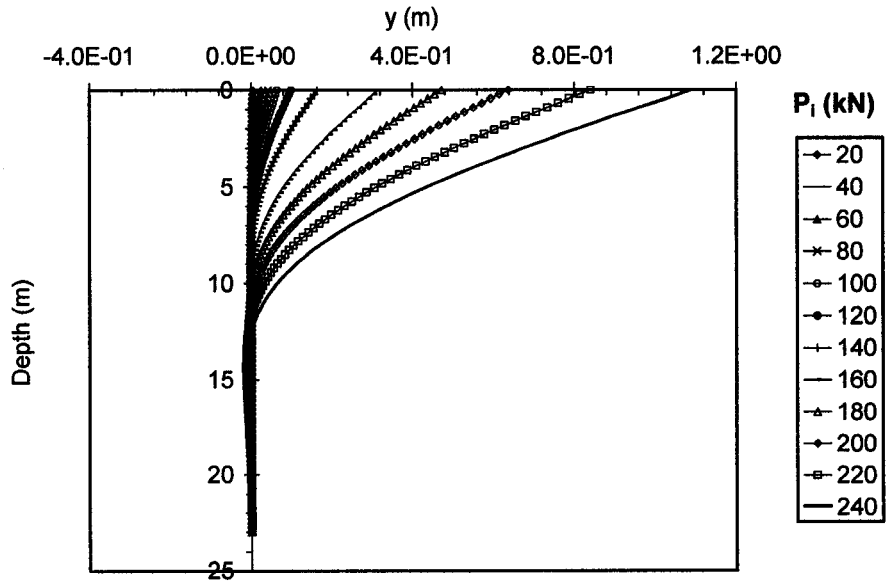

Fig. E.3 Distributions of lateral deflections at the primary structure y along the depth of the pile for sensitivity analysis of top lateral displacement δy_t for free head single pile with length L = 10T subjected to lateral forces P_i (kN)

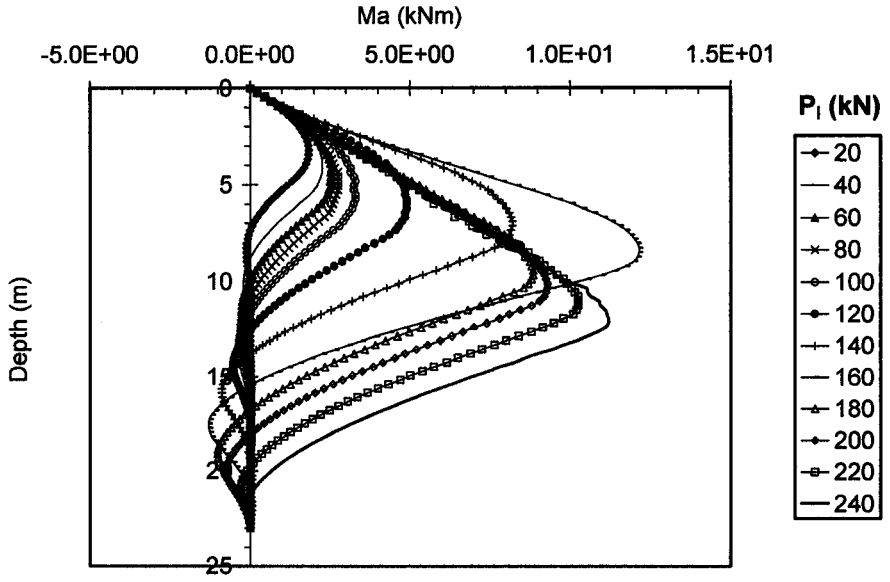

Fig. E.4 Distributions of bending moments M_a along the depth of the pile at the adjoint structure for sensitivity analysis of top lateral displacement δy_t for free head single pile with length L = 10T subjected to lateral forces P_i (kN)

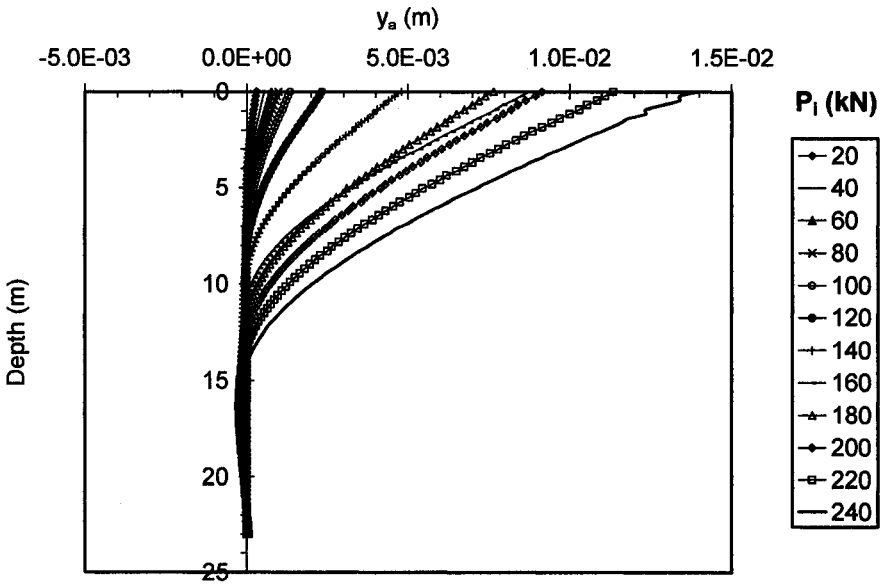

Fig. E.5 Distributions of lateral deflections at the adjoint structure y_a along the depth of the pile for sensitivity analysis of top lateral displacement δy_t for free head single pile with length L = 10T subjected to lateral forces P_i (kN)

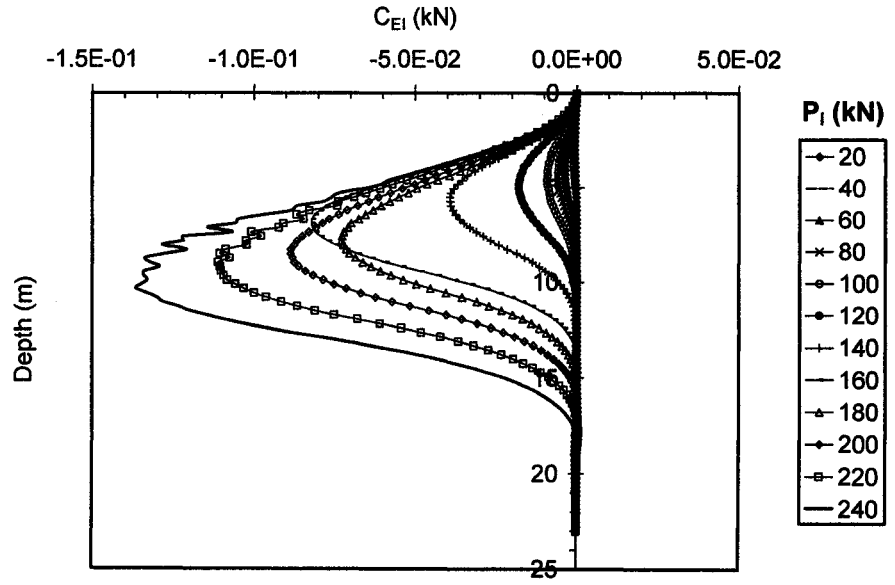

Fig. E.6 Distributions of sensitivity operators C_{EI} affecting the changes of δy_t due to the variations of the design variable δEI for free head single pile with length L = 10T subjected to lateral forces P_i (kN)

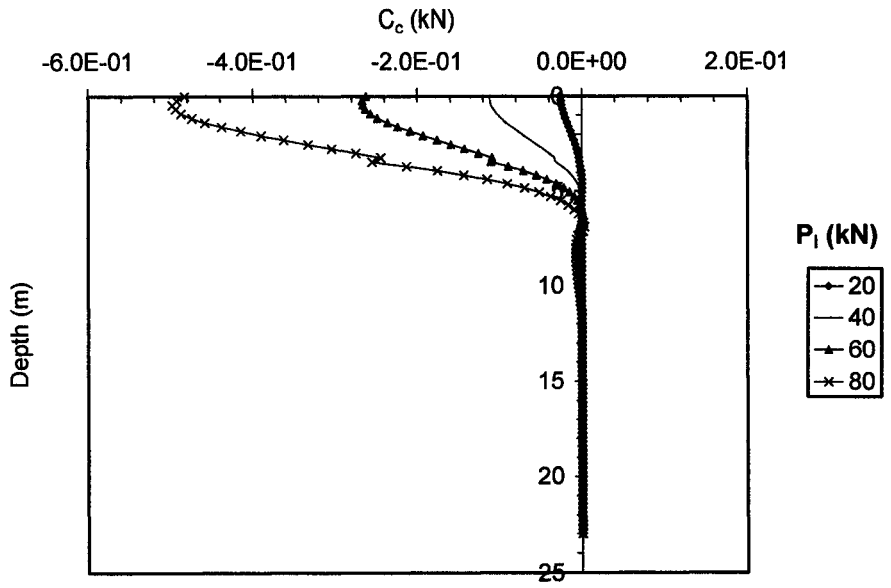

Fig. E.7a Distributions of sensitivity operators C_c affecting the changes of δy_t due to the variations of the design variable δc for free head single pile with length L = 10T subjected to lateral forces P_i (kN)

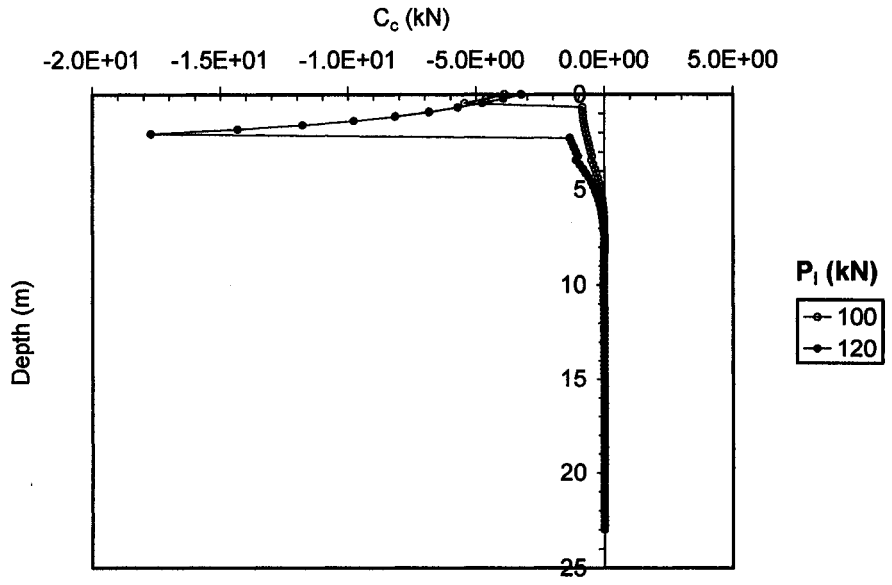

Fig. E.7b Distributions of sensitivity operators C_c affecting the changes of δy_t due to the variations of the design variable δc for free head single pile with length L = 10T subjected to lateral forces P_i (kN)

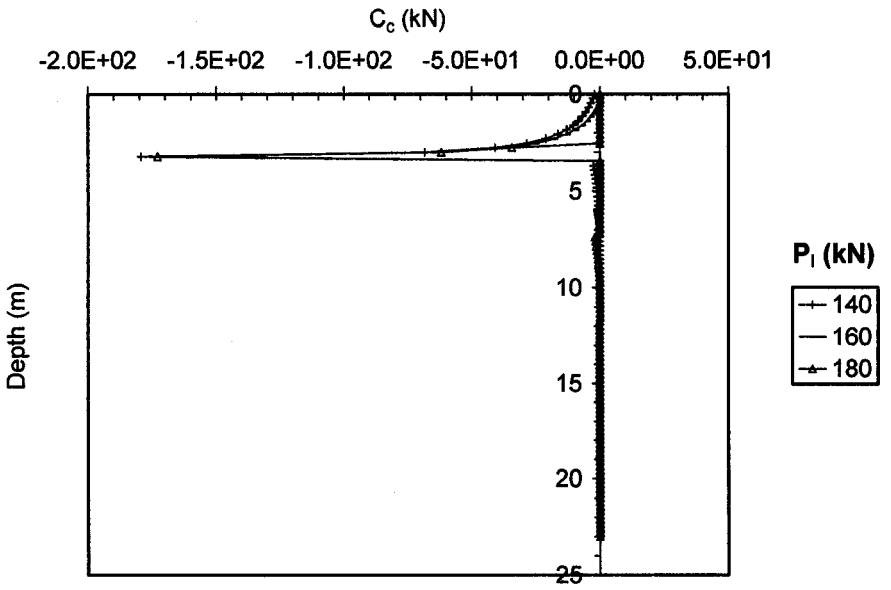

Fig. E.7c Distributions of sensitivity operators C_c affecting the changes of δy_t due to the variations of the design variable δc for free head single pile with length L = 10T subjected to lateral forces P_i (kN)

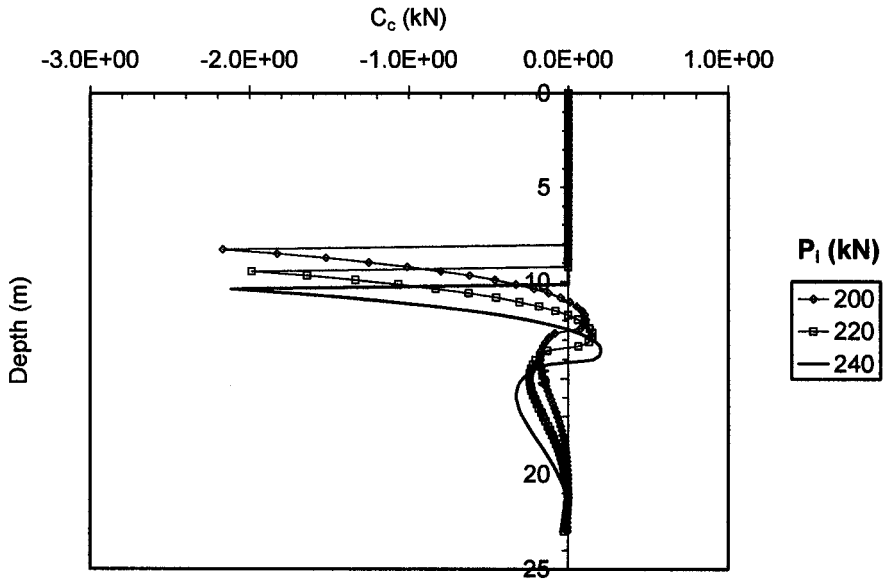

Fig. E.7d Distributions of sensitivity operators C_c affecting the changes of δy_t due to the variations of the design variable δc for free head single pile with length L = 10T subjected to lateral forces P_i (kN)

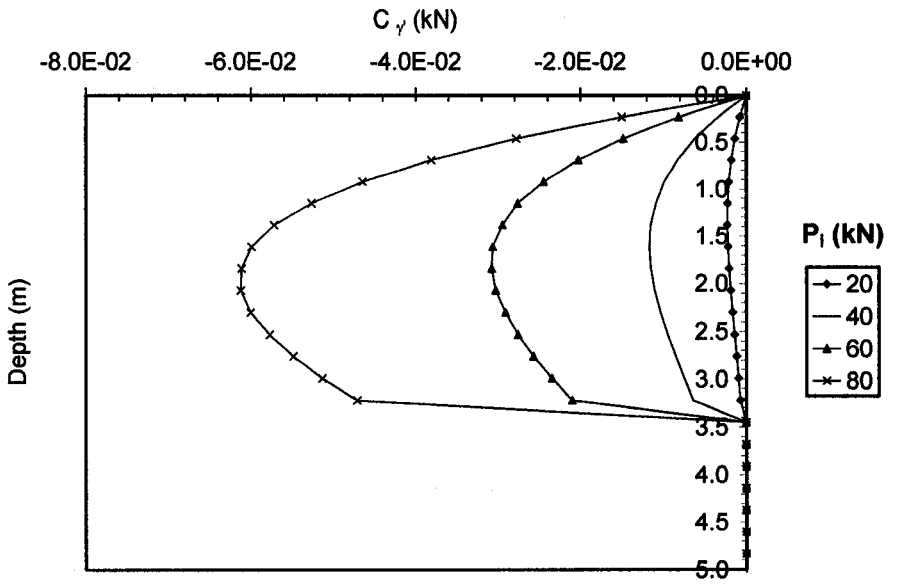

Fig. E.8a Distributions of sensitivity operators $C_{\gamma'}$ affecting the changes of δy_t due to the variations of the design variable $\delta\gamma'$ for free head single pile with length L = 10T subjected to lateral forces P_i (kN)

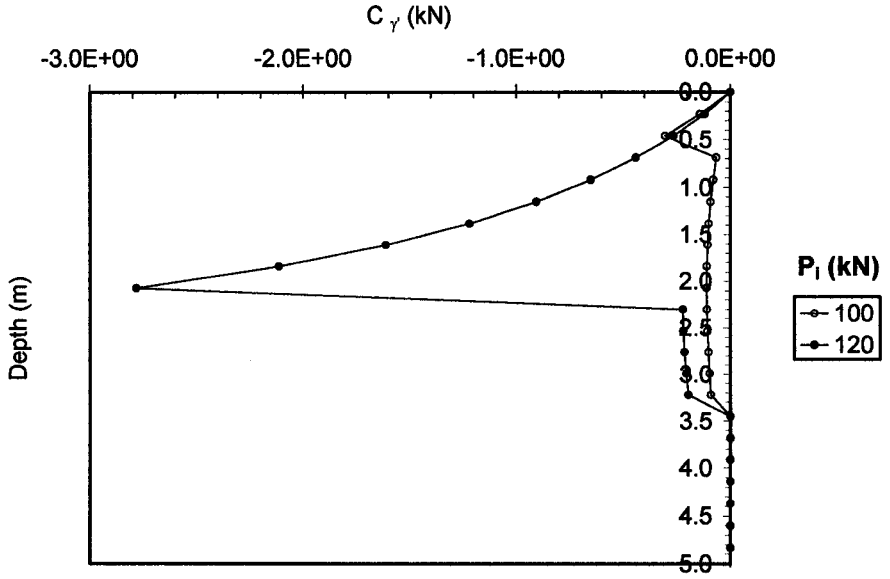

Fig. E.8b Distributions of sensitivity operators $C_{\gamma'}$ affecting the changes of δy_t due to the variations of the design variable $\delta\gamma'$ for free head single pile with length L = 10T subjected to lateral forces P_i (kN)

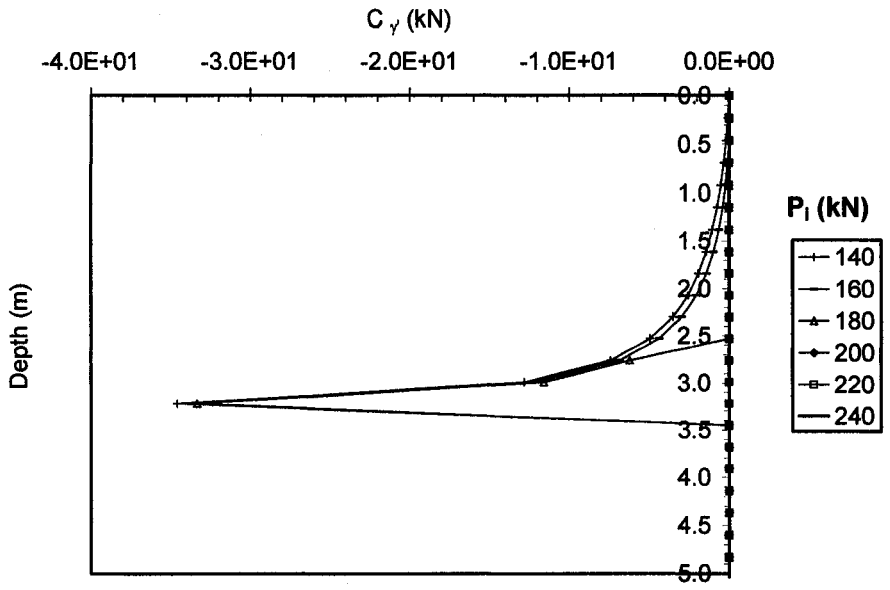

Fig. E.8c Distributions of sensitivity operators $C_{\gamma'}$ affecting the changes of δy_t due to the variations of the design variable $\delta\gamma'$ for free head single pile with length L = 10T subjected to lateral forces P_i (kN)

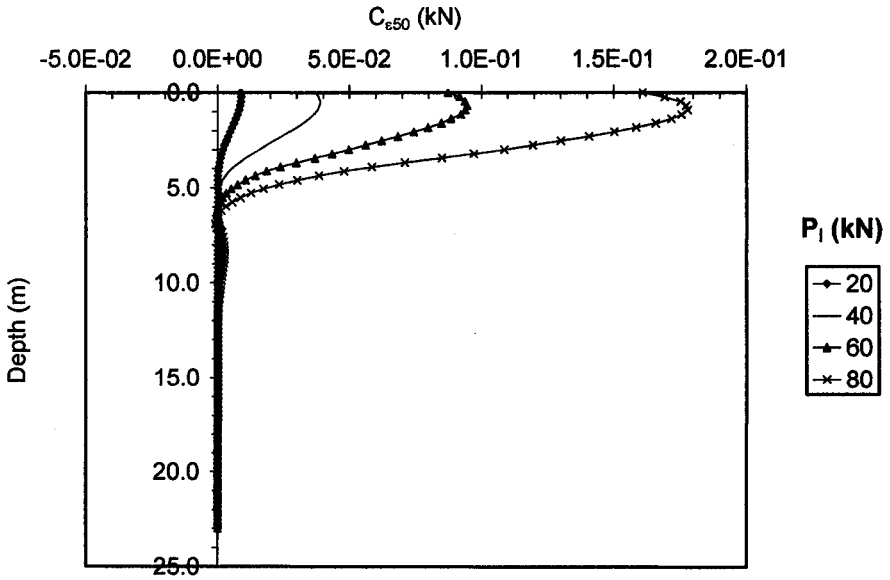

Fig. E.9a Distributions of sensitivity operators $C_{\varepsilon 50}$ affecting the changes of δy_t due to the variations of the design variable $\delta\varepsilon_{50}$ for free head single pile with length L = 10T subjected to lateral forces P_i (kN)

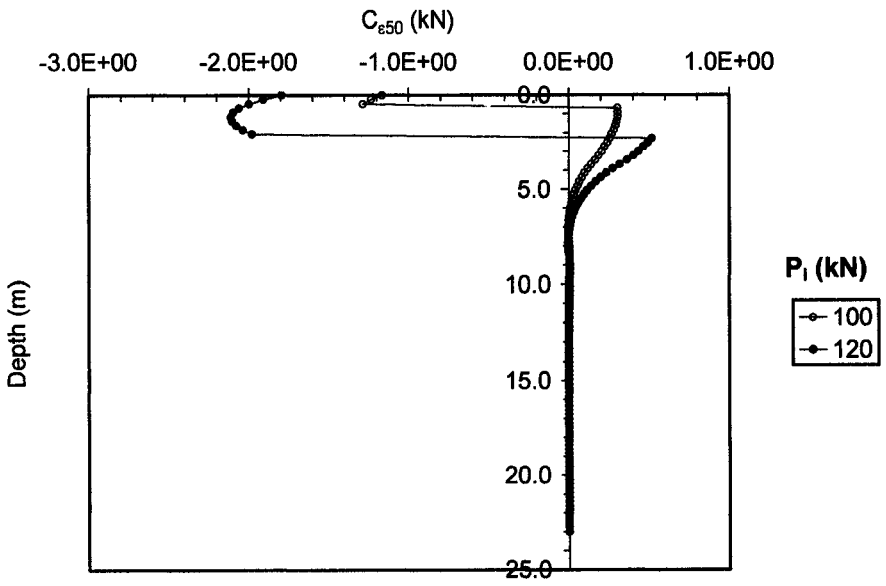

Fig. E.9b Distributions of sensitivity operators $C_{\varepsilon 50}$ affecting the changes of δy_t due to the variations of the design variable $\delta\varepsilon_{50}$ for free head single pile with length L = 10T subjected to lateral forces P_i (kN)

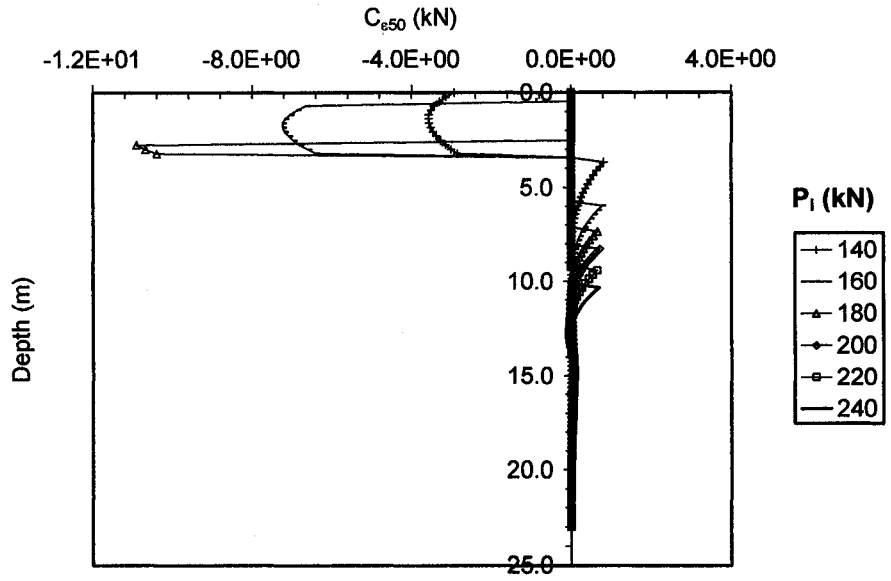

Fig. E.9c Distributions of sensitivity operators $C_{\varepsilon 50}$ affecting the changes of δy_t due to the variations of the design variable $\delta\varepsilon_{50}$ for free head single pile with length L = 10T subjected to lateral forces P_i (kN)

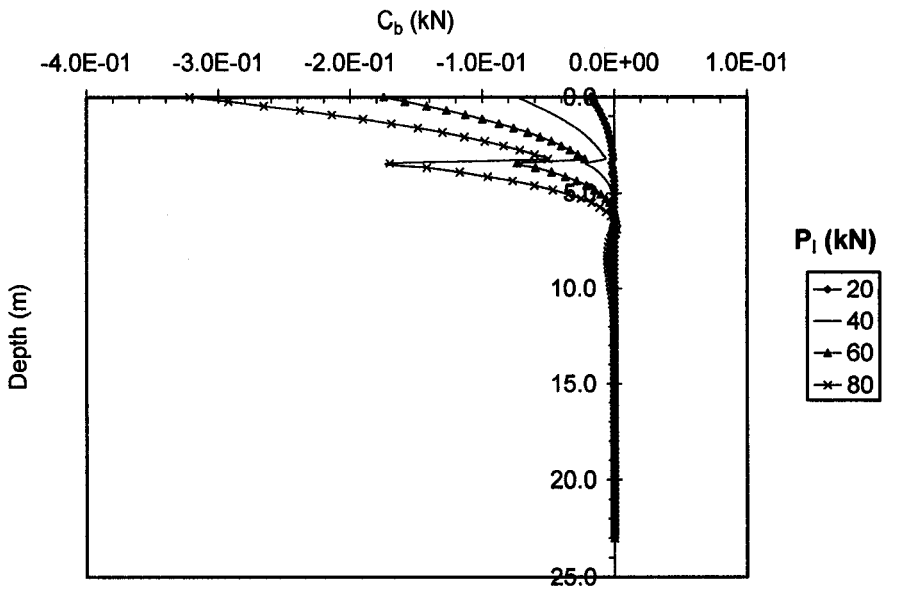

Fig. E.10a Distributions of sensitivity operators C_b affecting the changes of δy_t due to the variations of the design variable δb for free head single pile with length L = 10T subjected to lateral forces P_i (kN)

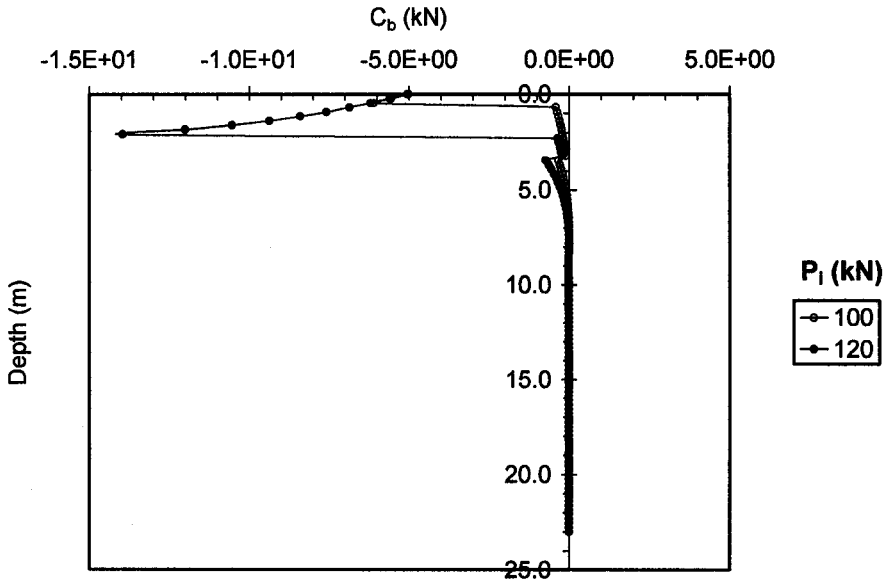

Fig. E.10b Distributions of sensitivity operators C_b affecting the changes of δy_t due to the variations of the design variable δb for free head single pile with length L = 10T subjected to lateral forces P_i (kN)

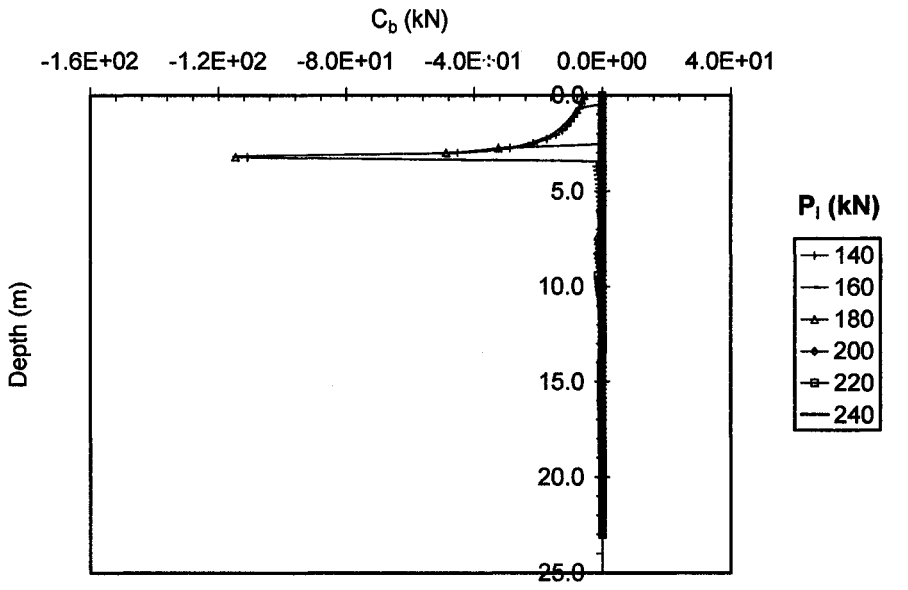

Fig. E.10c Distributions of sensitivity operators C_b affecting the changes of δy_t due to the variations of the design variable δb for free head single pile with length L = 10T subjected to lateral forces P_i (kN)

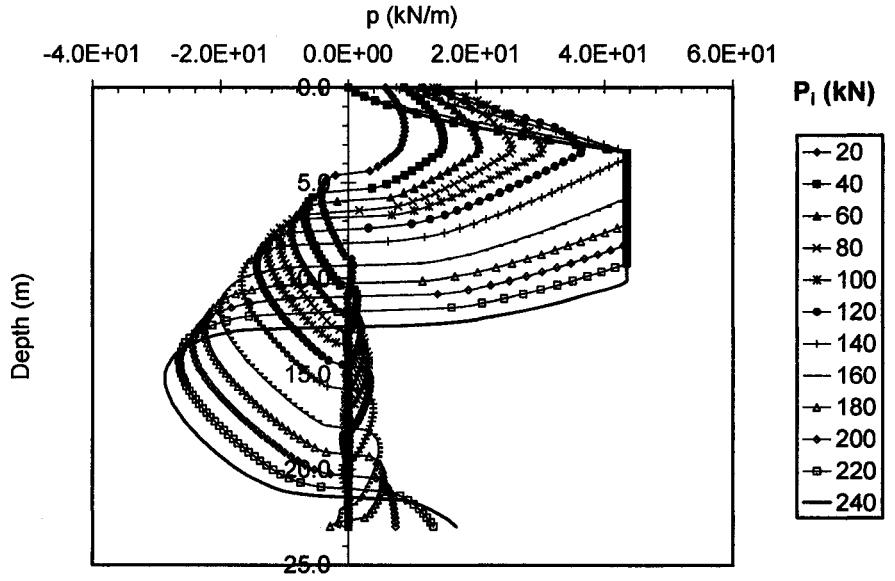

Fig. E.11 Distributions of soil reaction p at the primary structure along the depth of the pile for sensitivity analysis of top lateral displacement δy_t for free head single pile with length L = 10T subjected to lateral forces P_i (kN)

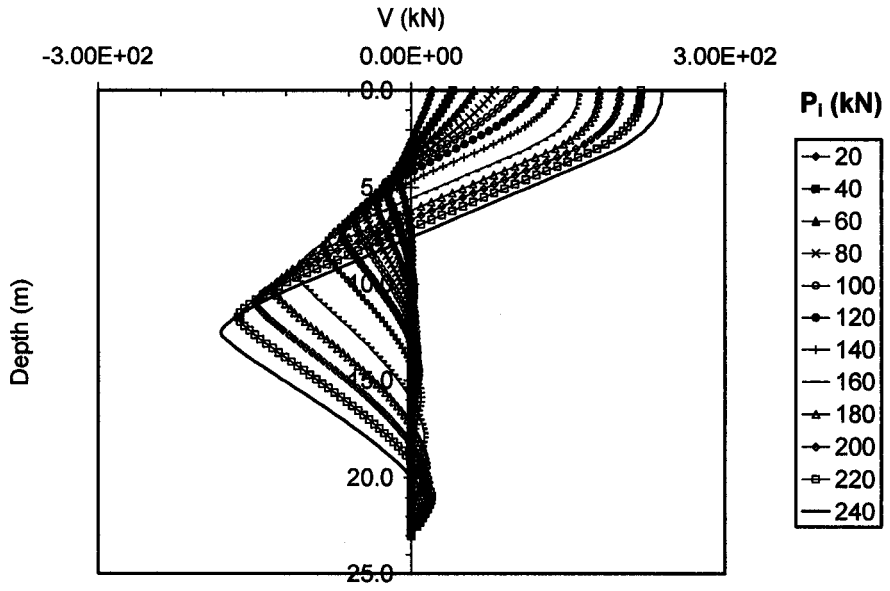

Fig. E.12 Distributions of shear forces V at the primary structure along the depth of the pile for sensitivity analysis of top lateral displacement δy_t for free head single pile with length L = 10T subjected to lateral forces P_i (kN)

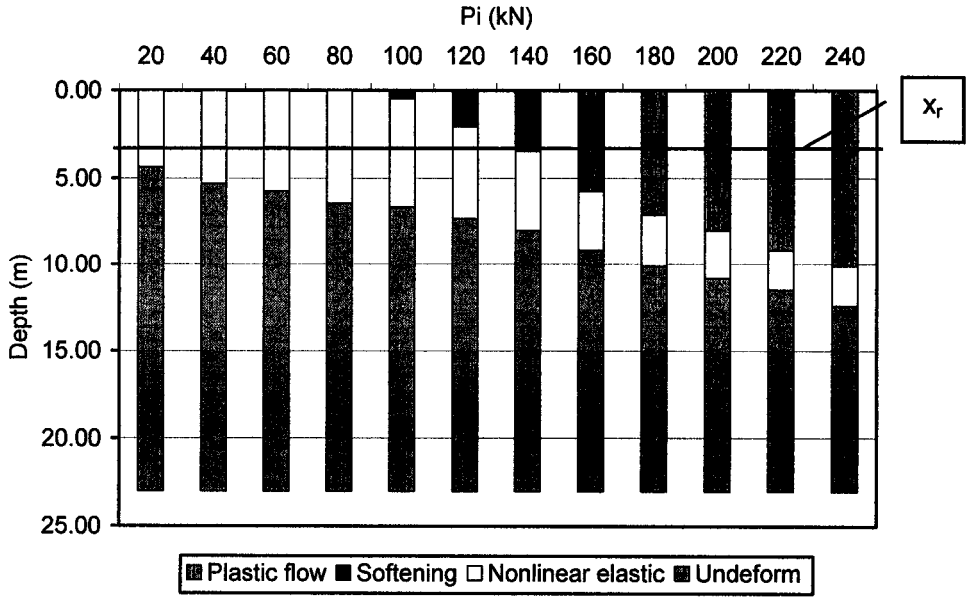

Fig. E.13 Quantitative assessment of the location and the size of soil phases developed with depth determined based on the distributions of sensitivity operators affecting δy_t for free head single pile with length L = 10T subjected to lateral forces P_i (kN)

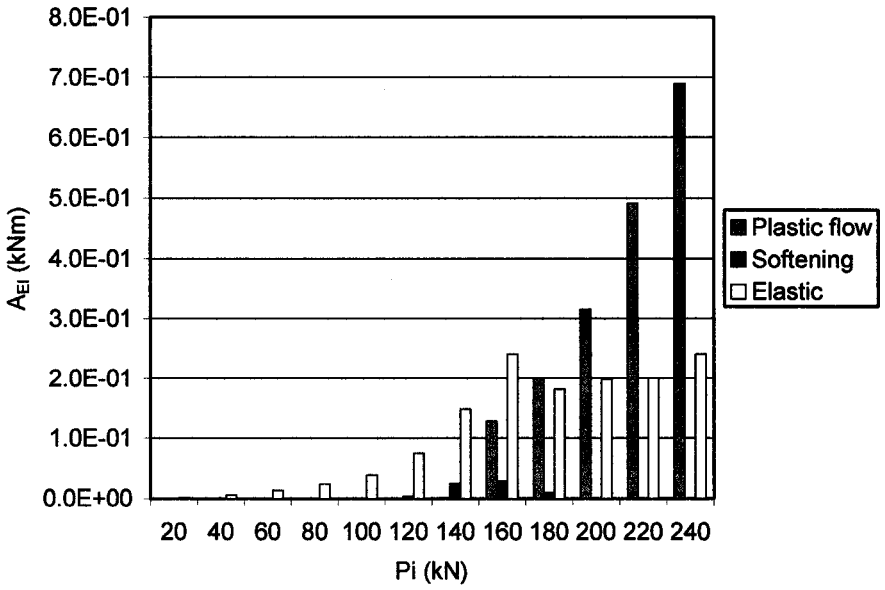

Fig. E.14a Quantitative assessment of sensitivity A_{EI} associated with development of nonlinear elastic, linear softening, and plastic flow stages in the soil along the pile axis that affect δy_t for free head single pile with length L = 10T subjected to lateral forces P_i (kN)

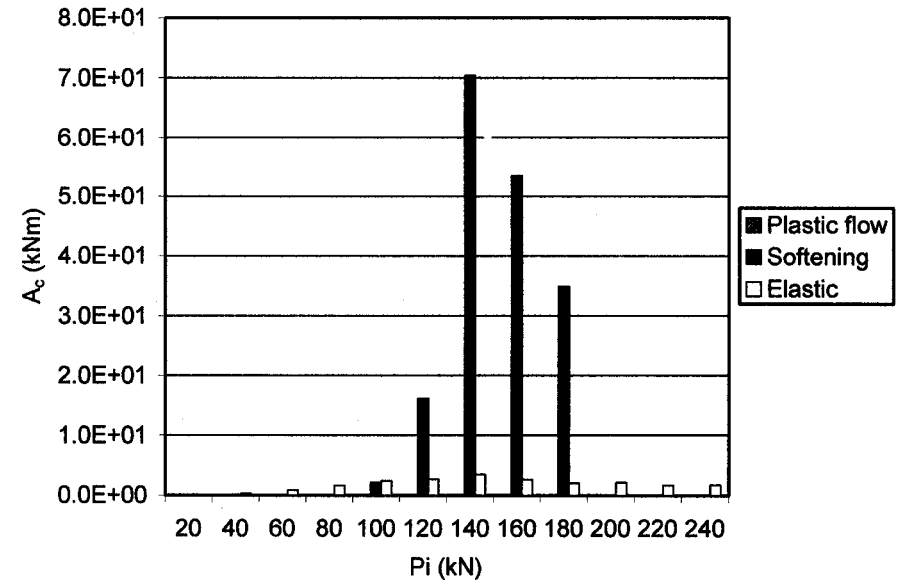

Fig. E.14b Quantitative assessment of sensitivity A_c associated with development of nonlinear elastic, linear softening, and plastic flow stages in the soil along the pile axis that affect δy_t for free head single pile with length L = 10T subjected to lateral forces P_i (kN)

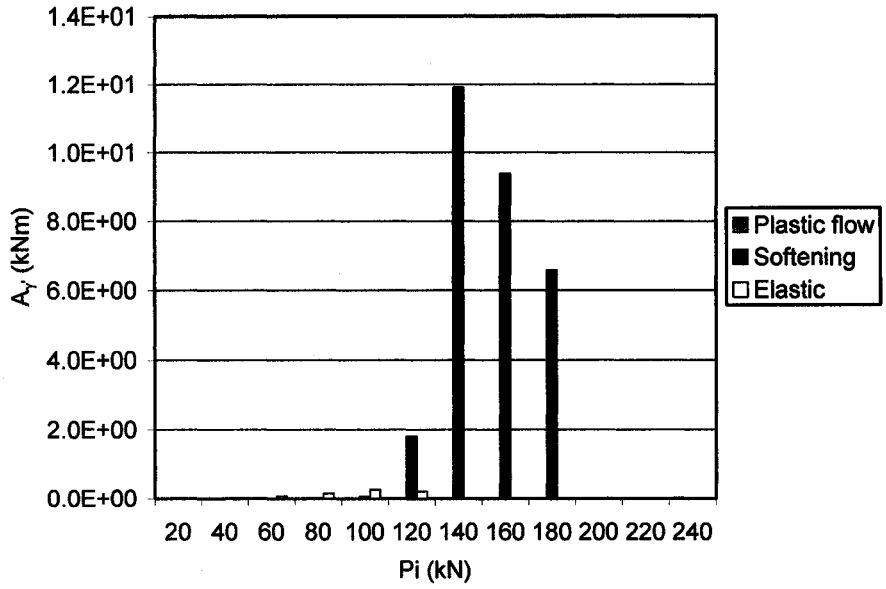

Fig. E.14c Quantitative assessment of sensitivity A_γ associated with development of nonlinear elastic, linear softening, and plastic flow stages in the soil along the pile axis that affect δy_t for free head single pile with length L = 10T subjected to lateral forces P_i (kN)

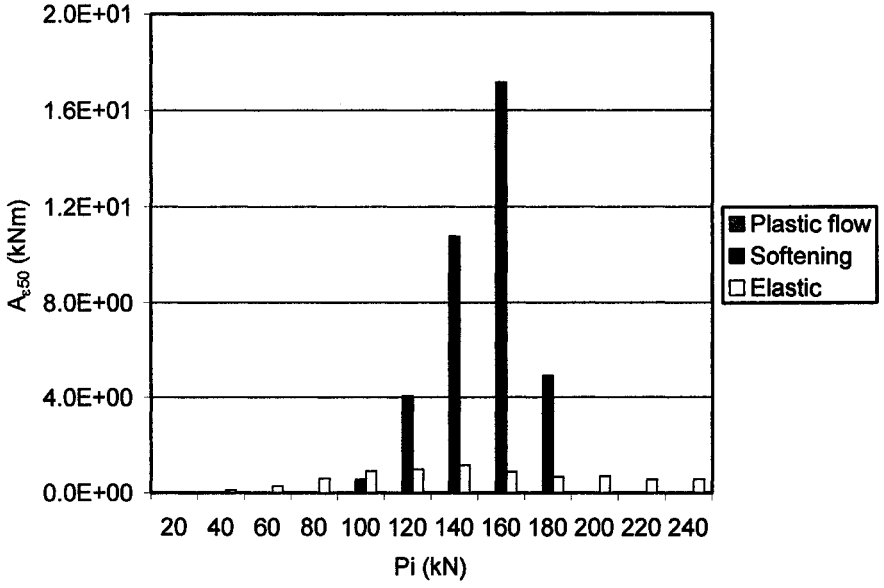

Fig. E.14d Quantitative assessment of sensitivity $A_{\varepsilon 50}$ associated with development of nonlinear elastic, linear softening, and plastic flow stages in the soil along the pile axis that affect δy_t for free head single pile with length L = 10T subjected to lateral forces P_i (kN)

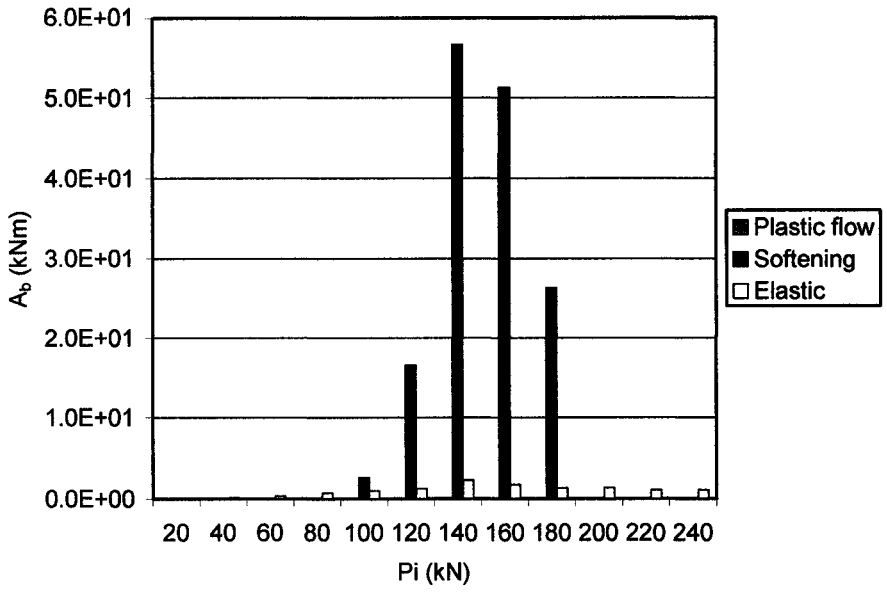

Fig. E.14e Quantitative assessment of sensitivity A_b associated with development of nonlinear elastic, linear softening, and plastic flow stages in the soil along the pile axis that affect δy_t for free head single pile with length L = 10T subjected to lateral forces P_i (kN)

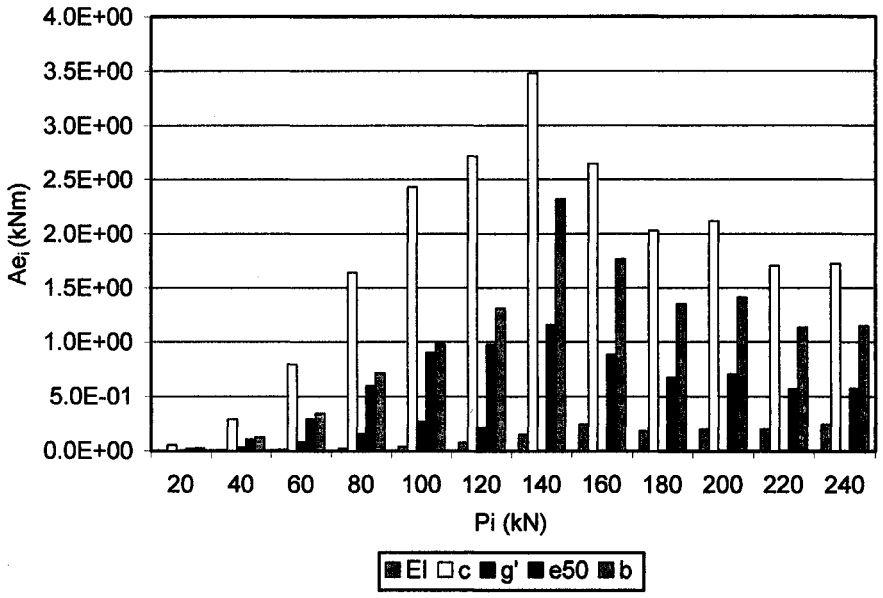

Fig. E.14f Quantitative assessment of sensitivities Ae_i that contains Ae_{EI}, Ae_c, $Ae_{\gamma'}$, $Ae_{\varepsilon 50}$, and Ae_b associated with the development of the nonlinear elastic stage in the soil along the pile axis that affect δy_t for free head single pile with length L = 10T subjected to lateral forces P_i (kN)

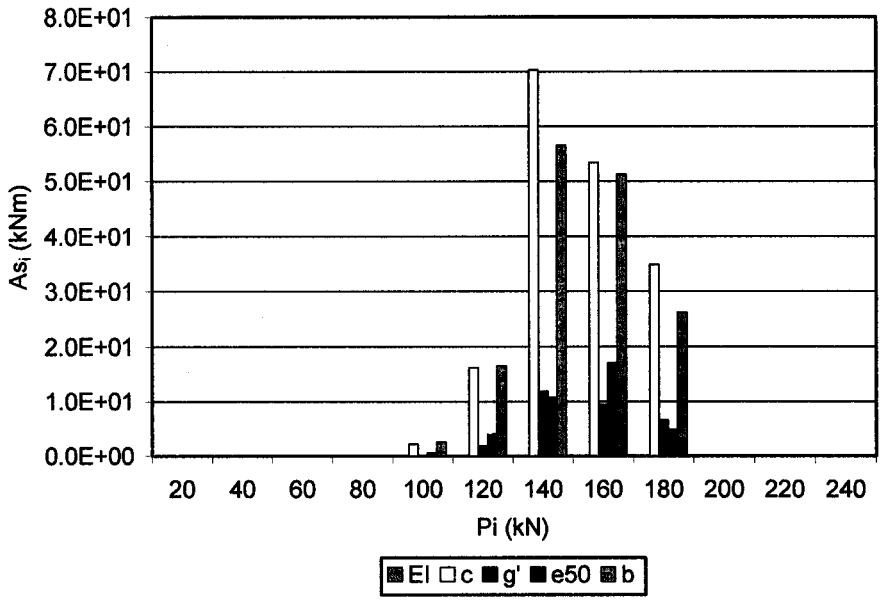

Fig. E.14g Quantitative assessment of sensitivities As_i that contains As_{EI}, As_c, $As_{\gamma'}$, $As_{\varepsilon 50}$, and As_b associated with the development of the linear softening stage in the soil along the pile axis that affect δy_t for free head single pile with length L = 10T subjected to lateral forces P_i (kN)

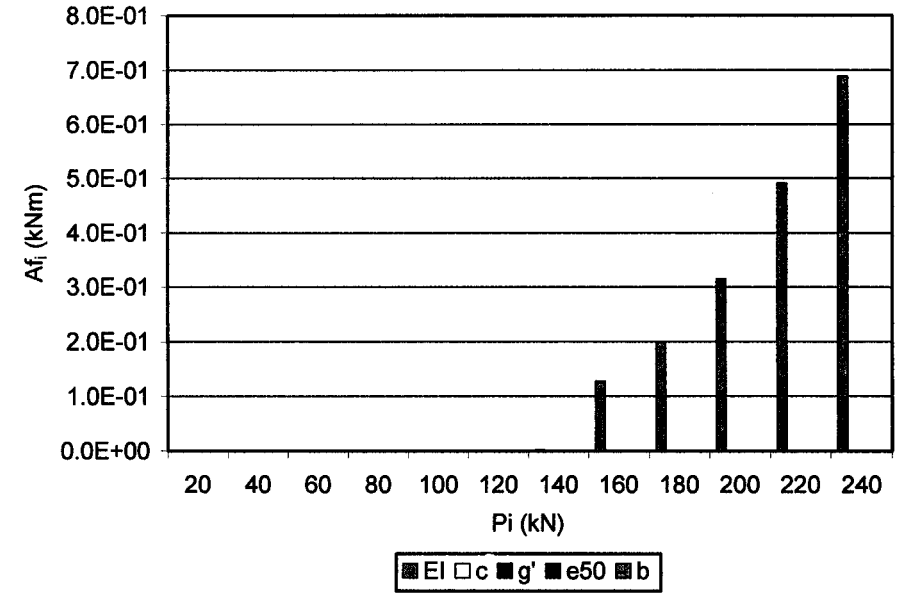

Fig. E.14h Quantitative assessment of sensitivities Af_i that contains Af_{EI}, Af_c, $Af_{\gamma'}$, $Af_{\varepsilon 50}$, and Af_b associated with the development of the plastic flow stage in the soil along the pile axis that affect δy_t for free head single pile with length L = 10T subjected to lateral forces P_i (kN)

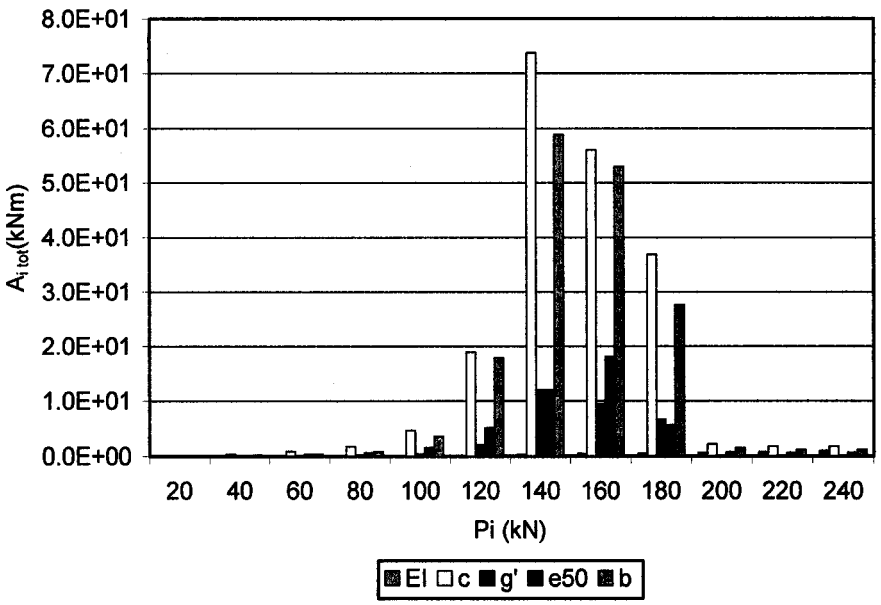

Fig. E.14i Quantitative assessment of sensitivities $A_{i\ tot}$ that contains (A_{EI}, A_c, $A_{\gamma'}$, $A_{\varepsilon 50}$, and A_b)$_{tot}$ associated with the development of three stages in the soil along the pile axis that affect δy_t for free head single pile with length L = 10T subjected to lateral forces P_i (kN)

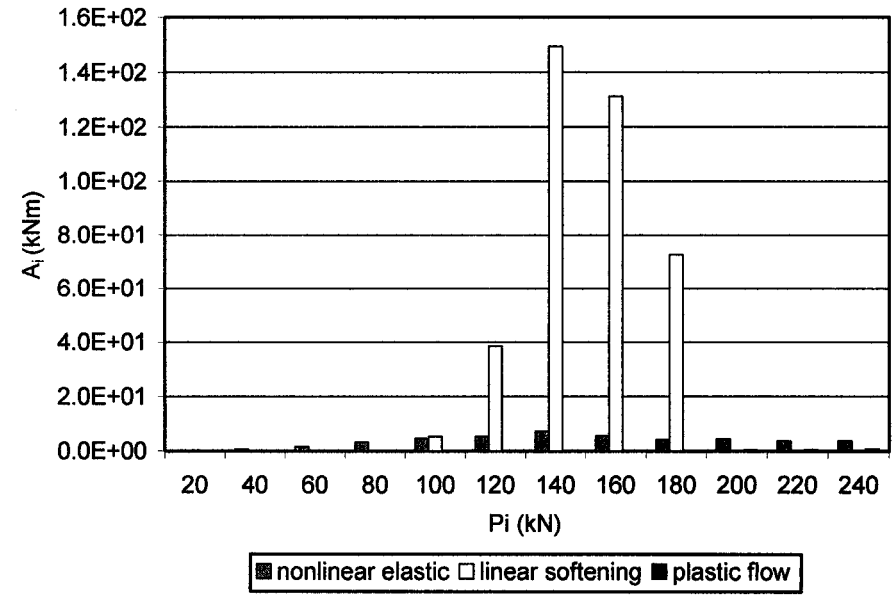

Fig. E.14j.1 Quantitative assessment of sensitivities A_i that is summation of (A_{EI}, A_c, $A_{\gamma'}$, $A_{\varepsilon 50}$, and A_b)$_i$ of each soil stage that affect δy_t for free head single pile with length L = 10T subjected to lateral forces P_i (kN)

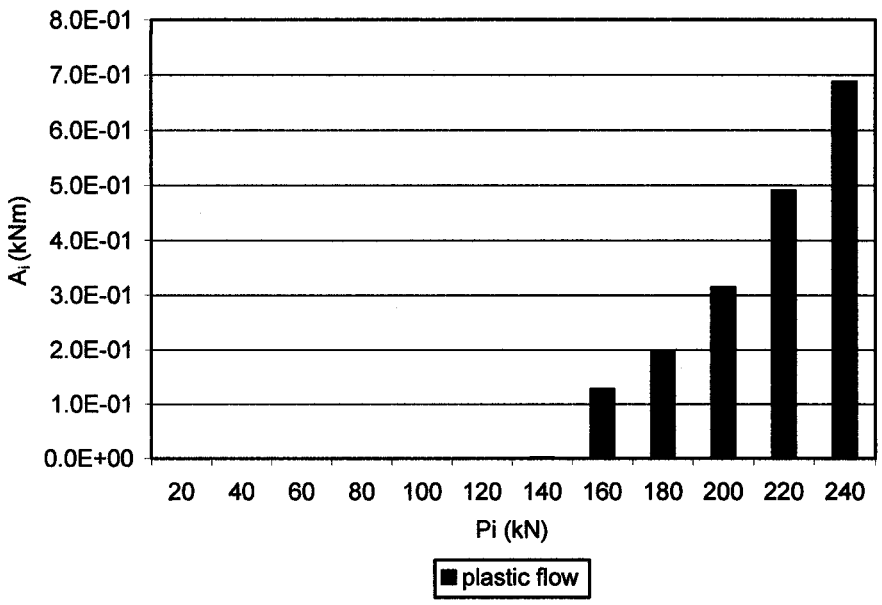

Fig. E.14j.2 Quantitative assessment of sensitivities A_i that is summation of (A_{EI}, A_c, $A_{\gamma'}$, $A_{\varepsilon 50}$, and A_b)$_i$ of each soil stage that affect δy_t for free head single pile with length L = 10T subjected to lateral forces P_i (kN)

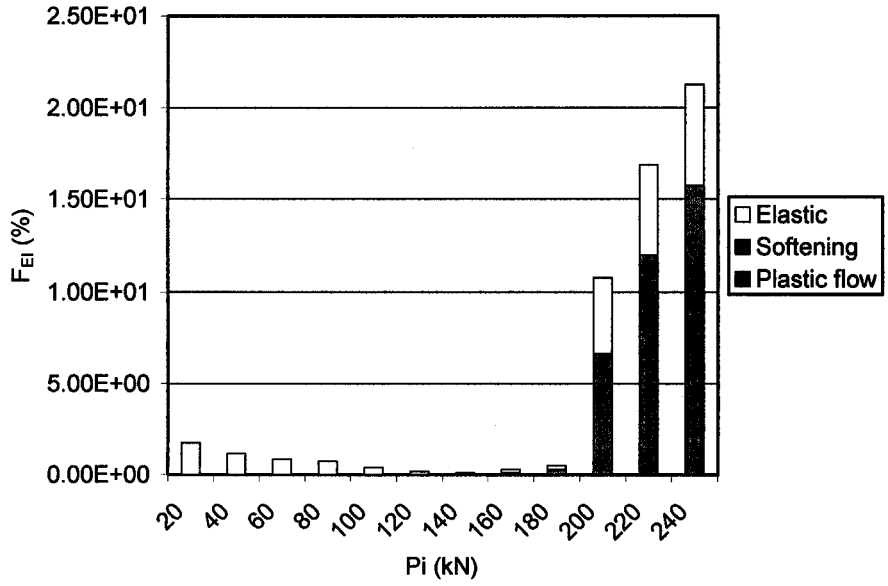

Fig. E.15a Quantitative assessment (in %) of relative sensitivity factors F_{EI} that affect δy_t for free head single pile with length L = 10T subjected to lateral forces P_i (kN)

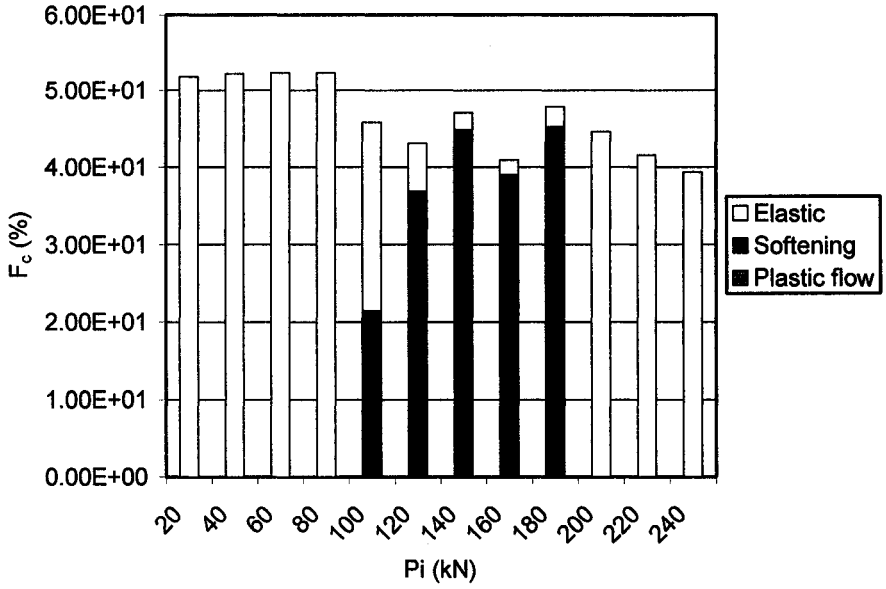

Fig. E.15b Quantitative assessment (in %) of relative sensitivity factors F_c that affect δy_t for free head single pile with length L = 10T subjected to lateral forces P_i (kN)

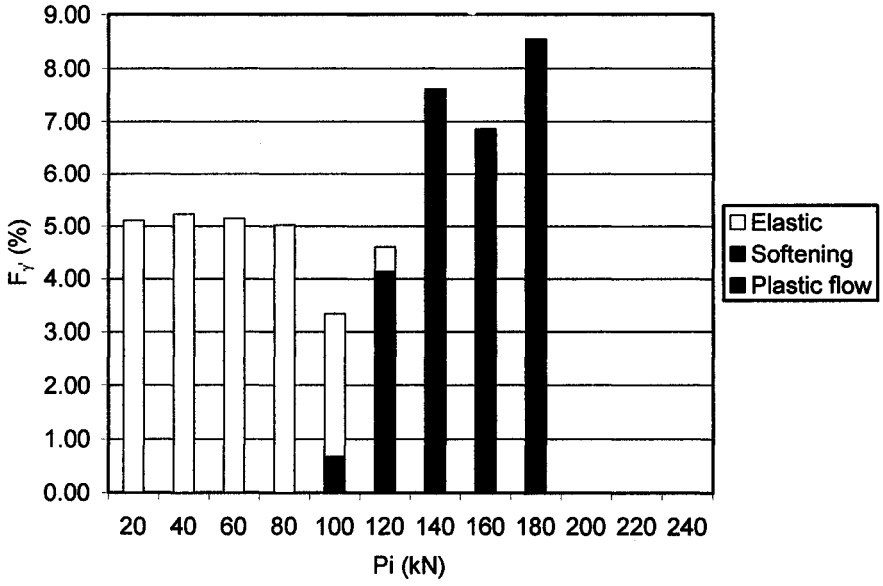

Fig. E.15c Quantitative assessment (in %) of relative sensitivity factors F_γ that affect δy_t for free head single pile with length L = 10T subjected to lateral forces P_i (kN)

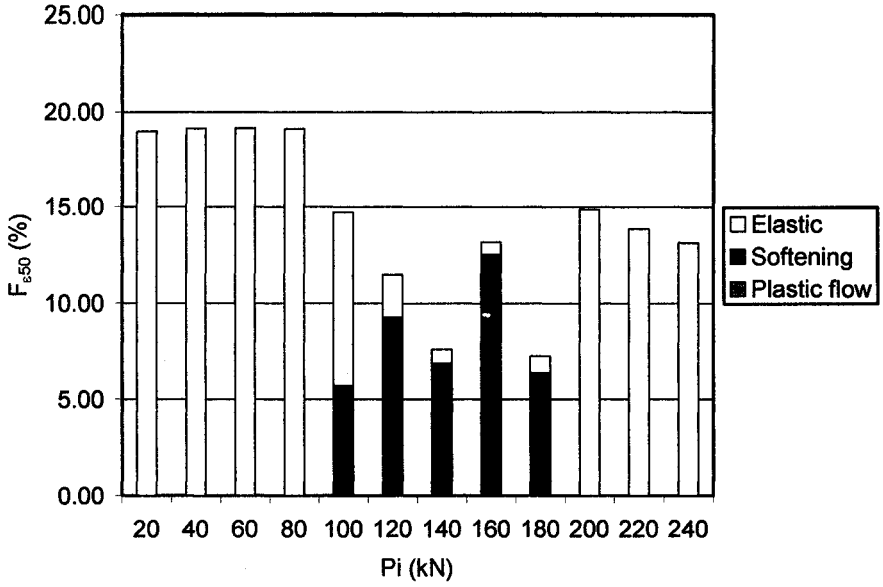

Fig. E.15d Quantitative assessment (in %) of relative sensitivity factors $F_{\varepsilon 50}$ that affect δy_t for free head single pile with length L = 10T subjected to lateral forces P_i (kN)

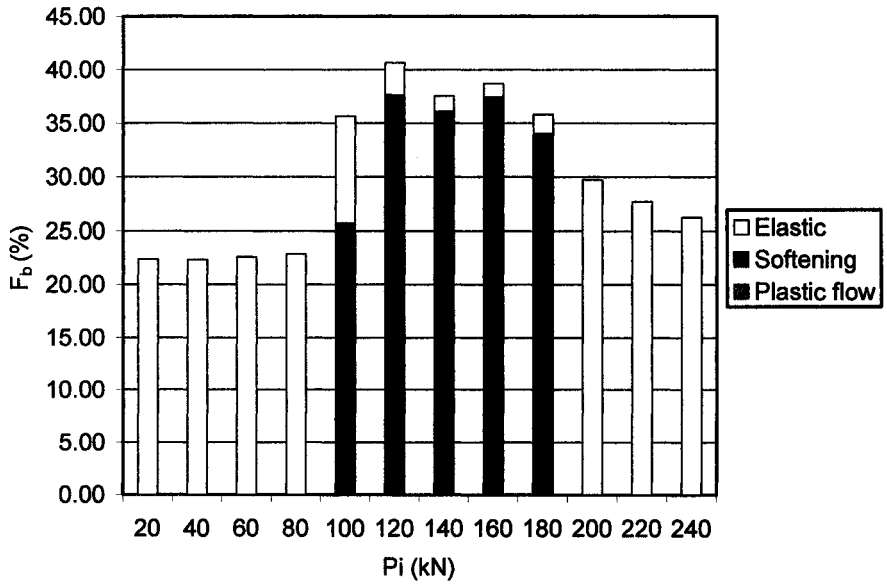

Fig. E.15e Quantitative assessment (in %) of relative sensitivity factors F_b that affect δy_t for free head single pile with length L = 10T subjected to lateral forces P_i (kN)

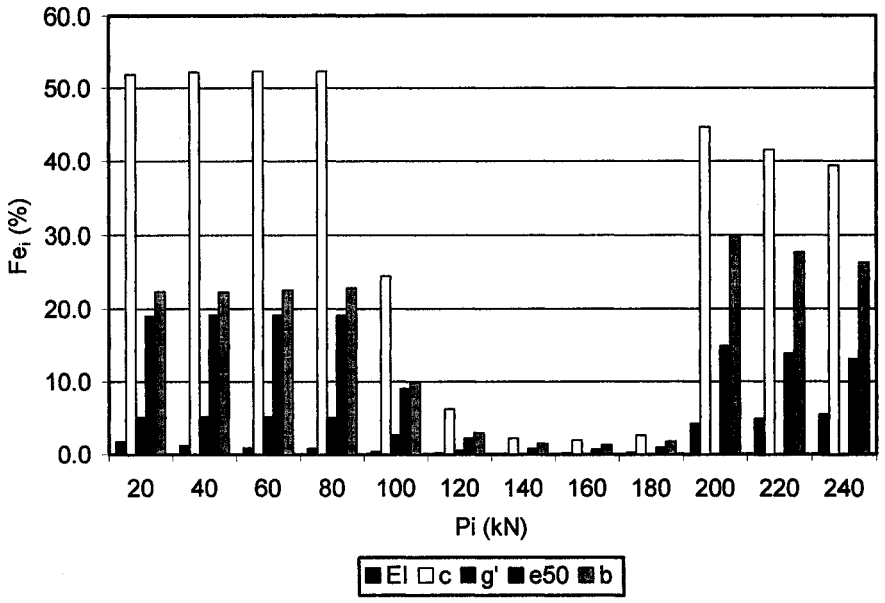

Fig. E.15f Quantitative assessment (in %) of relative sensitivity factors Fe_i that contains Fe_{EI}, Fe_c, $Fe_{\gamma'}$, $Fe_{\varepsilon 50}$, and Fe_b associated with the nonlinear elastic soil stage developed along the pile axis that affect δy_t for free head single pile with length L = 10T subjected to lateral forces P_i (kN)

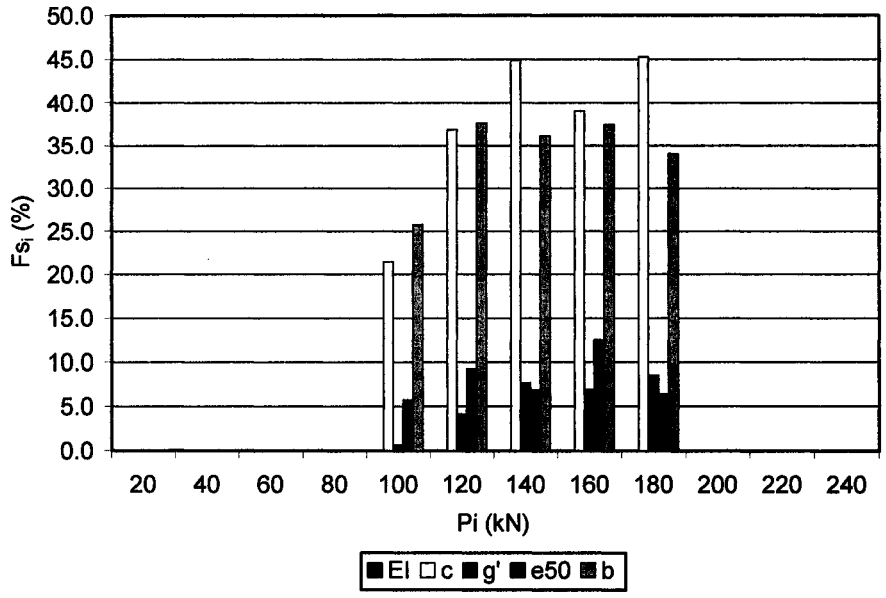

Fig. E.15g Quantitative assessment (in %) of relative sensitivity factors Fs_i that contains Fs_{EI}, Fs_c, $Fs_{\gamma'}$, $Fs_{\varepsilon 50}$, and Fs_b associated with the linear softening stage developed along the pile axis that affect δy_t for free head single pile with length L = 10T subjected to lateral forces P_i (kN)

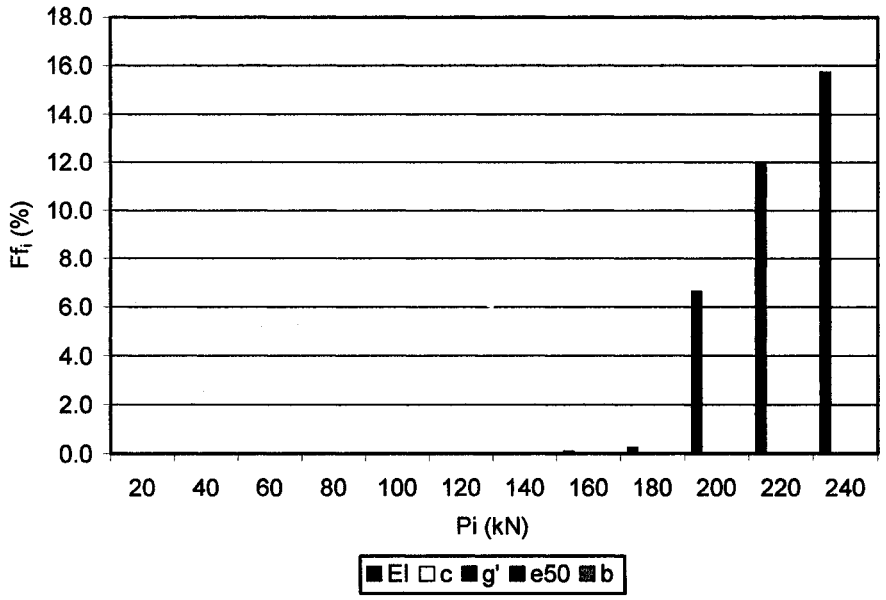

Fig. E.15h Quantitative assessment (in %) of relative sensitivity factors Ff_i that contains Ff_{EI}, Ff_c, $Ff_{\gamma'}$, $Ff_{\varepsilon 50}$, and Ff_b associated with the nonlinear elastic soil stage developed along the pile axis that affect δy_t for free head single pile with length L = 10T subjected to lateral forces P_i (kN)

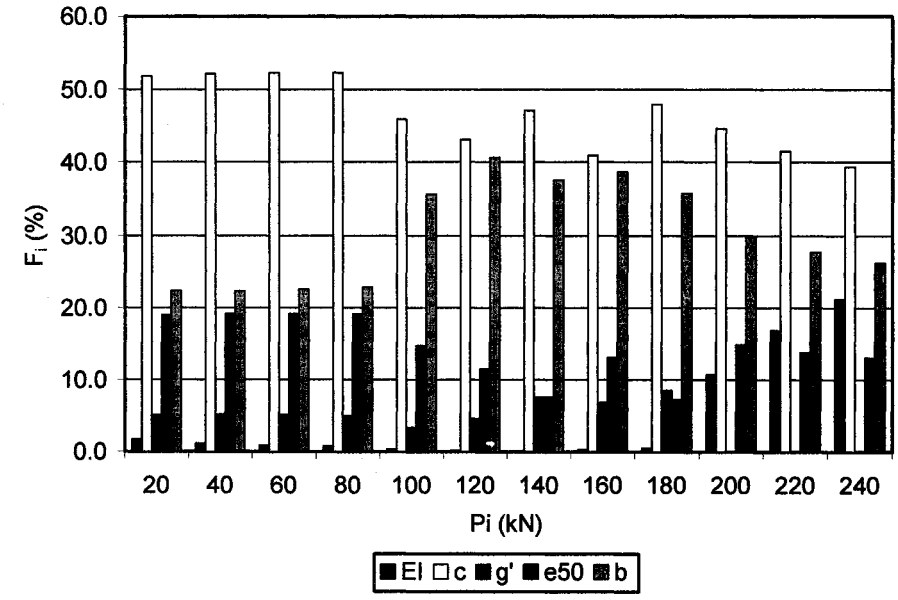

Fig. E.15i Quantitative assessment (in %) of relative sensitivity factors F_i that contains F_{EI}, F_c, $F_{\gamma'}$, $F_{\varepsilon 50}$, and F_b associated with all soil stages developed along the pile axis that affect δy_t for free head single pile with length L = 10T subjected to lateral forces P_i (kN)

APPENDIX F:

Sensitivity analysis of top lateral displacement δy_t for single fixed head pile with length L = 3T subjected to lateral forces Pi

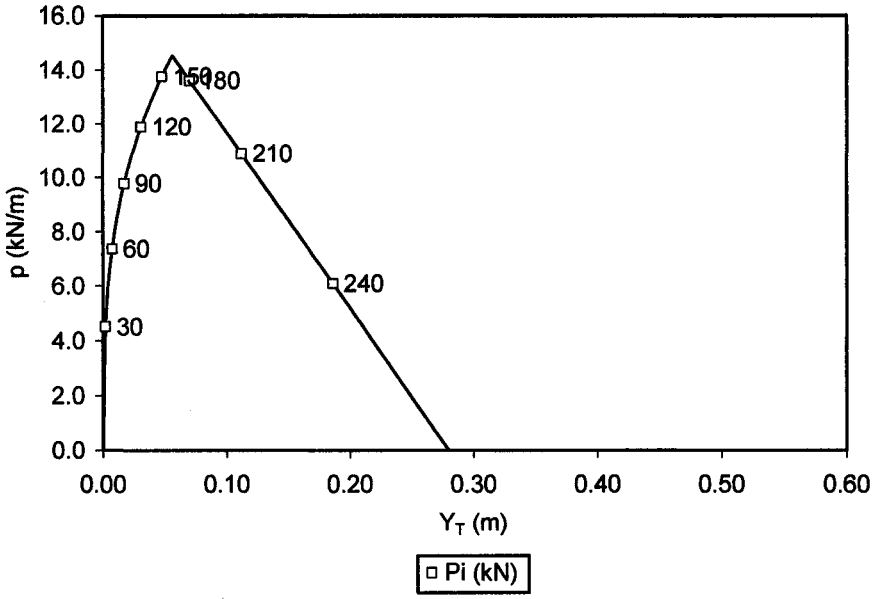

Fig. F.1 Soil reaction p at the top surface (expressed in terms of lateral loading) vs. lateral displacement generated by lateral loading applied to the pile for sensitivity analysis of top lateral displacement δy_t for fixed head single pile with length L = 3T subjected to lateral forces P_i (kN)

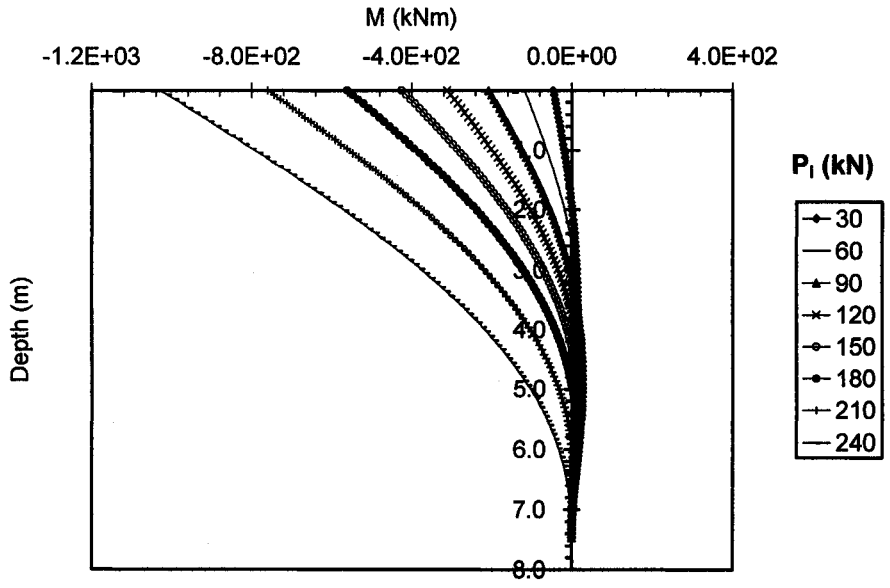

Fig. F.2 Distributions of bending moments at the primary structure M along the depth of the pile for sensitivity analysis of top lateral displacement δy_t for fixed head single pile with length L = 3T subjected to lateral forces P_i (kN)

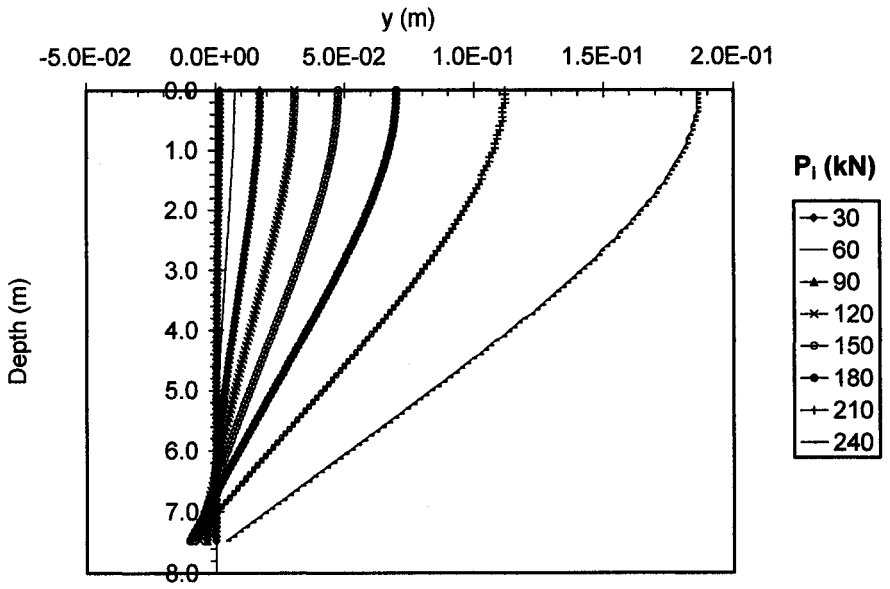

Fig. F.3 Distributions of lateral deflections at the primary structure y along the depth of the pile for sensitivity analysis of top lateral displacement δy_t for fixed head single pile with length L = 3T subjected to lateral forces P_i (kN)

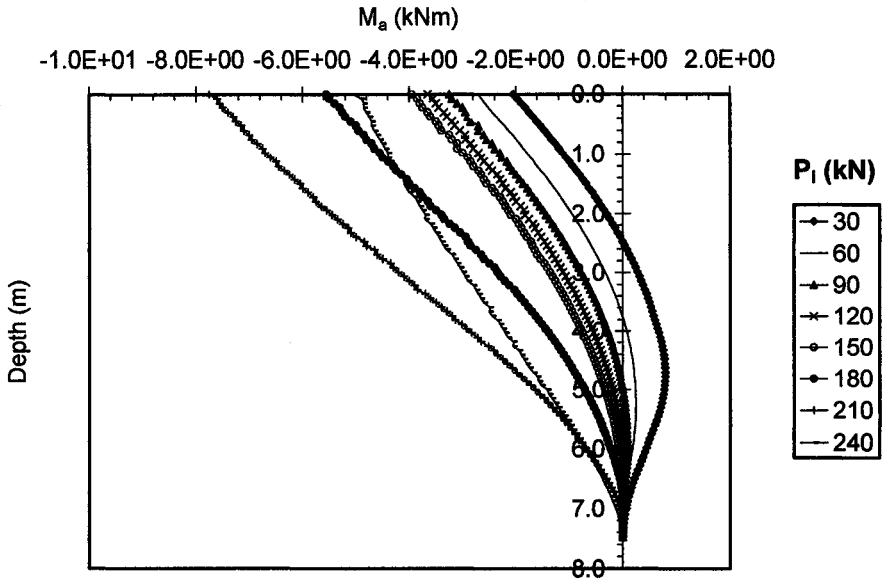

Fig. F.4 Distributions of bending moments M_a along the depth of the pile at the adjoint structure for sensitivity analysis of top lateral displacement δy_t for fixed head single pile with length L = 3T subjected to lateral forces P_i (kN)

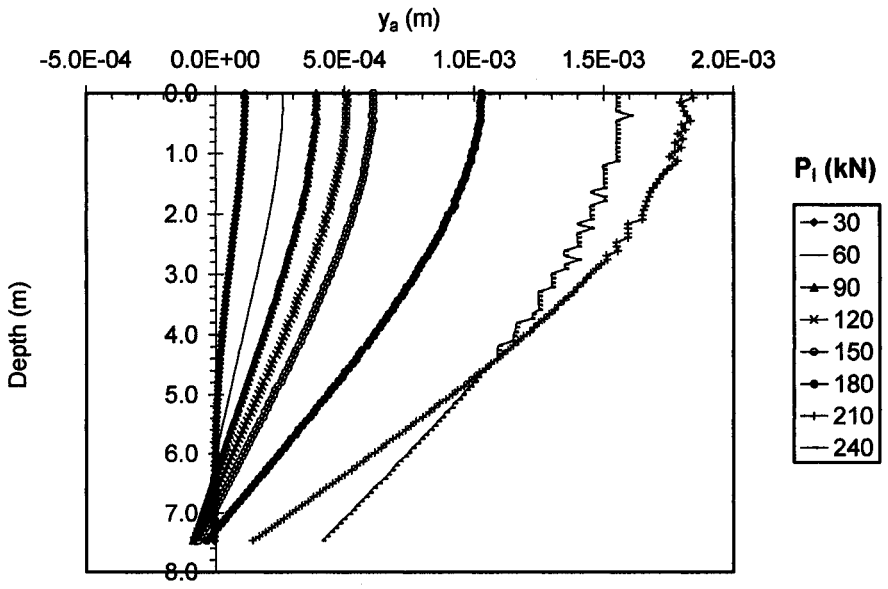

Fig. F.5 Distributions of lateral deflections at the adjoint structure y_a along the depth of the pile for sensitivity analysis of top lateral displacement δy_t for fixed head single pile with length L = 3T subjected to lateral forces P_i (kN)

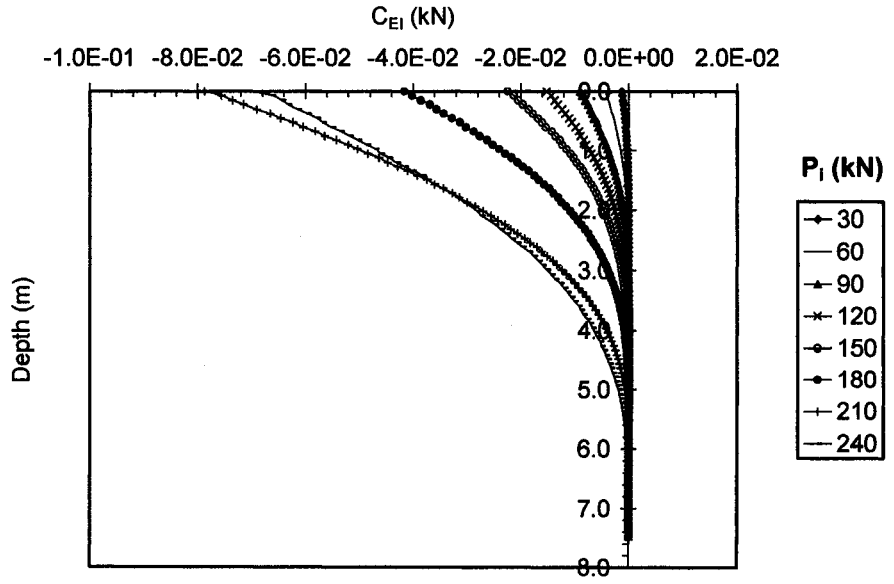

Fig. F.6 Distributions of sensitivity operators C_{EI} affecting the changes of δy_t due to variations of the design variable δEI for fixed head single pile with length L = 3T subjected to lateral forces P_i (kN)

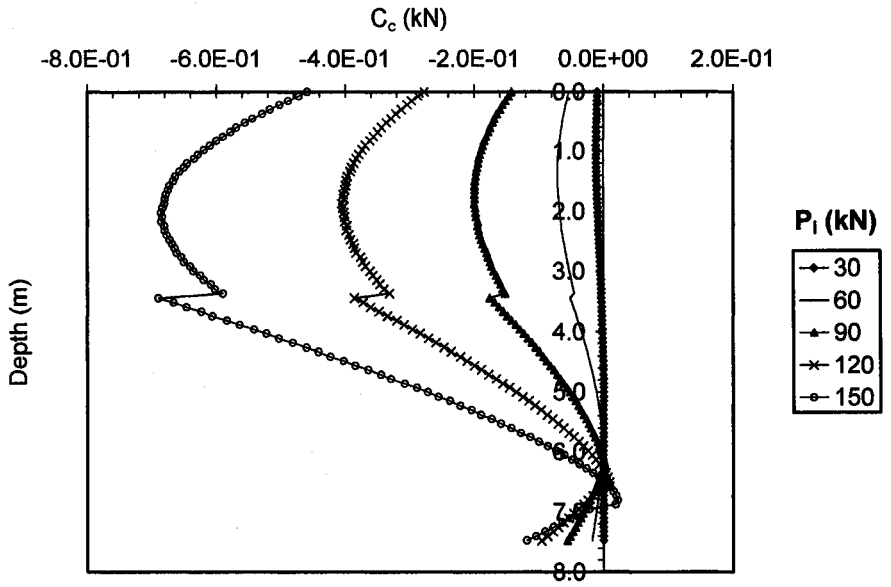

Fig. F.7a Distributions of sensitivity operators C_c affecting the changes of δy_t due to variations of the design variable δc for fixed head single pile with length L = 3T subjected to lateral forces P_i (kN)

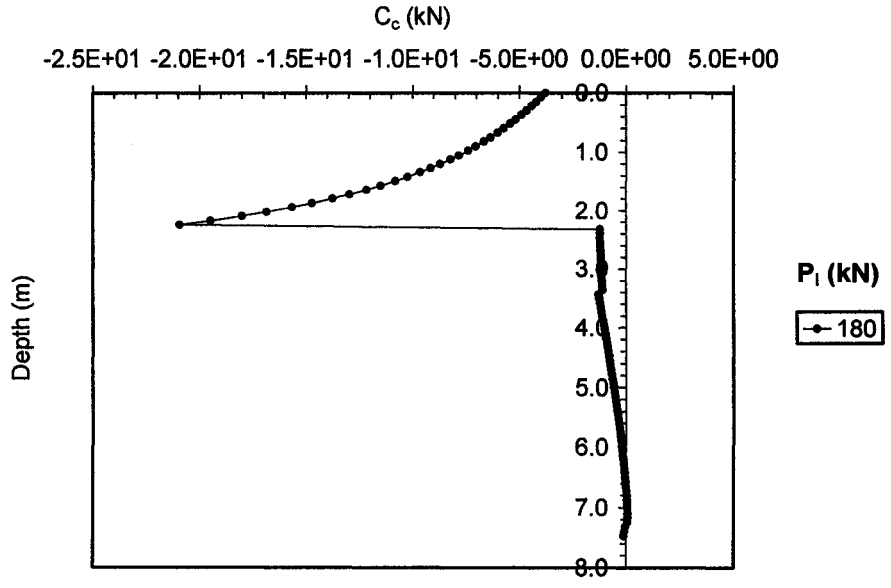

Fig. F.7b Distributions of sensitivity operators C_c affecting the changes of δy_t due to variations of the design variable δc for fixed head single pile with length L = 3T subjected to lateral forces P_i (kN)

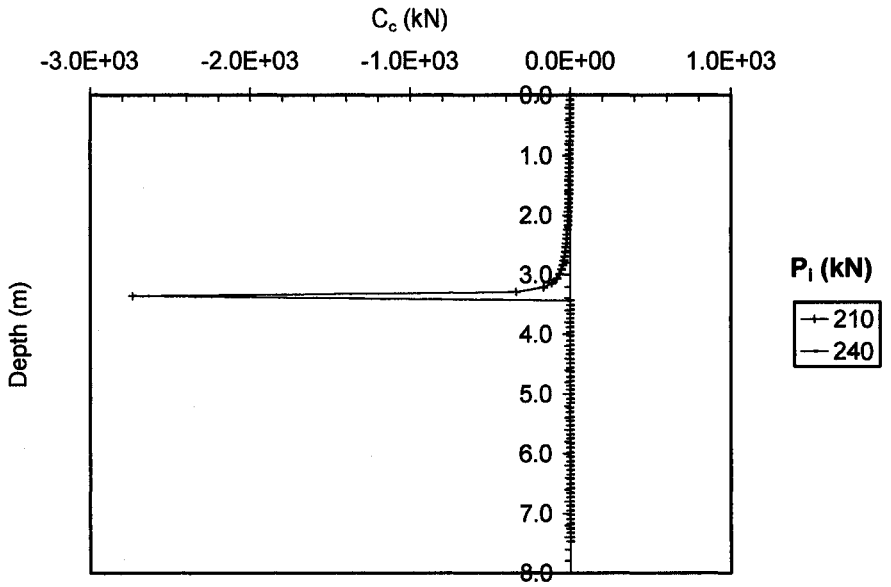

Fig. F.7c Distributions of sensitivity operators C_c affecting the changes of δy_t due to variations of the design variable δc for fixed head single pile with length L = 3T subjected to lateral forces P_i (kN)

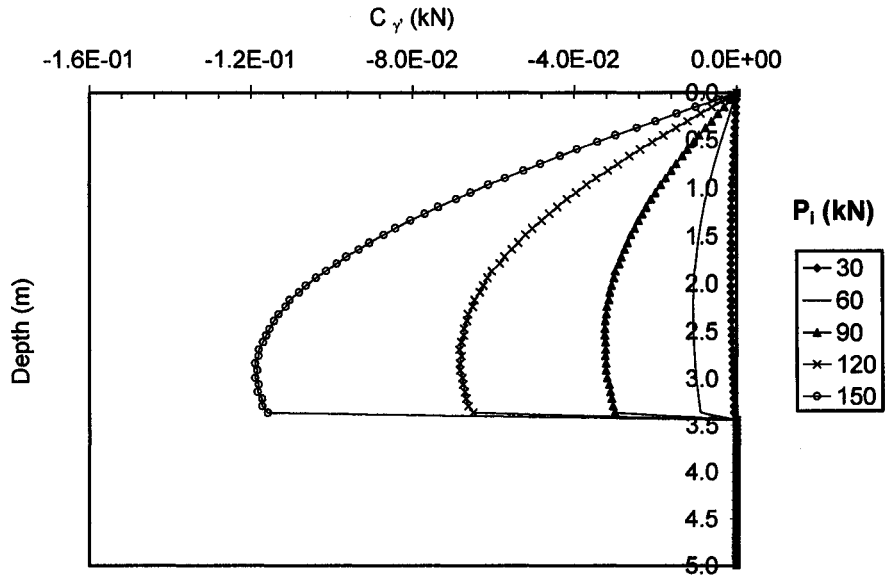

Fig. F.8a Distributions of sensitivity operators $C_{\gamma'}$ affecting the changes of δy_t due to variations of the design variable $\delta\gamma'$ for fixed head single pile with length L = 3T subjected to lateral forces P_i (kN)

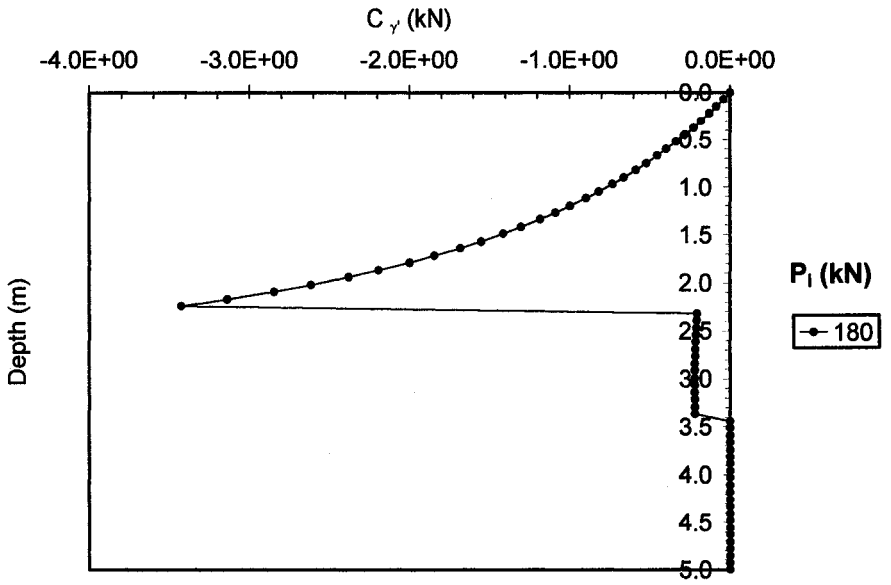

Fig. F.8b Distributions of sensitivity operators $C_{\gamma'}$ affecting the changes of δy_t due to variations of the design variable $\delta\gamma'$ for fixed head single pile with length L = 3T subjected to lateral forces P_i (kN)

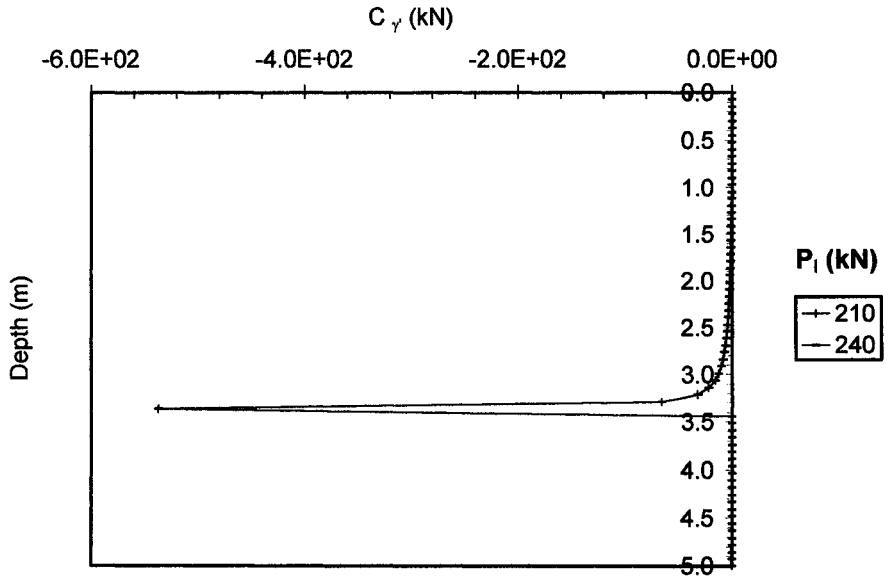

Fig. F.8c Distributions of sensitivity operators $C_{\gamma'}$ affecting the changes of δy_t due to variations of the design variable $\delta\gamma'$ for fixed head single pile with length L = 3T subjected to lateral forces P_i (kN)

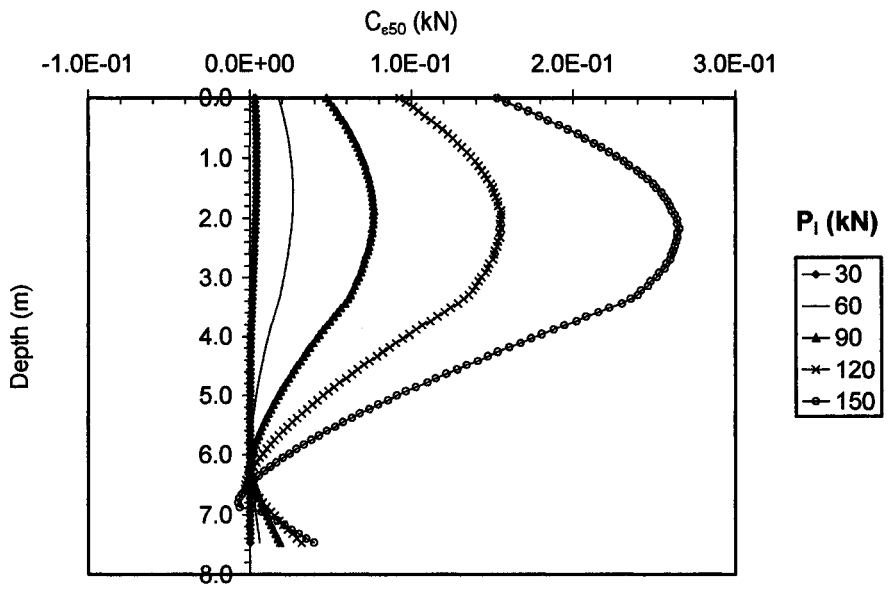

Fig. F.9a Distributions of sensitivity operators $C_{\varepsilon 50}$ affecting the changes of δy_t due to variations of the design variable $\delta\varepsilon_{50}$ for fixed head single pile with length L = 3T subjected to lateral forces P_i (kN)

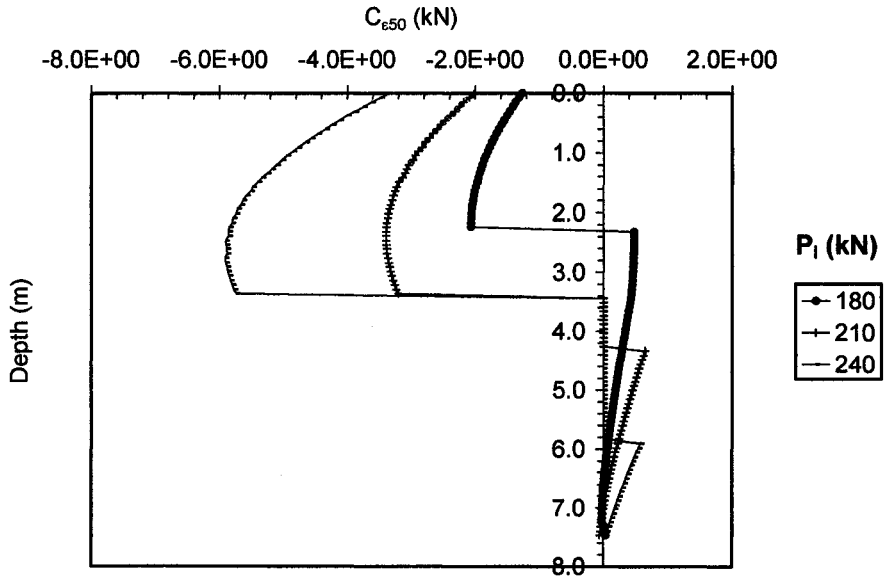

Fig. F.9b Distributions of sensitivity operators $C_{\varepsilon 50}$ affecting the changes of δy_t due to variations of the design variable $\delta\varepsilon_{50}$ for fixed head single pile with length L = 3T subjected to lateral forces P_i (kN)

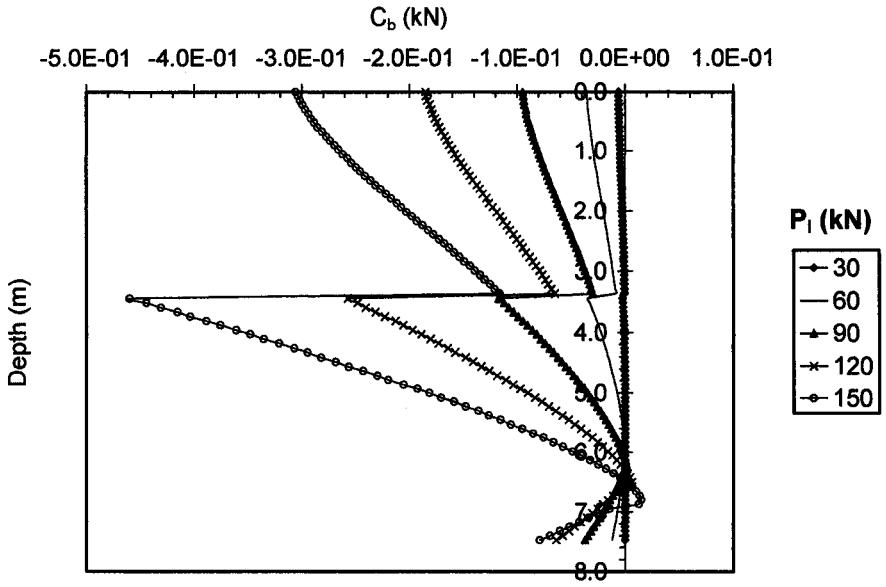

Fig. F.10a Distributions of sensitivity operators C_b affecting the changes of δy_t due to variations of the design variable δb for fixed head single pile with length L = 3T subjected to lateral forces P_i (kN)

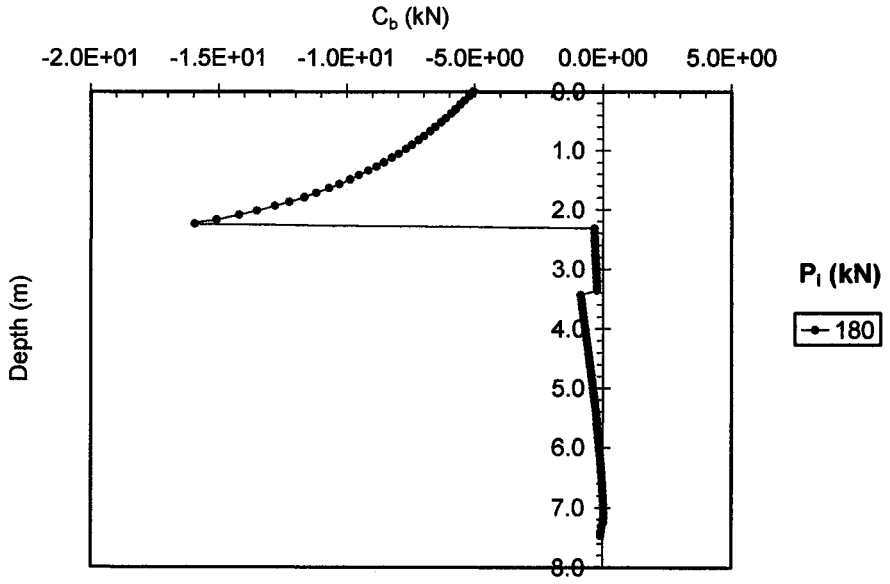

Fig. F.10b Distributions of sensitivity operators C_b affecting the changes of δy_t due to variations of the design variable δb for fixed head single pile with length L = 3T subjected to lateral forces P_i (kN)

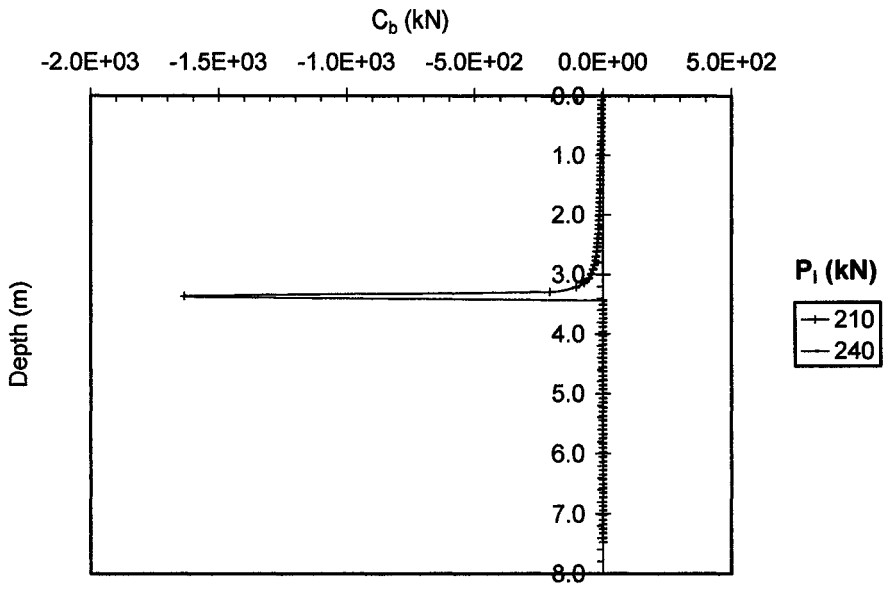

Fig. F.10c Distributions of sensitivity operators C_b affecting the changes of δy_t due to variations of the design variable δb for fixed head single pile with length L = 3T subjected to lateral forces P_i (kN)

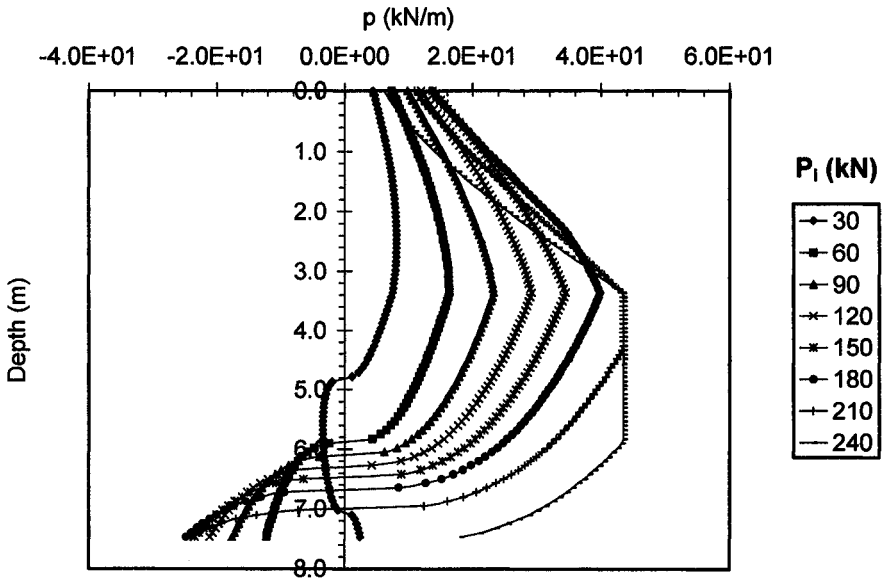

Fig. F.11 Distributions of soil reaction p at the primary structure along the depth of the pile for sensitivity analysis of top lateral displacement δy_t for fixed head single pile with length L = 3T subjected to lateral forces P_i (kN)

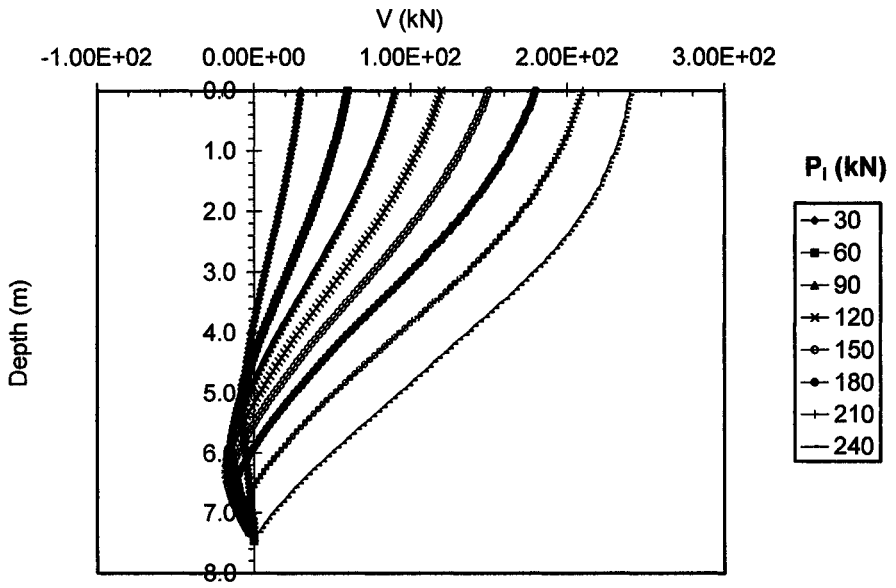

Fig. F.12 Distributions of shear forces V at the primary structure along the depth of the pile for sensitivity analysis of top lateral displacement δy_t for fixed head single pile with length L = 3T subjected to lateral forces P_i (kN)

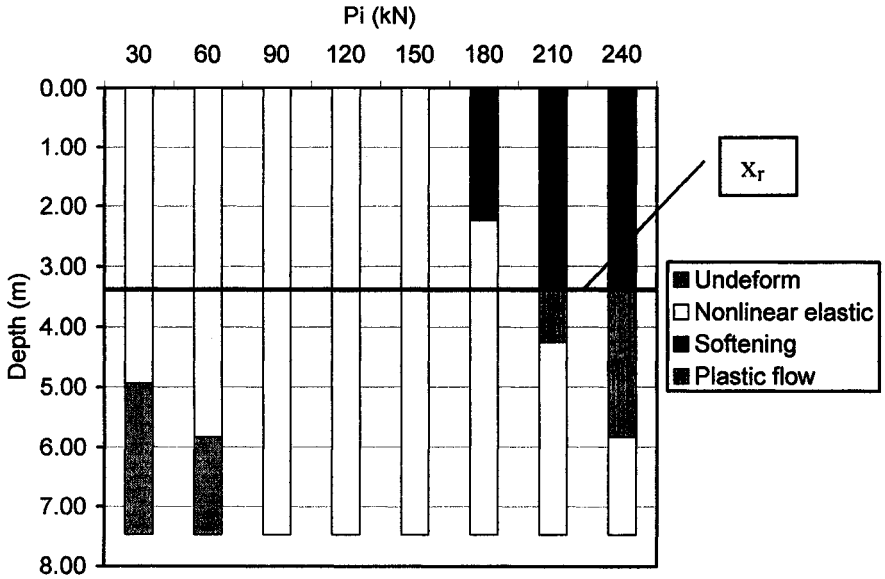

Fig. F.13 Quantitative assessment of location and size of soil phases developed with depth determined based on the distributions of sensitivity operators affecting δy_t for fixed head single pile with length L = 3T subjected to lateral forces P_i (kN)

APPENDIX G:

Sensitivity analysis of top lateral displacement δy_t for single fixed head pile with length L = 10T subjected to lateral forces P_i

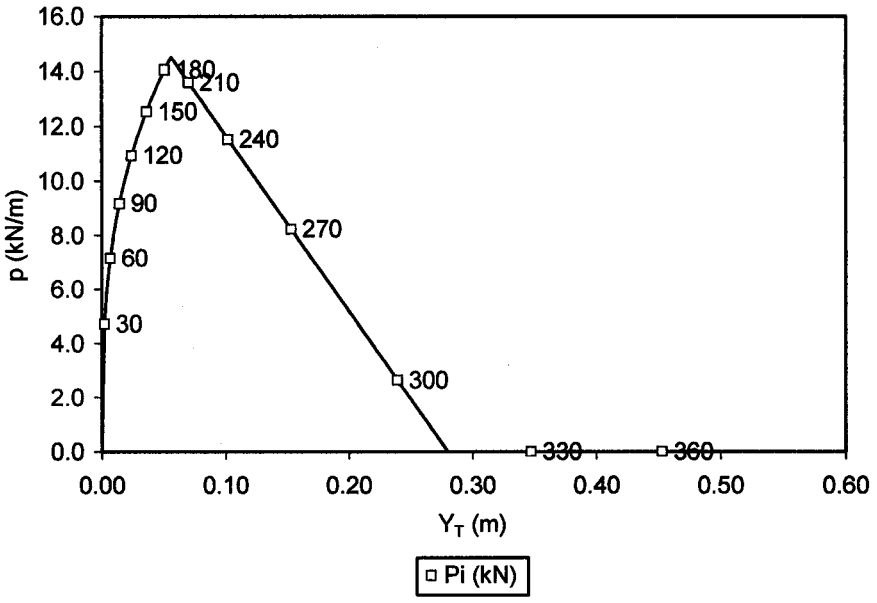

Fig. G.1 Soil reaction p at the top surface (expressed in terms of lateral loading) vs. lateral displacement generated by lateral loading applied to the pile for sensitivity analysis of top lateral displacement δy_t for fixed head single pile with length L = 10T subjected to lateral forces P_i (kN)

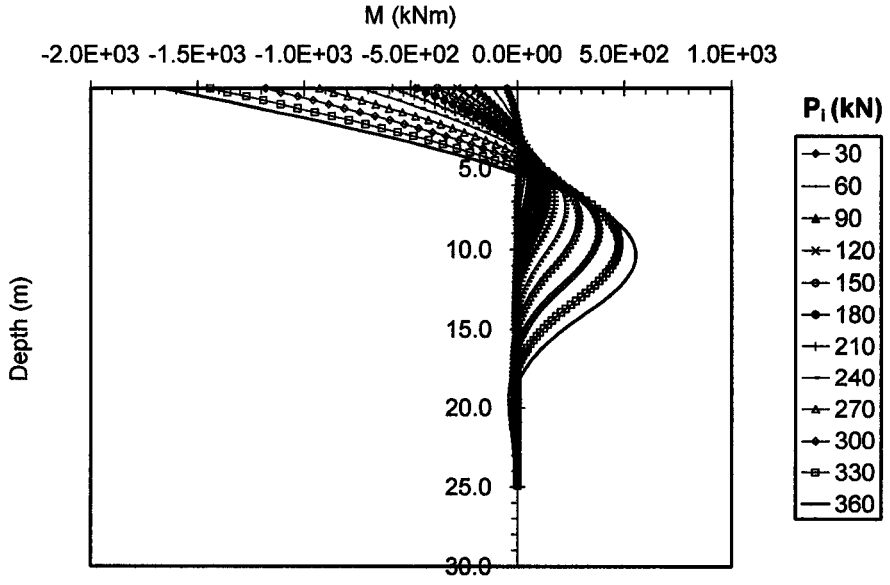

Fig. G.2 Distributions of bending moments at the primary structure M along the depth of the pile for sensitivity analysis of top lateral displacement δy_t for fixed head single pile with length L = 10T subjected to lateral forces P_i (kN)

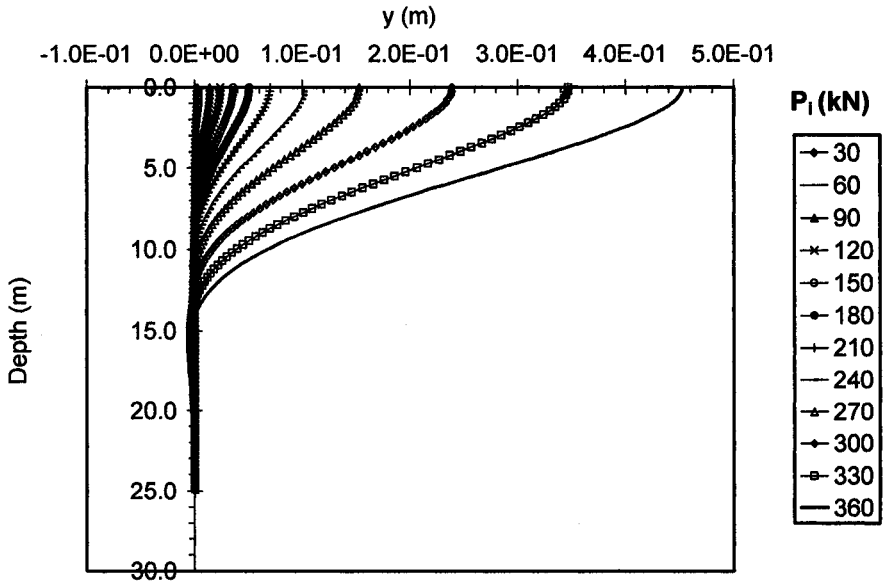

Fig. G.3 Distributions of lateral deflections at the primary structure y along the depth of the pile for sensitivity analysis of top lateral displacement δy_t for fixed head single pile with length L = 10T subjected to lateral forces P_i (kN)

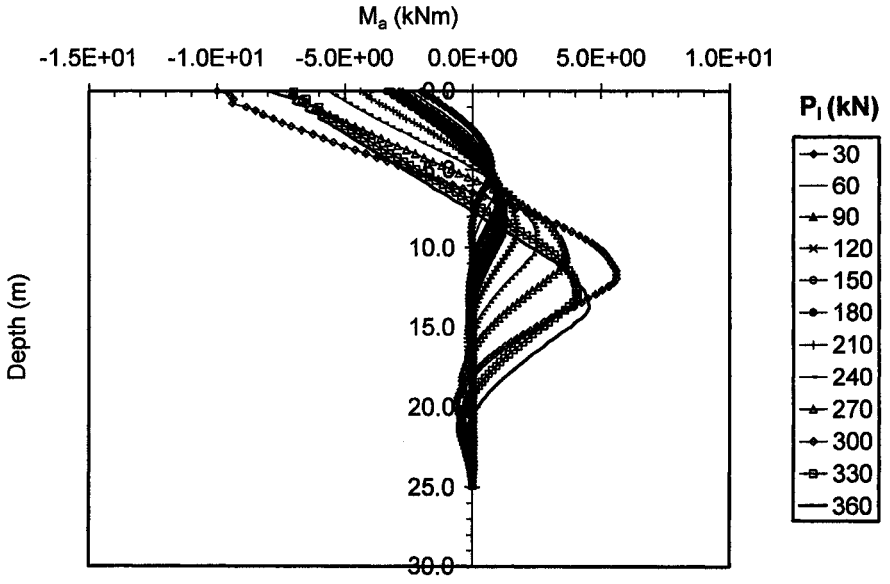

Fig. G.4 Distributions of bending moments M_a along the depth of the pile at the adjoint structure for sensitivity analysis of top lateral displacement δy_t for fixed head single pile with length L = 10T subjected to lateral forces P_i (kN)

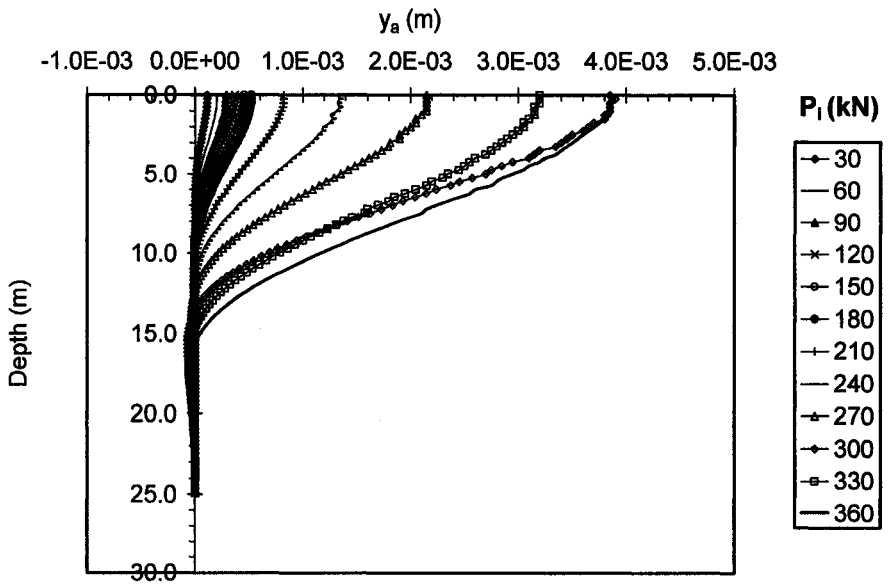

Fig. G.5 Distributions of lateral deflections at the adjoint structure y_a along the depth of the pile for sensitivity analysis of top lateral displacement δy_t for fixed head single pile with length L = 10T subjected to lateral forces P_i (kN)

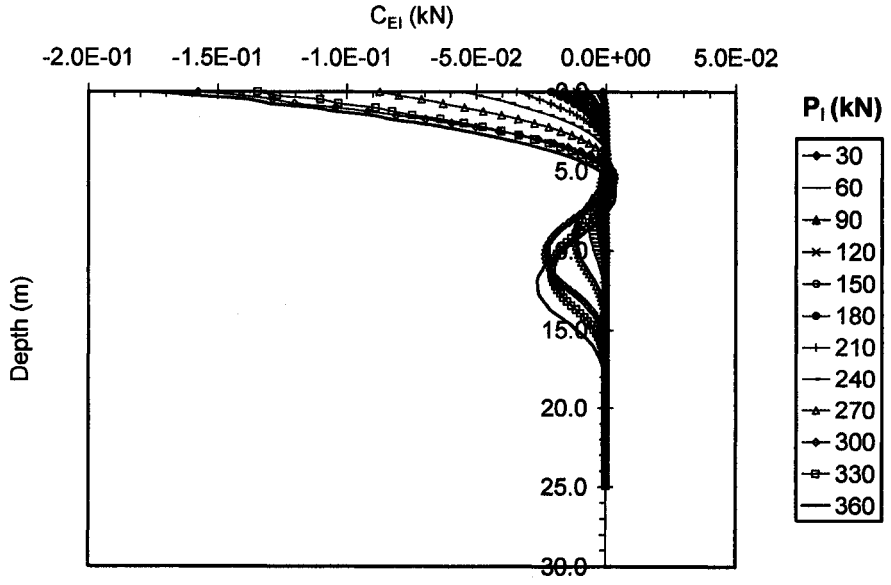

Fig. G.6 Distributions of sensitivity operators C_{EI} affecting the changes of δy_t due to the variations of the design variable δEI for fixed head single pile with length L = 10T subjected to lateral forces P_i (kN)

APPENDIX J:

Sensitivity analysis of top angle of rotation $\delta\varphi_t$ for single free head pile with length L = 3T subjected to lateral forces Pi

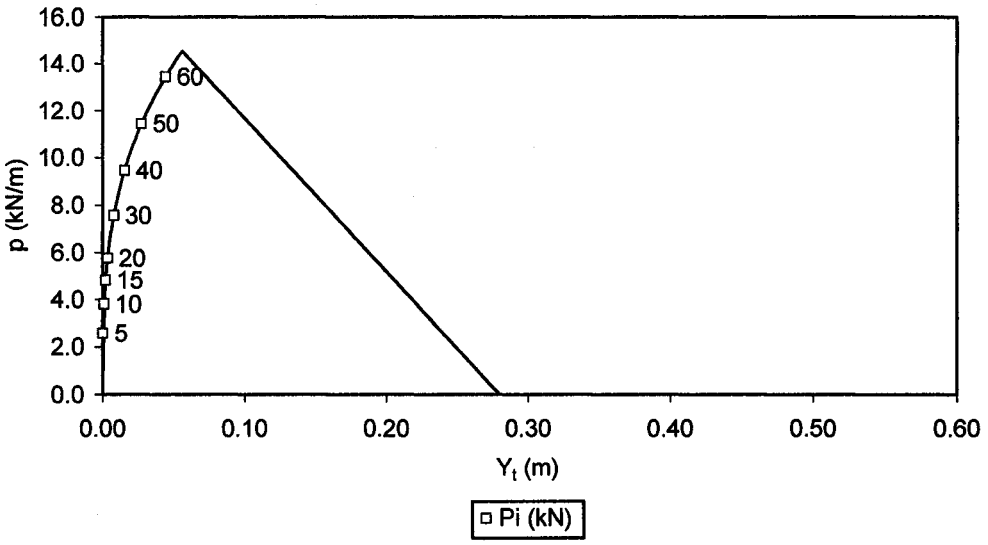

Fig. J.1 Soil reaction p at the top surface (expressed in terms of lateral loading) vs. lateral displacement generated by lateral loading applied to the pile for sensitivity analysis of top angle of rotation $\delta\varphi_t$ for free head single pile with length L = 3T subjected to lateral forces P_i (kN)

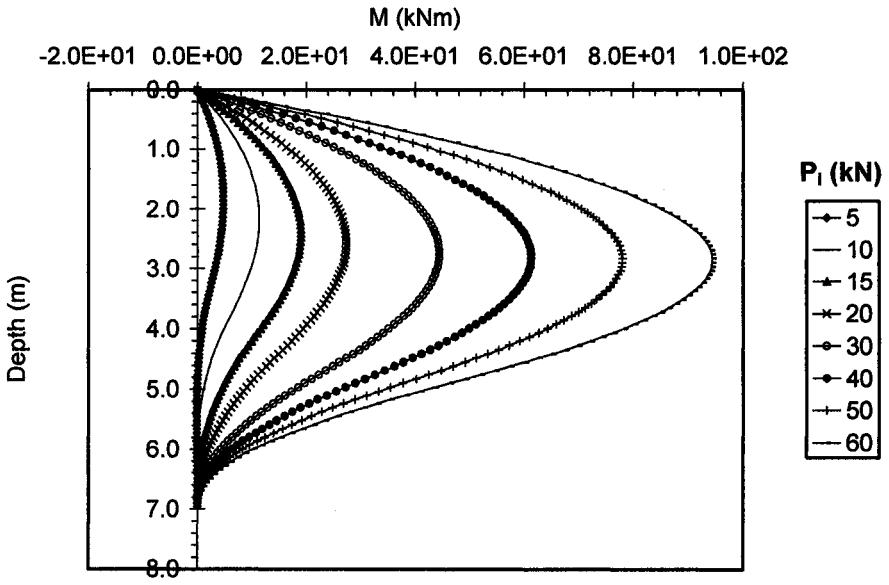

Fig. J.2 Distributions of bending moments at the primary structure M along the depth of the pile for sensitivity analysis of top angle of rotation $\delta\varphi_t$ for free head single pile with length L = 3T subjected to lateral forces P_i (kN)

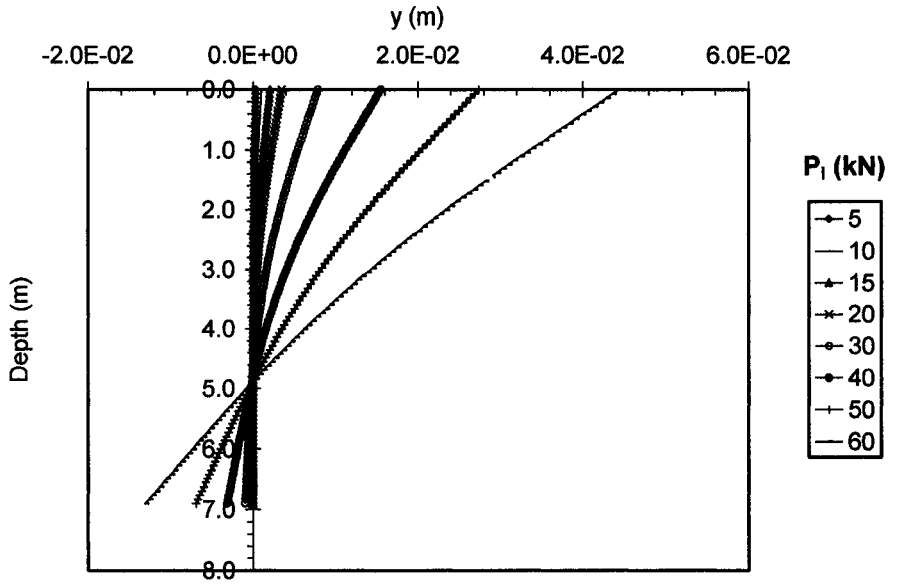

Fig. J.3 Distributions of lateral deflections at the primary structure y along the depth of the pile for sensitivity analysis of top angle of rotation $\delta\varphi_t$ for free head single pile with length L = 3T subjected to lateral forces P_i (kN)

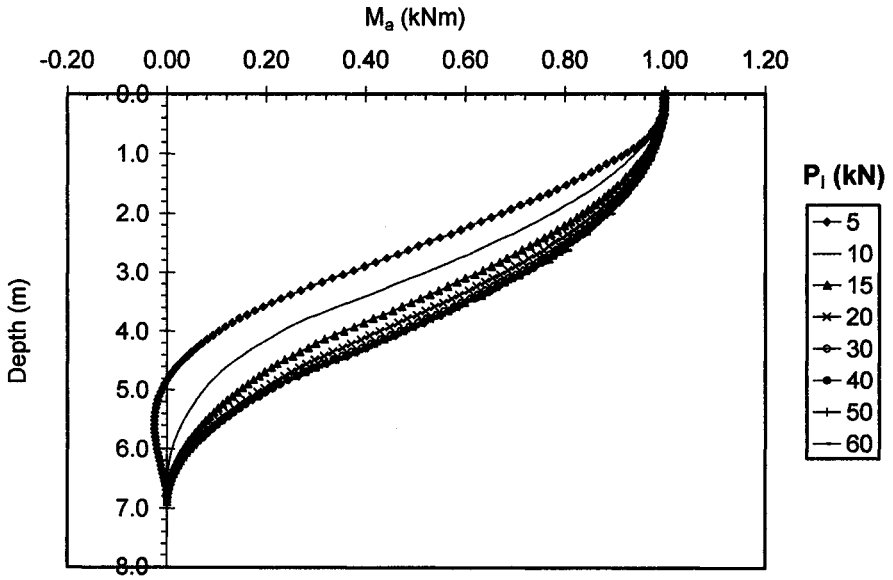

Fig. J.4 Distributions of bending moments M_a along the depth of the pile at the adjoint structure for sensitivity analysis of top angle of rotation $\delta\varphi_t$ for free head single pile with length L = 3T subjected to lateral forces P_i (kN)

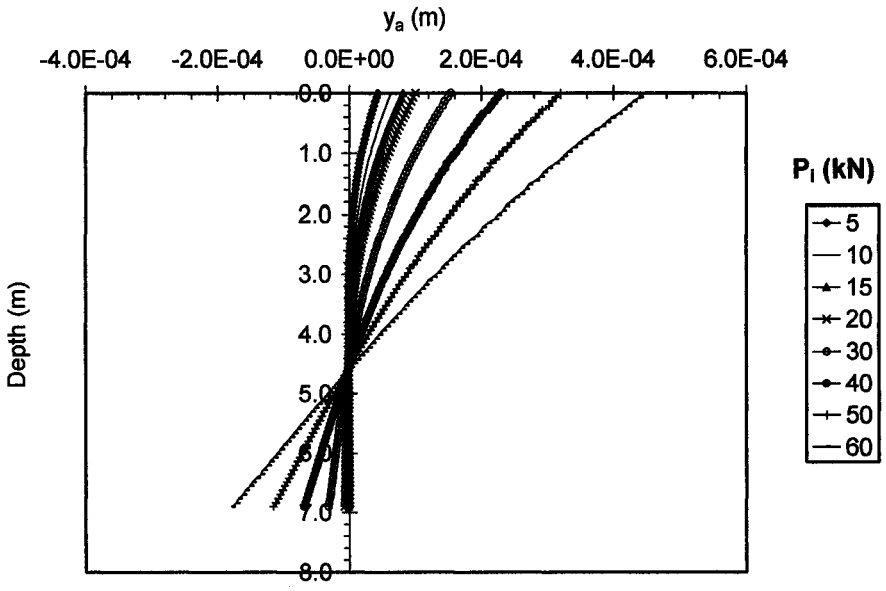

Fig. J.5 Distributions of lateral deflections at the adjoint structure y_a along the depth of the pile for sensitivity analysis of top angle of rotation $\delta\varphi_t$ for free head single pile with length L = 3T subjected to lateral forces P_i (kN)

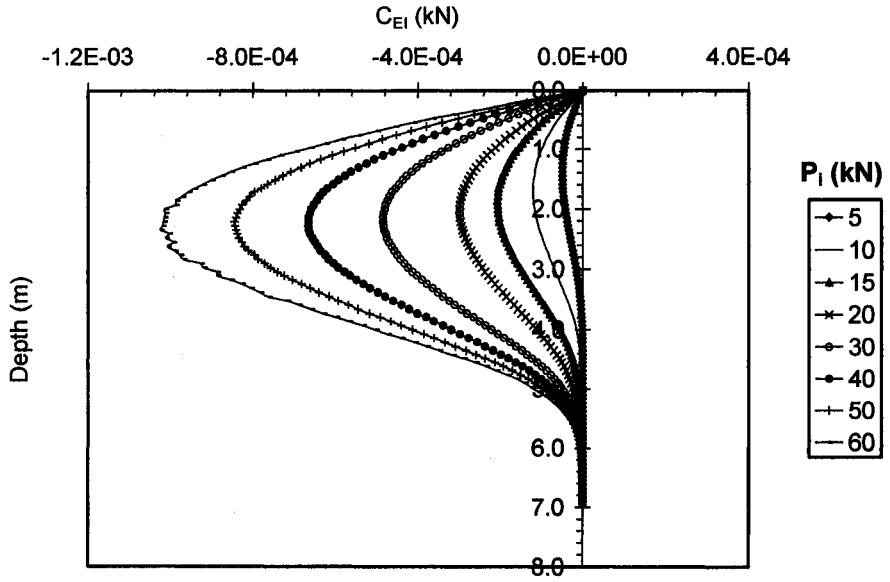

Fig. J.6 Distributions of sensitivity operators C_{EI} affecting the changes of $\delta\varphi_t$ due to variations of the design variable δEI for free head single pile with length L = 3T subjected to lateral forces P_i (kN)

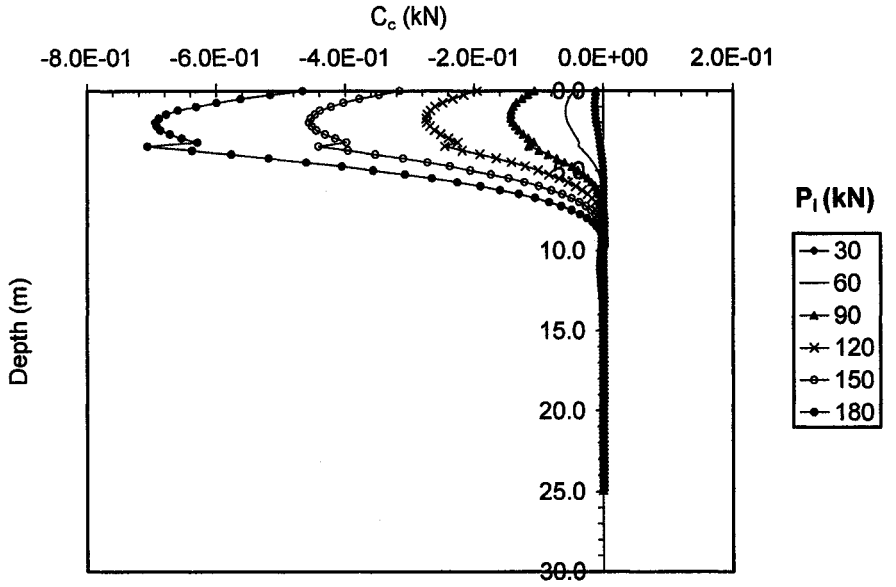

Fig. G.7a Distributions of sensitivity operators C_c affecting the changes of δy_t due to the variations of the design variable δc for fixed head single pile with length L = 10T subjected to lateral forces P_i (kN)

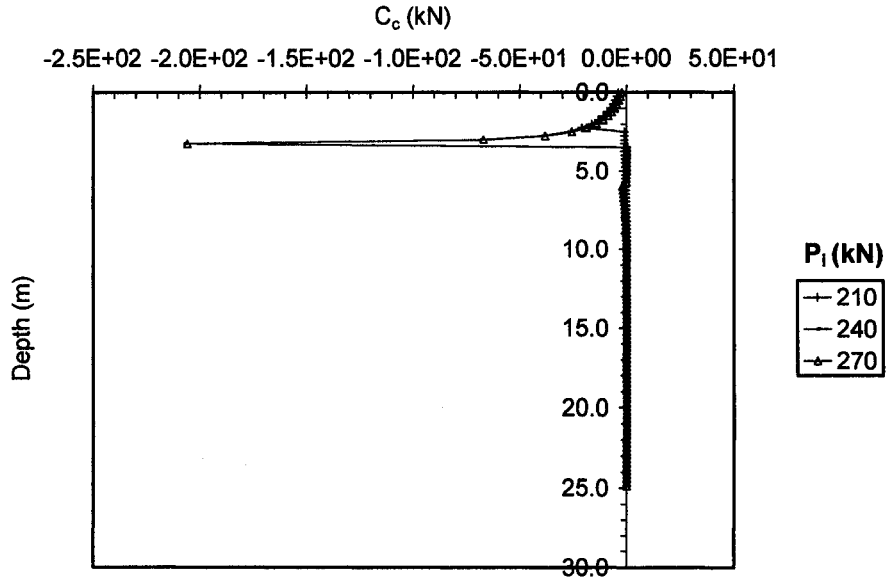

Fig. G.7b Distributions of sensitivity operators C_c affecting the changes of δy_t due to the variations of the design variable δc for fixed head single pile with length L = 10T subjected to lateral forces P_i (kN)

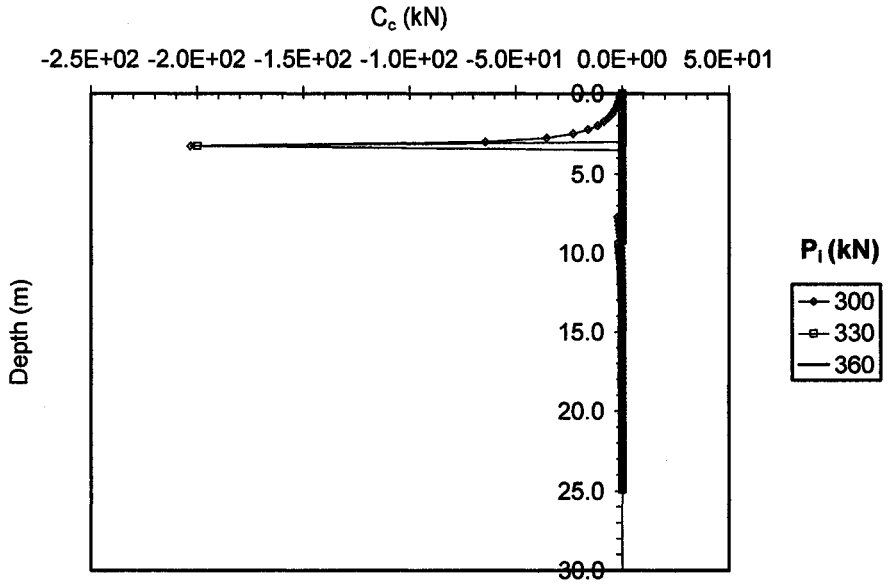

Fig. G.7c Distributions of sensitivity operators C_c affecting the changes of δy_t due to the variations of the design variable δc for fixed head single pile with length L = 10T subjected to lateral forces P_i (kN)

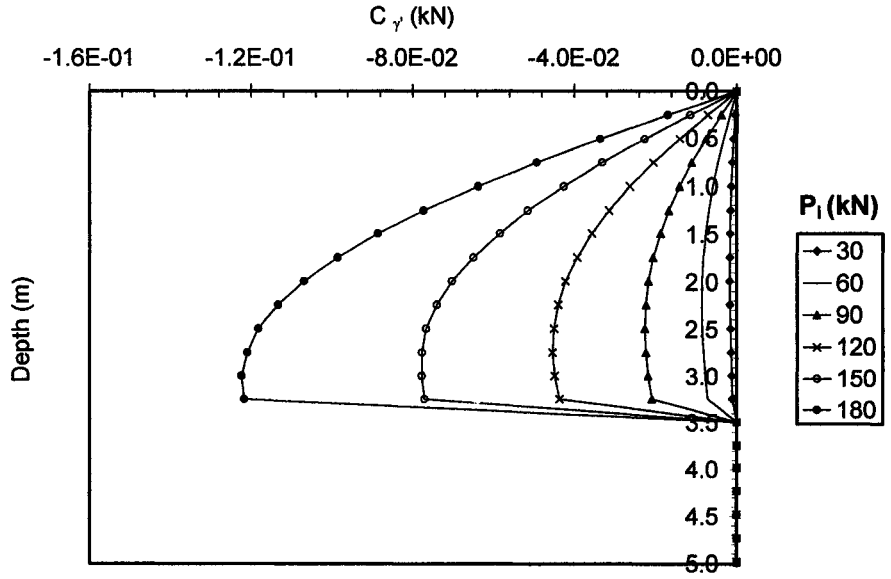

Fig. G.8a Distributions of sensitivity operators $C_{\gamma'}$ affecting the changes of δy_t due to the variations of the design variable $\delta\gamma'$ for fixed head single pile with length L = 10T subjected to lateral forces P_i (kN)

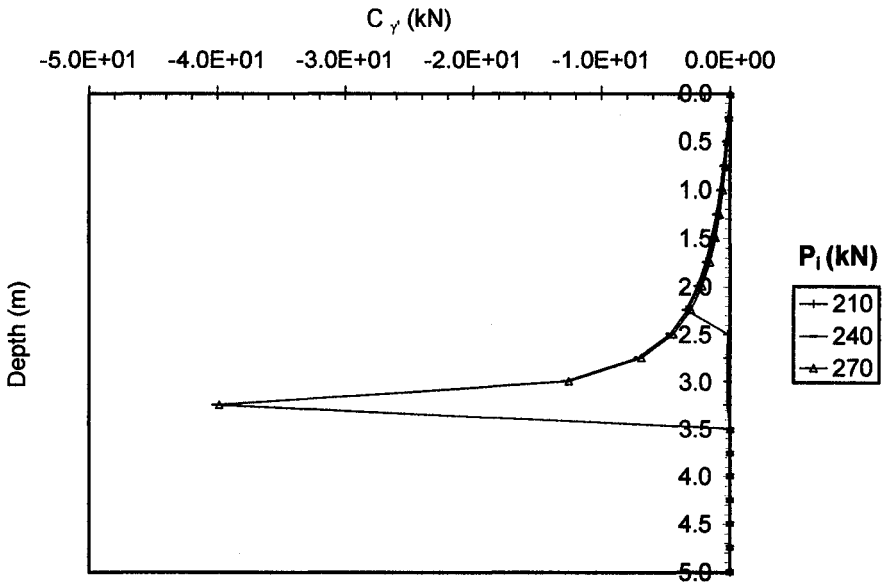

Fig. G.8b Distributions of sensitivity operators $C_{\gamma'}$ affecting the changes of δy_t due to the variations of the design variable $\delta\gamma'$ for fixed head single pile with length L = 10T subjected to lateral forces P_i (kN)

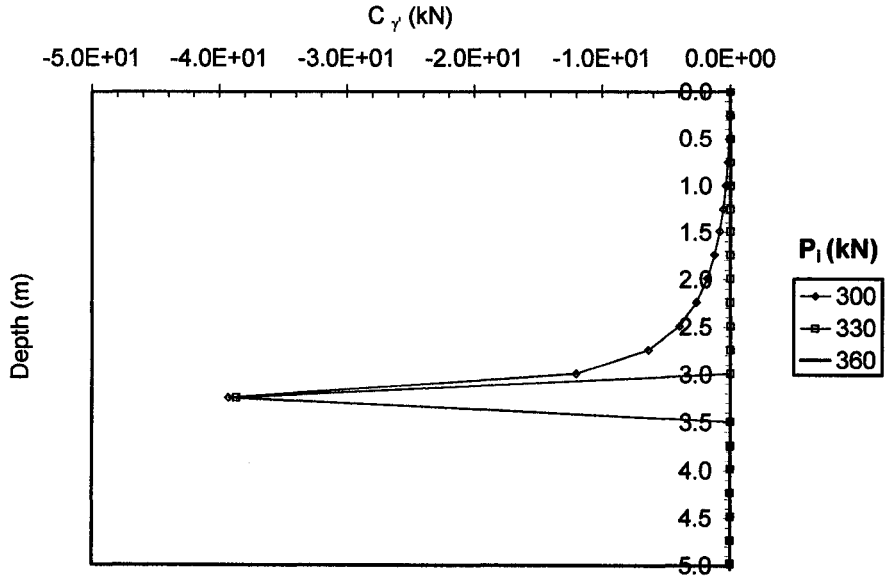

Fig. G.8c Distributions of sensitivity operators $C_{\gamma'}$ affecting the changes of δy_t due to the variations of the design variable $\delta\gamma'$ for fixed head single pile with length L = 10T subjected to lateral forces P_i (kN)

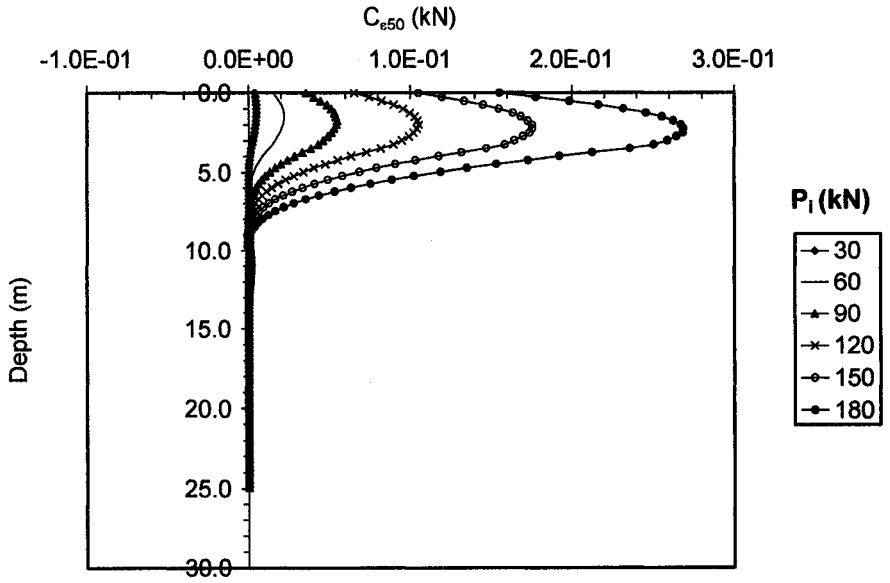

Fig. G.9a Distributions of sensitivity operators $C_{\varepsilon 50}$ affecting the changes of δy_t due to the variations of the design variable $\delta\varepsilon_{50}$ for fixed head single pile with length L = 10T subjected to lateral forces P_i (kN)

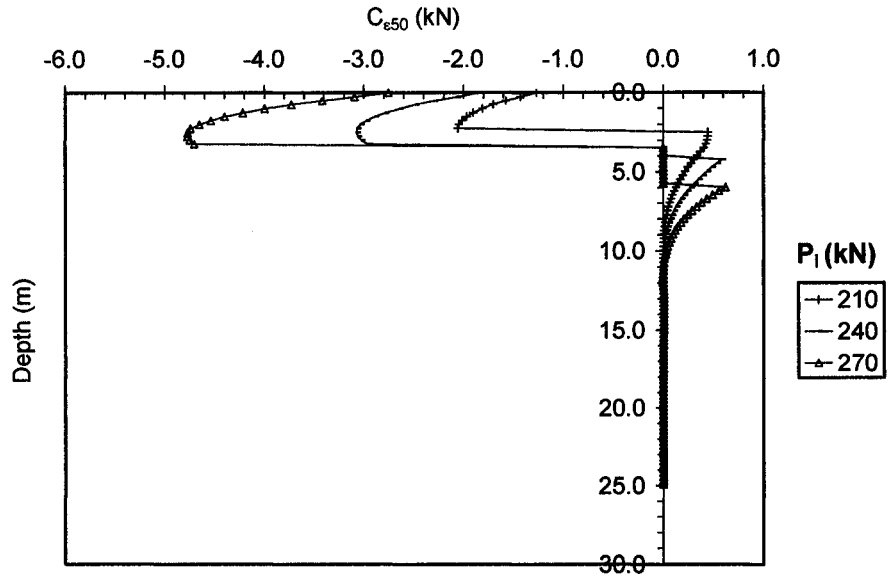

Fig. G.9b Distributions of sensitivity operators $C_{\varepsilon 50}$ affecting the changes of δy_t due to the variations of the design variable $\delta\varepsilon_{50}$ for fixed head single pile with length L = 10T subjected to lateral forces P_i (kN)

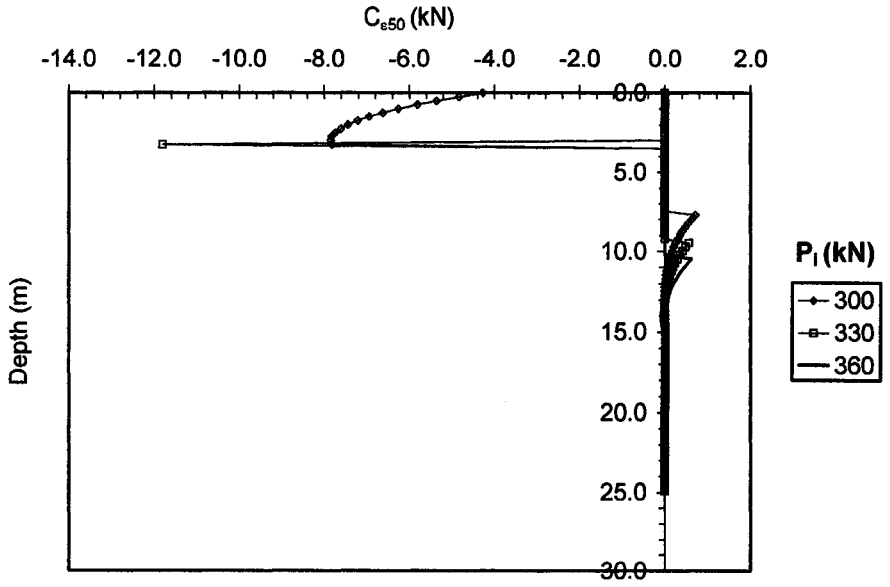

Fig. G.9c Distributions of sensitivity operators $C_{\varepsilon 50}$ affecting the changes of δy_t due to the variations of the design variable $\delta\varepsilon_{50}$ for fixed head single pile with length L = 10T subjected to lateral forces P_i (kN)

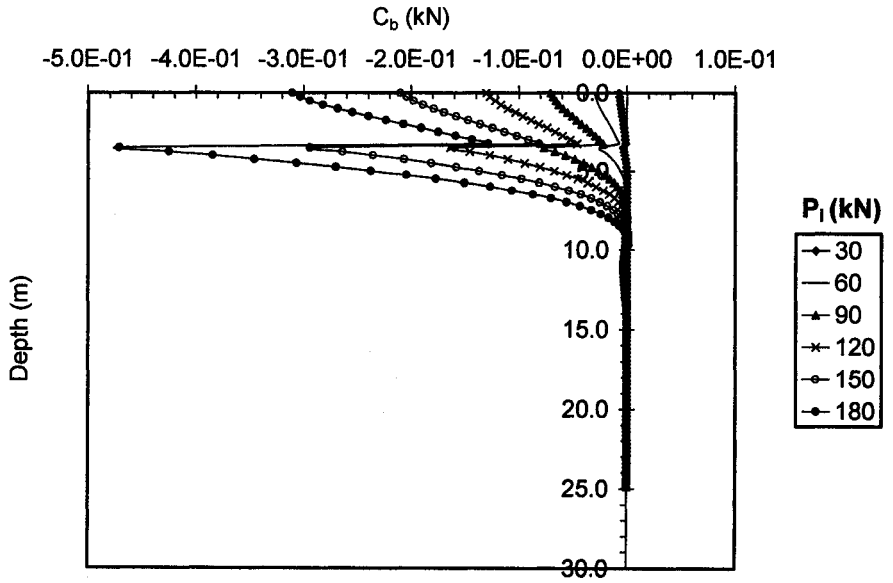

Fig. G.10a Distributions of sensitivity operators C_b affecting the changes of δy_t due to the variations of the design variable δb for fixed head single pile with length L = 10T subjected to lateral forces P_i (kN)

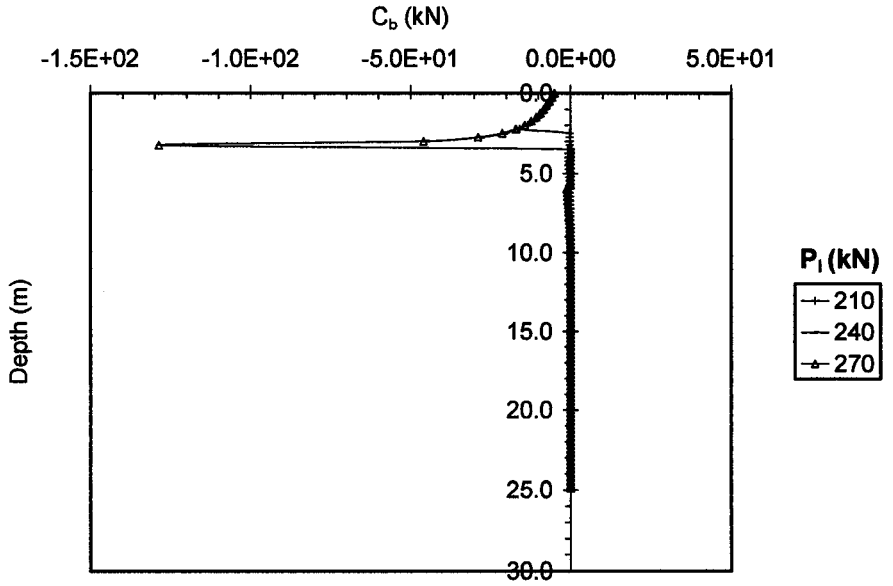

Fig. G.10b Distributions of sensitivity operators C_b affecting the changes of δy_t due to the variations of the design variable δb for fixed head single pile with length L = 10T subjected to lateral forces P_i (kN)

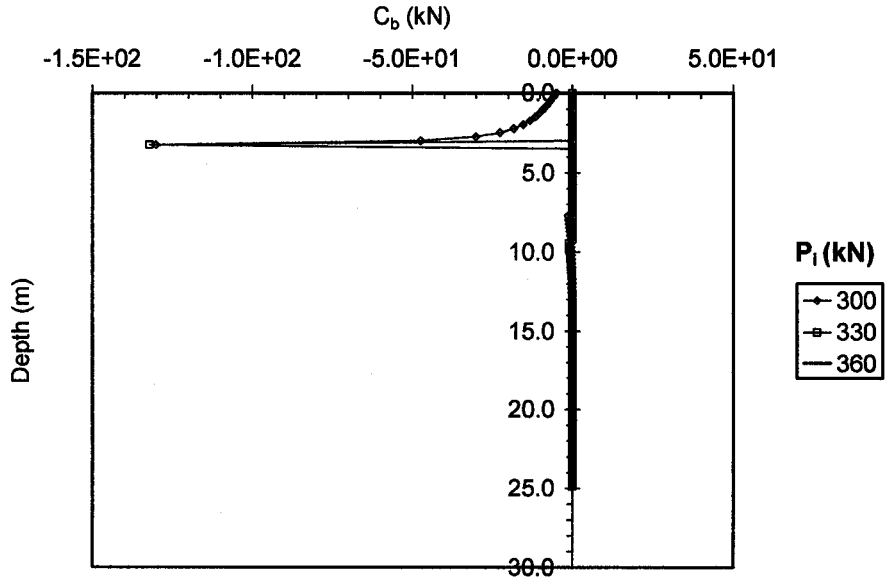

Fig. G.10c Distributions of sensitivity operators C_b affecting the changes of δy_t due to the variations of the design variable δb for fixed head single pile with length L = 10T subjected to lateral forces P_i (kN)

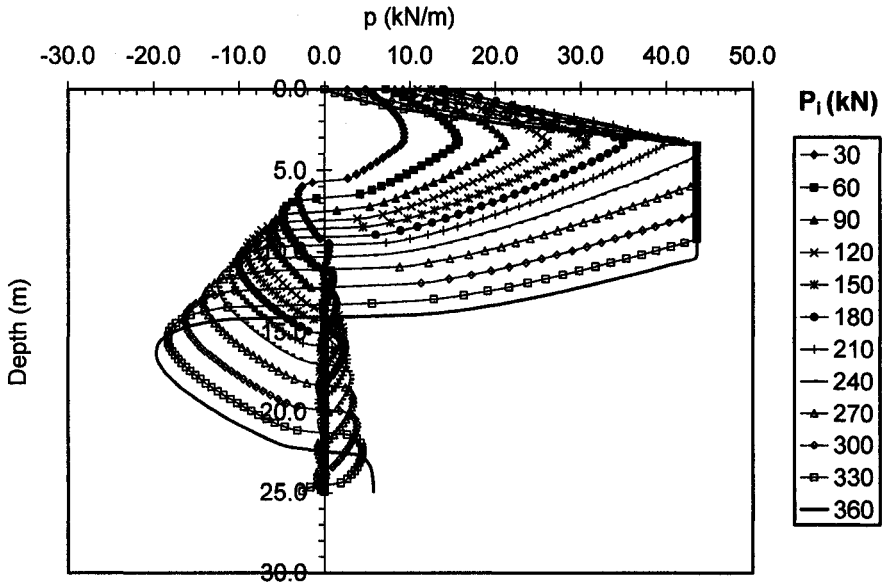

Fig. G.11 Distributions of soil reaction p at the primary structure along the depth of the pile for sensitivity analysis of top lateral displacement δy_t for fixed head single pile with length L = 10T subjected to lateral forces P_i (kN)

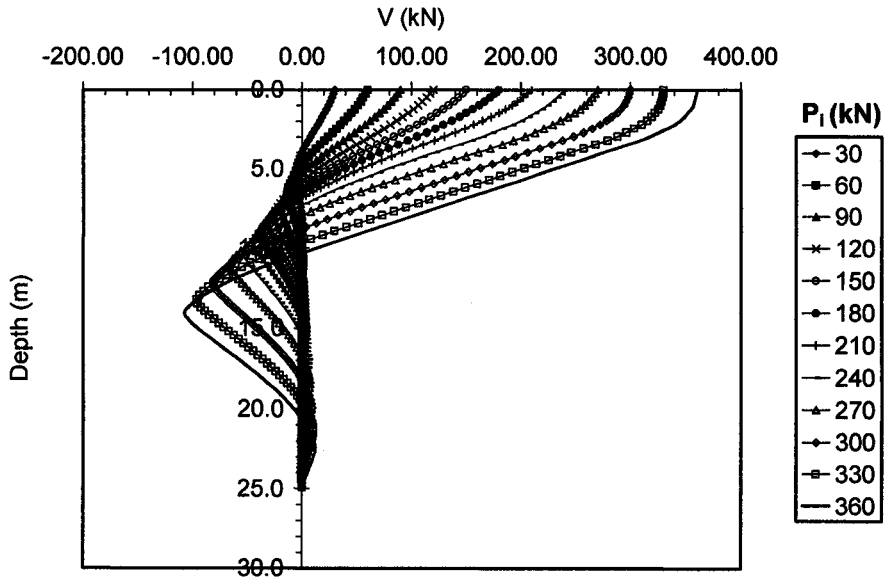

Fig. G.12 Distributions of shear forces V at the primary structure along the depth of the pile for sensitivity analysis of top lateral displacement δy_t for fixed head single pile with length L = 10T subjected to lateral forces P_i (kN)

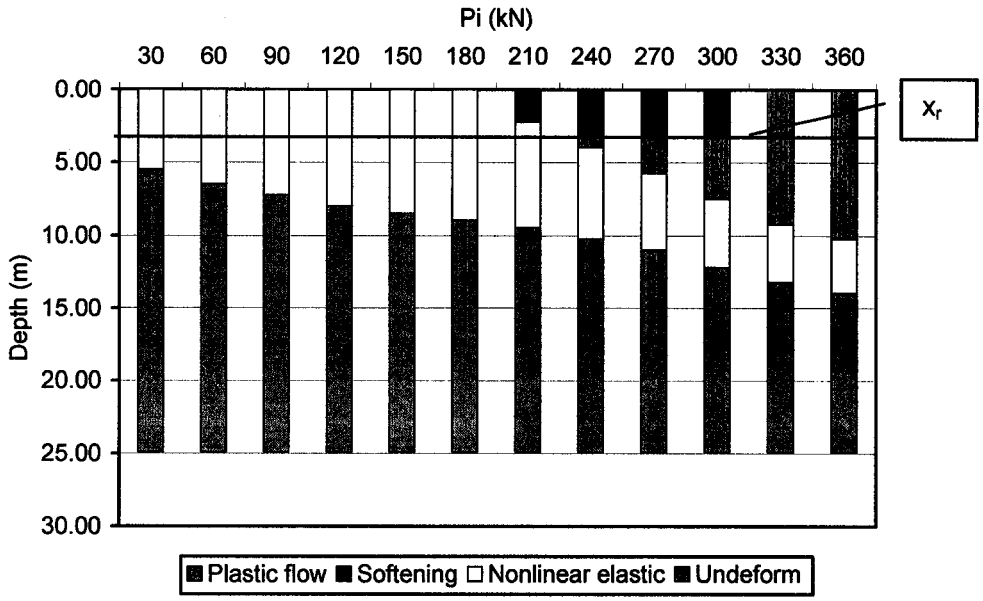

Fig. G.13 Quantitative assessment of the location and the size of soil phases developed with depth of the pile determined based on the distributions of sensitivity operators affecting δy_t for fixed head single pile with length L = 10T subjected to lateral forces P_i (kN)

APPENDIX H:

Sensitivity analysis of top lateral displacement δy_t for single free head pile with length L = 3T subjected to bending moments M_i

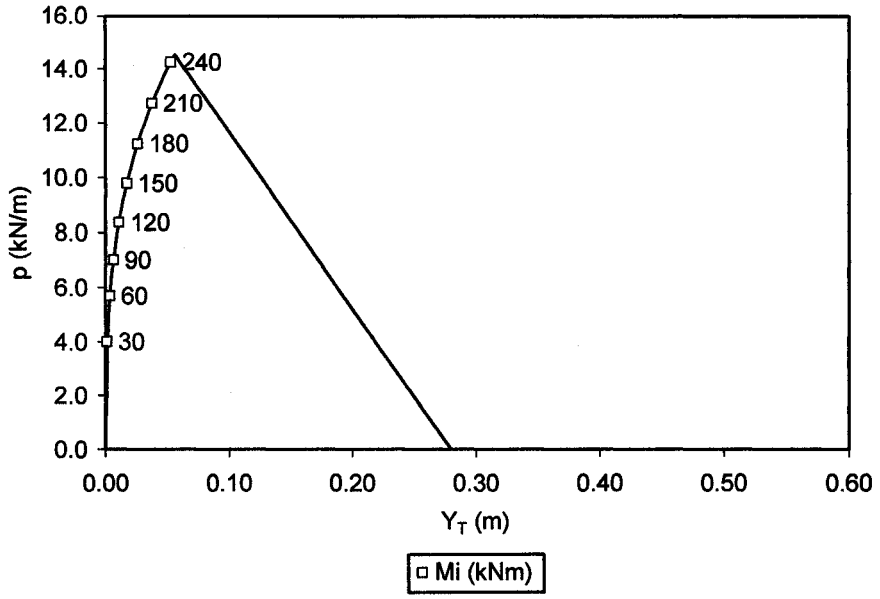

Fig. H.1 Soil reaction p at the top surface (expressed in terms of lateral loading) vs. lateral displacement generated by lateral loading applied to the pile for sensitivity analysis of top lateral displacement δy_t for free head single pile with length L = 3T subjected to bending moments M_i (kNm)

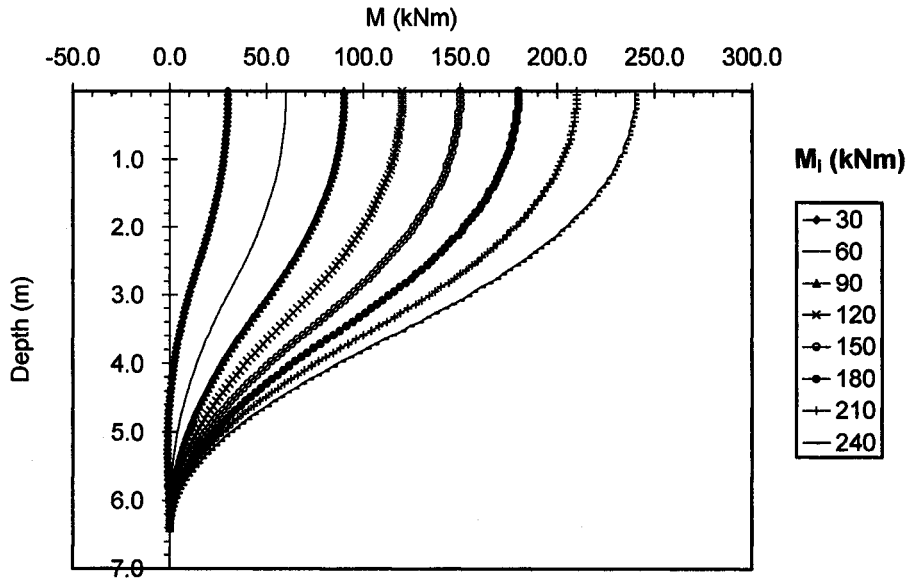

Fig. H.2 Distributions of bending moments at the primary structure M along the depth of the pile for sensitivity analysis of top lateral displacement δy_t for free head single pile with length L = 3T subjected to bending moments M_i (kNm)

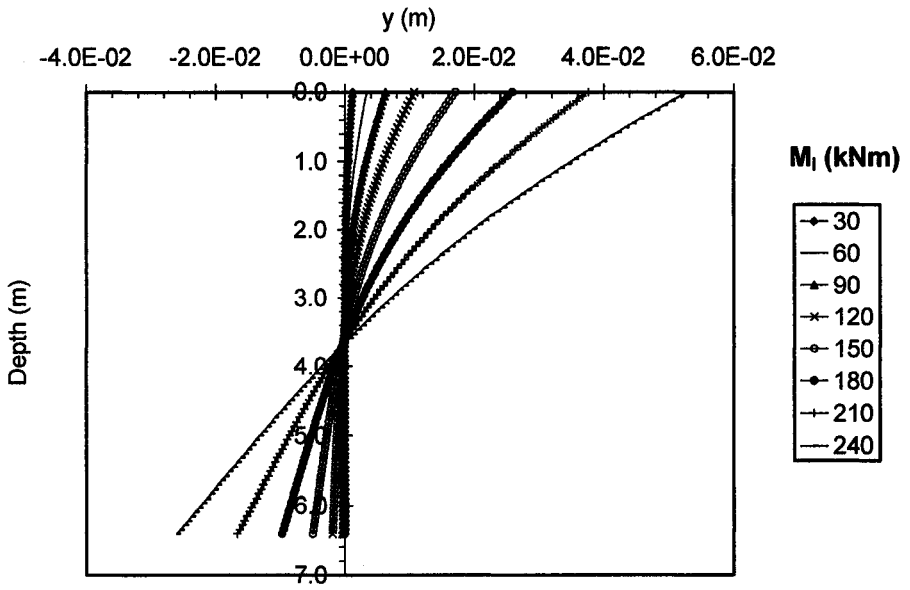

Fig. H.3 Distributions of lateral deflections at the primary structure y along the depth of the pile for sensitivity analysis of top lateral displacement δy_t for free head single pile with length L = 3T subjected to bending moments M_i (kNm)

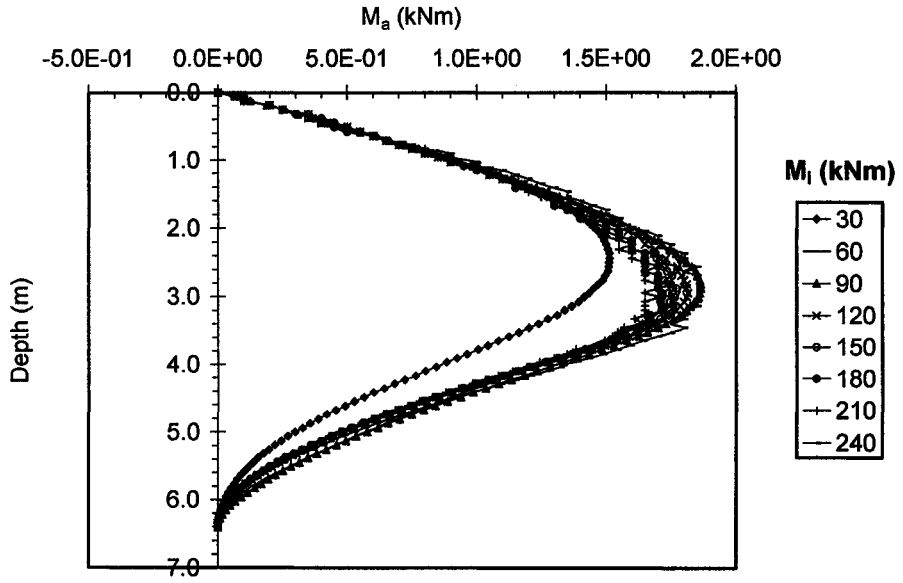

Fig. H.4 Distributions of bending moments M_a along the depth of the pile at the adjoint structure for sensitivity analysis of top lateral displacement δy_t for free head single pile with length L = 3T subjected to bending moments M_i (kNm)

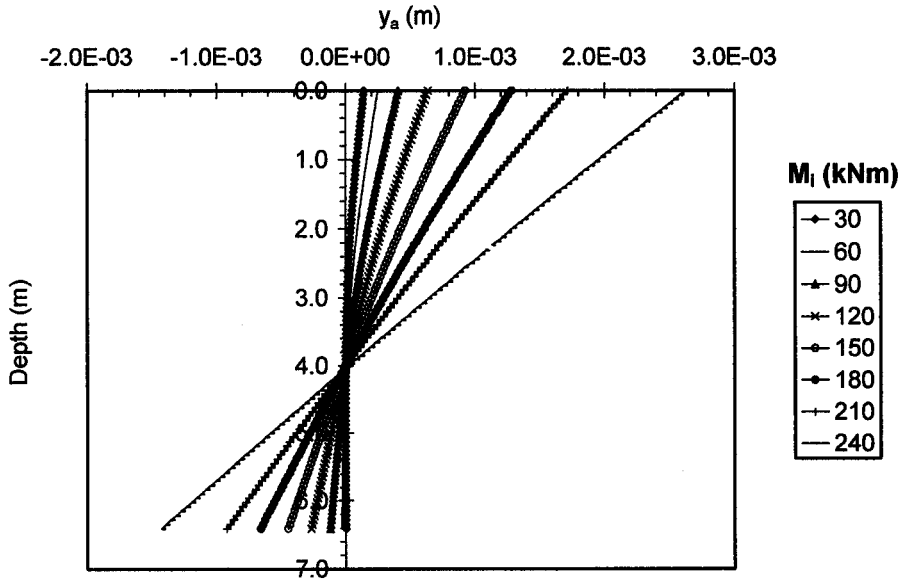

Fig. H.5 Distributions of lateral deflections at the adjoint structure y_a along the depth of the pile for sensitivity analysis of top lateral displacement δy_t for free head single pile with length L = 3T subjected to bending moments M_i (kNm)

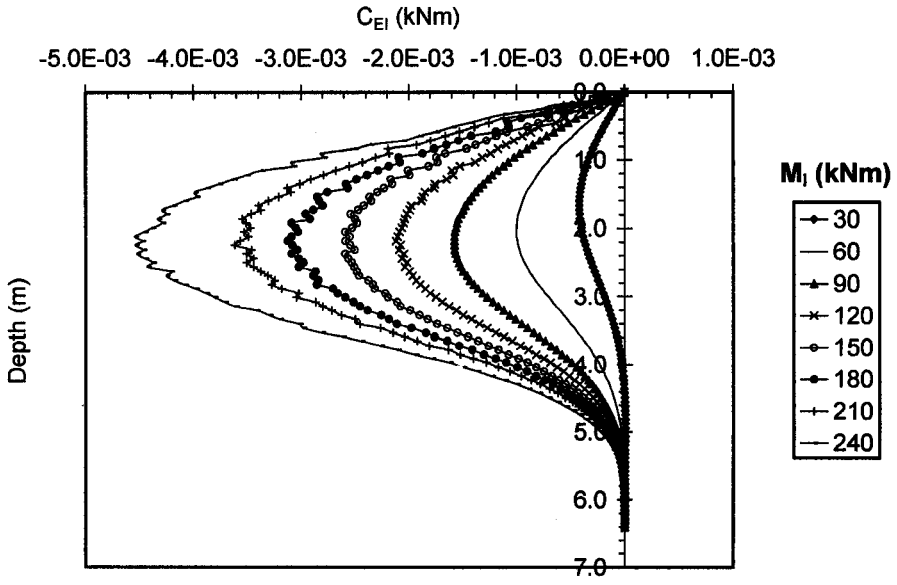

Fig. H.6 Distributions of sensitivity operators C_{EI} affecting the changes of δy_t due to the variations of the design variable δEI for free head single pile with length L = 3T subjected to bending moments M_i (kNm)

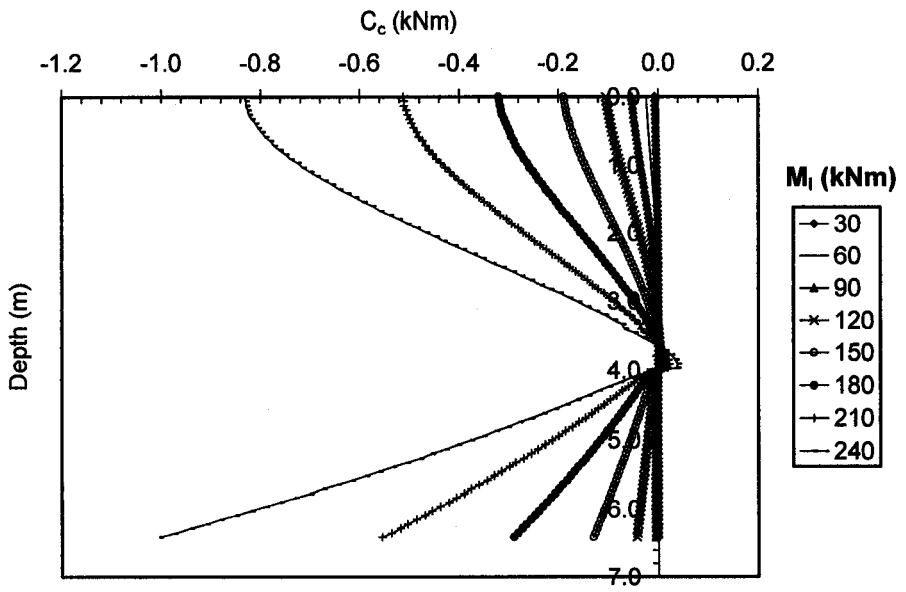

Fig. H.7 Distributions of sensitivity operators C_c affecting the changes of δy_t due to the variations of the design variable δc for free head single pile with length L = 3T subjected to bending moments M_i (kNm)

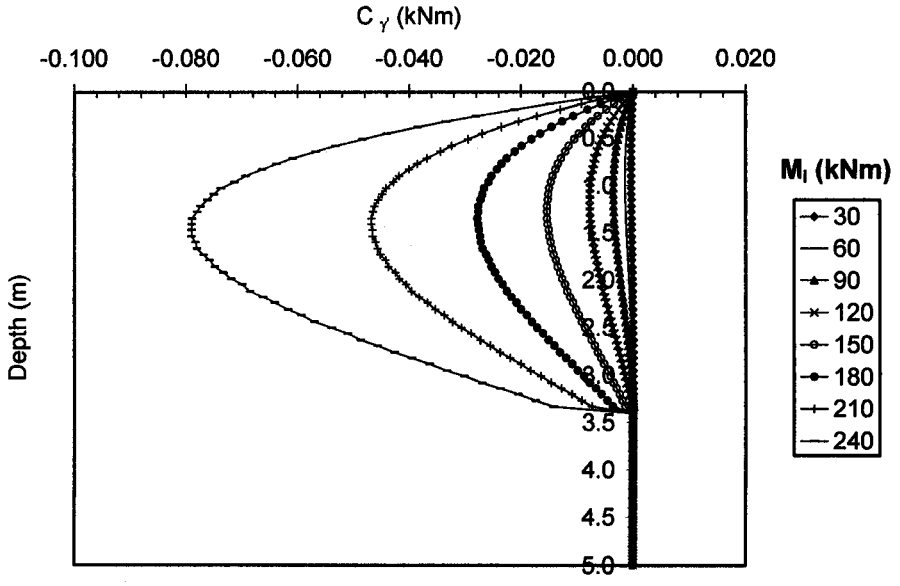

Fig. H.8 Distributions of sensitivity operators $C_{\gamma'}$ affecting the changes of δy_t due to the variations of the design variable $\delta\gamma'$ for free head single pile with length L = 3T subjected to bending moments M_i (kNm)

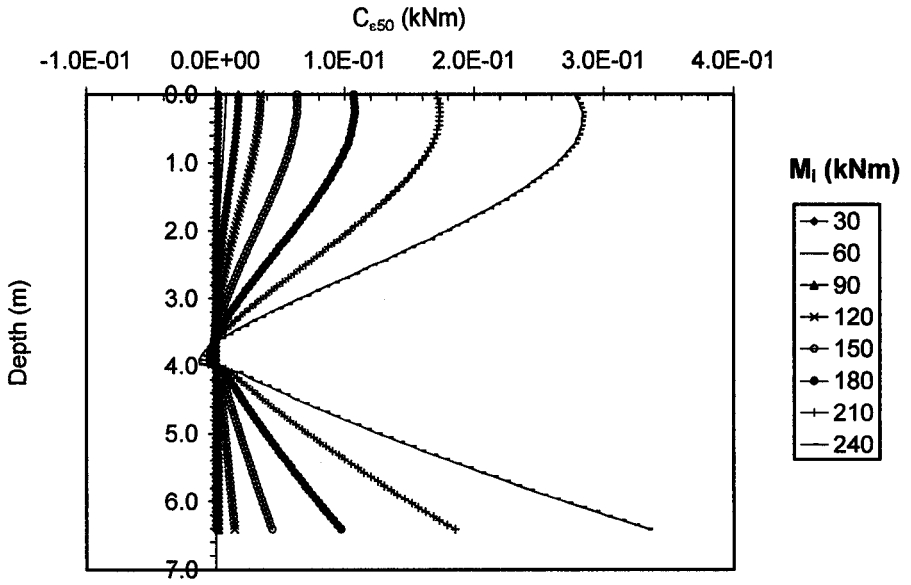

Fig. H.9 Distributions of sensitivity operators $C_{\varepsilon 50}$ affecting the changes of δy_t due to the variations of the design variable $\delta\varepsilon_{50}$ for free head single pile with length L = 3T subjected to bending moments M_i (kNm)

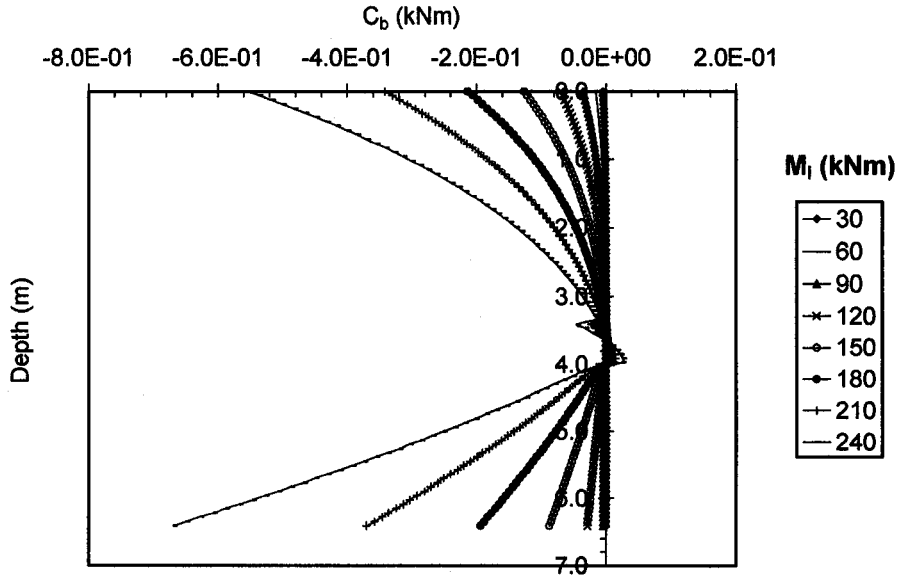

Fig. H.10 Distributions of sensitivity operators C_b affecting the changes of δy_t due to the variations of the design variable δb for free head single pile with length L = 3T subjected to bending moments M_i (kNm)

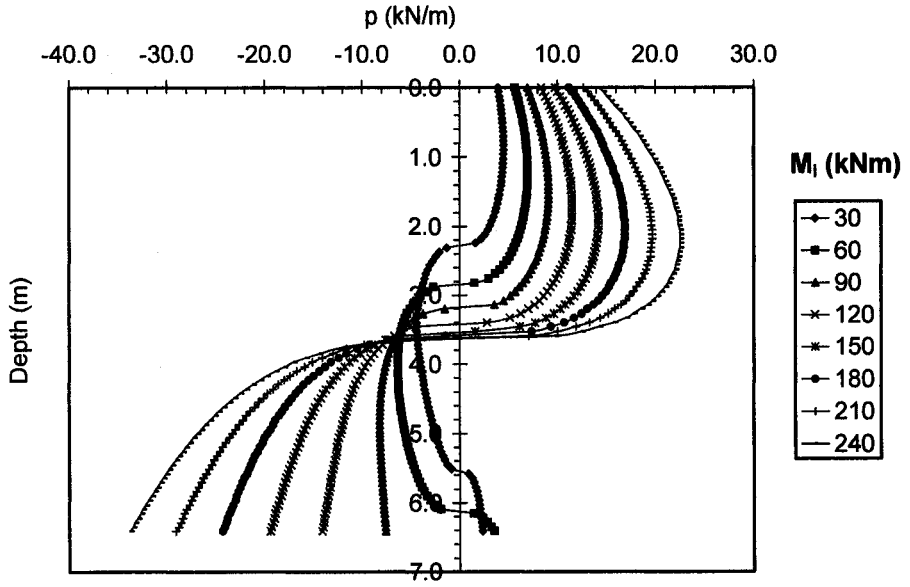

Fig. H.11 Distributions of soil reaction p at the primary structure along the depth of the pile for sensitivity analysis of top lateral displacement δy_t for free head single pile with length L = 3T subjected to bending moments M_i (kNm)

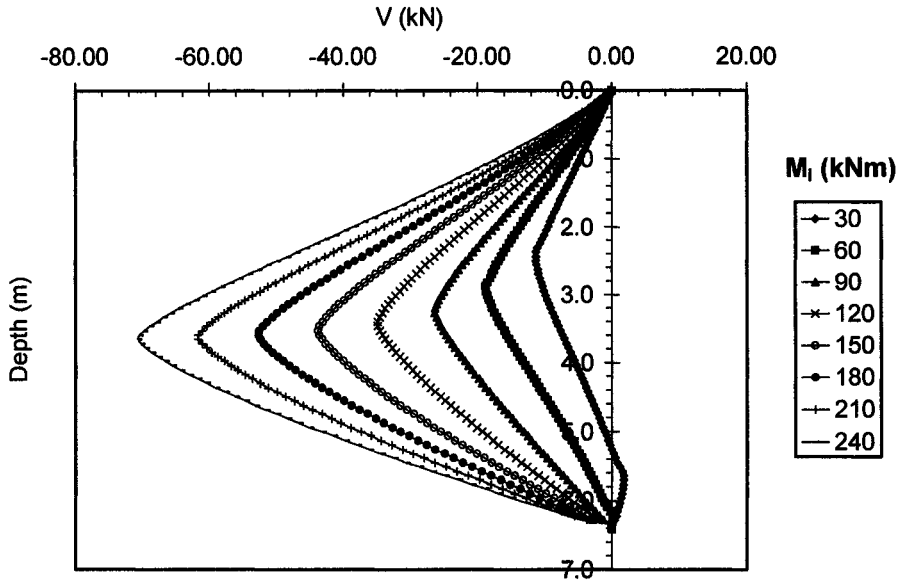

Fig. H.12 Distributions of shear forces V at the primary structure along the depth of the pile for sensitivity analysis of top lateral displacement δy_t for free head single pile with length L = 3T subjected to bending moments M_i (kNm)

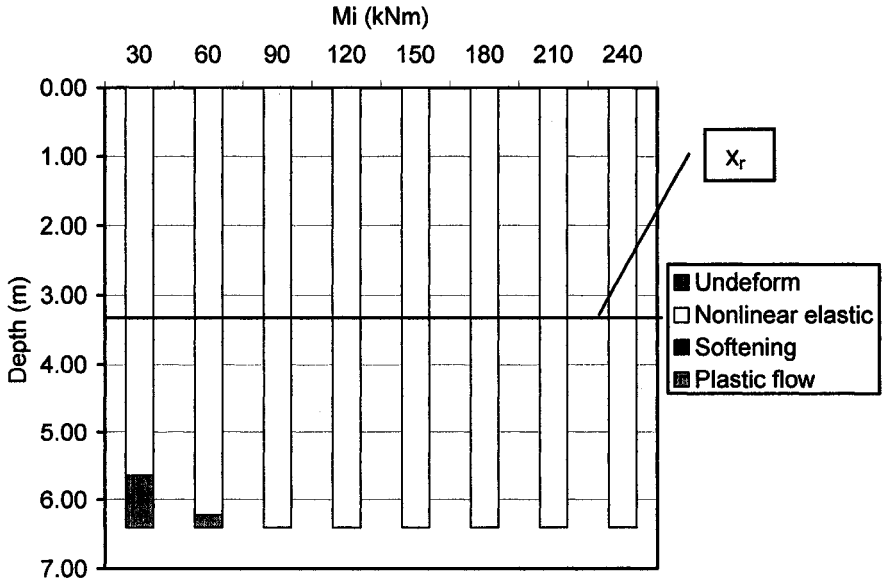

Fig. H.13 Quantitative assessment of the location and the size of soil phases developed with depth determined based on the distributions of sensitivity operators affecting δy_t for free head single pile with length L = 3T subjected to bending moments M_i (kNm)

APPENDIX I:

Sensitivity analysis of top lateral displacement δy_t for single free head pile with length L = 10T subjected to bending moments M_i

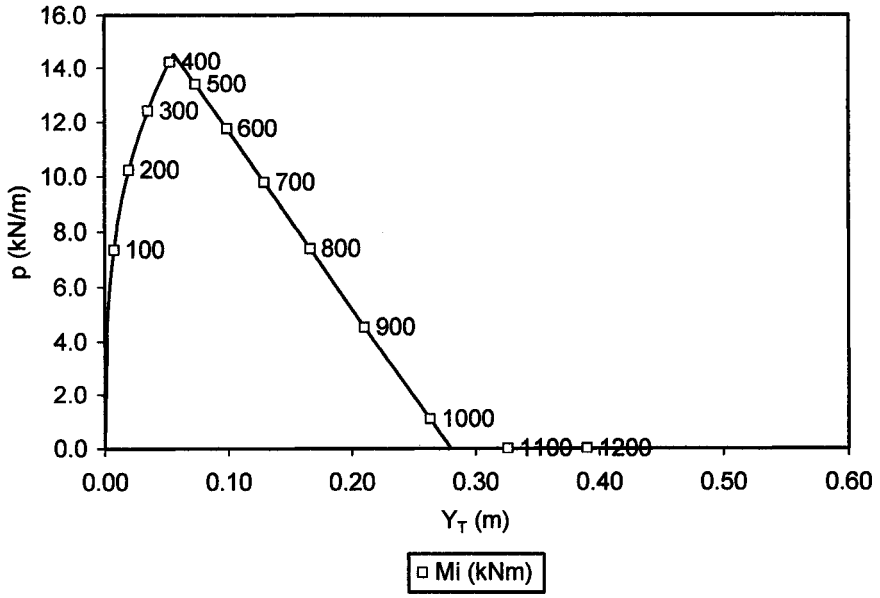

Fig. I.1 Soil reaction p at the top surface (expressed in terms of lateral loading) vs. lateral displacement generated by lateral loading applied to the pile for sensitivity analysis of top lateral displacement δy_t for free head single pile with length L = 10T subjected to bending moments M_i (kNm)

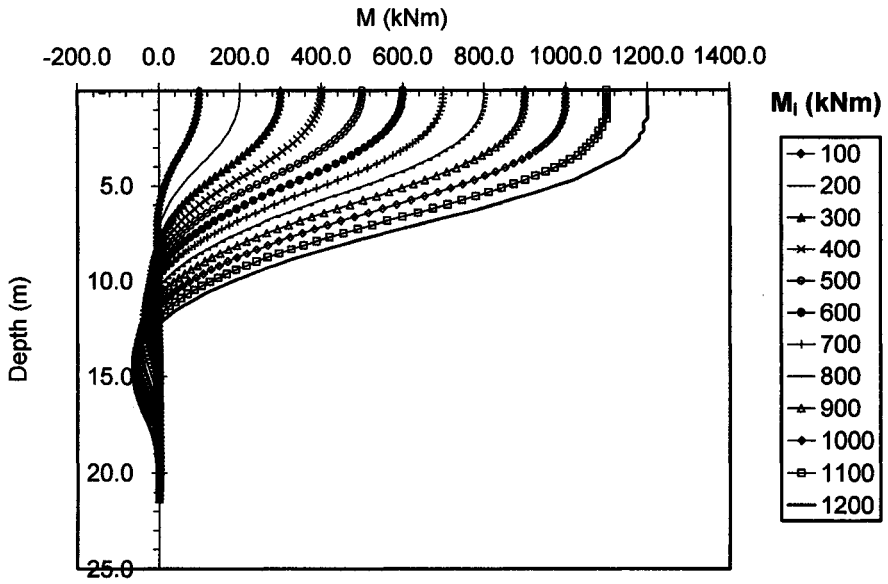

Fig. I.2 Distributions of bending moments at the primary structure M along the depth of the pile for sensitivity analysis of top lateral displacement δy_t for free head single pile with length L = 10T subjected to bending moments M_i (kNm)

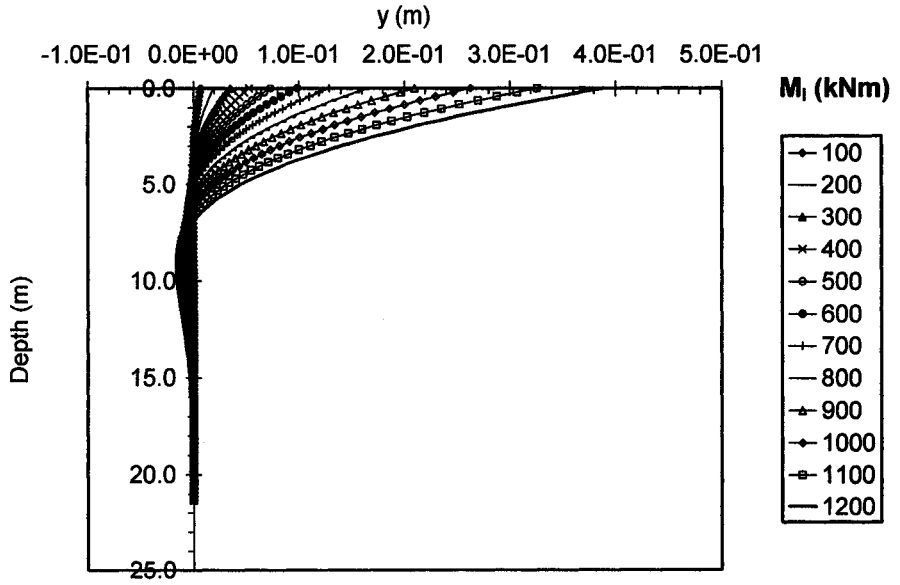

Fig. I.3 Distributions of lateral deflections at the primary structure y along the depth of the pile for sensitivity analysis of top lateral displacement δy_t for free head single pile with length L = 10T subjected to bending moments M_i (kNm)

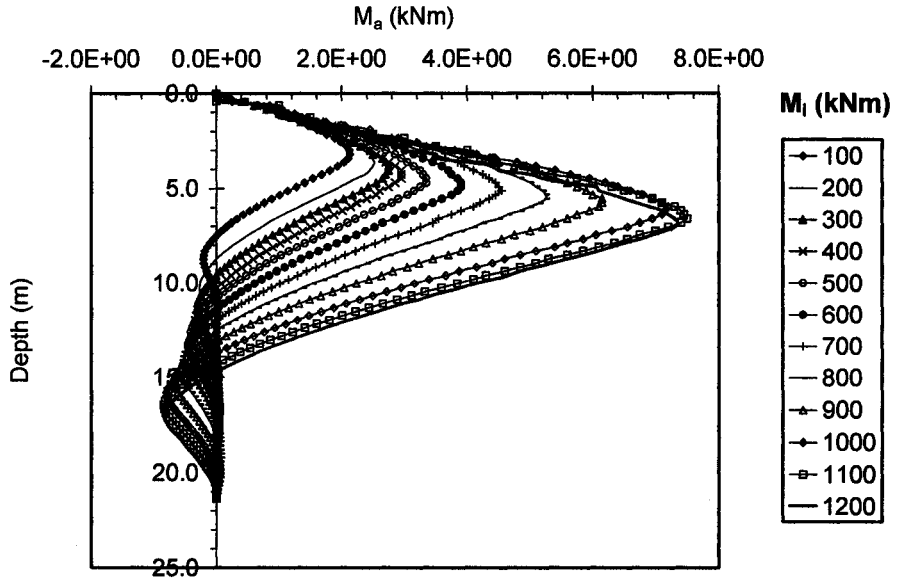

Fig. I.4 Distributions of bending moments M_a along the depth of the pile at the adjoint structure for sensitivity analysis of top lateral displacement δy_t for free head single pile with length L = 10T subjected to bending moments M_i (kNm)

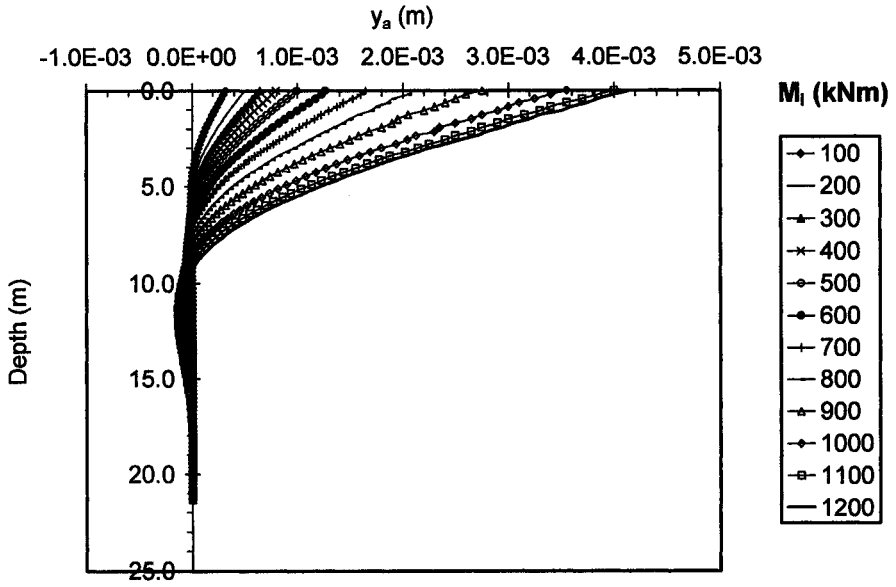

Fig. I.5 Distributions of lateral deflections at the adjoint structure y_a along the depth of the pile for sensitivity analysis of top lateral displacement δy_t for free head single pile with length L = 10T subjected to bending moments M_i (kNm)

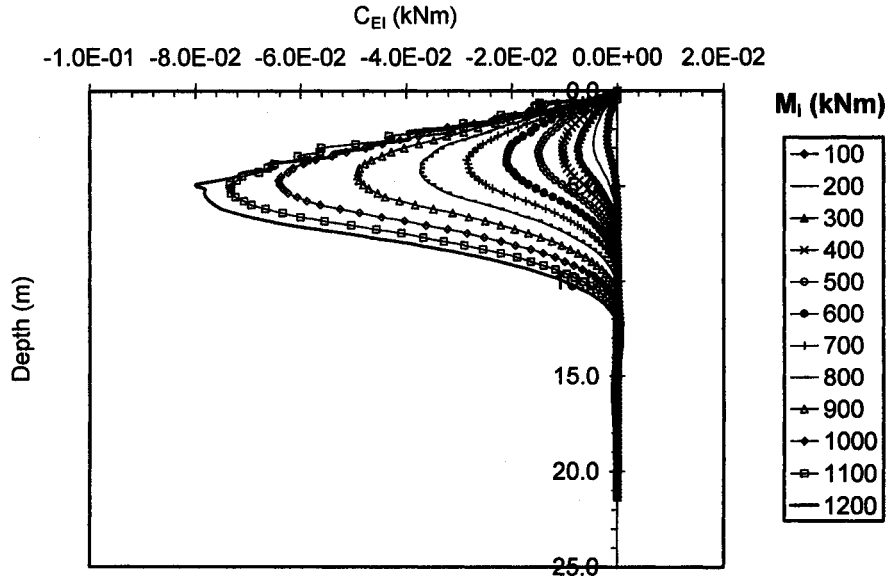

Fig. I.6 Distributions of sensitivity operators C_{EI} affecting the changes of δy_t due to variations of the design variable δEI for free head single pile with length L = 10T subjected to bending moments M_i (kNm)

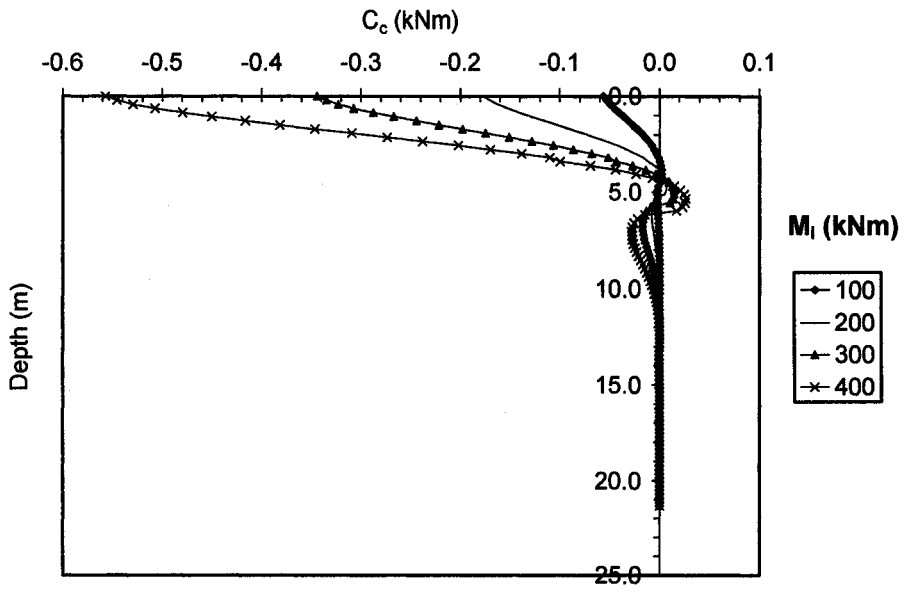

Fig. I.7a Distributions of sensitivity operators C_c affecting the changes of δy_t due to variations of the design variable δc for free head single pile with length L = 10T subjected to bending moments M_i (kNm)

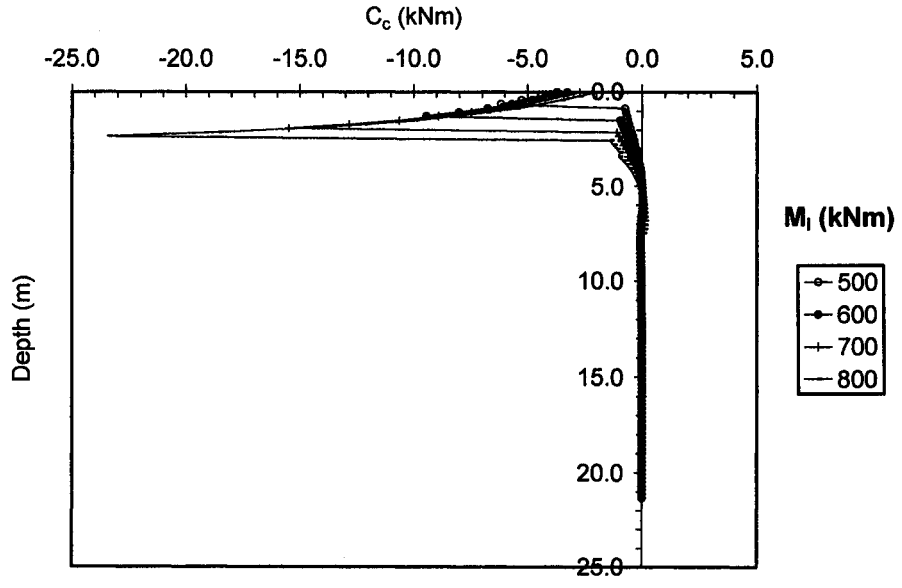

Fig. I.7b Distributions of sensitivity operators C_c affecting the changes of δy_t due to variations of the design variable δc for free head single pile with length L = 10T subjected to bending moments M_i (kNm)

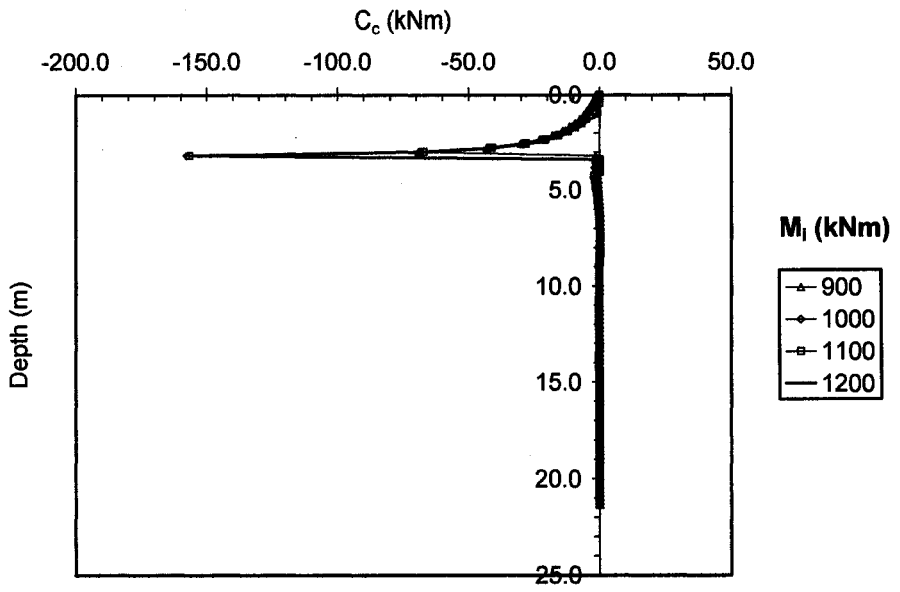

Fig. I.7c Distributions of sensitivity operators C_c affecting the changes of δy_t due to variations of the design variable δc for free head single pile with length L = 10T subjected to bending moments M_i (kNm)

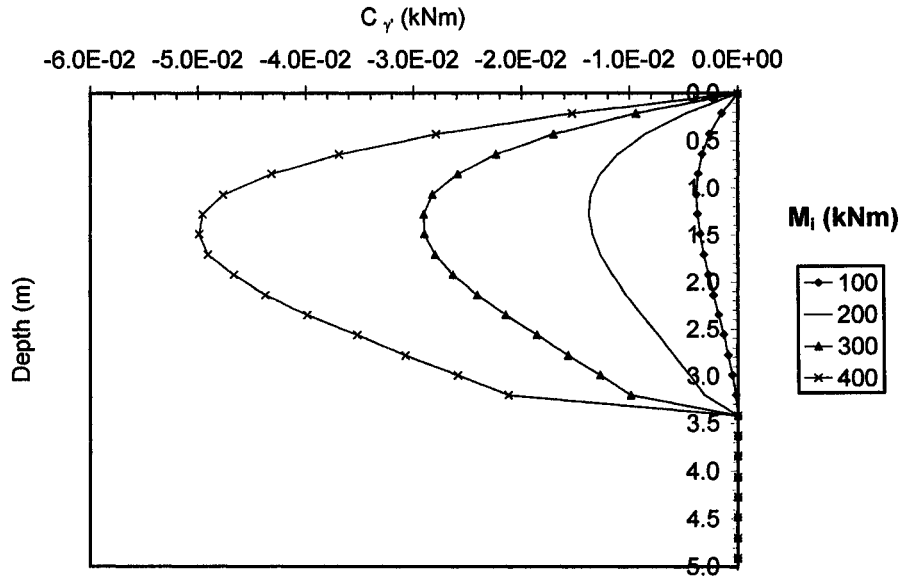

Fig. I.8a Distributions of sensitivity operators $C_{\gamma'}$ affecting the changes of δy_t due to variations of the design variable $\delta\gamma'$ for free head single pile with length L = 10T subjected to bending moments M_i (kNm)

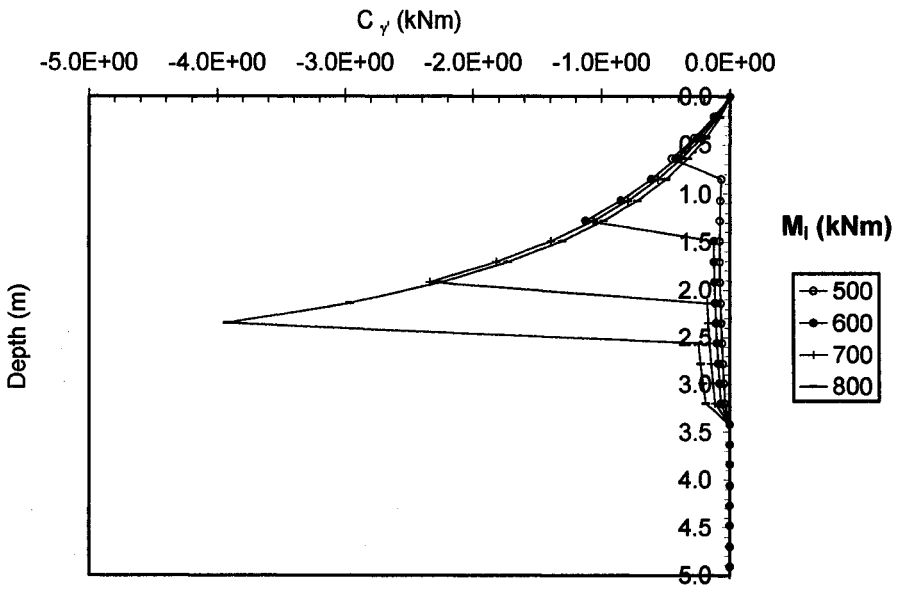

Fig. I.8b Distributions of sensitivity operators $C_{\gamma'}$ affecting the changes of δy_t due to variations of the design variable $\delta\gamma'$ for free head single pile with length L = 10T subjected to bending moments M_i (kNm)

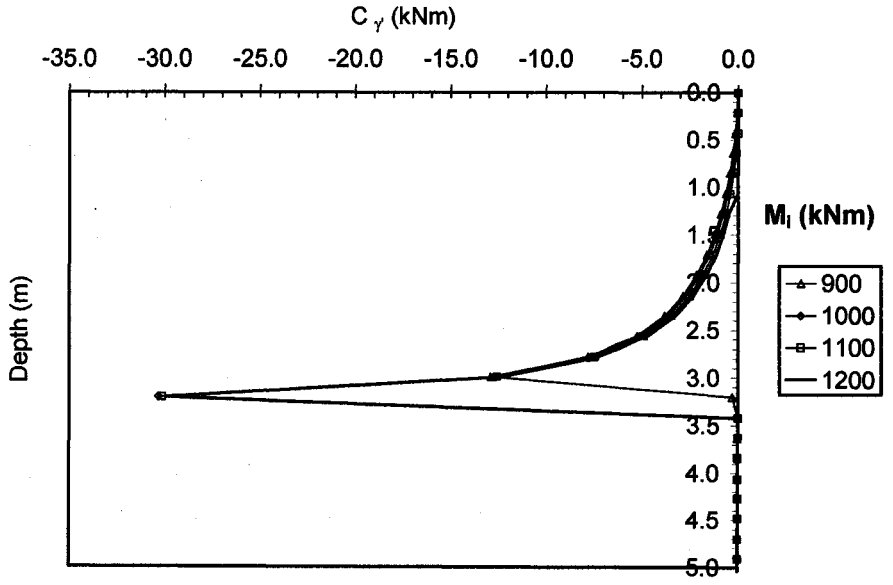

Fig. I.8c Distributions of sensitivity operators $C_{\gamma'}$ affecting the changes of δy_t due to variations of the design variable $\delta\gamma'$ for free head single pile with length L = 10T subjected to bending moments M_i (kNm)

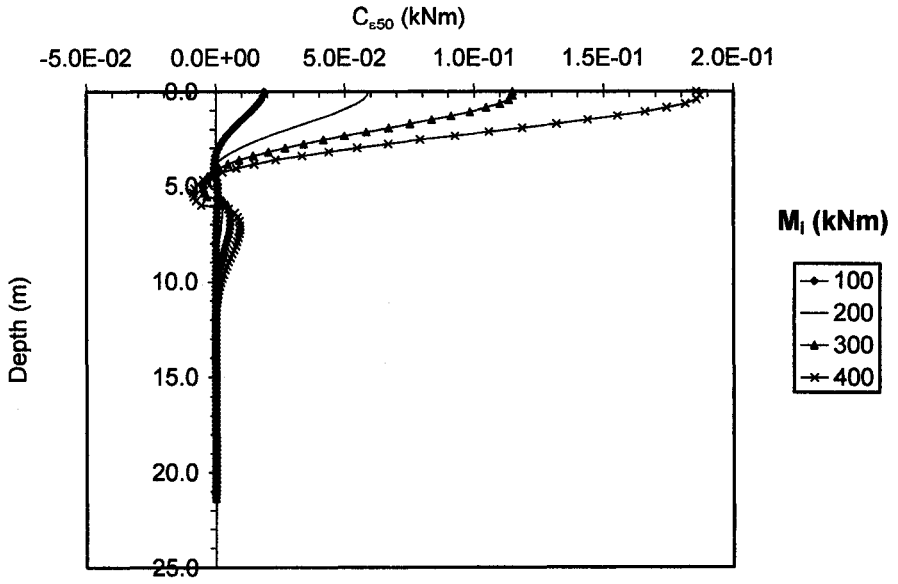

Fig. I.9a Distributions of sensitivity operators $C_{\varepsilon 50}$ affecting the changes of δy_t due to variations of the design variable $\delta\varepsilon_{50}$ for free head single pile with length L = 10T subjected to bending moments M_i (kNm)

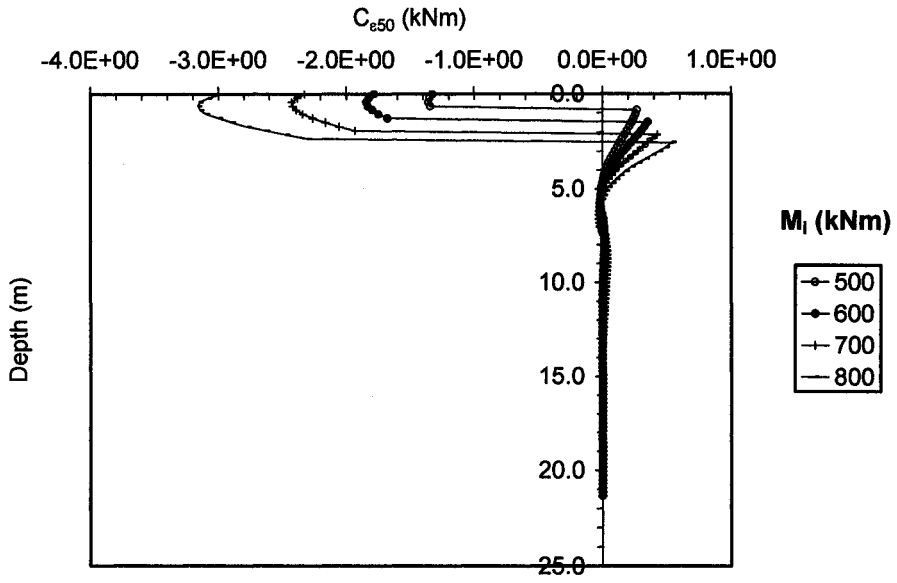

Fig. I.9b Distributions of sensitivity operators $C_{\varepsilon 50}$ affecting the changes of δy_t due to variations of the design variable $\delta\varepsilon_{50}$ for free head single pile with length L = 10T subjected to bending moments M_i (kNm)

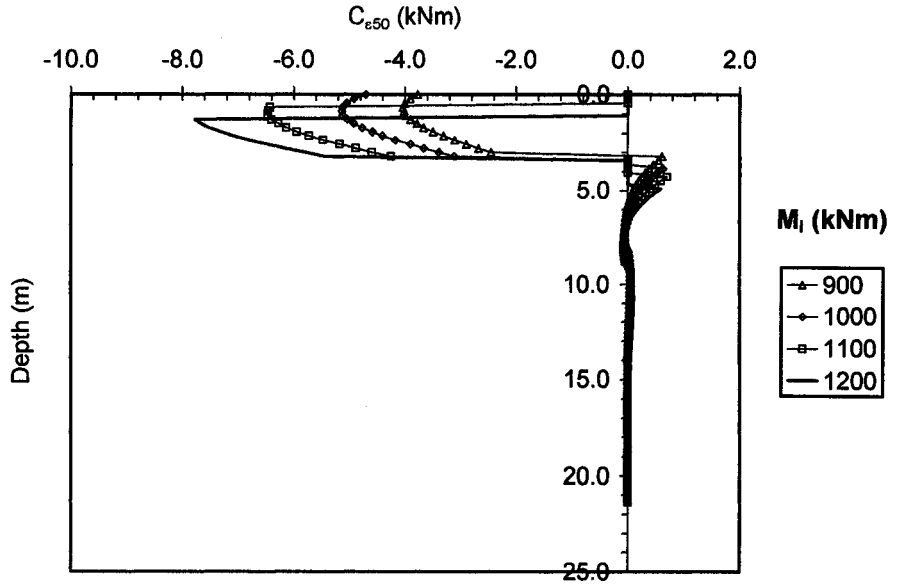

Fig. I.9c Distributions of sensitivity operators $C_{\varepsilon 50}$ affecting the changes of δy_t due to variations of the design variable $\delta\varepsilon_{50}$ for free head single pile with length L = 10T subjected to bending moments M_i (kNm)

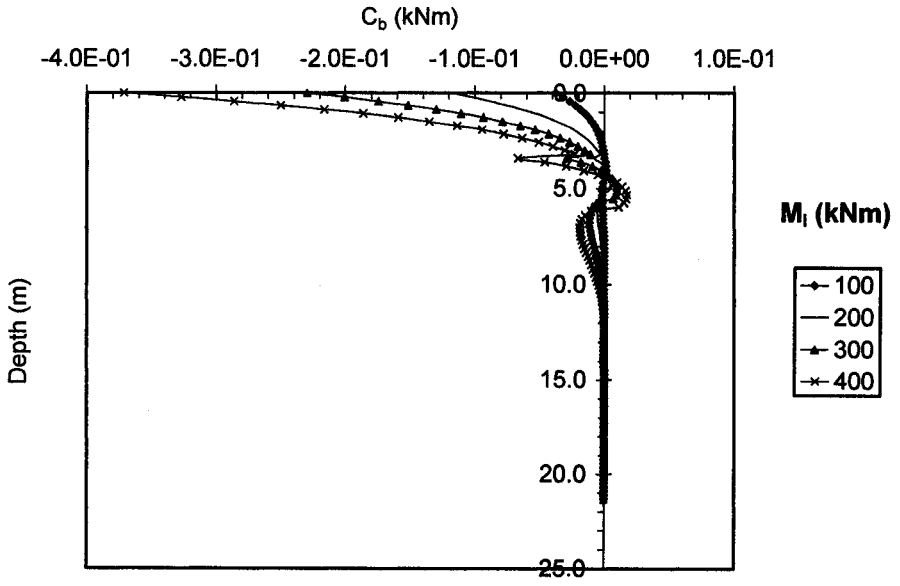

Fig. I.10a Distributions of sensitivity operators C_b affecting the changes of δy_t due to variations of the design variable δb for free head single pile with length L = 10T subjected to bending moments M_i (kNm)

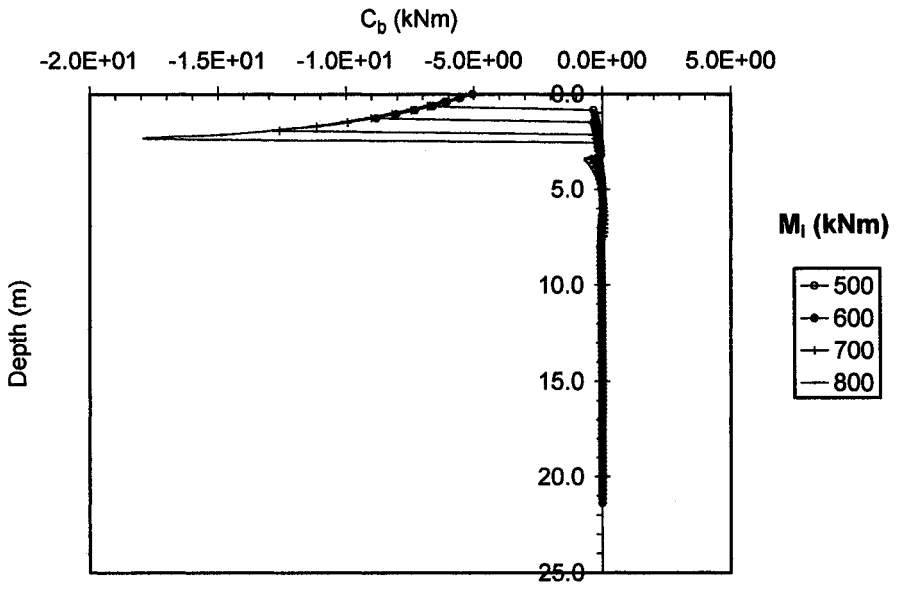

Fig. I.10b Distributions of sensitivity operators C_b affecting the changes of δy_t due to variations of the design variable δb for free head single pile with length L = 10T subjected to bending moments M_i (kNm)

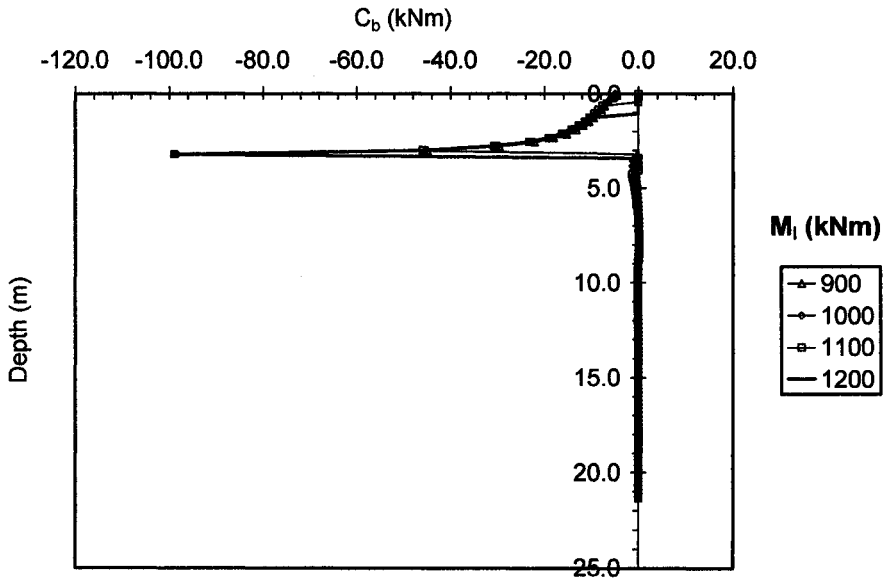

Fig. I.10c Distributions of sensitivity operators C_b affecting the changes of δy_t due to variations of the design variable δb for free head single pile with length L = 10T subjected to bending moments M_i (kNm)

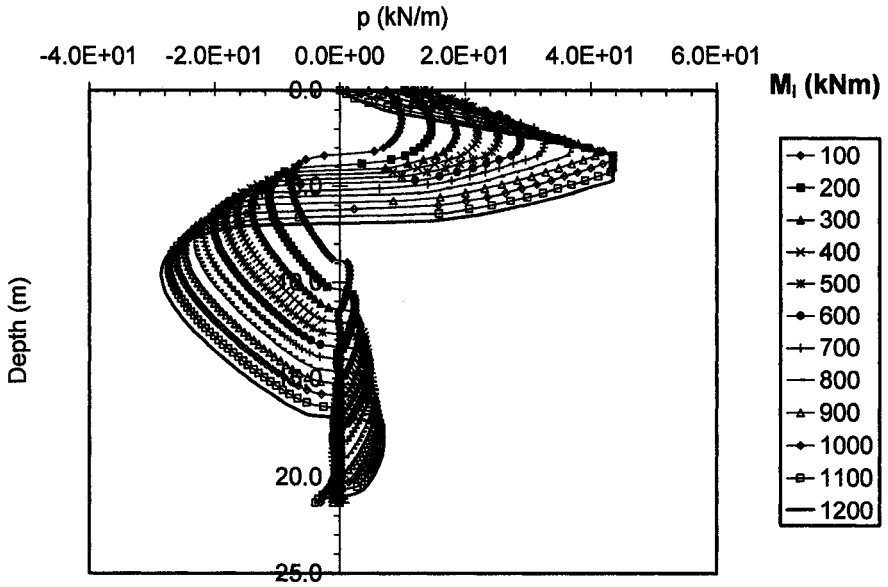

Fig. I.11 Distributions of soil reaction p at the primary structure along the depth of the pile for sensitivity analysis of top lateral displacement δy_t for free head single pile with length L = 10T subjected to bending moments M_i (kNm)

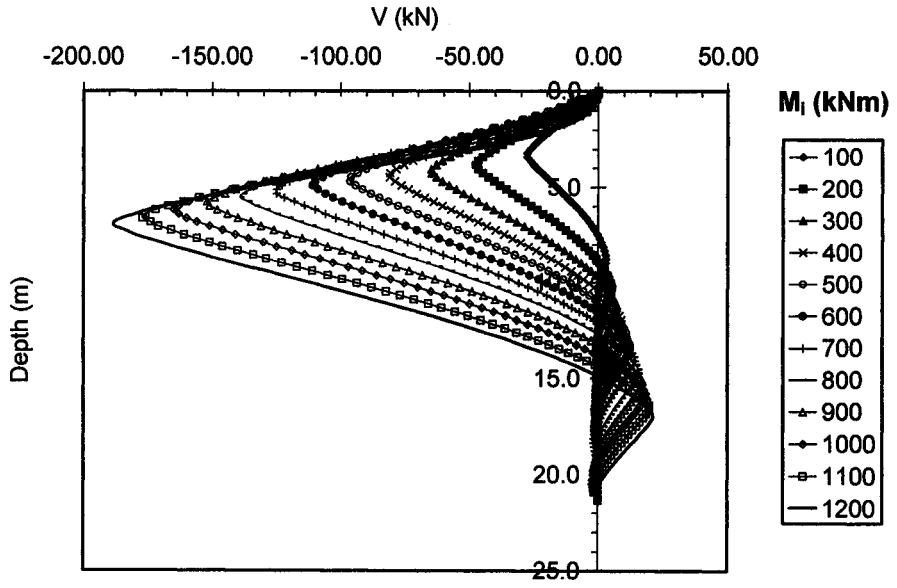

Fig. I.12 Distributions of shear forces V at the primary structure along the depth of the pile for sensitivity analysis of top lateral displacement δy_t for free head single pile with length L = 10T subjected to bending moments M_i (kNm)

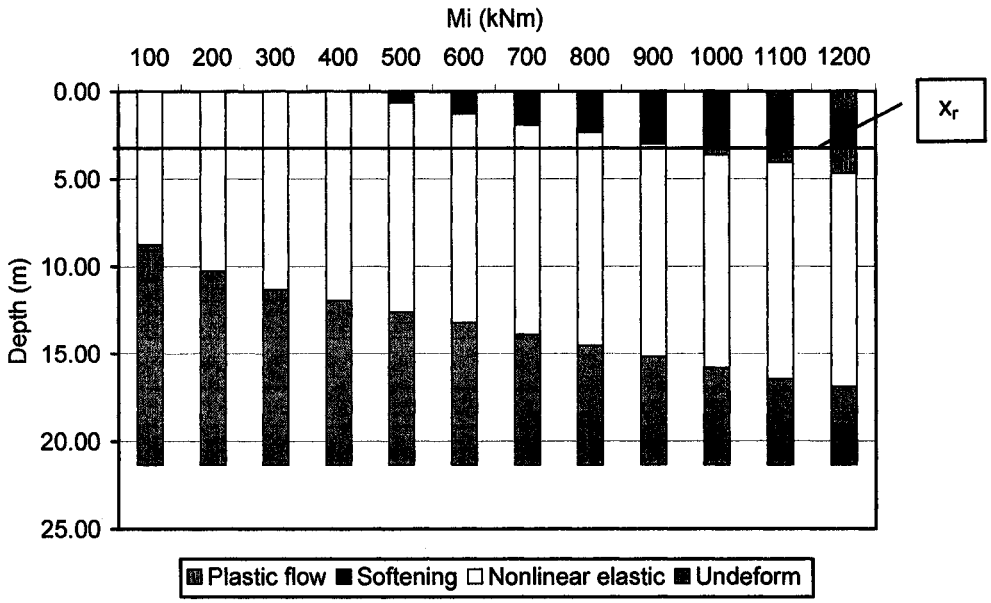

Fig. I.13 Quantitative assessment of the location and the size of soil phases developed with the depth determined based on the distributions of sensitivity operators affecting δy_t for free head single pile with length L = 10T subjected to bending moments M_i (kNm)

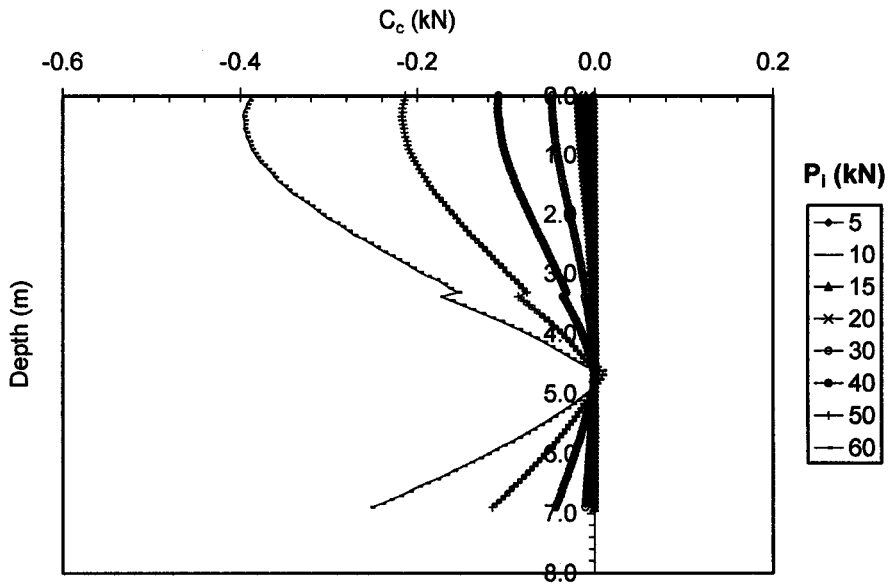

Fig. J.7 Distributions of sensitivity operators C_c affecting the changes of $\delta\varphi_t$ due to variations of the design variable δc for free head single pile with length L = 3T subjected to lateral forces P_i (kN)

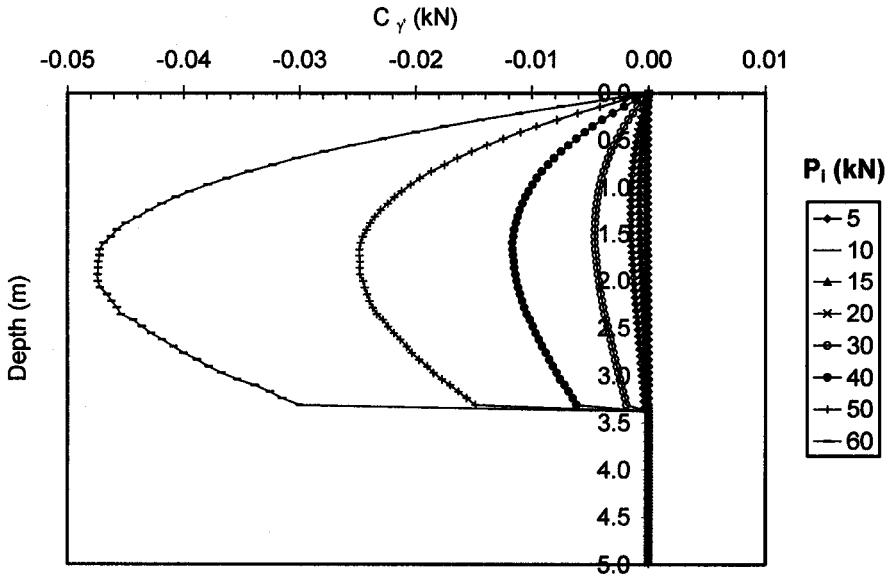

Fig. J.8 Distributions of sensitivity operators $C_{\gamma'}$ affecting the changes of $\delta\varphi_t$ due to variations of the design variable $\delta\gamma'$ for free head single pile with length L = 3T subjected to lateral forces P_i (kN)

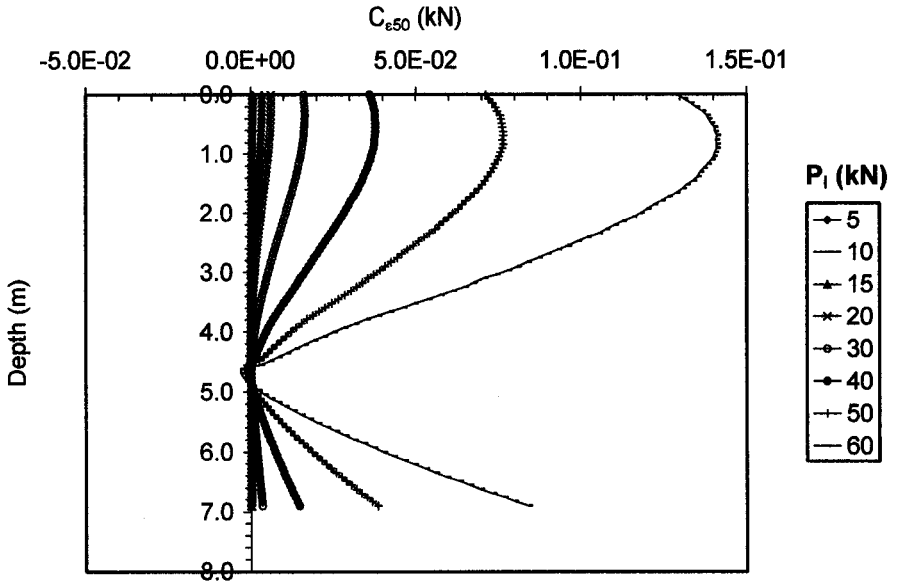

Fig. J.9 Distributions of sensitivity operators $C_{\varepsilon 50}$ affecting the changes of $\delta\varphi_t$ due to variations of the design variable $\delta\varepsilon_{50}$ for free head single pile with length L = 3T subjected to lateral forces P_i (kN)

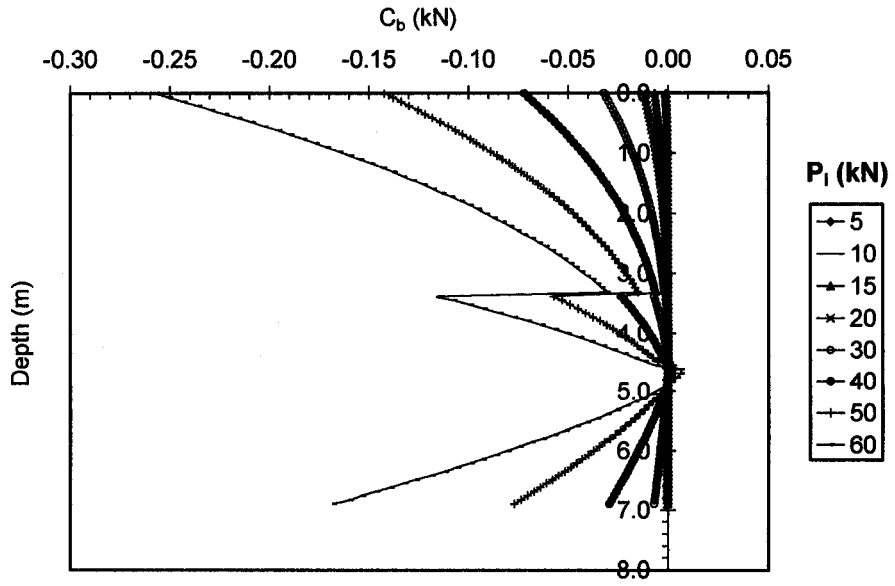

Fig. J.10 Distributions of sensitivity operators C_b affecting the changes of $\delta\varphi_t$ due to variations of the design variable δb for free head single pile with length L = 3T subjected to lateral forces P_i (kN)

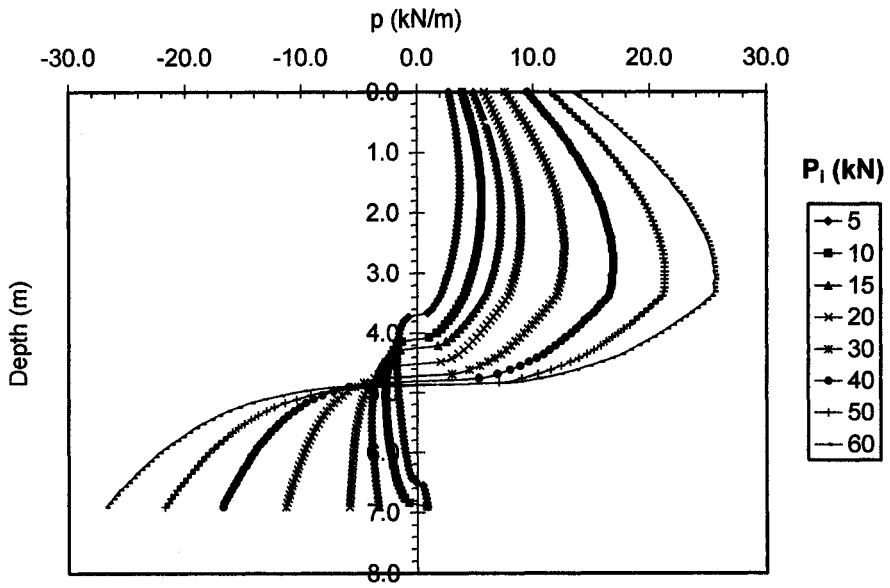

Fig. J.11 Distributions of soil reaction p at the primary structure along the depth of the pile for sensitivity analysis of top angle of rotation $\delta\varphi_t$ for free head single pile with length L = 3T subjected to lateral forces P_i (kN)

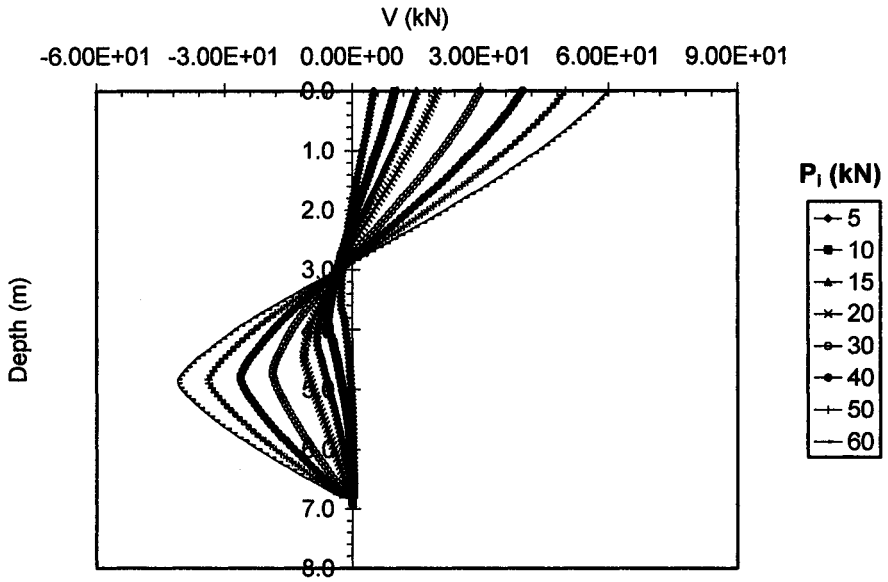

Fig. J.12 Distributions of shear forces V at the primary structure along the depth of the pile for sensitivity analysis of top angle of rotation $\delta\varphi_t$ for free head single pile with length L = 3T subjected to lateral forces P_i (kN)

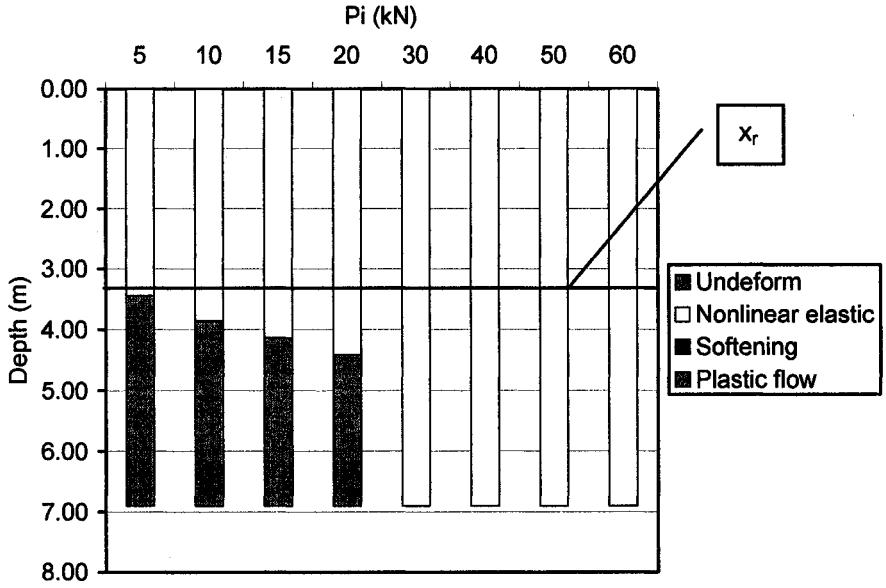

Fig. J.13 Quantitative assessment of the location and the size of the soil phases develop with the depth determined based on the distributions of sensitivity operators affecting $\delta\varphi_t$ for free head single pile with length L = 3T subjected to lateral forces P_i (kN)

APPENDIX K:

Sensitivity analysis of top angle of rotation $\delta\varphi_t$ for single free head pile with length L = 10T subjected to lateral forces Pi

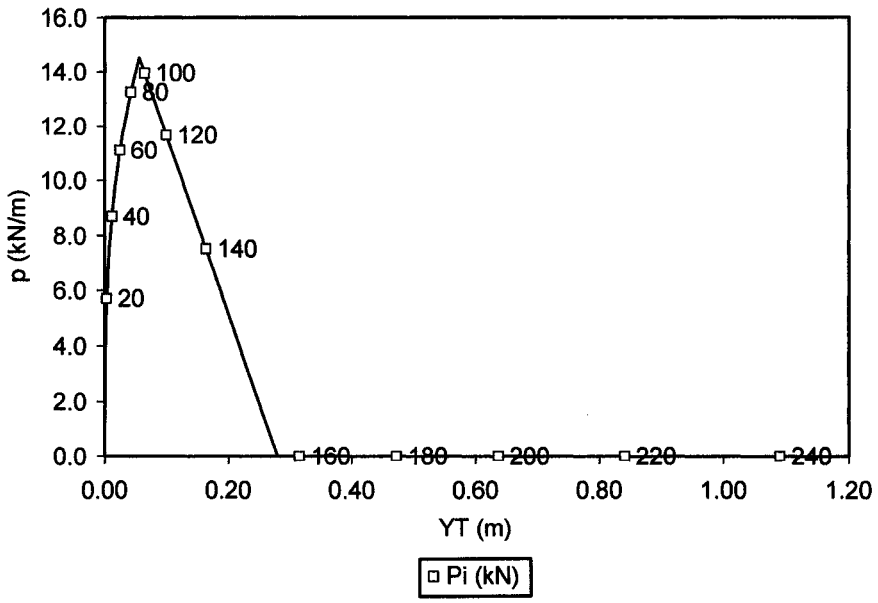

Fig. K.1 Soil reaction p at the top surface (expressed in terms of lateral loading) vs. lateral displacement generated by lateral loading applied to the pile for sensitivity analysis of top angle of rotation $\delta\varphi_t$ for free head single pile with length L = 10T subjected to lateral forces P_i (kN)

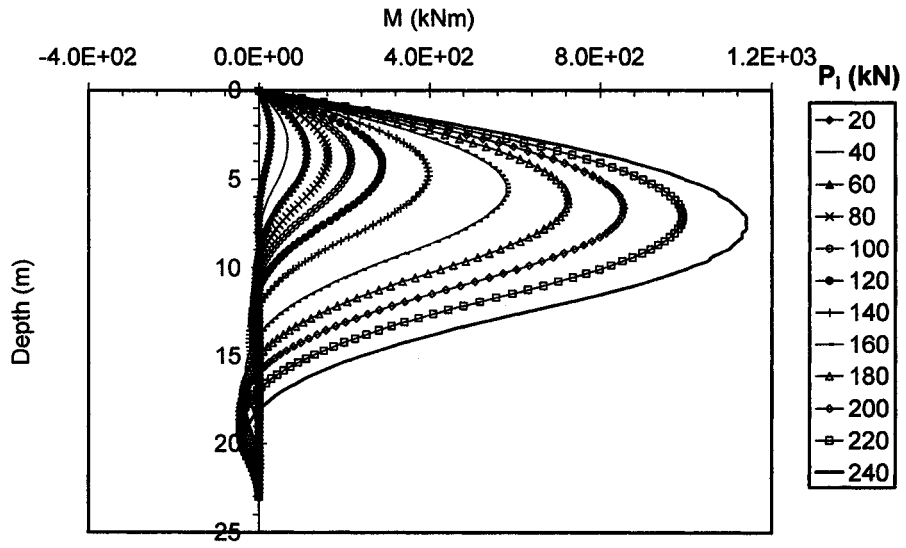

Fig. K.2 Distributions of bending moments at the primary structure M along the depth of the pile for sensitivity analysis of top angle of rotation $\delta\varphi_t$ for free head single pile with length L = 10T subjected to lateral forces P_i (kN)

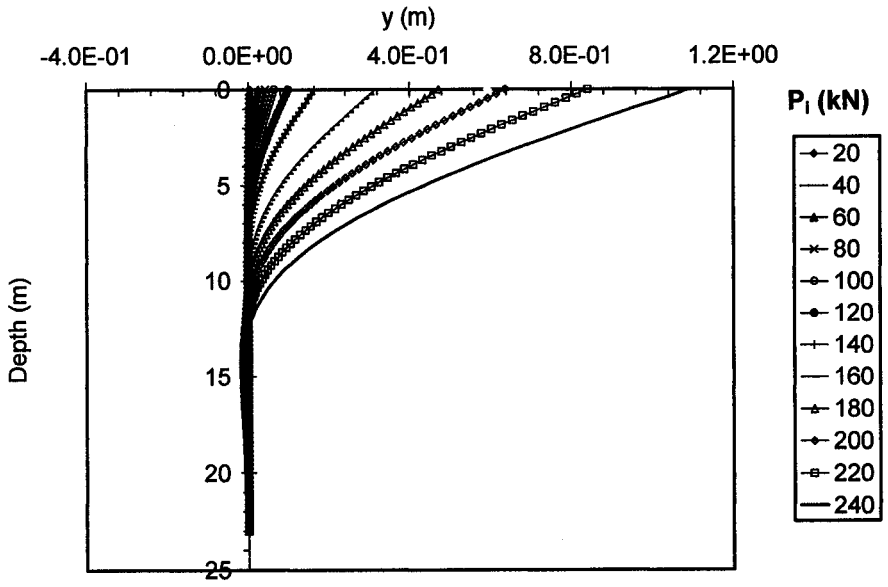

Fig. K.3 Distributions of lateral deflections at the primary structure y along the depth of the pile for sensitivity analysis of top angle of rotation $\delta\varphi_t$ for free head single pile with length L = 10T subjected to lateral forces P_i (kN)

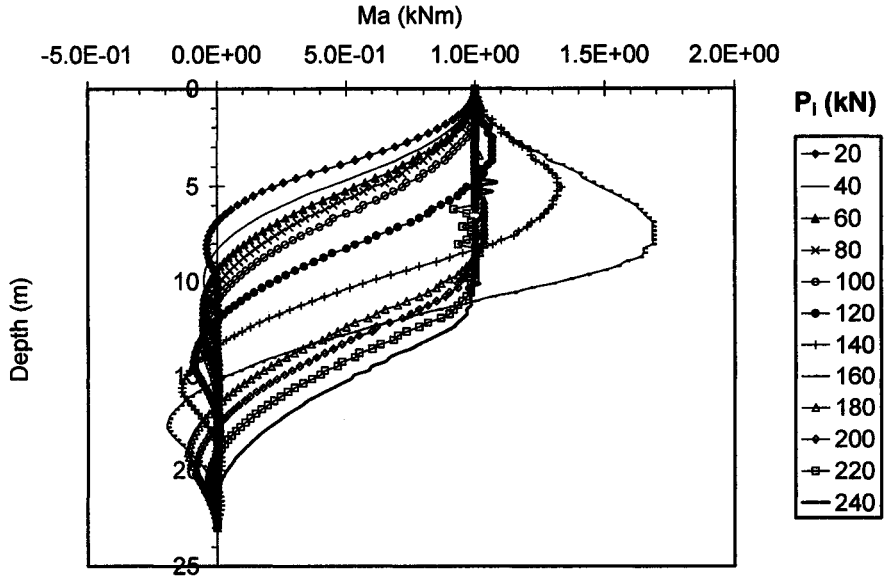

Fig. K.4 Distributions of bending moments M_a along the depth of the pile at the adjoint structure for sensitivity analysis of top angle of rotation $\delta\varphi_t$ for free head single pile with length L = 10T subjected to lateral forces P_i (kN)

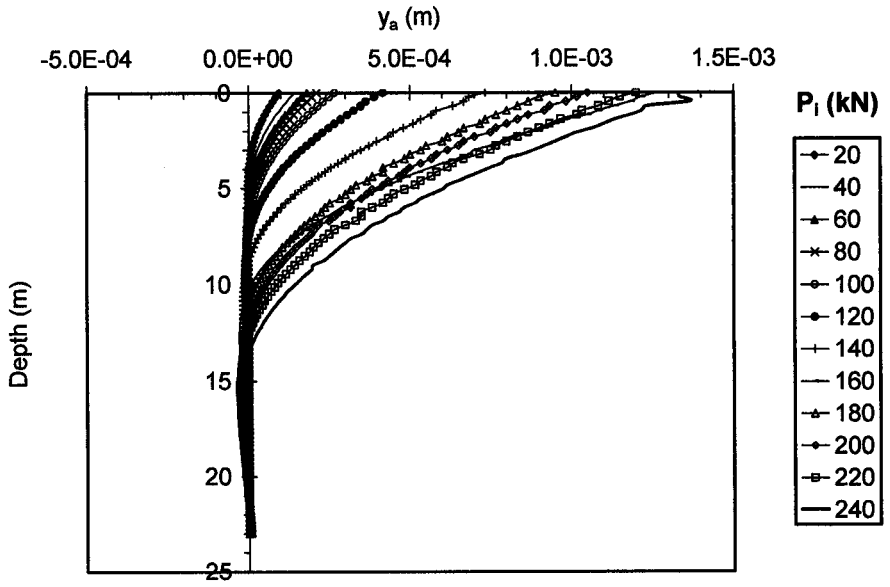

Fig. K.5 Distributions of lateral deflections at the adjoint structure y_a along the depth of the pile for sensitivity analysis of top angle of rotation $\delta\varphi_t$ for free head single pile with length L = 10T subjected to lateral forces P_i (kN)

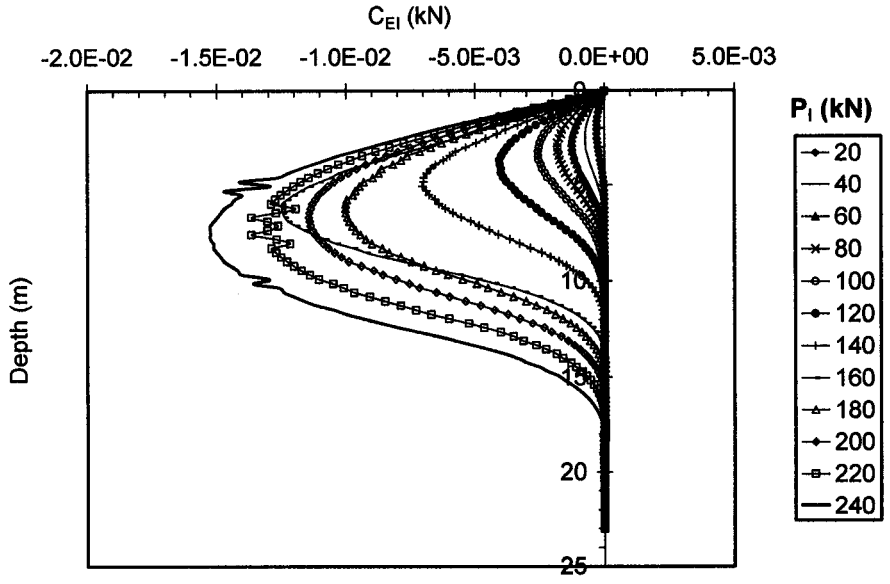

Fig. K.6 Distributions of sensitivity operators C_{EI} affecting the changes of $\delta\varphi_t$ due to variations of the design variable δEI for free head single pile with length L = 10T subjected to lateral forces P_i (kN)

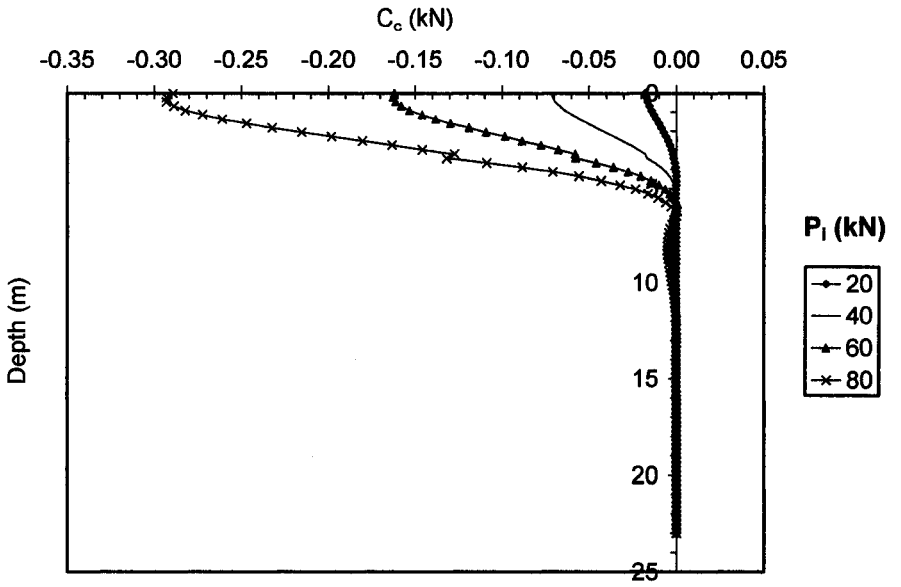

Fig. K.7a Distributions of sensitivity operators C_c affecting the changes of $\delta\varphi_t$ due to variations of the design variable δc for free head single pile with length L = 10T subjected to lateral forces P_i (kN)

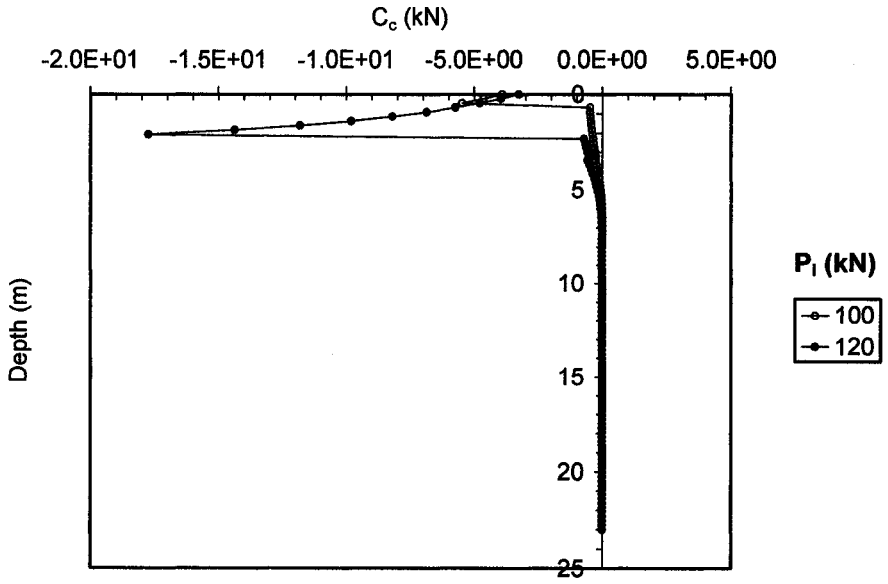

Fig. K.7b Distributions of sensitivity operators C_c affecting the changes of $\delta\varphi_t$ due to variations of the design variable δc for free head single pile with length L = 10T subjected to lateral forces P_i (kN)

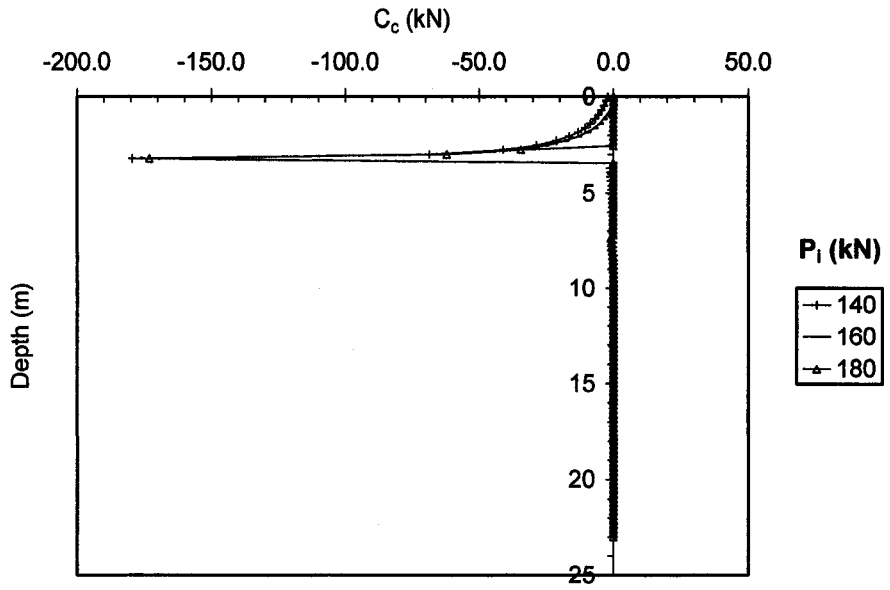

Fig. K.7c Distributions of sensitivity operators C_c affecting the changes of $\delta\varphi_t$ due to variations of the design variable δc for free head single pile with length L = 10T subjected to lateral forces P_i (kN)

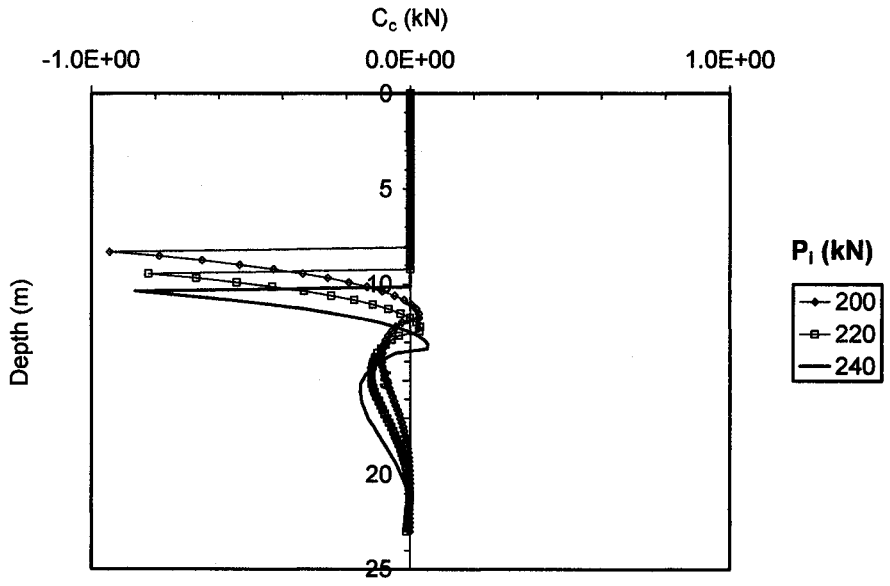

Fig. K.7d Distributions of sensitivity operators C_c affecting the changes of $\delta\varphi_t$ due to variations of the design variable δc for free head single pile with length L = 10T subjected to lateral forces P_i (kN)

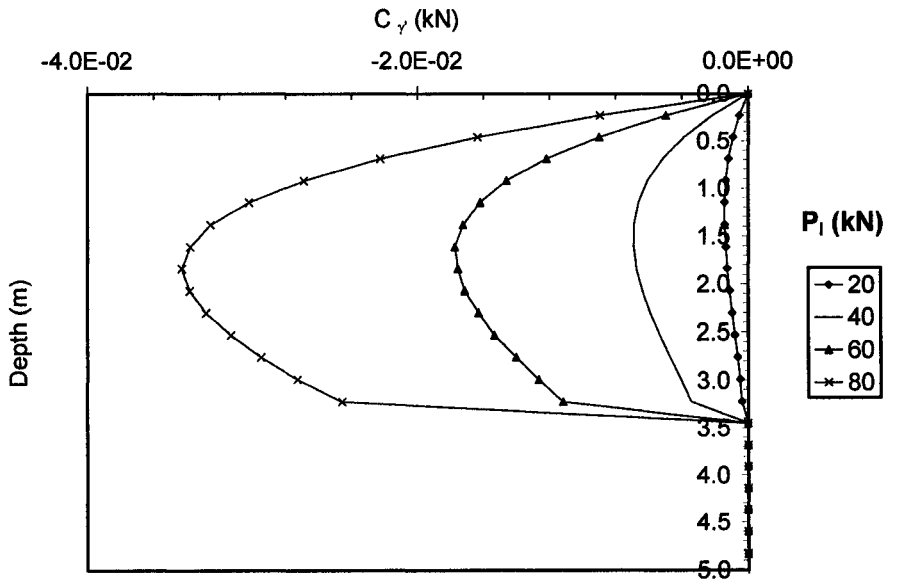

Fig. K.8a Distributions of sensitivity operators $C_{\gamma'}$ affecting the changes of $\delta\varphi_t$ due to variations of the design variable $\delta\gamma'$ for free head single pile with length L = 10T subjected to lateral forces P_i (kN)

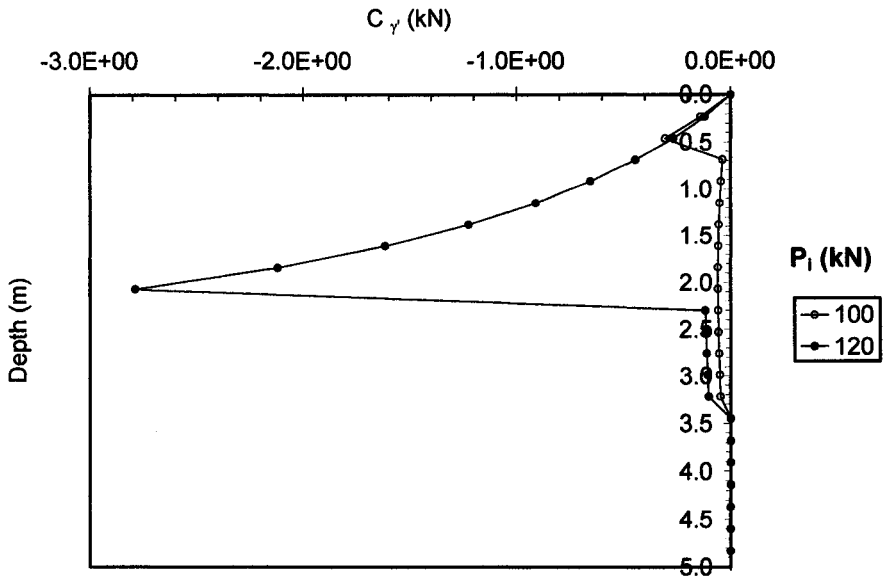

Fig. K.8b Distributions of sensitivity operators $C_{\gamma'}$ affecting the changes of $\delta\varphi_t$ due to variations of the design variable $\delta\gamma'$ for free head single pile with length L = 10T subjected to lateral forces P_i (kN)

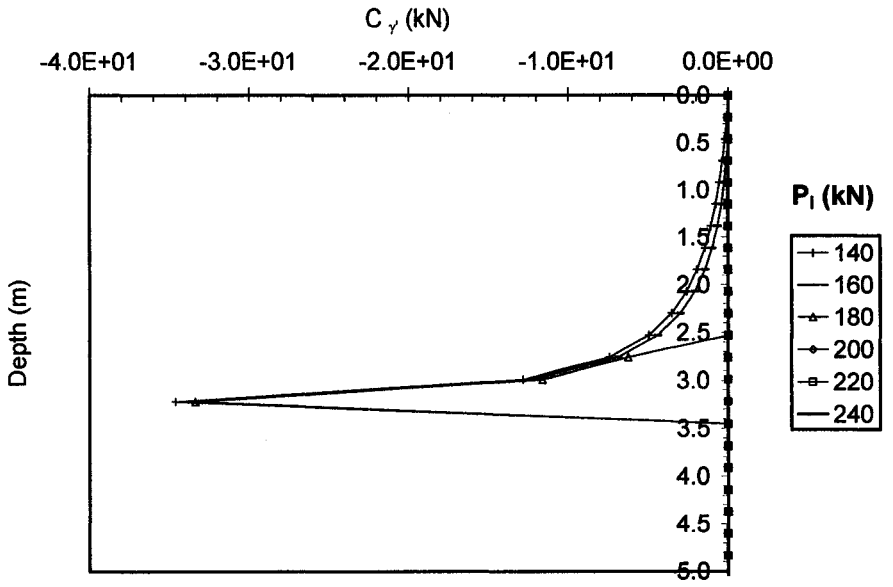

Fig. K.8c Distributions of sensitivity operators $C_{\gamma'}$ affecting the changes of $\delta\varphi_t$ due to variations of the design variable $\delta\gamma'$ for free head single pile with length L = 10T subjected to lateral forces P_i (kN)

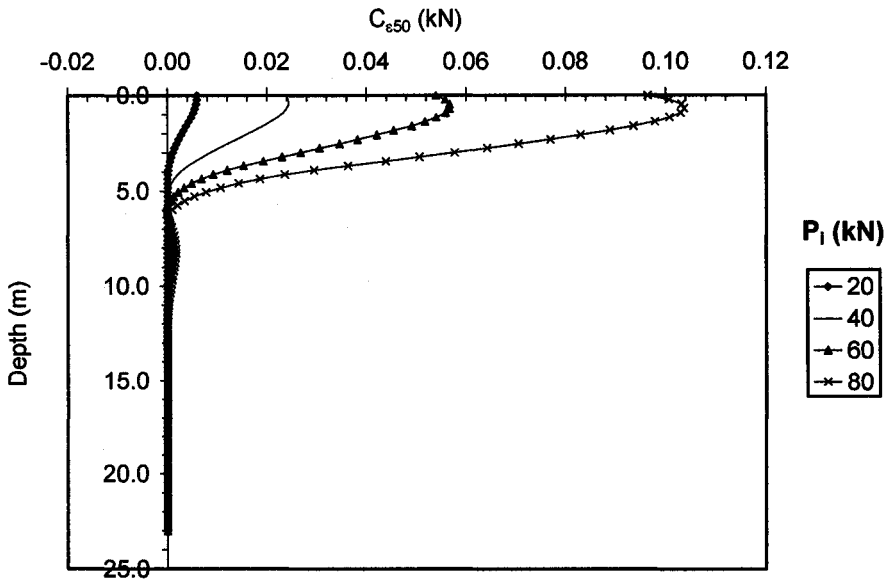

Fig. K.9a Distributions of sensitivity operators $C_{\varepsilon 50}$ affecting the changes of $\delta\varphi_t$ due to variations of the design variable $\delta\varepsilon_{50}$ for free head single pile with length L = 10T subjected to lateral forces P_i (kN)

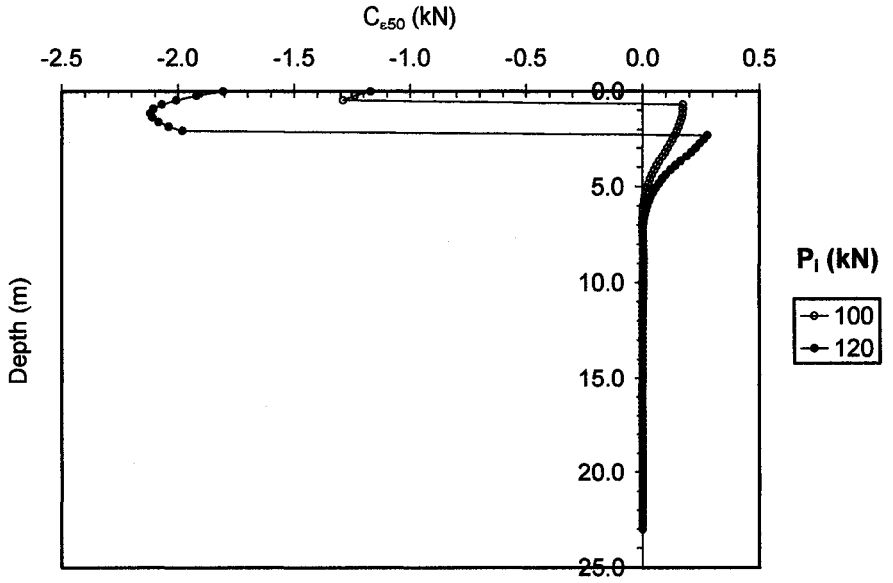

Fig. K.9b Distributions of sensitivity operators $C_{\varepsilon 50}$ affecting the changes of $\delta\varphi_t$ due to variations of the design variable $\delta\varepsilon_{50}$ for free head single pile with length L = 10T subjected to lateral forces P_i (kN)

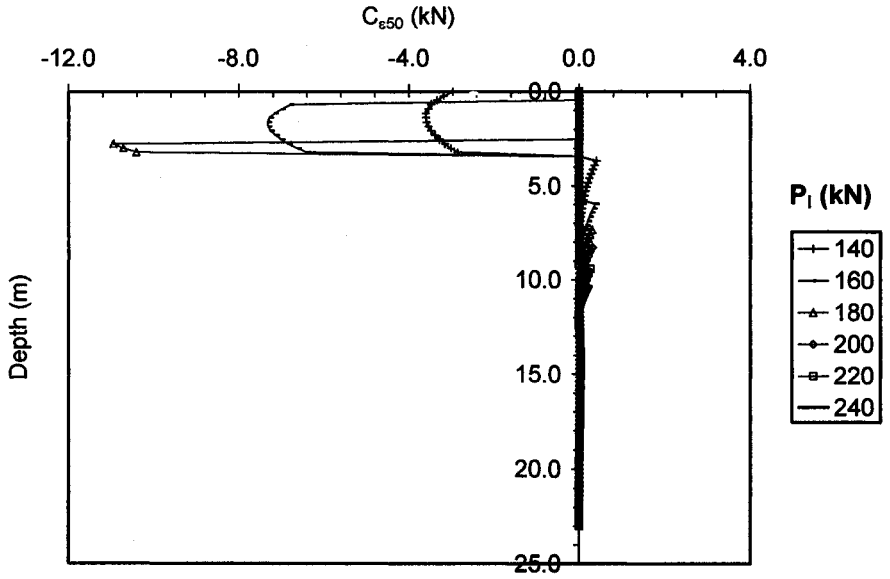

Fig. K.9c Distributions of sensitivity operators $C_{\varepsilon 50}$ affecting the changes of $\delta\varphi_t$ due to variations of the design variable $\delta\varepsilon_{50}$ for free head single pile with length L = 10T subjected to lateral forces P_i (kN)

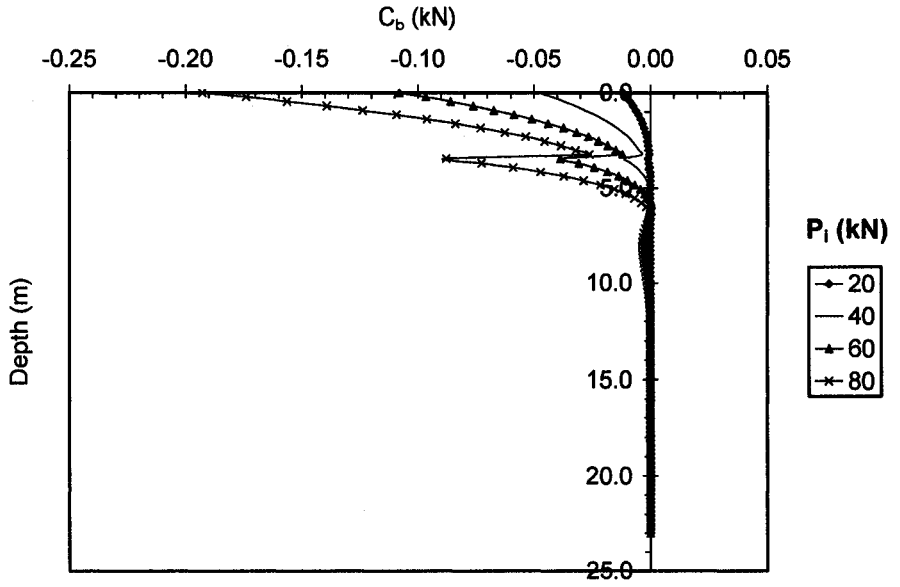

Fig. K.10a Distributions of sensitivity operators C_b affecting the changes of $\delta\varphi_t$ due to variations of the design variable δb for free head single pile with length L = 10T subjected to lateral forces P_i (kN)

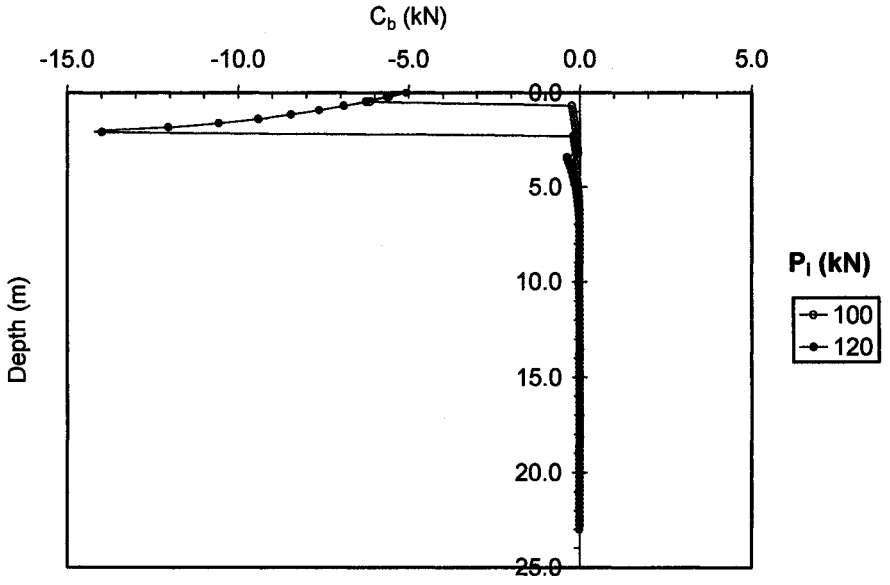

Fig. K.10b Distributions of sensitivity operators C_b affecting the changes of $\delta\varphi_t$ due to variations of the design variable δb for free head single pile with length L = 10T subjected to lateral forces P_i (kN)

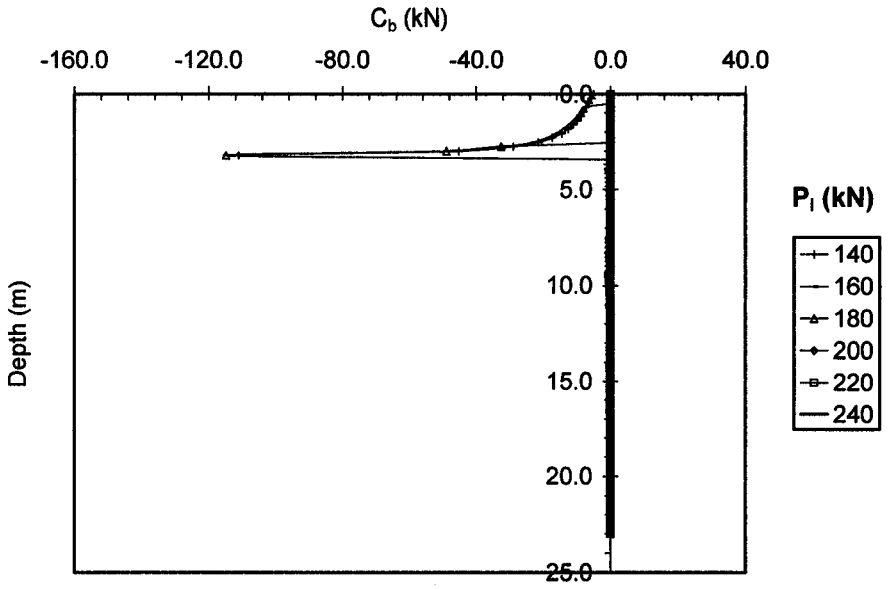

Fig. K.10c Distributions of sensitivity operators C_b affecting the changes of $\delta\varphi_t$ due to variations of the design variable δb for free head single pile with length L = 10T subjected to lateral forces P_i (kN)

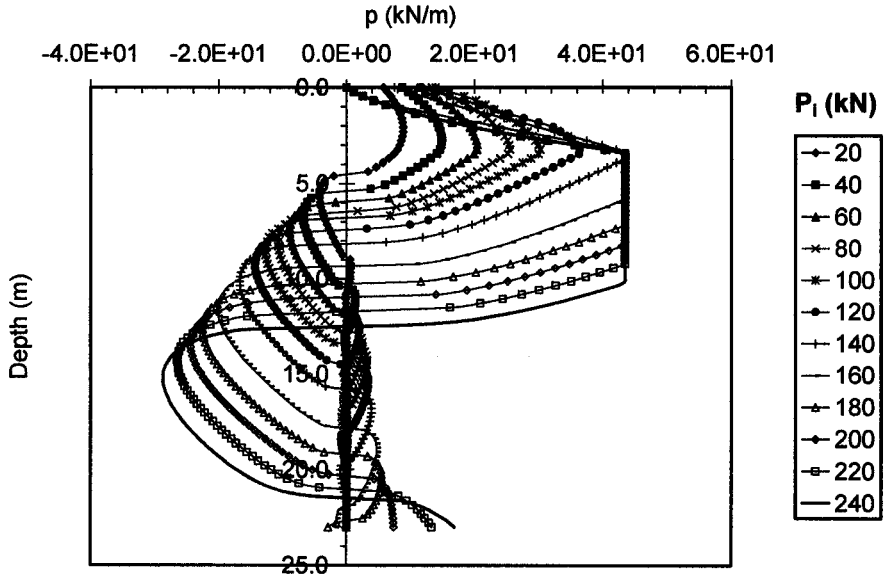

Fig. K.11 Distributions of soil reaction p at the primary structure along the depth of the pile for sensitivity analysis of top angle of rotation $\delta\varphi_t$ for free head single pile with length L = 10T subjected to lateral forces P_i (kN)

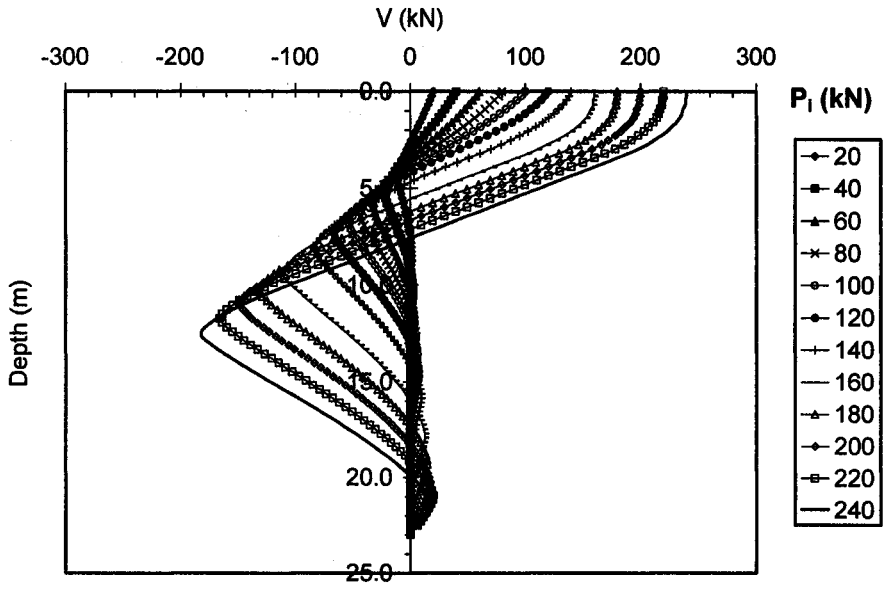

Fig. K.12 Distributions of shear forces V at the primary structure along the depth of the pile for sensitivity analysis of top angle of rotation $\delta\varphi_t$ for free head single pile with length L = 10T subjected to lateral forces P_i (kN)

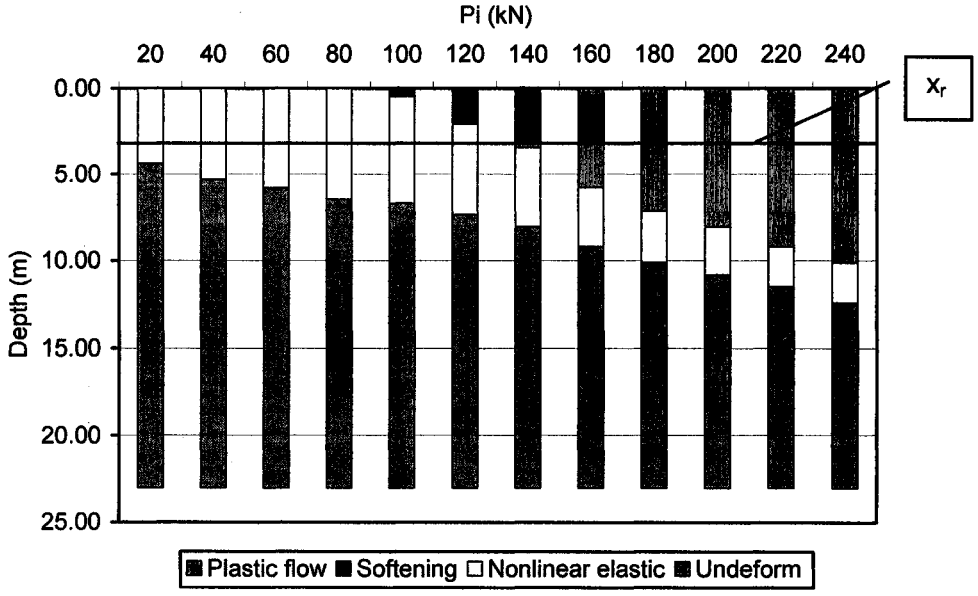

Fig. K.13 Quantitative assessment of the location and the size of the soil phases develop with the depth of the pile determined based on the distributions of sensitivity operators affecting $\delta\varphi_t$ for free head single pile with length L = 10T subjected to lateral forces P_i (kN)

APPENDIX L:

Sensitivity analysis of top angle of rotation $\delta\varphi_t$ for single free head pile with length L = 3T subjected to bending moments M_i

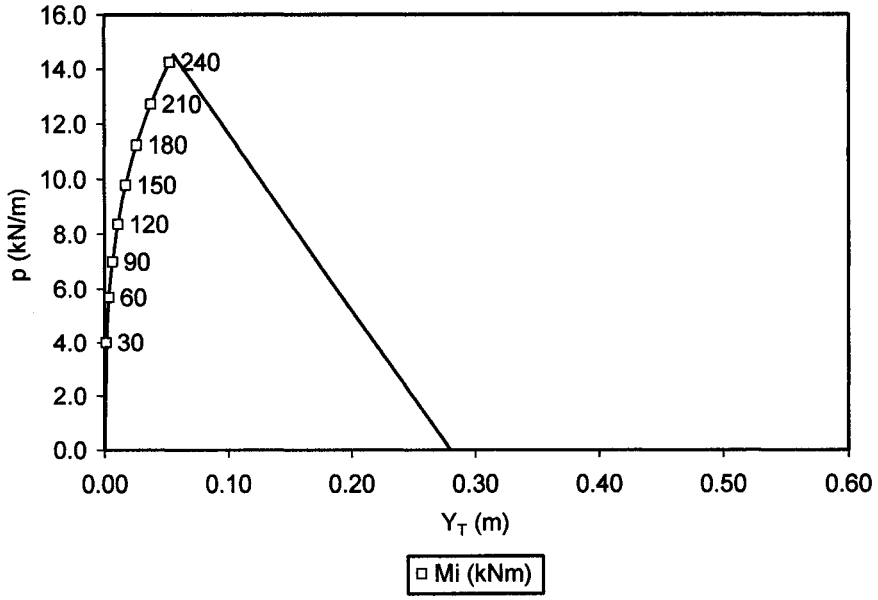

Fig. L.1 Soil reaction p at the top surface (expressed in terms of lateral loading) vs. lateral displacement generated by lateral loading applied to the pile for sensitivity analysis of top angle of rotation $\delta\varphi_t$ for free head single pile with length L = 3T subjected to bending moments M_i (kNm)

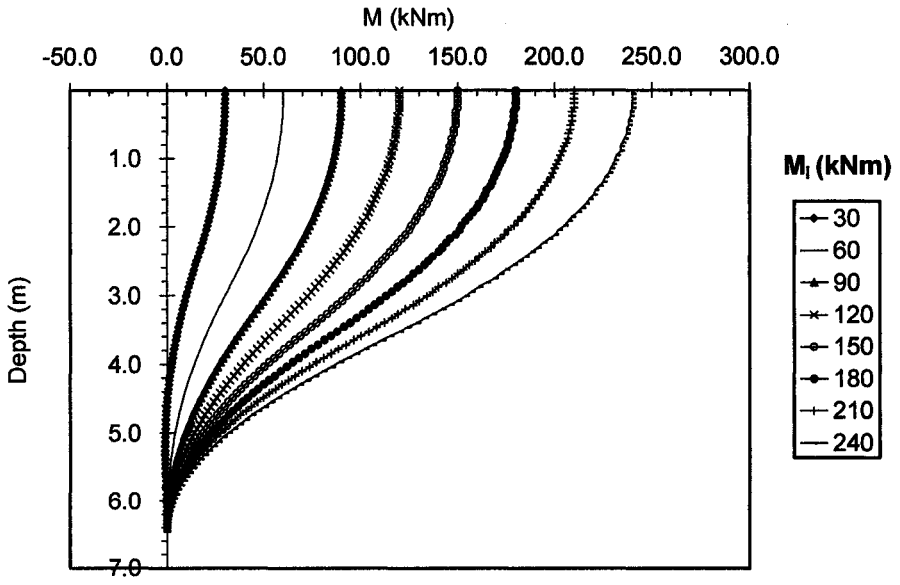

Fig. L.2 Distributions of bending moments at the primary structure M along the depth of the pile for sensitivity analysis of top angle of rotation $\delta\varphi_t$ for free head single pile with length L = 3T subjected to bending moments M_i (kNm)

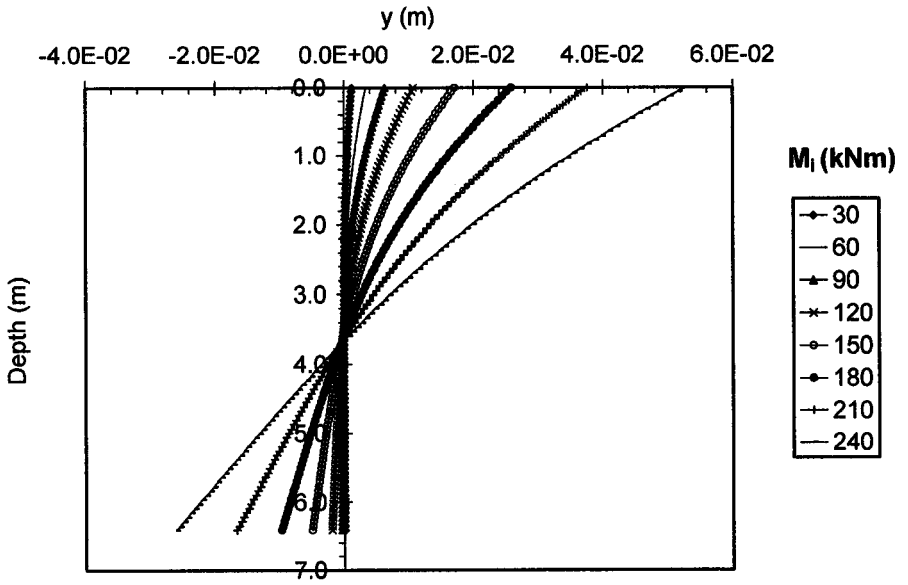

Fig. L.3 Distributions of lateral deflections at the primary structure y along the depth of the pile for sensitivity analysis of top angle of rotation $\delta\varphi_t$ for free head single pile with length L = 3T subjected to bending moments M_i (kNm)

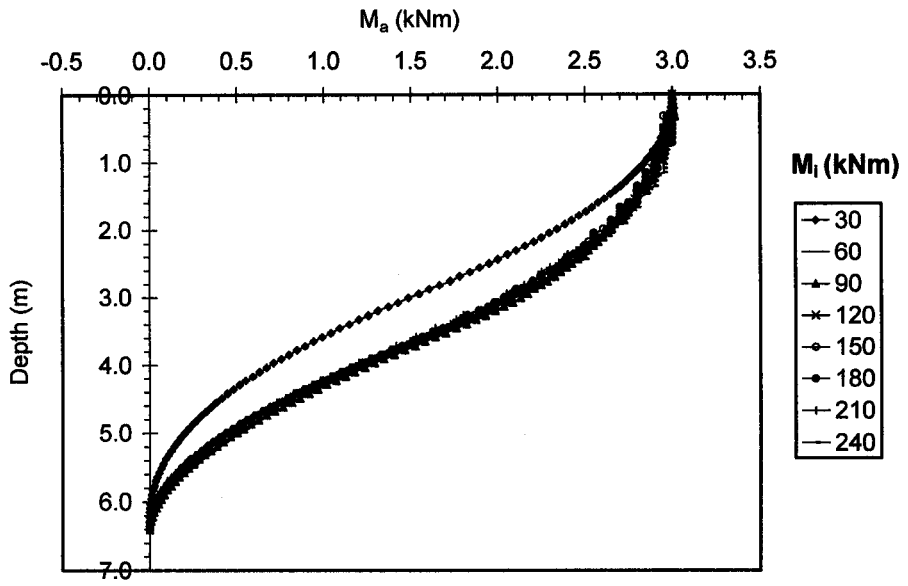

Fig. L.4 Distributions of bending moments M_a along the depth of the pile at the adjoint structure for sensitivity analysis of top angle of rotation $\delta\varphi_t$ for free head single pile with length L = 3T subjected to bending moments M_i (kNm)

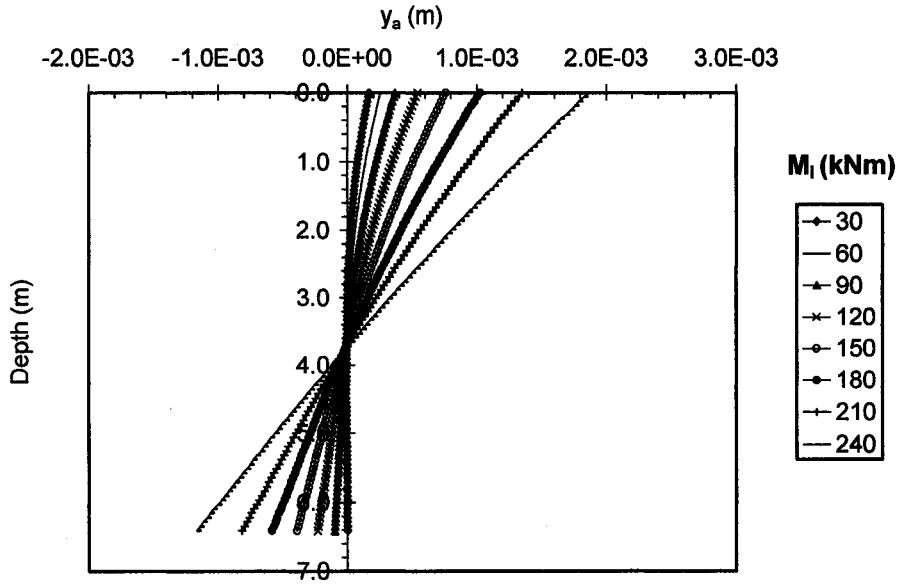

Fig. L.5 Distributions of lateral deflections at the adjoint structure y_a along the depth of the pile for sensitivity analysis of top angle of rotation $\delta\varphi_t$ for free head single pile with length L = 3T subjected to bending moments M_i (kNm)

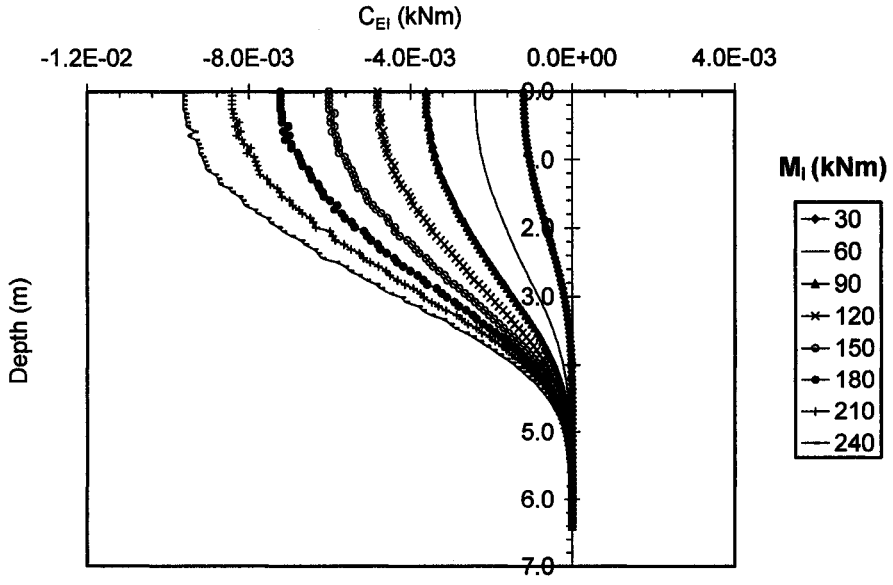

Fig. L.6 Distributions of sensitivity operators C_{EI} affecting the changes of $\delta\varphi_t$ due to variations of the design variable δEI for free head single pile with length L = 3T subjected to bending moments M_i (kNm)

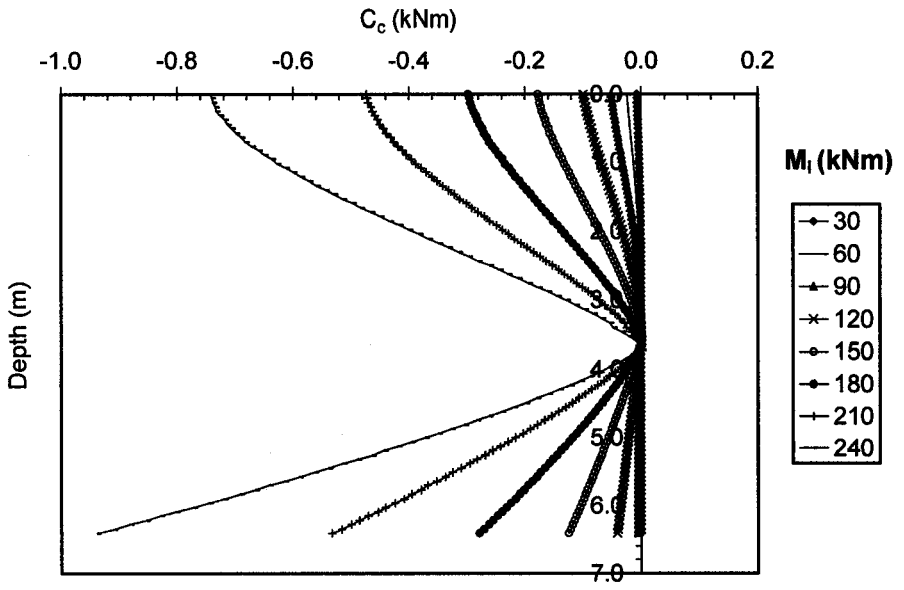

Fig. L.7 Distributions of sensitivity operators C_c affecting the changes of $\delta\varphi_t$ due to variations of the design variable δc for free head single pile with length L = 3T subjected to bending moments M_i (kNm)

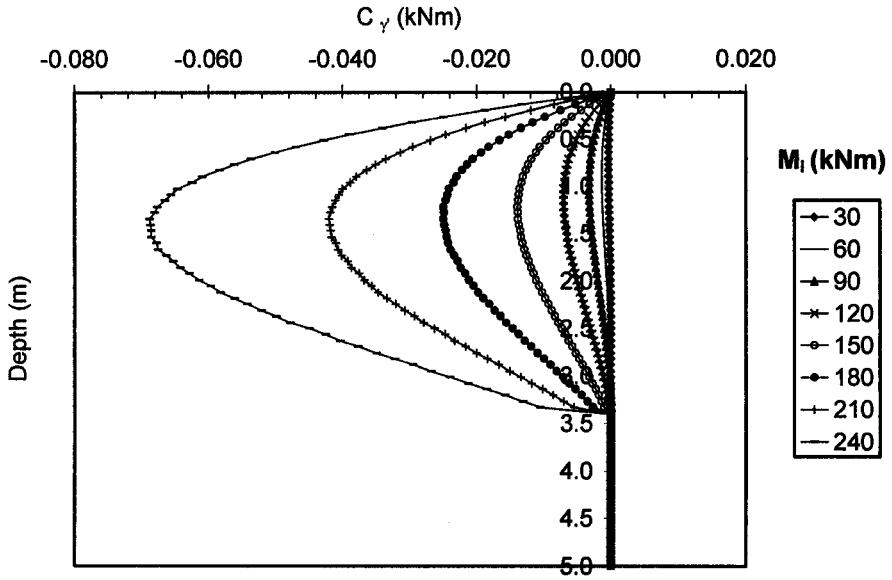

Fig. L.8 Distributions of sensitivity operators $C_{\gamma'}$ affecting the changes of $\delta\varphi_t$ due to variations of the design variable $\delta\gamma'$ for free head single pile with length L = 3T subjected to bending moments M_i (kNm)

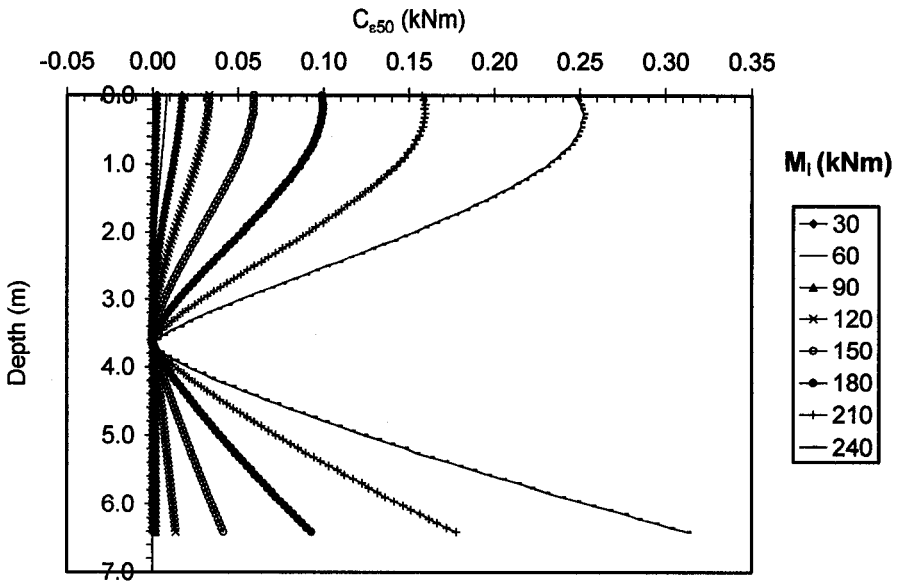

Fig. L.9 Distributions of sensitivity operators $C_{\varepsilon 50}$ affecting the changes of $\delta\varphi_t$ due to variations of the design variable $\delta\varepsilon_{50}$ for free head single pile with length L = 3T subjected to bending moments M_i (kNm)

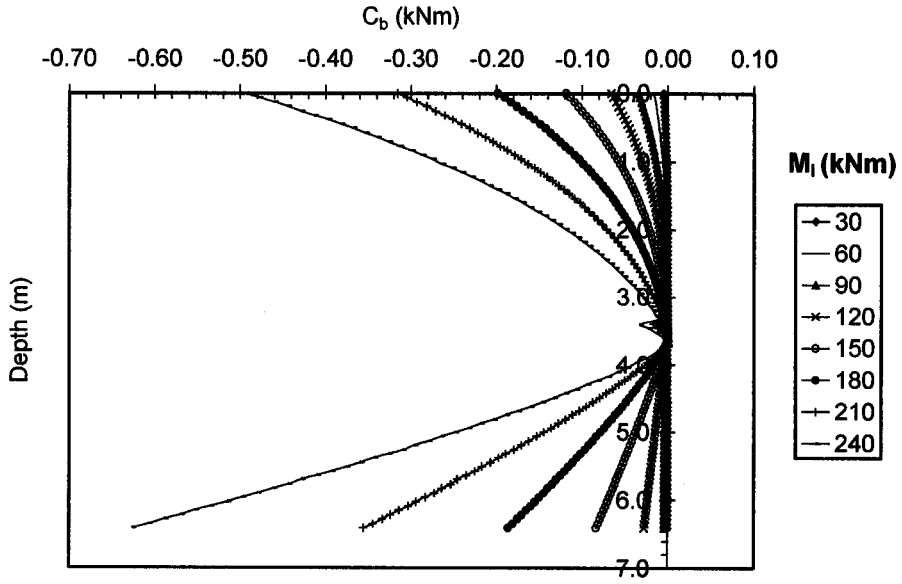

Fig. L.10 Distributions of sensitivity operators C_b affecting the changes of $\delta\varphi_t$ due to variations of the design variable δb for free head single pile with length L = 3T subjected to bending moments M_i (kNm)

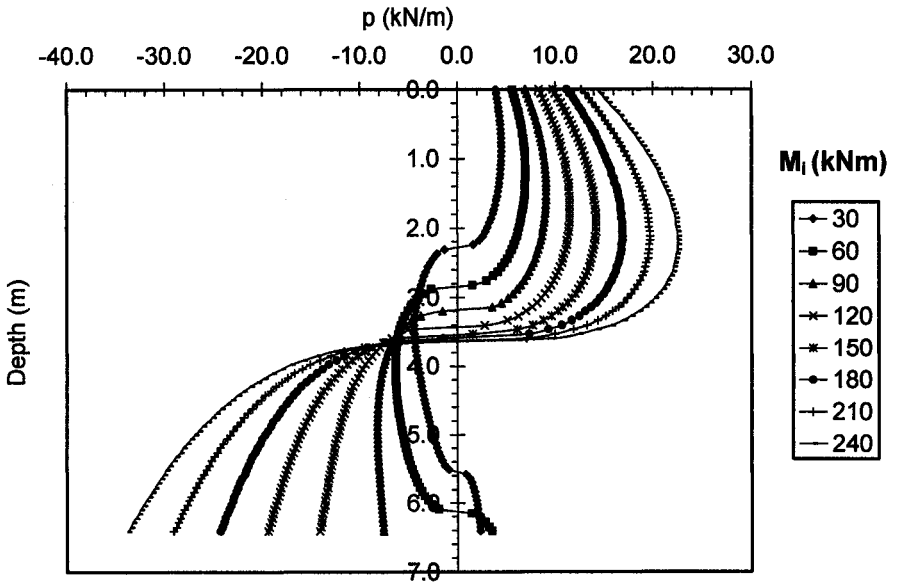

Fig. L.11 Distributions of soil reaction p at the primary structure along the depth of the pile for sensitivity analysis of top angle of rotation $\delta\varphi_t$ for free head single pile with length L = 3T subjected to bending moments M_i (kNm)

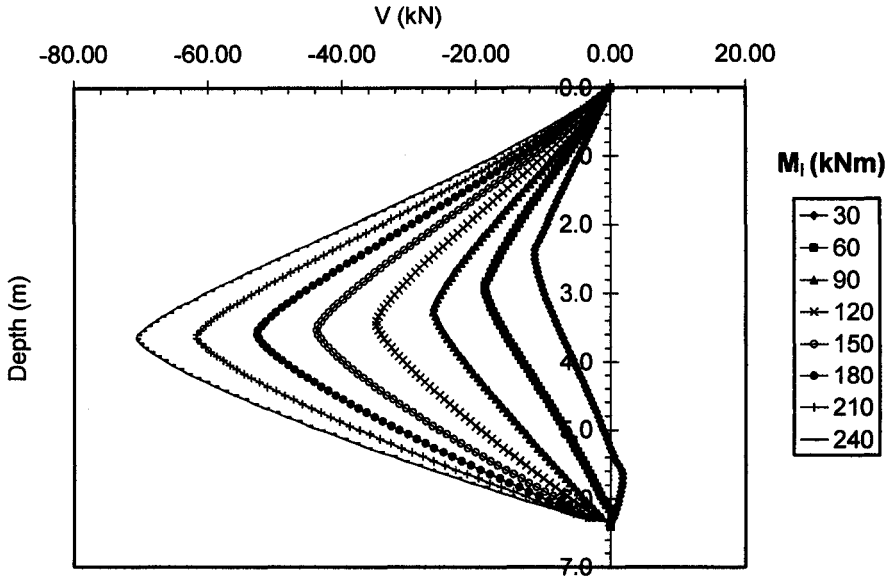

Fig. L.12 Distributions of shear forces V at the primary structure along the depth of the pile for sensitivity analysis of top angle of rotation $\delta\varphi_t$ for free head single pile with length L = 3T subjected to bending moments M_i (kNm)

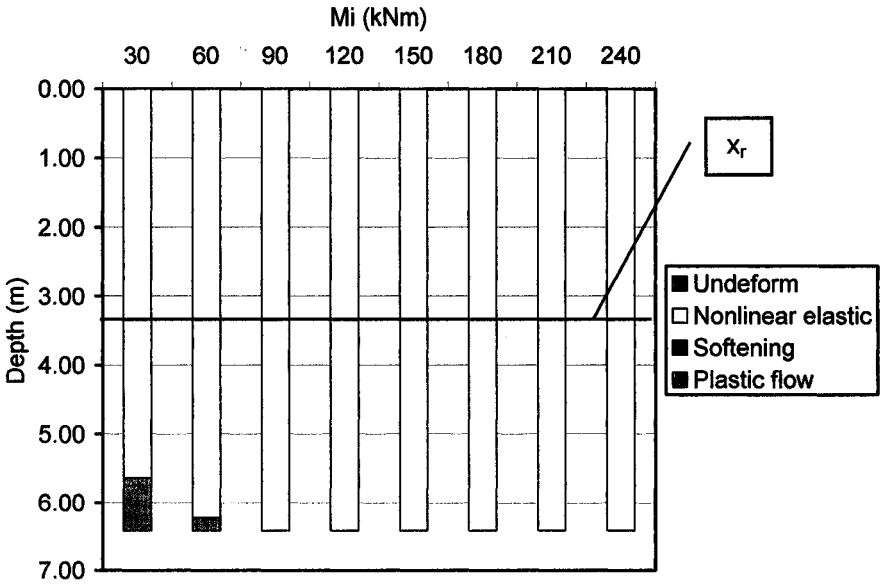

Fig. L.13 Quantitative assessment of the location and the size of the soil phases develop with the depth determined based on the distributions of sensitivity operators $\delta\varphi_t$ for free head single pile with length L = 3T subjected to bending moments M_i (kNm)

APPENDIX M:

Sensitivity analysis of top angle of rotation $\delta\varphi_t$ for single free head pile with length L = 10T subjected to bending moments M_i

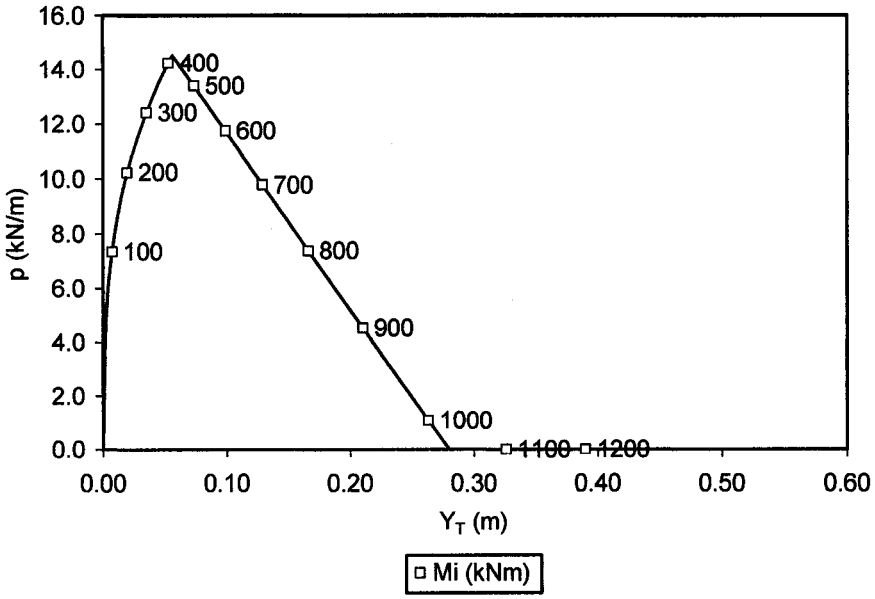

Fig. M.1 Soil reaction p at the top surface (expressed in terms of lateral loading) vs. lateral displacement generated by lateral loading applied to the pile for sensitivity analysis of top angle of rotation $\delta\varphi_t$ for free head single pile with length L = 10T subjected to bending moments M_i (kNm)

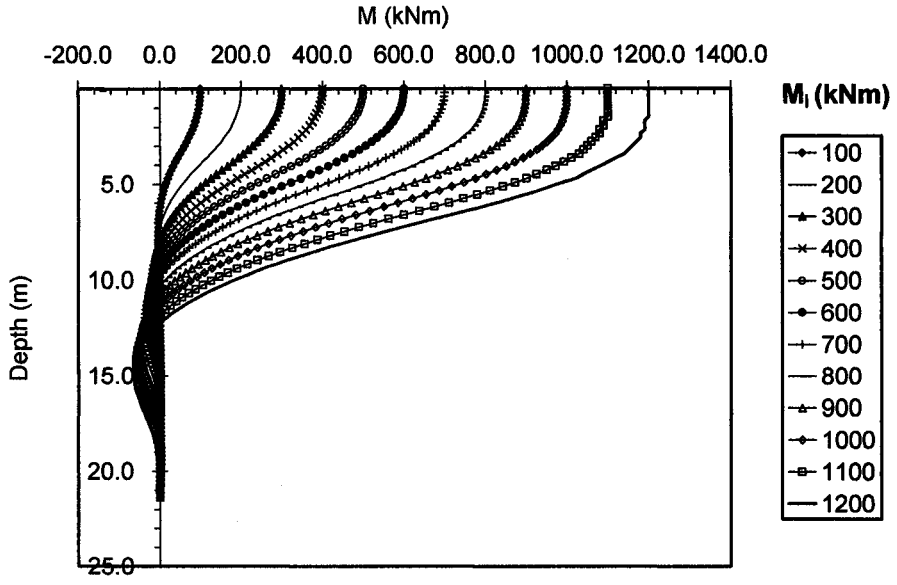

Fig. M.2 Distributions of bending moments at the primary structure M along the depth of the pile for sensitivity analysis of top angle of rotation $\delta\varphi_t$ for free head single pile with length L = 10T subjected to bending moments M_i (kNm)

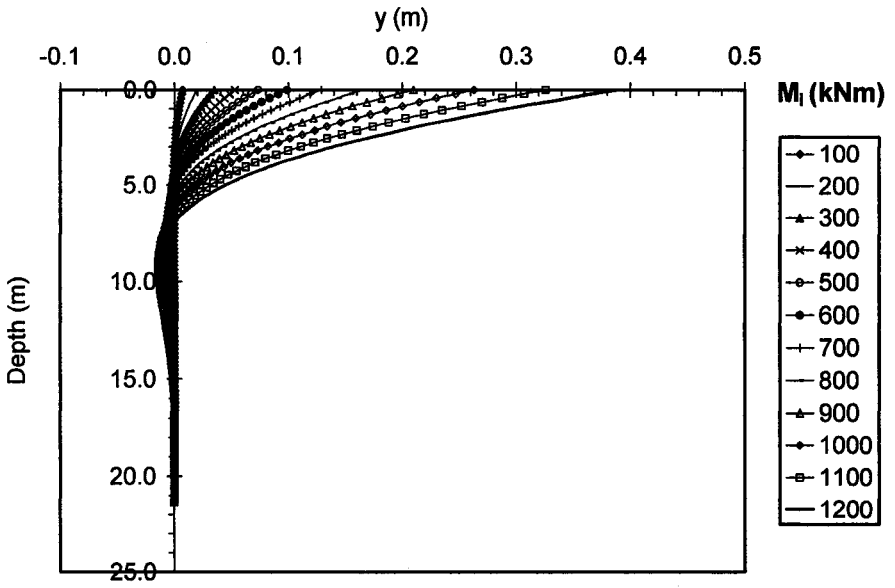

Fig. M.3 Distributions of lateral deflections at the primary structure y along the depth of the pile for sensitivity analysis of top angle of rotation $\delta\varphi_t$ for free head single pile with length L = 10T subjected to bending moments M_i (kNm)

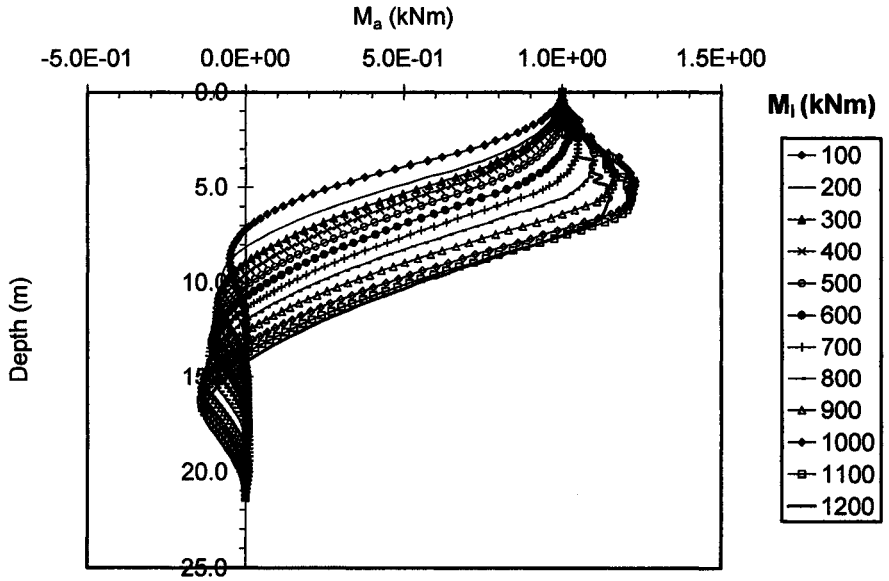

Fig. M.4 Distributions of bending moments M_a along the depth of the pile at the adjoint structure for sensitivity analysis of top angle of rotation $\delta\varphi_t$ for free head single pile with length L = 10T subjected to bending moments M_i (kNm)

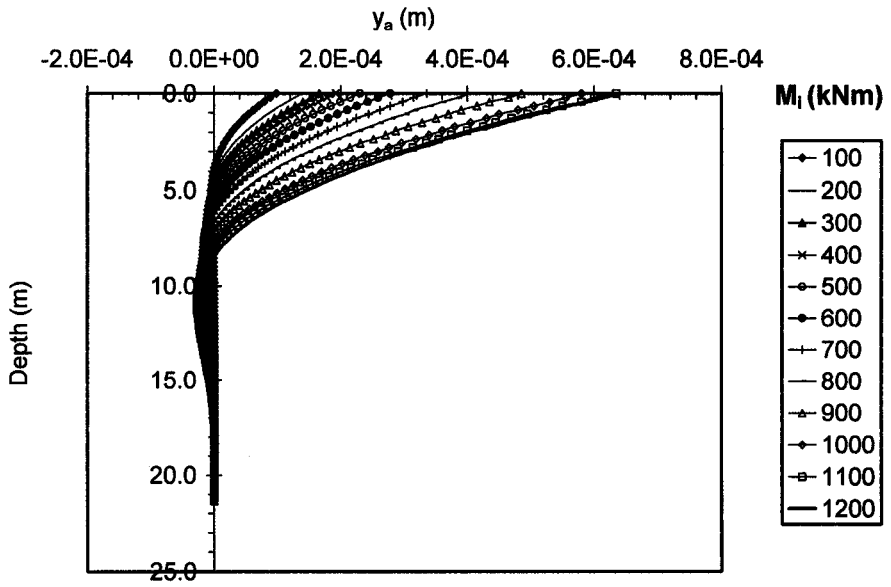

Fig. M.5 Distributions of lateral deflections at the adjoint structure y_a along the depth of the pile for sensitivity analysis of top angle of rotation $\delta\varphi_t$ for free head single pile with length L = 10T subjected to bending moments M_i (kNm)

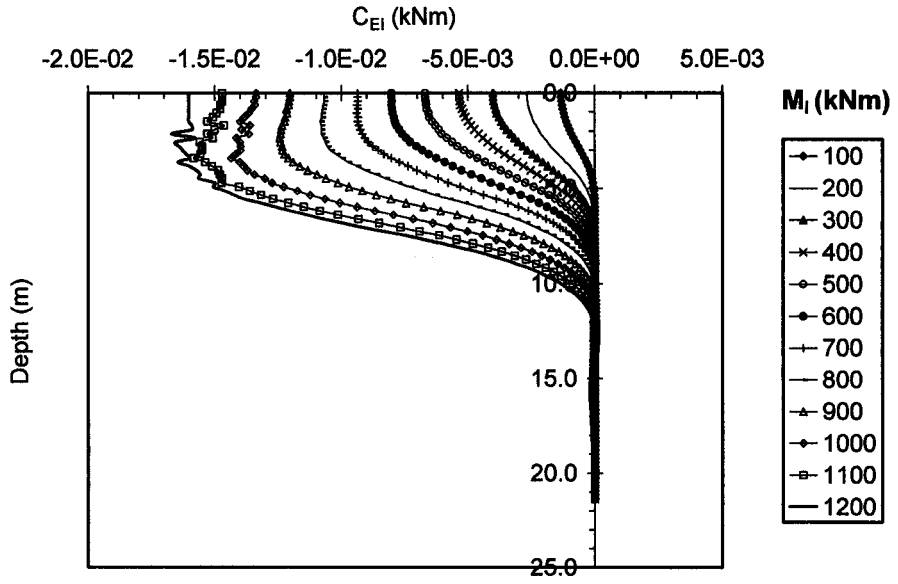

Fig. M.6a Distributions of sensitivity operators C_{EI} affecting the changes of $\delta\varphi_t$ due to variations of the design variable δEI for free head single pile with length L = 10T subjected to bending moments M_i (kNm)

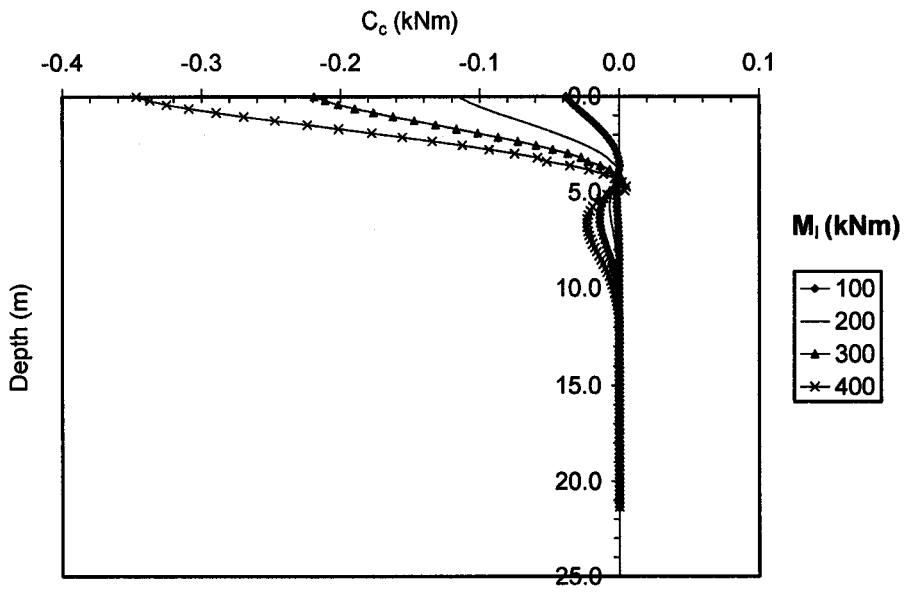

Fig. M.7a Distributions of sensitivity operators C_c affecting the changes of $\delta\varphi_t$ due to variations of the design variable δc for free head single pile with length L = 10T subjected to bending moments M_i (kNm)

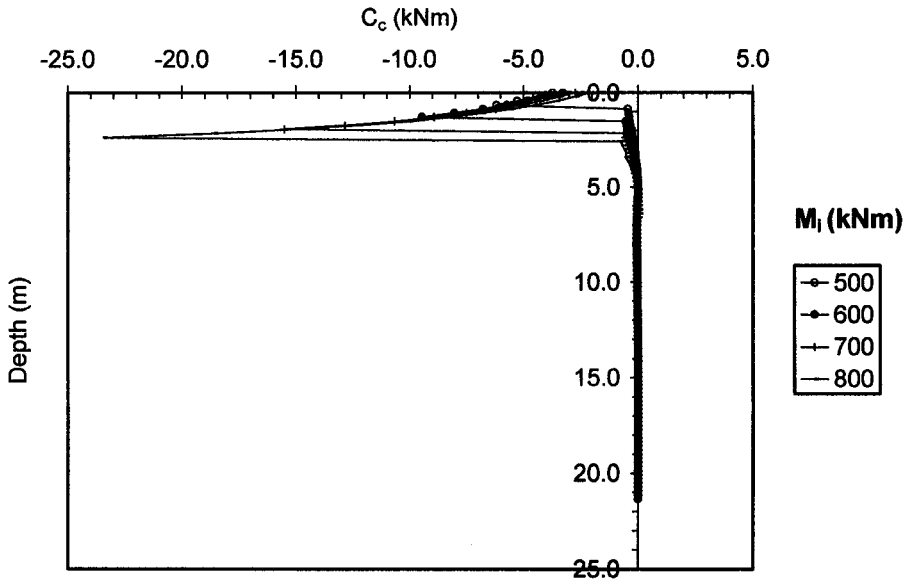

Fig. M.7b Distributions of sensitivity operators C_c affecting the changes of $\delta\varphi_t$ due to variations of the design variable δc for free head single pile with length L = 10T subjected to bending moments M_i (kNm)

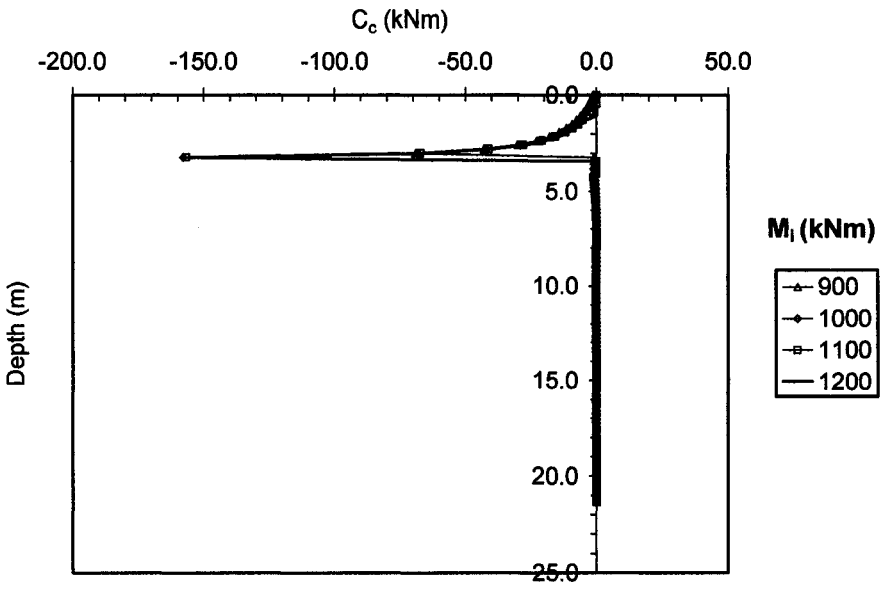

Fig. M.7c Distributions of sensitivity operators C_c affecting the changes of $\delta\varphi_t$ due to variations of the design variable δc for free head single pile with length L = 10T subjected to bending moments M_i (kNm)

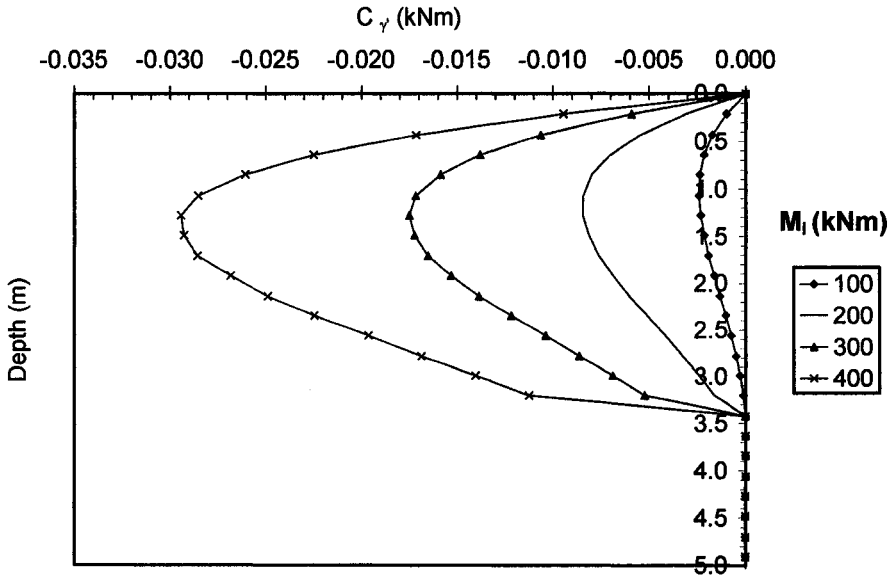

Fig. M.8a Distributions of sensitivity operators $C_{\gamma'}$ affecting the changes of $\delta\varphi_t$ due to variations of the design variable $\delta\gamma'$ for free head single pile with length L = 10T subjected to bending moments M_i (kNm)

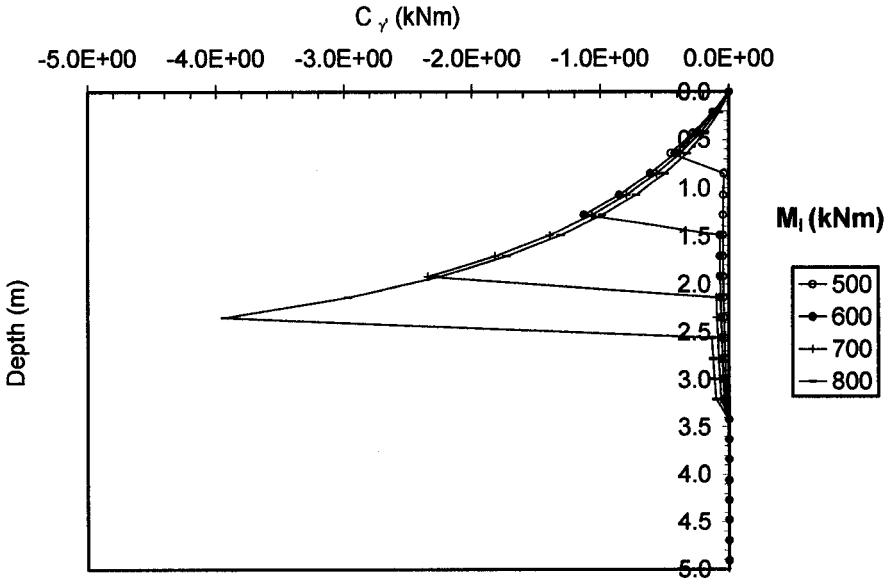

Fig. M.8b Distributions of sensitivity operators $C_{\gamma'}$ affecting the changes of $\delta\varphi_t$ due to variations of the design variable $\delta\gamma'$ for free head single pile with length L = 10T subjected to bending moments M_i (kNm)

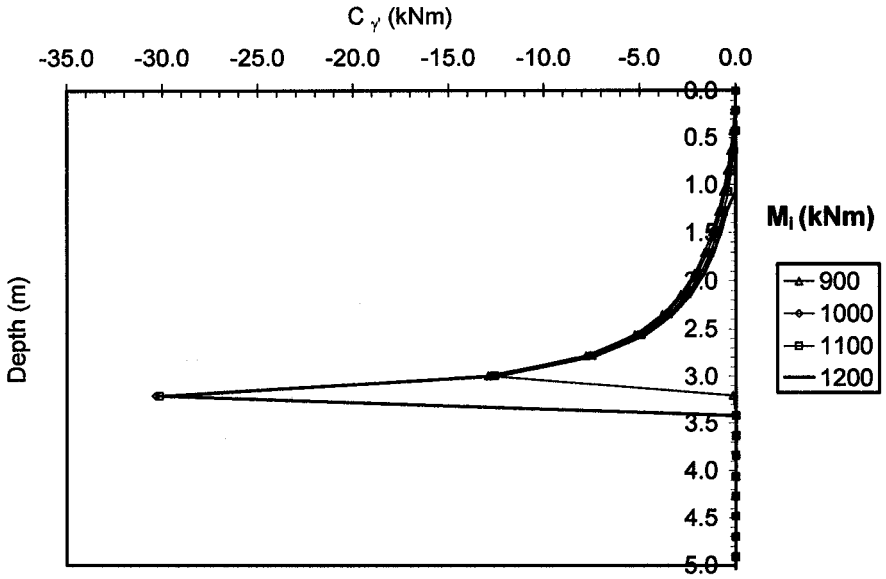

Fig. M.8c Distributions of sensitivity operators $C_{\gamma'}$ affecting the changes of $\delta\varphi_t$ due to variations of the design variable $\delta\gamma'$ for free head single pile with length L = 10T subjected to bending moments M_i (kNm)

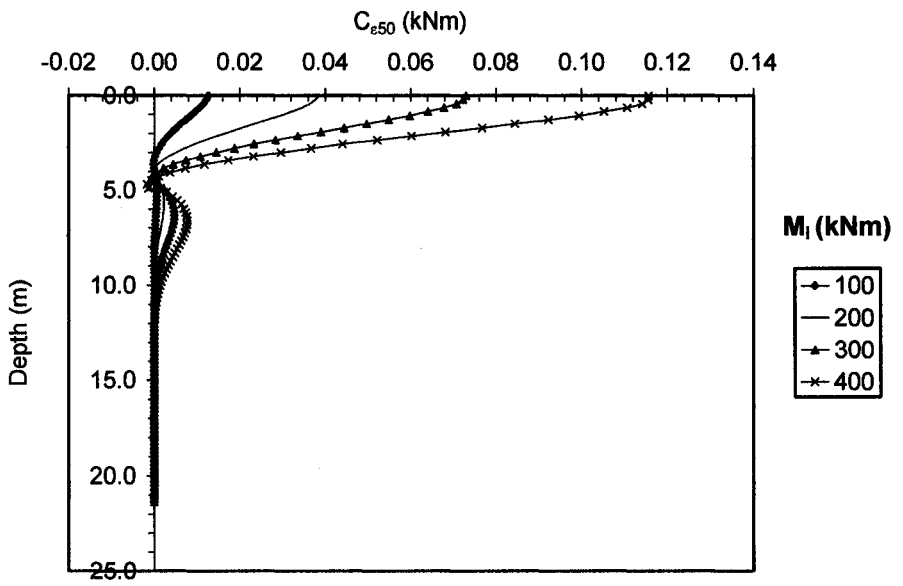

Fig. M.9a Distributions of sensitivity operators $C_{\varepsilon 50}$ affecting the changes of $\delta\varphi_t$ due to variations of the design variable $\delta\varepsilon_{50}$ for free head single pile with length L = 10T subjected to bending moments M_i (kNm)

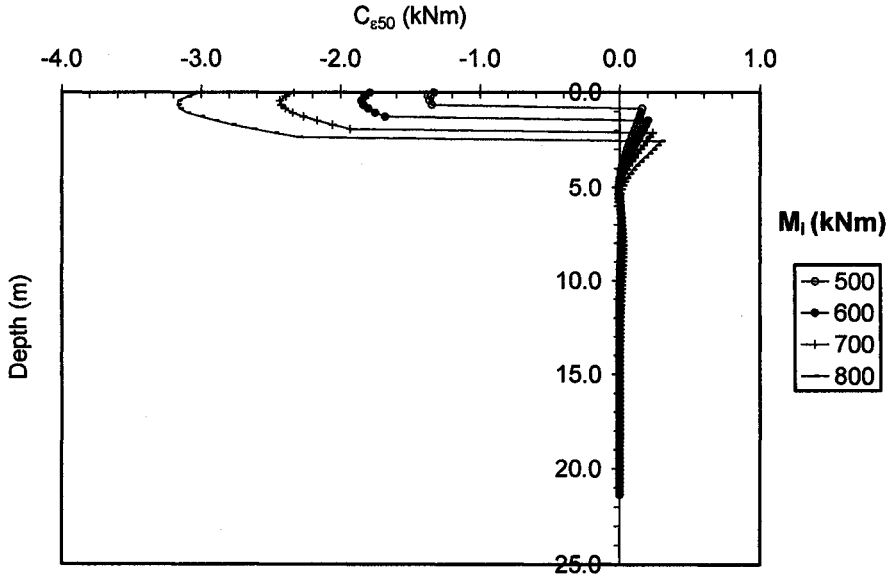

Fig. M.9b Distributions of sensitivity operators $C_{\varepsilon 50}$ affecting the changes of $\delta\varphi_t$ due to variations of the design variable $\delta\varepsilon_{50}$ for free head single pile with length L = 10T subjected to bending moments M_i (kNm)

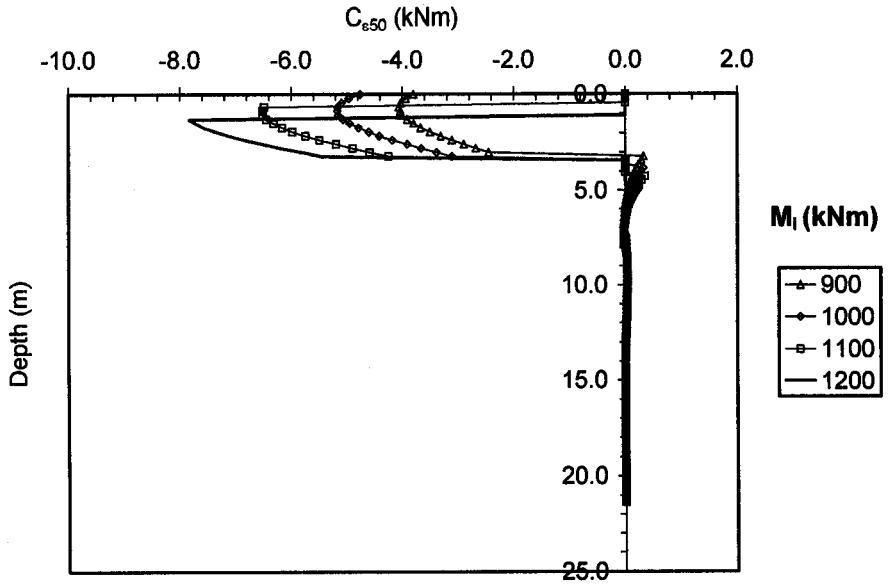

Fig. M.9c Distributions of sensitivity operators $C_{\varepsilon 50}$ affecting the changes of $\delta\varphi_t$ due to variations of the design variable $\delta\varepsilon_{50}$ for free head single pile with length L = 10T subjected to bending moments M_i (kNm)

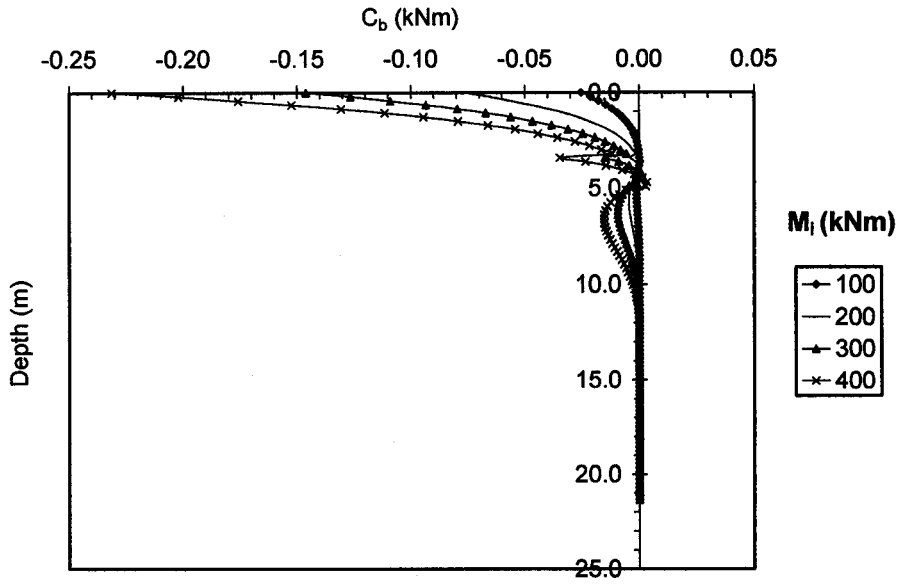

Fig. M.10a Distributions of sensitivity operators C_b affecting the changes of $\delta\varphi_t$ due to variations of the design variable δb for free head single pile with length L = 10T subjected to bending moments M_i (kNm)

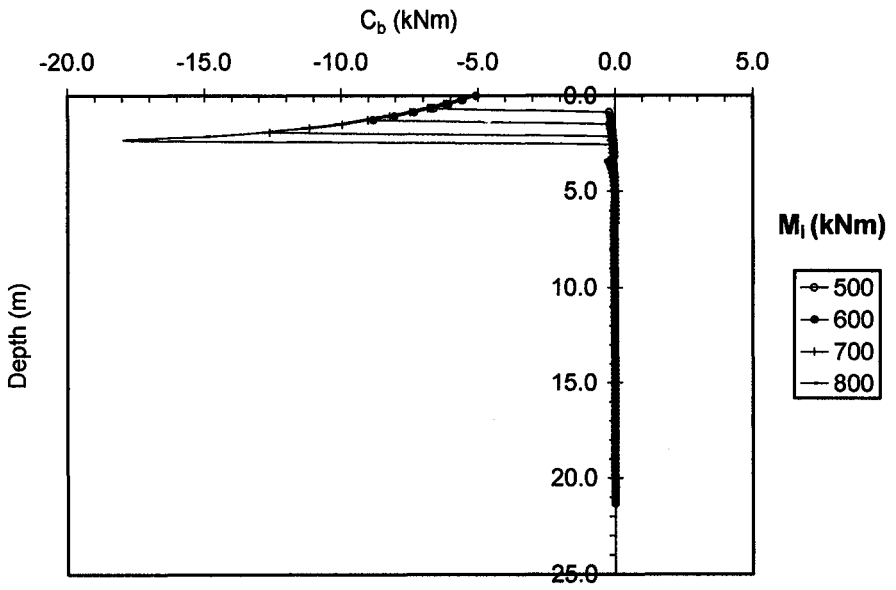

Fig. M.10b Distributions of sensitivity operators C_b affecting the changes of $\delta\varphi_t$ due to variations of the design variable δb for free head single pile with length L = 10T subjected to bending moments M_i (kNm)

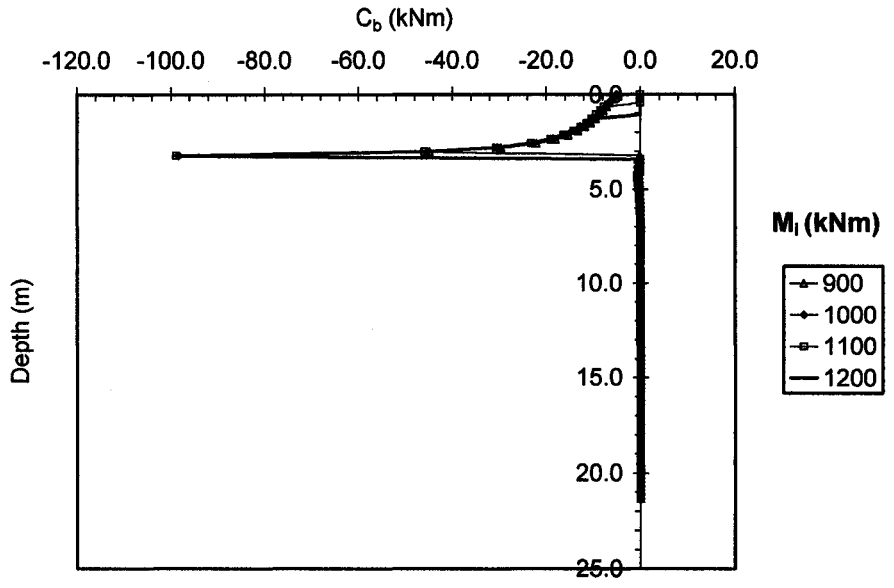

Fig. M.10c Distributions of sensitivity operators C_b affecting the changes of $\delta\varphi_t$ due to variations of the design variable δb for free head single pile with length L = 10T subjected to bending moments M_i (kNm)

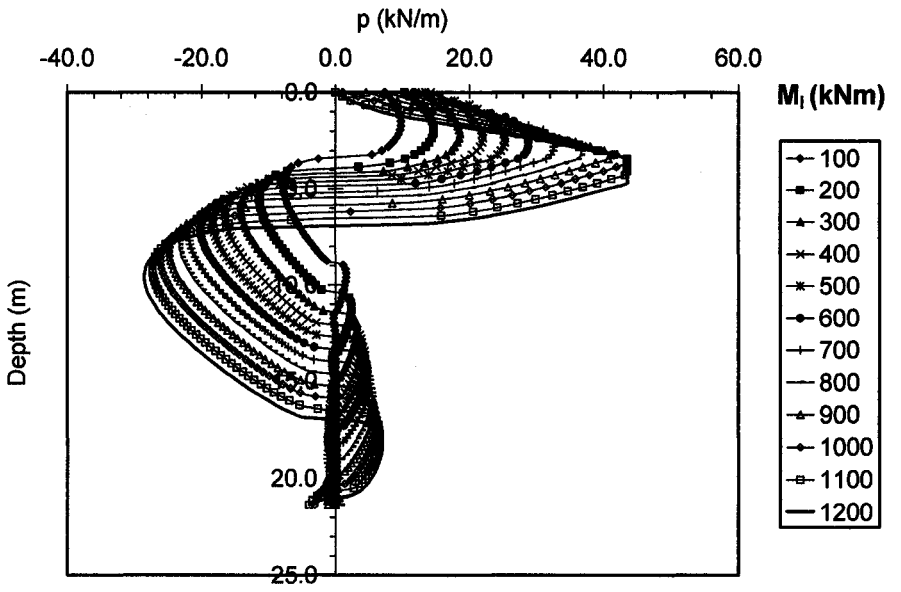

Fig. M.11 Distributions of soil reaction p at the primary structure along the depth of the pile for sensitivity analysis of top angle of rotation $\delta\varphi_t$ for free head single pile with length L = 10T subjected to bending moments M_i (kNm)

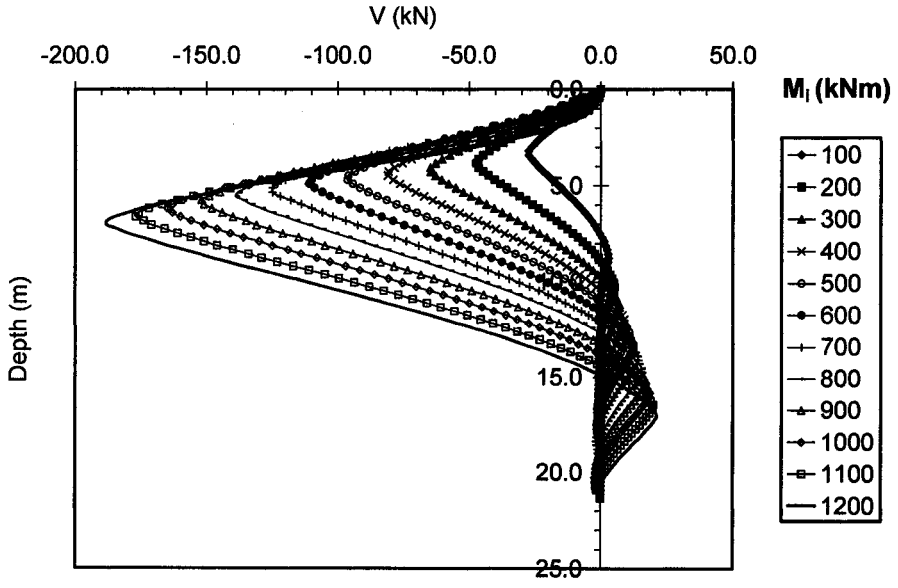

Fig. M.12 Distributions of shear forces V at the primary structure along the depth of the pile for sensitivity analysis of top angle of rotation $\delta\varphi_t$ for free head single pile with length L = 10T subjected to bending moments M_i (kNm)

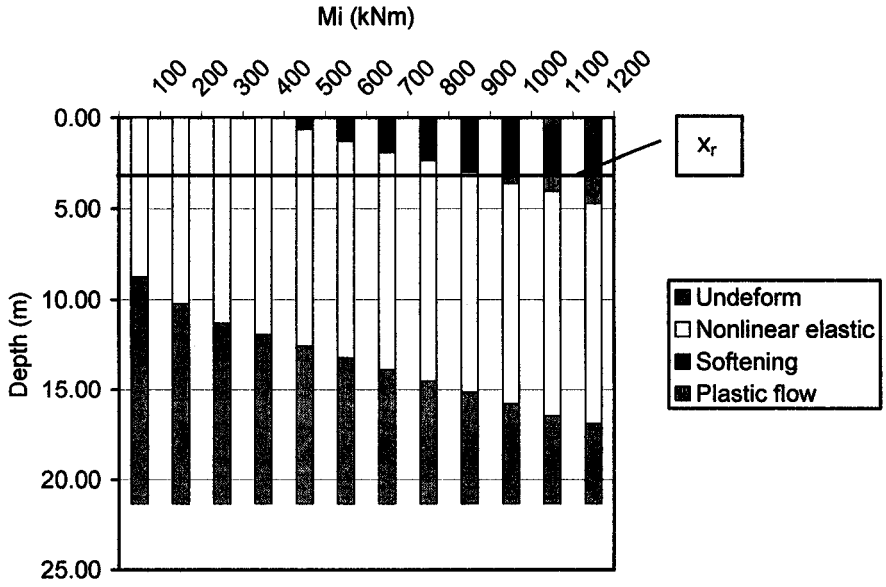

Fig. M.13 Quantitative assessment of the location and the size of the soil phases develop with the depth determined based on the distributions of sensitivity operators affecting $\delta\varphi_t$ for free head single pile with length L = 10T subjected to bending moments M_i (kNm)

APPENDIX N:

Efficiency of the pile groups Ge;
shear forces at the top V_t;
forces applied at the pile caps Pgi;
percentage of the forces carried by pile members; and
unit force Pg1
for groups of 3×3 piles having length L = 10T
with various spacings
(s = 2D, 3D, 4D, & 5D) in graphical form

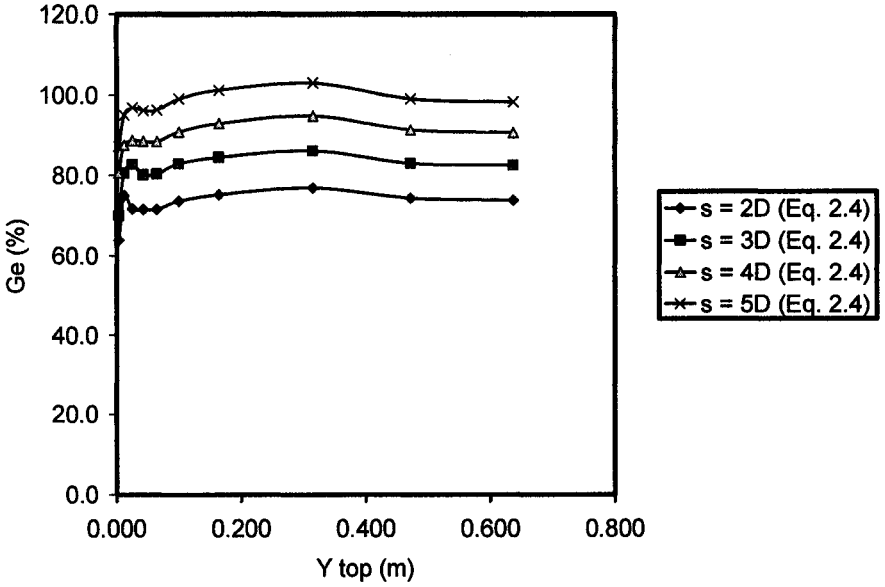

Fig. N.1a Efficiency of the group Ge of 3×3 piles with the various spacing s and the length L = 10T vs. top lateral displacement

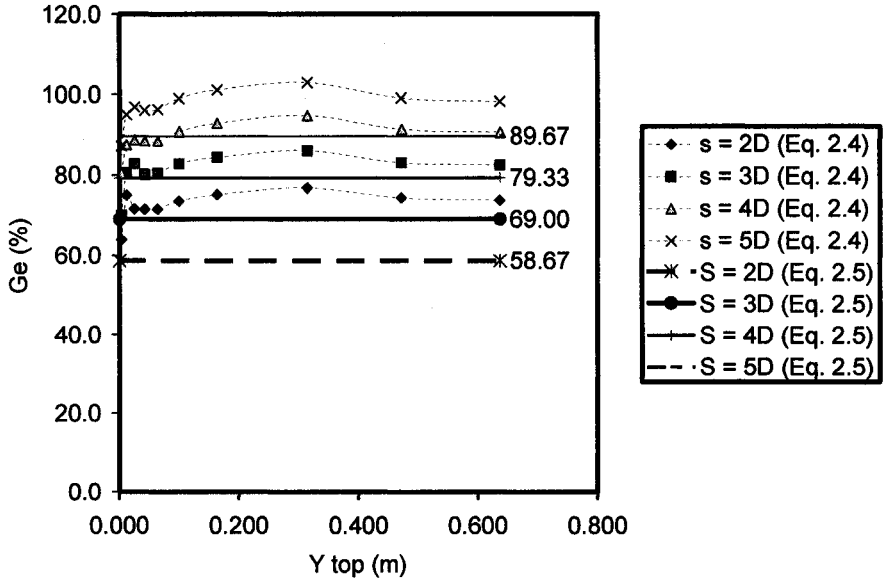

Fig. N.1b Efficiency of the group Ge of 3×3 piles with the various spacing s and the length L = 10T vs. top lateral displacement

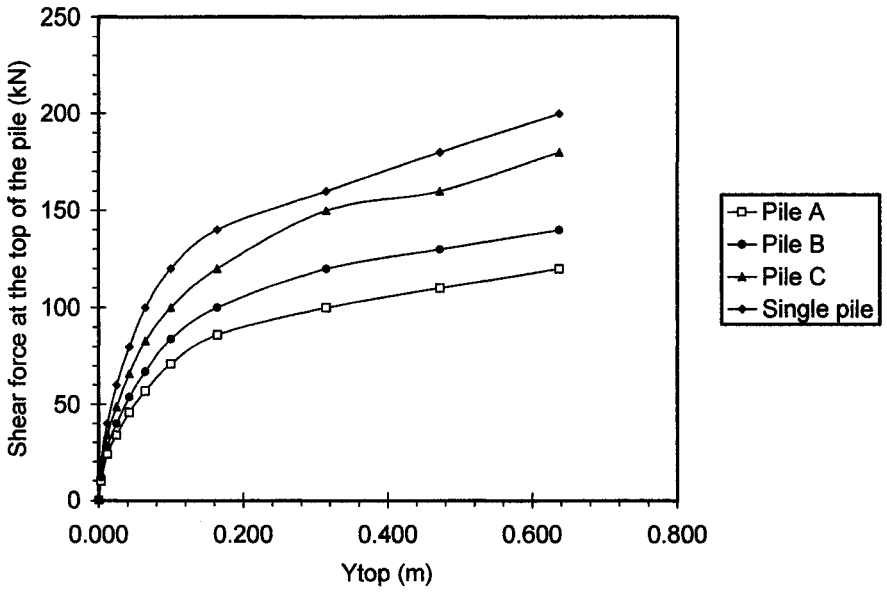

Fig. N.2a Shear forces at the top of pile members A (2nd trailing row), B (1st trailing row), and C (leading row) of the group of 3x3 piles with the spacing s = 2D and the length L = 10T vs. top lateral displacement

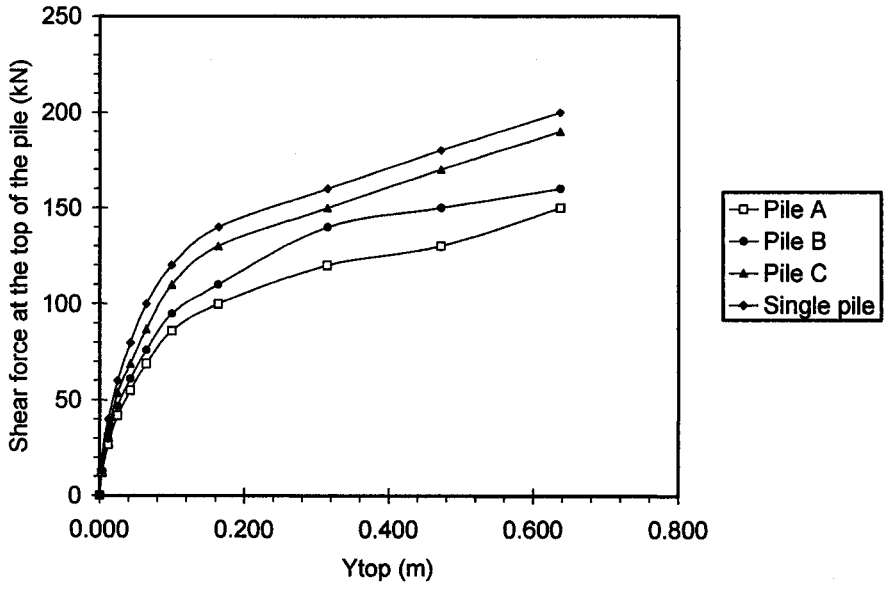

Fig. N.2b Shear forces at the top of pile members A (2nd trailing row), B (1st trailing row), and C (leading row) of the group of 3x3 piles with the spacing s = 3D and the length L = 10T vs. top lateral displacement

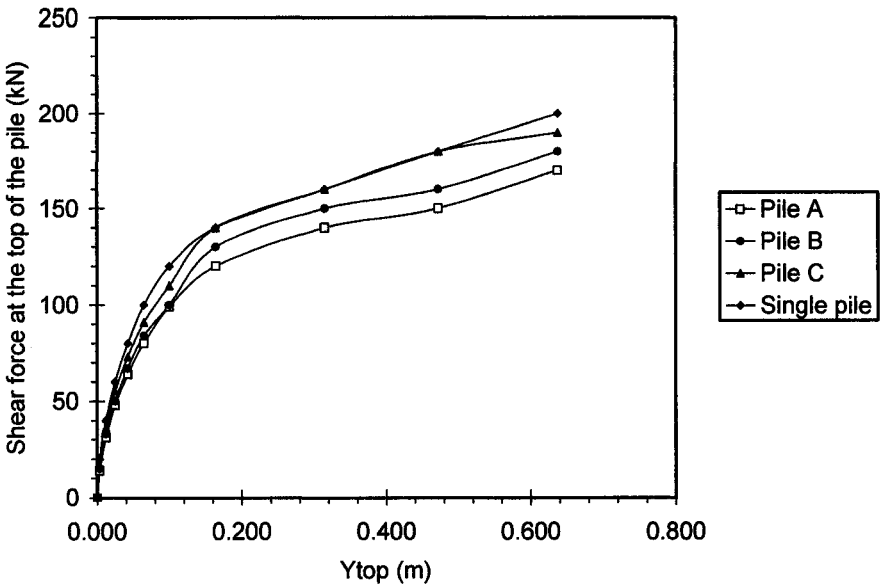

Fig. N.2c Shear forces at the top of pile members A (2nd trailing row), B (1st trailing row), and C (leading row) of the group of 3x3 piles with the spacing s = 4D and the length L = 10T vs. top lateral displacement

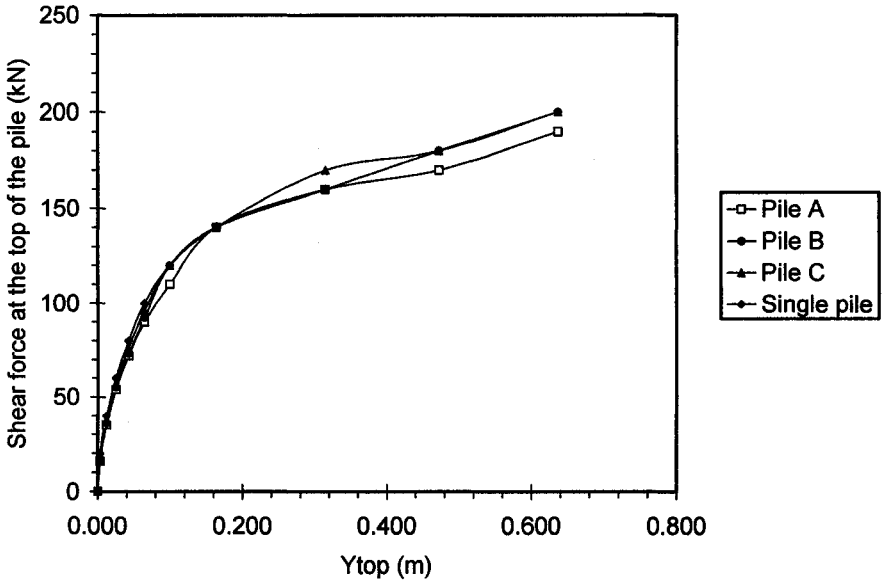

Fig. N.2d Shear forces at the top of pile members A (2nd trailing row), B (1st trailing row), and C (leading row) of the group of 3x3 piles with the spacing s = 5D and the length L = 10T vs. top lateral displacement

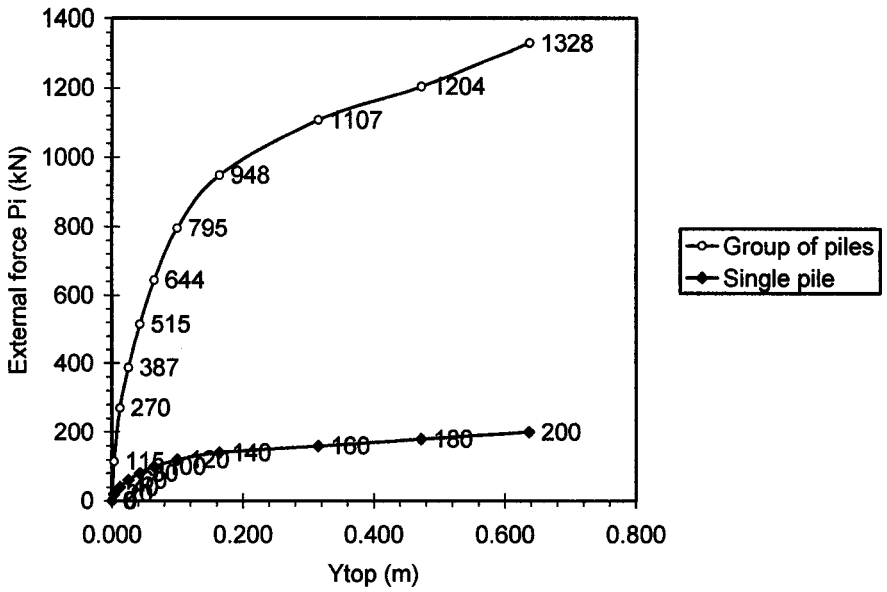

Fig. N.3a Forces Pi applied at the top of the group of 3x3 piles with the spacing s = 2D and the length L = 10T vs. top lateral displacement

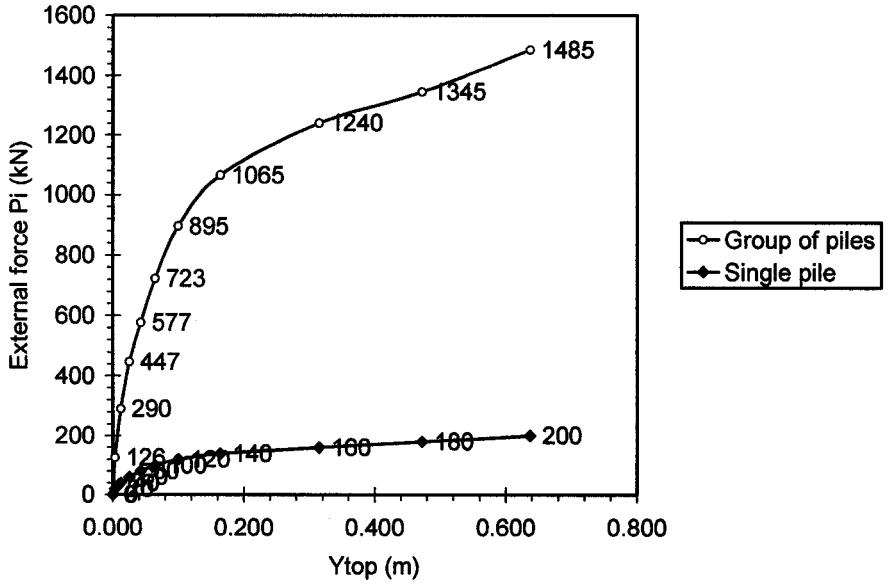

Fig. N.3b Forces Pi applied at the top of the group of 3x3 piles with the spacing s = 3D and the length L = 10T vs. top lateral displacement

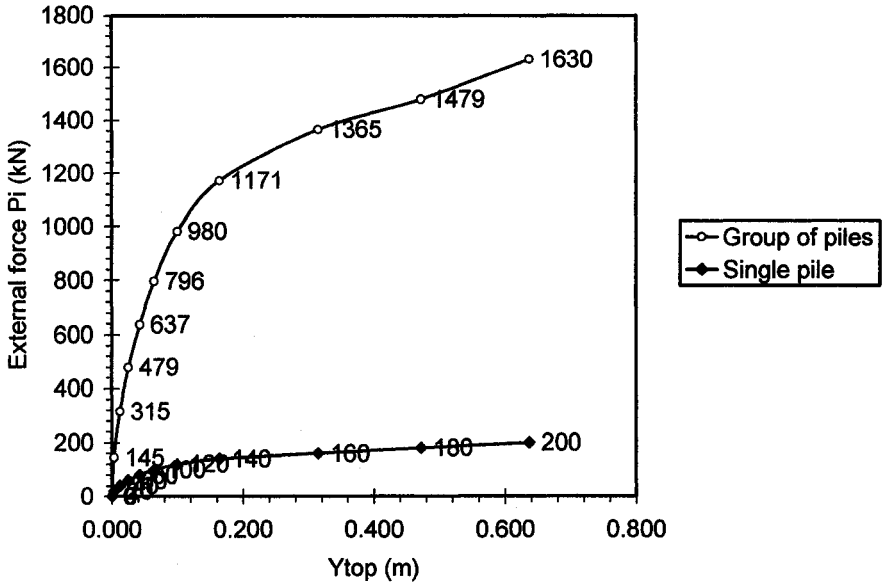

Fig. N.3c Forces Pi applied at the top of the group of 3x3 piles with the spacing s = 4D and the length L = 10T vs. top lateral displacement

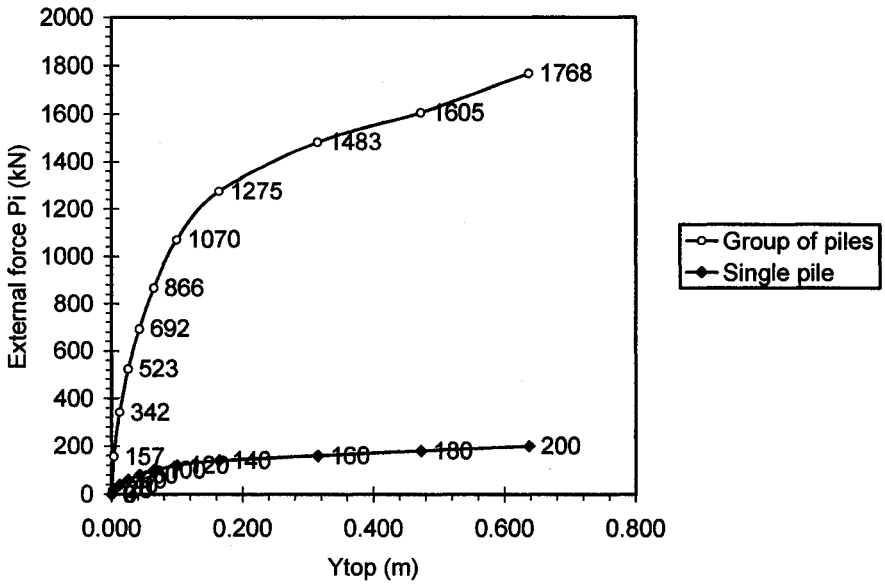

Fig. N.3d Forces Pi applied at the top of the group of 3x3 piles with the spacing s = 5D and the length L = 10T vs. top lateral displacement

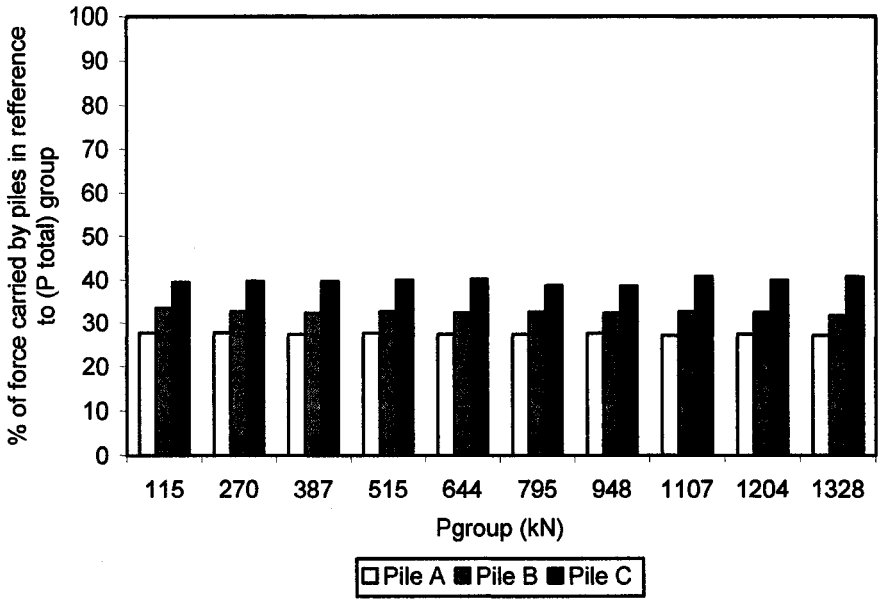

Fig. N.4a Percentage of force carried by the pile members A (2nd trailing row), B (1st trailing row), and C (leading row) of the group of 3x3 piles with the spacing s = 2D and the length L = 10T vs. top lateral displacement

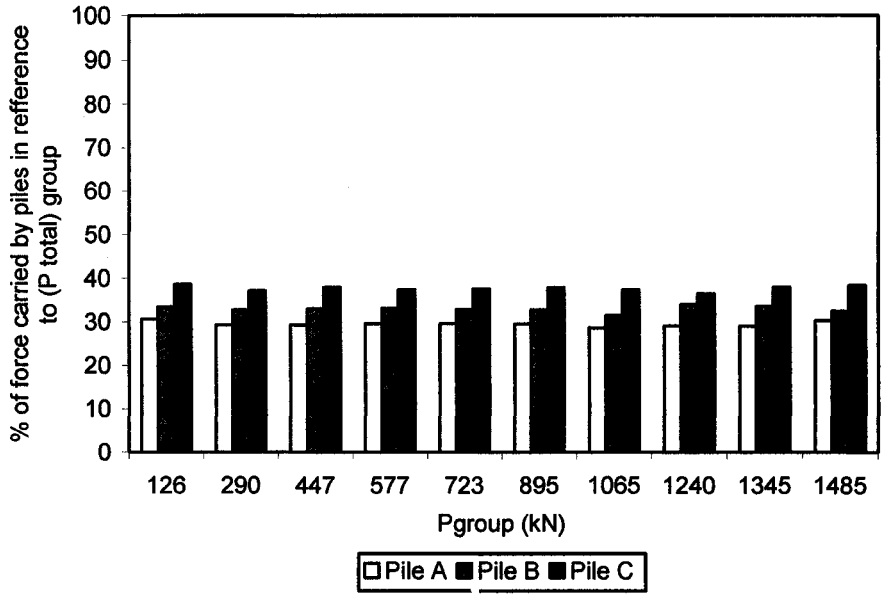

Fig. N.4b Percentage of force carried by the pile members A (2nd trailing row), B (1st trailing row), and C (leading row) of the group of 3x3 piles with the spacing s = 3D and the length L = 10T vs. top lateral displacement

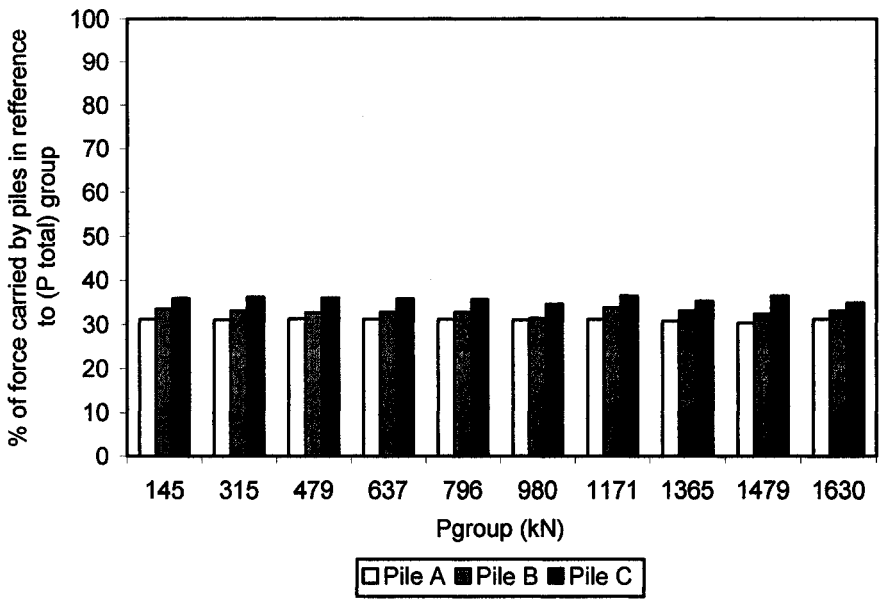

Fig. N.4c Percentage of force carried by the pile members A (2nd trailing row), B (1st trailing row), and C (leading row) of the group of 3x3 piles with the spacing s = 4D and the length L = 10T vs. top lateral displacement

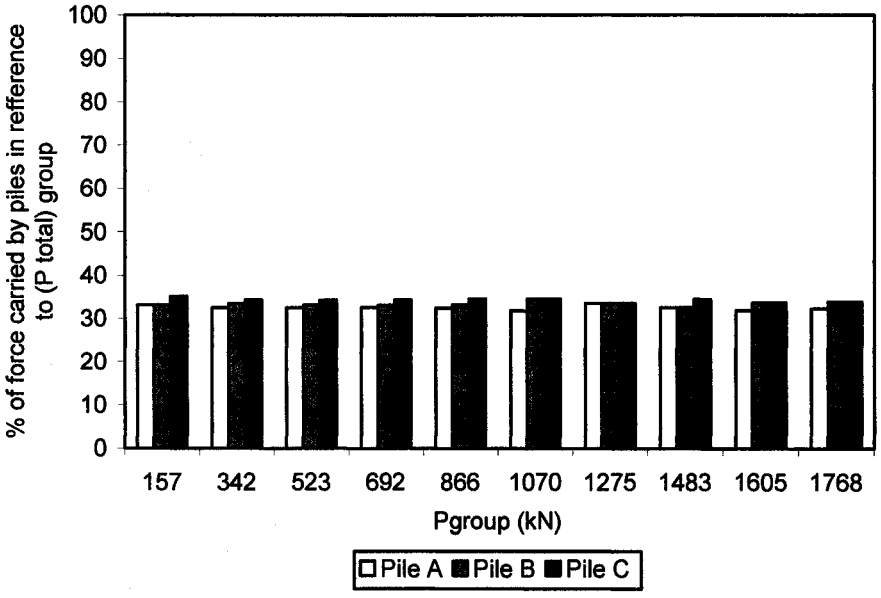

Fig. N.4d Percentage of force carried by the pile members A (2nd trailing row), B (1st trailing row), and C (leading row) of the group of 3x3 piles with the spacing s = 5D and the length L = 10T vs. top lateral displacement

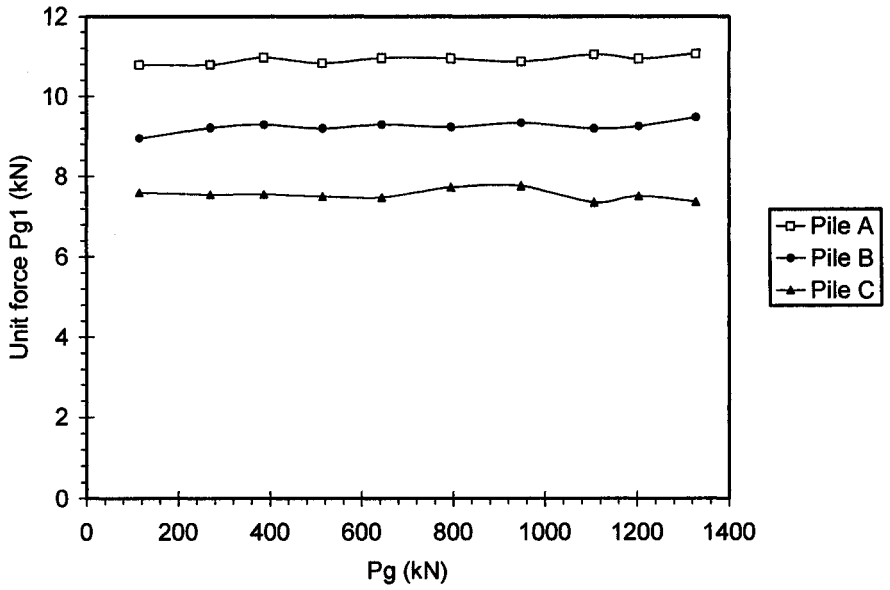

Fig. N.5a Unit forces Pg1 of pile members A (2nd trailing row), B (1st trailing row), and C (leading row) of the group of 3x3 piles with the spacing s = 2D and the length L = 10T vs. top lateral displacement

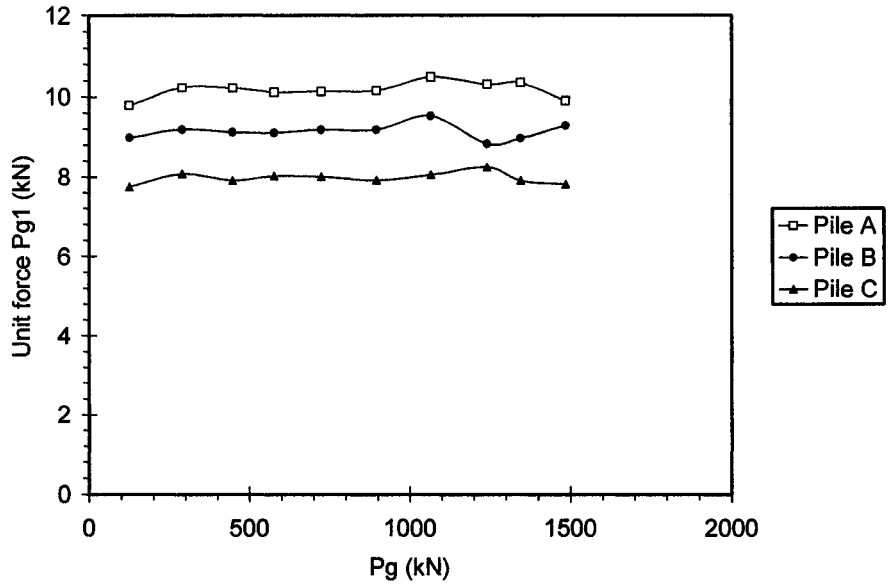

Fig. N.5b Unit forces Pg1 of pile members A (2nd trailing row), B (1st trailing row), and C (leading row) of the group of 3x3 piles with the spacing s = 3D and the length L = 10T vs. top lateral displacement

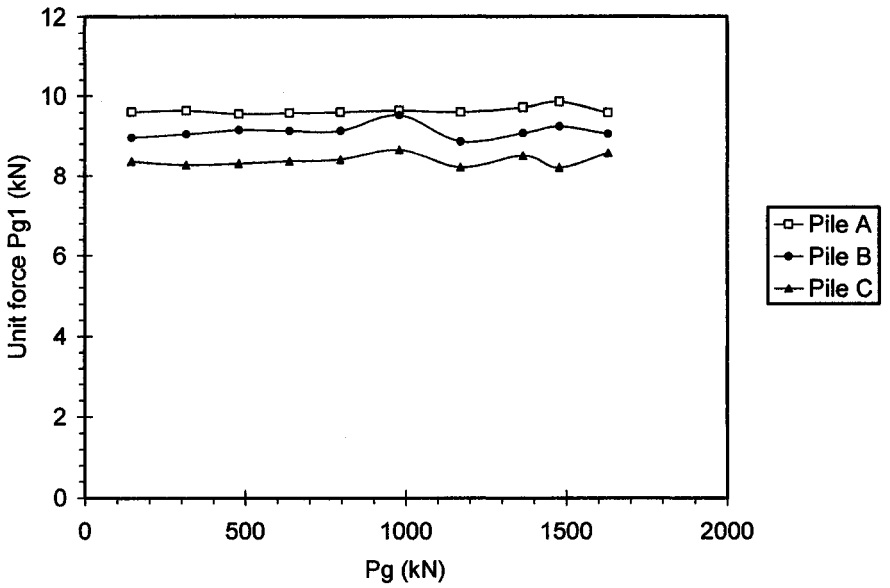

Fig. N.5c Unit forces Pg1 of pile members A (2nd trailing row), B (1st trailing row), and C (leading row) of the group of 3x3 piles with the spacing s = 4D and the length L = 10T vs. top lateral displacement

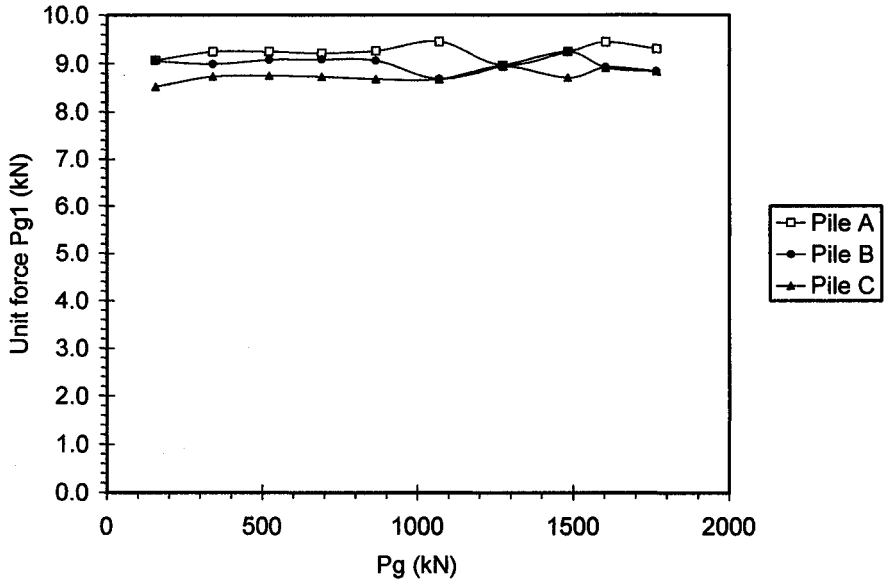

Fig. N.5d Unit forces Pg1 of pile members A (2nd trailing row), B (1st trailing row), and C (leading row) of the group of 3x3 piles with the spacing s = 5D and the length L = 10T vs. top lateral displacement

APPENDIX O:

Sensitivity analysis of top lateral displacement δy_t for pile member A (2^{nd} trailing row) of groups of 3×3 piles with length L = 10T and spacing s = 2D subjected to lateral forces Pi

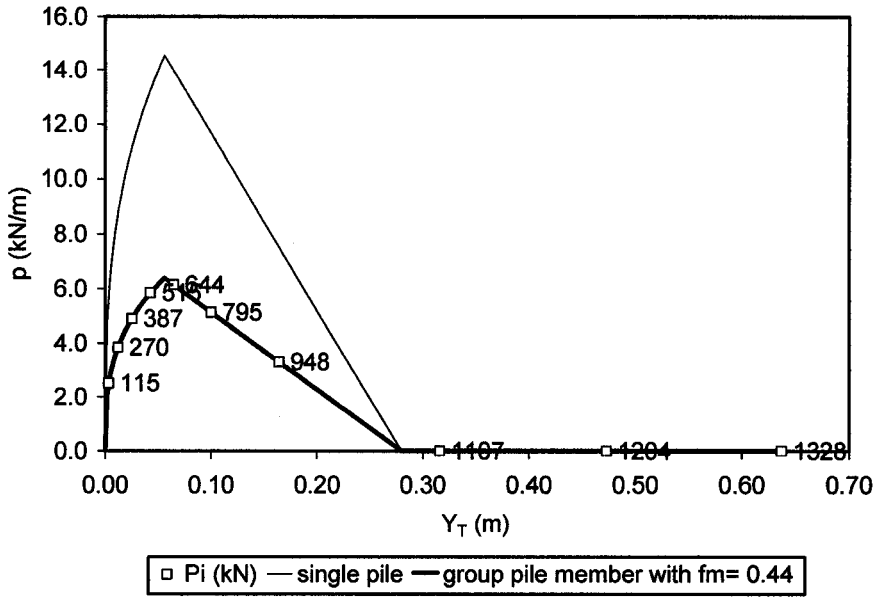

Fig. O.1 Soil reaction p at the top surface (expressed in terms of lateral loading) vs. lateral displacement generated by lateral loading applied to the pile for sensitivity analysis of top lateral displacement δy_t for pile member A (2nd trailing row) of groups of 3 x 3 piles with length L = 10T and spacing s = 2D subjected to lateral forces P_i (kN)

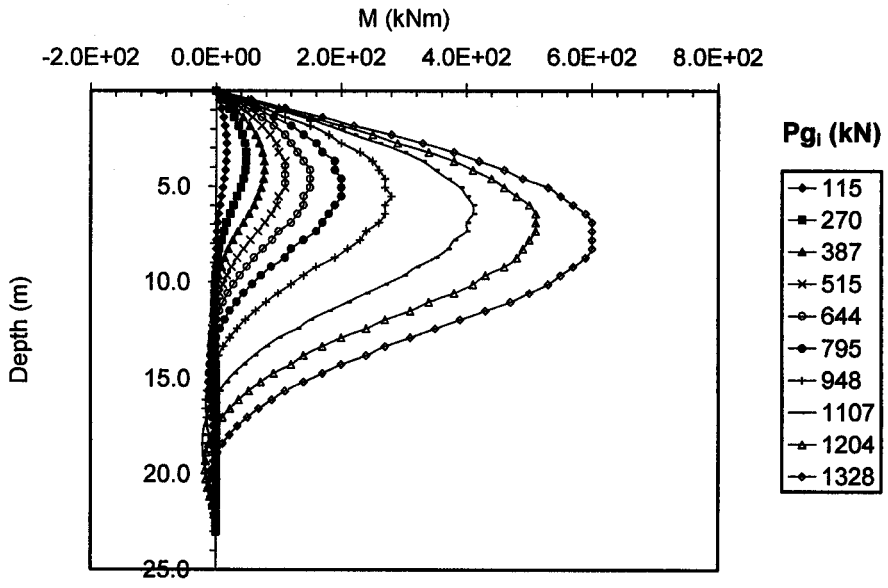

Fig. O.2 Distributions of bending moments at the primary structure M along the depth of the pile for sensitivity analysis of top lateral displacement δy_t for pile member A (2nd trailing row) of groups of 3 x 3 piles with length L = 10T and spacing s = 2D subjected to lateral forces P_i (kN)

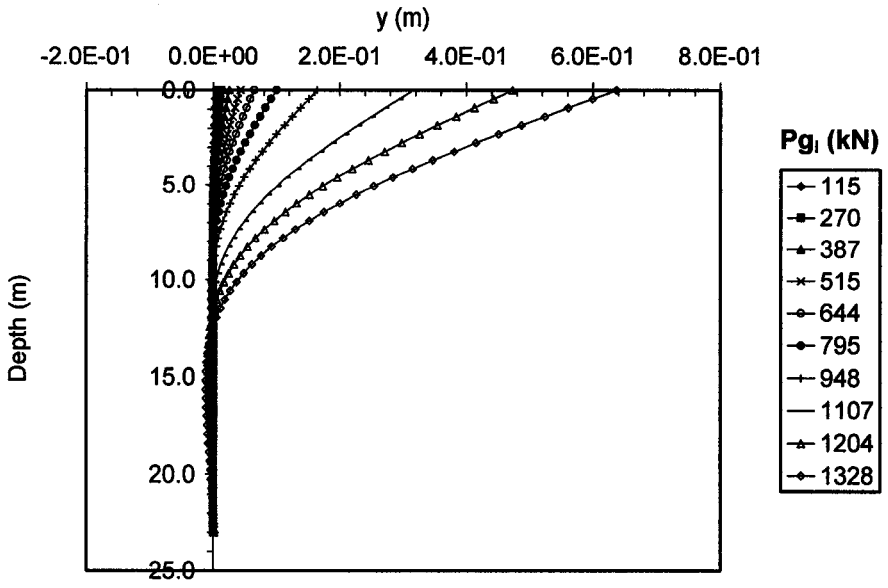

Fig. O.3 Distributions of lateral deflections at the primary structure y along the depth of the pile for sensitivity analysis of top lateral displacement δy_t for pile member A (2nd trailing row) of groups of 3 x 3 piles with length L = 10T and spacing s = 2D subjected to lateral forces P_i (kN)

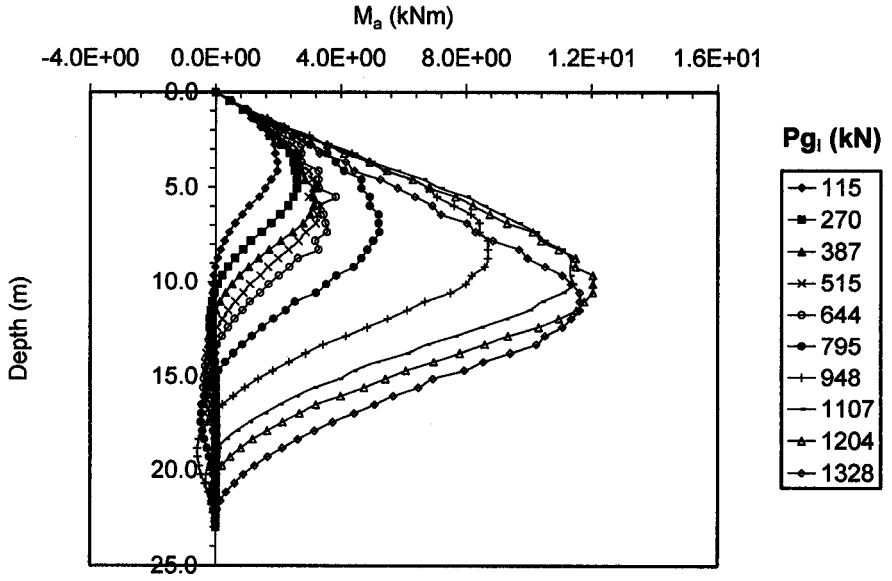

Fig. O.4 Distributions of bending moments M_a along the depth of the pile at the adjoint structure for sensitivity analysis of top lateral displacement δy_t for pile member A (2nd trailing row) of groups of 3 x 3 piles with length L = 10T and spacing s = 2D subjected to lateral forces P_i (kN)

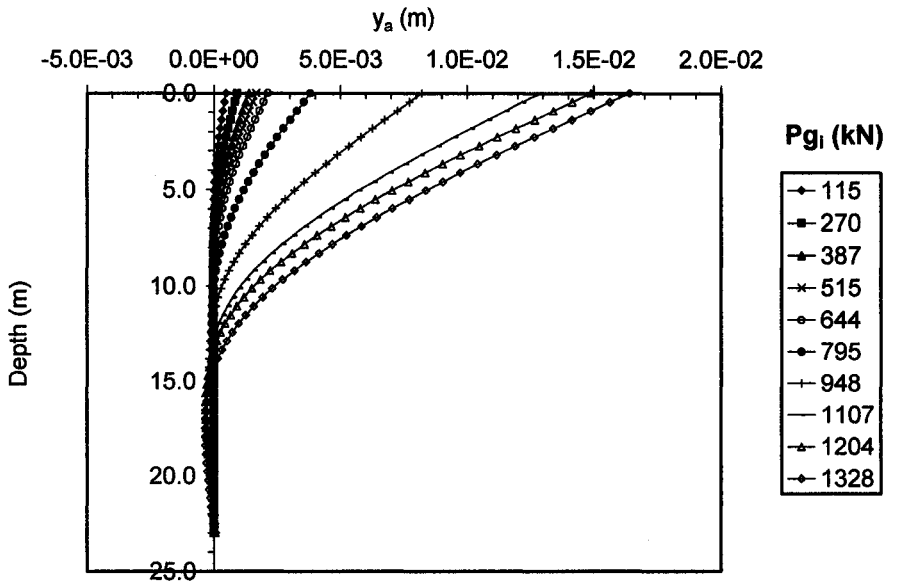

Fig. O.5 Distributions of lateral deflections at the adjoint structure y_a along the depth of the pile for sensitivity analysis of top lateral displacement δy_t for pile member A (2nd trailing row) of groups of 3 x 3 piles with length L = 10T and spacing s = 2D subjected to lateral forces P_i (kN)

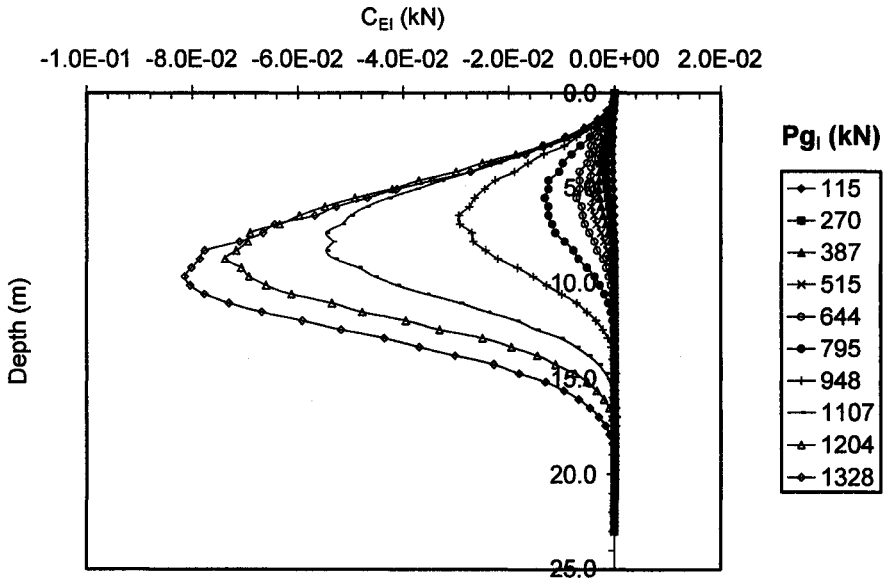

Fig. O.6 Distributions of sensitivity operators C_{EI} affecting the changes of δy_t due to variations of the design variable δEI for pile member A (2nd trailing row) of groups of 3 x 3 piles with length L = 10T and spacing s = 2D subjected to lateral forces P_i (kN)

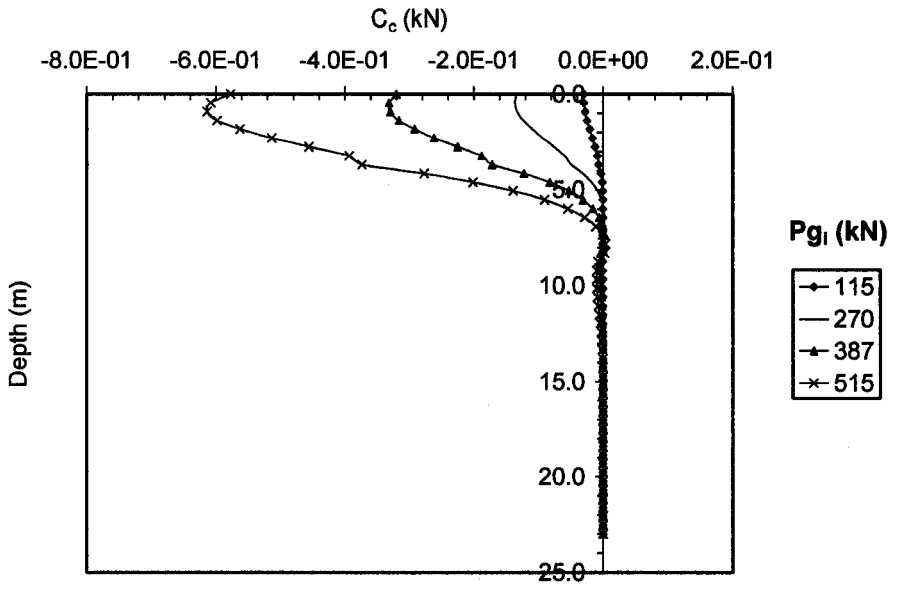

Fig. O.7a Distributions of sensitivity operators C_c affecting the changes of δy_t due to variations of the design variable δc for pile member A (2nd trailing row) of groups of 3 x 3 piles with length L = 10T and spacing s = 2D subjected to lateral forces P_i (kN)

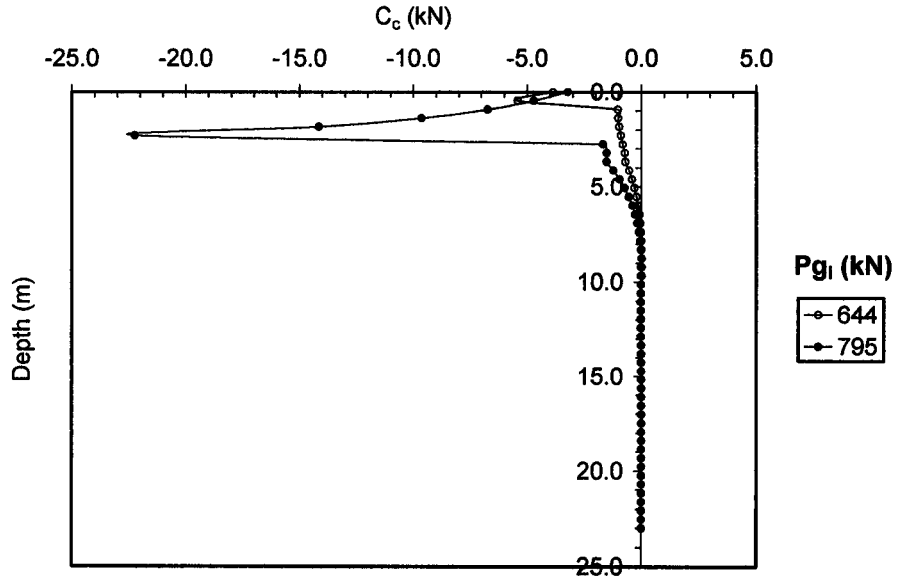

Fig. O.7b Distributions of sensitivity operators C_c affecting the changes of δy_t due to variations of the design variable δc for pile member A (2nd trailing row) of groups of 3 x 3 piles with length L = 10T and spacing s = 2D subjected to lateral forces P_i (kN)

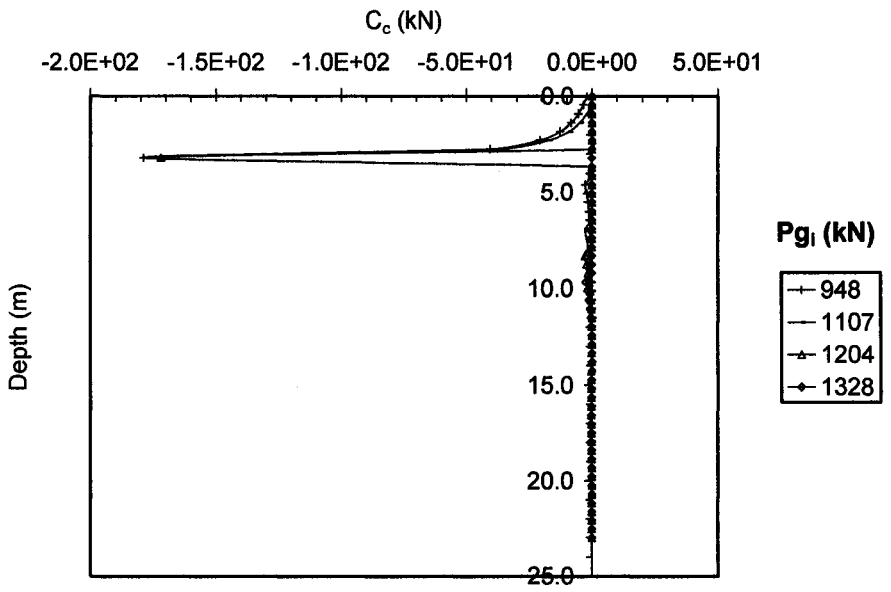

Fig. O.7c Distributions of sensitivity operators C_c affecting the changes of δy_t due to variations of the design variable δc for pile member A (2nd trailing row) of groups of 3 x 3 piles with length L = 10T and spacing s = 2D subjected to lateral forces P_i (kN)

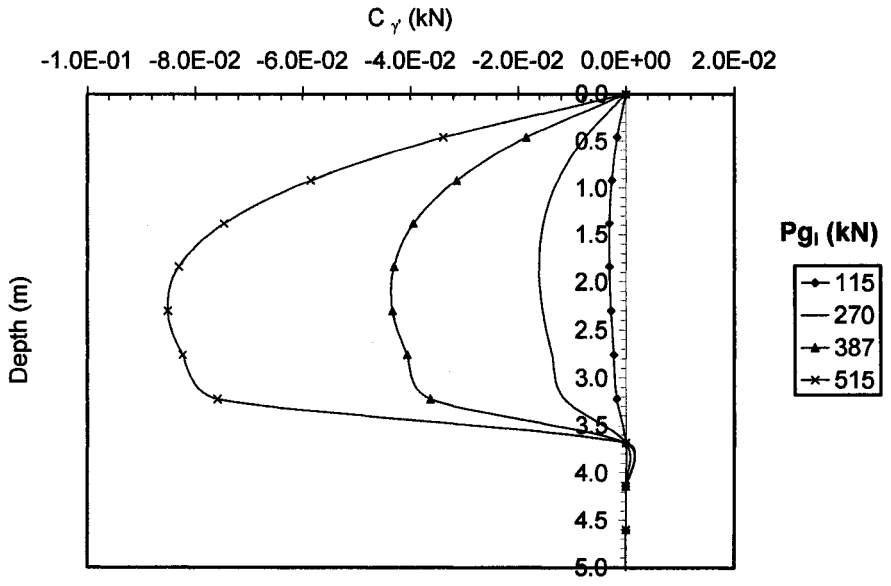

Fig. O.8a Distributions of sensitivity operators $C_{\gamma'}$ affecting the changes of δy_t due to variations of the design variable $\delta\gamma'$ for pile member A (2nd trailing row) of groups of 3 x 3 piles with length L = 10T and spacing s = 2D subjected to lateral forces P_i (kN)

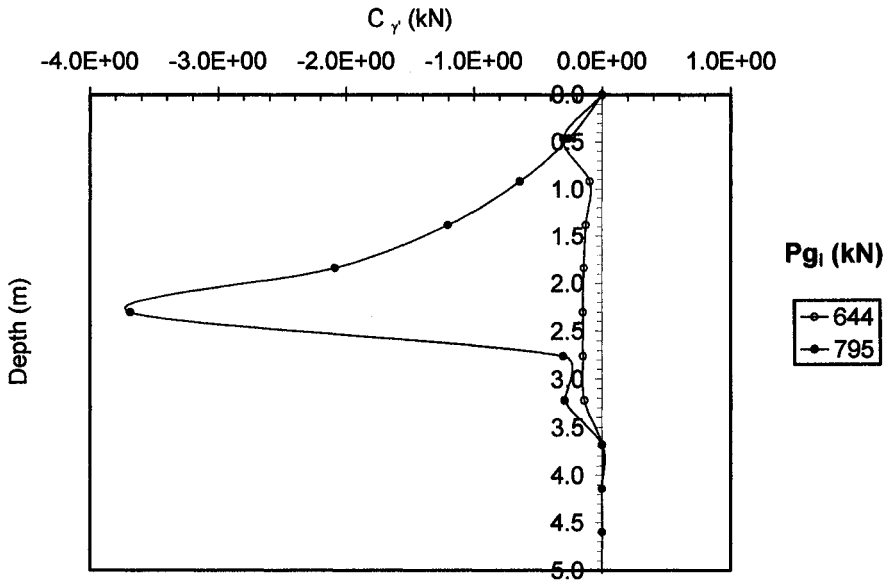

Fig. O.8b Distributions of sensitivity operators $C_{\gamma'}$ affecting the changes of δy_t due to variations of the design variable $\delta\gamma'$ for pile member A (2nd trailing row) of groups of 3 x 3 piles with length L = 10T and spacing s = 2D subjected to lateral forces P_i (kN)

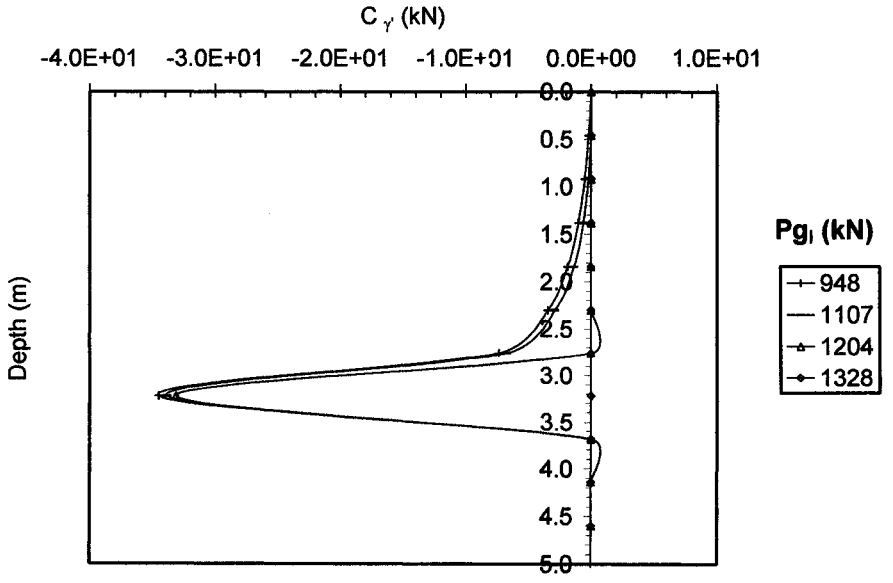

Fig. O.8c Distributions of sensitivity operators $C_{\gamma'}$ affecting the changes of δy_t due to variations of the design variable $\delta\gamma'$ for pile member A (2nd trailing row) of groups of 3 x 3 piles with length L = 10T and spacing s = 2D subjected to lateral forces P_i (kN)

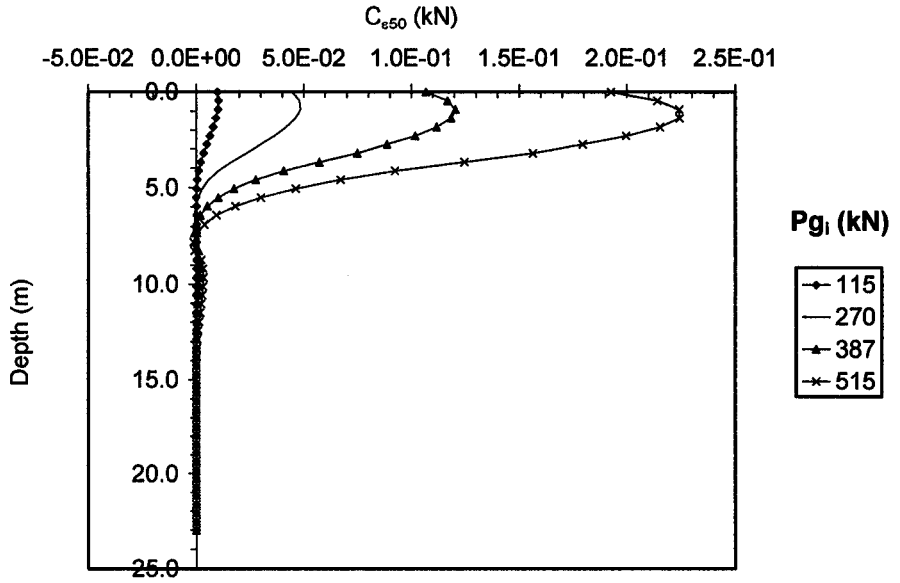

Fig. O.9a Distributions of sensitivity operators $C_{\varepsilon 50}$ affecting the changes of δy_t due to variations of the design variable $\delta\varepsilon_{50}$ for pile member A (2nd trailing row) of groups of 3 x 3 piles with length L = 10T and spacing s = 2D subjected to lateral forces P_i (kN)

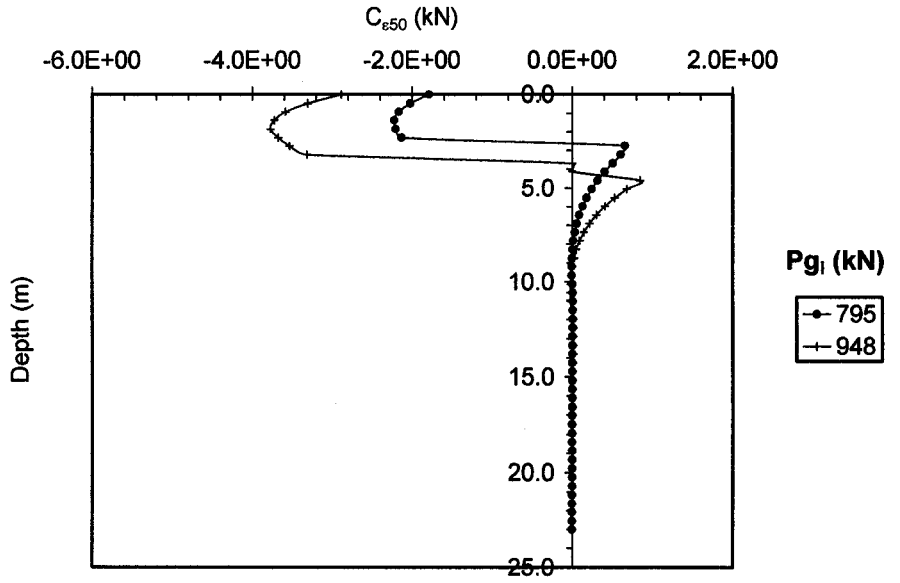

Fig. O.9b Distributions of sensitivity operators $C_{\varepsilon 50}$ affecting the changes of δy_t due to variations of the design variable $\delta\varepsilon_{50}$ for pile member A (2nd trailing row) of groups of 3 x 3 piles with length L = 10T and spacing s = 2D subjected to lateral forces P_i (kN)

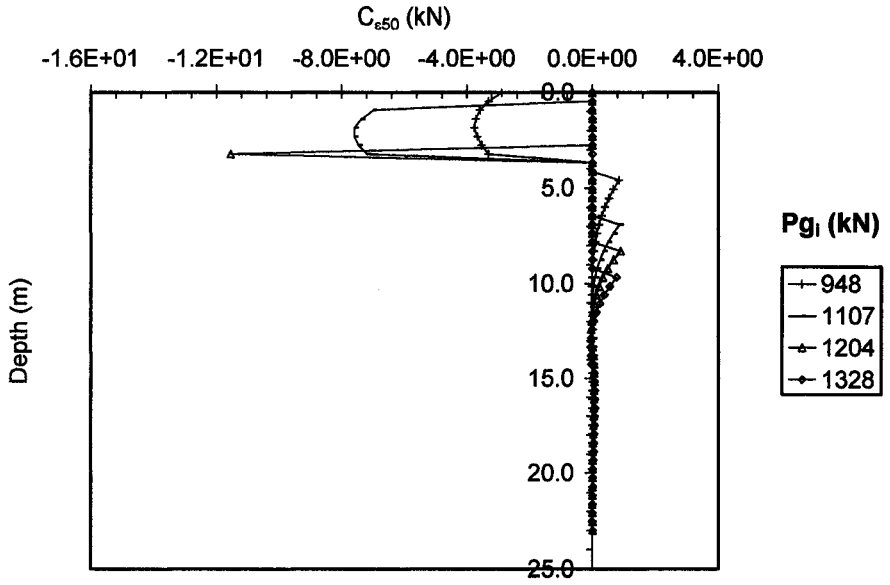

Fig. O.9c Distributions of sensitivity operators $C_{\varepsilon 50}$ affecting the changes of δy_t due to variations of the design variable $\delta \varepsilon_{50}$ for pile member A (2nd trailing row) of groups of 3 x 3 piles with length L = 10T and spacing s = 2D subjected to lateral forces P_i (kN)

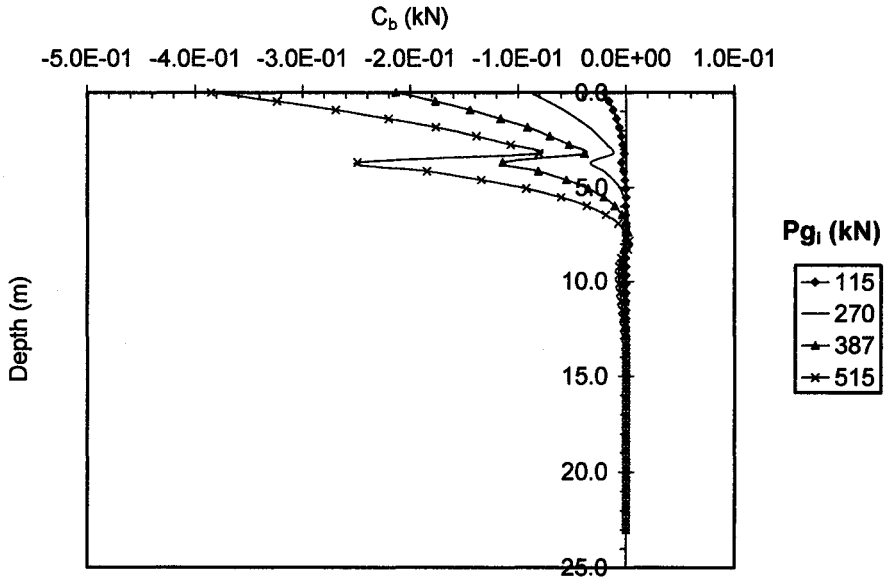

Fig. O.10a Distributions of sensitivity operators C_b affecting the changes of δy_t due to variations of the design variable δb for pile member A (2nd trailing row) of groups of 3 x 3 piles with length L = 10T and spacing s = 2D subjected to lateral forces P_i (kN)

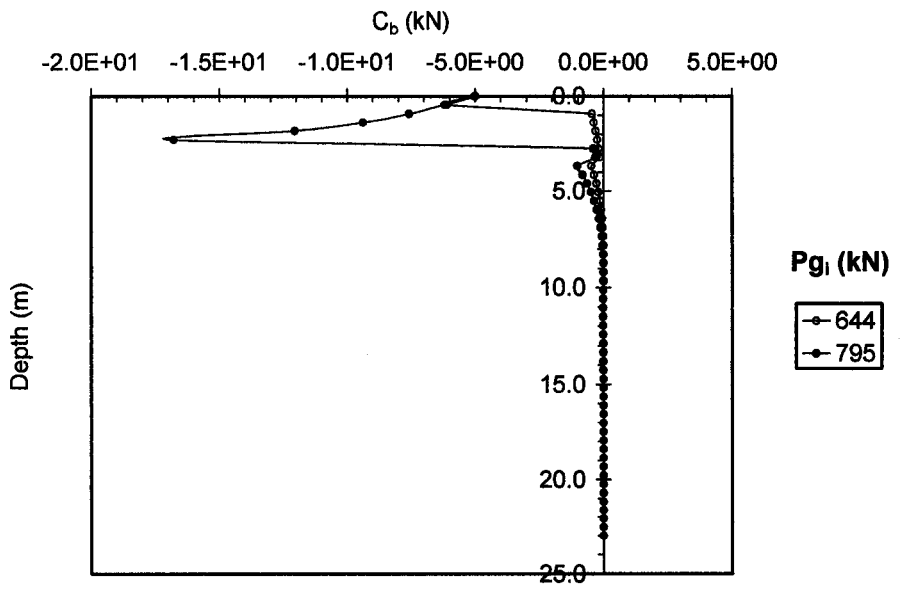

Fig. O.10b Distributions of sensitivity operators C_b affecting the changes of δy_t due to variations of the design variable δb for pile member A (2nd trailing row) of groups of 3 x 3 piles with length L = 10T and spacing s = 2D subjected to lateral forces P_i (kN)

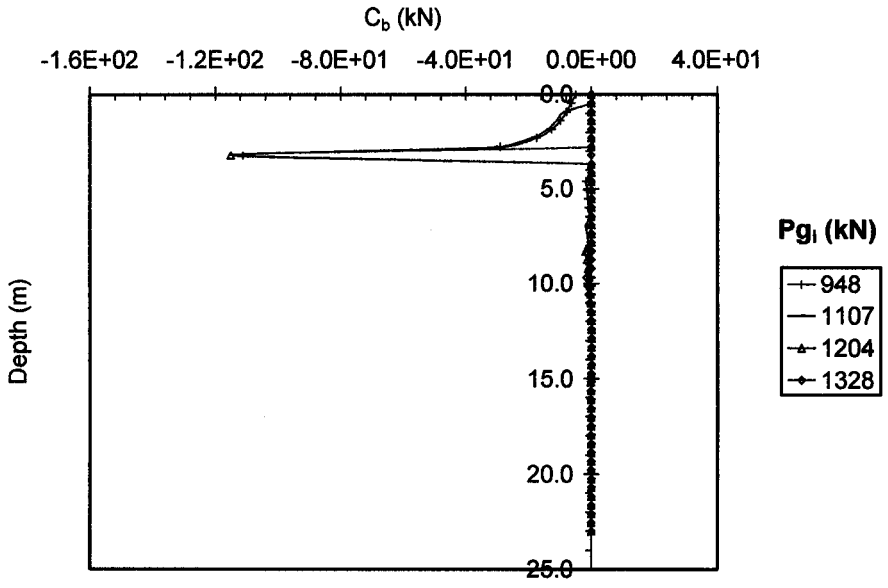

Fig. O.10c Distributions of sensitivity operators C_b affecting the changes of δy_t due to variations of the design variable δb for pile member A (2nd trailing row) of groups of 3 x 3 piles with length L = 10T and spacing s = 2D subjected to lateral forces P_i (kN)

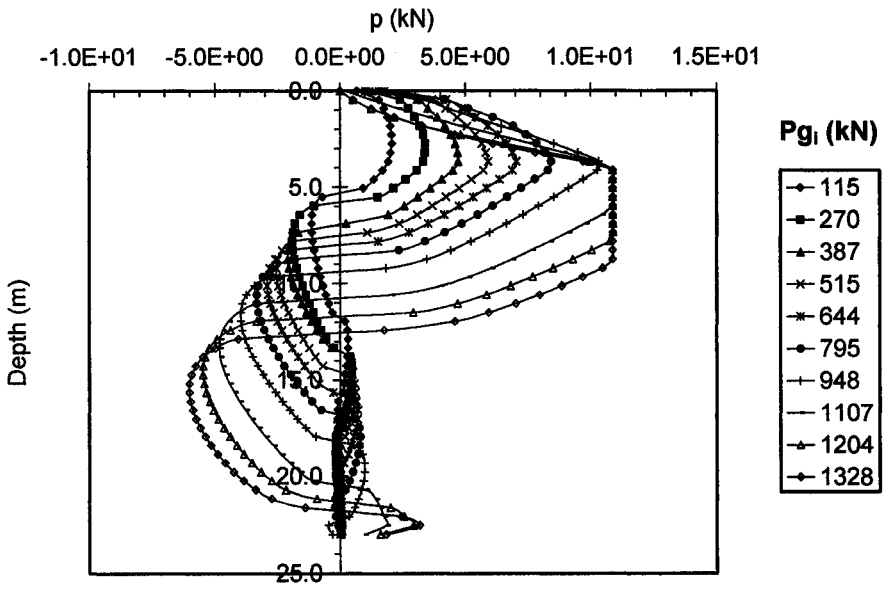

Fig. O.11 Distributions of soil reaction p at the primary structure along the depth of the pile for sensitivity analysis of top lateral displacement δy_t for pile member A (2nd trailing row) of groups of 3 x 3 piles with length L = 10T and spacing s = 2D subjected to lateral forces P_i (kN)

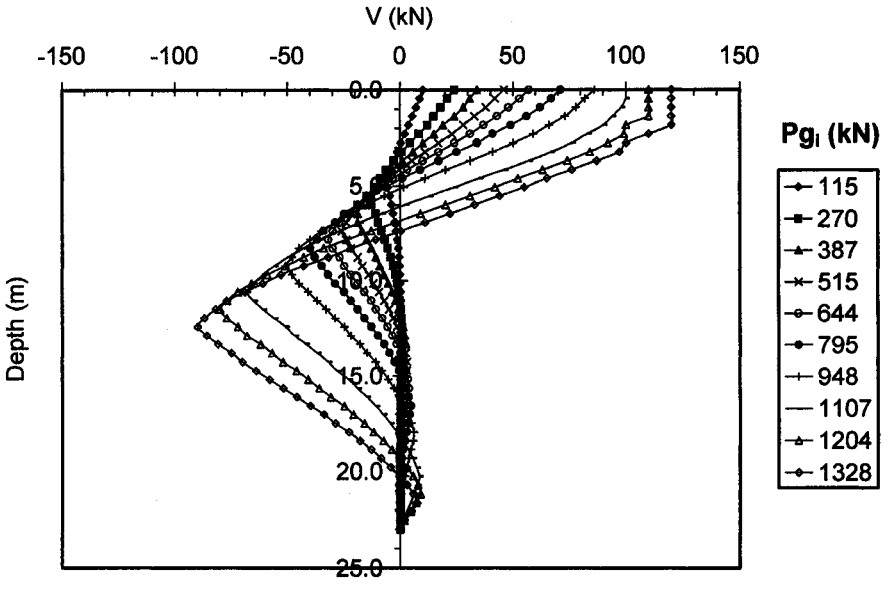

Fig. O.12 Distributions of shear forces V at the primary structure along the depth of the pile for sensitivity analysis of top lateral displacement δy_t for pile member A (2nd trailing row) of groups of 3 x 3 piles with length L = 10T and spacing s = 2D subjected to lateral forces P_i (kN)

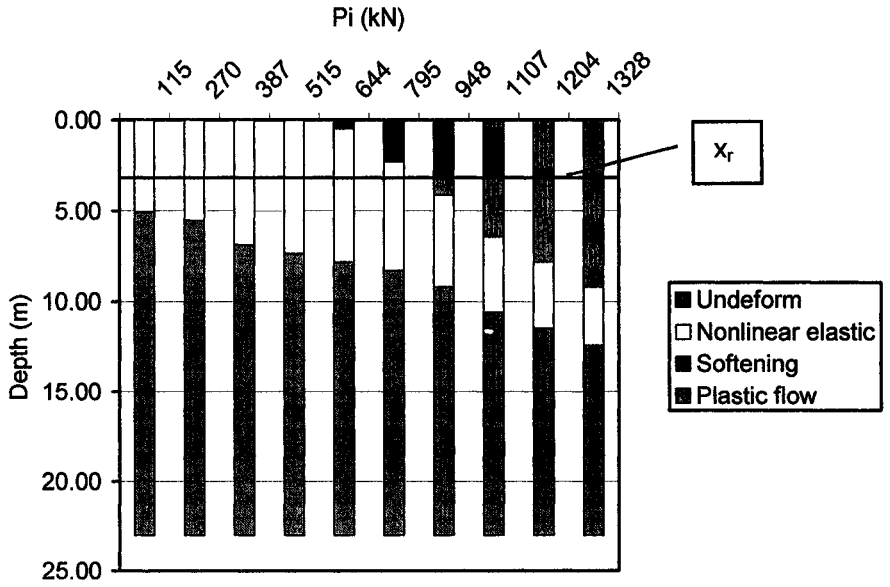

Fig. O.13 Quantitative assessment of the location and the size of the soil phases develop with the depth determined based on the distributions of sensitivity operators affecting δy_t for pile member A (2nd trailing row) of groups of 3 x 3 piles with length L = 10T and spacing s = 2D subjected to lateral forces P_i (kN)

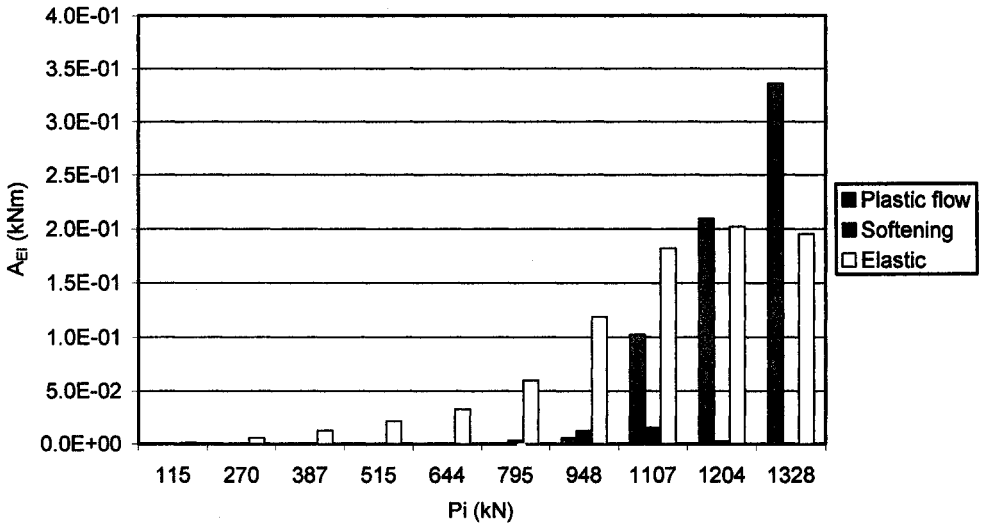

Fig. O.14a Quantitative assessment of A_{EI} of associated with specified soil's stages developed along the pile axis that affect δy_t for pile member A (2nd trailing row) of groups of 3 x 3 piles with length L = 10T and spacing s = 2D subjected to lateral forces P_i (kN)

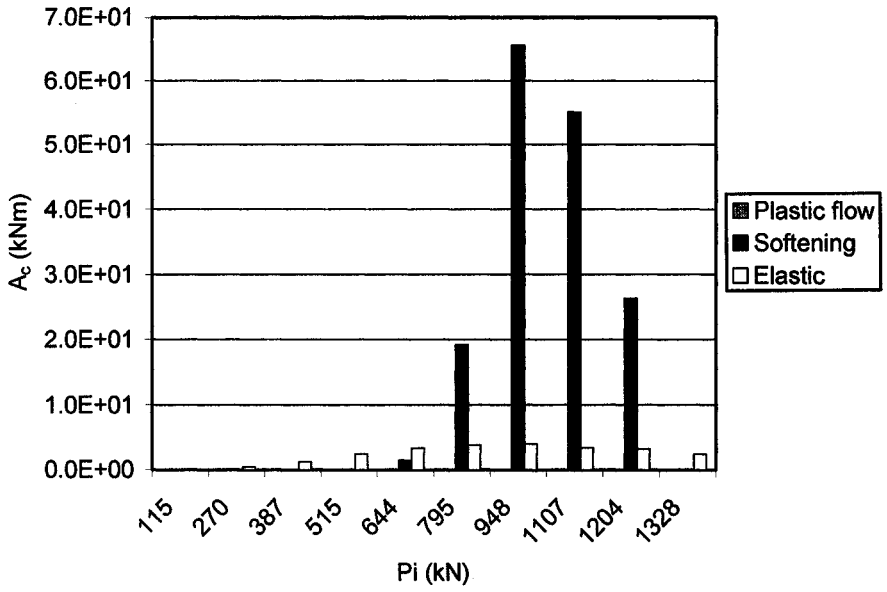

Fig. O.14b Quantitative assessment of A_c associated with specified soil's stages developed along the pile axis that affect δy_t for pile member A (2nd trailing row) of groups of 3 x 3 piles with length L = 10T and spacing s = 2D subjected to lateral forces P_i (kN)

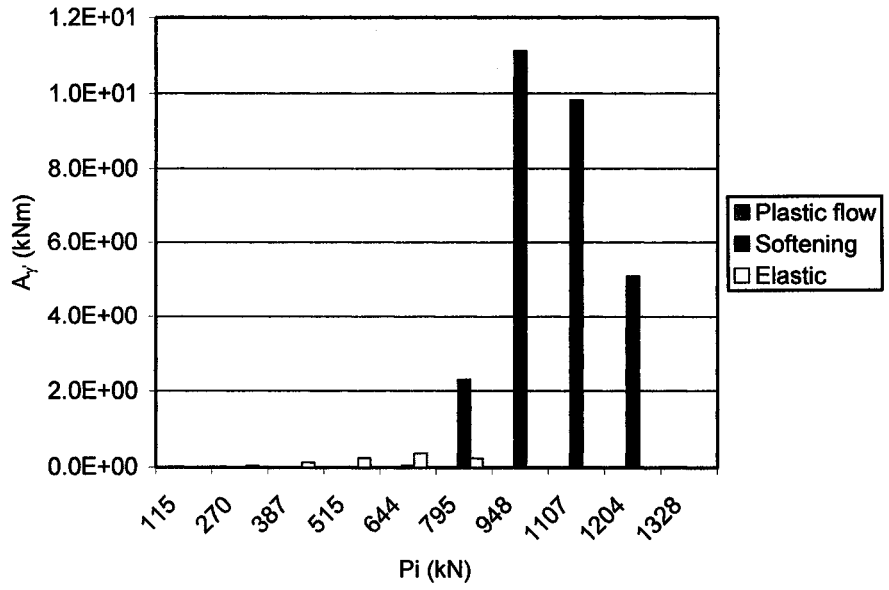

Fig. O.14c Quantitative assessment of A_γ associated with specified soil's stages developed along the pile axis that affect δy_t for pile member A (2nd trailing row) of groups of 3 x 3 piles with length L = 10T and spacing s = 2D subjected to lateral forces P_i (kN)

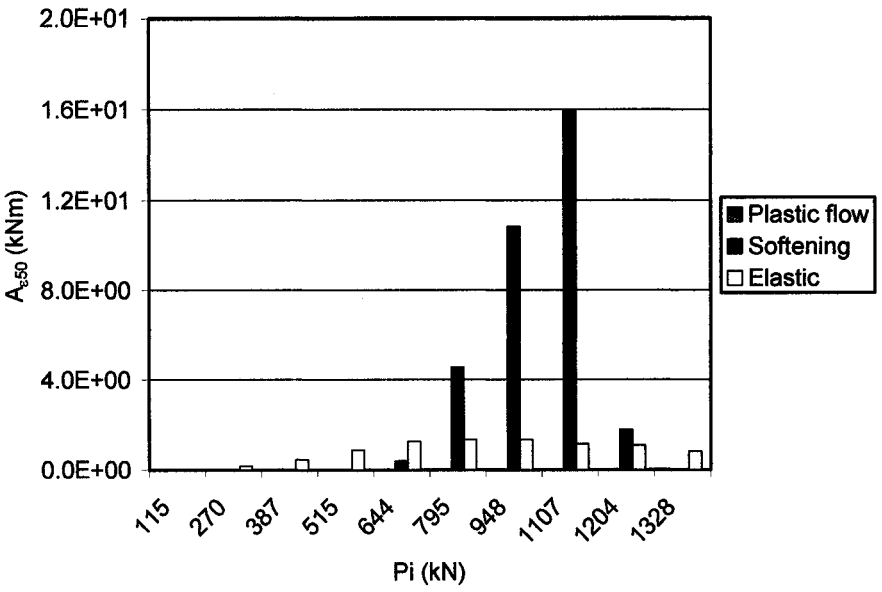

Fig. O.14d Quantitative assessment of $A_{\varepsilon 50}$ associated with specified soil's stages developed along the pile axis that affect δy_t for pile member A (2nd trailing row) of groups of 3 x 3 piles with length L = 10T and spacing s = 2D subjected to lateral forces P_i (kN)

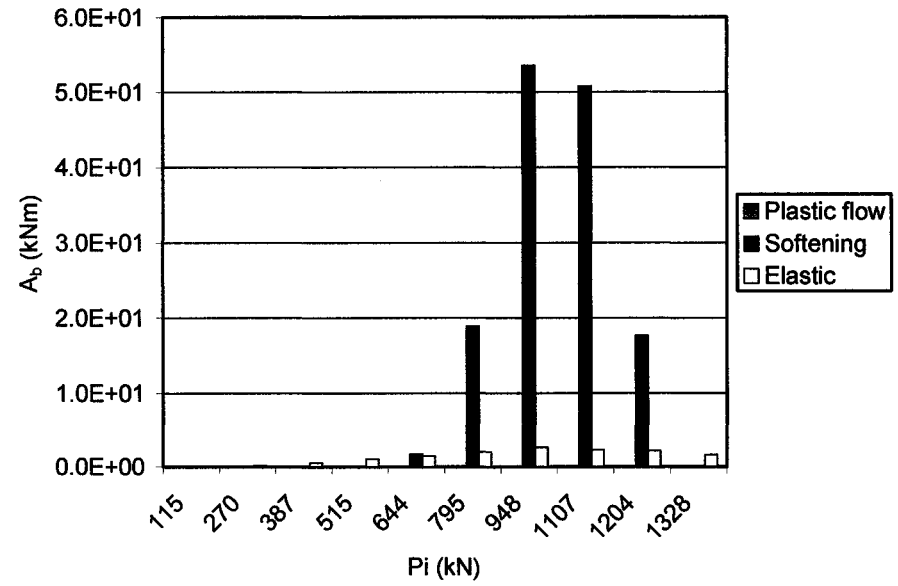

Fig. O.14e Quantitative assessment of A_b associated with specified soil's stages developed along the pile axis that affect δy_t for pile member A (2nd trailing row) of groups of 3 x 3 piles with length L = 10T and spacing s = 2D subjected to lateral forces P_i (kN)

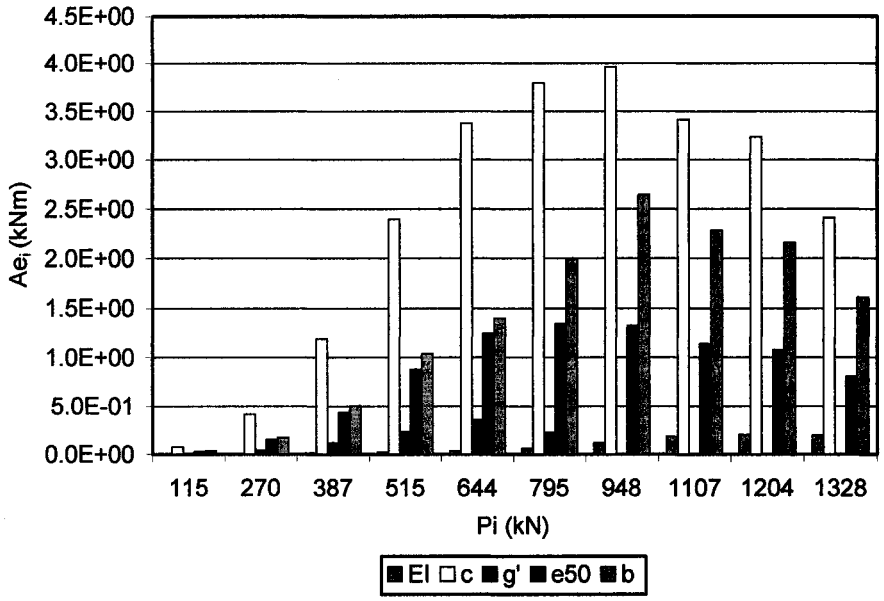

Fig. O.14f Quantitative assessment of sensitivities Ae_i that contains Ae_{EI}, Ae_c, $Ae_{\gamma'}$, $Ae_{\varepsilon 50}$, and Ae_b associated with the development of the nonlinear elastic stage in the soil along the pile axis that affect δy_t for pile member A (2nd trailing row) of groups of 3 x 3 piles with length L = 10T and spacing s = 2D subjected to lateral forces P_i (kN)

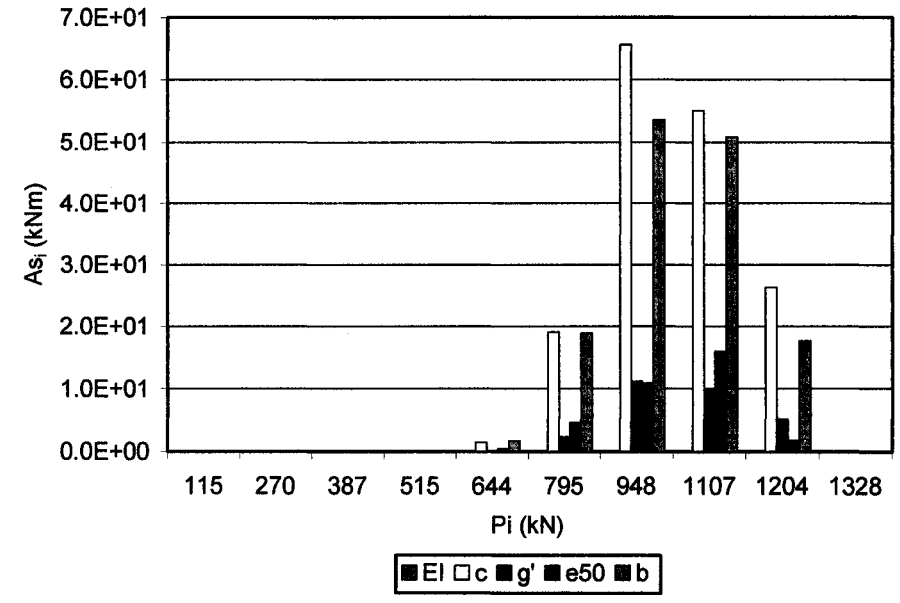

Fig. O.14g Quantitative assessment of sensitivities As_i that contains As_{EI}, As_c, $As_{\gamma'}$, $As_{\varepsilon 50}$, and As_b associated with the development of the linear softening stage in the soil along the pile axis that affect δy_t for pile member A (2nd trailing row) of groups of 3 x 3 piles with length L = 10T and spacing s = 2D subjected to lateral forces P_i (kN)

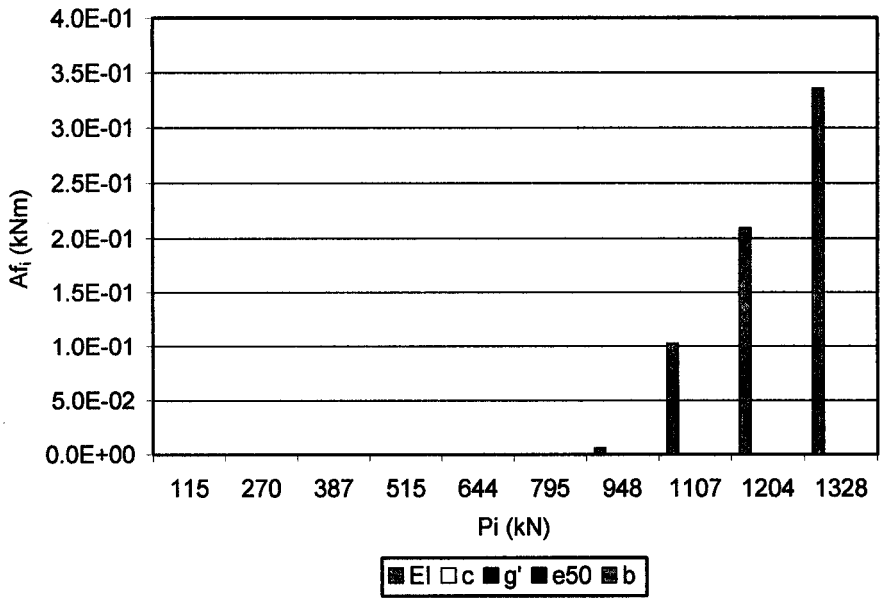

Fig. O.14h Quantitative assessment of sensitivities Af_i that contains Af_{EI}, Af_c, $Af_{\gamma'}$, $Af_{\varepsilon 50}$, and Af_b associated with the development of the plastic flow stage in the soil along the pile axis that affect δy_t for pile member A (2nd trailing row) of groups of 3 x 3 piles with length L = 10T and spacing s = 2D subjected to lateral forces P_i (kN)

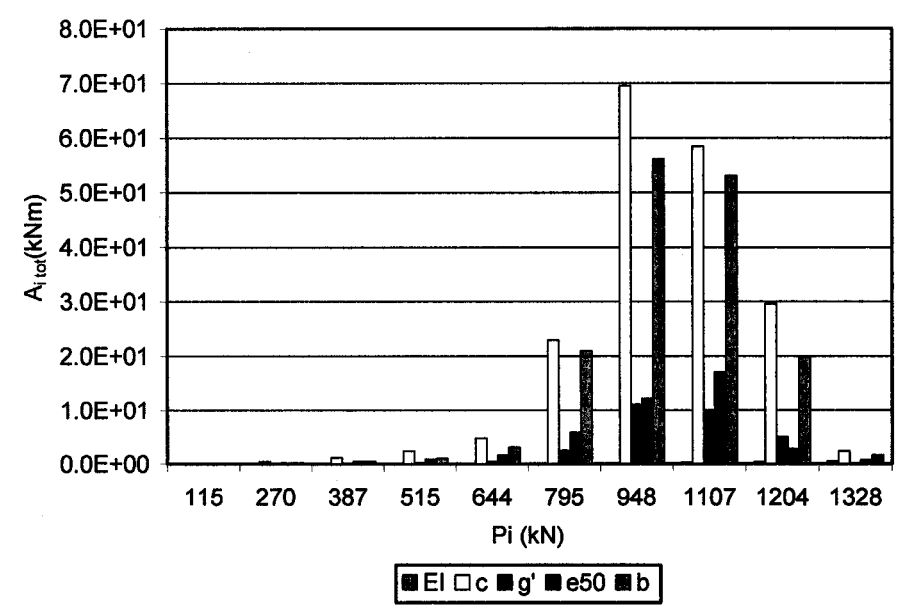

Fig. O.14i Quantitative assessment of sensitivities $A_{i\ tot}$ that contains $(A_{EI}, A_c, A_{\gamma'}, A_{\varepsilon 50}$, and $A_b)_{tot}$ associated with the development of three stages in the soil along the pile axis that affect δy_t for pile member A (2nd trailing row) of groups of 3 x 3 piles with length L = 10T and spacing s = 2D subjected to lateral forces P_i (kN)

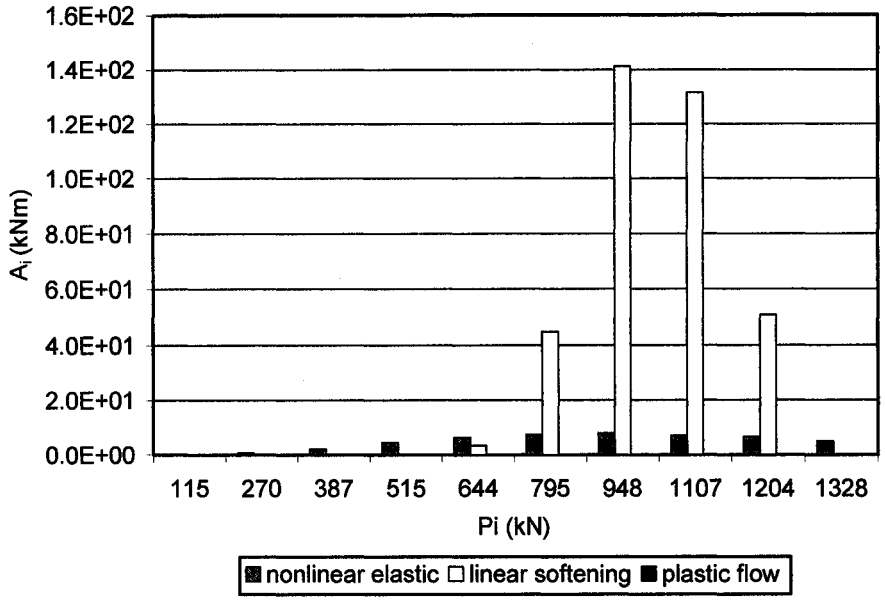

Fig. O.14j.1 Quantitative assessment of A_{tot} of the sensitivity analysis of δy_t for pile member A (2nd trailing row) of groups of 3 x 3 piles with length L = 10T and spacing s = 2D subjected to lateral forces P_i (kN)

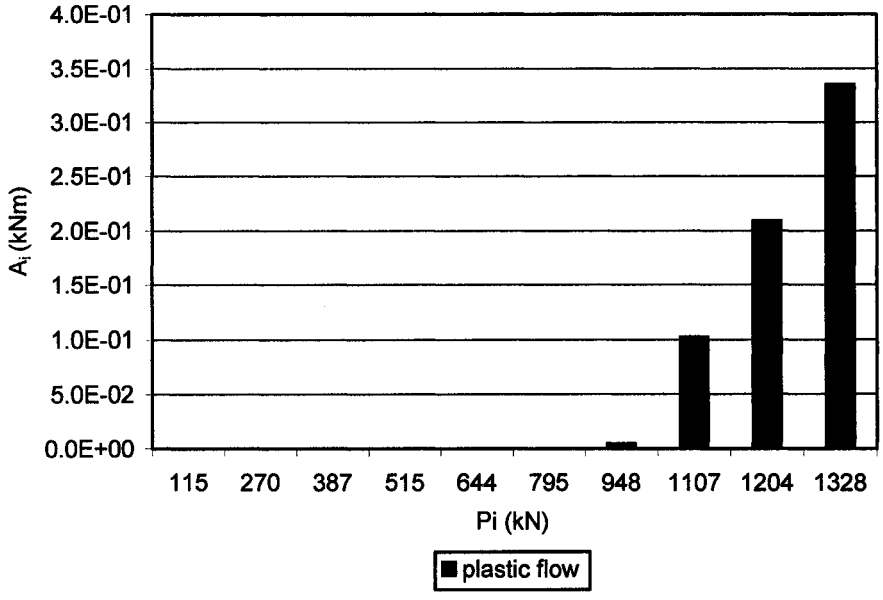

Fig. O.14j.2 Quantitative assessment of sensitivities A_{tot} that is summation of (A_{EI}, A_c, $A_{\gamma'}$, $A_{\varepsilon 50}$, and A_b)$_i$ of each soil stage that affect δy_t for pile member A (2nd trailing row) of groups of 3 x 3 piles with length L = 10T and spacing s = 2D subjected to lateral forces P_i (kN)

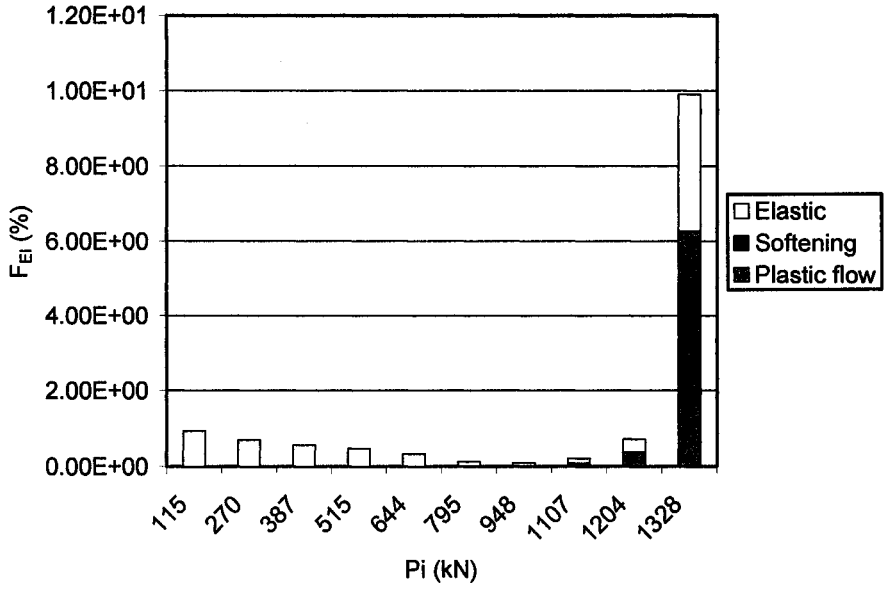

Fig. O.15a Quantitative assessment (in %) of relative sensitivity factors F_{EI} that affect δy_t for pile member A (2nd trailing row) of groups of 3 x 3 piles with length L = 10T and spacing s = 2D subjected to lateral forces P_i (kN)

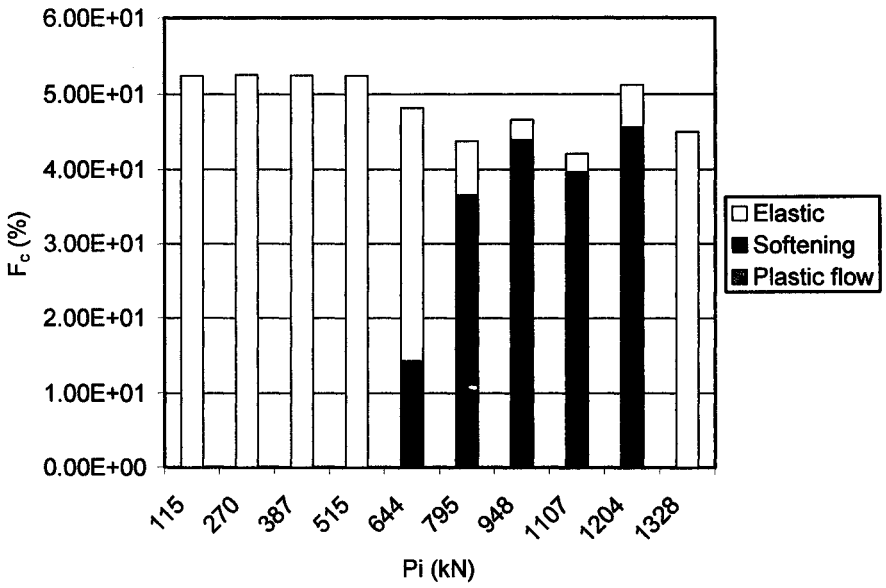

Fig. O.15b Quantitative assessment (in %) of relative sensitivity factors F_c that affect δy_t for pile member A (2nd trailing row) of groups of 3 x 3 piles with length L = 10T and spacing s = 2D subjected to lateral forces P_i (kN)

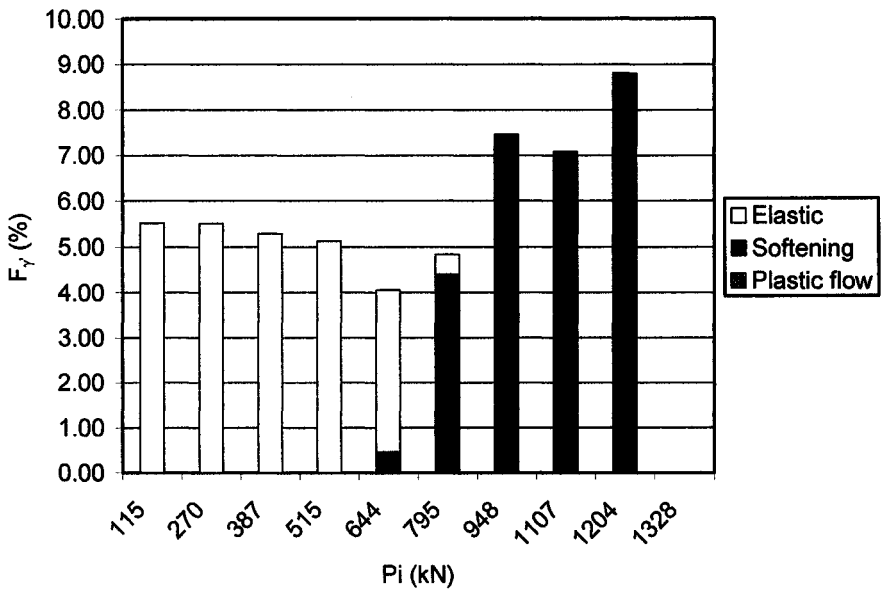

Fig. O.15c Quantitative assessment (in %) of relative sensitivity factors F_γ that affect δy_t for pile member A (2nd trailing row) of groups of 3 x 3 piles with length L = 10T and spacing s = 2D subjected to lateral forces P_i (kN)

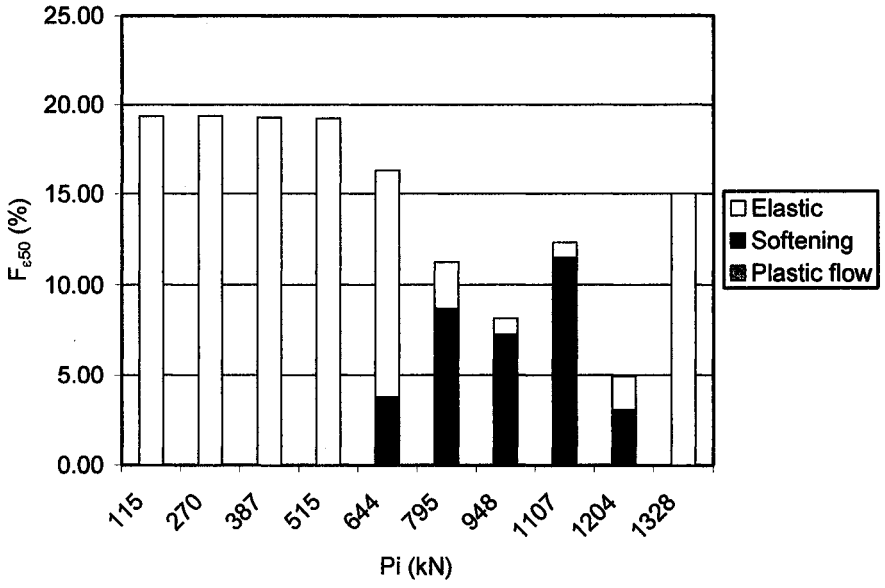

Fig. O.15d Quantitative assessment (in %) of relative sensitivity factors F_b that affect δy_t for pile member A (2nd trailing row) of groups of 3 x 3 piles with length L = 10T and spacing s = 2D subjected to lateral forces P_i (kN)

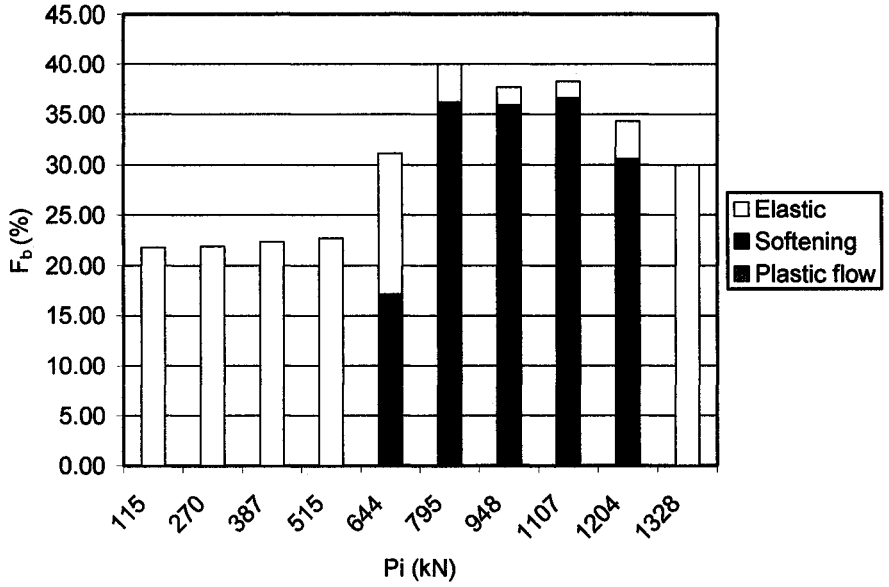

Fig. O.15e Quantitative assessment (in %) of relative sensitivity factors F_b that affect δy_t for pile member A (2nd trailing row) of groups of 3 x 3 piles with length L = 10T and spacing s = 2D subjected to lateral forces P_i (kN)

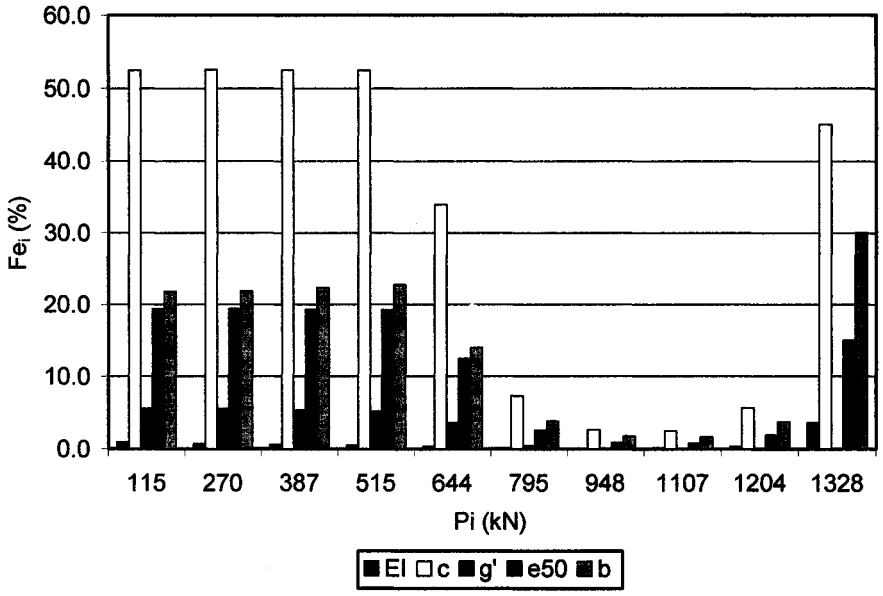

Fig. O.15f Quantitative assessment (in %) of relative sensitivity factors Fe_i that contains Fe_{EI}, Fe_c, $Fe_{\gamma'}$, $Fe_{\varepsilon 50}$, and Fe_b associated with the nonlinear elastic soil stage developed along the pile axis that affect δy_t for pile member A (2nd trailing row) of groups of 3 x 3 piles with length L = 10T and spacing s = 2D subjected to lateral forces P_i (kN)

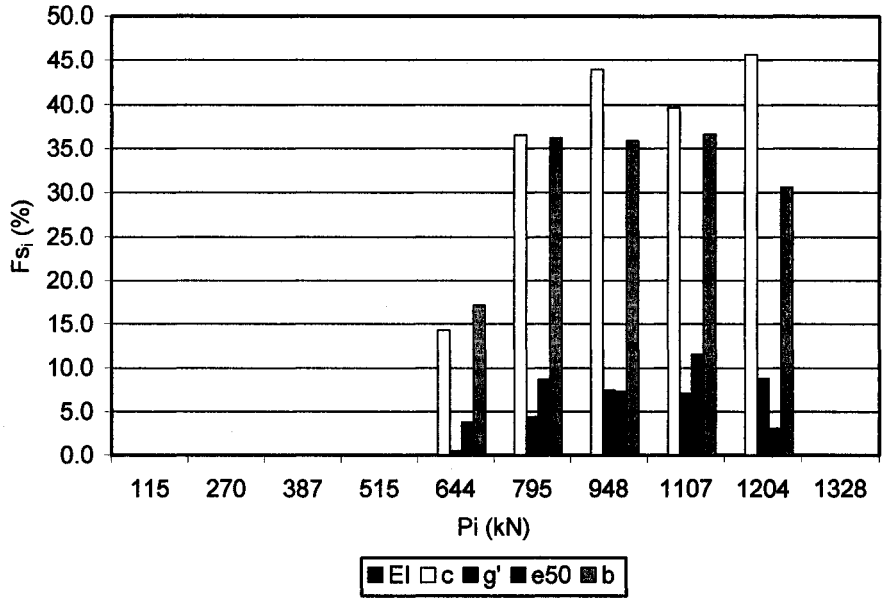

Fig. O.15g Quantitative assessment (in %) of relative sensitivity factors Fs_i that contains Fs_{EI}, Fs_c, $Fs_{\gamma'}$, $Fs_{\varepsilon 50}$, and Fs_b associated with the linear softening stage developed along the pile axis that affect δy_t for pile member A (2nd trailing row) of groups of 3 x 3 piles with length L = 10T and spacing s = 2D subjected to lateral forces P_i (kN)

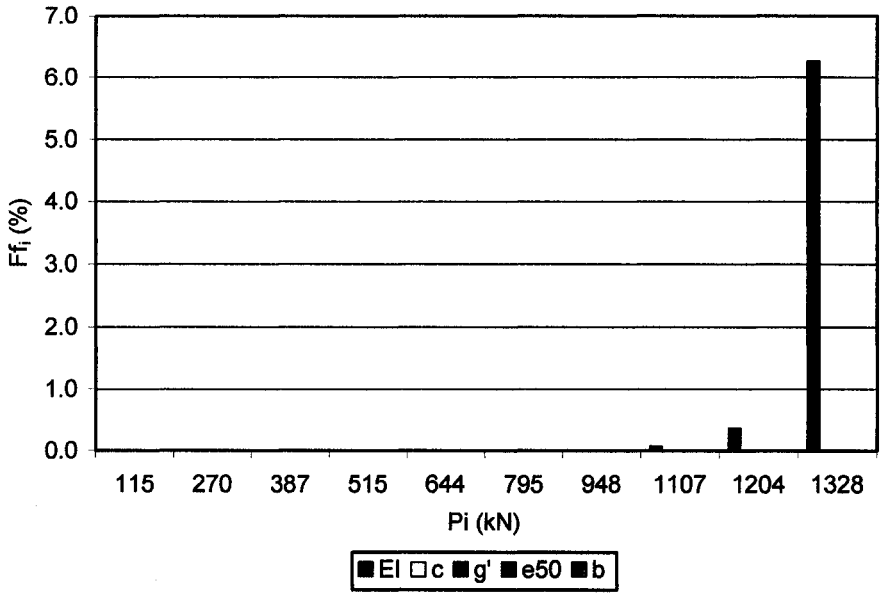

Fig. O.15h Quantitative assessment (in %) of relative sensitivity factors Ff_i that contains Ff_{EI}, Ff_c, $Ff_{\gamma'}$, $Ff_{\varepsilon 50}$, and Ff_b associated with the nonlinear elastic soil stage developed along the pile axis that affect δy_t for pile member A (2nd trailing row) of groups of 3 x 3 piles with length L = 10T and spacing s = 2D subjected to lateral forces P_i (kN)

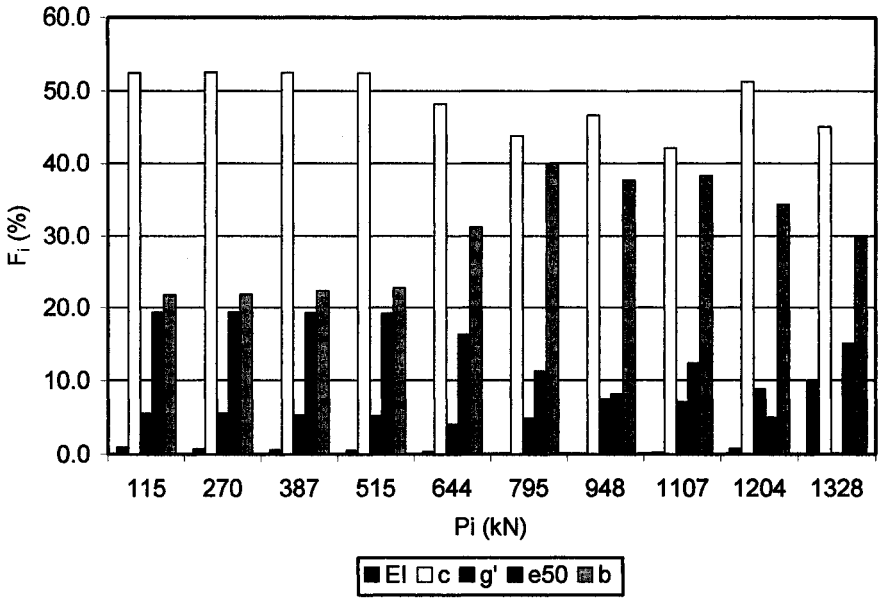

Fig. O.15i Quantitative assessment (in %) of relative sensitivity factors F_i that contains F_{EI}, F_c, $F_{\gamma'}$, $F_{\varepsilon 50}$, and F_b associated with all soil stages developed along the pile axis that affect δy_t for pile member A (2nd trailing row) of groups of 3 x 3 piles with length L = 10T and spacing s = 2D subjected to lateral forces P_i (kN)

APPENDIX P:

Comparison of the sensitivity analysis of top lateral displacement δy_t for pile member A, B, C, and D of group of 3×3 piles with length L = 10T and spacing s = 2D subjected to lateral forces P1, P2, P3

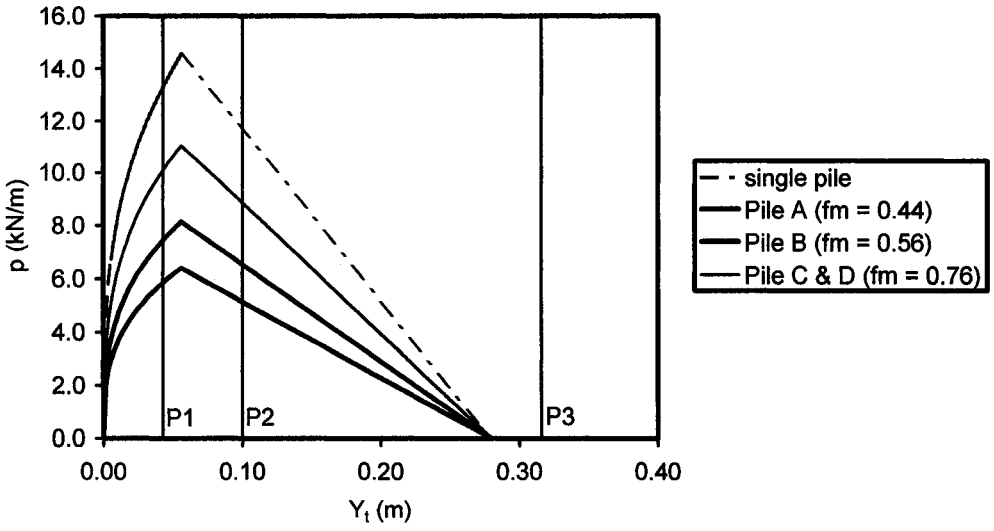

Fig. P.1 Soil reaction p at the top surface (expressed in terms of lateral loading) vs. lateral displacement generated by lateral loading applied to the pile for sensitivity analysis of top lateral displacement δy_t for pile members A (2nd trailing row), B (1st trailing row), C (middle pile in leading row), and D (corner pile in leading row) of group of 3 x 3 piles with length L = 10T and spacing s = 2D subjected to lateral forces P_i (kN)

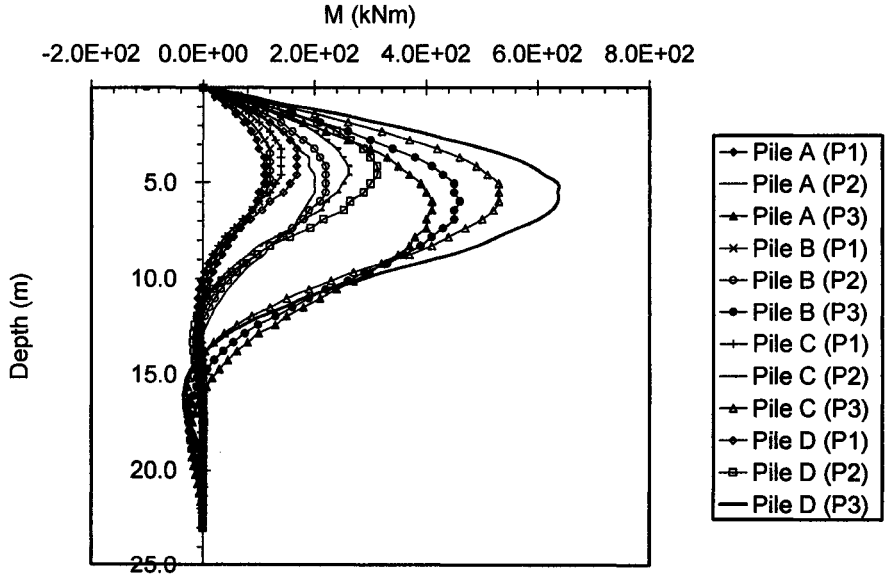

Fig. P.2 Distributions of bending moments at the primary structure M along the depth of the pile for sensitivity analysis of top lateral displacement δy_t for pile members A (2nd trailing row), B (1st trailing row), C (middle pile in leading row), and D (corner pile in leading row) of group of 3 x 3 piles with length L = 10T and spacing s = 2D subjected to lateral forces P_i (kN)

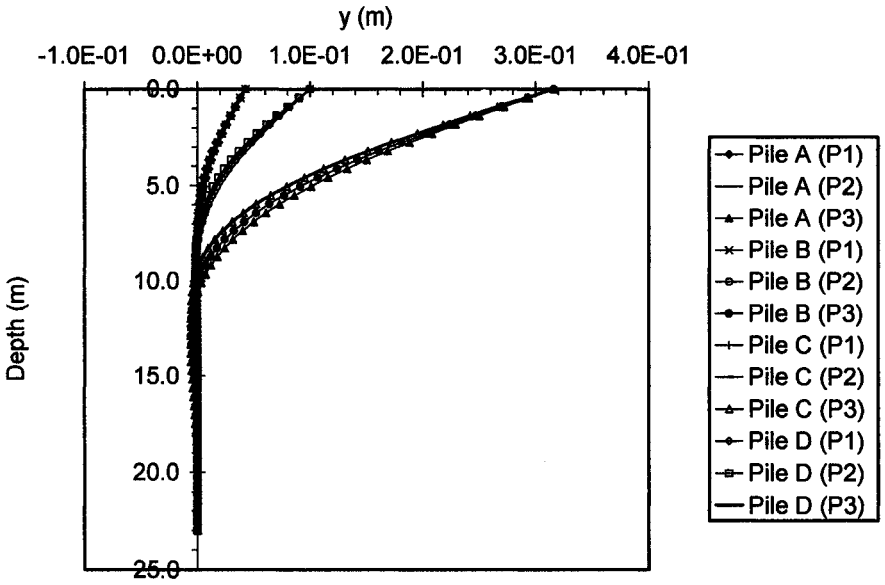

Fig. P.3 Distributions of lateral deflections at the primary structure y along the depth of the pile for sensitivity analysis of top lateral displacement δy_t for pile members A (2nd trailing row), B (1st trailing row), C (middle pile in leading row), and D (corner pile in leading row) of group of 3 x 3 piles with length L = 10T and spacing s = 2D subjected to lateral forces P_i (kN)

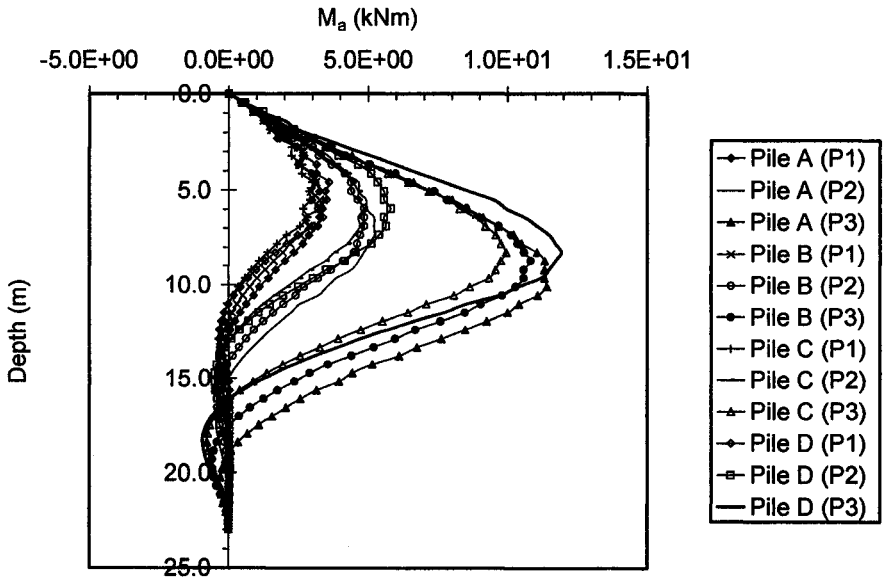

Fig. P.4 Distributions of bending moments M_a along the depth of the pile at the adjoint structure for sensitivity analysis of top lateral displacement δy_t for pile members A (2nd trailing row), B (1st trailing row), C (middle pile in leading row), and D (corner pile in leading row) of group of 3 x 3 piles with length L = 10T and spacing s = 2D subjected to lateral forces P_i (kN)

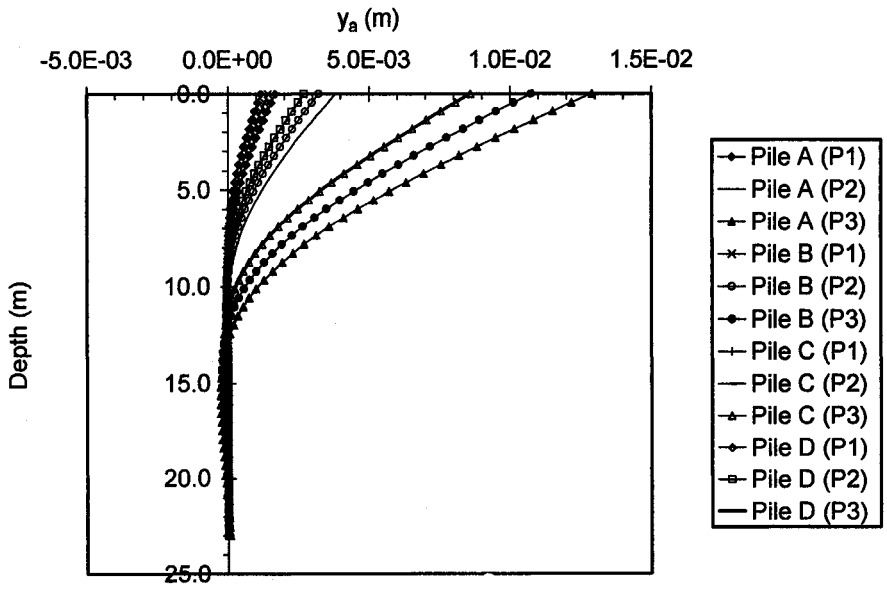

Fig. P.5 Distributions of lateral deflections at the adjoint structure y_a along the depth of the pile for sensitivity analysis of top lateral displacement δy_t for pile members A (2nd trailing row), B (1st trailing row), C (middle pile in leading row), and D (corner pile in leading row) of group of 3 x 3 piles with length L = 10T and spacing s = 2D subjected to lateral forces P_i (kN)

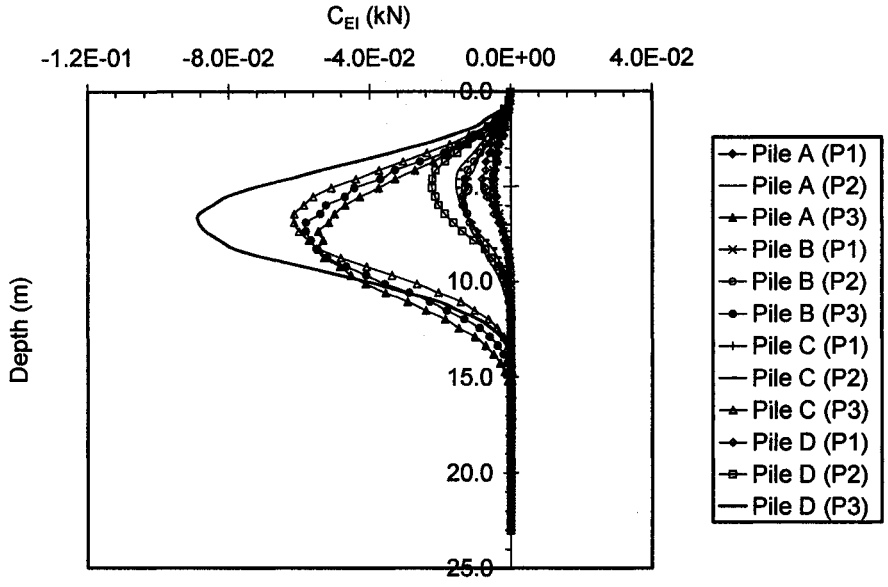

Fig. P.6 Distributions of sensitivity operators C_{EI} affecting the changes of δy_t due to variations of the design variable δEI for pile members A (2nd trailing row), B (1st trailing row), C (middle pile in leading row), and D (corner pile in leading row) of group of 3 x 3 piles with length L = 10T and spacing s = 2D subjected to lateral forces P_i (kN)

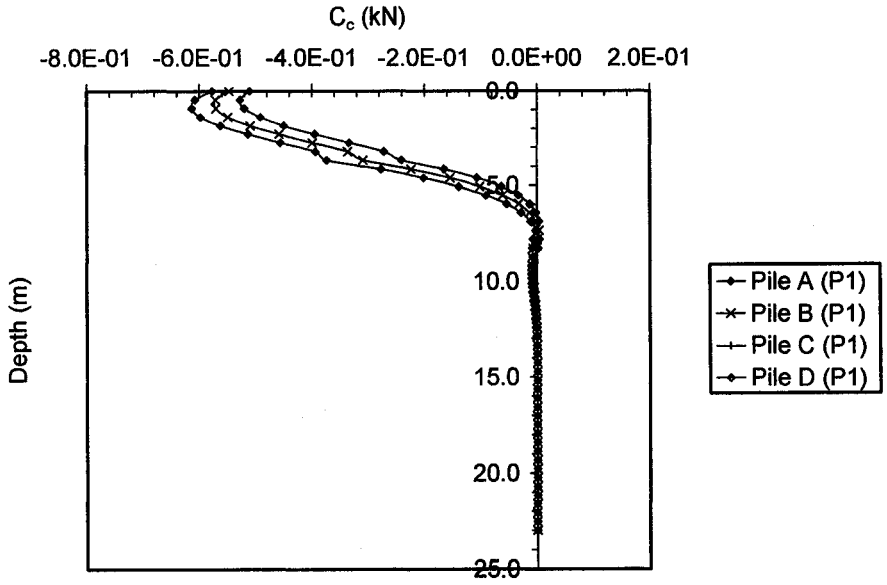

Fig. P.7a Distributions of sensitivity operators C_c affecting the changes of δy_t due to variations of the design variable δc for pile members A (2nd trailing row), B (1st trailing row), C (middle pile in leading row), and D (corner pile in leading row) of group of 3 x 3 piles with length L = 10T and spacing s = 2D subjected to lateral forces P_i (kN)

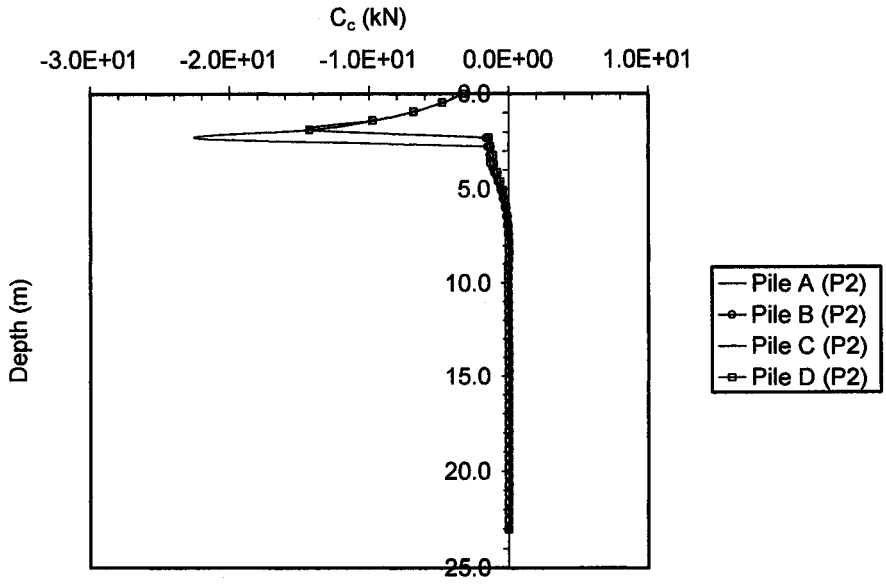

Fig. P.7b Distributions of sensitivity operators C_c affecting the changes of δy_t due to variations of the design variable δc for pile members A (2nd trailing row), B (1st trailing row), C (middle pile in leading row), and D (corner pile in leading row) of group of 3 x 3 piles with length L = 10T and spacing s = 2D subjected to lateral forces P_i (kN)

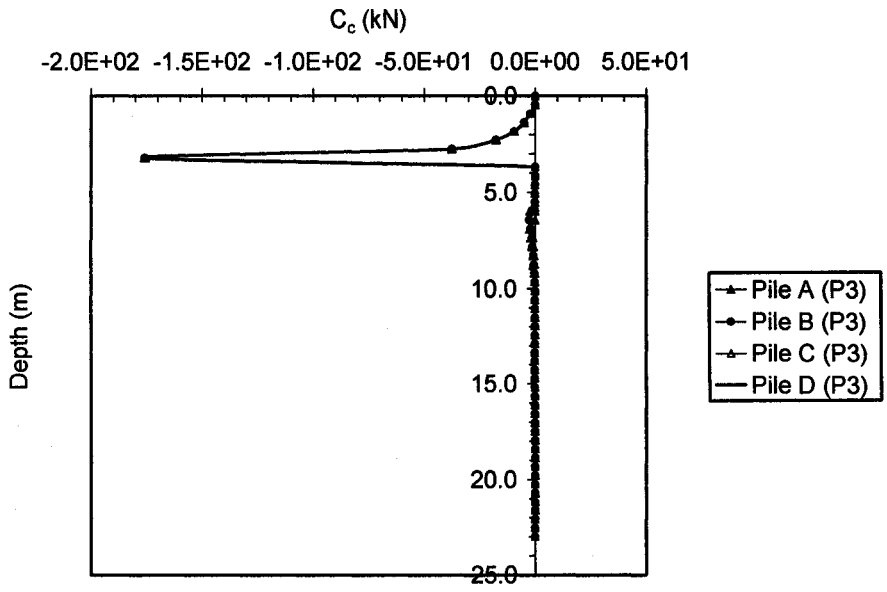

Fig. P.7c Distributions of sensitivity operators C_c affecting the changes of δy_t due to variations of the design variable δc for pile members A (2nd trailing row), B (1st trailing row), C (middle pile in leading row), and D (corner pile in leading row) of group of 3 x 3 piles with length L = 10T and spacing s = 2D subjected to lateral forces P_i (kN)

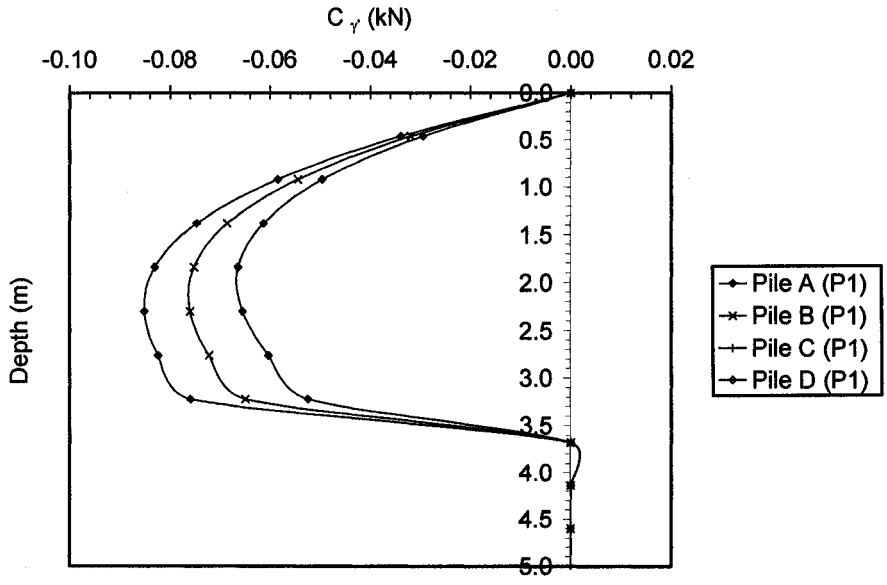

Fig. P.8a Distributions of sensitivity operators $C_{\gamma'}$ affecting the changes of δy_t due to variations of the design variable $\delta\gamma'$ for pile members A (2nd trailing row), B (1st trailing row), C (middle pile in leading row), and D (corner pile in leading row) of group of 3 x 3 piles with length L = 10T and spacing s = 2D subjected to lateral forces P_i (kN)

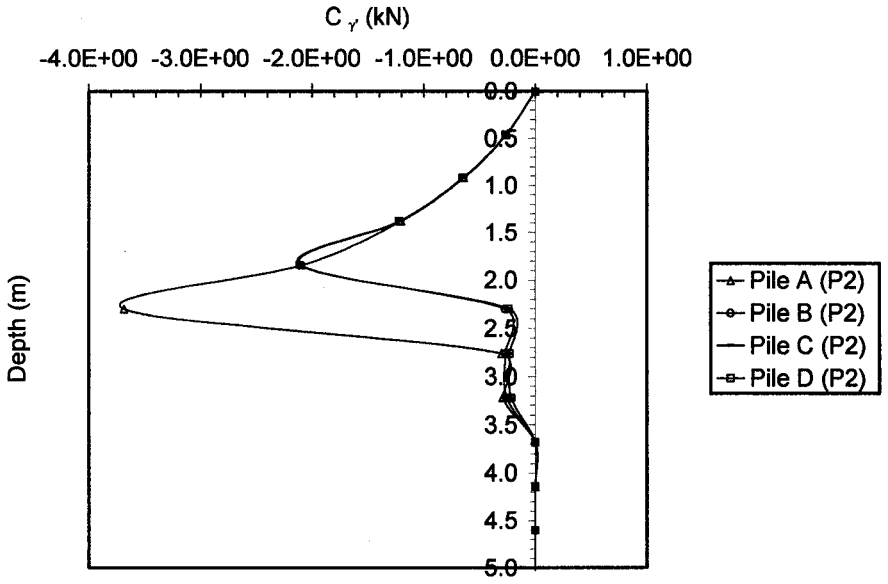

Fig. P.8b Distributions of sensitivity operators $C_{\gamma'}$ affecting the changes of δy_t due to variations of the design variable $\delta\gamma'$ for pile members A (2nd trailing row), B (1st trailing row), C (middle pile in leading row), and D (corner pile in leading row) of group of 3 x 3 piles with length L = 10T and spacing s = 2D subjected to lateral forces P_i (kN)

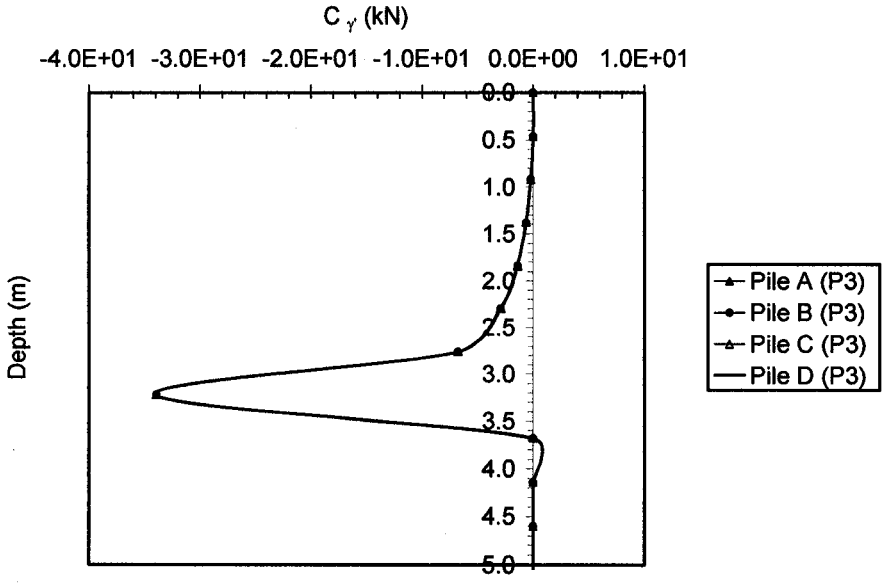

Fig. P.8c Distributions of sensitivity operators $C_{\gamma'}$ affecting the changes of δy_t due to variations of the design variable $\delta\gamma'$ for pile members A (2nd trailing row), B (1st trailing row), C (middle pile in leading row), and D (corner pile in leading row) of group of 3 x 3 piles with length L = 10T and spacing s = 2D subjected to lateral forces P_i (kN)

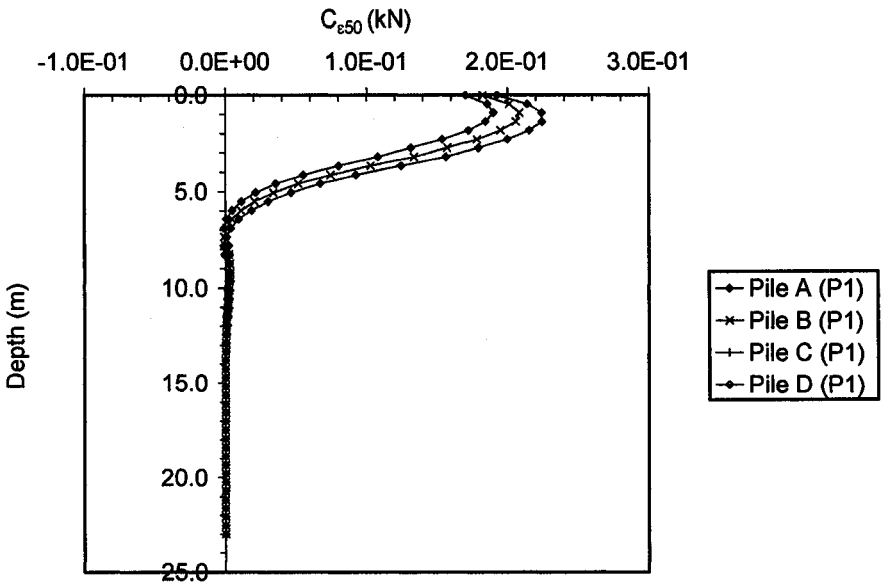

Fig. P.9a Distributions of sensitivity operators $C_{\varepsilon 50}$ affecting the changes of δy_t due to variations of the design variable $\delta\varepsilon_{50}$ for pile members A (2nd trailing row), B (1st trailing row), C (middle pile in leading row), and D (corner pile in leading row) of group of 3 x 3 piles with length L = 10T and spacing s = 2D subjected to lateral forces P_i (kN)

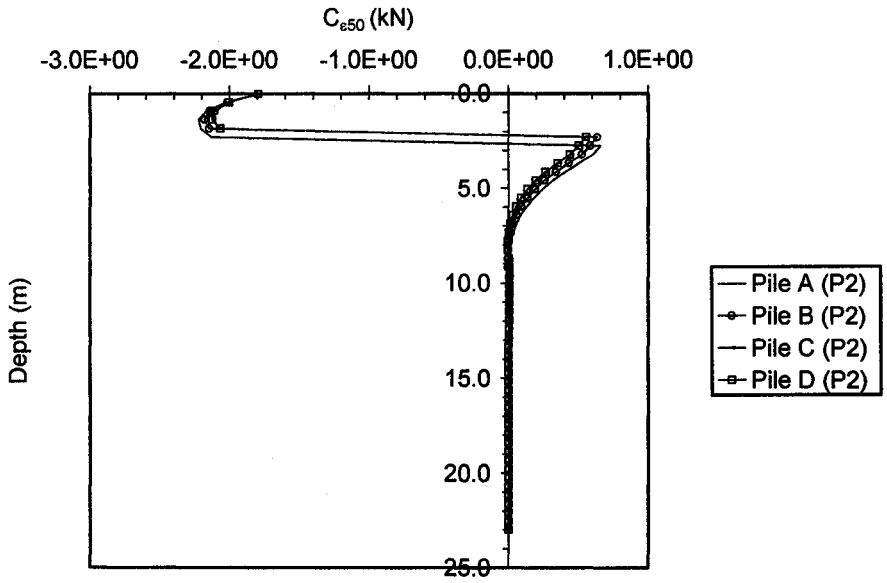

Fig. P.9b Distributions of sensitivity operators $C_{\varepsilon 50}$ affecting the changes of δy_t due to variations of the design variable $\delta\varepsilon_{50}$ for pile members A (2nd trailing row), B (1st trailing row), C (middle pile in leading row), and D (corner pile in leading row) of group of 3 x 3 piles with length L = 10T and spacing s = 2D subjected to lateral forces P_i (kN)

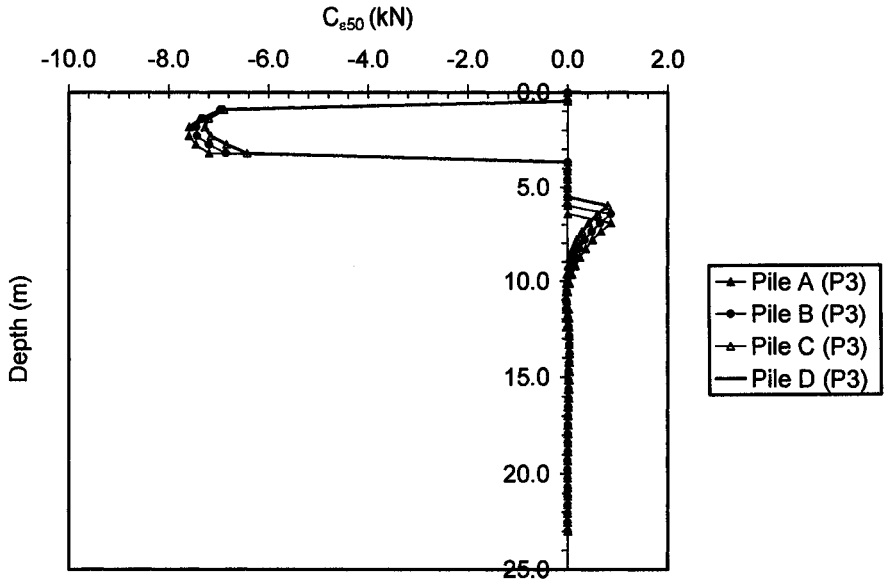

Fig. P.9c Distributions of sensitivity operators $C_{\varepsilon 50}$ affecting the changes of δy_t due to variations of the design variable $\delta\varepsilon_{50}$ for pile members A (2nd trailing row), B (1st trailing row), C (middle pile in leading row), and D (corner pile in leading row) of group of 3 x 3 piles with length L = 10T and spacing s = 2D subjected to lateral forces P_i (kN)

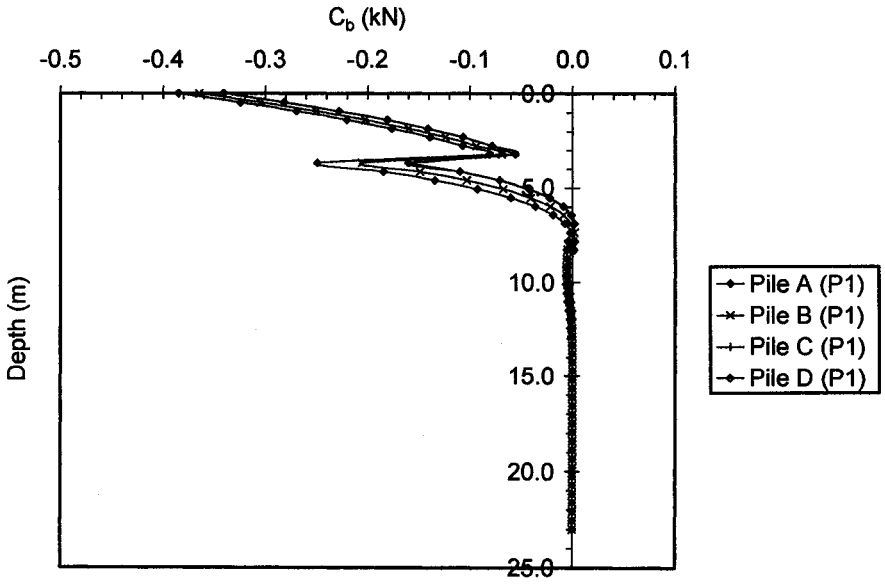

Fig. P.10a Distributions of sensitivity operators C_b affecting the changes of δy_t due to variations of the design variable δb for pile members A (2nd trailing row), B (1st trailing row), C (middle pile in leading row), and D (corner pile in leading row) of group of 3 x 3 piles with length L = 10T and spacing s = 2D subjected to lateral forces P_i (kN)

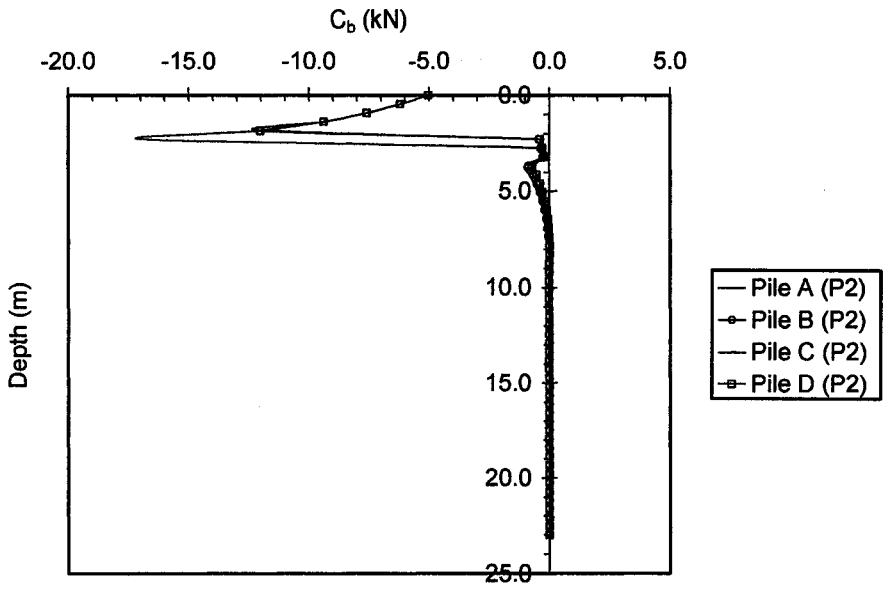

Fig. P.10b Distributions of sensitivity operators C_b affecting the changes of δy_t due to variations of the design variable δb for pile members A (2nd trailing row), B (1st trailing row), C (middle pile in leading row), and D (corner pile in leading row) of groups of 3 x 3 piles with length L = 10T and spacing s = 2D subjected to lateral forces P_i (kN)

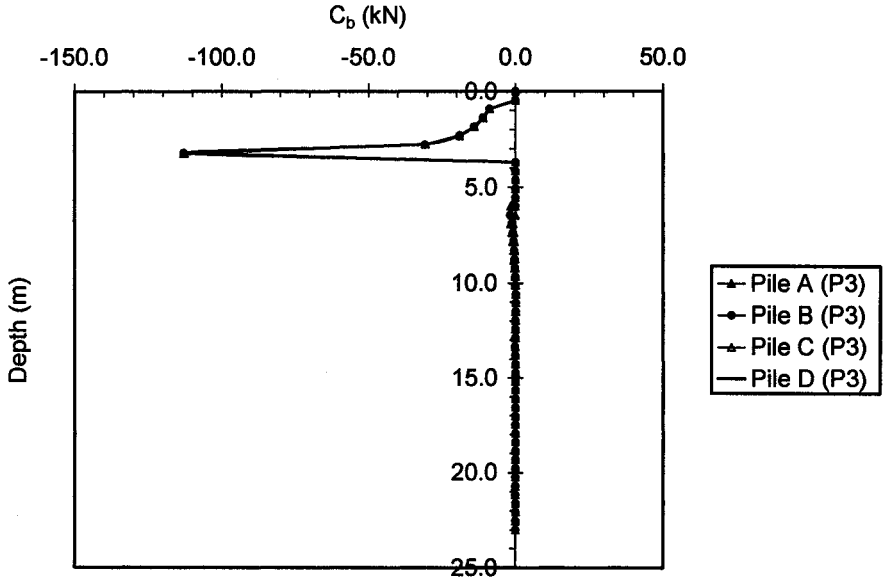

Fig. P.10c Distributions of sensitivity operators C_b affecting the changes of δy_t due to variations of the design variable δb for pile members A (2nd trailing row), B (1st trailing row), C (middle pile in leading row), and D (corner pile in leading row) of group of 3 x 3 piles with length L = 10T and spacing s = 2D subjected to lateral forces P_i (kN)

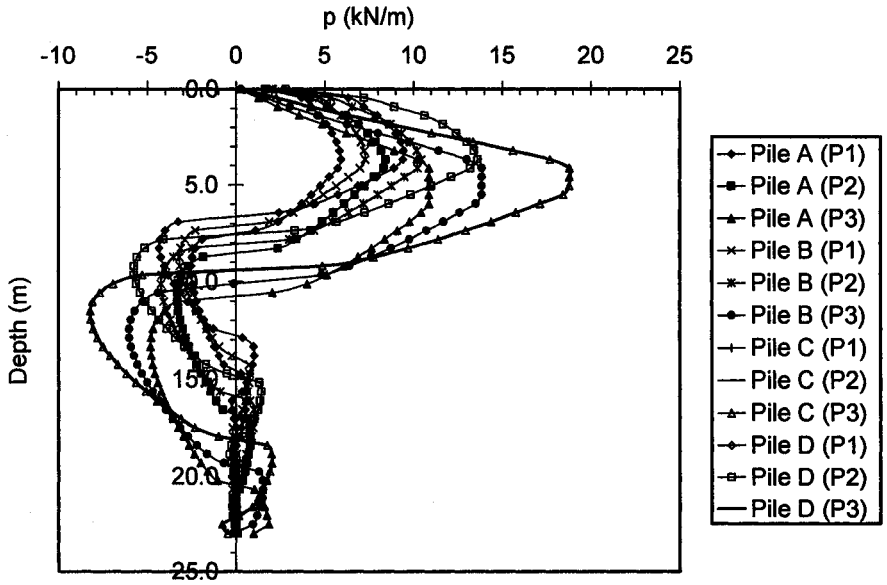

Fig. P.11 Distributions of soil reaction p at the primary structure along the depth of the pile for sensitivity analysis of top lateral displacement δy_t for pile members A (2nd trailing row), B (1st trailing row), C (middle pile in leading row), and D (corner pile in leading row) of group of 3 x 3 piles with length L = 10T and spacing s = 2D subjected to lateral forces P_i (kN)

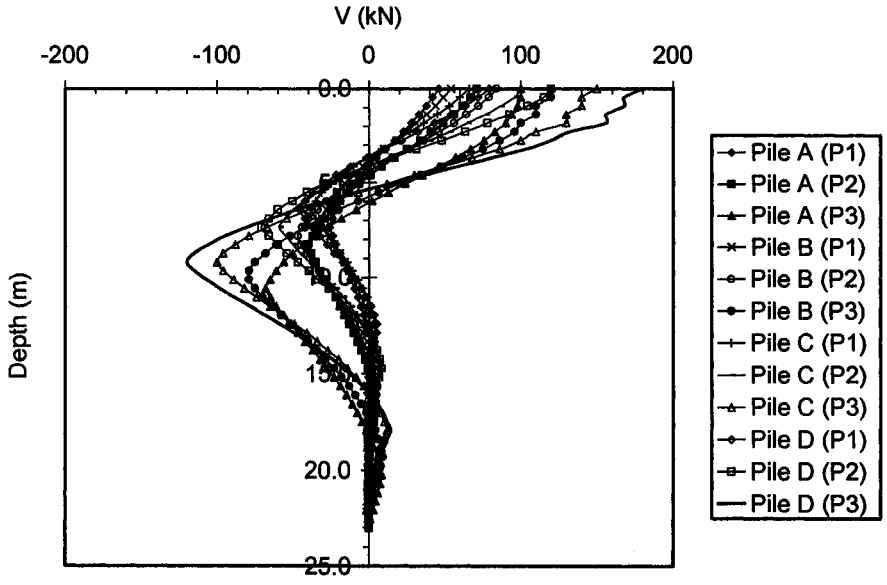

Fig. P.12 Distributions of shear forces V at the primary structure p along the depth of the pile for sensitivity analysis of top lateral displacement δy_t for pile members A (2nd trailing row), B (1st trailing row), C (middle pile in leading row), and D (corner pile in leading row) of group of 3 x 3 piles with length L = 10T and spacing s = 2D subjected to lateral forces P_i (kN)

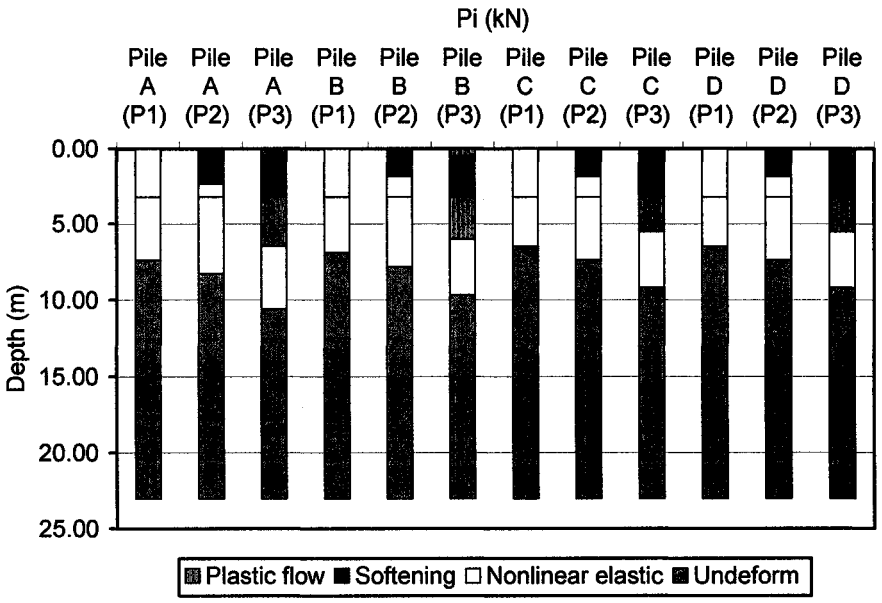

Fig. P.13 Quantitative assessment of the location and the size of the soil phases developed with depth determined based on the distributions of sensitivity operators affecting δy_t for pile members A (2nd trailing row), B (1st trailing row), C (middle pile in leading row), and D (corner pile in leading row) of group of 3 x 3 piles with length L = 10T and spacing s = 2D subjected to lateral forces P_i (kN)

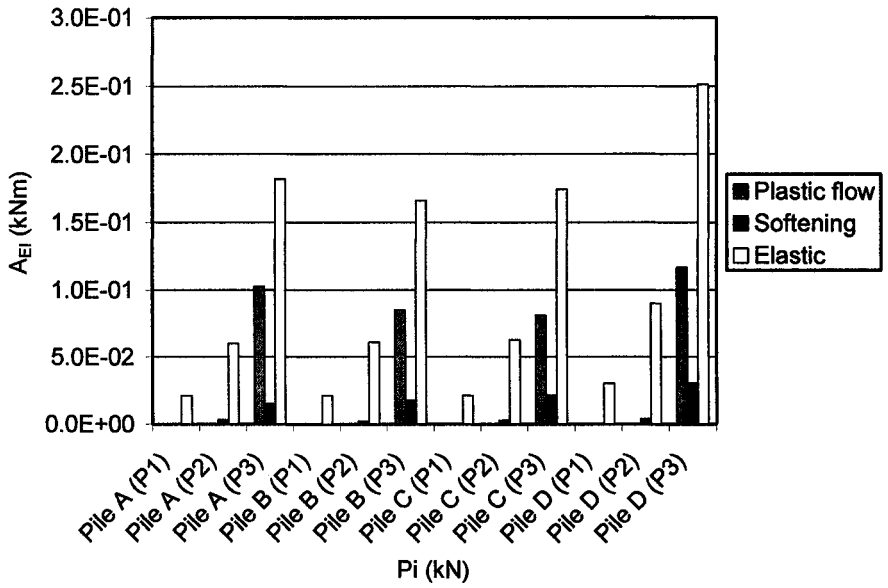

Fig. P.14a Quantitative assessment of sensitivity A_{EI} associated with development of nonlinear elastic, linear softening, and plastic flow stages in the soil along the pile axis that affect δy_t for pile members A (2nd trailing row), B (1st trailing row), C (middle pile in leading row), and D (corner pile in leading row) of group of 3 x 3 piles with length L = 10T and spacing s = 2D subjected to lateral forces P_i (kN)

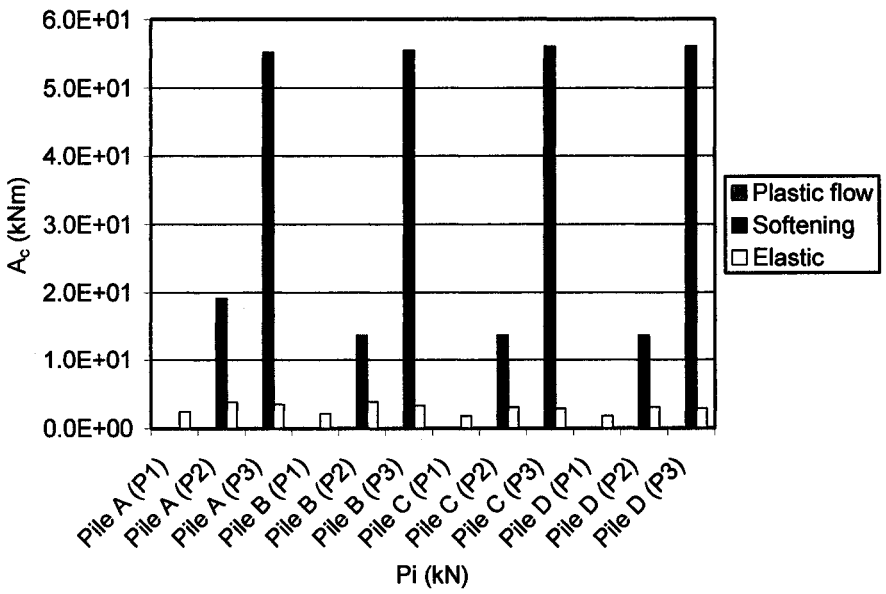

Fig. P.14b Quantitative assessment of sensitivity A_c associated with development of nonlinear elastic, linear softening, and plastic flow stages in the soil along the pile axis that affect δy_t for pile members A (2nd trailing row), B (1st trailing row), C (middle pile in leading row), and D (corner pile in leading row) of group of 3 x 3 piles with length L = 10T and spacing s = 2D subjected to lateral forces P_i (kN)

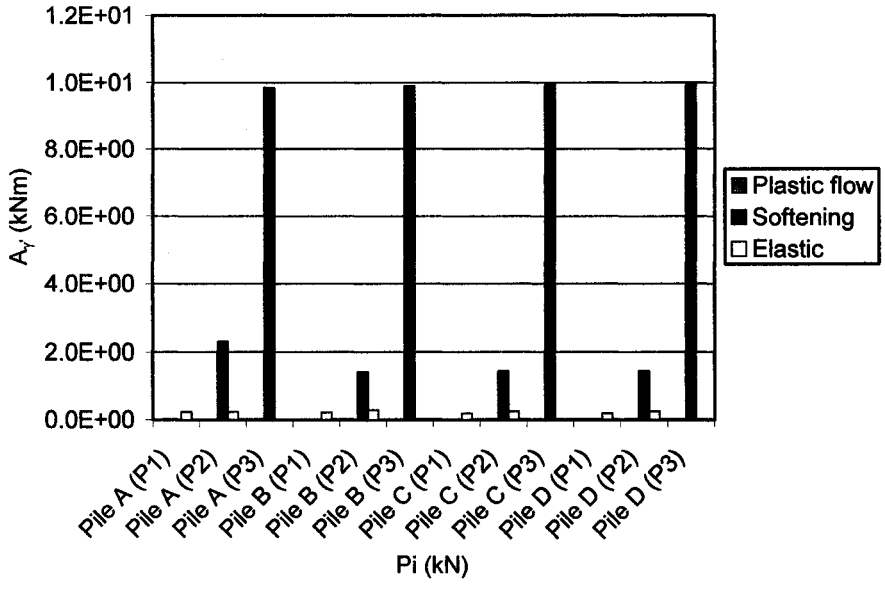

Fig. P.14c Quantitative assessment of sensitivity A_γ associated with development of nonlinear elastic, linear softening, and plastic flow stages in the soil along the pile axis that affect δy_t for pile members A (2nd trailing row), B (1st trailing row), C (middle pile in leading row), and D (corner pile in leading row) of group of 3 x 3 piles with length L = 10T and spacing s = 2D subjected to lateral forces P_i (kN)

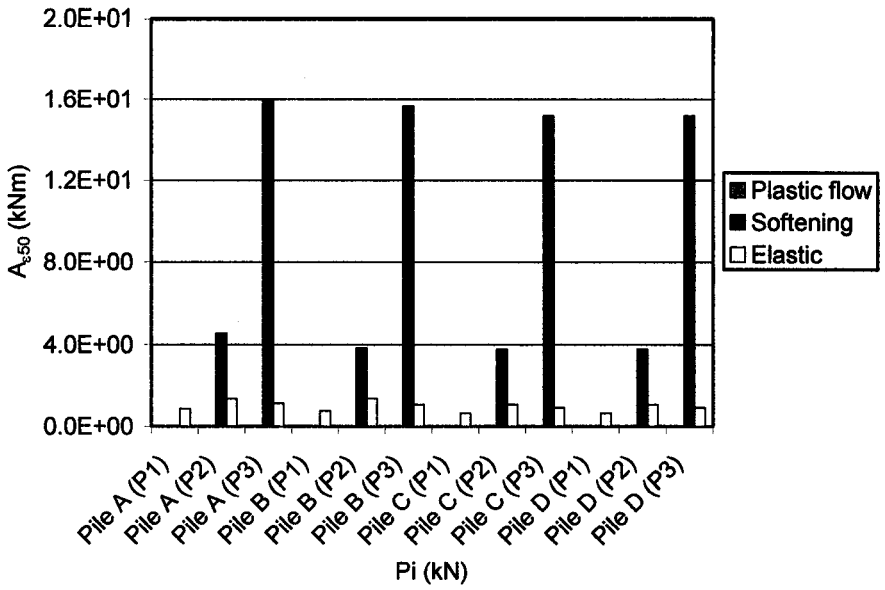

Fig. P.14d Quantitative assessment of sensitivity $A_{\varepsilon 50}$ associated with development of nonlinear elastic, linear softening, and plastic flow stages in the soil along the pile axis that affect δy_t for pile members A (2nd trailing row), B (1st trailing row), C (middle pile in leading row), and D (corner pile in leading row) of group of 3 x 3 piles with length L = 10T and spacing s = 2D subjected to lateral forces P_i (kN)

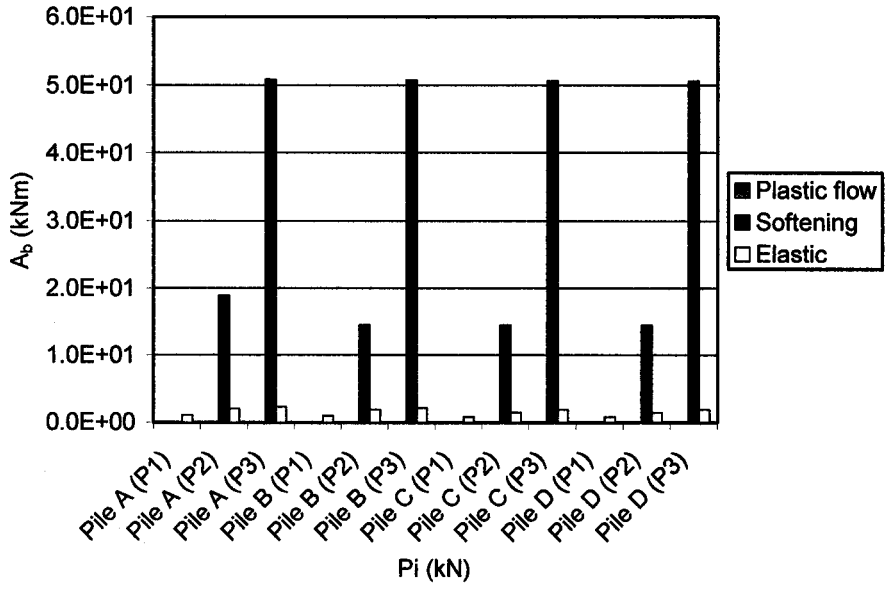

Fig. P.14e Quantitative assessment of sensitivity A_b associated with development of nonlinear elastic, linear softening, and plastic flow stages in the soil along the pile axis that affect δy_t for pile members A (2nd trailing row), B (1st trailing row), C (middle pile in leading row), and D (corner pile in leading row) of group of 3 x 3 piles with length L = 10T and spacing s = 2D subjected to lateral forces P_i (kN)

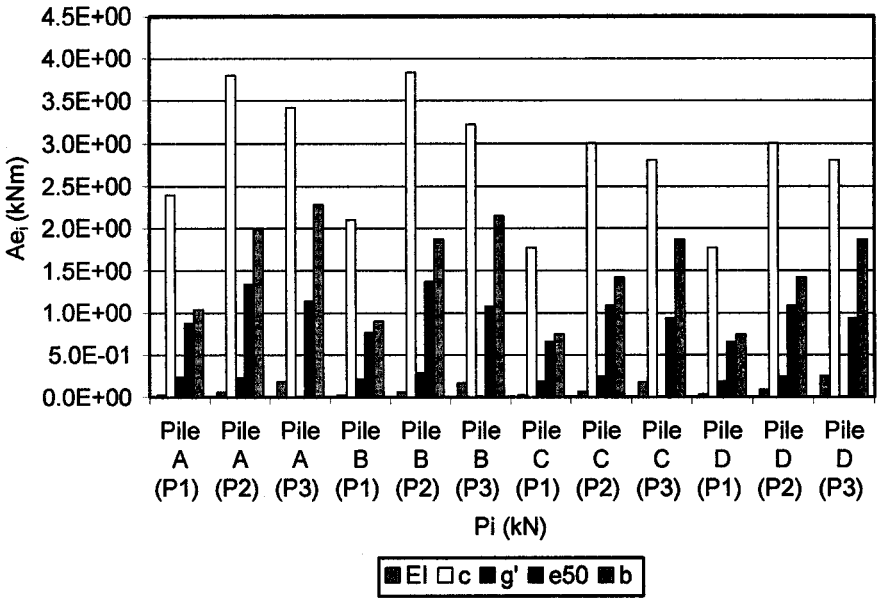

Fig. P.14f Quantitative assessment of sensitivities Ae_i that contains Ae_{EI}, Ae_c, $Ae_{\gamma'}$, $Ae_{\varepsilon 50}$, and Ae_b associated with the development of the nonlinear elastic stage in the soil along the pile axis that affect δy_t for pile members A (2nd trailing row), B (1st trailing row), C (middle pile in leading row), and D (corner pile in leading row) of group of 3 x 3 piles with length L = 10T and spacing s = 2D subjected to lateral forces P_i (kN)

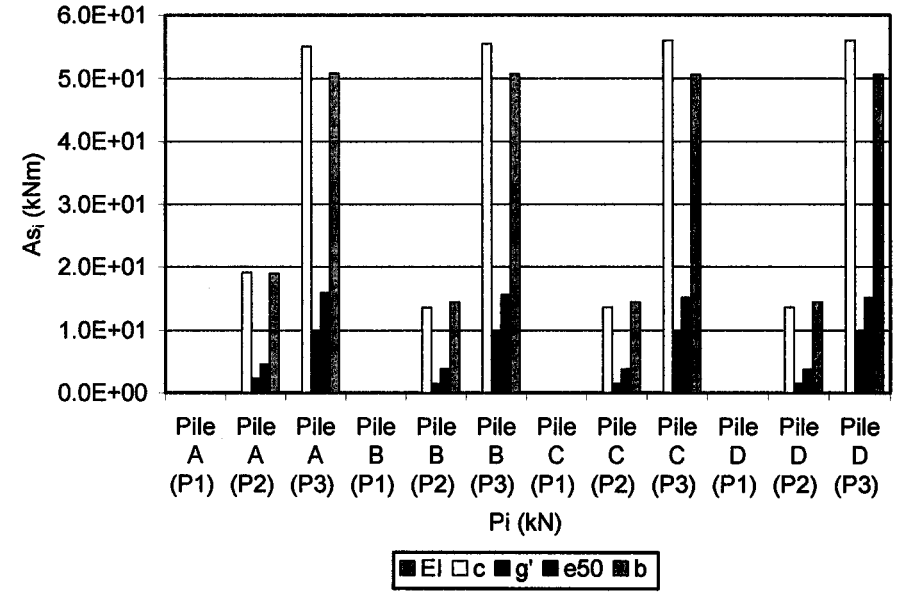

Fig. P.14g Quantitative assessment of As_i that contains As_{EI}, As_c, $As_{\gamma'}$, $As_{\varepsilon 50}$, and As_b associated with the development of the linear softening stage in the soil along the pile axis that affect δy_t for pile members A (2nd trailing row), B (1st trailing row), C (middle pile in leading row), and D (corner pile in leading row) of group of 3 x 3 piles with length L = 10T and spacing s = 2D subjected to lateral forces P_i (kN)

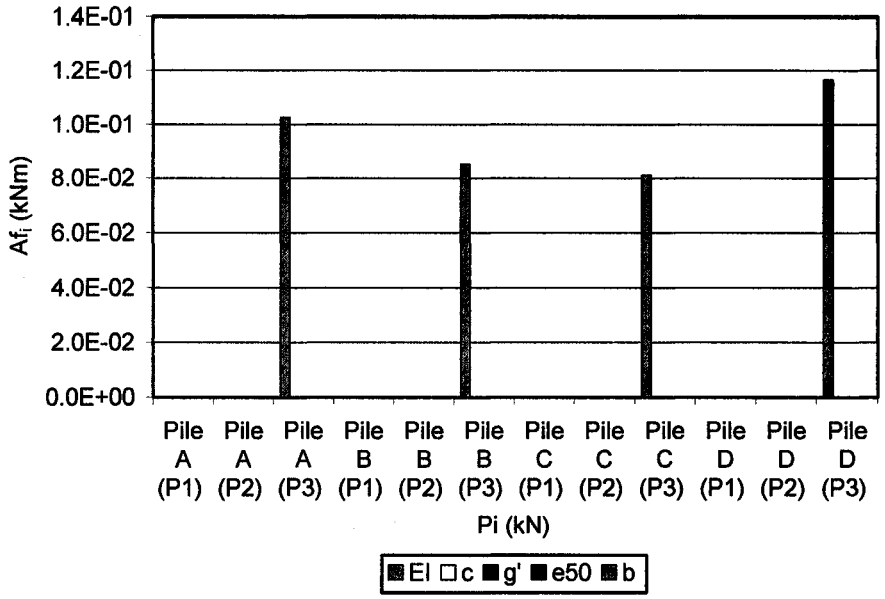

Fig. P.14h Quantitative assessment of sensitivities Af_i that contains Af_{EI}, Af_c, $Af_{\gamma'}$, $Af_{\varepsilon 50}$, and Af_b associated with the development of the plastic flow stage in the soil along the pile axis that affect δy_t for pile members A (2nd trailing row), B (1st trailing row), C (middle pile in leading row), and D (corner pile in leading row) of group of 3 x 3 piles with length L = 10T and spacing s = 2D subjected to lateral forces P_i (kN)

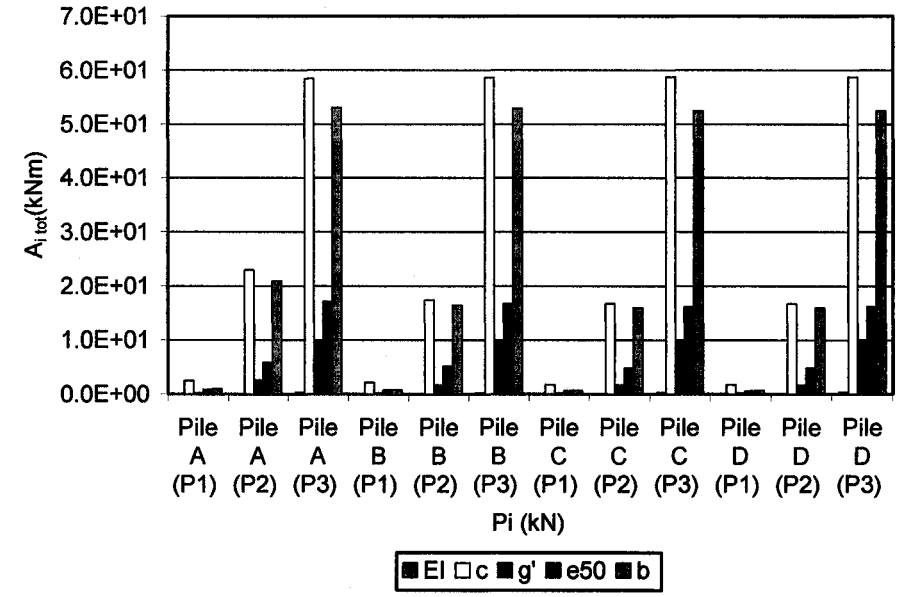

Fig. P.14i Quantitative assessment of sensitivities $A_{i\ tot}$ that contains $(A_{EI}, A_c, A_{\gamma'}, A_{\varepsilon 50}$, and $A_b)_{tot}$ associated with the development of three stages in the soil along the pile axis that affect δy_t for pile members A (2nd trailing row), B (1st trailing row), C (middle pile in leading row), and D (corner pile in leading row) of group of 3 x 3 piles with length L = 10T and spacing s = 2D subjected to lateral forces P_i (kN)

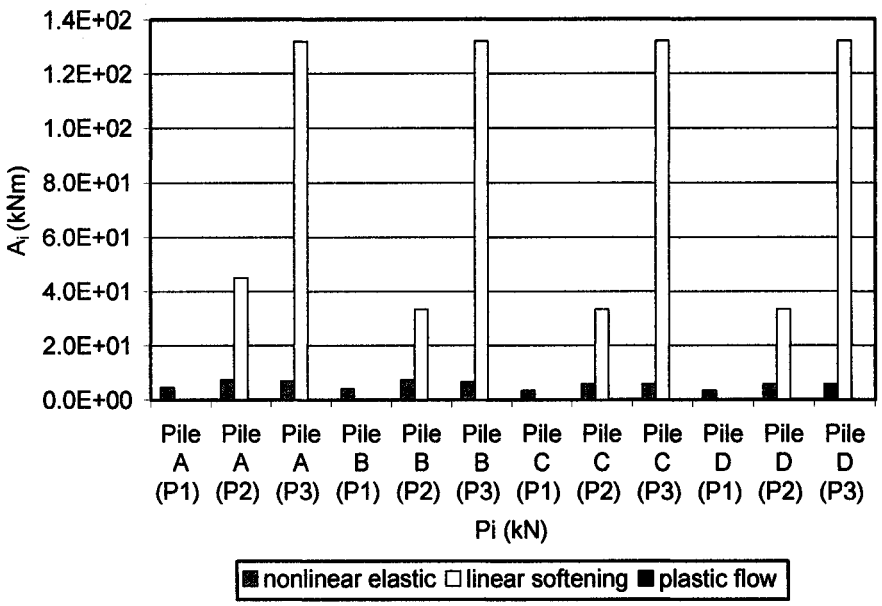

Fig. P.14j.1 Quantitative assessment of sensitivities A_{tot} that is summation of (A_{EI}, A_c, $A_{\gamma'}$, $A_{\varepsilon 50}$, and A_b)$_i$ of each soil stage that affect assessment of A_{tot} of the sensitivity analysis of δy_t for pile members A (2nd trailing row), B (1st trailing row), C (middle pile in leading row), and D (corner pile in leading row) of group of 3 x 3 piles with length L = 10T and spacing s = 2D subjected to lateral forces P_i (kN)

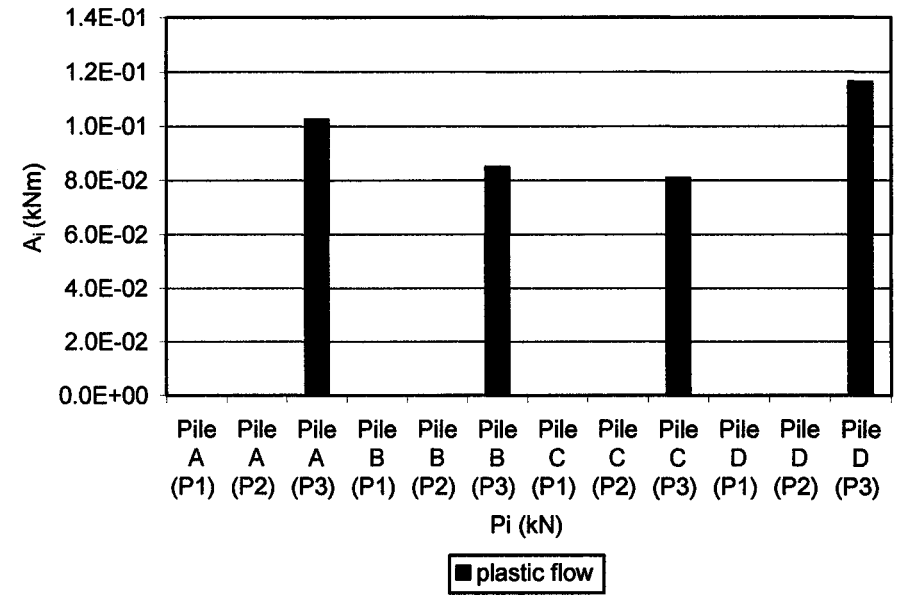

Fig. P.14j.2 Quantitative assessment of sensitivities A_{tot} that is summation of (A_{EI}, A_c, $A_{\gamma'}$, $A_{\varepsilon 50}$, and A_b)$_i$ of each soil stage that affect δy_t for pile members A (2nd trailing row), B (1st trailing row), C (middle pile in leading row), and D (corner pile in leading row) of group of 3 x 3 piles with length L = 10T and spacing s = 2D subjected to lateral forces P_i (kN)

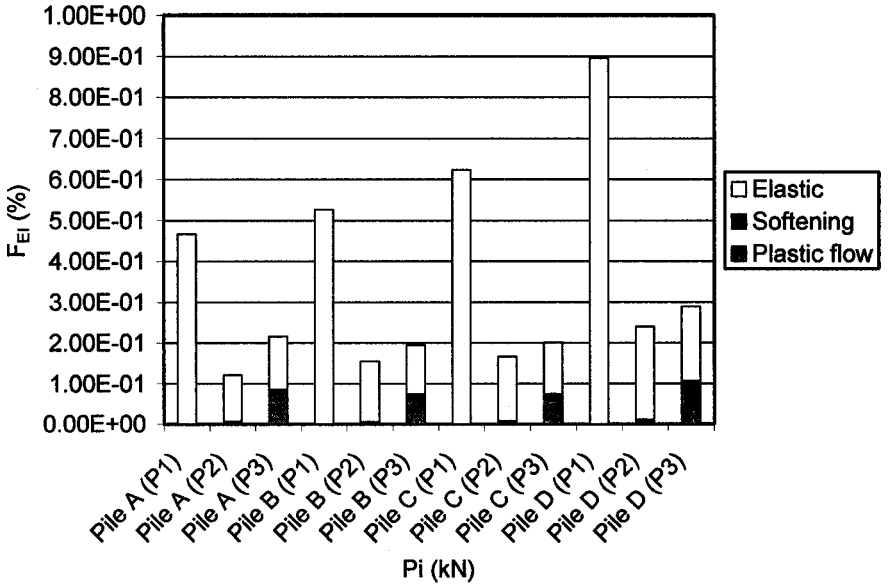

Fig. P.15a Quantitative assessment (in %) of relative sensitivity factors F_{EI} that affect δy_t for pile members A (2nd trailing row), B (1st trailing row), C (middle pile in leading row), and D (corner pile in leading row) of group of 3 x 3 piles with length L = 10T and spacing s = 2D subjected to lateral forces P_i (kN)

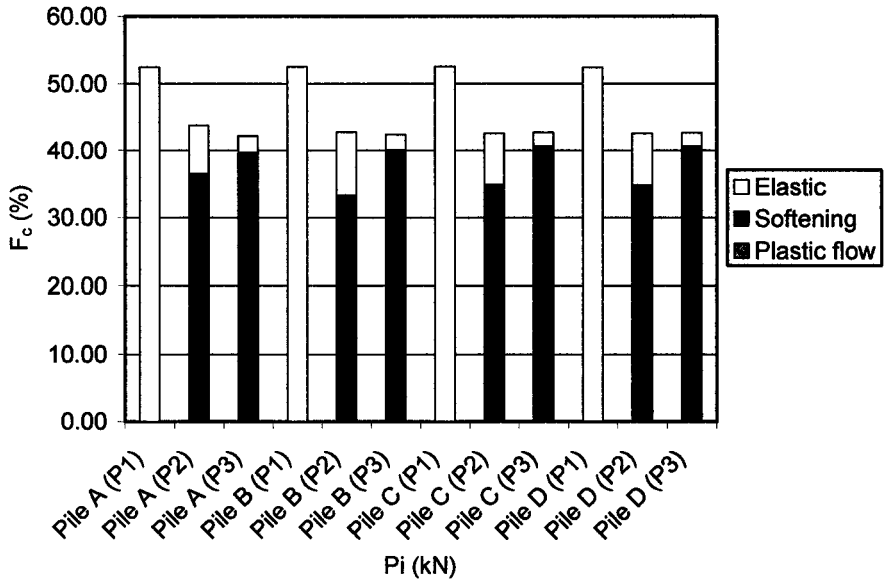

Fig. P.15b Quantitative assessment (in %) of relative sensitivity factors F_c that affect δy_t for pile members A (2nd trailing row), B (1st trailing row), C (middle pile in leading row), and D (corner pile in leading row) of group of 3 x 3 piles with length L = 10T and spacing s = 2D subjected to lateral forces P_i (kN)

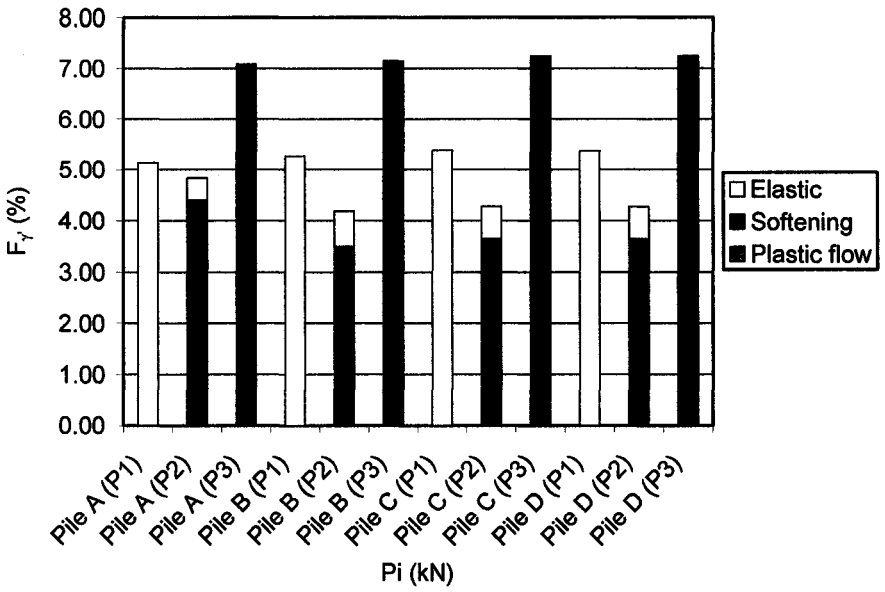

Fig. P.15c Quantitative assessment (in %) of relative sensitivity factors $F_{\varepsilon 50}$ that affect δy_t for pile members A (2nd trailing row), B (1st trailing row), C (middle pile in leading row), and D (corner pile in leading row) of group of 3 x 3 piles with length L = 10T and spacing s = 2D subjected to lateral forces P_i (kN)

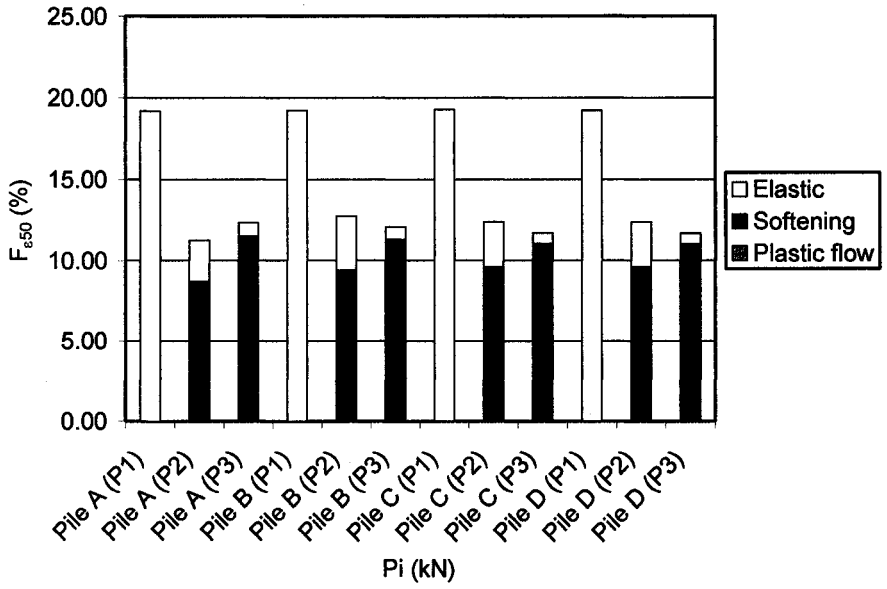

Fig. P.15d Quantitative assessment (in %) of relative sensitivity factors $F_{\varepsilon 50}$ that affect δy_t for pile members A (2nd trailing row), B (1st trailing row), C (middle pile in leading row), and D (corner pile in leading row) of group of 3 x 3 piles with length L = 10T and spacing s = 2D subjected to lateral forces P_i (kN)

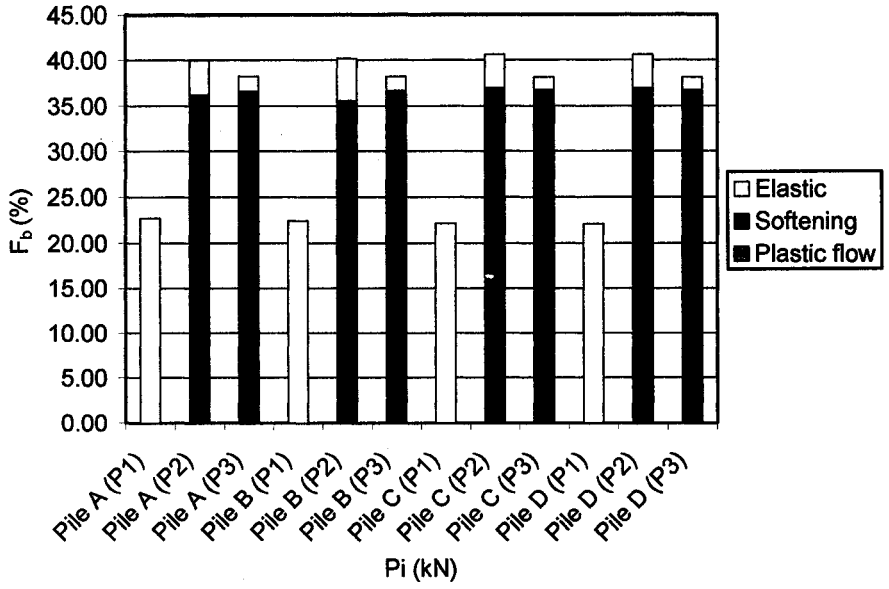

Fig. P.15e Quantitative assessment (in %) of relative sensitivity factors F_b that affect δy_t for pile members A (2nd trailing row), B (1st trailing row), C (middle pile in leading row), and D (corner pile in leading row) of group of 3 x 3 piles with length L = 10T and spacing s = 2D subjected to lateral forces P_i (kN)

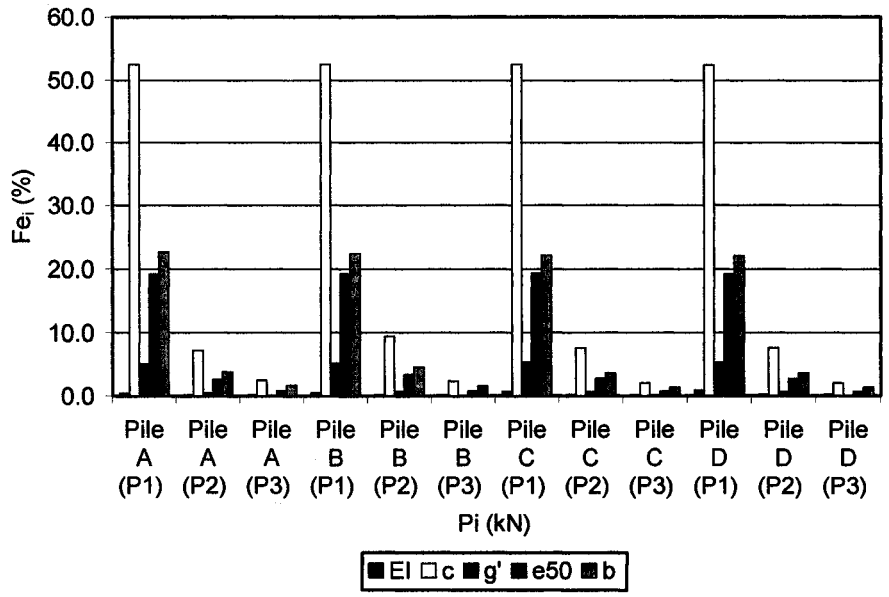

Fig. P.15f Quantitative assessment (in %) of relative sensitivity factors Fe_i that contains Fe_{EI}, Fe_c, $Fe_{\gamma'}$, $Fe_{\varepsilon 50}$, and Fe_b associated with the nonlinear elastic soil stage developed along the pile axis that affect δy_t for pile members A (2nd trailing row), B (1st trailing row), C (middle pile in leading row), and D (corner pile in leading row) of group of 3 x 3 piles with length L = 10T and spacing s = 2D subjected to lateral forces P_i (kN)

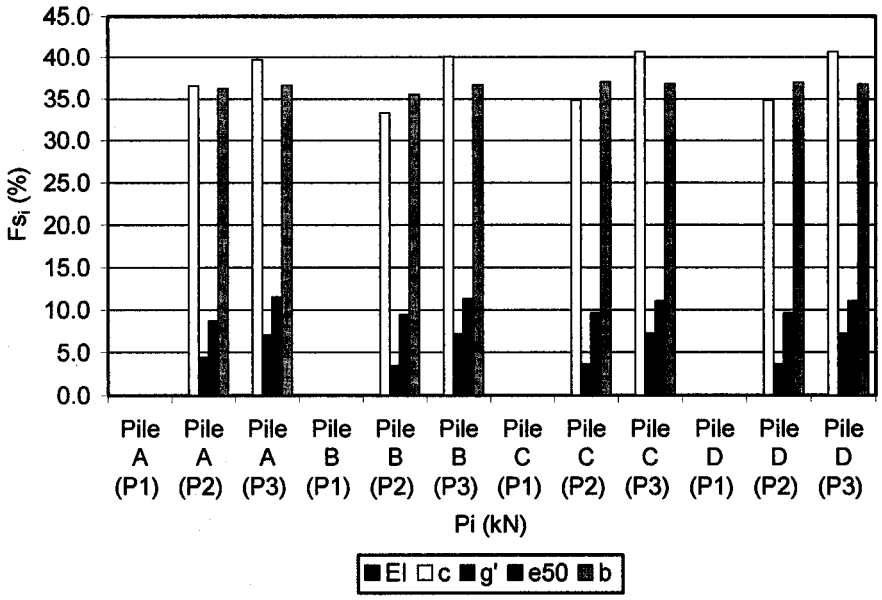

Fig. P.15g Quantitative assessment (in %) of relative sensitivity factors Fs_i that contains Fs_{EI}, Fs_c, $Fs_{\gamma'}$, $Fs_{\varepsilon 50}$, and Fs_b associated with the linear softening stage developed along the pile axis that affect δy_t for pile members A (2nd trailing row), B (1st trailing row), C (middle pile in leading row), and D (corner pile in leading row) of group of 3 x 3 piles with length L = 10T and spacing s = 2D subjected to lateral forces P_i (kN)

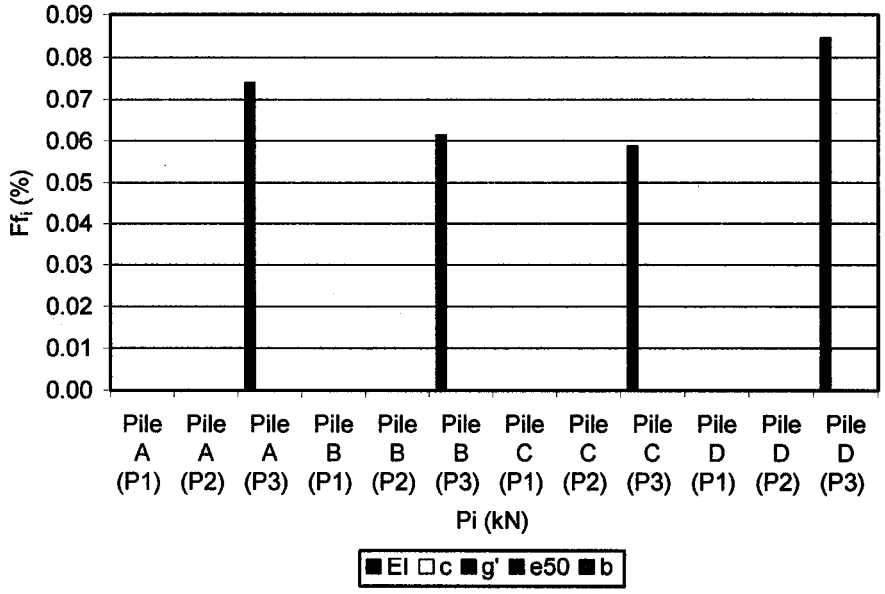

Fig. P.15h Quantitative assessment (in %) of relative sensitivity factors Ff_i that contains Ff_{EI}, Ff_c, $Ff_{\gamma'}$, $Ff_{\varepsilon 50}$, and Ff_b associated with the nonlinear elastic soil stage developed along the pile axis that affect δy_t for pile members A (2nd trailing row), B (1st trailing row), C (middle pile in leading row), and D (corner pile in leading row) of group of 3x3 piles with length L=10T and spacing s = 2D subjected to lateral forces P_i (kN)

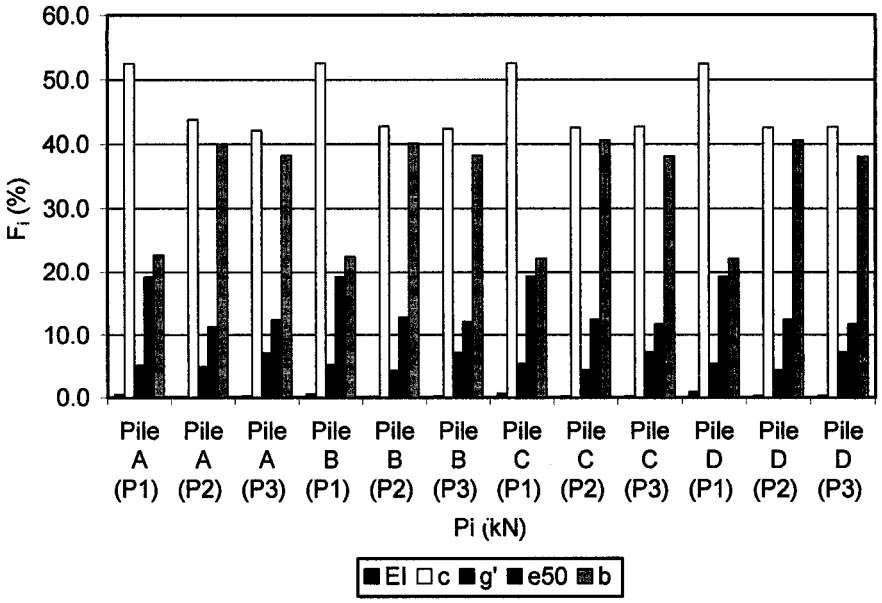

Fig. P.15i Quantitative assessment (in %) of relative sensitivity factors F_i that contains F_{EI}, F_c, $F_{\gamma'}$, $F_{\varepsilon 50}$, and F_b associated with all soil stages developed along the pile axis that affect δy_t for pile members A (2nd trailing row), B (1st trailing row), C (middle pile in leading row), and D (corner pile in leading row) of group of 3 x 3 piles with length L = 10T and spacing s = 2D subjected to lateral forces P_i (kN)

APPENDIX Q:

Comparison of the sensitivity analysis of top lateral displacement δy_t for pile member A (2^{nd} trailing row) of groups of 3×3 piles with various spacing (s = 2D, 3D, 4D, 5D) & single pile with length L = 10T subjected to lateral forces P1, P2, P3

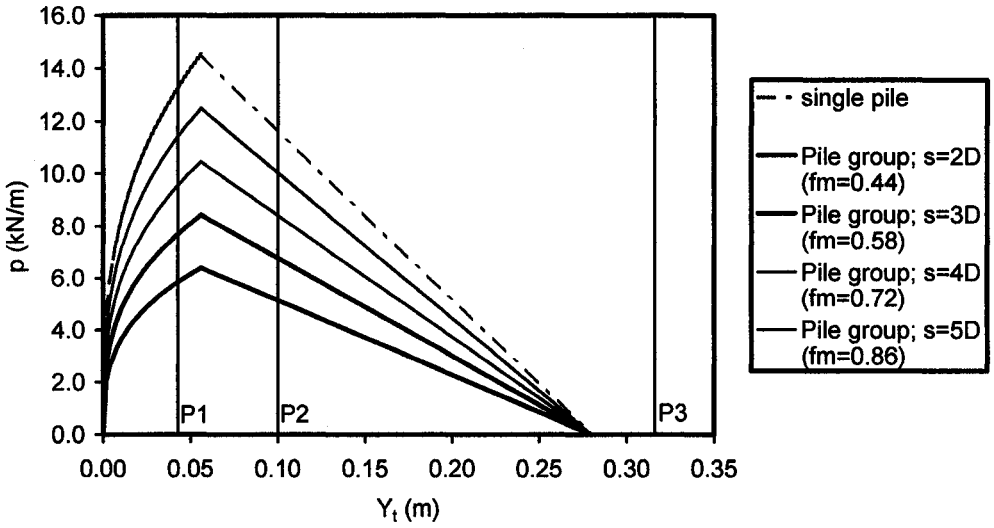

Fig. Q.1 Soil reaction p at the top surface (expressed in terms of lateral loading) vs. lateral displacement generated by lateral loading applied to the pile for sensitivity analysis of top lateral displacement δy_t for pile member A (2nd trailing row) of group of 3 x 3 piles with various spacing and single pile with length L = 10T subjected to lateral forces P_i (kN)

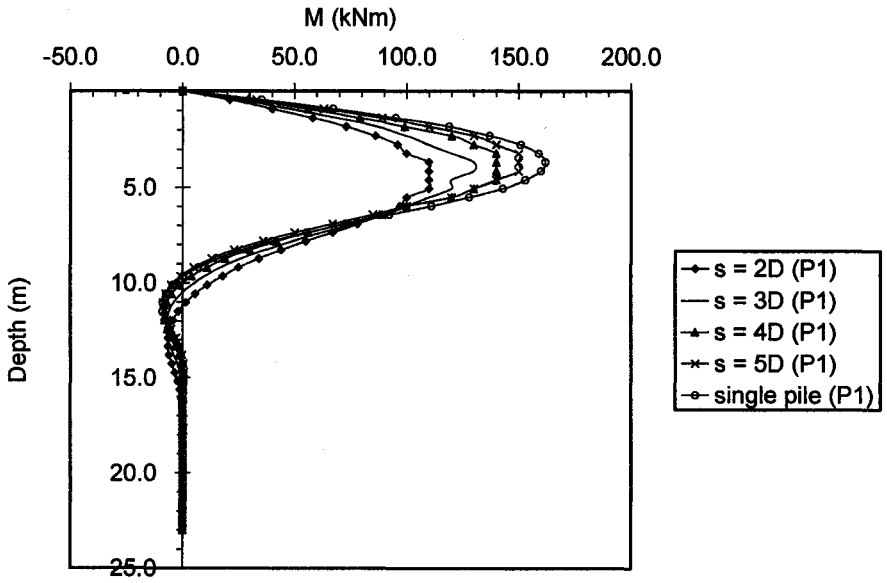

Fig. Q.2a Distributions of bending moments at the primary structure M along the depth of the pile for sensitivity analysis of top lateral displacement δy_t for pile member A (2nd trailing row) of group of 3 x 3 piles with various spacing and single pile with length L = 10T subjected to lateral forces P1

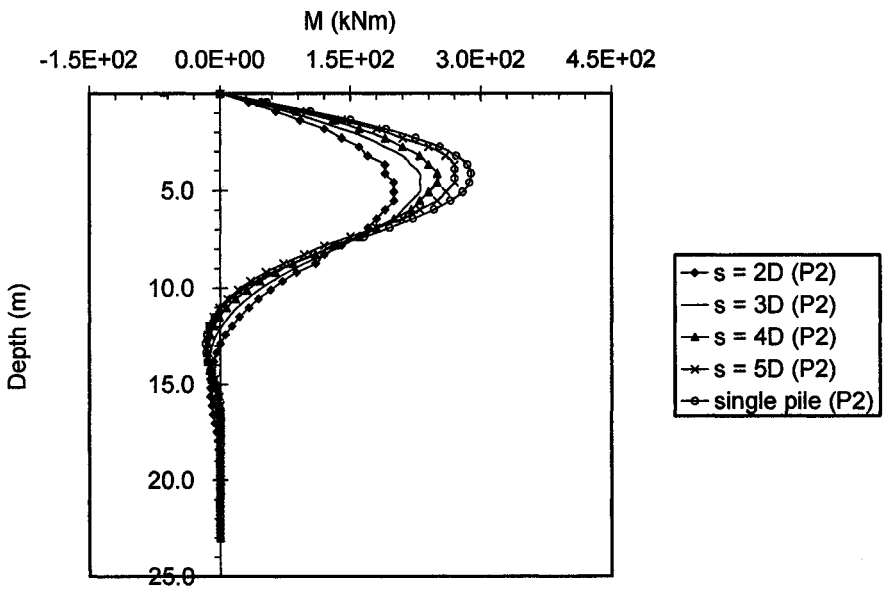

Fig. Q.2b Distributions of bending moments at the primary structure M along the depth of the pile for sensitivity analysis of top lateral displacement δy_t for pile member A (2nd trailing row) of group of 3 x 3 piles with various spacing and single pile with length L = 10T subjected to lateral forces P2

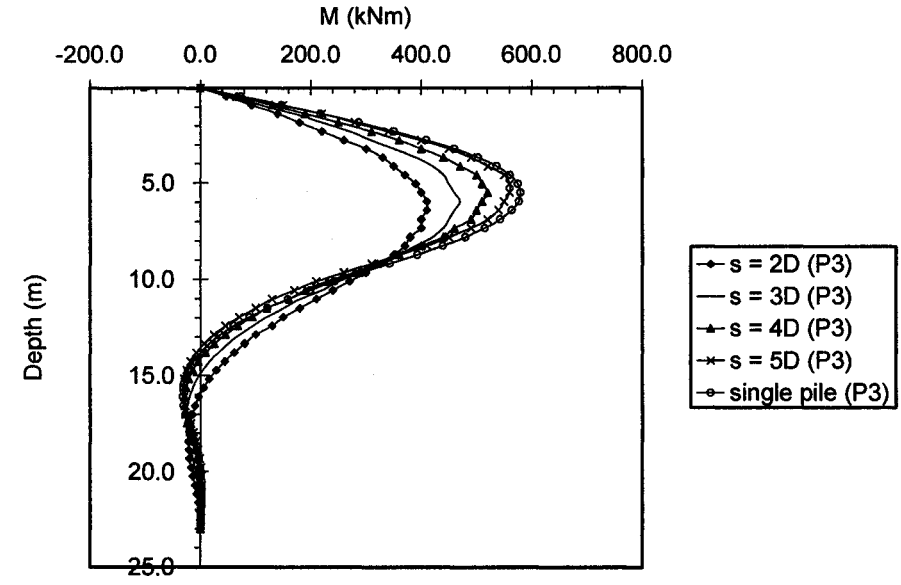

Fig. Q.2c Distributions of bending moments at the primary structure M along the depth of the pile for sensitivity analysis of top lateral displacement δy_t for pile member A (2nd trailing row) of group of 3 x 3 piles with various spacing and single pile with length L = 10T subjected to lateral forces P3

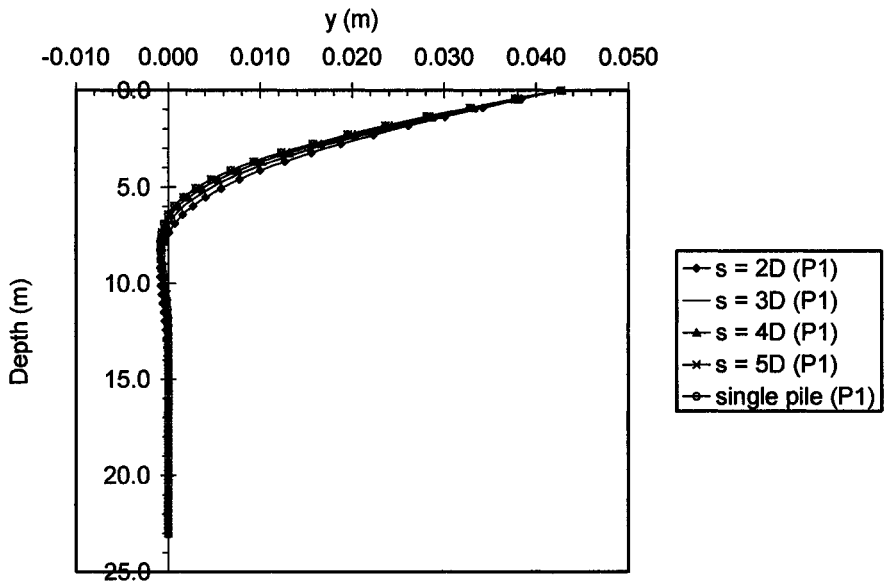

Fig. Q.3a Distributions of lateral deflections at the primary structure y along the depth of the pile for sensitivity analysis of top lateral displacement δy_t for pile member A (2nd trailing row) of group of 3 x 3 piles with various spacing and single pile with length L = 10T subjected to lateral forces P1

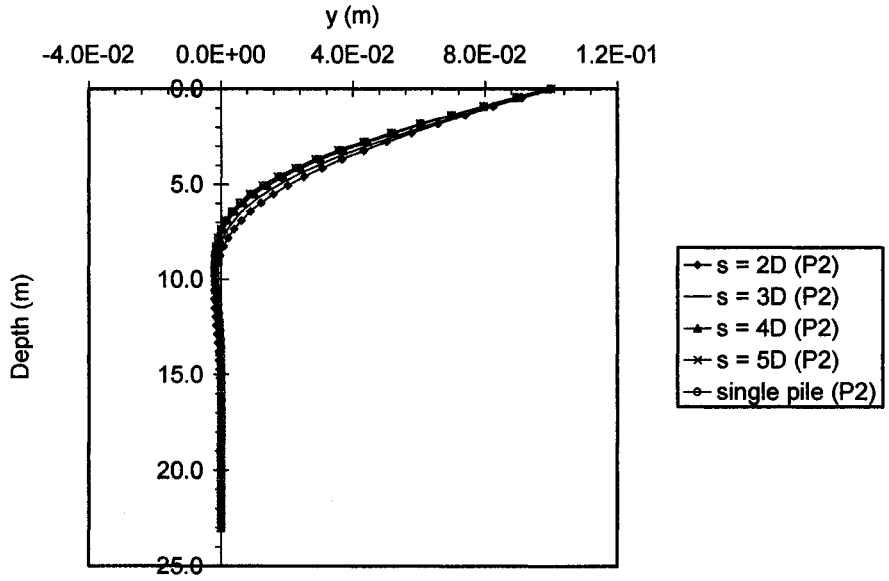

Fig. Q.3b Distributions of lateral deflections at the primary structure y along the depth of the pile for sensitivity analysis of top lateral displacement δy_t for pile member A (2nd trailing row) of group of 3 x 3 piles with various spacing and single pile with length L = 10T subjected to lateral forces P2

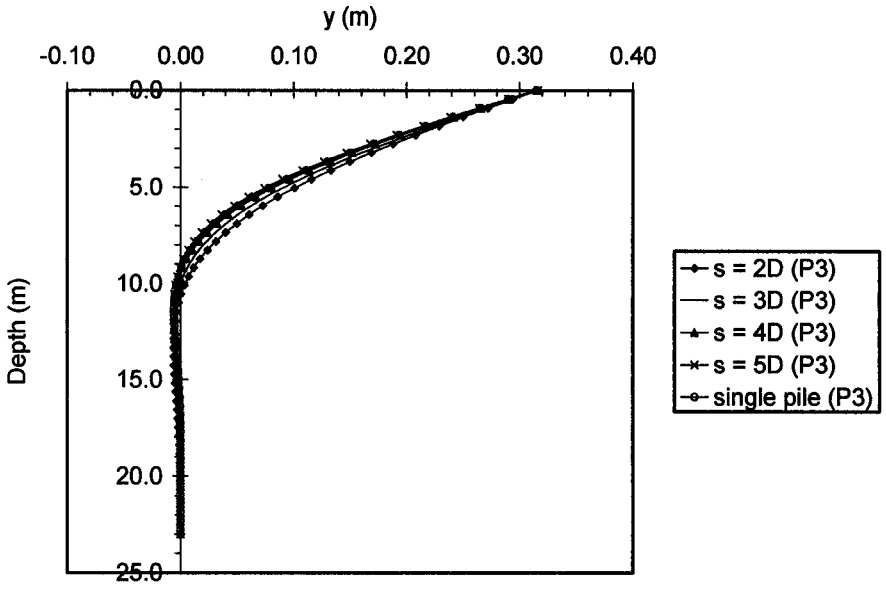

Fig. Q.3c Distributions of lateral deflections at the primary structure y along the depth of the pile for sensitivity analysis of top lateral displacement δy_t for pile member A (2nd trailing row) of group of 3 x 3 piles with various spacing and single pile with length L = 10T subjected to lateral forces P3

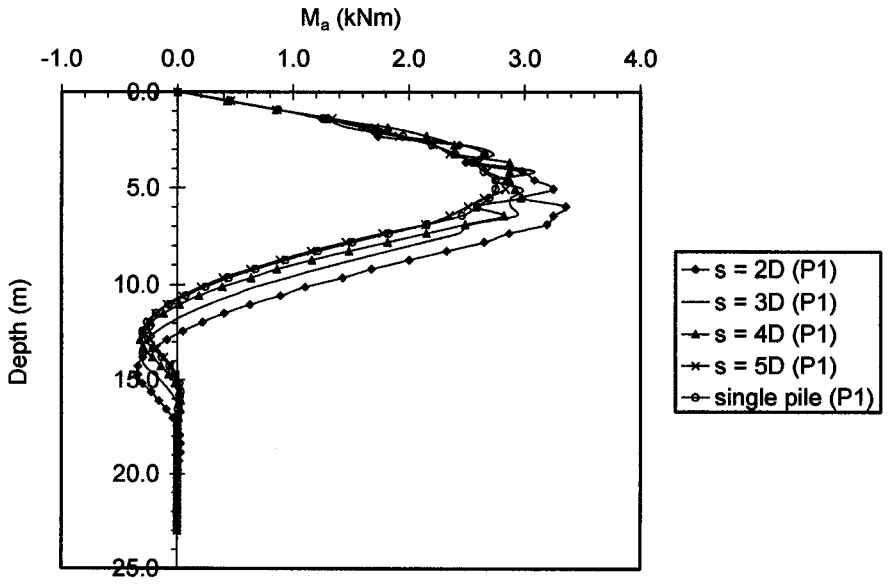

Fig. Q.4a Distributions of bending moments M_a along the depth of the pile at the adjoint structure for sensitivity analysis of top lateral displacement δy_t for pile member A (2nd trailing row) of group of 3 x 3 piles with various spacing and single pile with length L = 10T subjected to lateral forces P1

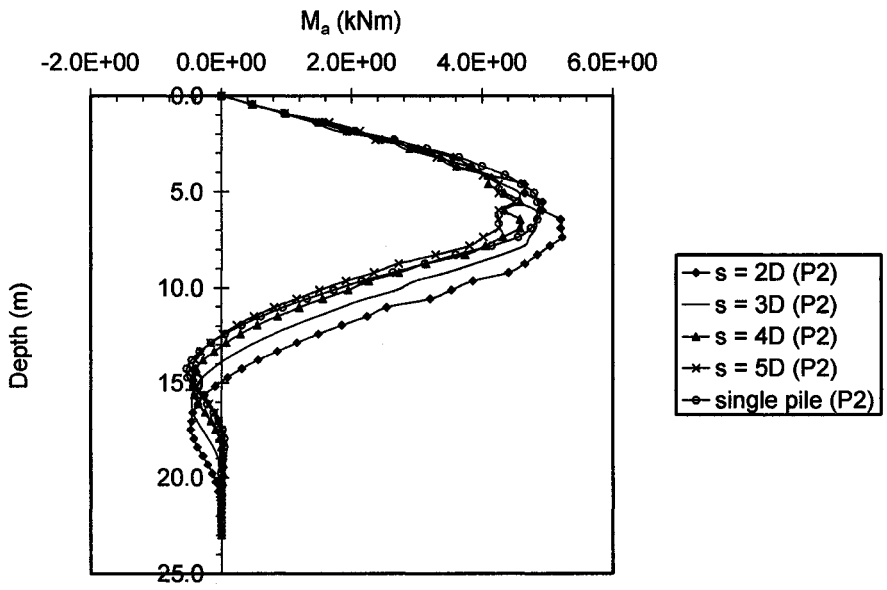

Fig. Q.4b Distributions of bending moments M_a along the depth of the pile at the adjoint structure for sensitivity analysis of top lateral displacement δy_t for pile member A (2nd trailing row) of group of 3 x 3 piles with various spacing and single pile with length L = 10T subjected to lateral forces P2

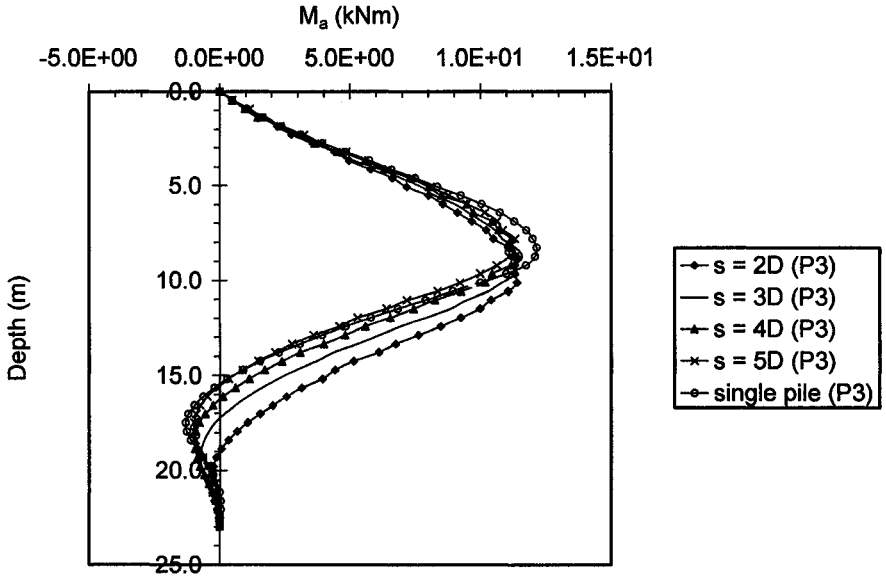

Fig. Q.4c Distributions of bending moments M_a along the depth of the pile at the adjoint structure for sensitivity analysis of top lateral displacement δy_t for pile member A (2nd trailing row) of group of 3 x 3 piles with various spacing and single pile with length L = 10T subjected to lateral forces P3

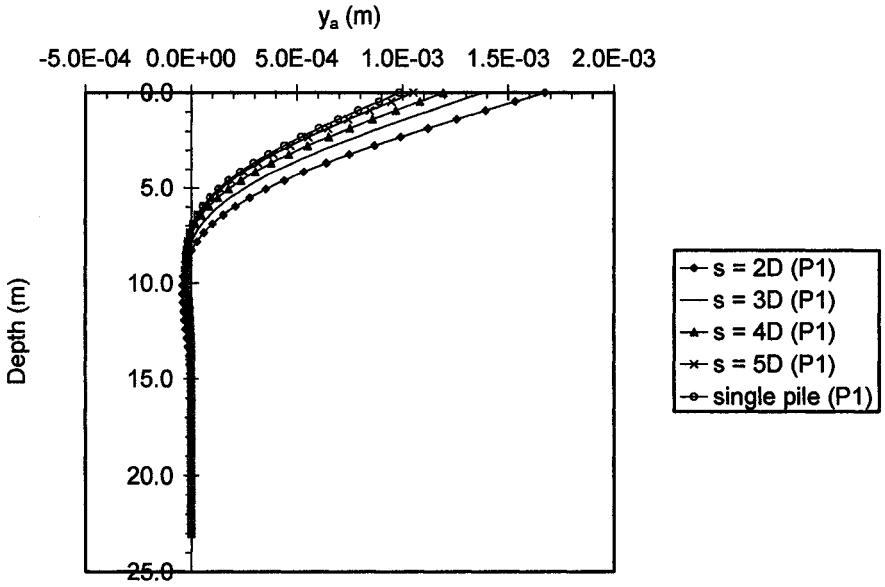

Fig. Q.5a Distributions of lateral deflections at the adjoint structure y_a along the depth of the pile for sensitivity analysis of top lateral displacement δy_t for pile member A (2nd trailing row) of group of 3 x 3 piles with various spacing and single pile with length L = 10T subjected to lateral forces P1

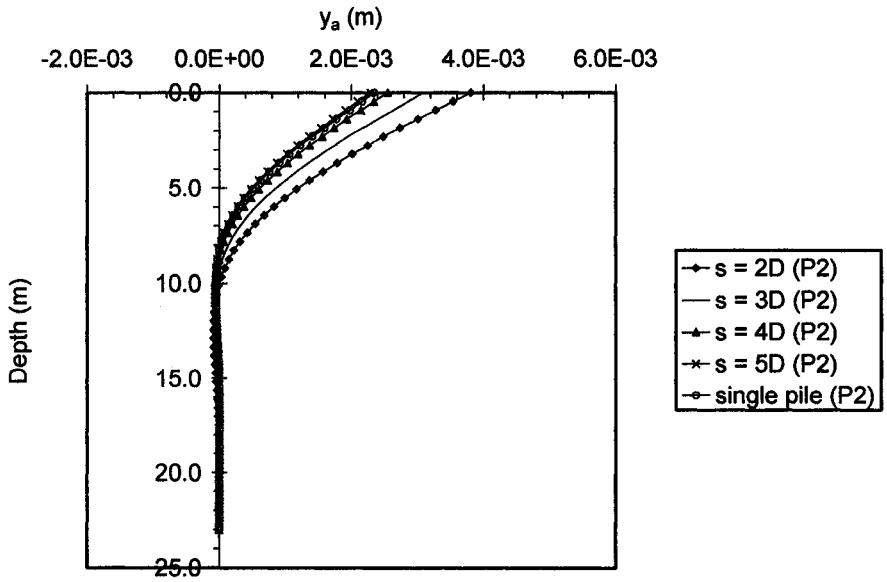

Fig. Q.5b Distributions of lateral deflections at the adjoint structure y_a along the depth of the pile for sensitivity analysis of top lateral displacement δy_t for pile member A (2nd trailing row) of group of 3 x 3 piles with various spacing and single pile with length L = 10T subjected to lateral forces P2

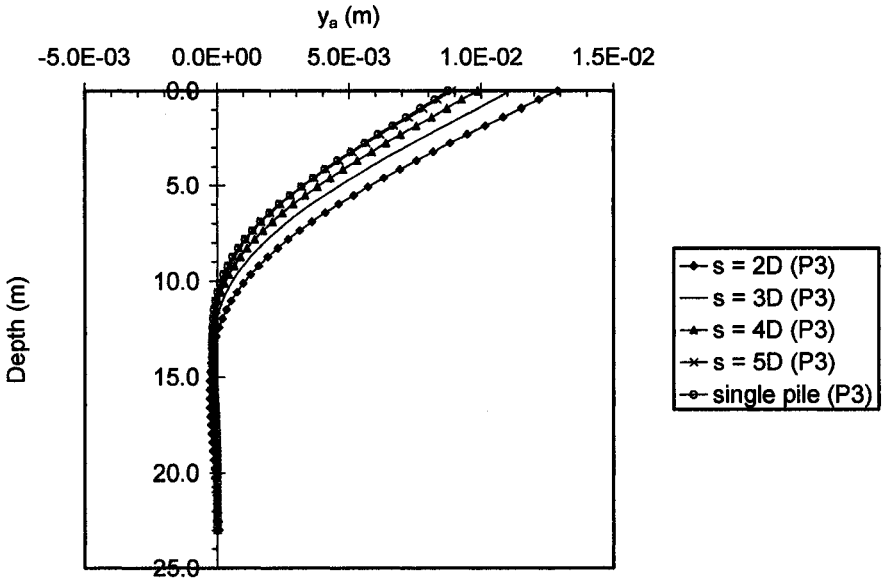

Fig. Q.5c Distributions of lateral deflections at the adjoint structure y_a along the depth of the pile for sensitivity analysis of top lateral displacement δy_t for pile member A (2nd trailing row) of group of 3 x 3 piles with various spacing and single pile with length L = 10T subjected to lateral forces P3

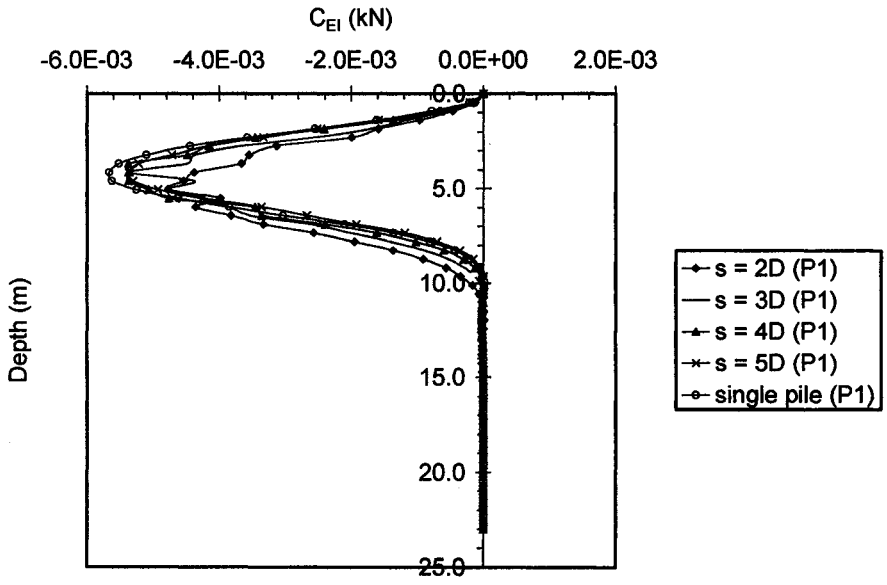

Fig. Q.6a Distributions of sensitivity operators C_{EI} affecting the changes of δy_t due to variations of the design variable δEI for pile member A (2nd trailing row) of group of 3 x 3 piles with various spacing and single pile with length L = 10T subjected to lateral forces P1

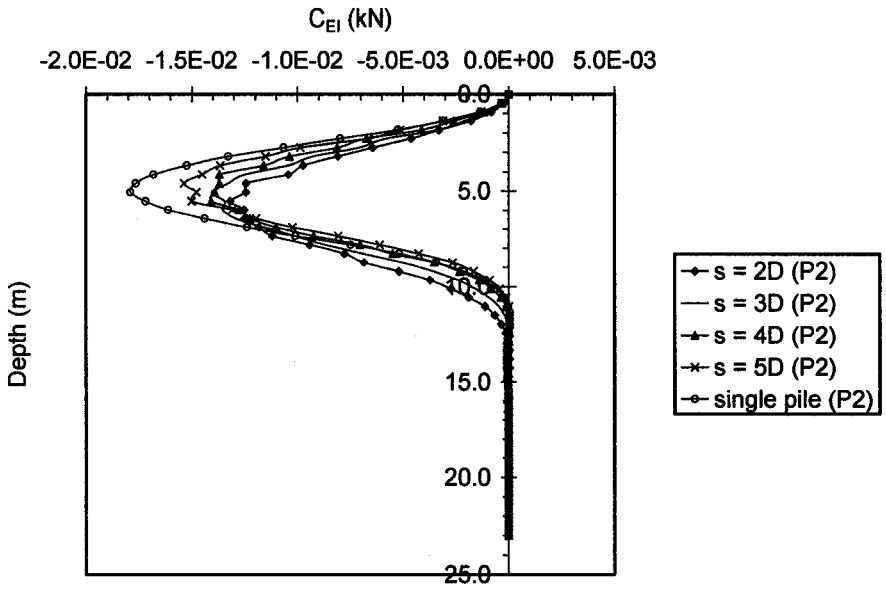

Fig. Q.6b Distributions of sensitivity operators C_{EI} affecting the changes of δy_t due to variations of the design variable δEI for pile member A (2nd trailing row) of group of 3 x 3 piles with various spacing and single pile with length L = 10T subjected to lateral forces P2

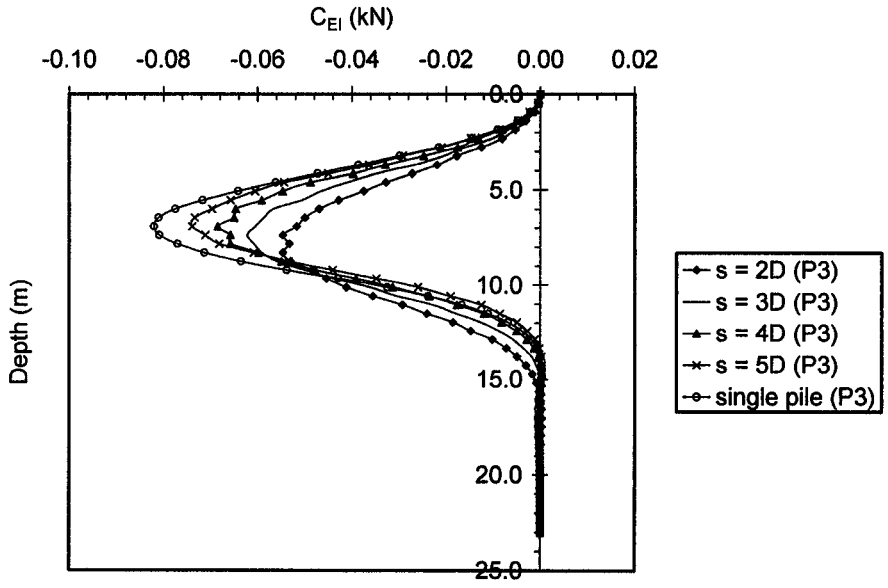

Fig. Q.6c Distributions of sensitivity operators C_{EI} affecting the changes of δy_t due to variations of the design variable δEI for pile member A (2nd trailing row) of group of 3 x 3 piles with various spacing and single pile with length L = 10T subjected to lateral forces P3

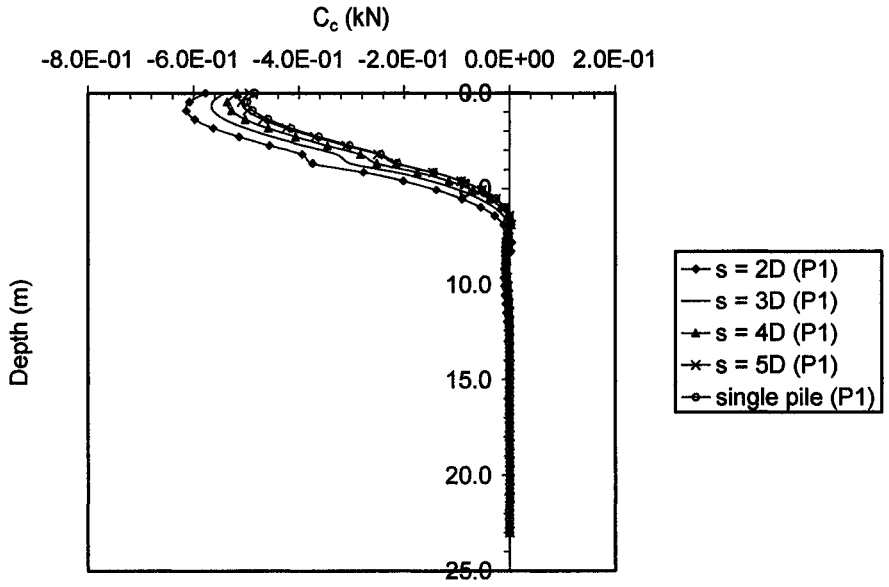

Fig. Q.7a Distributions of sensitivity operators C_c affecting the changes of δy_t due to variations of the design variable δc for pile member A (2nd trailing row) of group of 3 x 3 piles with various spacing and single pile with length L = 10T subjected to lateral forces P1

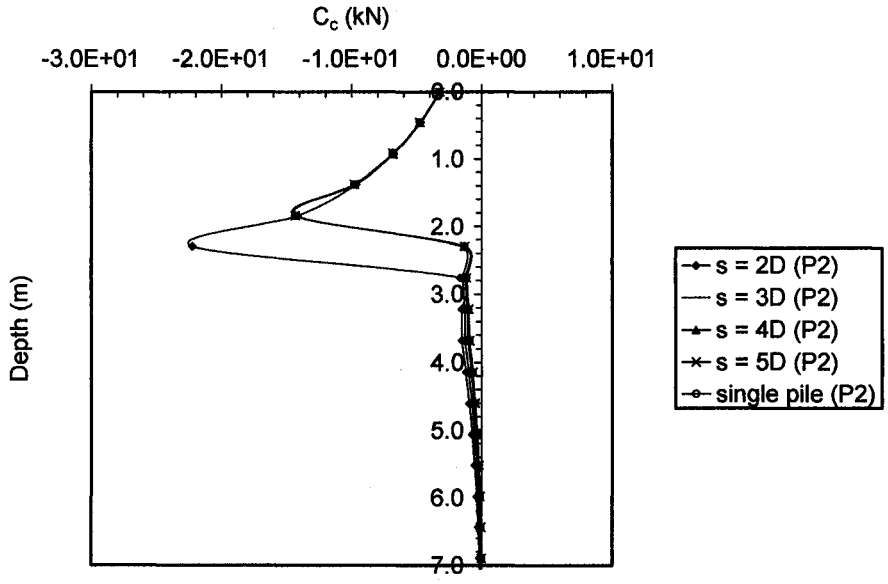

Fig. Q.7b Distributions of sensitivity operators C_c affecting the changes of δy_t due to variations of the design variable δc for pile member A (2nd trailing row) of group of 3 x 3 piles with various spacing and single pile with length L = 10T subjected to lateral forces P2

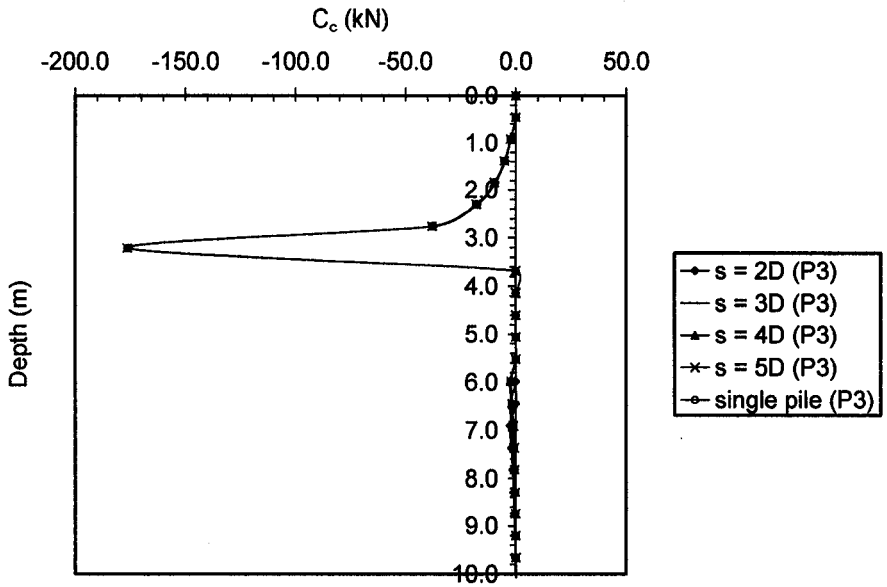

Fig. Q.7c Distributions of sensitivity operators C_c affecting the changes of δy_t due to variations of the design variable δc for pile member A (2nd trailing row) of group of 3 x 3 piles with various spacing and single pile with length L = 10T subjected to lateral forces P3

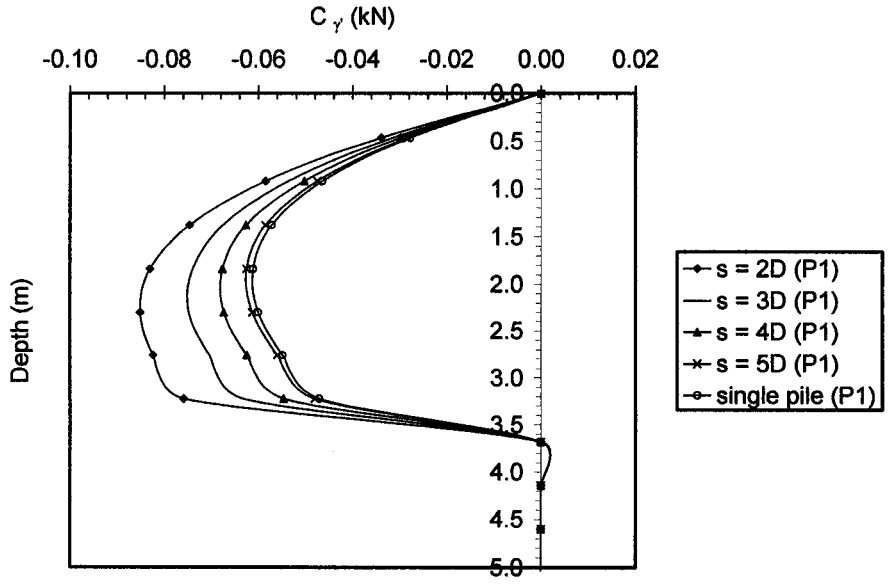

Fig. Q.8a Distributions of sensitivity operators $C_{\gamma'}$ affecting the changes of δy_t due to variations of the design variable $\delta\gamma'$ for pile member A (2nd trailing row) of group of 3 x 3 piles with various spacing and single pile with length L = 10T subjected to lateral forces P1

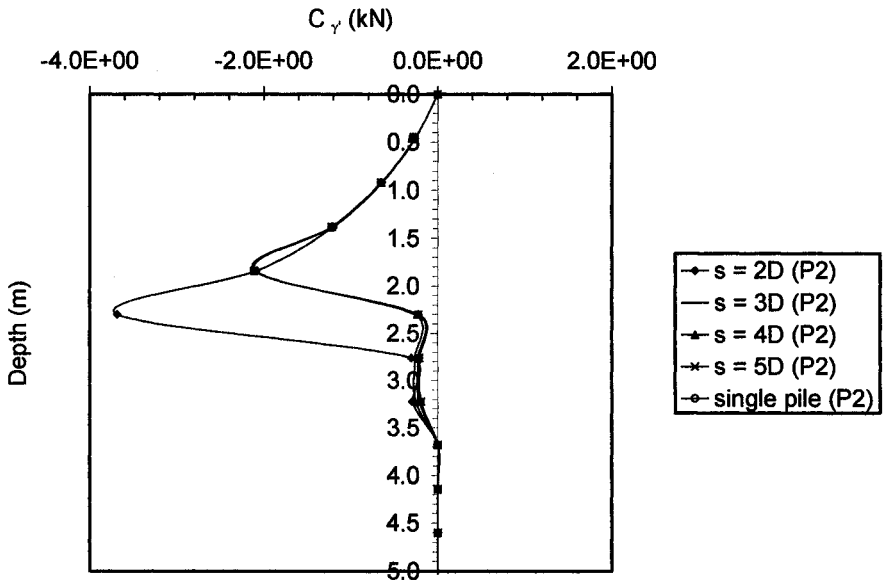

Fig. Q.8b Distributions of sensitivity operators $C_{\gamma'}$ affecting the changes of δy_t due to variations of the design variable $\delta\gamma'$ for pile member A (2nd trailing row) of group of 3 x 3 piles with various spacing and single pile with length L = 10T subjected to lateral forces P2

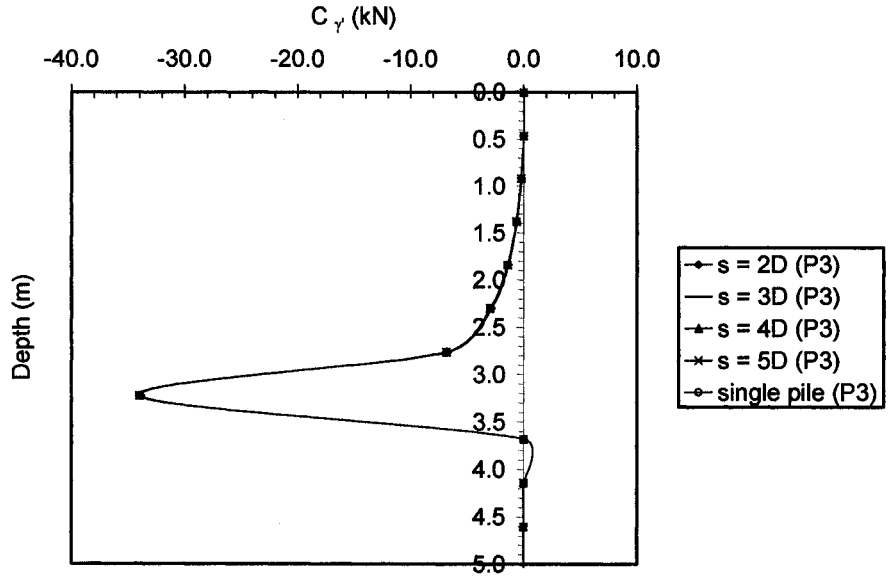

Fig. Q.8c Distributions of sensitivity operators $C_{\gamma'}$ affecting the changes of δy_t due to variations of the design variable $\delta\gamma'$ for pile member A (2nd trailing row) of group of 3 x 3 piles with various spacing and single pile with length L = 10T subjected to lateral forces P3

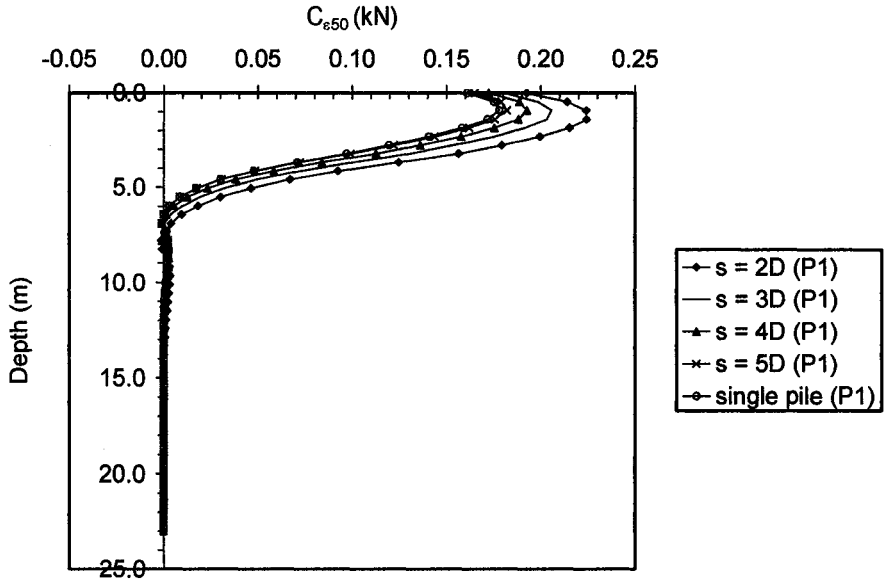

Fig. Q.9a Distributions of sensitivity operators $C_{\varepsilon 50}$ affecting the changes of δy_t due to variations of the design variable $\delta\varepsilon_{50}$ for pile member A (2nd trailing row) of groups of 3 x 3 piles with various spacing and single pile with length L = 10T subjected to lateral forces P1

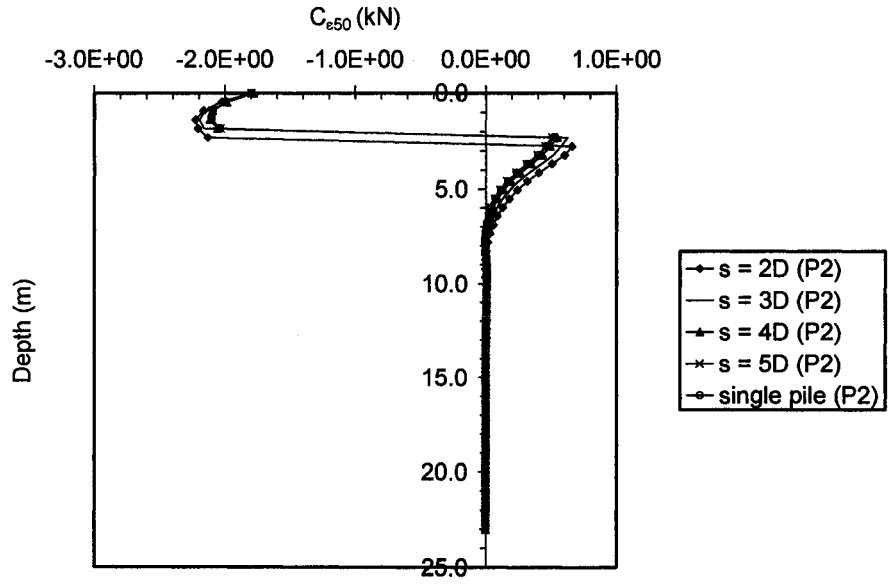

Fig. Q.9b Distributions of sensitivity operators $C_{\varepsilon 50}$ affecting the changes of δy_t due to variations of the design variable $\delta\varepsilon_{50}$ for pile member A (2nd trailing row) of groups of 3 x 3 piles with various spacing and single pile with length L = 10T subjected to lateral forces P2

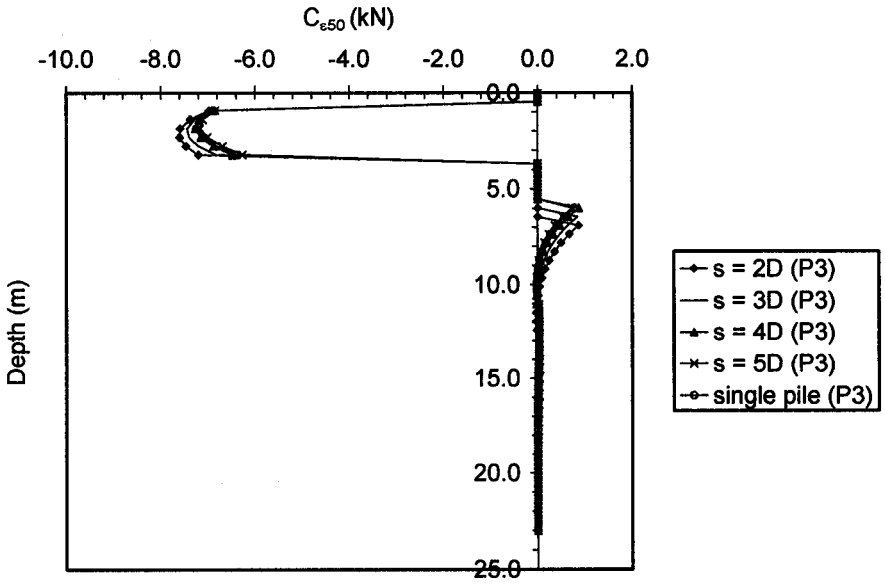

Fig. Q.9c Distributions of sensitivity operators $C_{\varepsilon 50}$ affecting the changes of δy_t due to the variations of the design variable $\delta\varepsilon_{50}$ for pile member A (2nd trailing row) of groups of 3 x 3 piles with various spacing and single pile with length L = 10T subjected to lateral forces P3

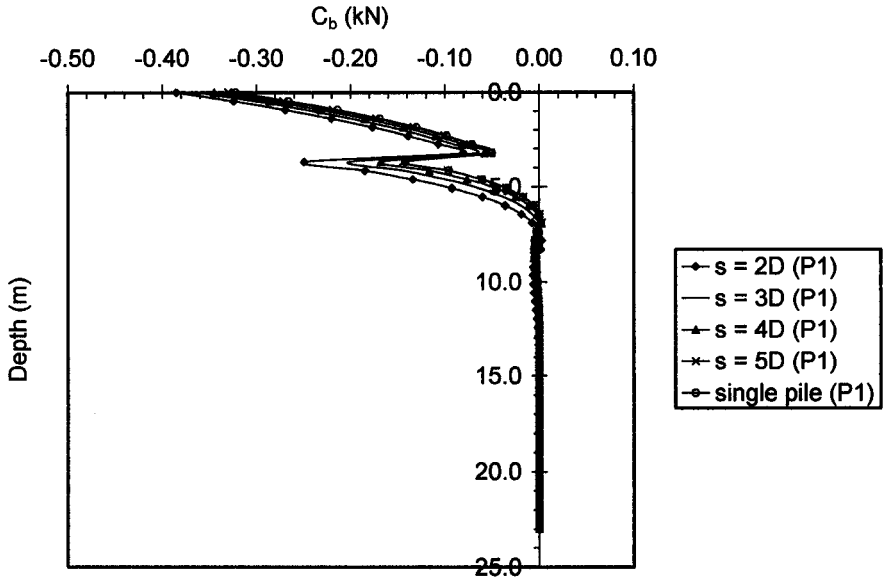

Fig. Q.10a Distributions of sensitivity operators C_b affecting the changes of δy_t due to the variations of the design variable δb for pile member A (2nd trailing row) of groups of 3 x 3 piles with various spacing and single pile with length L = 10T subjected to lateral forces P1

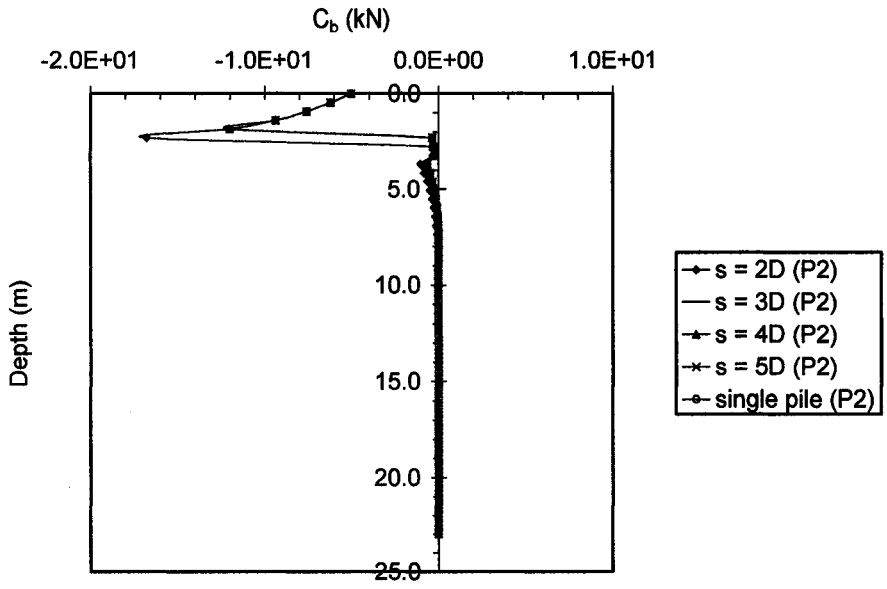

Fig. Q.10b Distributions of sensitivity operators C_b affecting the changes of δy_t due to the variations of the design variable δb for pile member A (2nd trailing row) of groups of 3 x 3 piles with various spacing and single pile with length L = 10T subjected to lateral forces P2

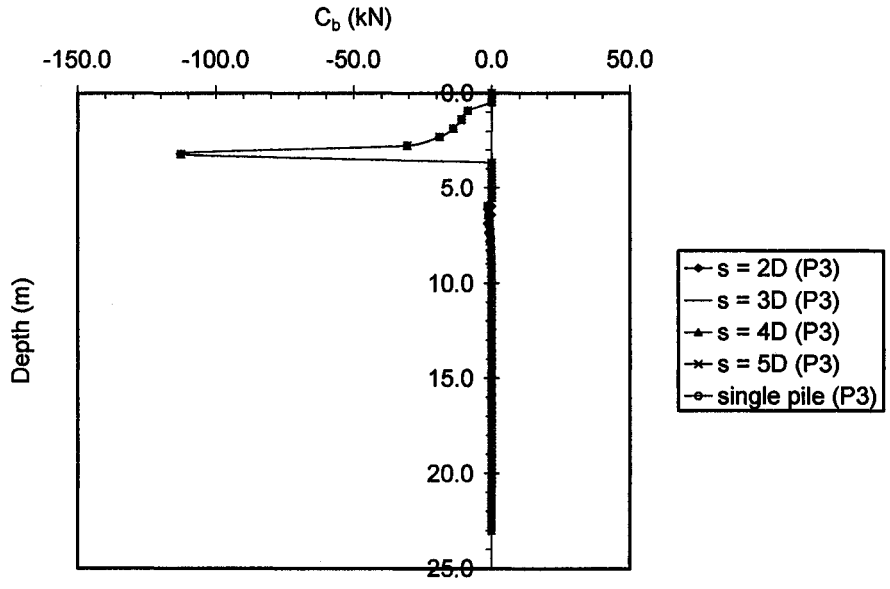

Fig. Q.10c Distributions of sensitivity operators C_b affecting the changes of δy_t due to the variations of the design variable δb for pile member A (2nd trailing row) of groups of 3 x 3 piles with various spacing and single pile with length L = 10T subjected to lateral forces P3

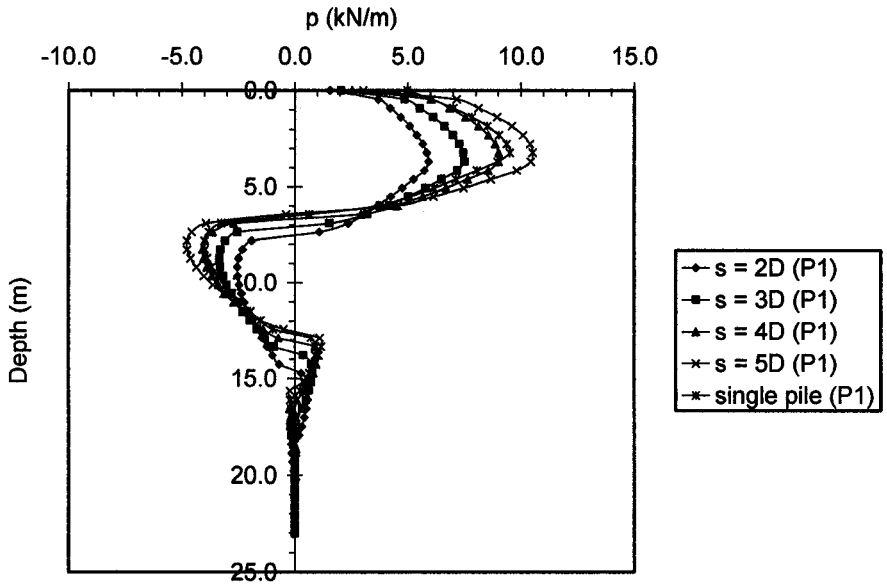

Fig. Q.11a Distributions of soil reaction p at the primary structure along the depth of the pile for sensitivity analysis of top lateral displacement δy_t for pile member A (2nd trailing row) of group of 3 x 3 piles with various spacing and single pile with length L = 10T subjected to lateral forces P1

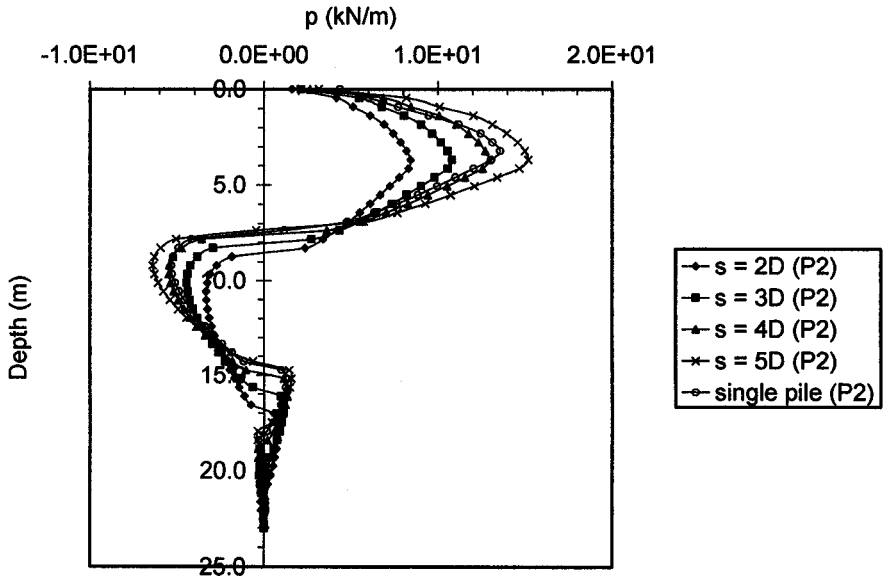

Fig. Q.11b Distributions of soil reaction p at the primary structure p along the depth of the pile for sensitivity analysis of top lateral displacement δy_t for pile member A (2nd trailing row) of group of 3 x 3 piles with various spacing and single pile with length L = 10T subjected to lateral forces P2

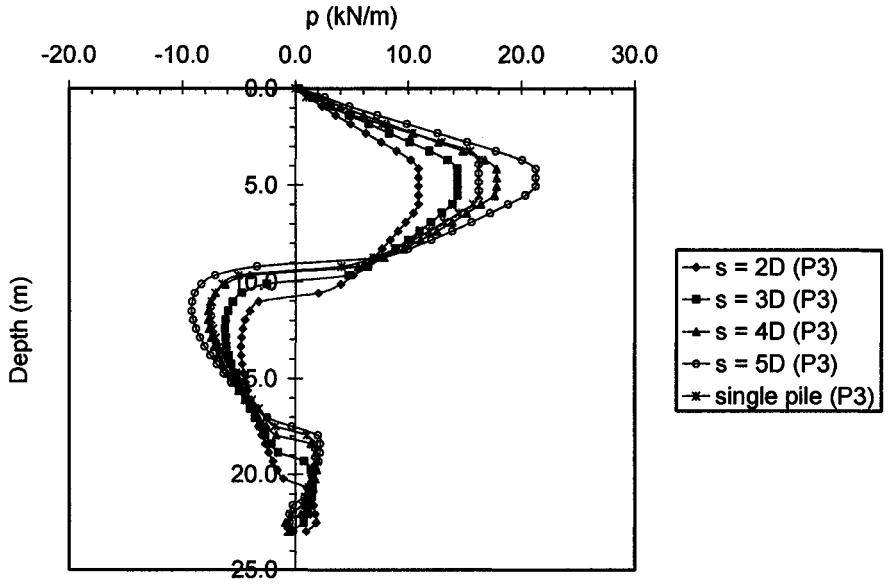

Fig. Q.11c Distributions of soil reaction p at the primary structure p along the depth of the pile for sensitivity analysis of top lateral displacement δy_t for pile member A (2nd trailing row) of group of 3 x 3 piles with various spacing and single pile with length L = 10T subjected to lateral forces P3

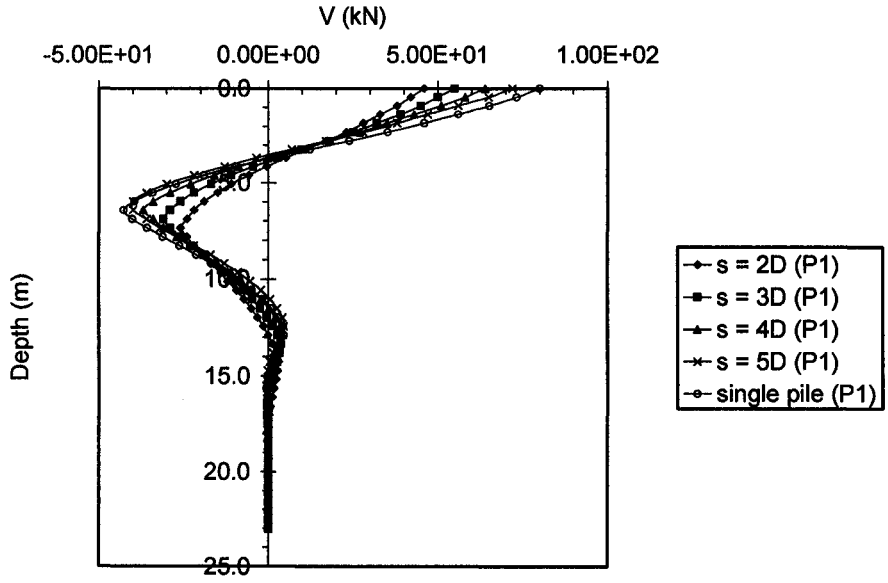

Fig. Q.12a Distributions of shear forces V at the primary structure p along the depth of the pile for sensitivity analysis of top lateral displacement δy_t for pile member A (2nd trailing row) of group of 3 x 3 piles with various spacing and single pile with length L = 10T subjected to lateral forces P1

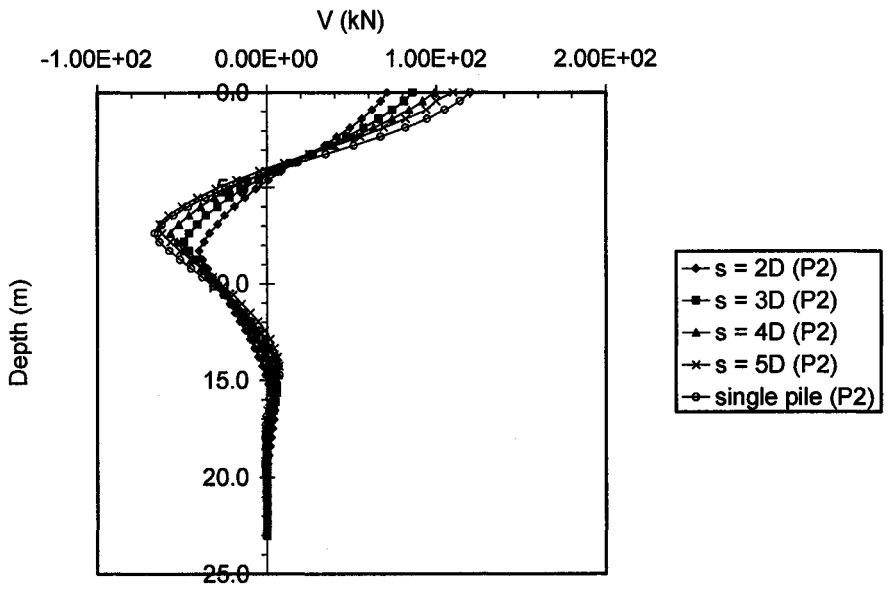

Fig. Q.12b Distributions of shear forces V at the primary structure p along the depth of the pile for sensitivity analysis of top lateral displacement δy_t for pile member A (2nd trailing row) of group of 3 x 3 piles with various spacing and single pile with length L = 10T subjected to lateral forces P2

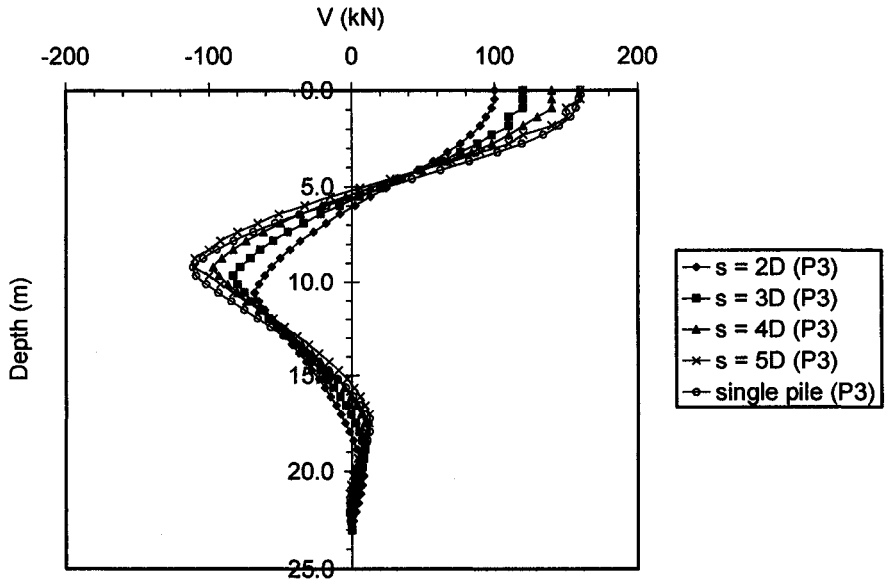

Fig. Q.12c Distributions of shear forces V at the primary structure p along the depth of the pile for sensitivity analysis of top lateral displacement δy_t for pile member A (2nd trailing row) of group of 3 x 3 piles with various spacing and single pile with length L = 10T subjected to lateral forces P3

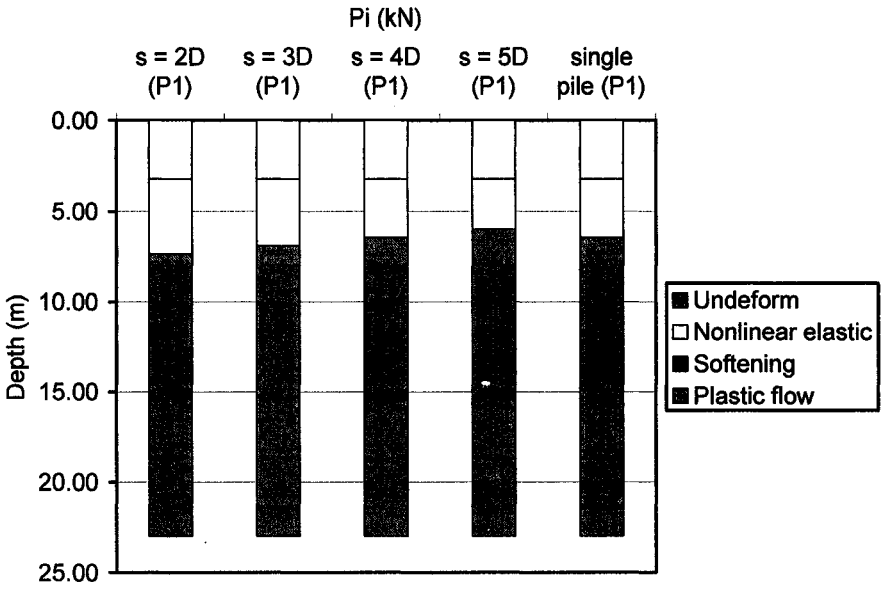

Fig. Q.13a Quantitative assessment of location and size of soil phases develop with depth determined based on the distributions of sensitivity operators δy_t for pile member A (2nd trailing row) of group of 3 x 3 piles with various spacing and single pile with length L = 10T subjected to lateral forces P1

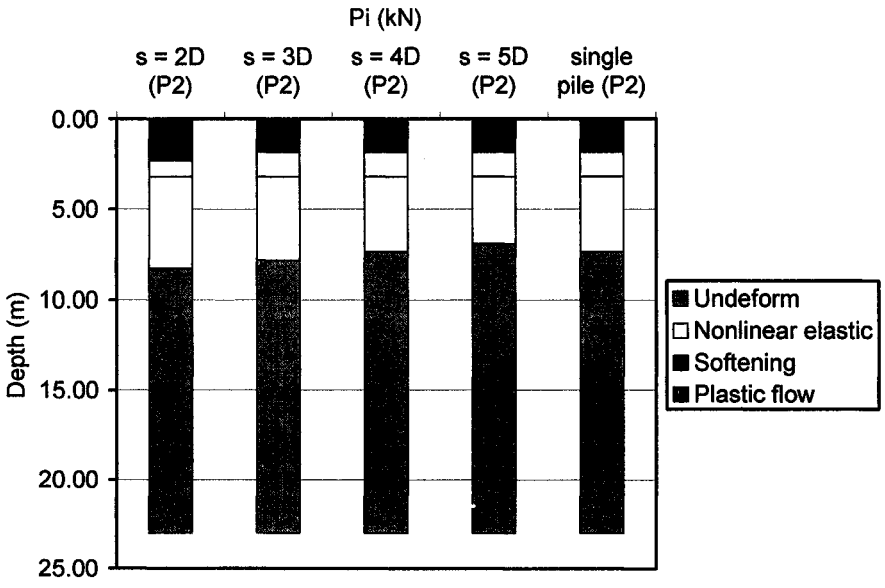

Fig. Q.13b Quantitative assessment of location and size of soil phases develop with depth determined based on the distributions of sensitivity operators δy_t for pile member A (2nd trailing row) of group of 3 x 3 piles with various spacing and single pile with length L = 10T subjected to lateral forces P2

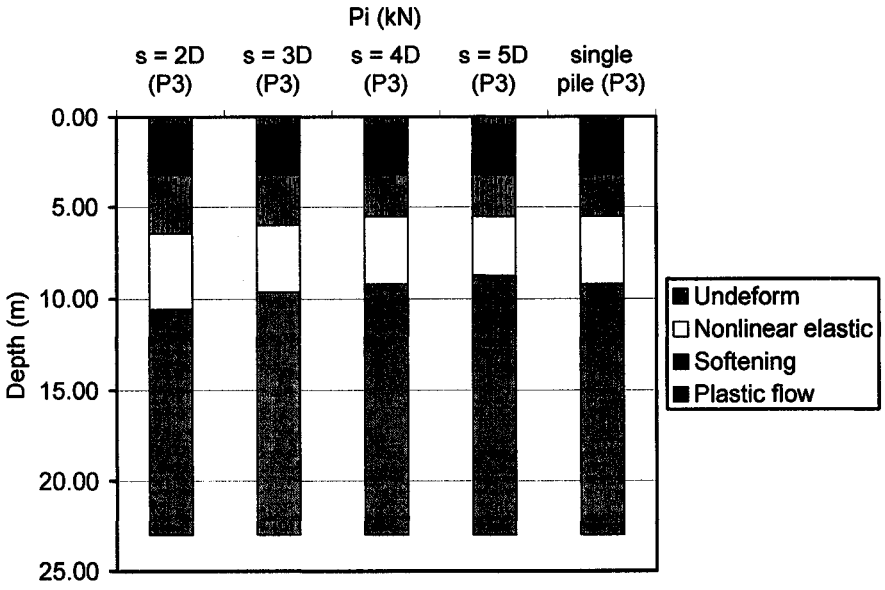

Fig. Q.13c Quantitative assessment of location and size of soil phases develop with depth determined based on the distributions of sensitivity operators δy_t for pile member A (2nd trailing row) of group of 3 x 3 piles with various spacing and single pile with length L = 10T subjected to lateral forces P3

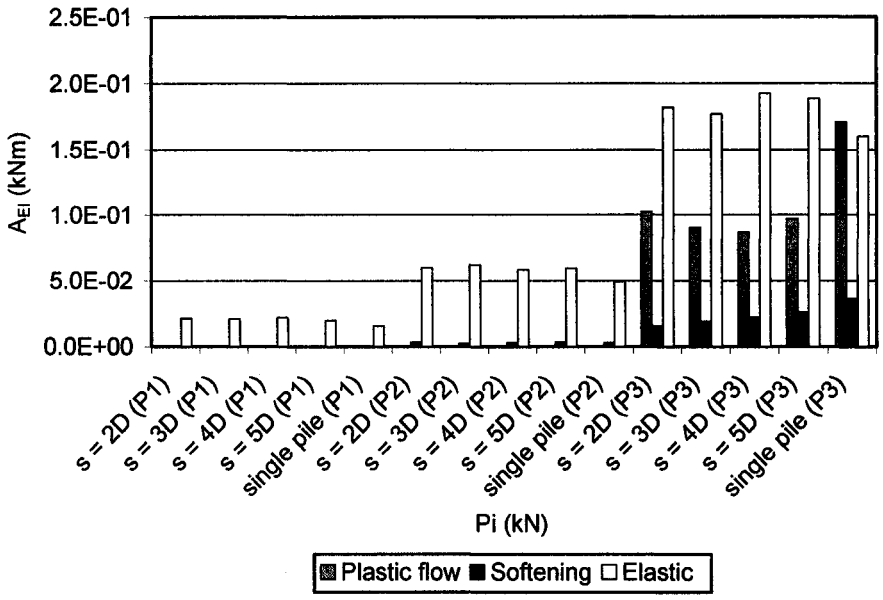

Fig. Q.14a Quantitative assessment of sensitivity A_{EI} associated with development of nonlinear elastic, linear softening, and plastic flow stages in the soil along the pile axis that affect δy_t for pile member A (2nd trailing row) of group of 3 x 3 piles with various spacing and single pile with length L = 10T subjected to lateral forces P_i (kN)

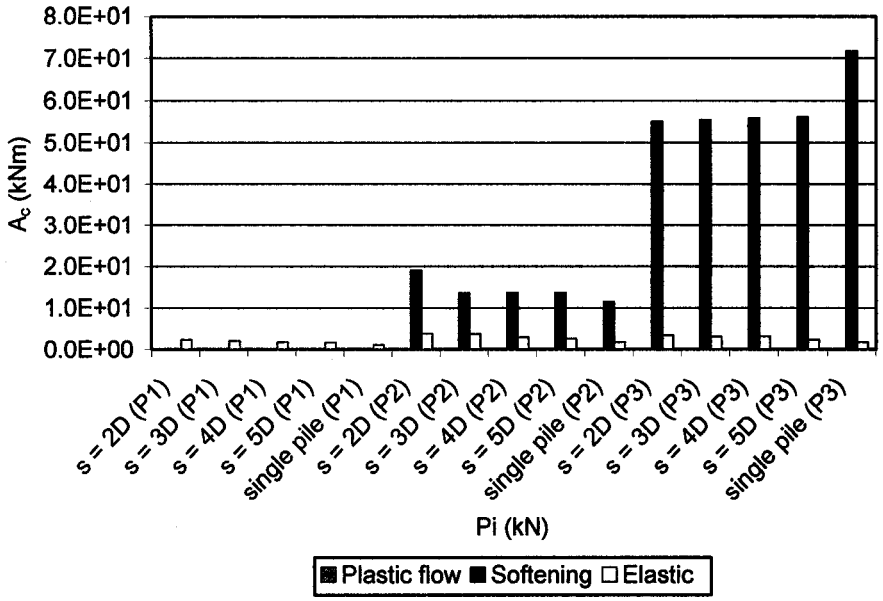

Fig. Q.14b Quantitative assessment of sensitivity A_c associated with development of nonlinear elastic, linear softening, and plastic flow stages in the soil along the pile axis that affect δy_t for pile member A (2nd trailing row) of group of 3 x 3 piles with various spacing and single pile with length L = 10T subjected to lateral forces P_i (kN)

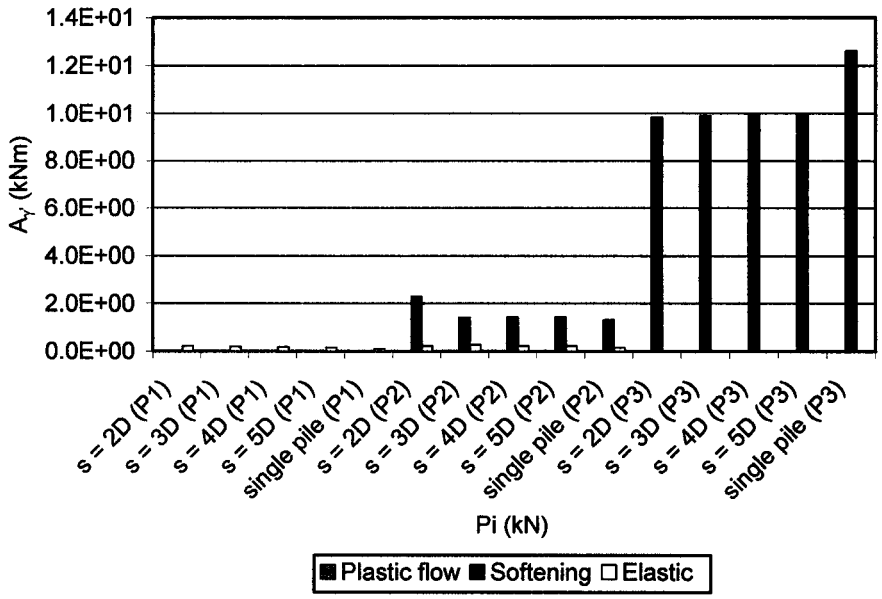

Fig. Q.14c Quantitative assessment of sensitivity A_γ associated with development of nonlinear elastic, linear softening, and plastic flow stages in the soil along the pile axis that affect δy_t for pile member A (2nd trailing row) of group of 3 x 3 piles with various spacing and single pile with length L = 10T subjected to lateral forces P_i (kN)

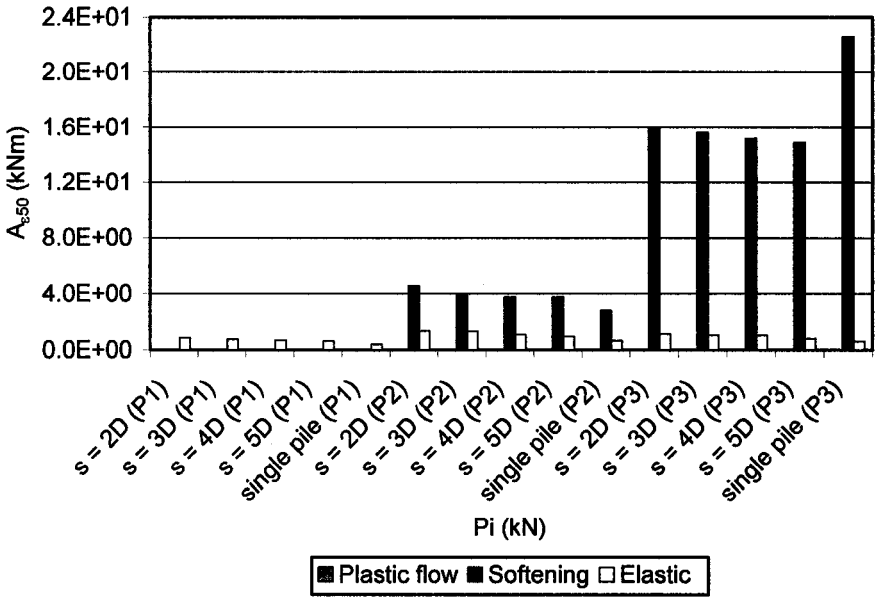

Fig. Q.14d Quantitative assessment of sensitivity $A_{\varepsilon 50}$ associated with development of nonlinear elastic, linear softening, and plastic flow stages in the soil along the pile axis that affect δy_t for pile member A (2nd trailing row) of group of 3 x 3 piles with various spacing and single pile with length L = 10T subjected to lateral forces P_i (kN)

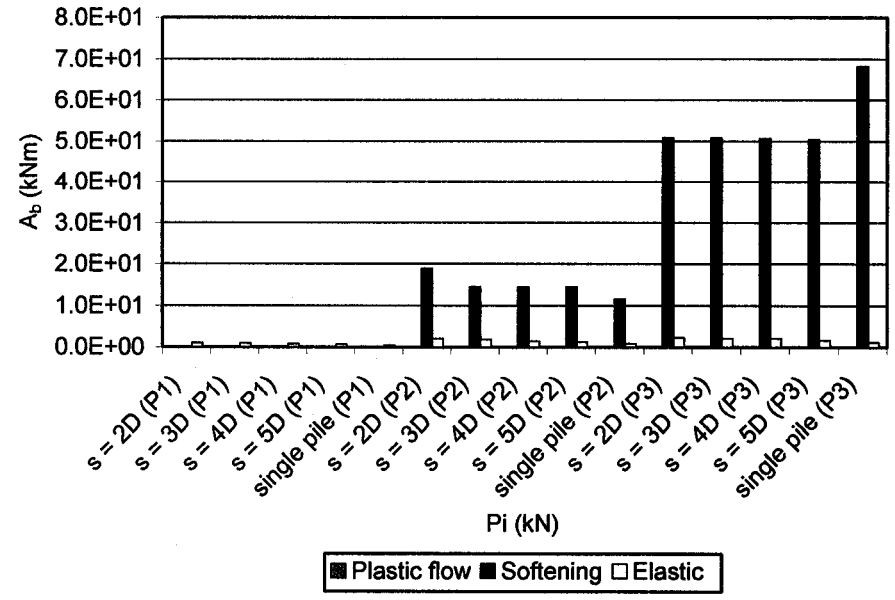

Fig. Q.14e Quantitative assessment of sensitivity A_b associated with development of nonlinear elastic, linear softening, and plastic flow stages in the soil along the pile axis that affect δy_t for pile member A (2nd trailing row) of group of 3 x 3 piles with various spacing and single pile with length L = 10T subjected to lateral forces P_i (kN)

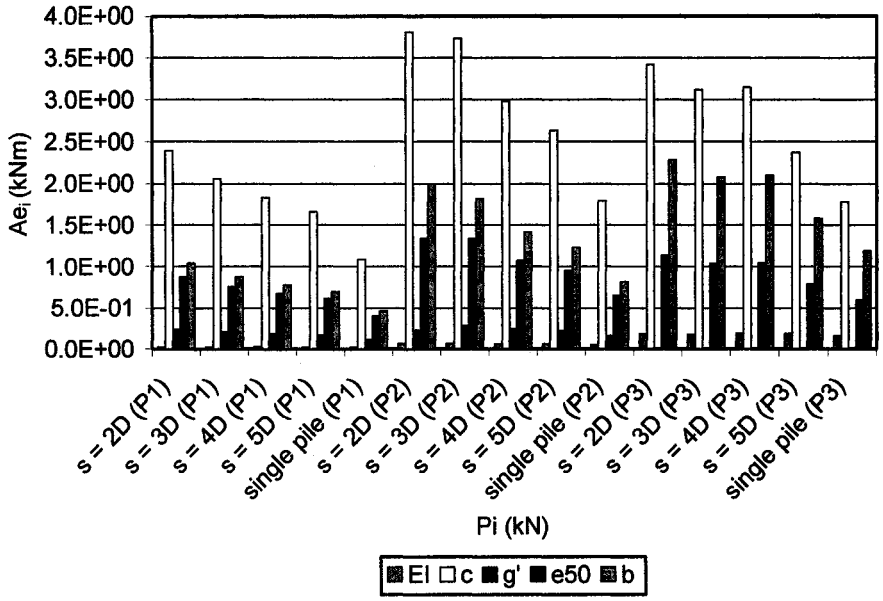

Fig. Q.14f Quantitative assessment of sensitivities Ae_i that contains Ae_{EI}, Ae_c, $Ae_{\gamma'}$, $Ae_{\varepsilon 50}$, and Ae_b associated with the development of the nonlinear elastic stage in the soil along the pile axis that affect δy_t for pile member A (2nd trailing row) of group of 3 x 3 piles with various spacing and single pile with length L = 10T subjected to lateral forces P_i (kN)

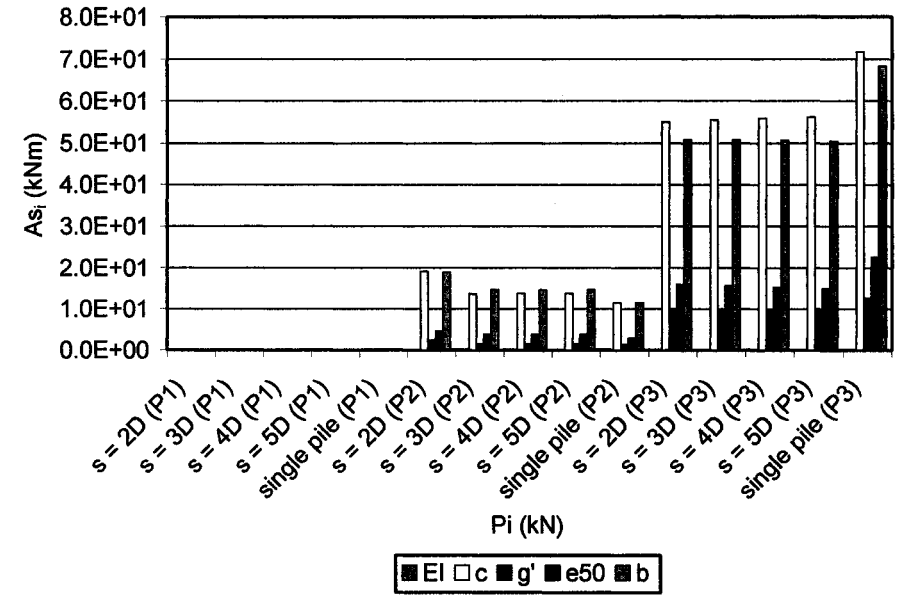

Fig. Q.14g Quantitative assessment of sensitivities As_i that contains As_{EI}, As_c, $As_{\gamma'}$, $As_{\varepsilon 50}$, and As_b associated with the development of the linear softening stage in the soil along the pile axis that affect δy_t for pile member A (2nd trailing row) of group of 3 x 3 piles with various spacing and single pile with length L = 10T subjected to lateral forces P_i (kN)

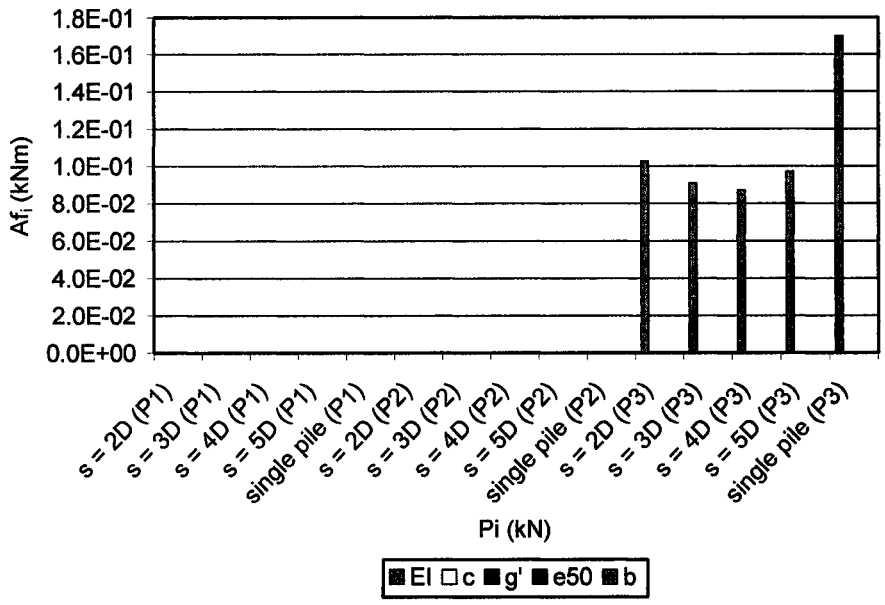

Fig. Q.14h Quantitative assessment of sensitivities Af_i that contains Af_{EI}, Af_c, $Af_{\gamma'}$, $Af_{\varepsilon 50}$, and Af_b associated with the development of the plastic flow stage in the soil along the pile axis that affect δy_t for pile member A (2nd trailing row) of group of 3 x 3 piles with various spacing and single pile with length L = 10T subjected to lateral forces P_i (kN)

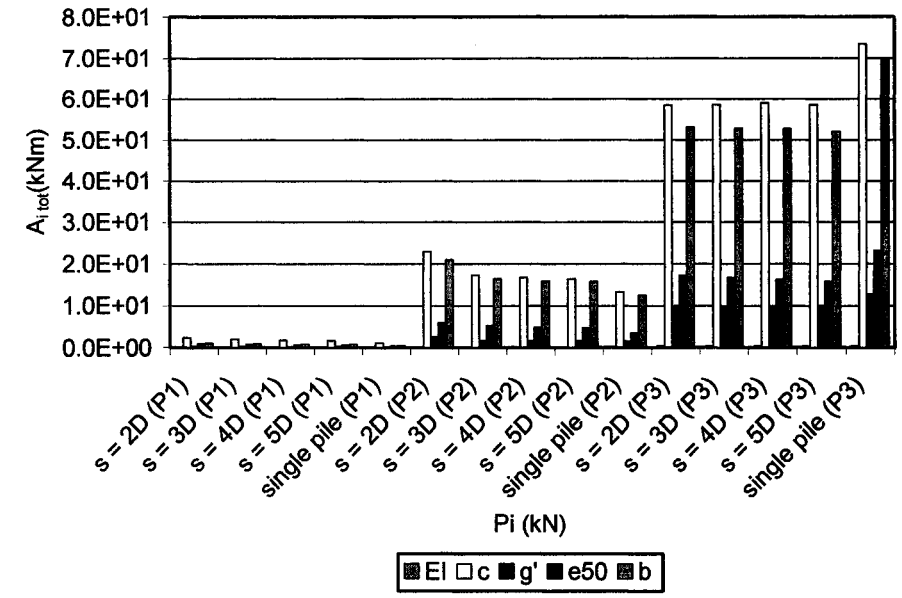

Fig. Q.14i Quantitative assessment of sensitivities $A_{i\ tot}$ that contains (A_{EI}, A_c, $A_{\gamma'}$, $A_{\varepsilon 50}$, and A_b)$_{tot}$ associated with the development of three stages in the soil along the pile axis that affect δy_t for pile member A (2nd trailing row) of group of 3 x 3 piles with various spacing and single pile with length L = 10T subjected to lateral forces P_i (kN)

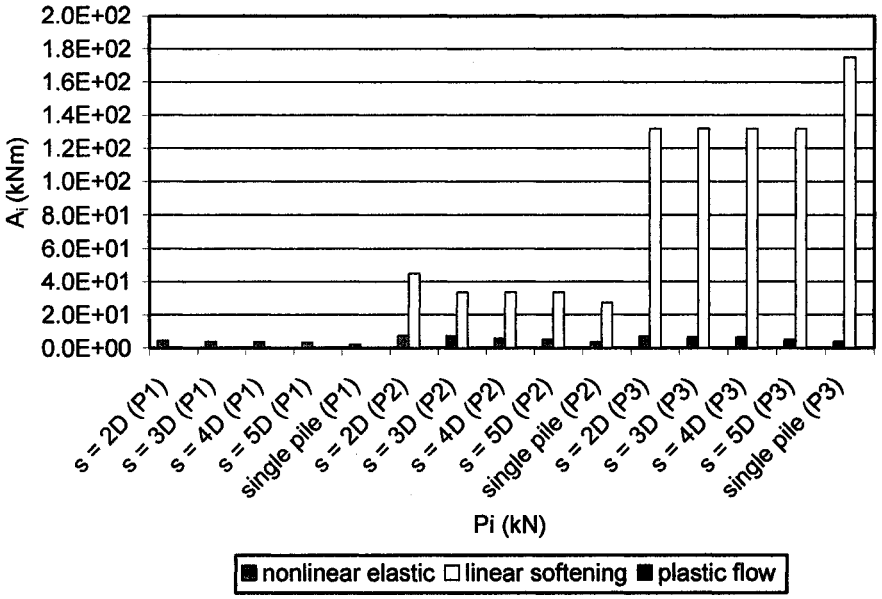

Fig. Q.14j.1 Quantitative assessment of sensitivities A_i that is summation of (A_{EI}, A_c, $A_{\gamma'}$, $A_{\varepsilon 50}$, and A_b)$_i$ of each soil stage that affect δy_t for pile member A (2nd trailing row) of group of 3 x 3 piles with various spacing and single pile with length L = 10T subjected to lateral forces P_i (kN)

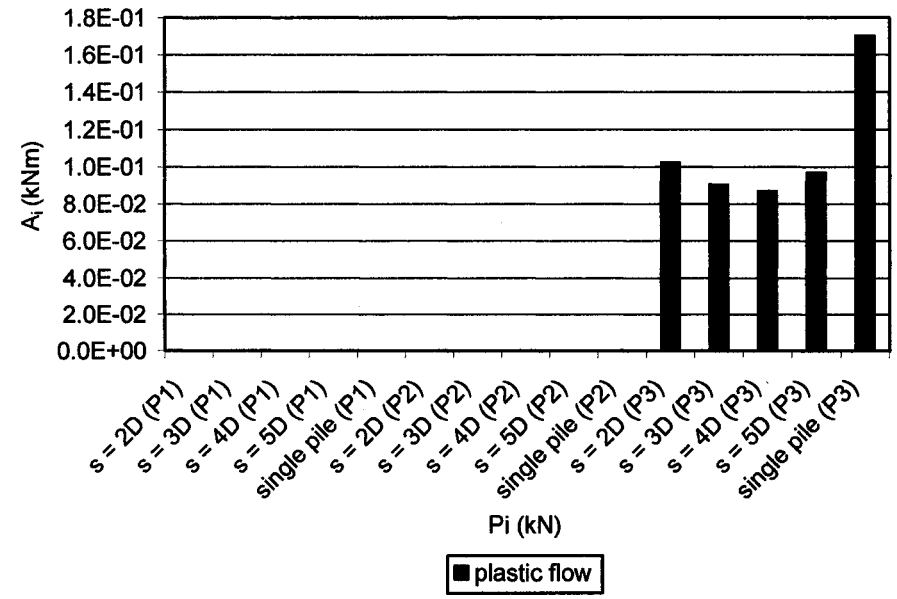

Fig. Q.14j.2 Quantitative assessment of sensitivities A_i that is summation of (A_{EI}, A_c, $A_{\gamma'}$, $A_{\varepsilon 50}$, and A_b)$_i$ of each soil stage that affect δy_t for pile member A (2nd trailing row) of group of 3 x 3 piles with various spacing and single pile with length L = 10T subjected to lateral forces P_i (kN)

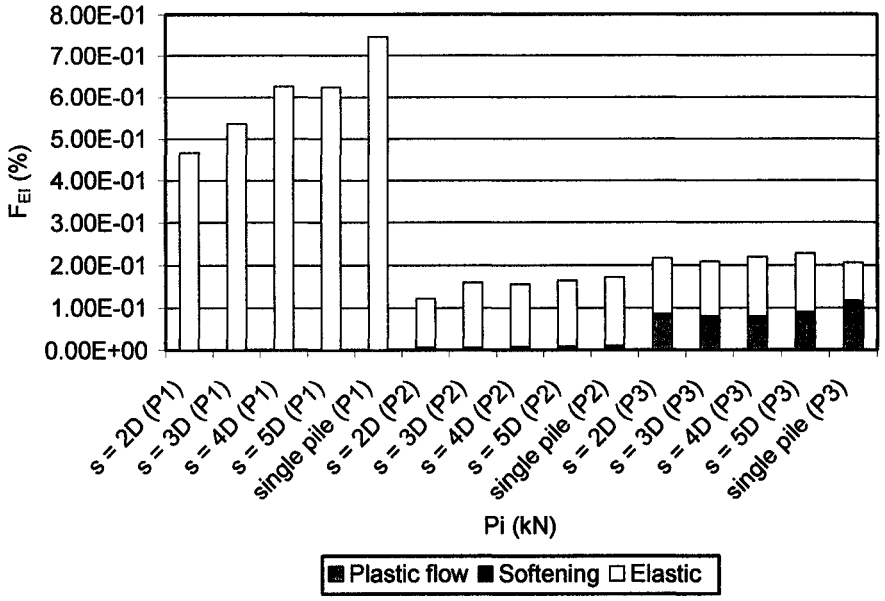

Fig. Q.15a Quantitative assessment (in %) of relative sensitivity factors F_{EI} that affect δy_t for pile member A (2nd trailing row) of group of 3 x 3 piles with various spacing and single pile with length L = 10T subjected to lateral forces P_i (kN)

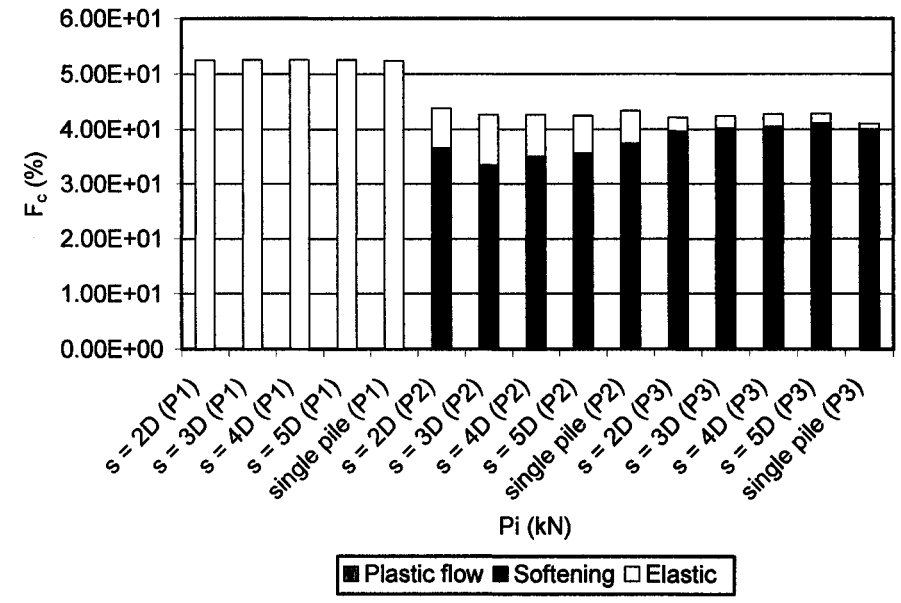

Fig. Q.15b Quantitative assessment (in %) of relative sensitivity factors F_c that affect δy_t for pile member A (2nd trailing row) of group of 3 x 3 piles with various spacing and single pile with length L = 10T subjected to lateral forces P_i (kN)

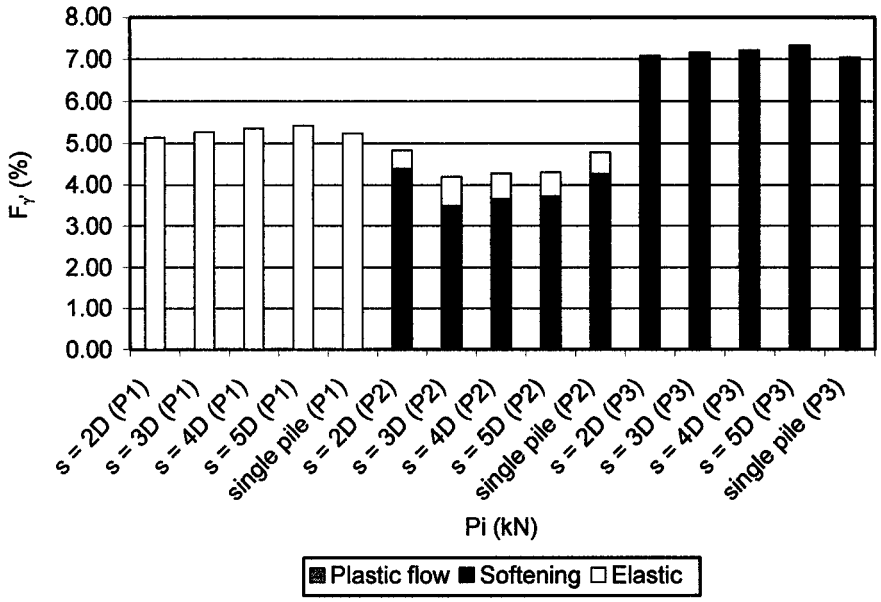

Fig. Q.15c Quantitative assessment (in %) of relative sensitivity factors F_γ that affect δy_t for pile member A (2nd trailing row) of group of 3 x 3 piles with various spacing and single pile with length L = 10T subjected to lateral forces P_i (kN)

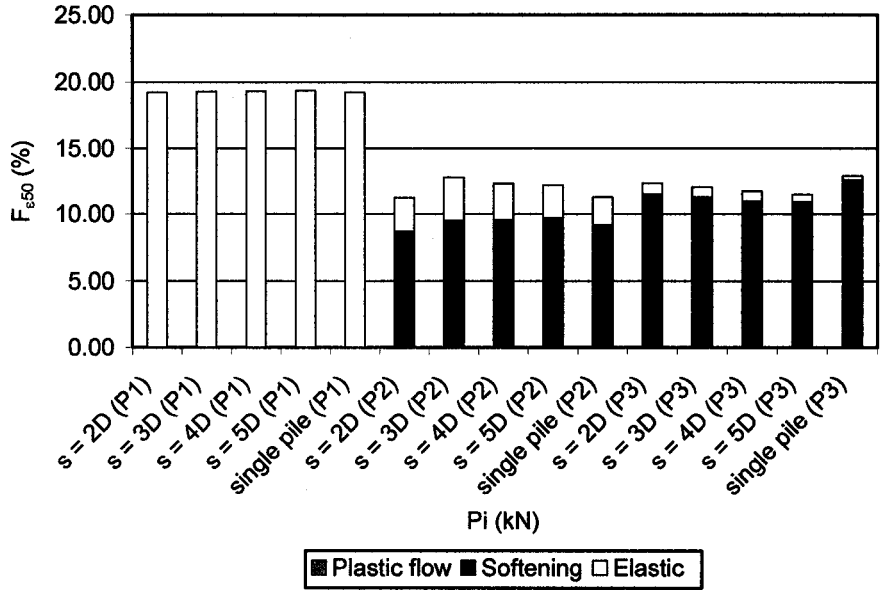

Fig. Q.15d Quantitative assessment (in %) of relative sensitivity factors $F_{\varepsilon 50}$ that affect δy_t for pile member A (2nd trailing row) of group of 3 x 3 piles with various spacing and single pile with length L = 10T subjected to lateral forces P_i (kN)

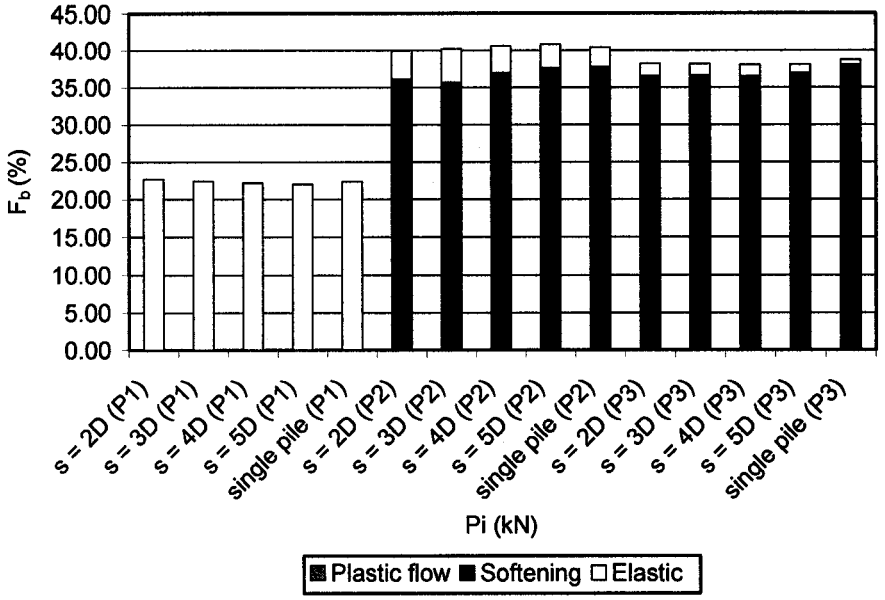

Fig. Q.15e Quantitative assessment (in %) of relative sensitivity factors F_b that affect δy_t for pile member A (2nd trailing row) of group of 3 x 3 piles with various spacing and single pile with length L = 10T subjected to lateral forces P_i (kN)

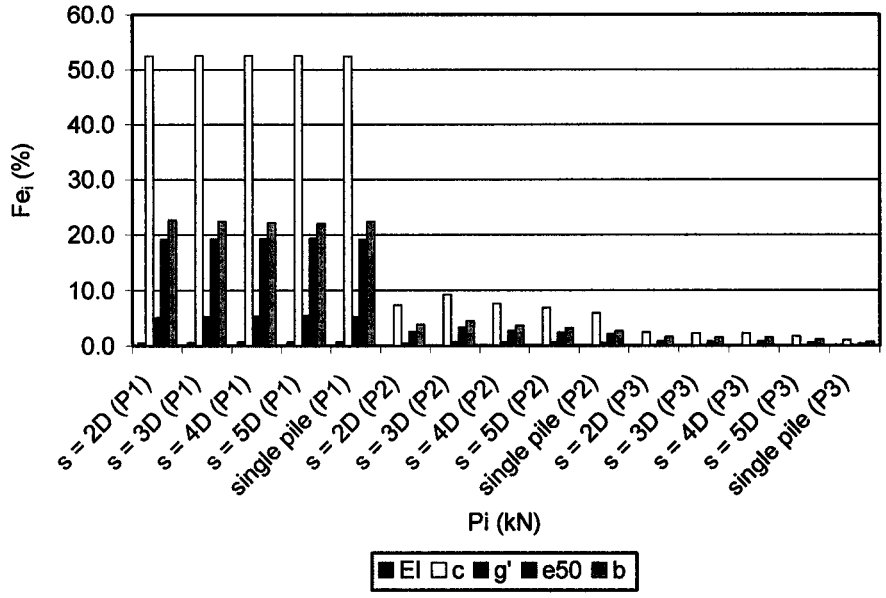

Fig. Q.15f Quantitative assessment (in %) of relative sensitivity factors Fe_i that contains Fe_{EI}, Fe_c, $Fe_{\gamma'}$, $Fe_{\varepsilon 50}$, and Fe_b associated with the nonlinear elastic soil stage developed along the pile axis that affect δy_t for pile member A (2nd trailing row) of group of 3 x 3 piles with various spacing and single pile with length L = 10T subjected to lateral forces P_i (kN)

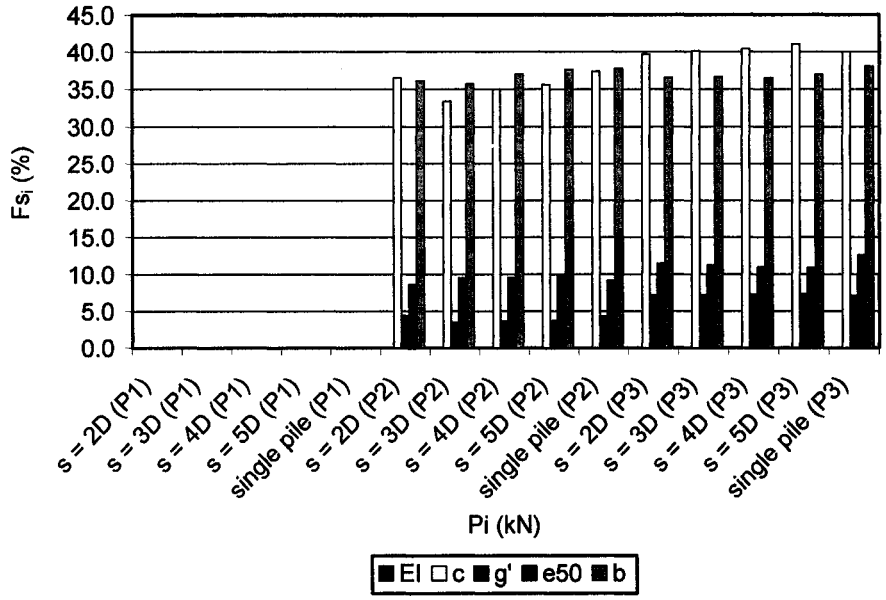

Fig. Q.15g Quantitative assessment (in %) of relative sensitivity factors Fs_i that contains Fs_{EI}, Fs_c, $Fs_{\gamma'}$, $Fs_{\varepsilon 50}$, and Fs_b associated with the linear softening stage developed along the pile axis that affect δy_t for pile member A (2nd trailing row) of group of 3 x 3 piles with various spacing and single pile with length L = 10T subjected to lateral forces P_i (kN)

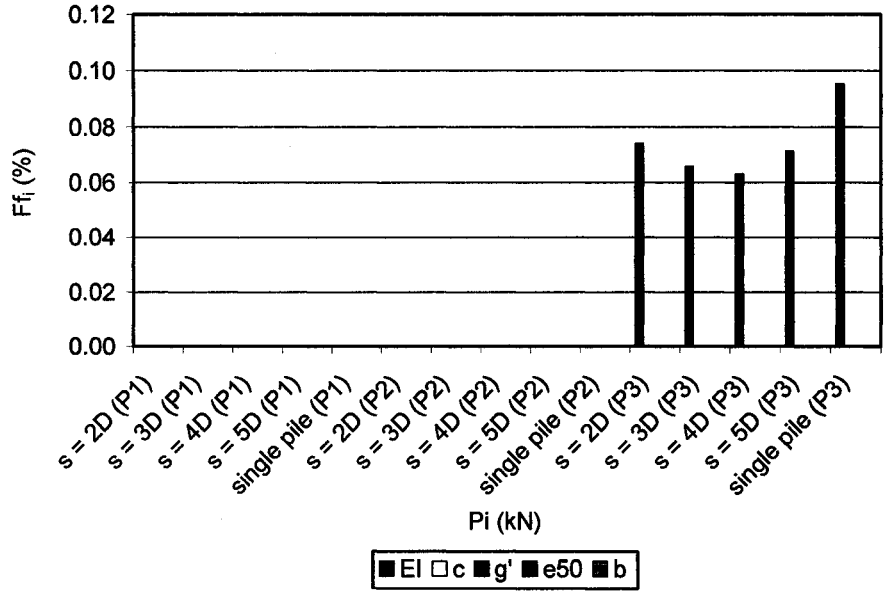

Fig. Q.15h Quantitative assessment (in %) of relative sensitivity factors Ff_i that contains Ff_{EI}, Ff_c, $Ff_{\gamma'}$, $Ff_{\varepsilon 50}$, and Ff_b associated with the nonlinear elastic soil stage developed along the pile axis that affect Ff_i associated with plastic flow soil phase of the sensitivity analysis of δy_t for pile member A (2nd trailing row) of group of 3 x 3 piles with various spacing and single pile with length L = 10T subjected to lateral forces P_i (kN)

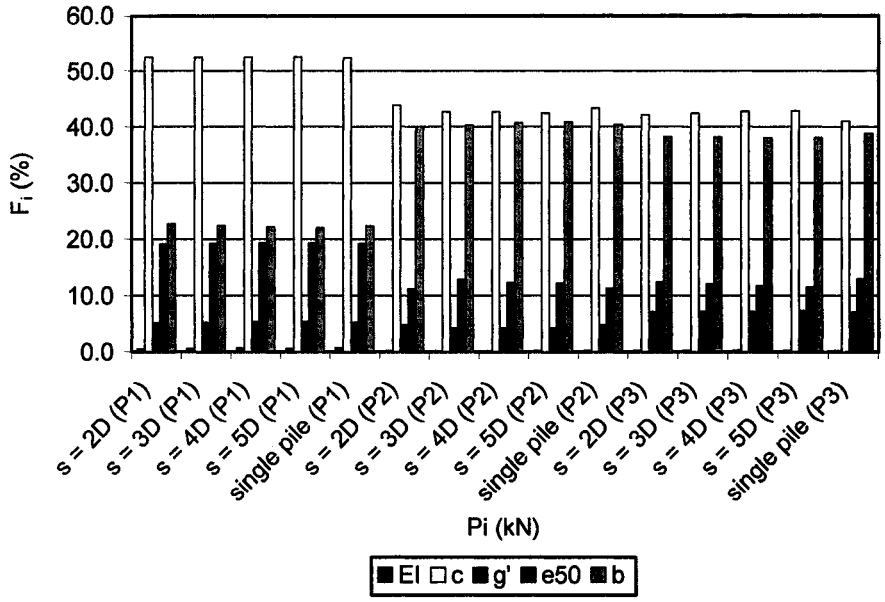

Fig. Q.15i Quantitative assessment (in %) of relative sensitivity factors F_i that contains F_{EI}, F_c, $F_{\gamma'}$, $F_{\varepsilon 50}$, and F_b associated with all soil stages developed along the pile axis that affect F_i associated with all phases of the sensitivity analysis of δy_t for pile member A (2nd trailing row) of group of 3 x 3 piles with various spacing and single pile with length L = 10T subjected to lateral forces P_i (kN)

APPENDIX R:

Comparison of the quantitative assessments of sensitivities A and relative sensitivity factors F of free head single isolated piles with various lengths

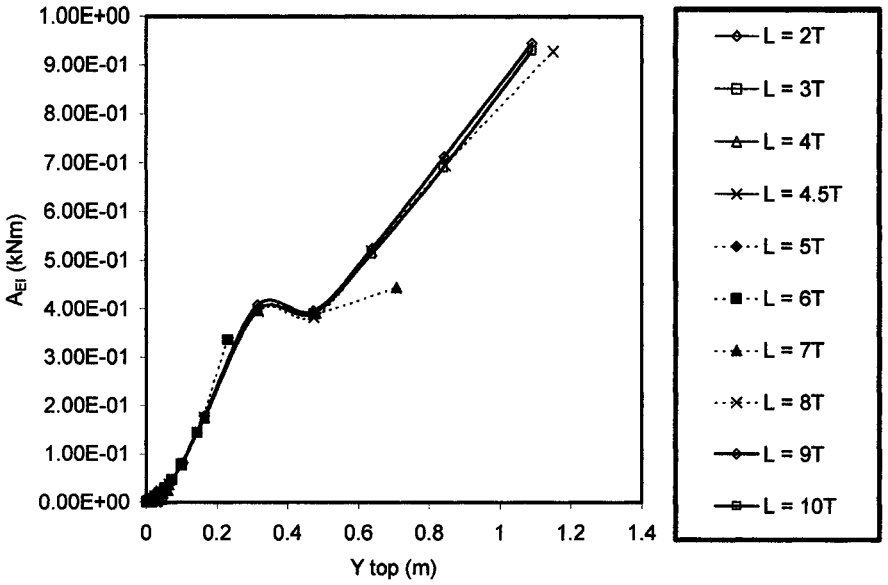

Fig. R.1a The quantitative assessment of sensitivities A_{EI} affecting δy_t of free head single piles subjected to lateral forces Pi (kN) with various lengths vs. the lateral displacement at the top of the pile

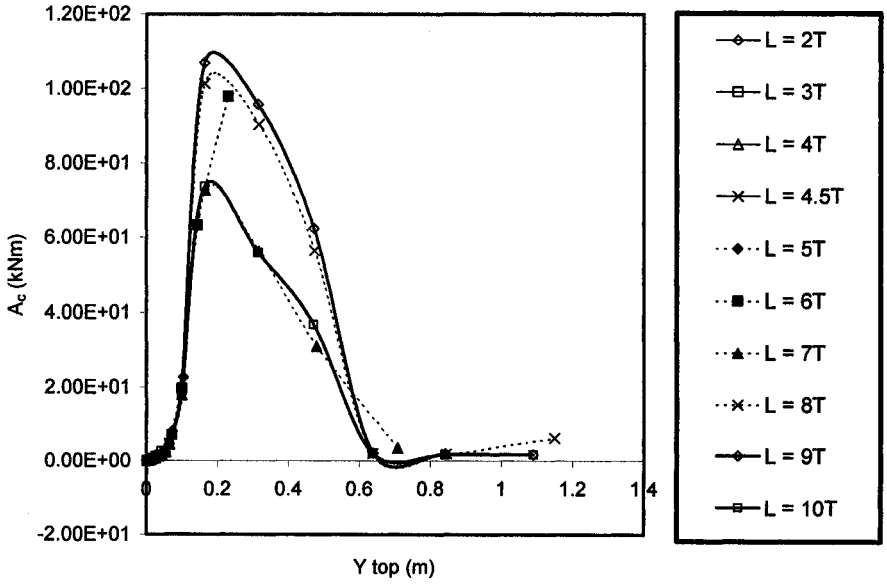

Fig. R.1b The quantitative assessment of sensitivities A_c affecting δy_t of free head single piles subjected to lateral forces Pi (kN) with various lengths vs. the lateral displacement at the top of the pile

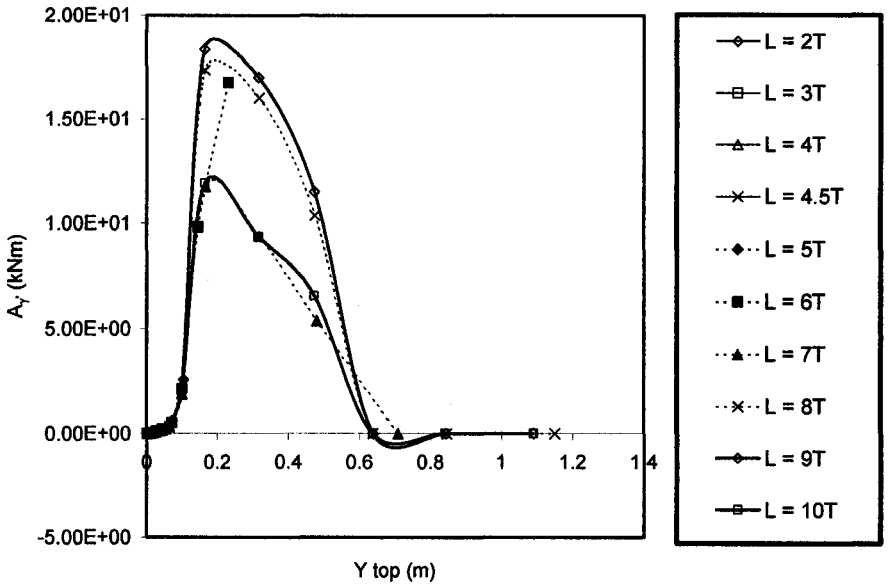

Fig. R.1c The quantitative assessment of sensitivities A_γ affecting δy_t of free head single piles subjected to lateral forces Pi (kN) with various lengths vs. the lateral displacement at the top of the pile

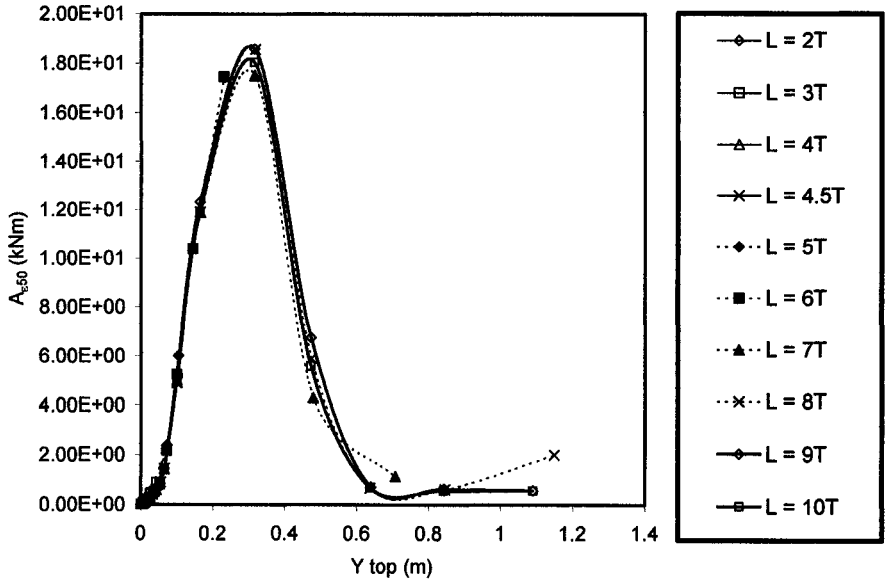

Fig. R.1d The quantitative assessment of sensitivities $A_{\varepsilon 50}$ affecting δy_t of free head single piles subjected to lateral forces Pi (kN) with various lengths vs. the lateral displacement at the top of the pile

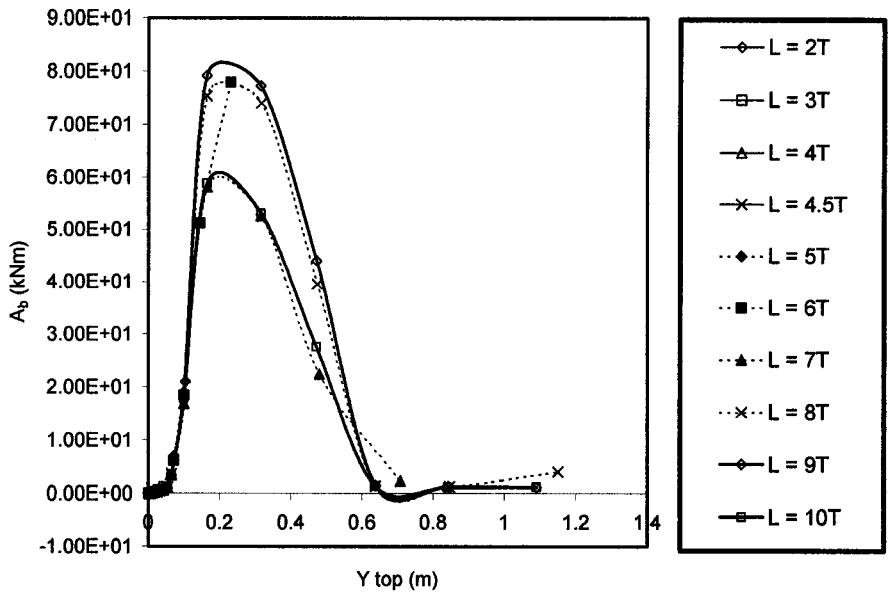

Fig. R.1e The quantitative assessment of sensitivities A_b affecting δy_t of free head single piles subjected to lateral forces Pi (kN) of free head single piles with various lengths vs. the lateral displacement at the top of the pile

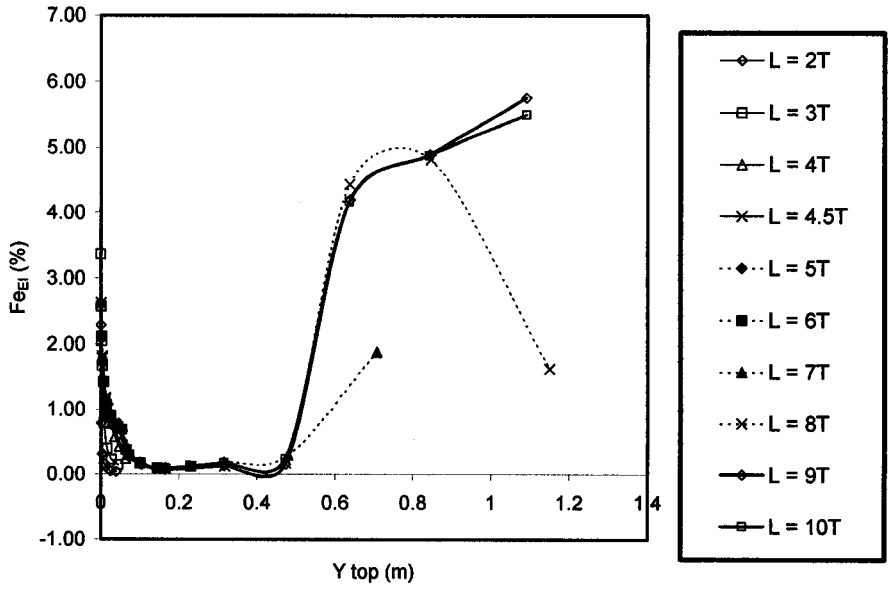

Fig. R.2a The quantitative assessment of relative sensitivity factors Fe_{EI} associated with soil's elastic stage affecting δy_t of free head single piles subjected to lateral forces Pi (kN) with various lengths vs. the lateral displacement at the top of the pile

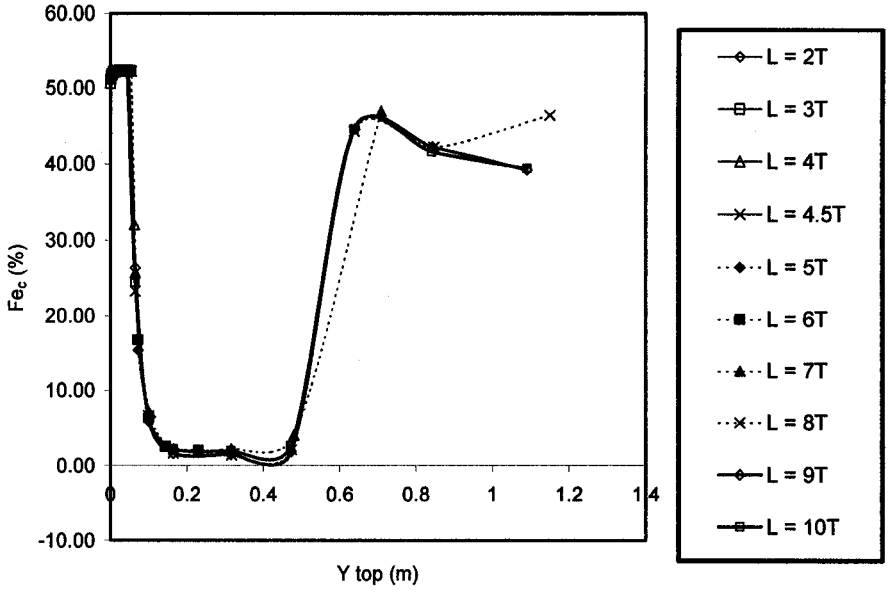

Fig. R.2b The quantitative assessment of relative sensitivity factors Fe_c associated with soil's elastic stage affecting δy_t of free head single piles subjected to lateral forces Pi (kN) with various lengths vs. the lateral displacement at the top of the pile

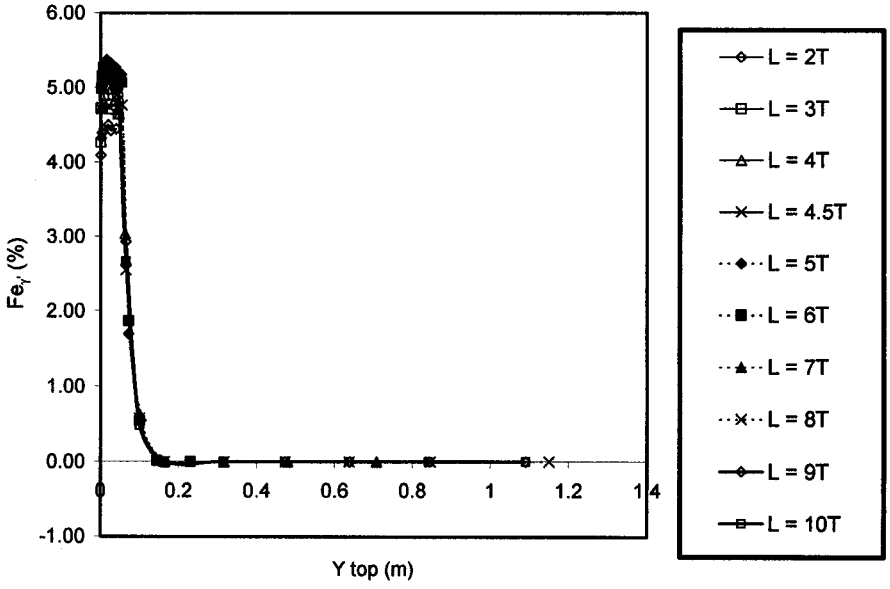

Fig. R.2c The quantitative assessment of relative sensitivity factors Fe_γ associated with soil's elastic stage affecting δy_t of free head single piles subjected to lateral forces Pi (kN) with various lengths vs. the lateral displacement at the top of the pile

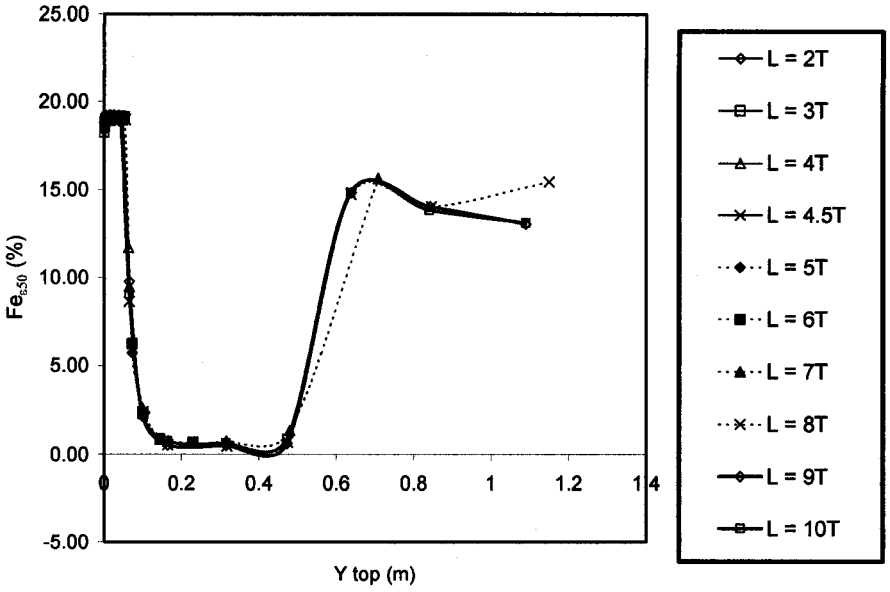

Fig. R.2d The quantitative assessment of relative sensitivity factors $Fe_{\varepsilon 50}$ associated with soil's elastic stage affecting δy_t of free head single piles subjected to lateral forces Pi (kN) with various lengths vs. the lateral displacement at the top of the pile

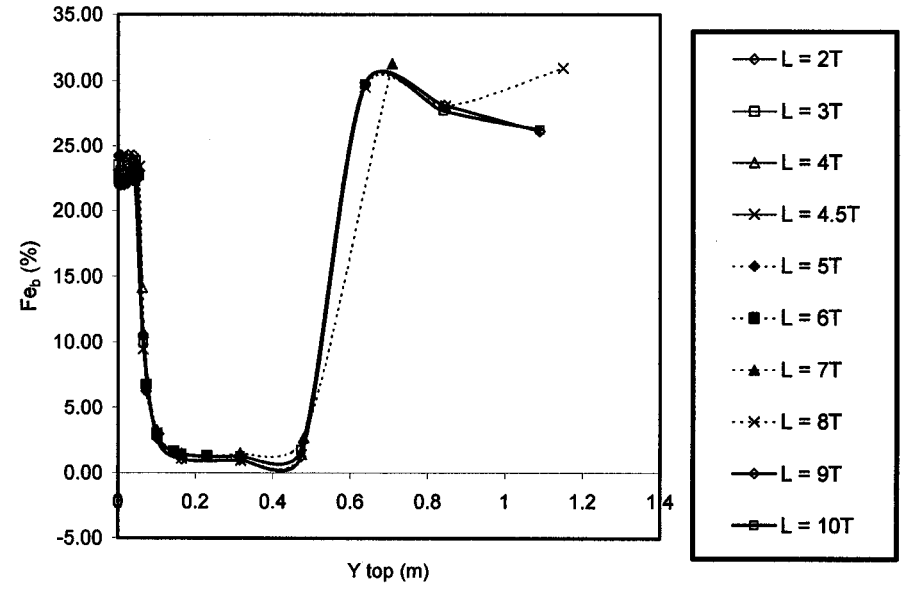

Fig. R.2e The quantitative assessment of relative sensitivity factors Fe_b associated with soil's elastic stage affecting δy_t of free head single piles subjected to lateral forces Pi (kN) with various lengths vs. the lateral displacement at the top of the pile

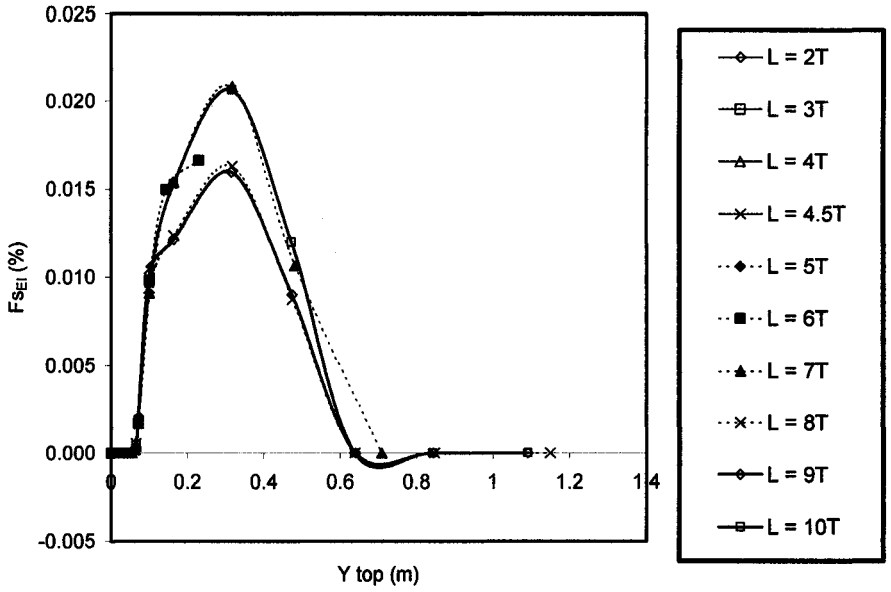

Fig. R.3a The quantitative assessment of relative sensitivity factors Fs_{EI} associated with soil's linear softening stage affecting δy_t of free head single piles subjected to lateral forces Pi (kN) with various lengths vs. the lateral displacement at the top of the pile

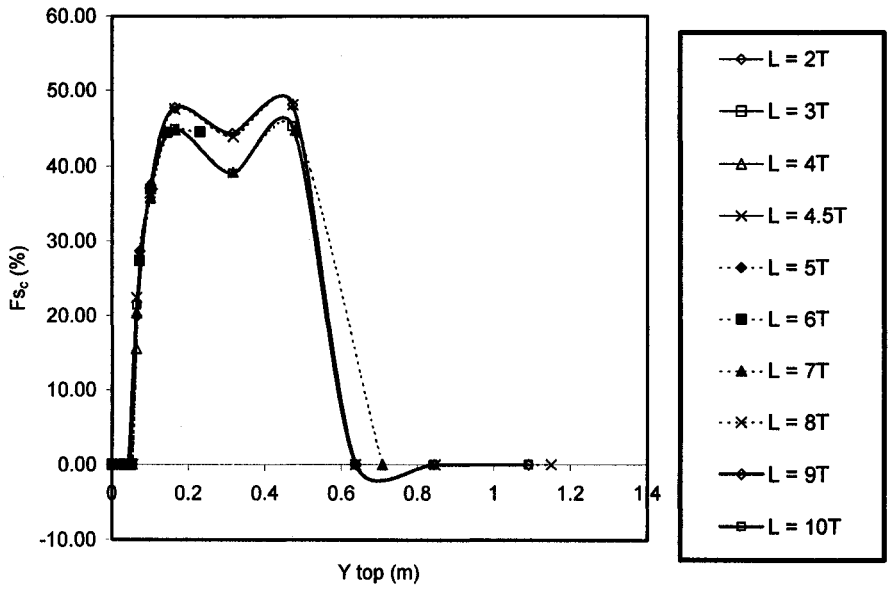

Fig. R.3b The quantitative assessment of relative sensitivity factors Fs_c associated with soil's linear softening stage affecting δy_t of free head single piles subjected to lateral forces Pi (kN) with various lengths vs. the lateral displacement at the top of the pile

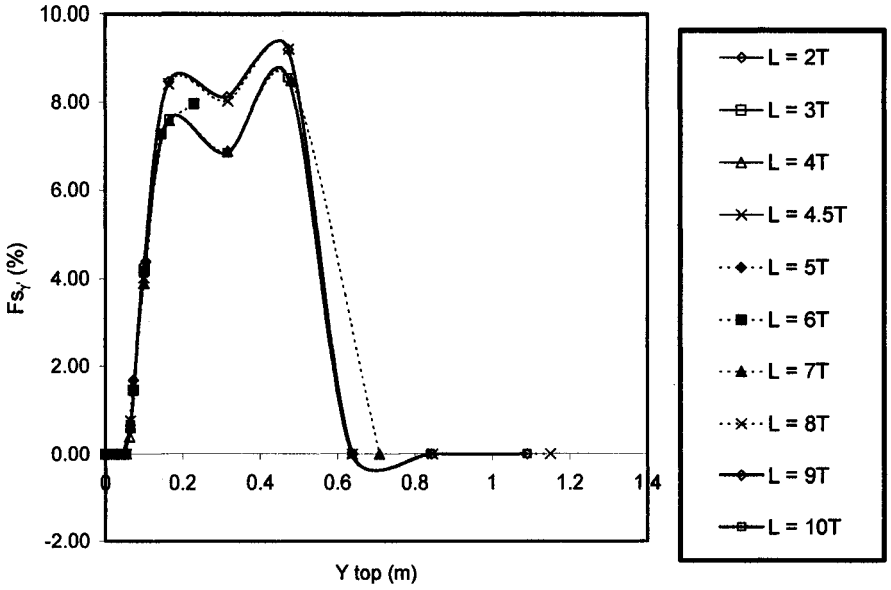

Fig. R.3c The quantitative assessment of relative sensitivity factors Fs_γ associated with soil's linear softening stage affecting δy_t of free head single piles subjected to lateral forces Pi (kN) with various lengths vs. the lateral displacement at the top of the pile

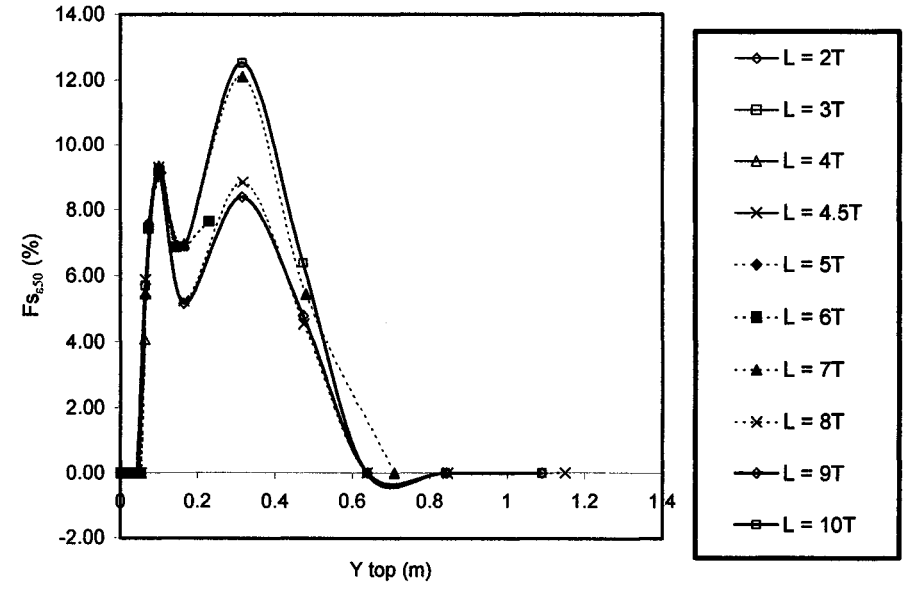

Fig. R.3d The quantitative assessment of relative sensitivity factors $Fs_{\varepsilon 50}$ associated with soil's linear softening stage affecting δy_t of free head single piles subjected to lateral forces Pi (kN) with various lengths vs. the lateral displacement at the top of the pile

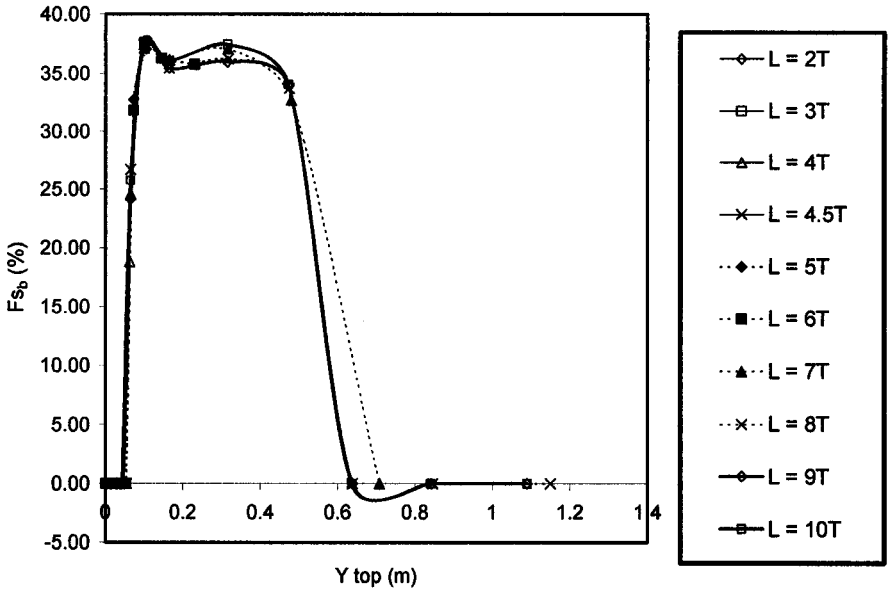

Fig. R.3e The quantitative assessment of relative sensitivity factors Fs_b associated with soil's linear softening stage affecting δy_t of free head single piles subjected to lateral forces Pi (kN) with various lengths vs. the lateral displacement at the top of the pile

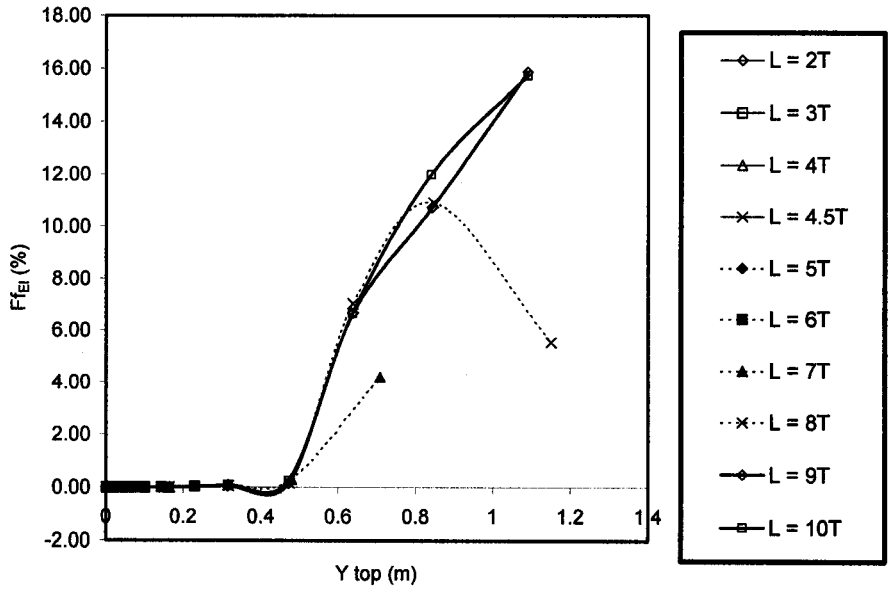

Fig. R.4a The quantitative assessment of relative sensitivity factors Ff_{EI} associated with soil's plastic flow stage affecting δy_t of free head single piles subjected to lateral forces Pi (kN) with various lengths vs. the lateral displacement at the top of the pile

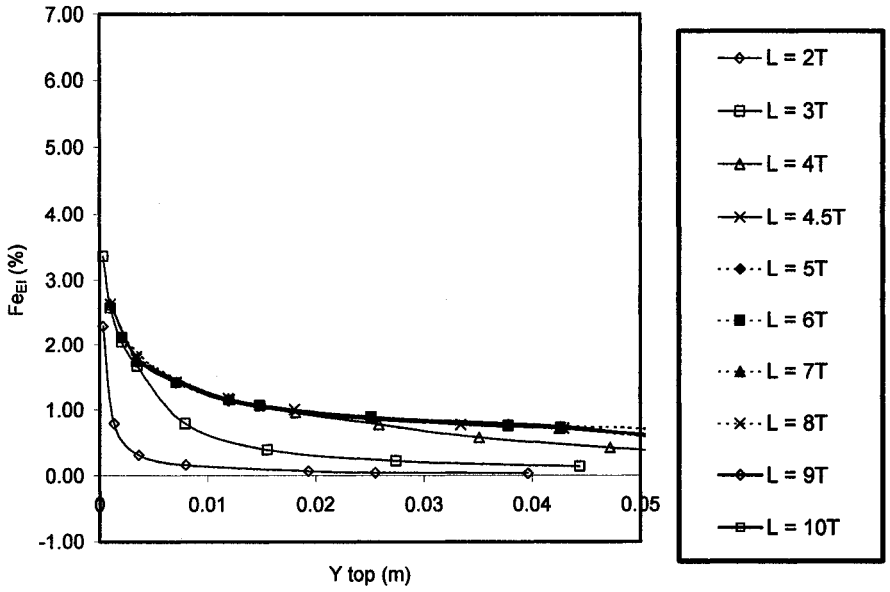

Fig. R.5a The quantitative assessment of relative sensitivity factors Fe_{EI} associated with soil's elastic stage affecting δy_t of free head single piles subjected to lateral forces Pi (kN) with various lengths vs. the lateral displacement at the top of the pile for $y_{top} < 0.05$ m

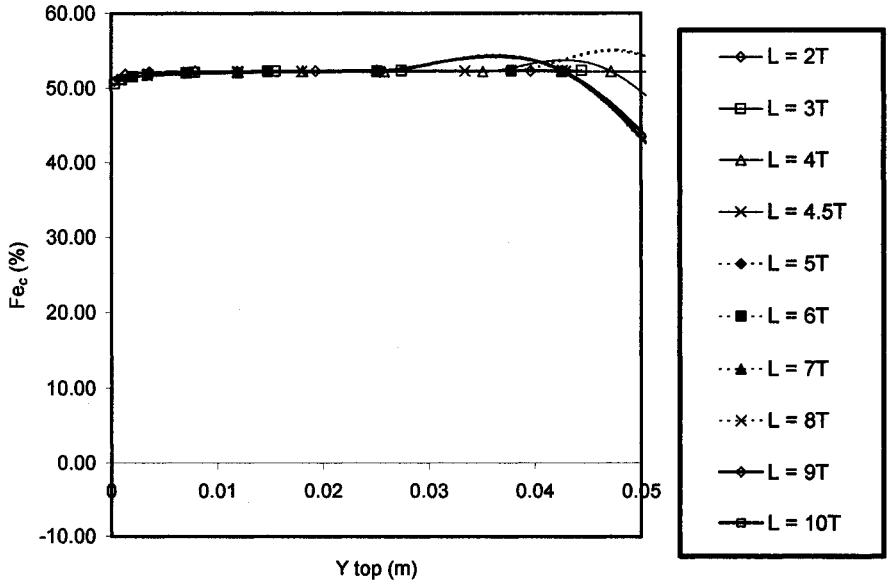

Fig. R.5b The quantitative assessment of relative sensitivity factors Fe_c associated with soil's elastic stage affecting δy_t of free head single piles subjected to lateral forces Pi (kN) with various lengths vs. the lateral displacement at the top of the pile for $y_{top} < 0.05$ m

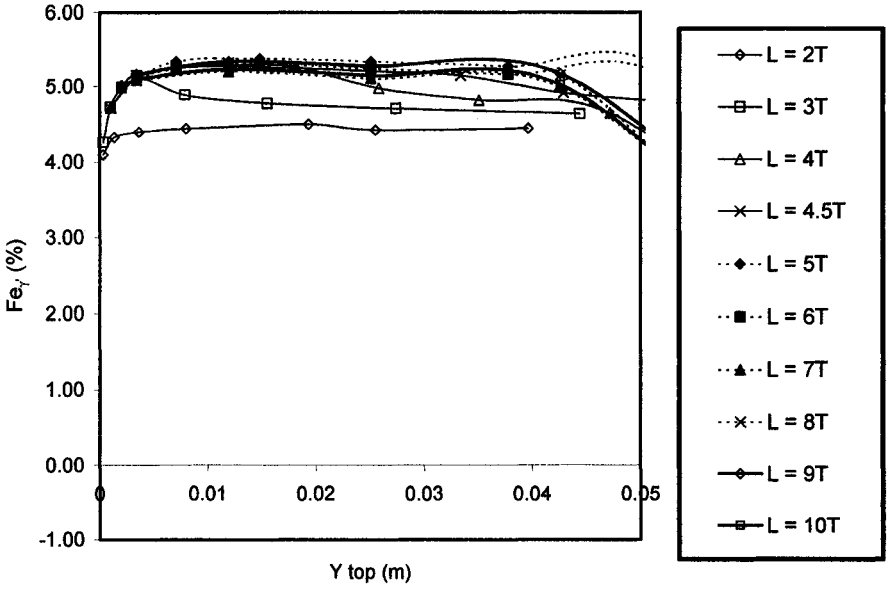

Fig. R.5c The quantitative assessment of relative sensitivity factors Fe_γ associated with soil's elastic stage affecting δy_t of free head single piles subjected to lateral forces Pi (kN) with various lengths vs. the lateral displacement at the top of the pile for $y_{top} < 0.05$ m

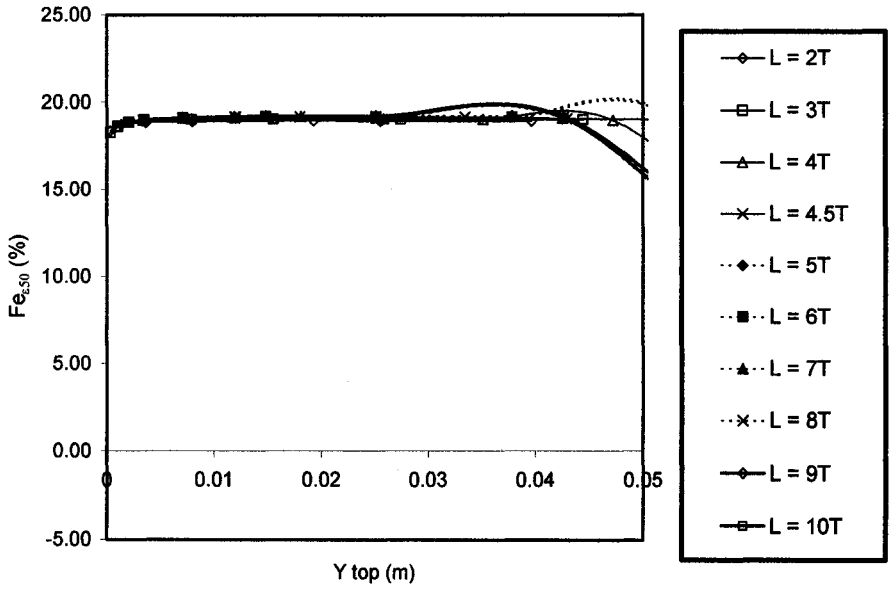

Fig. R.5d The quantitative assessment of relative sensitivity factors $Fe_{\varepsilon 50}$sociated with soil's elastic stage affecting δy_t of free head single piles subjected to lateral forces Pi (kN) with various lengths vs. the lateral displacement at the top of the pile for $y_{top} < 0.05$ m

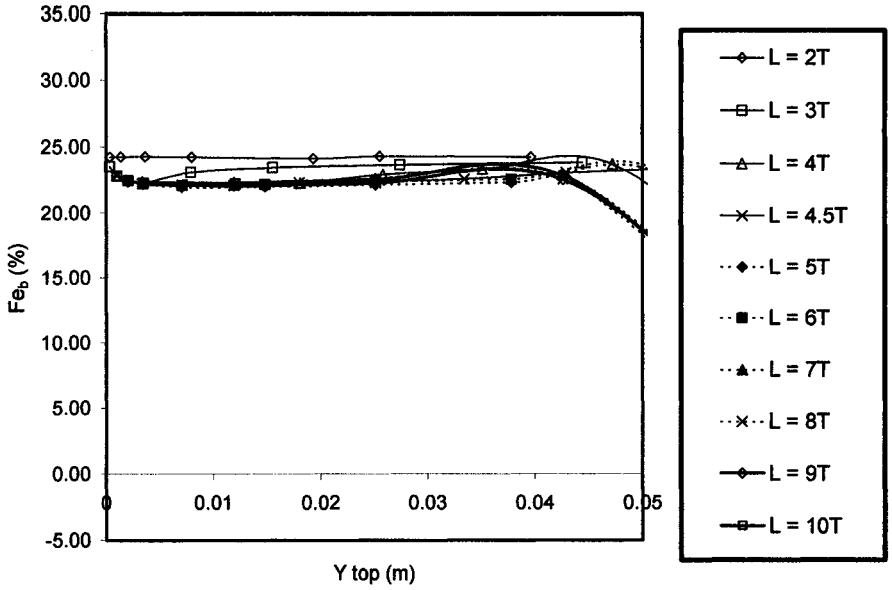

Fig. R.5e The quantitative assessment of relative sensitivity factors Fe_b associated with soil's elastic stage affecting δy_t of free head single piles subjected to lateral forces Pi (kN) with various lengths vs. the lateral displacement at the top of the pile for $y_{top} < 0.05$ m

APPENDIX S:

Comparison of the quantitative assessments of sensitivities *A* and relative sensitivity factors *F* of groups of 3×3 piles with various spacing and length L = 10T

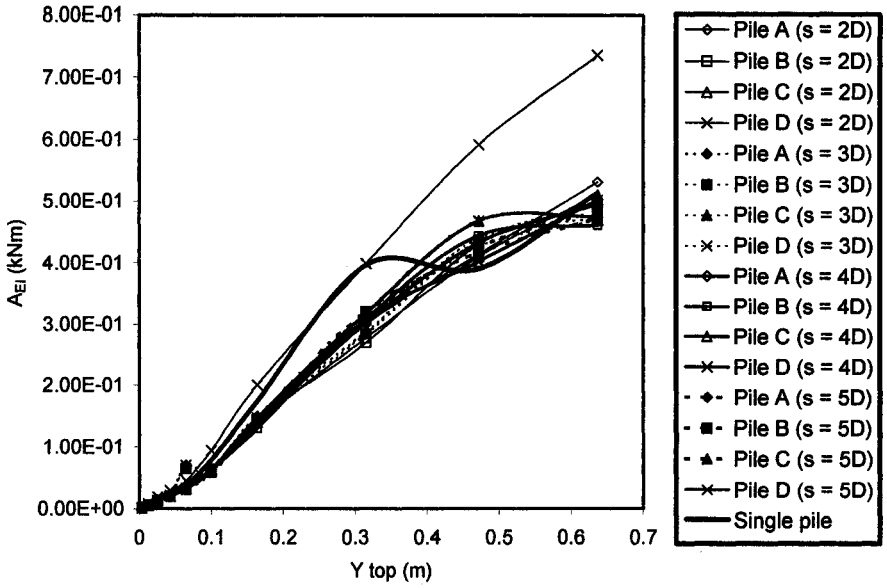

Fig. S.1a The quantitative assessment of sensitivities A_{EI} affecting δy_t of pile members of the groups of 3x3 piles subjected to lateral forces Pg_i (kN) with various spacing and length L = 10T vs. the lateral displacement at the top of the pile

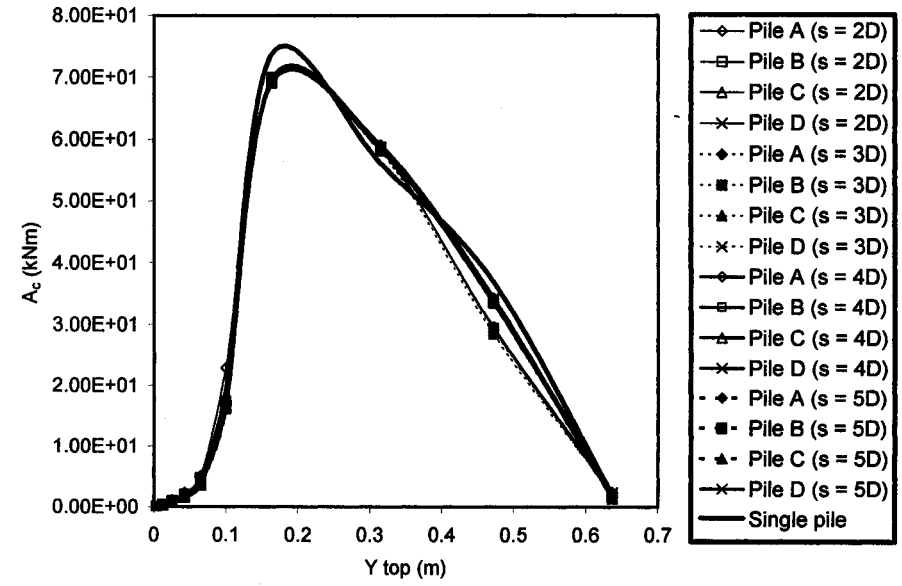

Fig. S.1b The quantitative assessment of sensitivities A_c affecting δy_t of pile members of the groups of 3x3 piles subjected to lateral forces Pg_i (kN) with various spacing and length L = 10T vs. the lateral displacement at the top of the pile

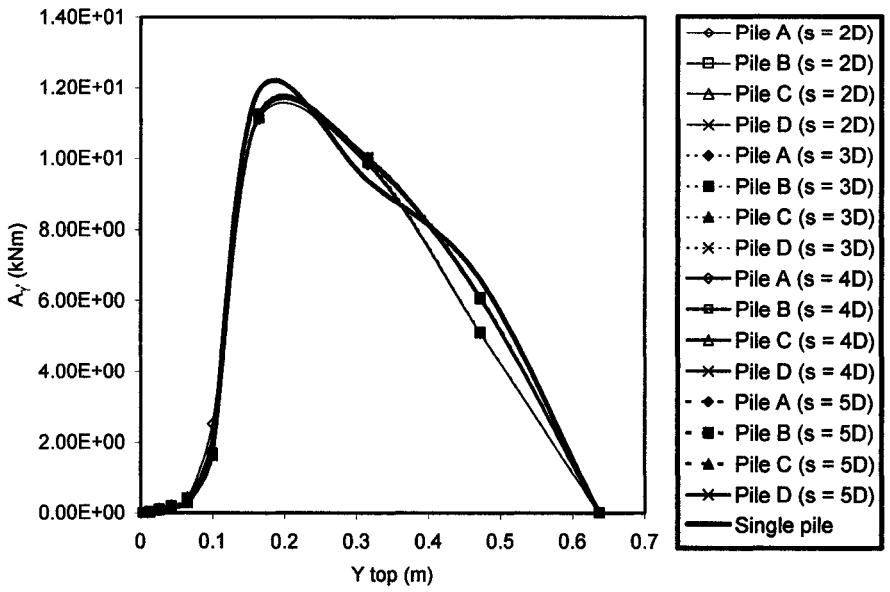

Fig. S.1c The quantitative assessment of sensitivities A_γ affecting δy_t of pile members of the groups of 3x3 piles subjected to lateral forces Pg_i (kN) with various spacing and length L = 10T vs. the lateral displacement at the top of the pile

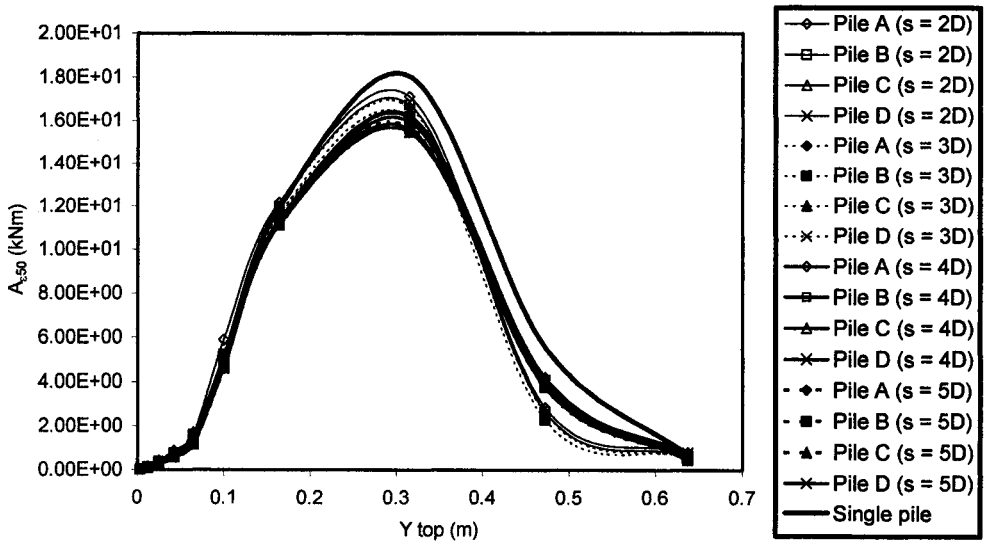

Fig. S.1d The quantitative assessment of sensitivities $A_{\varepsilon 50}$ affecting δy_t of pile members of the groups of 3x3 piles subjected to lateral forces Pg_i (kN) with various spacing and length L = 10T vs. the lateral displacement at the top of the pile

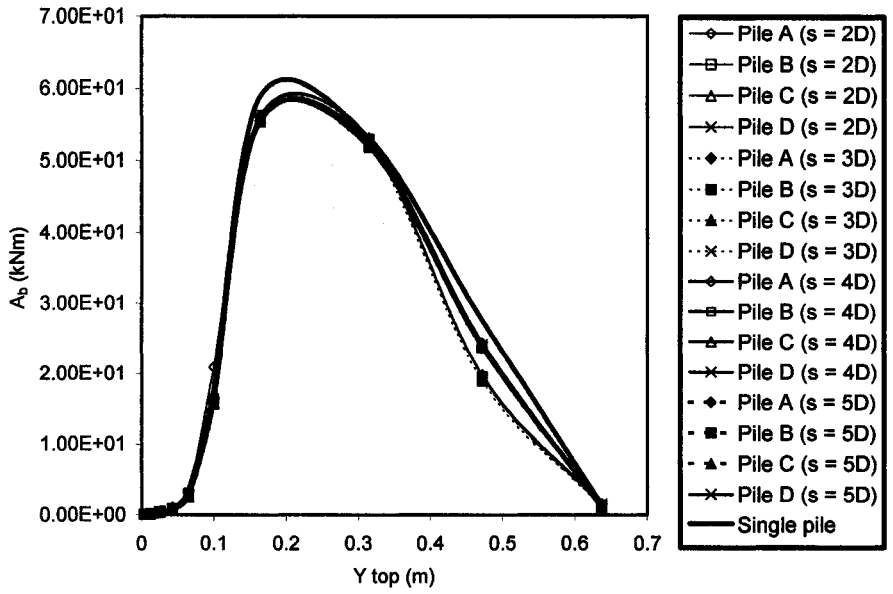

Fig. S.1e The quantitative assessment of sensitivities A_b affecting δy_t of pile members of the groups of 3x3 piles subjected to lateral forces Pg_i (kN) with various spacing and length L = 10T vs. the lateral displacement at the top of the pile

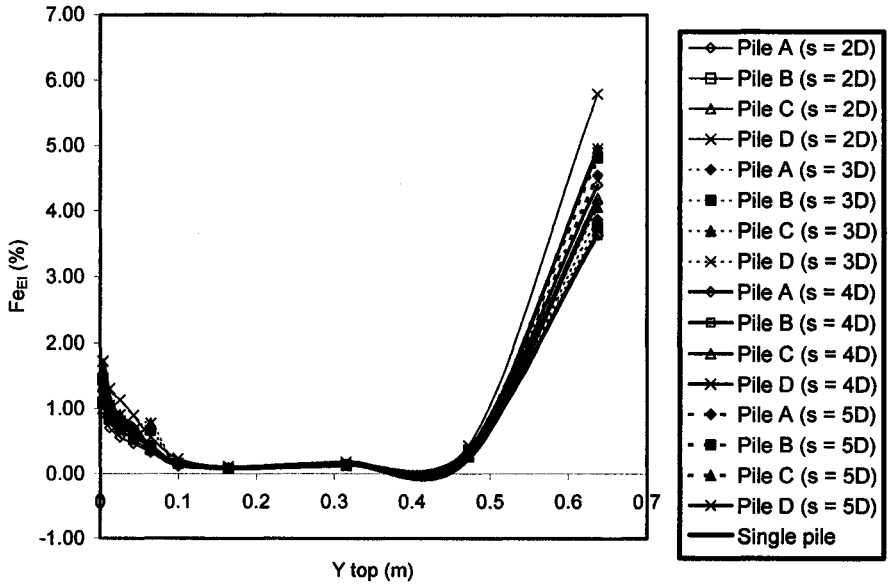

Fig. S.2a The quantitative assessment of relative sensitivity factors Fe_{EI} associated with development of soil's elastic stage along the pile axis affecting δy_t of pile members of the groups of 3x3 piles subjected to lateral forces Pg_i (kN) with various spacing and length L = 10T vs. the lateral displacement at the top of the pile

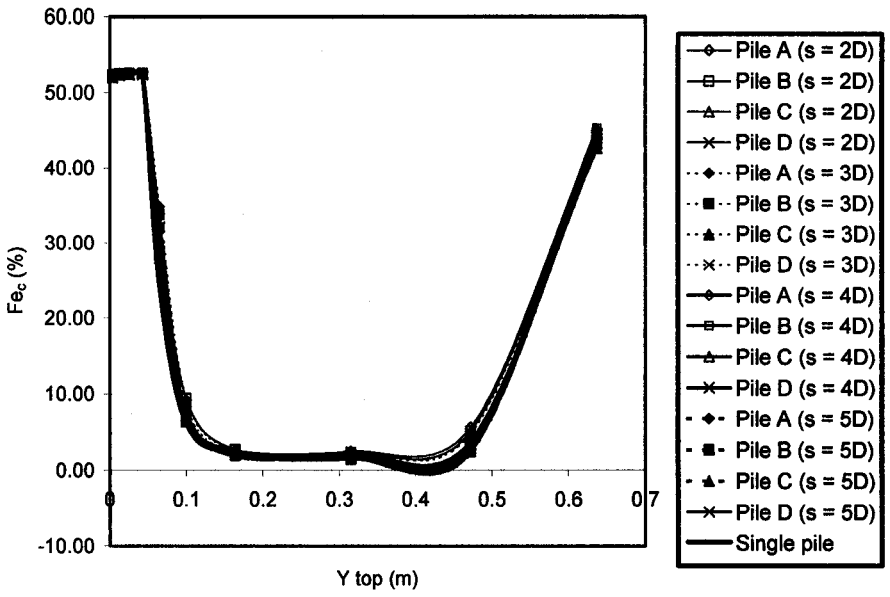

Fig. S.2b The quantitative assessment of relative sensitivity factors Fe_c associated with development of soil's elastic stage along the pile axis affecting δy_t of pile members of the groups of 3x3 piles subjected to lateral forces Pg_i (kN) with various spacing and length L = 10T vs. the lateral displacement at the top of the pile

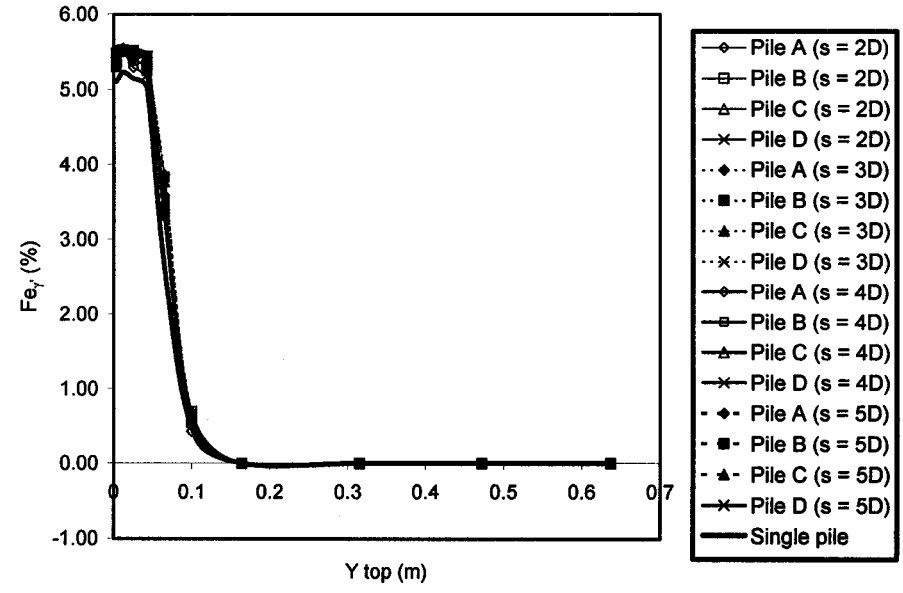

Fig. S.2c The quantitative assessment of relative sensitivity factors $Fe_{\gamma'}$ associated with development of soil's elastic stage along the pile axis affecting δy_t of pile members of the groups of 3x3 piles subjected to lateral forces Pg_i (kN) with various spacing and length L = 10T vs. the lateral displacement at the top of the pile

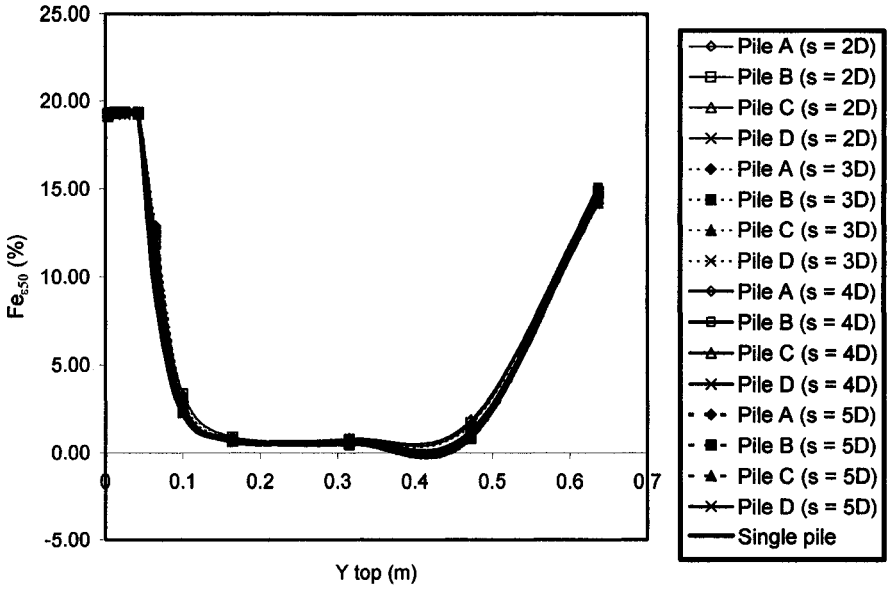

Fig. S.2d The quantitative assessment of relative sensitivity factors $Fe_{\varepsilon 50}$ associated with development of soil's elastic stage along the pile axis affecting δy_t of pile members of the groups of 3x3 piles subjected to lateral forces Pg_i (kN) with various spacing and length L = 10T vs. the lateral displacement at the top of the pile

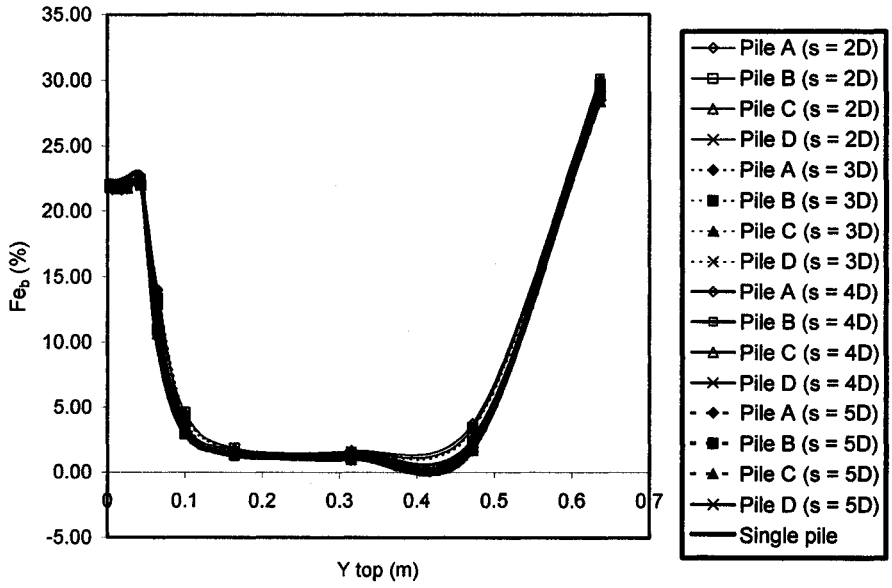

Fig. S.2e The quantitative assessment of relative sensitivity factors Fe_b associated with development of soil's elastic stage along the pile axis affecting δy_t of pile members of the groups of 3x3 piles subjected to lateral forces Pg_i (kN) with various spacing and length L = 10T vs. the lateral displacement at the top of the pile

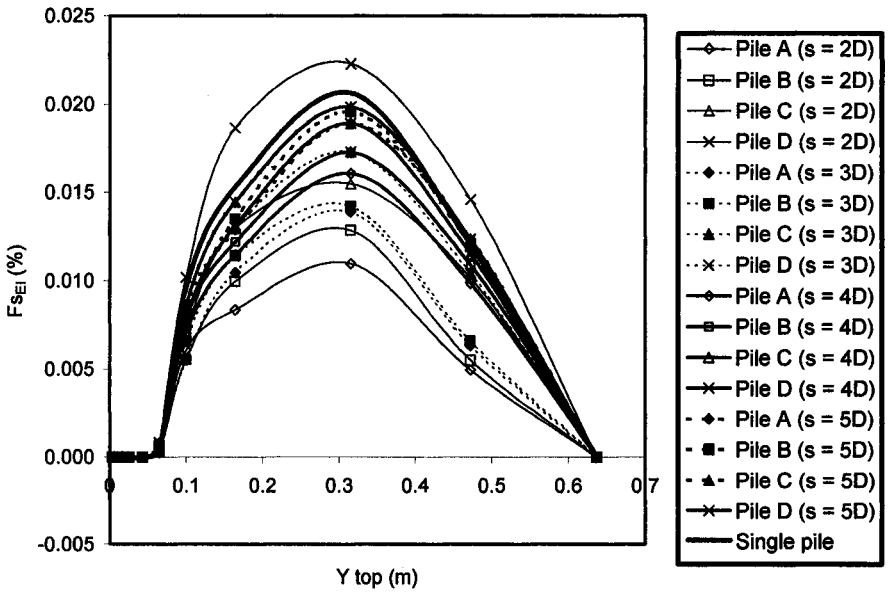

Fig. S.3a The quantitative assessment of relative sensitivity factors Fs_{EI} associated with development of soil's linear softening stage along the pile axis affecting δy_t of pile members of the groups of 3x3 piles subjected to lateral forces Pg_i (kN) with various spacing and length L = 10T vs. the lateral displacement at the top of the pile

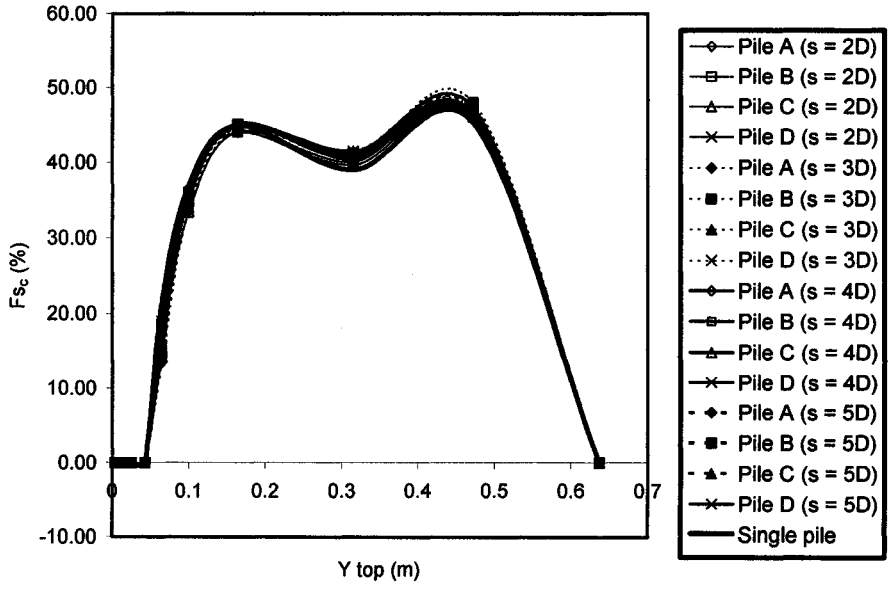

Fig. S.3b The quantitative assessment of relative sensitivity factors Fs_c associated with development of soil's linear softening stage along the pile axis affecting δy_t of pile members of the groups of 3x3 piles subjected to lateral forces Pg_i (kN) with various spacing and length L = 10T vs. the lateral displacement at the top of the pile

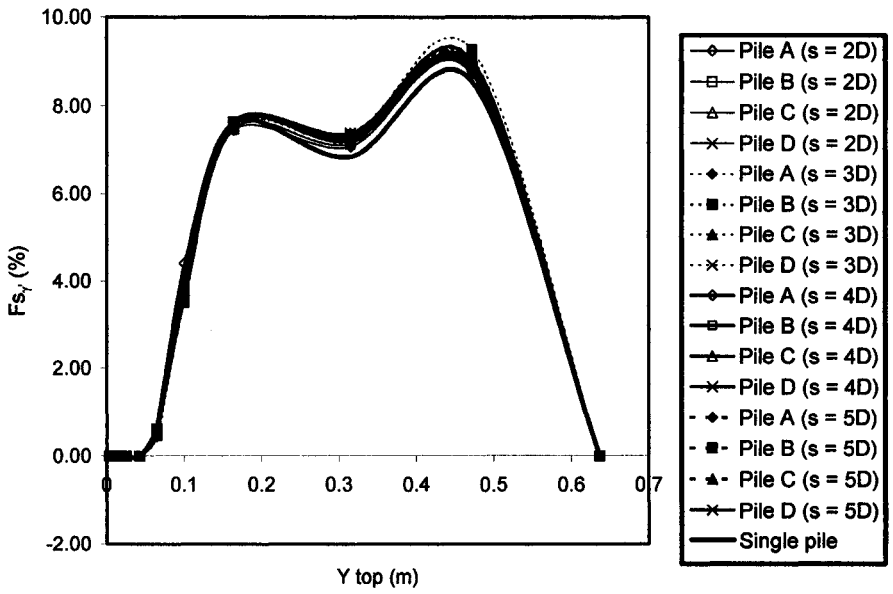

Fig. S.3c The quantitative assessment of relative sensitivity factors $Fs_{\gamma'}$ associated with development of soil's linear softening stage along the pile axis affecting δy_t of pile members of the groups of 3x3 piles subjected to lateral forces Pg_i (kN) with various spacing and length L = 10T vs. the lateral displacement at the top of the pile

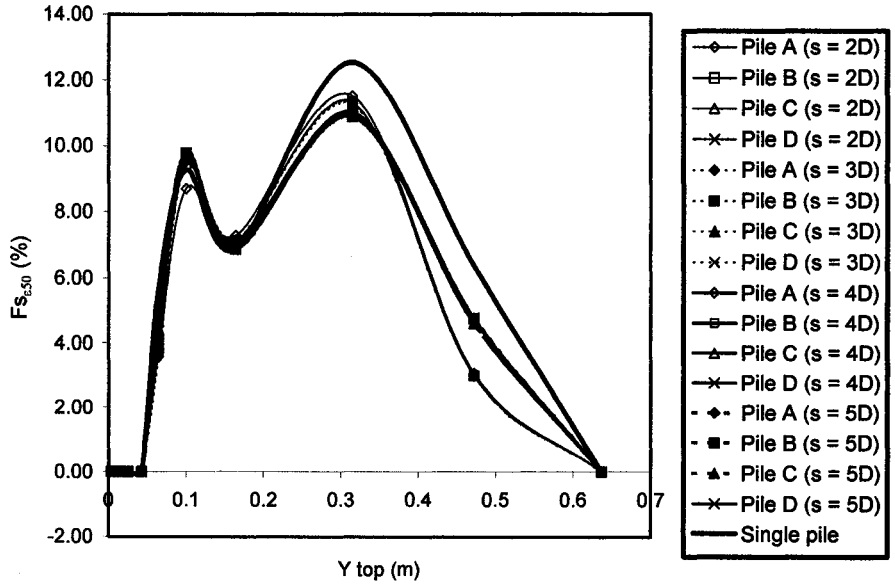

Fig. S.3d The quantitative assessment of relative sensitivity factors $Fs_{\varepsilon 50}$ associated with development of soil's linear softening stage along the pile axis affecting δy_t of pile members of the groups of 3x3 piles subjected to lateral forces Pg_i (kN) with various spacing and length L = 10T vs. the lateral displacement at the top of the pile

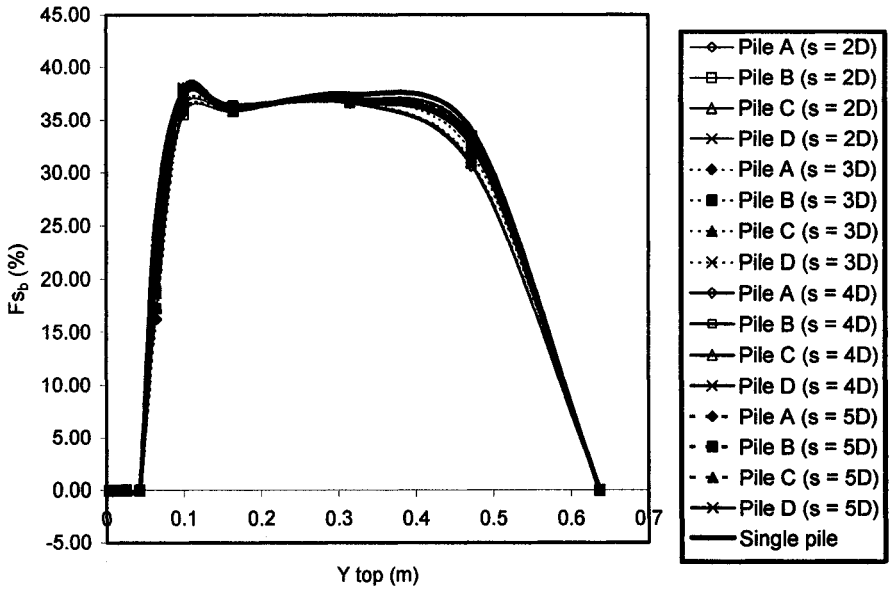

Fig. S.3e The quantitative assessment of relative sensitivity factors Fs_b associated with development of soil's linear softening stage along the pile axis affecting δy_t of pile members of the groups of 3x3 piles subjected to lateral forces Pg_i (kN) with various spacing and length L = 10T vs. the lateral displacement at the top of the pile

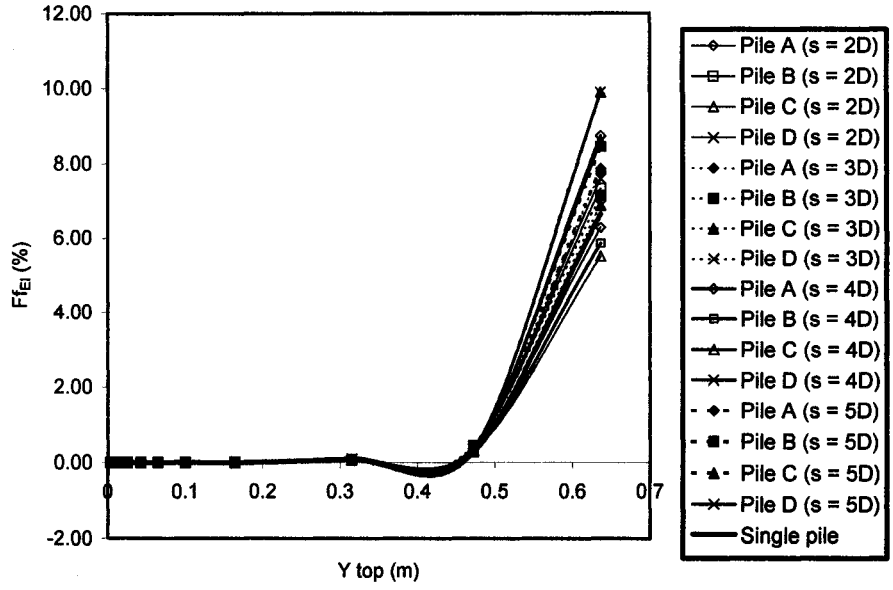

Fig. S.4a The quantitative assessment of relative sensitivity factors Ff_{EI} associated with development of soil's plastic flow stage along the pile axis affecting δy_t of pile members of the groups of 3x3 piles subjected to lateral forces Pg_i (kN) with various spacing and length L = 10T vs. the lateral displacement at the top of the pile

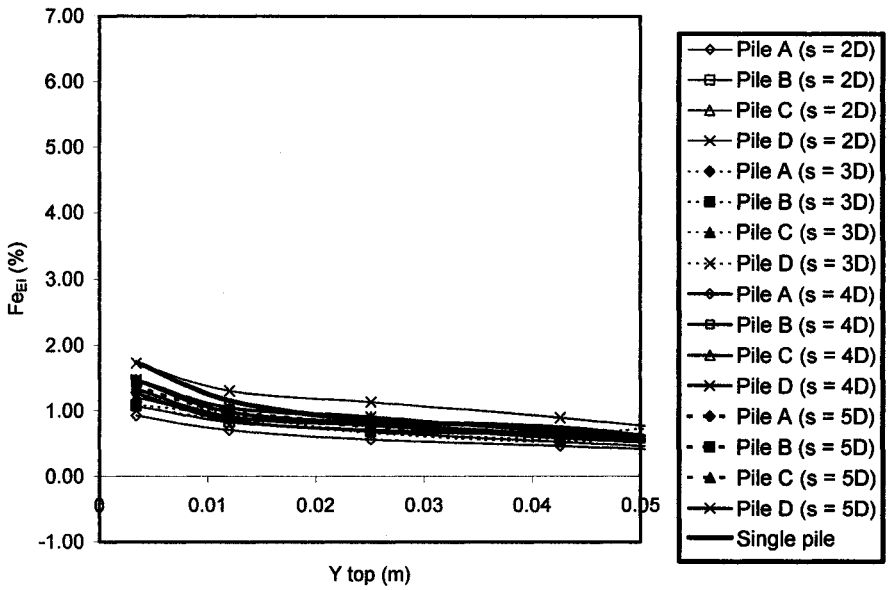

Fig. S.5a The quantitative assessment of relative sensitivity factors Fe_{EI} associated with development of soil's elastic stage along the pile axis affecting δy_t of pile members of the groups of 3x3 piles subjected to lateral forces Pg_i (kN) with various spacing and length L = 10T vs. the lateral displacement at the top of the pile for $y_{top} < 0.05$ m

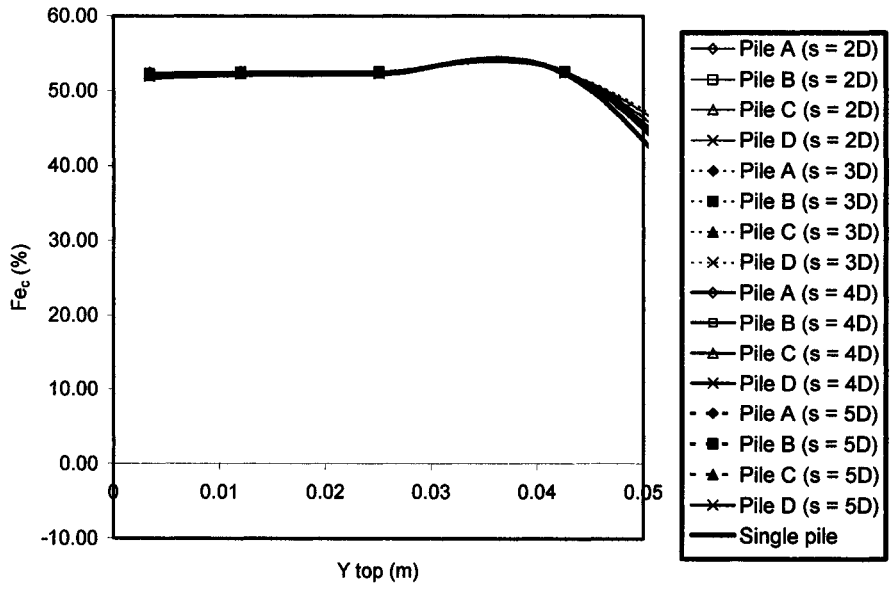

Fig. S.5b The quantitative assessment of relative sensitivity factors Fe_c associated with development of soil's elastic stage along the pile axis affecting δy_t of pile members of the groups of 3x3 piles subjected to lateral forces Pg_i (kN) with various spacing and length L = 10T vs. the lateral displacement at the top of the pile for $y_{top} < 0.05$ m

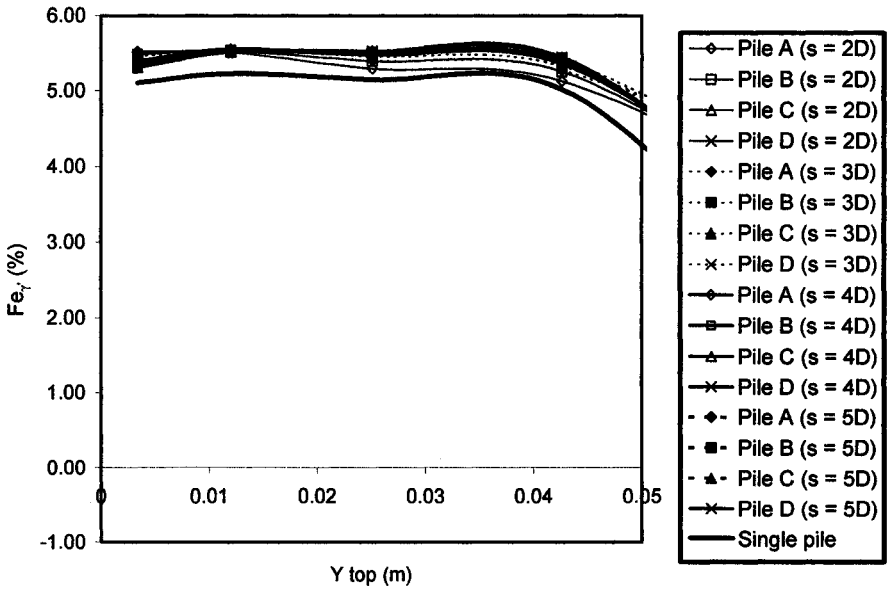

Fig. S.5c The quantitative assessment of relative sensitivity factors Fe_γ associated with development of soil's elastic stage along the pile axis affecting δy_t of pile members of the groups of 3x3 piles subjected to lateral forces Pg_i (kN) with various spacing and length L = 10T vs. the lateral displacement at the top of the pile for $y_{top} < 0.05$ m

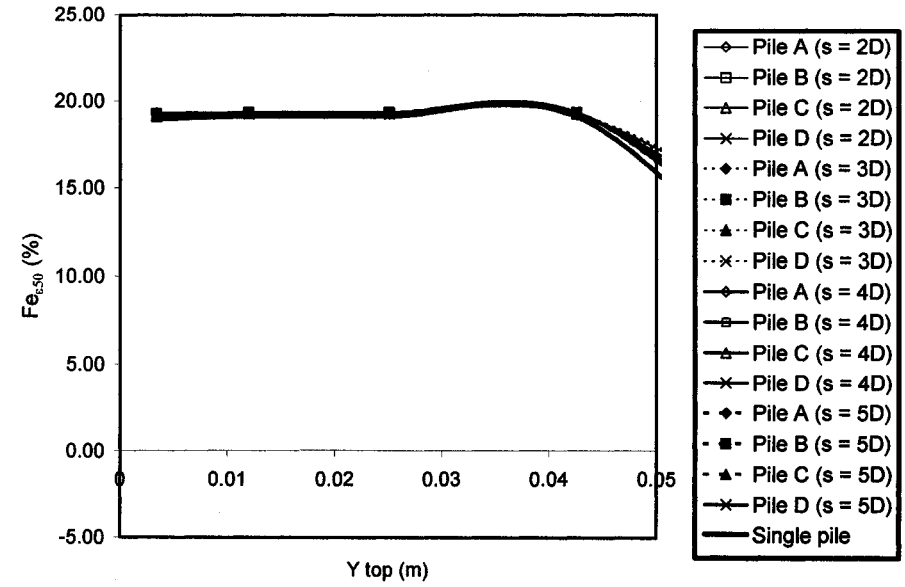

Fig. S.5d The quantitative assessment of relative sensitivity factors $Fe_{\varepsilon 50}$ associated with development of soil's elastic stage along the pile axis affecting δy_t of pile members of the groups of 3x3 piles subjected to lateral forces Pg_i (kN) with various spacing and length L = 10T vs. the lateral displacement at the top of the pile for $y_{top} < 0.05$ m

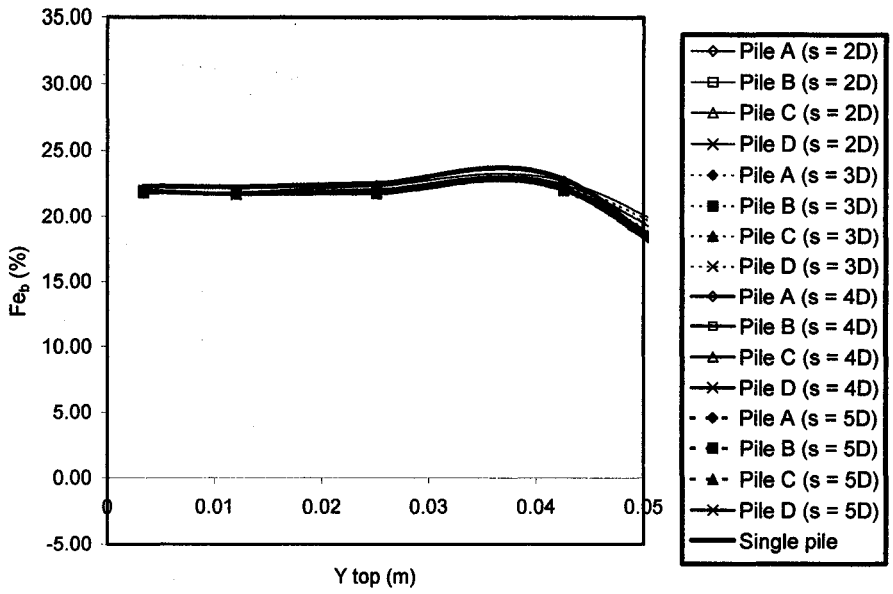

Fig. S.5e The quantitative assessment of relative sensitivity factors Fe_b associated with development of soil's elastic stage along the pile axis affecting δy_t of pile members of the groups of 3x3 piles subjected to lateral forces Pg_i (kN) with various spacing and length L = 10T vs. the lateral displacement at the top of the pile for $y_{top} < 0.05$ m

VITA AUCTORIS

Deni Gunawan Priyanto Putro was born on July 31, 1977 in Grobogan, Central Java, Indonesia. After he graduated from YSKI Senior High School in 1995, he entered Petra Christian University, Surabaya, Indonesia where he obtained a B.Eng in Civil Engineering in 2000. From there he went to University of Windsor starting in May 2001. He is currently a candidate for M.A.Sc in Civil Engineering at the University of Windsor and hopes to graduate in Fall 2002.